U.S. DEPARTMENT OF ENERGY | Energy Efficiency & Renewable Energy

MARCH 2015

2014

VEHICLE TECHNOLOGIES OFFICE

FY 2014 Annual Progress Report - Advanced Combustion Engine Research and Development

This document highlights work sponsored by agencies of the U.S. Government. Neither the U.S. Government nor any agency thereof, nor any of their employees, makes any warranty, express or implied, or assumes any legal liability or responsibility for the accuracy, completeness, or usefulness of any information, apparatus, product, or process disclosed, or represents that its use would not infringe privately owned rights. Reference herein to any specific commercial product, process, or service by trade name, trademark, manufacturer, or otherwise does not necessarily constitute or imply its endorsement, recommendation, or favoring by the U.S. Government or any agency thereof. The views and opinions of authors expressed herein do not necessarily state or reflect those of the U.S. Government or any agency thereof.

U.S. Department of Energy
1000 Independence Avenue, S.W.
Washington, D.C. 20585-0121

FY 2014 PROGRESS REPORT FOR ADVANCED COMBUSTION ENGINE RESEARCH AND DEVELOPMENT

Energy Efficiency and Renewable Energy
Vehicle Technologies Office

Approved by Gurpreet Singh
Program Manager, Advanced Combustion Engine R&D
Vehicle Technologies Office

December 2014

Acknowledgement

We would like to express our sincere appreciation to Alliance Technical Services, Inc. and Oak Ridge National Laboratory for their technical and artistic contributions in preparing and publishing this report.

In addition, we would like to thank all the participants for their contributions to the programs and all the authors who prepared the project abstracts that comprise this report.

Table of Contents

I. INTRODUCTION

I.1 Program Overview and Status

DEVELOPING ADVANCED COMBUSTION ENGINE TECHNOLOGIES

On behalf of the Vehicle Technologies Office (VTO) of the U.S. Department of Energy (DOE), we are pleased to introduce the Fiscal Year (FY) 2014 Annual Progress Report for the Advanced Combustion Engine (ACE) Program. The VTO mission is to develop more energy-efficient and environmentally friendly highway transportation technologies that will enable the United States to use significantly less petroleum, and reduce greenhouse gas and other regulated emissions while meeting or exceeding drivers' performance expectations. The ACE Program supports VTO's mission by addressing critical technical barriers in commercializing higher efficiency, very low emissions, advanced combustion engines for passenger and commercial vehicles that meet future federal emissions regulations.

Dramatically improving the efficiency of internal combustion engines (ICEs) is one of the most promising and cost-effective approaches to increasing the fuel economy of the U.S. vehicle fleet over the next several decades. ICEs already offer outstanding drivability and reliability to over 230 million highway transportation vehicles in the U.S., while future technology improvements are expected to make them substantially more efficient. Engine efficiency improvements alone can potentially increase fuel economy by 35% to 50% for passenger vehicles and by 30% for commercial vehicles with accompanying carbon dioxide (the primary greenhouse gas) reduction. Even greater vehicle fuel economy improvement is expected when more efficient engines are coupled with advanced hybrid electric powertrains. Advanced combustion engines could greatly reduce U.S. transportation petroleum consumption to achieve economic, environmental, and energy security benefits. The Energy Information Administration Annual Energy Outlook 2014 reference case scenario forecasts that even in 2040, over 99% of all highway transportation vehicles sold will still have ICEs.

The ACE R&D Program set the following goals for advanced combustion engines to achieve passenger and commercial vehicle fuel economy improvements:

- By 2015, increases the efficiency of ICEs for passenger vehicles resulting in fuel economy improvements of 25% for gasoline vehicles and 40% for diesel vehicles, compared to baseline 2009 gasoline vehicles, and by 2020, achieve fuel economy improvements of 35% and 50% for gasoline and diesel vehicles, respectively.
- By 2015, increase the efficiency of ICEs for commercial vehicles from 42% (2009 baseline) to 50% (20% improvement) and by 2020, further improve engine efficiency to 55% (30% improvement) with demonstrations on commercial vehicle platforms.
- By 2015, increase the fuel economy of passenger vehicles by at least 5% with thermoelectric generators that convert energy from engine waste heat to electricity.

The passenger and commercial vehicle goals will be met while utilizing advanced fuel formulations that can incorporate non-petroleum-based blending agents to enhance combustion efficiency and reduce petroleum dependence. The ACE Program undertakes R&D activities to improve the efficiency of engines for highway transportation vehicles. The Program supports a well-balanced R&D effort that spans fundamental research, applied technology development, and prototype demonstration. The ACE Program includes collaborations with industry, national laboratories, and universities in these activities to address critical technology barriers and R&D needs of advanced combustion engines that are common between passenger and commercial vehicle applications.

The ACE Program launched two initiatives in FY 2010, namely the SuperTruck Initiative and the Advanced Technology Powertrains for Light-Duty Vehicles (ATP-LD), to address the first two goals. These initiatives continued in FY 2014 and are on track to accomplish the stated FY 2015 goals. More than $100 million from the American Recovery and Reinvestment Act and a private cost share of 50% support nearly $375 million in total research, development and demonstration projects across the country. The four SuperTruck projects focus on cost-effective measures to improve the freight efficiency of Class 8 long-haul trucks by 50%, of which 20% will come from engine efficiency improvements alone. The ATP-LD projects focus on increasing the fuel economy of passenger vehicles by at least 25% using only engine/powertrain improvements.

Through an enabling technologies FY 2012 solicitation, DOE awarded six cost-shared (from 20% to 50%) contracts to competitively selected teams of suppliers and vehicle manufacturers to develop and demonstrate innovations capable of achieving breakthrough engine and powertrain system efficiencies while meeting federal emission standards for passenger and commercial vehicles that include long-haul tractor trailers. These projects continued in FY 2014 to address the technical barriers inhibiting wider use of these advanced enabling engine technologies in the mass market.

Three-year university research grants totaling $12 million (equally split between DOE and the National Science Foundation) were awarded in FY 2013 and continued through FY 2014. These grants were competitively selected through an FY 2012 joint solicitation under a Memorandum of Understanding between DOE/VTO and the National Science Foundation. Under these grants, the universities are partnered with industry and national laboratories to advance transformative ideas to develop the enabling understanding for improving the efficiency of ICEs. The grants cover a diverse array of topics that bring to bear experiments, modeling and analyses to enable more efficient low-temperature combustion processes in ICEs. Among the universities/university team(s) receiving grants, nine are focused on improving engine combustion efficiency and three are focused on reducing emissions.

Three projects initiated in FY 2011 continued in FY 2014 to develop thermoelectric generators with cost-competitive advanced thermoelectric materials that will improve passenger vehicle fuel economy by at least 5% in FY 2015.

This introduction outlines the nature, current focus, recent progress, and future directions of the ACE Program. The ACE Program's R&D activities are planned in conjunction with U.S. DRIVE (Driving Research and Innovation for Vehicle efficiency and Energy sustainability) and the 21st Century Truck partnerships. ACE R&D activities are closely coordinated with the relevant activities of the Fuel and Lubricant Technologies Program and the Materials Technology Program, also within VTO, due to the importance of clean fuels and advanced materials in achieving high efficiency and low emissions in engines.

CURRENT TECHNICAL FOCUS AREAS AND OBJECTIVES

The VTO ACE Program focuses on R&D of advanced engine combustion strategies that will increase the efficiency beyond current state-of-the-art engines and reduce engine-out emissions of nitrogen oxides (NOx) and particulate matter (PM) to near-zero levels. Engine combustion research focuses on three major combustion strategies: a) low temperature combustion (LTC) (including homogeneous charge compression ignition, pre-mixed charge compression ignition, reactivity controlled compression ignition); b) lean-burn (or dilute) gasoline combustion; and c) clean diesel combustion. In parallel, research is underway to increase emission control systems efficiency and durability to comply with emissions regulations at an acceptable cost and with reduced dependence on precious metals.

The ACE Program objectives are the following:

- Further the fundamental understanding of advanced combustion strategies that simultaneously show higher efficiencies and very low emissions, and the effects of critical factors such as fuel spray characteristics, in-cylinder air motion, heat transfer and others. Address critical barriers associated with gasoline- and diesel-based advanced engines, as well as renewable fuels.
- Improve the effectiveness and durability of emission control (exhaust aftertreatment) devices to complement advanced combustion strategies, as well as reduce their dependence on precious metals to reduce cost, which is another barrier to penetration of advanced combustion engines in the passenger and commercial vehicle markets.
- Develop precise and flexible engine controls to facilitate adjustments of parameters that allow advanced combustion engines to operate over a wider range of engine speed/load conditions.
- Develop key enabling technologies such as sensors for control systems and engine diagnostics, and components for thermal energy recovery.
- Further advance engine technologies such as turbo-machinery, flexible valve systems, advanced combustion systems, and fuel system components to reduce parasitic losses and other losses to the environment.

- Further develop approaches to producing useful work from engine waste heat such as through incorporation of bottoming cycles or thermoelectric generators that convert energy in the engine exhaust directly to electricity.
- Improve integration of advanced engine/emissions technologies with hybrid-electric systems for greater vehicle fuel economy with lowest possible emissions.

The ACE Program maintains close collaboration with industry through a number of working groups and teams, and utilizes these networks for setting goals, adjusting priorities of research, and tracking progress. These collaborative groups include the Advanced Combustion and Emission Control Tech Team of the U.S.DRIVE Partnership and the Engine Systems Team of the 21st Century Truck Partnership. Focused efforts are carried out under the Advanced Combustion Memorandum of Understanding (which includes auto manufacturers, engine companies, fuel suppliers, national laboratories, and universities) and the CLEERS (Cross-Cut Lean Exhaust Emission Reduction Simulation) activity for the Advanced Engine Cross-Cut Team.

TECHNOLOGY STATUS AND KEY BARRIERS

Significant advances in engine combustion, emission controls, fuel injection, turbo-machinery, and other advanced engine technologies continue to increase the thermal efficiency of ICEs with simultaneous reductions in emissions. With these advances, gasoline and diesel engines continue to be attractive engine options for conventional vehicles. In addition, these engines can be readily adapted to use natural gas and biofuels such as ethanol and biodiesel, and can be integrated with hybrid and plug-in hybrid electric vehicle powertrains.

LTC strategies such as homogeneous charge compression ignition, pre-mixed charge compression ignition, and reactivity controlled compression ignition exhibit high efficiency with significant reductions in engine-out emissions of NOx and PM to levels that remove or reduce the requirements for exhaust aftertreatment. Progress in LTC strategies continue to expand the operational range covering speed/load combinations consistent with light-duty and heavy-duty drive cycles. Significant R&D effort has focused on allowing independent control of the intake/exhaust valves relative to piston motion and on other improvements in air-handling and engine controls. These address major challenges of fuel mixing, conditioning of intake air, combustion timing control, and expansion of the operational range. Many of these technologies are transitioning to the vehicle market.

Spark-ignition (SI) gasoline engines power the majority of the U.S. light-duty vehicle fleet and generally operate with stoichiometric combustion to allow use of highly cost-effective three-way catalysts for emission control. Engine technology advances in recent years contributing to substantial improvements in gasoline engine efficiency include direct fuel injection, flexible valve systems, improved combustion chamber design, and reduced mechanical friction. Lean-burn gasoline engines have been introduced in countries with less stringent emissions regulations. These engines have higher efficiencies at part load but require more costly lean-NOx emission controls to meet the more stringent U.S. emissions regulations. Advances in lean-burn gasoline emission controls are critical for introducing this higher efficiency technology in the U.S. market.

Attaining the high efficiency potential of lean-burn gasoline technology requires a better understanding of the dynamics of fuel-air mixture preparation; the challenge is in creating combustible mixtures near the spark plug and away from cylinder walls in an overall lean environment. Research focuses on developing a comprehensive understanding of intake air flows and fuel sprays, as well as their interactions with the combustion chamber surfaces over a wide operating range and generating appropriate turbulence to enhance flame speed. Improved simulation tools are being developed for optimizing the lean-burn systems over the wide range of potential intake systems, piston geometries, and injector designs. Another challenge is the reliable ignition and combustion of lean (dilute) fuel-air mixtures. Robust, high-energy ignition systems and mixture control methods, are also being developed to reduce combustion variability at lean and highly boosted conditions. Several new ignition systems have been proposed (e.g., high-energy plugs, plasma, corona, laser, etc.) and need to be investigated.

Diesel engines are also well-suited for light-duty vehicle applications, delivering fuel economies that are considerably higher than comparable SI engines. Key developments in combustion and emission controls combined with the availability of low sulfur fuel have enabled manufacturers to achieve the mandated emission levels and introduce additional diesel-powered models to the U.S. market. DOE research has contributed to all of these areas. However, diesels in passenger cars have limited market penetration in the U.S.

primarily due to the cost of the added components required to reduce emissions and higher diesel fuel price, hence research continues on increasing engine efficiency and reducing the cost of emissions compliance.

The heavy-duty diesel is the most common engine for commercial vehicles because of its high efficiency and outstanding durability. When R&D efforts over the last decade focused on meeting increasingly stringent heavy-duty engine emission standards, efficiency gains were modest. After meeting U.S. Environmental Protection Agency (EPA) 2010 emission standards for NOx and PM, efforts then turned to improving the engine efficiency. Continued aggressive R&D to improve boosting, thermal management, and the reduction and/or recovery of rejected thermal energy has resulted in current heavy-duty diesel engines efficiencies in the 42-43% range. Advanced combustion regimes and demonstrated waste heat recovery technologies can significantly improve overall engine efficiency to 55%.

The EPA in 2007 allowed the introduction of urea selective catalytic reduction (urea-SCR) technology for NOx control in Tier 2 light-duty vehicles, heavy-duty engines, and in other future diesel engine applications in the U.S. Strategies have been developed and implemented to supply the urea-water solution (given the name "diesel exhaust fluid") for vehicles. Using urea-SCR, light-duty manufacturers have been able to meet the Tier 2, Bin 5 emissions standard. All heavy-duty diesel vehicle manufacturers have adopted urea-SCR since it has a broader temperature range of effectiveness than competing means of NOx reduction and allows the engine/emission control system to achieve higher fuel efficiency. Although urea-SCR is a relatively mature catalyst technology, more support research is needed to aid formulation optimization and minimize degradation effects such as hydrocarbon fouling.

Due to the low exhaust temperature (150^{o}C) of advanced engines, emissions of NOx and PM are a significant challenge for lean-burn technologies including conventional and advanced diesel combustion strategies for light-and heavy-duty engines, as well as lean-burn gasoline engine. Numerous technologies are being investigated to reduce vehicle NOx emissions while minimizing the fuel penalty associated with operating these devices. These include advanced combustion strategies using high dilution levels to reduce in-cylinder NOx formation as well as post-combustion emission control (aftertreatment) devices.

Cost is a primary limitation to further adoption of current light-duty diesels. Complex engine and exhaust gas recirculation systems, and the larger catalyst volumes associated with lean-NOx traps (LNTs) and diesel particulate filters (DPFs) result in higher overall costs in comparison to conventional gasoline vehicle systems. LNTs are particularly cost-sensitive because they require platinum group metals, and the cost of these materials is high and volatile due to limited sources that are primarily mined in foreign countries. Improvements in the temperature range of operation for LNTs are also desired to reduce cost and enable success in the lean-gasoline engine application. Both LNTs and DPFs result in extra fuel use, or a "fuel penalty," as they require fueling changes in the engine for regeneration processes. Aggressive research has substantially decreased the combined fuel penalty for both devices to approximately 4% of total fuel flow; further reductions are possible. Since LNTs have a larger impact on fuel consumption than urea-SCR, most light-duty vehicle manufacturers appear to prefer SCR although urea replenishment is more of a challenge for light-duty customers as compared to heavy-duty vehicle users. Another improvement being pursued for LNT technology is to pair them with SCR catalysts. The advantage is that the SCR catalyst uses the NH_3 produced by the LNT so no urea is needed. Formulation and system geometries are being researched to reduce the overall precious metal content of LNT+SCR systems that reduces cost and makes the systems more feasible for light-duty vehicles.

The direct injection technology utilized for most advanced gasoline engines produces PM emissions that although smaller in mass than diesel particulates, may still represent significant emissions in terms of particulate number counts. PM emissions from dilute combustion gasoline engines are not fully understood; their morphology and chemical composition are also affected by combustion. There is a need to develop filtration systems for smaller diameter PM that are durable and with low fuel economy penalty. Fuel economy penalties are caused by increased back pressure and the need to regenerate the filter. The PM aftertreatment effectiveness can be sensitive to fuel sulfur or other contaminants (e.g., ash) and extended durability needs to be established and the feasibility of meeting future more stringent U.S. regulations has to be confirmed.

The significantly lower NOx and PM engine-out emission levels from advanced LTC strategies reduce the requirements for exhaust aftertreatment. However, higher hydrocarbon (HC) and carbon monoxide (CO) emissions require additional controls which are often a challenge with the low exhaust temperature characteristic of these combustion modes.

Complex and precise engine and emission controls require sophisticated feedback systems employing new types of sensors. A major advancement in this area for light-duty engines has been the introduction of in-cylinder pressure sensors integrated into the glow plug. Start-of-combustion sensors (other than the aforementioned pressure sensor) have been identified as a need, and several development projects have been completed. Sensors are also beneficial for the emission control system. NOx and PM sensors are under development and require additional advances to be cost-effective, accurate, and reliable. Upcoming regulations with increased requirements for onboard diagnostics will also challenge manufacturers trying to bring advanced fuel efficient solutions to market. The role of sensors and catalyst diagnostic approaches will be a key element of emission control research in the next few years.

Waste heat recovery approaches (e.g., bottoming cycles) are being implemented in heavy-duty diesel vehicles and explored for light-duty diesel and gasoline applications. Experiments have shown that bottoming cycles have the potential to improve vehicle fuel economy by as much as 10%. Thermoelectric generators can directly convert energy in the engine's exhaust to electricity for operating auxiliary loads and accessories. In current gasoline production passenger vehicles, roughly over 70% of the fuel energy is lost as waste heat from an engine operating at full power—about 35% to 40% is lost in the exhaust gases and another 30% to 35% is lost to the engine coolant. Several manufacturers intend to introduce thermoelectric generators in their cars later this decade in Europe and North America.

Thermoelectric devices for vehicle occupant comfort heating or cooling are more fuel efficient alternatives to the conventional mobile heating, ventilation and air conditioning systems. Estimates show that dispersed thermoelectric devices can maintain single occupant comfort conditioning with about one-sixth of the energy used by conventional systems that cool the entire driver and passenger cabin. The ACE Program and the California Energy Commission completed two projects to design and install zonal (dispersed) thermoelectric heating, ventilation and air conditioning systems in selected passenger vehicle models. A ride-and-drive demonstration was conducted at the successful projects close in early FY 2014.

FUTURE DIRECTIONS

The maximum theoretical ICE fuel conversion efficiency is considerably higher than the mid-40% peak values seen today. High irreversibility in traditional premixed or diffusion flames limits achievable efficiencies. Other contributing factors are heat losses during combustion/expansion, structural limits that constrain peak cylinder pressures, untapped exhaust energy, and mechanical friction. R&D efforts will continue to focus on operating the engine near peak efficiency over real-world driving cycles to improve the overall vehicle fuel economy. For SI engines, this means reducing the throttling losses with technologies such as lean-burn, high dilution, and variable geometry. Exhaust losses can be reduced with compound compression and expansion cycles made possible by variable valve timing, use of turbine expanders, regenerative heat recovery, and application of thermoelectric generators. These approaches could potentially increase light-duty vehicle fuel economy by 35% to 50%, and increase heavy-duty engine efficiency to 55%. The ACE Program will continue to pursue engine hardware changes needed to implement advanced combustion strategies. These include variable fuel injection geometries, turbo- and super-charging to produce very high manifold pressures, compound compression and expansion cycles, variable compression ratio technologies, and improved sensors and control methods. VTO will also continue to examine approaches that are a substantial departure from today's processes to gain larger reductions in combustion irreversibilities.

The ACE Program will continue to address the critical barriers common to both gasoline and diesel engines, with increased emphasis on the improvement of gasoline SI engines. Gasoline engines, including those using E85 (85% ethanol, 15% gasoline) flexible-fuel, can be made 20% to 25% more efficient through employment of direct injection, boosting/downsizing, and lean-burn.

The ACE Program will also continue to address emission control requirements for high-efficiency diesel and lean-burn gasoline engines to meet more stringent future emission standards. National laboratory and university projects will continue to focus on innovative emission control strategies that will reduce the cost and increase the performance and durability of NOx reduction and PM oxidation systems at 150°C exhaust temperatures. Project areas will include development of low-cost base metal catalysts (to replace expensive platinum group metals), lighter and more compact multifunctional components, new control strategies to lessen impact on fuel consumption, and improved sensors and onboard diagnostics. Also, simulations of the

catalyst technologies are being developed to enable industry to perform more cost-effective system integration during vehicle development.

The requirements of emission controls are expected to change as advanced combustion approaches evolve and engine-out emissions become cleaner. With the potential introduction of high-efficiency lean-burn gasoline engines, the ACE Program will undertake further R&D on emission controls for managing HC/CO emissions in addition to lean-NOx emission control which has previously focused on diesel engines. Engine-out PM emissions from direct injection gasoline engines, although lower in mass than the diesel engine, are also a concern due to smaller particle sizes and morphology.

The ACE Program will continue R&D of enabling technologies for more efficient, emission-compliant engine/powertrain systems. Research will focus on injector controls and fuel spray development, engine controls and sensors that are precise and flexible for enabling improved efficiency and emission reduction in advanced combustion engines. In addition to developing a better understanding of stochastic and deterministic in-cylinder processes that limit the speed/load range of many advanced combustion strategies. Control system technologies will facilitate adjustments to parameters such as intake air temperature, fuel injection timing, injection rate, variable valve timing, and exhaust gas recirculation to allow advanced combustion engines to operate over a wider range of engine speed/load conditions. The best combination of engine technologies should enable advanced combustion engines to meet maximum fuel economy and performance requirements. These include variable compression ratio, variable valve timing, variable boost, advanced sensors and ignition systems, and exhaust emission control devices (to control HC emissions at engine idling conditions) in an integrated system. Research on advanced sensors will address upcoming EPA onboard diagnostic requirements, improve understanding of emission control aging, and develop models that are integral to the diagnostic method.

The ACE Program will conclude the thermoelectric generator projects in FY 2015. These projects will demonstrate cost-competitiveness of thermoelectric generators for selected passenger vehicle platforms. The projects will also show reduction in cost of thermoelectric materials, cost-competitive manufacturing at the production scale for the vehicle market, and demonstrate durable for vehicle applications.

The remainder of this report highlights progress achieved during FY 2014. The following 66 abstracts of industry, university, and national laboratory projects provide an overview of the exciting work being conducted to address critical technical barriers and challenges to commercializing higher efficiency, advanced ICEs for light-duty passenger vehicles, and medium- to heavy-duty commercial vehicles. We are encouraged by the technical progress realized under this dynamic program in FY 2014, but we also remain cognizant of the significant technical hurdles that lay ahead, especially those to further improve efficiency while meeting the light-duty EPA Tier 3 emission standards and future heavy-duty engine standards for the full useful life of these vehicles.

Gurpreet Singh, Program Manager
Advanced Combustion Engine Program
Vehicle Technologies Office

Kenneth C. Howden
Vehicle Technologies Office

Roland M. Gravel
Vehicle Technologies Office

Leo Breton
Vehicle Technologies Office

I.2 Project Highlights

The following projects highlight progress made in the Advanced Combustion Engine Program during FY 2014.

COMBUSTION RESEARCH

The objective of these projects is to identify how to achieve more efficient combustion with reduced emissions from advanced technology engines.

- Sandia National Laboratories is providing the physical understanding of the in-cylinder combustion processes needed to minimize the fuel consumption and the carbon footprint of automotive diesel engines while maintaining compliance with emissions standards. In FY 2014 they, (1) Upgraded fuel injection capabilities to allow several closely spaced injection events within a single cycle; (2) Acquired and installed a state-of-the-art injection quantity and rate bench and applied it to determine the effects of both fuel properties and operating parameters on the fuel injection rate; (3) Examined the evolution of the in-cylinder flow for three different swirl ratios and characterized the evolution of flow asymmetry throughout the compression stroke; (4) Extended computational fluid dynamics code capabilities to allow efficient use of parallel computing capabilities; and (5) Examined the impact of a full-engine grid on calculations of fuel spray asymmetries and near-top-dead center turbulence levels. (Miles, report II.1)
- Sandia National Laboratories is developing a fundamental understanding of how in-cylinder controls can improve efficiency and reduce pollutant emissions of advanced low-temperature combustion (LTC) technologies. In FY 2014 they, (1) Tracked the spatial and temporal soot precursor evolution, which aided LTC computer model validation for codes used by industry (Cummins, Convergent Science); (2) Identified the key features and dependencies of injector dribble throughout the engine cycle, which point to areas for further injector development; and (3) Experimentally verified the existence and magnitude of the end-of-injection entrainment wave that was previously predicted by computer models of various complexities, which helps to justify further development of injection rate-shaping to tailor mixing. (Musculus, report II.2)
- Sandia National Laboratories is facilitating improvement of engine spray combustion modeling, accelerating the development of cleaner, more efficient engines. In FY 2014 they, (1) Organized ECN3, the third workshop of the Engine Combustion Network, with over 150 Web and in-person attendees focused on experimental and modeling advancement. Led the year-long experimental/modeling exchange on targets to identify the state of the art and in-spray combustion modeling and remedying known weaknesses; (2) Quantified the formaldehyde formation on plane with simultaneous high-speed schlieren along a line of sight to reveal the ignition location and timing for diesel sprays; and (3) Developed quantitative soot and soot radiation datasets for diesel ECN "Spray A" and variants. (Pickett, report II.3)

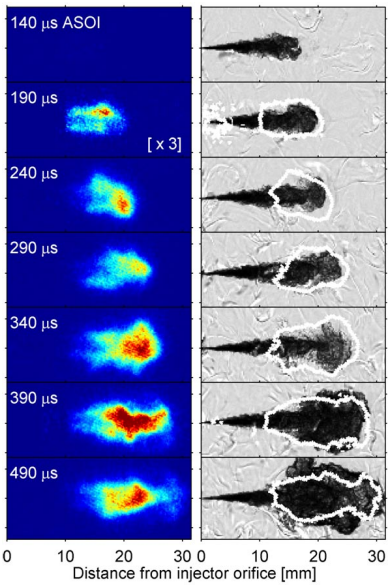

Time Sequence of Formaldehyde Formation (left panels) and Schlieren Images of the Fuel Injected (right panels) (Pickett, report II.3)

- Sandia National Laboratories is providing the fundamental understanding (science-base) required to overcome the technical barriers to the development of practical low-temperature gasoline combustion (LTGC) engines by industry. In FY 2014 they, (1) Analyzed how a Miller cycle would affect maximum load over a range of intake boost pressure for both premixed and partial fuel stratification fueling strategies; (2) Conducted extensive study of combustion noise level and ringing intensity over a range of loads, intake-boost pressures, CA50s (crank angles at which 50% of the combustion heat release has occurred), speeds, and pressure rise rates; (3) Conducted an in-depth investigation of all potential factors affecting measurement of thermal efficiency and developed methods to correct for errors and eliminate uncertainties; (4) Evaluated the potential for improving thermal efficiency over the load range by better

optimizing partial fuel stratification fuel distributions; (5) Collaborated with University of California, Berkeley and General Motors on computational fluid dynamics modeling of partial fuel stratification operation in our LTGC engine and comparisons of computational fluid dynamics and experimental results; and (6) Supported development of chemical-kinetic mechanisms at Lawrence Livermore National Laboratory for LTGC operation with ethanol-gasoline blends. (Dec, report II.4)

- Sandia National Laboratories is developing robust automotive low-temperature gasoline combustion (LTGC) strategies that improve fuel economy and reduce pollutant emissions. In FY 2014 they, (1) Quantified negative valve overlap period species that influence main-cycle ignition through dump sampling and gas chromatograph measurements; (2) Clarified importance of select hydrocarbon species on main-cycle ignition through the application of CHEMKIN-PRO models; (3) Performed exploratory vacuum ultraviolet mass spectroscopy experiments at the Lawrence Berkeley National Laboratory synchrotron to obtain detailed information about negative valve overlap sample speciation; and (4) Published a report that details advanced gasoline ignition system challenges and opportunities, and started lab facility upgrades to enable future ignition research. (Ekoto, report II.5)
- Argonne National Laboratory is developing physics-based nozzle flow and spray models, high-fidelity turbulence models, reduced chemical-kinetic models, and high-performance computing tool development on codes used by the industry for internal combustion engines applications. In 2014, (1) Three-dimensional, transient, turbulent in-nozzle flow simulations have been performed; (2) Demonstrated that an Eulerian-Eulerian approach is more suitable to mimic the spray distribution; and (3) Developed and validated a 163 species-based reduced reaction mechanism for a mixture of n-dodecane and m-xylene as a surrogate for diesel fuel. (Som, report II.6)
- Argonne National Laboratory is studying the mechanisms of spray atomization by performing detailed, quantitative measurements in the near-nozzle region of sprays from fuel injectors. In FY 2014 they, (1) Completed measurements of the internal geometry of all 12 samples of the ECN "Spray G" gasoline injectors; (2) Organized the Internal Geometry and Nozzle Flow topic at the ECN3 Workshop; (3) In collaboration with University of Massachusetts Amherst, completed simulations of cavitating nozzle flows and compared them to X-ray measurements; and (4) Completed the fabrication of a new spray chamber which was used to perform three-dimensional tomography of sprays at elevated pressure and temperature. (Powell, report II.7)

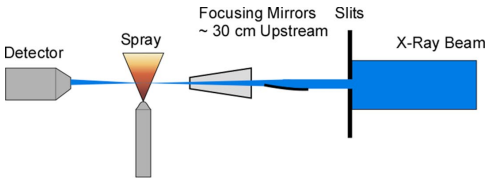

X-Ray Measurement of Fuel Injection Sprays (Powell, report II.7)

- Sandia National Laboratories is combining unique state-of-the-art simulation capability based on the large-eddy simulation (LES) technique and apply high-resolution LES and first principles models at conditions unattainable using direct numerical simulation to complement key experiments and bridge gap between basic/applied research. In FY 2014 they, (1) Established an improved understanding of the transient structure of reacting diesel jets that demonstrated the effects of real-fluid thermodynamics and transport; (2) Using these data, a systematic study of high pressure transient mixing processes served to quantify the envelope of relevant physical conditions just prior to autoignition; and (3) Provided a detailed framework for simultaneous development of advanced combustion closures with optimized chemical mechanisms that efficiently capture turbulence-chemistry interactions and cool/hot flame ignition with equal fidelity. (Oefelein, report II.8)
- Argonne National Laboratory is collaborating with combustion researchers within DOE's Offices of Basic Energy Sciences and Vehicle Technologies Office programs to develop and validate predictive chemical kinetic models for a range of transportation-relevant fuels. In FY 2014 they, (1) Acquired new measurements for a research grade gasoline, multi-component surrogate blends, and measurements of these fuels doped with a reactivity modifier, 2-ethylhexyl nitrate; (2) Developed chemical kinetic models for these fuels and compared predictions with experimental data, highlighting sensitive reaction pathways which should be further investigated in order to improve the chemical kinetic model predictions; and (3) Developed an approach to quantify, from rapid compression machine data, extents of low- and intermediate-temperature heat release which occur prior to the main ignition event. (Goldsborough, report II.9)

- Lawrence Livermore National Laboratory is developing detailed chemical kinetic models for fuel components and combining the component models into surrogate fuel models to represent real transportation fuels. In FY 2014 they, (1) Developed a chemical kinetic model for tri-methylbenzene, a surrogate component surrogate diesel fuel; (2) Developed a chemical kinetic model for n-butyl-cyclohexane, a surrogate component for diesel fuel; (3) Developed a chemical kinetic model for tetralin, a surrogate component for diesel fuel; and (4) Performed detailed chemical kinetic modeling of surrogates of gasoline fuels. (Pitz, report II.10)
- Lawrence Livermore National Laboratory is gaining fundamental and practical insight into high-efficiency clean-combustion regimes through numerical simulations and experiments, and developing and applying numerical tools to simulate high efficiency clean combustion by combining multidimensional fluid mechanics with chemical kinetics. In FY 2014 they, (1) Implemented algorithms for fast chemical solutions of small to moderate mechanism sizes enabling faster engine simulations; (2) Made improvements and generalizations to the chemistry solver interface to computational fluid dynamics codes, making it more widely applicable/available to engine researchers and designers; and (3) Further developed chemical integration algorithms for graphics processing units to enable use of massively parallel architectures for engine simulations. (Whitesides, report II.11)
- Lawrence Livermore National Laboratory is accelerating development and deployment of high-efficiency clean-combustion engine concepts through deeper understanding of complex fluid and chemistry interactions. In FY 2014 they, (1) Completed a detailed code profile that identifies when the multispecies transport algorithms dominate the simulation cost for kinetically controlled engine design; (2) Created a suite of mechanism development tools for reaction analysis and error detection; (3) Accelerated the design of a new gasoline mechanism to study the impact of cetane enhancers on formation of oxides of nitrogen using the new suite of tools; and (4) Adapted all major algorithms in the Lawrence Livermore National Laboratory chemistry solver to the graphical processing unit. (McNenly, report II.12)
- Los Alamos National Laboratory is developing algorithms and software for the advancement of speed, accuracy, robustness, and range of applicability of the KIVA internal engine combustion modeling—to be more predictive, and providing KIVA software that is easier to maintain and is easier to add models to than the current KIVA. In FY 2014 they, (1) Finished developing underlying discretization to an hp-adaptive predictor-corrector split using a Petrov-Galerkin finite element method for multi-species flow inclusive the chemistry input system and setup; (2) Validated three-dimensional local-arbitrary Lagrangian-Eulerian moving parts algorithm/code with extensive error and convergence analysis; (3) Developed a plasma kernel spark model, to supply heat at a single node based on engine manufacturer-specified spark current; and (4) Developed a dynamic large-eddy simulation turbulence modeling for wall-bounded flows, and will be especially applicable to internal combustion engine modeling. (Carrington, report II.13)
- Oak Ridge National Laboratory is developing and applying innovative strategies that maximize the benefit of high-performance computing resources and predictive simulation to support accelerated design and development of advanced engines to meet future fuel economy and emissions goals. In FY 2014 they, (1) Supported three ongoing efforts with direct industry collaboration; (2) Developed and demonstrated computational frameworks for managing massively parallel simulation and optimization jobs on Oak Ridge National Laboratory's Titan supercomputer; and (3) Observed significant variation in predicted combustion performance at highly dilute conditions due to stochastic variability in initial spray conditions. (Edwards, report II.14)
- Argonne National Laboratory is optimizing engine operating conditions to use low cetane fuel to achieve clean, high-efficiency engine operation and demonstrating the use of low-temperature combustion as an enabling technology for high-efficiency vehicles. In FY 2014 they, (1) Achieved idle (-0.2 bar brake mean effective pressure) to 20-bar brake mean effective pressure using only 87 anti-knock index fuel; (2) Attained a 30% fuel economy improvement using low-temperature combustion in a conventional powertrain vehicle over a similar port fuel injected vehicle on the combined Urban Dynamometer

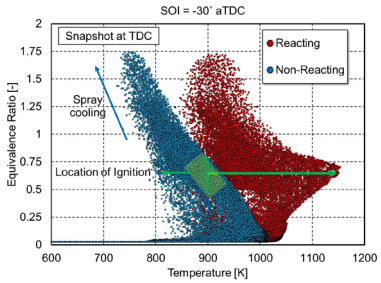

Reactivity Phi-T Plot for Unreacting and Reacting Simulation for Gasoline Compression Ignition Engine (Ciatti, report II.15)

Driving Schedule and Highway Fuel Economy Test cycles in a 2007 Cadillac vehicle; and (3) Utilized high-fidelity simulations at Argonne to explore three-dimensional assessments of in-cylinder reactivity. (Ciatti, report II.15)

- Argonne National Laboratory is quantifying efficiency potential and combustion stability limitations of advanced gasoline direct injection engines, extending the lean and exhaust gas recirculation dilution tolerance of light-duty gasoline direct injection engines, and developing a three-dimensional computational fluid dynamics methodology to analyze and predict cyclic variability in gasoline direct injection engines. In FY 2014 they, (1) Completed evaluation of spark-based ignition systems under dilute operation with focus on ignition energy and release profile; (2) Collaborated with Sandia National Laboratories to improve numerical modeling of conventional as well as alternative ignition systems; (3) Validated Reynolds-averaged Navier-Stokes modeling; and (4) Free-air delivered laser system successfully implemented on the existing engine hardware and tested yielding improved combustion stability for dilute operation. (Wallner, report II.16)
- Oak Ridge National Laboratory is characterizing dynamics of cyclic variability that limits dilution levels in spark-ignition engines, evaluating potential engine efficiency gains resulting from effective control of cyclic variations, and demonstrating dilution limit extension through active control to reduce cyclic variability. In FY 2014 they, (1) Characterized sensitivity of control parameters to data sampling quality and determined that symbolic analysis approach is robust for reduced-quality data; (2) Determined that dual-timescale control is necessary for high exhaust gas recirculation control strategies to be effective; and (3) Determined that effective dual-timescale next-cycle control strategies have the potential to yield an additional three point reduction in coefficient of variation relative to single-timescale control with a 5% overall fuel efficiency improvement at a high exhaust gas recirculation, 2,000 rpm/4-bar brake mean effective pressure operating condition, based on available deterministic information. (Kaul, report II.17)
- Oak Ridge National Laboratory is developing and evaluating the potential of high-efficiency clean combustion (HECC) strategies with production viable hardware and aftertreatment on multi-cylinder engines. In FY 2014 they, (1) Attained the 2014 technical target of developing a reactivity-controlled compression ignition engine map suitable for use in vehicle system drive cycle simulations; (2) Attained the 2014 technical target of demonstrating greater than 25% improvement in modeled fuel economy with multi-mode reactivity-controlled compression ignition operation as compared to a 2009 port fuel injected gasoline engine baseline; and (3) Performed drive cycle estimations of fuel economy and emissions using vehicle systems modeling with experimental data with multi-mode reactivity-controlled compression ignition/conventional diesel combustion operation. (Curran, report II.18)

University of Wisconsin Reactivity-Controlled Compression Ignition Hybrid Vehicle on the ORNL Chassis Dynamometer undergoing Drive Cycle Evaluations (Curran, report II.18)

- Oak Ridge National Laboratory is defining and analyzing specific advanced pathways to improve the energy conversion efficiency of internal combustion engines with emphasis on thermodynamic opportunities afforded by new approaches to combustion. In FY 2014 they, (1) Published a collaborative study with Sandia National Laboratories on the chemistry of in-cylinder reforming; (2) Commissioned a new flexible multi-cylinder engine experiment capable of two reforming strategies: an internal in-cylinder reforming strategy and an external exhaust gas recirculation loop reforming strategy; and (3) Characterized performance, temperature dependency, and sulfur tolerance of a rhodium reforming catalyst. (Daw, report II.19)
- Oak Ridge National Laboratory is improving engine efficiency through better combustion uniformity, developing and applying diagnostics to resolve combustion-uniformity drivers, understanding origins of combustion non-uniformity and develop mitigation strategies, and addressing critical barriers to engine efficiency and market penetration. In FY 2014 they, (1) Developed multi-color multi-species exhaust gas recirculation probe for simultaneous CO_2, H_2O, temperature and pressure measurements; and (2) Applied multi-color multi-species exhaust gas recirculation probe to Cooperative Research and Development Agreement and SuperTruck projects to assess specific hardware, validate and improve numerical design tools, and gain fundamental insights into performance drivers. (Partridge, report II.20)

- Oak Ridge National Laboratory is developing high-fidelity neutron imaging capabilities and employing the technique to aid improved design and control of complex advanced combustion systems, and help to guide model validation and input. In FY 2014 they, (1) Recorded higher resolution computed tomography scan of commercial gasoline direct injector; (2) Initiated gasoline particulate filter-focused study; and (3) In collaboration with the Massachusetts Institute of Technology, used the technique to quantify ash loading density profiles in a series of ash-filled samples. (Toops, report II.21)
- Michigan Technological University is performing a comprehensive characterization of high injection pressure dimethyl ether (DME) spray combustion under lean-burn conditions: investigate the characteristics of DME spray combustion for use in internal combustion engines and whether these characteristics affect burning rates, quenching limits, and emissions under engine-representative conditions. In FY 2014 they, (1) Designed and fabricated the DME injector window mounted in the combustion vessel test facility; (2) Fabricated the fuel delivery system of hydraulically activated electronic unit injector operated by oil-intensified system along with interface controller; (3) Measured the rate of injection for DME and diesel fuel with various injection pressures; (4) Conducted experiment of non-vaporizing, vaporizing, and combusting spray in the Michigan Technological University combustion vessel and autoignition using a rapid compression machine; and (5) Developed various DME detailed and reduced chemistries for predictive tool modeling. (Lee, report II.22)
- The University of New Hampshire is using collaborative experiments and numerical simulations to investigate unsteady reciprocating effects on heat transfer in piston engines. In FY 2014 they, (1) Designed, built, and tested a constant temperature wall-plate to study heat transfer in controlled experiments with simulated conditions found in engines; (2) Validated a two-wavelength infrared surface temperature measurement technique against simultaneous thermocouple and thermographic phosphor measurements; (3) Demonstrated a four-layer thin-film optical coating design to extend the two-wavelength infrared surface temperature measurement technique to fired engine conditions; (4) Performed direct numerical simulation of reciprocal channel flow with heat transfer for flow regimes with strong non-equilibrium behaviors and compared the results to Reynolds-averaged Navier-Stokes models; and (5) Developed an exact integral method to evaluate wall heat flux suitable for experimental data. The method also provides a means to connect wall heat flux to bulk flow dynamics. (White, report II.23)

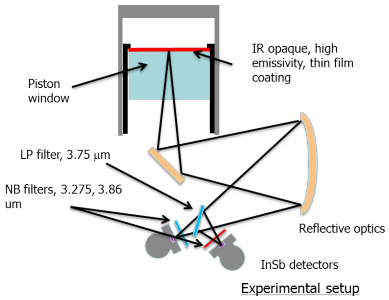

Experimental Setup to Measure In-Cylinder Surface Temperature Using the Two-Wavelength Infrared Temperature Diagnostic (White, report II.23)

- Stanford University is conducting detailed measurements and developing advanced modeling capabilities to improve current understanding about heat transfer, thermal stratification, and non-equilibrium coupling processes in the near-wall region of internal combustion engines that are operated under low-temperature combustion conditions. In FY 2014 they, (1) Achieved high frame-rate micro-particle image velocimetry measurements in operating engine with spatial accuracy for surface position of 30 ±0.5 μm; (2) Demonstrated the potential of 3-pentanone laser-induced-fluorescence measurements to identify structures of local temperature variations in optical engine; (3) Created several post-processing tools to examine near-wall region and transient boundary-layer effects in direct numeric simulation; and (4) Developed non-equilibrium wall models and demonstrated the significance of pressure gradients near top-dead center that induced by large in-cylinder vortical structure. (Ihme, report II.24)
- The University of California, Berkeley is demonstrating extension of engine load and speed limits using partial fuel stratification (PFS) compared to homogeneous charge compression ignition, and developing validated models of PFS. In FY 2014 they, (1) Demonstrated that low-temperature heat release (LTHR) and intermediate temperature heat release (ITHR) increase with intake pressure boost for gasoline, becoming active above about 1.3-1.4 bar for 0% ethanol, above about 1.7-1.8 bar for 10% ethanol, and above about 2.2 bar for 20% ethanol; (2) Quantified the effect of start-of-injection timing on PFS with a certification gasoline; (3) Developed and validated a model of the Sandia engine in CONVERGE™ CFD; (4) Quantified the ability of available chemical kinetic mechanisms to predict the pressure-boost onset of LTHR and ITHR for gasoline and the effect of ethanol addition to gasoline on LTHR/ITHR; and (5) Quantified the

effect of fuel stratification on flame propagation velocity using a numerical model for hydrogen-air flames. (Dibble, report II.25)

- Michigan State University is examining the active radicals generated in the turbulent jet ignition (TJI) process through both rapid compression machine and optically accessible engine experiments and developing a new large-eddy simulation modeling technique to model the TJI system. In FY 2014 they, (1) Designed, fabricated and tested the generation 3 TJI system in a rapid compression machine; (2) Developed TJI control system for a rapid compression machine and preliminary model-based closed-loop combustion control system based on a 2.0-L 4-cylinder engine with TJI; (3) Demonstrated lean limit extension capability of TJI in the rapid compression machine; and (4) Conducted large-eddy simulation/filtered mass density function modeling of propane in a closed chamber and preliminary large-eddy simulation/filtered mass density function simulations of TJI in a coupled prechamber rapid compression machine. (Toulson, report II.26)
- The University of Connecticut is developing a predictive turbulent combustion model that is universally applicable to mixed regimes of combustion including elements of both premixed and non-premixed flames in the presence of local limit phenomena such as extinction and autoignition. In FY 2014 they, (1) Developed and validated reduced mechanisms for gasoline and diesel surrogates; (2) Implemented the reduced mechanisms into Argonne's large-eddy simulation and Reynolds-averaged Navier-Stokes codes for engine simulations; (3) Performed chemical explosive mode analysis-based computational diagnostics of Sandia's direct numerical simulation datasets to extract critical flame features; and (4) Performed direct numerical simulation-based scalar dissipation rate modeling for a premixed hydrogen flame. (Lu, report II.27)

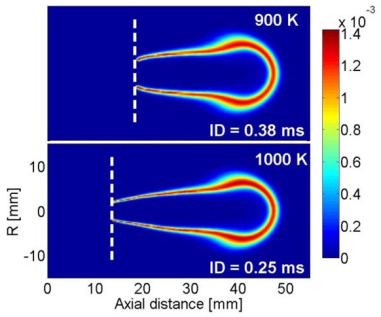

Flame Shapes Indicated by OH Mass Fraction at 900 K and 1,000 K Ambient Conditions (Lu, report II.27)

- Clemson University is elucidating the impact of thermal barrier coatings on low-temperature combustion efficiency, operating range and emissions; developing ceramic and metallic piston coatings that increase thermal and combustion efficiency without decreasing volumetric efficiency; and developing simulation tools to predict temperature gradients and coating surface temperature swings. In FY 2014, (1) Temperature limits of the piston aluminum alloy were determined through the investigation of surface hardness variations with temperature; (2) Process parameters were developed for spraying both a dense yttria-stabilized zirconia coating and a coating with inter-pass boundaries reducing the thermal conductivity by a factor of two (0.62 W/mK); and (3) ANSYS was used to create a finite element analysis model of a thermal barrier coated piston and determine the flow of heat through the barrier coating layers and the metal piston. (Filippi, report II.28)
- The Pennsylvania State University is quantifying effects of radiative heat transfer and turbulent fluctuations in composition and temperature on combustion, emissions, and heat losses in internal combustion engines; developing computational fluid dynamics-based models to capture these effects in simulations of in-cylinder processes in internal combustion engines; and exercising models to explore advanced combustion concepts for internal combustion engines to develop next-generation high-efficiency engines. In FY 2014 they, (1) Implemented radiative transfer equation solvers in OpenFOAM®, and coupled the radiation calculations with liquid fuel-spray models; (2) Mapped out a "radiation state space" to identify engine-relevant conditions where radiative heat transfer and turbulence-chemistry-radiation interactions are expected to be most prominent; and (3) Quantified radiative emission in a heavy-duty diesel engine by post-processing earlier simulation results. (Haworth, report II.29)
- Yale University is measuring quantitative sooting tendencies for a wide range of diesel and biodiesel fuel components, and developing a mixing rule that can be used to define surrogate fuel mixtures that mimic the sooting behavior of real diesel fuels. In FY 2014 they, (1) Rebuilt the burner and fuel system and verified with time-resolved measurements that flames could be doped with diesel fuels without condensation; (2) Validated the laser-induced incandescence quantitative sooting tendencies for several diesel and biodiesel components; and (3) Prepared 32 diesel surrogate component mixtures that follow

an optimized scheme for determining properties of the individual components and measured sooting tendencies. (Pfefferle, report II.30)

- Argonne National Laboratory is evaluating the impacts of low-temperature combustion technology on fuel economy and engine-out emissions using vehicle simulations and engine in the loop, and comparing the fuel economy benefits of low-temperature combustion technology to port fuel injection and spark-ignited direct injection technologies by using simulations. In FY 2014 they, (1) Quantified the fuel economy benefits of low-temperature combustion for a mild hybrid powertrain, belt-integrated starter-generator; and (2) Updated the fuel economy benefits of low-temperature combustion for a conventional powertrain with improved low-load steady-state brake specific fuel consumption data on low-temperature combustion from the Argonne Engine Research Group. (Shidore, report II.31)

EMISSION CONTROL R&D

The following project highlights summarize the advancements made in emission control technologies to both reduce exhaust emissions and reduce the energy needed for emission control system operation.

- Oak Ridge National Laboratory is coordinating the Cross-Cut Lean Exhaust Emission Reduction Simulation (CLEERS) activity for the DOE Advanced Engine Cross-Cut Team. In FY 2014 they, (1) Continued leadership of the CLEERS Planning Committee; (2) Facilitated CLEERS Focus teleconferences, which continue to have strong domestic and international participation (typically 30-50 participants); (3) Provided regular update reports to DOE Advanced Combustion Engine Cross-Cut Team; (4) Organized the 2014 DOE Cross-Cut Workshop on Lean Emissions Reduction Simulation (CLEERS Workshop) at the University of Michigan - Dearborn on April 29-May 1, 2014; (5) Maintained the CLEERS website (www.cleers.org), including the CLEERS bibliographic database; and (6) Supported the Advanced Combustion and Emissions Control Low Temperature Aftertreatment Team in developing an evaluation protocol for low-temperature oxidation catalysts. (Daw, report III.1)
- Oak Ridge National Laboratory is collaborating with Pacific Northwest National Laboratory to support industry in the development of accurate simulation tools for the design of catalytic emissions control systems that enable advanced high-efficiency combustion engines to meet emissions regulations while maximizing fuel efficiency. In FY 2014 they, (1) Conducted detailed measurements of N_2O formation as a function of time and catalyst location during lean-NOx trap regeneration. Identified the chemical pathways leading to N_2O formation upon the switch from rich regeneration back to lean trapping conditions; (2) Proposed new mechanisms for NO oxidation and NO selective catalytic reduction over a small pore copper zeolite that are consistent with measured reaction rates and observed surface intermediates; and (3) Refined measurement and analysis techniques for quantifying NH_3 adsorption enthalpies on zeolite selective catalytic reduction catalysts. Measured impacts of catalyst state on NH_3 adsorption enthalpy as a function of coverage on a commercial small pore copper zeolite. (Daw, report III.2)
- Pacific Northwest National Laboratory is promoting the development of improved computational tools for simulating realistic full-system performance of lean-burn engines and the associated emissions control systems, and providing the practical and scientific understanding and analytical base required to enable the development of efficient, commercially viable emissions control solutions for ultra-high-efficiency vehicles. In FY 2014 (1) Analysis of data previously collected in cooperative experiments with Oak Ridge National Laboratory revealed important differences between particulate populations produced by stoichiometric and lean stratified combustion; (2) Continued to obtain highly relevant fundamental insights into the properties of Cu-chabhazite zeolite-based selective catalytic reduction catalysts that are recognized internationally as leading the research; (3) Micro-scale flow and filtration simulations of multi-functional exhaust filters showed how the three-dimensional location of catalysts affects backpressure during soot loading; and (4) Completed studies of candidate new lean-NOx trap materials for high temperature applications. Initiated

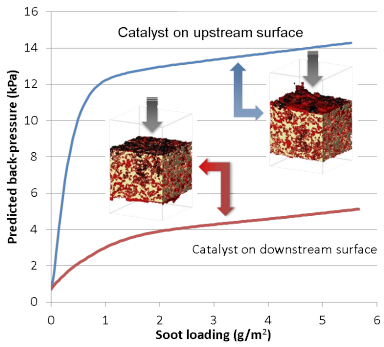

Simulation results showing dramatically different back-pressure profiles with respect to soot loading as a multi-functional filter is exposed to exhaust from different orientations. (Stewart, report III.3)

new studies on passive NOx adsorbers for low-temperature aftertreatment of NOx emissions. (Stewart, report III.3)

- Pacific Northwest National Laboratory is identifying approaches to significantly improve both the high- and low-temperature performance, and the stability of the catalytic oxides of nitrogen reduction technologies via a pursuit of a more fundamental understanding. In FY 2014, (1) Based on prior literature reports, several synthesis efforts were carried out at Pacific Northwest National Laboratory to prepare model chabhazite zeolite-based catalysts; (2) Catalysts were characterized before and after incorporation of Fe by nuclear magnetic resonance, Mossbauer, and Fourier transform infrared spectroscopies; (3) Baseline reactivity measurements were performed on these catalysts in preparation for mechanistic studies of high- and low-temperature performance loss; (4) New chabhazite zeolite-based formulations were discovered and their initial "standard" selective catalytic reduction performance has been assessed; and (5) The synthesis, characterization of stability of a variety of model K-titania catalysts were completed this year. (Peden, report III.4)
- Pacific Northwest National Laboratory is developing and demonstrating mixed metal oxide-based catalysts as a low-cost replacement for platinum in the oxidation of NO to NO_2 in lean engine exhaust, an essential first step in controlling oxides of nitrogen emissions. In FY 2014, (1) The extensive isotope exchange between MnO_x/CeO_2 and $^{15}N^{18}O$ clearly shows that the oxygen mobility in these catalysts is very high indeed; (2) NO decomposition is facile on MnO_x/CeO_2 catalysts even at 300 K. In addition to N_2O, N_2 formation was also observed; (3) Upon NO exposure, the initially formed hyponitrite and nitrite species on MnO_x/CeO_2 transform to nitrates. This transformation is accelerated in the presence of gas phase O_2; (4) A physical mixture of MnO_x and CeO_2 exhibits comparable NO oxidation activity to the catalyst prepared by incipient wetness with the same composition; and (5) Using DFT we have shown that the presence of Mn^{4+} ions enhances the activity of nearby CeO_2, and NO oxidation can also proceed on Mn_2O_4 "clusters." (Szanyi, report III.5)
- Pacific Northwest National Laboratory is developing an improved understanding of selective catalytic reduction (SCR) and diesel particulate filter (DPF) integration for application to on-road heavy-duty diesel emission reduction. In FY 2014 they, (1) Investigated the relationship between soot loading behavior and SCR catalyst concentration and location in SCR-DPF samples has led to greater understanding of the pathway towards improved SCR-DPF integration and increased SCR catalyst loading in excess of 150 g/L; (2) SCR reaction rate measurements at different NO_2/oxides of nitrogen ratios in the presence of soot has led to improved understanding of the nature of the impact of soot on oxides of nitrogen conversion, and a greater level of understanding of strategies for improved SCR predictive modeling of integrated SCR-DPF systems; and (3) Fundamental understanding of the impact and nature of SCR reaction on passive soot oxidation has been developed, leading to a greater understanding of the potential pathways towards maximizing the passive soot oxidation exhibited in SCR-DPF systems for heavy-duty diesel deployment. (Rappe, report III.6)
- Oak Ridge National Laboratory is developing emission control technologies that perform at low temperatures (<150ºC) to enable fuel-efficient engines with low exhaust temperatures to meet emission regulations, and identifying advancements in technologies that will enable commercialization of advanced combustion engine vehicles. In FY 2014 they, (1) Completed support investigation of innovative Au@Cu (core@shell) catalyst for oxidation; (2) Successfully added ZrO_2 to SiO_2 support for Pd catalyst to achieve high surface area support with better activity; (3) Discovered a new catalyst that has no platinum-grade metal based on Cu-Ce-Co oxides that does not demonstrate inhibition between hydrocarbon and CO oxidation processes (which commonly limit platinum-grade metal-based catalysts); and (4) Initiated study of trapping materials. (Toops, report III.7)
- Oak Ridge National Laboratory is assessing and characterizing catalytic emission control technologies for lean-gasoline engines, and identifying strategies for reducing the costs, improving the performance, and minimizing the fuel penalty associated with

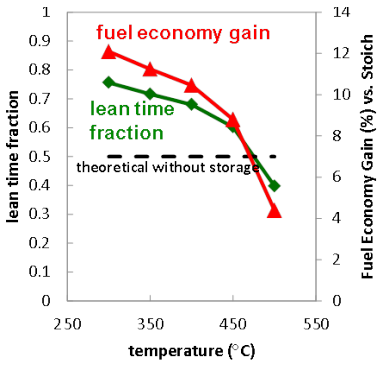

Lean Time Fraction and Associated Predicted Fuel Economy Gain as a Function of Temperature (Parks, report III.8)

emission controls for lean-gasoline engines. In FY 2014 they, (1) Determined that hydrogen concentration is not a limitation at air-to-fuel ratios associated with peak NH_3 production over the three-way catalyst; (2) Evaluated the concept of adding a oxides of nitrogen storage component to the three-way catalyst for increasing net NH_3 production; discovered that the relative advantage of the oxides of nitrogen storage component addition is a strong function of temperature, with lower temperatures giving more improvement in fuel economy; and (3) Constructed and commissioned a synthetic exhaust gas catalyst aging apparatus with the capability to age catalysts under a stoichiometric-rich-stoichiometric-lean sequence per industry guidance (based on communication with collaborating partners General Motors and Umicore). (Parks, report III.8)

- Oak Ridge National Laboratory is researching the fundamental chemistry of automotive catalysts, identifying strategies for enabling self-diagnosing catalyst systems, and addressing critical barriers to market penetration. In FY 2014 they, (1) Characterized spatiotemporal intra-catalyst performance of hydrothermally aged commercial Cu-SAPO-34 selective catalytic reduction catalyst under standard and fast selective catalytic reduction conditions; (2) Developed improved SpaciMS analysis codes for improved quantification and enabling nitrogen and stoichiometry balances; and (3) Demonstrated non-invasive nature of SpaciMS capillary sampling methodology used for Cooperative Research and Development Agreement measurements. (Partridge, III.9)

- Argonne National Laboratory is determining detailed mechanisms of gasoline particulate filter filtration/regeneration processes, and evaluating filter performance in consideration of backpressure increase, particulate matter mass, and number emission reduction efficiencies to suggest an optimized filter substrate structure for gasoline direct-injection engines. In FY 2014, (1) Accurate soot number measurements were enabled using a scanning mobility particle sizer; (2) Raman spectroscopy and pair distribution function analyses using synchrotron X-rays were used to evaluate carbon crystalline structures of gasoline direct-injection particulate matter taken under various engine operating conditions; (3) Extensive oxidation experiments by thermogravimetric analyzer were performed for gasoline direct-injection soot containing different ash fractions to understand ash effects on soot oxidation kinetics; (4) Particulate matter-reducing effects were examined with a three-way catalyst as a function of engine operating conditions; and (5) gasoline particulate filter filtration and regeneration experiments were performed, along with micro-imaging, to evaluate unique characteristics of gasoline particulate filter filtration and regeneration processes. (Seong, report III.10)

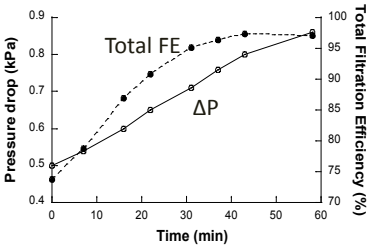

Pressure Drop and Number-Based Filtration Efficiency (FE) as a Function of Time after Particulate Matter Loading in a Filter (Seong, report III.10)

- Pacific Northwest National Laboratory is seeking to shorten development time of filtration technologies for future engines and developing modeling approaches relevant to the likely key challenge for gasoline particulate filtration—high number efficiency at high exhaust temperatures. In FY 2014, (1) Micro X-Ray computed tomography data were obtained for seven additional substrate samples in support of ongoing filtration experiments; (2) Extensive analysis was carried out to characterize the three-dimensional structure of porous filter materials and identify features and length scales tied to performance; (3) Three-dimensional micro-scale simulations were carried out to support the development of improved reduced order device-scale modeling tools; and (4) A third round of cooperative experiments at the University of Wisconsin Engine Research Center was successfully completed. (Stewart, report III.11)

- Pacific Northwest National Laboratory is investigating a number of candidate low-temperature oxidation catalysts as fresh materials, and after realistic laboratory- and engine-aging; obtaining a better understanding of fundamental characteristics and various aging factors in both thermal and chemical aspects that impact the long-term performance of these candidate low-temperature oxidation catalysts. In FY 2014, (1) Cu/CeO_2-ZrO_2 catalysts have been prepared by impregnating Cu on both home-made (CZ and C4Z1) and commercial (GMR5 and GMR6) support materials; (2) Very high initial CO oxidation activity was observed on the home-made CZCu catalyst (50% CO conversion was achieved at 150°C). However, the activity of all Cu catalyst supported on home-made CeO_2-ZrO_2 dropped dramatically after high-temperature hydrothermal aging; (3) Commercial CeO_2-ZrO_2 catalysts contain both Pr and La ions. These additives may stabilize the CeO_2-ZrO_2 mixed oxides, and also, may help to establish and maintain high Cu dispersion; and (4) Ce4+ ions in the commercial support GMR6 can be reduced to Ce3+ much more

extensively than in home-made mixed oxides. This probably enhances their oxygen donating abilities, and therefore, their oxidation activities. (Peden, report III.12)

- Purdue University is synthesizing Cu-SSZ-13 catalysts that are exceptionally well defined at the microscopic level, including control of number and type of active sites. In FY 2014 they, (1) Showed that isolated Cu ions near the six member rings of SSZ-13 are the dominant active sites for standard selective catalytic reduction (473 K) and are present in both oxidized (CuI) and reduced (CuII) forms; (2) Performed *operando* X-ray absorption spectroscopy reactant cutoff experiments at Argonne National Laboratory to isolate the species that contribute to Cu reduction and oxidation during standard selective catalytic reduction; (3) Synthesized a series of solid SSZ-13 samples with varying Si/Al ratio (ranging from 4-140) using three different synthesis methods; (4) Developed new experimental NH_3 titration methods to characterize the dynamic nature of active sites in Cu-SSZ-13 before and during selective catalytic reduction reactions; and (4) Computed spectroscopies of Cu sites and their interactions with a variety of reactants in SSZ-13 and SAPO-34 throughout the redox cycle. (Ribeiro, report III.13)
- The University of Houston is predicting binary and ternary metal alloy catalyst compositions for enhanced CO, NO and hydrocarbon oxidation from first principles density functional theory and verify through kinetic and mechanistic studies, and developing enhanced low-temperature CO, hydrocarbon and NO oxidation catalysts through zoning and profiling of metal and ceria components. In FY 2014 they, (1) Discovered a novel water-mediated reaction mechanism for CO oxidation on supported metal catalysts at low temperatures; (2) Developed the first iteration of a computational screening model for simultaneous CO and NO oxidation; (3) Developed a kinetic model of oxides of nitrogen reduction on a lean-NOx trap with $H_2/CO/C_3H_6$ as reductants; and (4) Characterized the performance of $Pt/Pd/Al_2O_3$ oxidation catalysts with different Pt:Pd ratios for CO and C_3H_6 oxidation and developed kinetic expressions. (Epling, report III.14)
- The University of Kentucky Center for Applied Energy Research is improving the low-temperature performance of catalyst-based oxides of nitrogen (NOx) mitigation systems by designing materials which can function as either passive NOx adsorbers or low-temperature lean-NOx trap catalysts. In FY 2014, (1) The fundamentals of NOx storage and release on Al_2O_3, Pt/Al_2O_3 and Pt/La-A l_2O_3 in the temperature range 80-160ºC were investigated by means of microreactor and in situ diffuse reflectance infrared Fourier transform spectroscopy experiments; (2) Pt/CeO_2-ZrO_2 was identified as a promising material for passive NOx adsorber applications; and (3) Ceria-based mixed oxides incorporating Pr were identified as promising materials for lean-NOx trap catalysts intended for low-temperature operation, due to the fast kinetics of nitrate decomposition they exhibit under rich conditions. (Crocker, report III.15)

HIGH-EFFICIENCY ENGINE TECHNOLOGIES

The objective of these projects is to research and develop technologies for more efficient clean engine/powertrain systems to improve passenger and commercial vehicle fuel economy.

- Cummins Inc. is engaged in developing and demonstrating advanced diesel engine technologies to significantly improve engine thermal efficiency while meeting U.S. Environmental Protection Agency 2010 emissions. In FY 2014 they, (1) Demonstrated the SuperTruck Demo 2 vehicle with 86% freight efficiency improvement on a 24-hour cycle, which includes overnight hoteling and operating the Texas highway drive cycle route; (2) Demo 2 also demonstrated a 76% freight efficiency improvement on the Texas highway drive cycle; (3) Demonstrated a Li-ion battery pack auxiliary power unit capabilities to support full sleeper cab hotel loads; (4) Validated an advanced transmission efficiency model; (5) Completed an alternate fuel compression ignition, i.e. dual-fuel multi-cylinder engine build and initial testing with cylinder-to-cylinder and cycle-to-cycle control system; (6) Completed an initial conventional diesel engine technologies roadmap to 55% thermal efficiency; (7) Completed selective analytical validation tests in a conventional diesel single-cylinder engine of revised injector and piston configurations; and (8) Completed multi-cylinder engine tests to validate analysis of both conventional diesel and alternate fuel compression ignition technologies. (Koeberlein, report IV.1)
- Detroit Diesel Corporation is conducting a demonstration of a 50% total increase in vehicle freight efficiency measured in ton-miles per gallon, with at least 20% improvement through the development of a heavy-duty diesel engine; and development of a heavy-duty diesel engine capable of achieving 50% brake

thermal efficiency on a dynamometer under a load representative of a level road at 65 mph. In FY 2014 they, (1) Demonstrated a combined 50.2% brake thermal efficiency in the laboratory on the SuperTruck demonstration engine and waste heat recovery systems, meeting the 2014 project targets; (2) Development continued on the core diesel engine technology with the best results to date being an engine brake thermal efficiency of 47.9%; (3) The waste heat recovery system design for vehicle integration completed; (4) Prototype A-sample SuperTruck vehicle built and utilized as a test bed for functional integration of the various complex technologies; (5) Successful integration of waste heat recovery, hybrid and high voltage systems, controllers and network architecture, new cooling layout, new hydraulic systems, and powertrain; (6) Lessons learned from A-sample build and integration in early FY 2014, applied to the build-up of final demonstration truck builds in late FY 2014; and (7) The final high-efficiency engine hardware, including optimized turbocharger and aftertreatment systems, installed and running on the demonstration vehicle. (Singh, report IV.2)

- Volvo is identifying concepts and technologies that have potential to achieve 55% brake thermal efficiency (BTE) in a heavy-duty diesel engine and demonstrating a heavy-duty diesel engine capable of achieving 50% BTE at the end of the SuperTruck project. In FY 2014 they, (1) Validated computational fluid dynamics combustion models against single-cylinder engine test data with primary reference fuel 87 surrogate fuel; (2) Evaluated several concepts capable of 55% BTE; (3) Engine test results together with verified sub-systems add up to 47.9% BTE without waste heat recovery for the 50% BTE demonstrator powertrain; and (4) Transported probability density function combustion computational fluid dynamics tool used for the 55% BTE concept engine work where we enter new regimes and explore advanced injection strategies. (Amar, report IV.3)
- Navistar, Inc. is using advanced engine technologies to develop a heavy-duty diesel engine capable of achieving 50% or better brake thermal efficiency on a dynamometer under a load representative of a level road at 65 mph; In FY 2014 they, (1) Conducted a study on the impact of effective compression ratio, comparing early intake valve closing and late intake valve closing valve strategies for dual-fuel operation at a mid-load operating condition; (2) Completed investigation on important combustion parameters, such as compression ratio, peak cylinder pressure and their impact on thermal efficiency; extensive investigation of conventional diffusive diesel combustion; (3) Conducted advanced combustion investigation by varying combustion parameters such as fuel injection strategy; (4) Demonstrated combustion efficiencies from 47.6% to 48.1% through contributing combustion system and engine system features. (Zukouski, report IV.4)
- Delphi is developing, implementing, and demonstrating fuel consumption reduction technologies using a new low-temperature combustion process: gasoline direct-injection compression ignition (GDCI). In FY 2014, (1) Engine calibration mapping tests were performed over a broad speed and load range on performance dynamometers in support of vehicle controls development; (2) The GDCI vehicle, which was completed at the end of FY 2013, underwent a full debug of controllers and wiring; (3) Control algorithms for the GDCI combustion system and control hardware were integrated into the demonstration vehicle including cooled exhaust gas recirculation control, cold-start improvements, fuel timing control and transient control algorithms; and (4) Completed GDCI vehicle warm Federal Test Procedure testing revealing a 39% improvement in fuel economy over the baseline port-fuel-injected vehicle. Tailpipe emissions, however, did not meet the targeted Tier 2 Bin 2 standard. (Confer, report IV.5)

Gasoline Direct-Injection Compression Ignition Demonstration Vehicle at the Delphi Technical Center in Auburn Hills, Michigan (Confer, report IV.5)

- Ford Motor Company is demonstrating 25% fuel economy improvement in a mid-sized sedan using a downsized, advanced gasoline turbocharged direct injection engine capable of meeting Tier 3 Super Ultra-Low Emissions Vehicle 30 emissions on the Federal Test Procedure 75 cycle. In FY 2014 they, (1) Completed build of a total of 12 engines for project support (2) Completed Engine #2 transient emissions verification testing, including steady-state cold fluids development and transient cold start development; (3) Completed powertrain/vehicle integration tasks for Vehicles #1–4, including removal of existing powertrain, prep for new powertrain, prep for new advanced integrated and supporting powertrain systems, and installation of new powertrain; and (4) Completed Vehicles #1–4 powertrain/

vehicle control verification on hoist; all systems functional and responsive per design intent. (Wagner, report IV.6)

- Cummins Inc. is demonstrating 40% fuel economy improvement over a baseline gasoline V-8 pickup truck with Tier 2 Bin 2 tailpipe emissions compliance. In FY 2014 they, (1) Completed demonstration of Tier 2 Bin 5 demonstration with the ATLAS diesel engine and vehicle; and (2) Completed demonstration of Tier 2 Bin 2 engine-out emissions demonstration in a test cell using an ATLAS engine. (Ruth, report IV.7)
- Robert Bosch LLC is improving light-duty vehicle fuel economy by 25% with minimum performance penalties while achieving Super Ultra-Low Emission Vehicle level emissions with gasoline. In FY 2014 they, (1) Upgraded two 2009 Cadillac CTS vehicles with 3.6-L port-fuel-injection 6-cylinder engines to ACCESS prototype vehicles with 2.0-L turbocharged direct injection 4-cylinder multi-mode combustion capable engines; (2) Achieved the project target of greater than 25% fuel economy improvement in the prototype vehicle on combined Federal Test Procedure 75 and Highway Fuel Economy Test drive cycles over the baseline vehicles, and identified measures to attain Super Ultra-Low Emission Vehicle emissions; and (3) Demonstrated spark-ignition, spark-assisted compression ignition multi-mode combustion in the prototype vehicle during real-world driving conditions. (Yilmaz, report IV.8)
- Chrysler Group LLC is demonstrating 25% improvement in combined Federal Test Procedure (FTP) City and Highway fuel economy for the Chrysler minivan, and accelerating the development of highly efficient engine and powertrain systems for light-duty vehicles, while meeting future emissions standards. In FY 2014, (1) Base calibrations were developed and refined; (2) Cold-start/FTP calibration and testing in a powertrain test cell has been completed; (3) Several FTP tests have been run and cold-start calibration improvements evaluated; (4) Hardware changes to improve the engine warm-up rate were procured and installed in the Alpha 2 engines; (5) Thermal and ancillary load management refinement continued in the development vehicle, but was not used during the demonstration vehicle tests; and (6) Several FTP tests were completed with calibration refinements that helped exceed the fuel economy goal. (Reese, report IV.9)
- Filter Sensing Technologies, Inc. is demonstrating and quantifying improvements in efficiency and greenhouse gas reductions through improved diesel particulate filter (DPF) sensing, controls, and low-pressure drop components. In FY 2014 they, (1) Developed pre-production radio frequency (RF) sensors capable of fast response (<1 second) and both single- and dual-antenna vector measurements, which received a 2014 R&D 100 Award; (2) Achieved Phase II performance targets of sensor accuracy within 10% of full-scale measurements relative to gravimetric standard with new and ash-aged DPFs simulating over 380,000 miles of on-road aging and ash accumulation; (3) Achieved 2014 technical objective of developing a stand-alone RF control system for a model year 2013, 13-L heavy-duty engine, which demonstrated a reduction in regeneration duration of 15% to 30% with RF-based sensing and control; and (4) Demonstrated on-road RF sensor durability through a 12-month fleet test of two sensor units installed on heavy-duty Volvo/Mack vehicles operated in New York City. (Sappok, report IV.10)
- General Motors is applying and evaluating the enabling technologies of hydrogen-augmented exhaust gas recirculation (EGR), two spark plugs per cylinder, increased compression ratio with a low surface area to volume ratio combustion chamber, increased charge motion (tumble and/or swirl), dual gasoline direct injection (GDI)/port fuel injection (PFI) fuel system and a variable geometry turbocharger system to a current GM-boosted spark ignition engine. In FY 2014, (1) Phase 4 turbocharged 2.0-L engine with dedicated EGR, 12.0:1 compression ratio, two spark plugs per cylinder, intake port swirl plate, dual GDI/PFI fuel system and variable geometry turbocharger has been tested to establish the fuel consumption and full load performance of this specification compared to the baseline; and (2) Phase 5 turbocharged 2.0-L engine with dedicated EGR, 12.0:1 compression ratio, Dual Coil Offset ignition system, intake port swirl plate, dual GDI/PFI fuel system and variable geometry turbocharger is being tested to establish the fuel consumption and full-load performance of this specification compared to the baseline. (Keating, report IV.11)

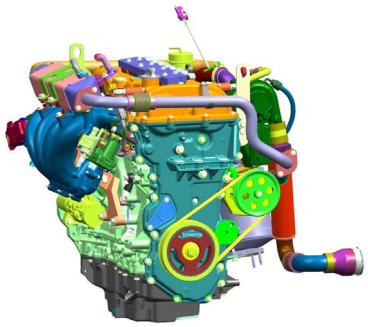

Phase 4 Dedicated EGR Engine Packaged for a General Motors Mid-sized Vehicle (Keating, report IV.11)

- Eaton Corporation is demonstrating fuel economy improvement and emissions reduction through organic Rankine cycle (ORC) waste heat recovery (WHR) systems utilizing a roots expander on heavy-duty diesel engines. In FY 2014 they, (1) Refined and updated thermodynamic system model for ORC with roots expander; (2) Built and evaluated multistage roots expander with water as working fluid on ORC test stand; (3) Correlated objective ORC test data to the analytical predictions for the multistage expander; (4) Developed engine controls for the ORC system with roots expander; and (5) Completed ORC system installation on a 13.5-L John Deere engine. (Subramanian, report IV.12)
- MAHLE Powertrain is demonstrating thermal efficiency of 45% on a light-duty gasoline engine platform while demonstrating potential to meet U.S. Environmental Protection Agency emissions regulations, and a 30% predicted vehicle drive cycle fuel economy improvement over an equivalent conventional port-fuel-injected gasoline engine with variable cam phasing. In FY 2014 they, (1) Completed boosted single-cylinder thermodynamic engine testing with Phase 2A Turbulent Jet Ignition designs and Phase 2B Turbulent Jet Ignition designs; (2) Completed pre-chamber injector spray targeting optimization; (3) Initiated Turbulent Jet Ignition operating strategy development; and (4) Successfully correlated computational fluid dynamics model to wide open throttle, lean, auxiliary fueled pre-chamber experimental results. Blaxill, report IV.13)
- ENVERA LLC is developing a high-efficiency variable compression ratio (VCR) engine having variable valve actuation and an advanced high-efficiency supercharger to obtain up to a 40% improvement in fuel economy when replacing current production V-8 engines with the new small displacement VCR engine. In FY 2014 they, (1) Completed computer-aided design and development of the VCR cranktrain, mechanism, actuator system and crankcase; (2) Generated mass-production feasible valve lift and duration profiles; (3) Constructed GT-POWER model of the VCR engine; (4) Initiated evaluation of boosting system options using GT-POWER modeling; and (5) Developed engine management system component and needs specification. (Mendler, report IV.14)
- Robert Bosch LLC is developing an intake air oxygen (IAO2) sensor which directly and accurately measures the oxygen concentration in the intake manifold. In FY 2014, (1) An exhaust gas recirculation (EGR) control algorithm that utilizes an IAO2 sensor was developed, calibrated, and implemented in a rapid-prototype engine control unit for dynamometer cell validation at Clemson University. The control algorithm predicts cylinder-by-cylinder EGR percentages based on intake system models and IAO2 sensor readings; (2) Engine and vehicle simulation results suggest that maximum fuel economy gain potential when using an IAO2 sensor for EGR control is approximately 1-2% for spark-ignition engines; and (3) Testing and validation of design concept for IAO2, which was completed in Phase I. Focus of component design and research continued to be on the subsystems sensor connector and housing as well as the protection tube. (Schnabel, report IV.15)
- Los Alamos National Laboratory is developing oxides of nitrogen (NOx) and ammonia (NH_3) sensors for diesel emission control systems. In FY 2014, (1) Sensor quantitatively tracks NOx and hydrocarbon concentration in engine dynamometer testing performed both during start up and when operated in EGR step mode; (2) Demonstrated 5 ppm NH_3 sensitivity in a Pt/ytrria-stabilized zirconia/Au sensor manufactured by ESL ElectroScience. Also demonstrated stable performance over 1,000 hours of operation in the laboratory; and (3) Demonstrated an effective overcoat layer to improve sensor durability in engine environments. (Mukundan, report IV.16)

SOLID STATE ENERGY CONVERSION

Several projects are being pursued to capture waste heat from advanced combustion engines in both light- and heavy-duty vehicles using thermoelectrics (TEs). Following are highlights of the development of these technologies during FY 2014.

- Gentherm Inc. is preparing a detailed production cost analysis for a thermoelectric generator (TEG) for passenger vehicle volumes of 100,000 units per year and a discussion of how costs will be reduced in manufacturing. In FY 2014 they developed manufacturing processes for fabrication of TE materials and engines, designed, built and tested TE cartridges, scaled up manufacturing of cartridges, developed models of the cartridge and TEG, integrated these in a vehicle, experimentally confirmed the cartridge model, designed light- and heavy-duty vehicle generators, scaled up the TEG fabrication concept by

developing mass production design and tooling, bench tested partial light-duty vehicle TEGs, developed test tools, and developed and installed materials manufacturing tools. (Jovovic, report V.1)

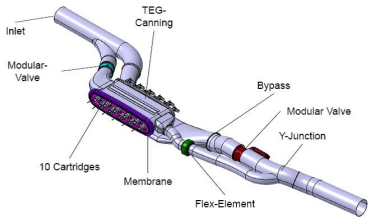

Design of a Light-Duty Vehicle Thermoelectric Generator System Designed by Tenneco (Jovovic, report V.1)

- General Motors is overcoming major obstacles to the commercialization of automotive TEG systems, developing an overall TEG system including all necessary vehicle controls and electrical systems and fully integrated onto a light-duty vehicle, and is demonstrating fuel economy improvement of 5% over the US06 drive cycle. In FY 2014 they, (1) Produced 6,300 skutterudite TE legs with diffusion barriers and metallization layers, and these legs were used to fabricate over 120 skutterudite TE modules for the initial TEG prototype; (2) Verified that the skutterudite modules maintain beginning-of-life performance after 2,000 hours continuous in-gradient operation and 250 thermal cycles; (3) Used a thermal model to predict that peak power of 1,600 W and average power of 900 W are achievable in a full-size truck over the US06 drive cycle; and (4) Demonstrated that rare earth-free p-type skutterudites can exhibit comparable thermoelectric figure of merit values to rare earth-containing p-type skutterudite formulations. (Salvador, report V.2)
- GMZ Energy is demonstrating a robust, thermally cyclable TE exhaust waste heat recovery system that will provide approximately a 5% fuel efficiency improvement for a light-duty vehicle platform, and is developing an initial design/concept for a 1-kW TEG in the exhaust stream of a Bradley Fighting Vehicle. In FY 2014, (1) A device efficiency of 6.5% was measured, where the hot-side and cold-side temperatures were 600ºC and 100ºC, respectively. 2% degradation in power output was measured for a TE module subjected to 1,000 thermal cycles, between 600ºC and 100ºC; (2) The heat exchanger design for the automotive TEG was finalized. The TEG is predicted to generate ~190 W for the average exhaust conditions over the US06 drive cycle. The TEG is currently in fabrication; (3) New NbFeSb-based half-Heuslers compositions have been developed. An analysis based on the cost of raw materials indicate that the cost of these new compositions is >50% less than conventional half-Heusler materials with a high Hf content; (4) An advanced testing plan for measuring the effect of a TEG on the fuel economy of a mid-sized passenger vehicle has been developed. Chassis dynamometer testing has been performed on the vehicle platform in order to establish a fuel economy baseline; and (5) A $1/5^{th}$ scale TEG, for the Bradley Fighting Vehicle application, was fabricated and tested. (Cleary, report V.3)
- Argonne National Laboratory is establishing requirements for a TEG to provide cost-effective power for hybrid electric vehicles when subjected to U.S. Environmental Protection Agency standard test procedures, quantifying fuel economy benefits from the EPA two-cycle procedure, developing a TEG model based on published information that can simulate the effect of exhaust flow interruptions, and is estimating the net present value of the fuel savings. In FY 2014 they, (1) Analyzed the fuel-saving potential of auxiliary power sources over the two-cycle procedure for three types of vehicles; (2) Developed a TEG model that reflects the effect of heat stored on the hot and cold surfaces of TEG; and (3) Evaluated the impact of thermal reservoirs and the possibility of optimizing the number of TEG modules. (Vijayagopal, report V.4)

I.3 Honors and Special Recognitions/Patents

HONORS AND SPECIAL RECOGNITIONS

1. Invited Speaker: "In-Cylinder Measurements of Mixture Formation: Linkage to HC/CO Emissions from Light-Duty Diesel Engines," Miles PC. 13th Hyundai · Kia International Powertrain Conference, Gyeongi, S. Korea, Oct. 24–25, 2013. (Miles, report II.1)

2. Invited Seminar: "Physical Fluid Dynamics in Reciprocating Engines," Miles PC. John Deere. Waterloo, IA, May 5, 2014. (Miles, report II.1)

3. SAE International Excellence in Oral Presentation Award (2014). (Pickett, report II.3)

4. High Performance Computing Innovation Excellence Award from International Data Corporation, June 2014. (Som, report II.6)

5. Invitee to US-Frontiers of Engineering workshop organized by National Academy of Sciences (only 100 people under the age of 45 were invited). (Som, report II.6)

6. Excellence in Oral Presentation Award, SAE World Congress, 2014. (Oefelein, report II.8)

7. Charles Westbrook and William Pitz recognized on the Thomson Reuters' list of The World's Most Influential Scientific Minds. (Pitz, report II.10)

8. McNenly, M.J. and Whitesides, R.A., Lawrence Livermore National Laboratory Director's Science and Technology Award for "Adaptive preconditioner solver for internal combustion engine computational fluid dynamics." (Whitesides, report II.11, and McNenly, report II.12)

9. Awarded two of the 42 DOE Office of Science 2014 ASCR Leadership Computing Challenge awards including 17.5 Mhrs and 15 Mhrs allocated on Titan. (Edwards, report II.14)

10. Invited Presentation: Bill Partridge, Jae-Soon Choi, Jim Parks, Maggie Connatser, Jon Yoo, Rodrigo Sanchez, Vitaly Prikhodko, Neal Currier, Sam Geckler, Mike Ruth, Rick Booth, David Koeberlein, Alex Yezerets. "Diagnostic Developments & Applications for Enabling Advanced-Efficiency Automotive Systems," Arnold Air Force Base, Arnold Engineering Development Complex, Manchester, Tennessee, November 21, 2013. (Partridge, report II.20)

11. Invited Presentation: Bill Partridge, Jae-Soon Choi, Jim Parks, Maggie Connatser, Jon Yoo, Rodrigo Sanchez, Vitaly Prikhodko, Neal Currier, Sam Geckler, Mike Ruth, Rick Booth, David Koeberlein, Alex Yezerets. "Diagnostic Developments & Applications for Enabling Advanced-Efficiency Automotive Systems," Mechanical and Aerospace Engineering Department, University of Central Florida, Orlando, Florida, March 28, 2014. (Partridge, report II.20)

12. Invited Presentation: Peden CHF. "Future Challenges for Catalytic Vehicle Emission Control." Presented by Chuck Peden (Invited Speaker) to the University of Toronto, Department of Chemical Engineering and Applied Chemistry, Toronto, ON, Canada, October 2013. (Stewart report III.3)

13. Invited Presentation: Gao, F; J Szanyi, and CHF Peden. "Cu/CHA materials for the selective catalytic reduction of NOx with NH3: Catalyst structure/function and mechanistic studies." Presented by Chuck Peden (Invited Speaker) at the 2013 AIChE National Meeting, San Francisco, CA, November 2013. (Stewart report III.3)

14. Invited Presentation: Gao F, J Szanyi, and CHF Peden. "Changing Nature of the Active Cu Species During NH3 SCR over Cu/CHA Catalysts." Presented by Chuck Peden (Invited Speaker) for the CLEERS Conference Call, January 2014. (Stewart report III.3)

15. Invited Presentation: Gao, F; JH Kwak, HY Zhu, J Szanyi, and CHF Peden. "Cu-CHA Catalysts for the Selective Catalytic Reduction of NOx with NH3: Catalyst Structure/Function and Mechanistic Studies." Presented by Chuck Peden (Invited Speaker) at the 247th ACS National Meeting, Dallas, TX, March 2014. (Stewart report III.3)

16. Invited Presentation: Zammit, M, C DiMaggio, M Smith, C Lambert, J Theis, C Kim, J Parks, J Pihl, S Daw, G Muntean, C Peden, K Rappe, K Birnbaum, D Tran, M Stewart, and K Howden. "Protocol Development Update." Presented by George Muntean (Invited Speaker) for the CLEERS Conference Call, April 2014. (Stewart report III.3)

17. Invited Presentation: Zelenyuk, A. "Detailed Characterization of Particulates Emitted by a Lean-Burn Gasoline Direct Injection Engine." Presented by Alla Zelenyuk (Invited Speaker) at the 18th Annual CLEERS Workshop, Dearborn, MI, April 2014. (Stewart report III.3)

18. Invited Presentation: Stewart, ML. "Microstructural features of catalyzed and uncatalyzed DPFs." Presented by Mark Stewart (Invited Seminar) at the Advanced Combustion Engine Tech Team Meeting, Southfield MI, May 2014. (Stewart report III.3)

19. Invited Presentation: Gao, F, GG Muntean, CHF Peden, K Rappe, ML Stewart, J Szanyi, DN Tran, and Y Wang. "CLEERS Aftertreatment Modeling and Analysis." Presented by George Muntean (Invited Speaker) at Vehicle Technologies Program Annual Merit Review and Peer Evaluation Meeting, Washington, DC, June 2014. (Stewart report III.3)

20. Invited Presentation: Peden CHF, F Gao, J Szanyi, JH Kwak, M Kollar, and Y Wang. "Cu-CHA zeolite materials for the selective catalytic reduction of NOx with NH3: Catalyst structure/function and mechanistic studies." Presented by Chuck Peden (Invited Speaker) at the Seventh Tokyo Conference on Advanced Catalytic Science and Technology (TOCAT7), Kyoto, Japan, June 2014. (Stewart report III.3)

21. Invited Presentation: Stewart, ML. "Microstructural features of catalyzed and uncatalyzed exhaust particulate filters." Presented by Mark Stewart (Invited Seminar) at Corning Incorporated Sullivan Park R&D Center, Corning, NY, July 2014. (Stewart report III.3)

22. Invited Presentation: Gao F, M Kollar, Y Wang, J Szanyi, and CHF Peden. "Understanding ammonia selective catalytic reduction kinetics over Cu/SSZ-13 from motion of the Cu ions." Presented by Feng Gao (Invited Speaker) at the 248th ACS National Meeting, San Francisco, CA, August 2014. (Stewart report III.3)

23. Invited Presentation: Gao F, M Kollar, Y Wang, J Szanyi, and CHF Peden. "Synthesis, characterization and evaluation of Cu/Fe-Chabazite catalysts for use in selective catalytic reduction (SCR) with ammonia." Presented by Chuck Peden (Invited Speaker) at the 247th ACS National Meeting, Dallas, TX, April 2014. (Peden, report III.4)

24. Invited Presentation: Gao, F, GG Muntean, J Szanyi, CHF Peden, N Currier, A Kumar, K Kamasamudram, J Li, J Luo, A Yezerets, M Castagnola, HY Chen, and H. Hess. "Enhanced High Temperature Performance of NOx Storage/Reduction (NSR) Materials." Presented by Chuck Peden (Invited Speaker) at the DOE Combustion and Emission Control Review, Washington, DC, June 2014. (Peden, report III.4)

25. Invited Presentation: Kollar M, F Gao, RK Kukkadapu, Y Wang, J Szanyi, and CHF Peden. "Fe/SSZ-13 as an NH3-SCR catalyst." Presented by Marton Kollar (Invited Speaker) at 2014 Postdoc Research Symposium, Richland, WA, July 2014. (Peden, report III.4)

26. Invited Presentation: Bill Partridge, Jae-Soon Choi, Jim Parks, Maggie Connatser, Jon Yoo, Rodrigo Sanchez, Vitaly Prikhodko, Neal Currier, Sam Geckler, Mike Ruth, Rick Booth, David Koeberlein, Alex Yezerets. "Diagnostic Developments & Applications for Enabling Advanced-Efficiency Automotive Systems," Knoxville-Oak Ridge Chapter of the American Institute of Chemical Engineers (AIChE), Knoxville, Tennessee, October 10, 2013. (Partridge, III.9)

27. Invited Presentation: Xavier Auvray, William Partridge, Jae-Soon Choi, Josh Pihl, Aleksey Yezerets, Krisha Kamasamudram, Neal Currier, Filipa Coehlo and Louise Olsson. "Modeling of NOx SCR with NH3 from axial species distribution measurements," Crosscut Workshop on Lean Emissions Reduction Simulation (CLEERS) Teleconference (intra- and international attendance via teleconference) Oak Ridge National Laboratory, October 17, 2013. (Partridge, III.9)

28. Invited Presentation: Szanyi, J, CHF Peden, CH Kim, W Li, SH Oh, and SJ Schmieg. "Thermally Stable Ultra-Low Temperature Oxidation Catalysts." Presented by Chuck Peden (Invited Speaker) at Vehicle Technologies Program Annual Merit Review and Peer Evaluation Meeting, Washington DC, June 2014. (Peden, report III.12)

29. Outstanding oral presentation award at the Michigan Catalysis Society, Spring 2014 meeting. (Ribeiro, report III.13)

30. Best Poster Award at Chicago Catalysis Society Spring 2014 Meeting, Naperville, Illinois. (Ribeiro, report III.13)

31. Third place poster presentation award at the Purdue Chemical Engineering Graduate Student Organization Symposium, Fall 2014. (Ribeiro, report III.13)

32. Third place poster presentation at Gordon Research Conference on Catalysis, June 2014. (Ribeiro, report III.13)

33. 2014 Early Career Excellence in Research Award, Purdue University College of Engineering. (Koeberlein, report IV.1)

34. 2014 Purdue University Faculty Scholar. (Koeberlein, report IV.1)

35. 2014 DOE Vehicle Technologies Office R&D Award. (Koeberlein, report IV.1)

36. R&D 100 Award for RF-DPFTM, Received from R&D Magazine for development of one of the top 100 new technologies of the year. (Sappok, report IV.10)

37. Diesel Progress Magazine, "A Matter of Frequency: Radio frequency technology key to Filter Sensing Technologies' DPF monitoring system," July 2014. (Sappok, report IV.10)

38. Best poster award for "Nanostructured Bulk High-Temperature Thermoelectric Generators for Efficient Power Generation." by Luke Schoensee et al., at the International Conference on Thermoelectrics, Nashville, TN, 2014. (Cleary, report V.3)

INVENTION AND PATENT DISCLOSURES

1. U.S. Patent Issued, No. 8,689,767 B1: Dec, J. E., Yang, Y., and Dronniou, N. "A Method for Operating Homogeneous Charge Compression Ignition Engines Using Conventional Gasoline," April 2014. (Dec, report II.4)

2. Provisional U.S. Patent Filed: Yang, Y. and Dec, J. E., "Bio-Ketones: Autoignition Characteristics and Their Potential as Fuels for HCCI Engines," Application number 61,981,389, April 2014. (Dec, report II.4)

3. L.C. Maxey, W.P. Partridge, S.A. Lewis, J.E. Parks "Optically Stimulated Differential Impedance Spectroscopy," United States Patent, Patent No. US 8,653,830, Date of Patent February 18, 2014. (Partridge, report II.20)

4. Stewart, ML, GG Muntean. "Process for modifying ceramic exhaust filter substrates to achieve greater fuel efficiency." Invention Disclosure, June 2014; #30626-E. (Stewart report III.3)

5. Stewart, ML, GG Muntean. "Software and methodology for identifying catalyst distribution in multi-function ceramic exhaust filters." Invention Disclosure, June 2014; #30616-E. (Stewart report III.3)

6. Stewart, ML, GG Muntean. "Process for modifying ceramic exhaust filter substrates to achieve greater fuel efficiency." Provisional Patent Application, July, 2014; #8753. (Stewart report III.3)

7. Gao, F, Y Wang, M Kollar, J Szanyi, CHF Peden. "Catalysts for Low Temperature Selective Catalytic Reduction of NOx with Ammonia." Invention Disclosure, February, 2014; #30561-E. (Peden, report III.4)

8. J. Larimore, L. Jiang, E. Hellström, S. Jade, and A. Stefanopoulou, "Real-Time Residual Mass Estimation with Adaptive Scaling," Application US 14/185,673, Filed on February 20, 2014. Pending (Yilmaz, report IV.8)

9. N. Ravi, J. Oudart, N. Chaturvedi, and D. Cook, "System and Method for Control of a Transient Between SI and HCCI Combustion Modes," Application US 14/185,278, Filed on February 20, 2014. Pending (Yilmaz, report IV.8)

10. J. Oudart, N. Ravi, and D. Cook, "System and Method for Control of a Transient Between SI and HCCI Combustion Modes," Application US 14/185,357, Filed on February 20, 2014. Pending (Yilmaz, report IV.8)

11. E. Hellström, A. Stefanopoulou, L. Jiang, J. Sterniak, N. Ravi, J. Oudart, J. Schwanke, "Mixed-Mode Combustion Control," Application US 14/221,989, Filed on March 21, 2014. Pending (Yilmaz, report IV.8)

12. E. Doran, D. Cook, J. Oudart, and N. Ravi, "Method of estimating duration of auto-ignition phase in a spark assisted compression ignition operation," Application US 61/821,102, Filed on May 8, 2014. Pending (Yilmaz, report IV.8)

13. Bromberg, L., Sappok, A., Koert, Parker, R., and Wong, V., "Microwave Sensing for Determination of Loading of Filters," United States Patent 7,679,374 (2010), European Patent granted 2014. (Sappok, report IV.10)

14. Bromberg, L., Sappok, A., and Koert, P., "Method and System for Controlling Filter Operation," United States Patent No. 8,384, 397, (2013), Japanese Patent granted 2014. (Sappok, report IV.10)

15. Sappok, A., Smith III, R., Bromberg, L., "Advanced Radio Frequency Sensing Probe," United States Patent Application No. 61,897,825, Filed 2013. (Sappok, report IV.10)

16. "Encapsulation of High Temperature Thermoelectric Modules" (7029.3495.001). The patent authors are James R. Salvador, Jeffrey S. Sakamoto, and Young-Sam Park. (Salvador, report V.2)

17. "Exhaust bypass control for exhaust heat recovery," M.G. Reynolds, J. Yang, G.P. Meisner, F.R. Stabler, P.H. De Bock, T.A. Anderson, P-006665 Chinese Patent CN 102,235,212: issued 16 October 2013, (U.S. patent 8,256,220 was issued 4 September 2012). (Salvador, report V.2)

18. "Thermoelectric generators incorporating phase-change materials for waste heat recovery from engine exhaust" G.P Meisner and J. Yang, US Patent 8,646,261 Issued 11 February 2014. (Salvador, report V.2)

19. Patent application number: 61969344, "NbFeSb-Based Half-Heusler Thermoelectric Materials and Methods of Making," G. Joshi, 2014. (Cleary, report V.3)

I.4 Future Project Directions

COMBUSTION RESEARCH

The focus in FY 2015 for combustion and related in-cylinder processes will continue to be on advancing the fundamental understanding of combustion processes in support of achieving efficiency and emissions goals. This will be accomplished through modeling of combustion, in-cylinder observation using optical and other imaging techniques, and parametric studies of engine operating conditions.

- Sandia National Laboratories is providing the physical understanding of the in-cylinder combustion processes needed to minimize the fuel consumption and the carbon footprint of automotive diesel engines while maintaining compliance with emissions standards. In FY 2015 Sandia plans to, (1) Examine the impact of "stepped-lip" piston bowl geometries on the in-cylinder flow development and the mixture preparation process and compare with conventional bowl geometries; (2) Investigate benefits of close-coupled pilot injections on mixture formation, combustion noise, and emissions and identify the physical processes dominating this behavior; and (3) Identify and investigate multiple injection strategies suitable for limiting cold-start hydrocarbon and CO emissions. (Miles, report II.1)
- Sandia National Laboratories is developing fundamental understanding of how in-cylinder controls can improve efficiency and reduce pollutant emissions of advanced low-temperature combustion technologies. In FY 2015 Sandia plans to, (1) Continue building a conceptual-model understanding of multiple-injection processes for both conventional diesel and low-temperature combustion; (2) Determine how combustion design affects heat transfer and efficiency; and (3) Continue to explore and upgrade fuel-injection technologies. (Musculus, report II.2)
- Sandia National Laboratories is facilitating improvement of engine spray combustion modeling, accelerating the development of cleaner, more efficient engines. In FY 2015 Sandia plans to, (1) Characterize multi-hole sprays compared to axial-hole sprays; (2) Quantify gasoline spray mixing over a range of conditions extending from flash boiling to late injection; and (3) Evaluate internal flows within transparent injectors, transitioning to near-field mixing and dispersion at the exit of the nozzle. (Pickett, report II.3)
- Sandia National Laboratories is providing the fundamental understanding (science-base) required to overcome the technical barriers to the development of practical low-temperature gasoline combustion (LTGC) engines by industry. In 2015 Sandia plans to, (1) Conduct a comprehensive investigation of the use of multiple injections to better optimize fuel distributions with direct-injection partial fuel stratification for LTGC; (2) Image fuel distributions in optical engine to guide selection of fuel-injection strategies for multiple-injection direct-injection partial fuel stratification to be applied in the metal engine; (3) Conduct multi-zone kinetic modeling to determine desired fuel distributions; (4) Conduct full evaluation of performance with new low-swirl, spark plug capable cylinder head; and (5) Apply turbocharger and friction models from General Motors to investigate how these real-engine effects would affect LTGC performance. (Dec, report II.4)
- Sandia National Laboratories is developing robust automotive low-temperature gasoline combustion (LTGC) strategies that improve fuel economy and reduce pollutant emissions. In FY 2015 Sandia plans to, (1) Evaluate potential advanced ignition technologies to widen LTGC operating envelopes; (2) Develop/apply diagnostics to measure fundamental ignition system processes; (3) Develop phenomenological models for novel ignition hardware and operating strategies; and (4) Collaborate with combustion chemistry modeling groups to improve kinetics mechanisms used for LTGC simulations. (Ekoto, report II.5)
- Argonne National Laboratory is developing physics-based nozzle flow and spray models, high-fidelity turbulence models, reduced chemical-kinetic models, and high-performance computing tool development on codes used by the industry for internal combustion engines applications. In 2015 they plan to, (1) Implement the best practices developed for large-eddy simulation calculations on engine simulations with different engine geometries available in literature; (2) Develop a near-nozzle Eulerian spray modeling approach which in principle is significantly different from a classical spray modeling approach which is Lagrangian in nature; and (3) Develop a multi-component surrogate (with four or five components)

mechanism for diesel fuel and validate against experimental data in constant volume chamber and single-cylinder engine. (Som, report II.6)

- Argonne National Laboratory is studying the mechanisms of spray atomization by performing detailed, quantitative measurements in the near-nozzle region of sprays from fuel injectors. In FY 2015, (1) The needle motion and fuel distribution of the Engine Combustion Network the "Spray G" gasoline direct-injection injectors will be measured using X-ray diagnostics, and will be made available to experimental and modeling partners in the Engine Combustion Network; (2) Measure the fuel/air mixing in a gasoline direct-injection system that is being used in engine tests of advanced combustion strategies; (3) Further studies of cavitation will be done to improve the community's understanding of this phenomenon and its impact on fuel/air mixing and injector internal flows; and (4) Studies of injector dribble will be performed. (Powell, report II.7)
- Sandia National Laboratories is combining unique state-of-the-art simulation capability based on the large-eddy simulation (LES) technique and apply high-resolution LES and first-principles models at conditions unattainable using direct numerical simulation to complement key experiments and bridge gap between basic/applied research. In FY 2015 they plan to continue to extend development of models and corresponding benchmark simulations to high-Reynolds-number, direct-injection processes for both diesel and gasoline direct injection engine applications over a wide range of pressures and temperatures, and perform detailed calculations and analysis of internal injector flow physics and heat transfer and extend treatment of complex geometry to optical engine configurations. (Oefelein, report II.8)
- Argonne National Laboratory is collaborating with combustion researchers within DOE's Offices of Basic Energy Sciences and Vehicle Technologies Office programs to develop and validate predictive chemical kinetic models for a range of transportation-relevant fuels. In FY 2015 they plan to, (1) Acquire measurements for gasoline/diesel surrogates and multi-component surrogate blends, as well as full-boiling range fuels, and mixtures of these with reactivity modifiers, including ethanol; (2) Improve methods to formulate surrogate fuel blends which can represent the autoignition behavior of real transportation fuels; (3) Further develop and utilize novel approaches for kinetic mechanism validation/improvement, including global sensitivity analysis, along with new targets such as rate of heat release and extents of low- and intermediate-temperature heat release; and (4) Test and validate the operational characteristics of a new, single-piston rapid compression machine. (Goldsborough, report II.9)
- Lawrence Livermore National Laboratory is developing detailed chemical kinetic models for fuel components and combining the component models into surrogate fuel models to represent real transportation fuels. In FY 2015 they plan to, (1) Continue to develop detailed chemical kinetic models for additional cycloalkanes for gasoline and diesel fuel; (2) Develop gasoline surrogate fuels for additional Fuels for Advanced Combustion Engines fuels; and (3) Develop improved models for incipient soot. (Pitz, report II.10)
- Lawrence Livermore National Laboratory is gaining fundamental and practical insight into high-efficiency clean-combustion regimes through numerical simulations and experiments, and developing and applying numerical tools to simulate high efficiency clean combustion by combining multidimensional fluid mechanics with chemical kinetics. In FY 2015 they plan to, (1) Continue solver development and licensing to improve robustness and availability; (2) Complete key features for practical use of graphical processing unit chemistry solvers for engine computational fluid dynamics; and (3) Continue full-engine simulations identifying key issues in simulation setup and analysis. (Whitesides, report II.11)
- Lawrence Livermore National Laboratory is accelerating development and deployment of high-efficiency clean-combustion engine concepts through deeper understanding of complex fluid and chemistry interactions. In FY 2015 they plan to, (1) Continue efforts to distribute the project's new software to industrial and academic partners, and to the multidimensional computational fluid dynamics software packages they use; (2) Improve the fluid transport calculation and other simulation bottlenecks that occur now that the chemistry solver is substantially faster; (3) Continue to create new combustion algorithms for the graphics processing unit; and (4) Explore more robust error theory for physical models in engine simulations to ensure that accuracy is maintained in a rigorous manner transparent to all users. (McNenly, report II.12)

- Los Alamos National Laboratory is developing algorithms and software for the advancement of speed, accuracy, robustness, and range of applicability of the KIVA internal engine combustion modeling—to be more predictive, and providing KIVA software that is easier to maintain and is easier to add models to than the current KIVA. In FY 2015 they plan to, (1) Continue developing the parallel system in the *hp*-adaptive finite element method; (2) Continue developing comprehensive comparative results to benchmark problems and to commercial software as part of the verification and validation of the algorithms; (3) Continue developing the implicit solver system for the predictor-corrector split finite element method system; (4) Validate the KIVA chemistry and spray with *hp*-adaptive scheme; (5) Continue developing the parallel solution method for the *hp*-adaptive predictor-corrector split algorithm; and (6) Continue to verify and validate combustion and spray models. (Carrington, report II.13)
- Oak Ridge National Laboratory is developing and applying innovative strategies that maximize the benefit of high-performance computing resources and predictive simulation to support accelerated design and development of advanced engines to meet future fuel economy and emissions goals. In FY 2015 they plan to continue collaboration with industry and the Lawrence Livermore National Laboratory to enable graphical processing unit implementation of Converge™ flow solvers and evaluate the resulting speed-up on Titan, and continue effort to couple injector and engine models to include in-cylinder spray development and combustion into the injector design optimization process. (Edwards, report II.14)
- Argonne National Laboratory is optimizing engine operating conditions to use low cetane fuel to achieve clean, high-efficiency engine operation and demonstrating the use of low-temperature combustion as an enabling technology for high-efficiency vehicles. In FY 2015 they plan to, (1) Continue to improve low-load operation using low-pressure diesel injection, reduced injector umbrella angles and reduced swirl to enhance local richness in the combustion chamber; (2) Use 10% ethanol-based 87 anti-knock index fuel to insure success using a more representative U.S. pump gasoline; (3) Explore the opportunity to utilize a turbo/supercharger combination to enhance intermediate temperature heat release to further enhance low-load operation; and (4) Conduct additional engine performance tests for Autonomie simulations to support low-temperature combustion development as applied to vehicles. (Ciatti, report II.15)
- Argonne National Laboratory is quantifying efficiency potential and combustion stability limitations of advanced gasoline direct-injection engines, extending the lean and exhaust gas recirculation dilution tolerance of light-duty gasoline direct-injection engines, and developing a three-dimensional computational fluid dynamics methodology to analyze and predict cyclic variability in gasoline direct-injection engines. In FY 2015 they plan to, (1) Improve the understanding of engine cyclic variability and contrast Reynolds-averaged Navier-Stokes against large-eddy simulation engine multi-cycle results in terms of accuracy and computational requirements; (2) Perform experiments and simulations to further the understanding of the basic interaction between ignition source and in-cylinder flow with the goal to improve flame propagation under dilute conditions; and (3) Develop and evaluate comprehensive numerical models for advanced ignition systems and validate with targeted experiments. (Wallner, report II.16)
- Oak Ridge National Laboratory is characterizing dynamics of cyclic variability that limits dilution levels in spark-ignition engines, evaluating potential engine efficiency gains resulting from effective control of cyclic variations, and demonstrating dilution limit extension through active control to reduce cyclic variability. In FY 2015 they plan to demonstrate impact of dual-timescale control strategies on exhaust gas recirculation dilution limit extension, and demonstrate applicability of short-timescale next-cycle control strategy to homogeneous lean combustion. (Kaul, report II.17)
- Oak Ridge National Laboratory is developing and evaluating the potential of high-efficiency clean combustion strategies with production viable hardware and aftertreatment on multi-cylinder engines. In FY 2015 they plan to, (1) Evaluate the role of advanced air handling and hybrid exhaust gas recirculation systems for reactivity-controlled compression ignition load expansion and potential efficiency increases; (2) Conduct transient dual- and single-fuel low-temperature combustion experiments in conjunction with exhaust aftertreatments including experiments investigating the effectiveness of a selective catalytic reduction/diesel oxidation catalyst system to store/oxidize high levels of CO/HC from reactivity-controlled compression ignition operation; (3) Analyze reactivity-controlled compression ignition particulate matter data to determine composition and nature of reactivity-controlled compression ignition particulate matter;

and (4) Conduct heavy-duty reactivity-controlled compression ignition experiments in collaboration with Cummins. (Curran, report II.18)

- Oak Ridge National Laboratory is defining and analyzing specific advanced pathways to improve the energy conversion efficiency of internal combustion engines with emphasis on thermodynamic opportunities afforded by new approaches to combustion. In FY 2015 they plan to, (1) Characterize in-cylinder reforming chemistry through speciation of reformate for parametric investigations of engine operating conditions; (2) Determine the in-cylinder reforming chemistry for multiple fuel types differing in H/C ratio; (3) Develop an engine operating strategy for exhaust gas recirculation loop reforming based on flow-reactor results of catalyst performance; and (4) Acquire a full-sized reforming catalyst for the thermochemical recuperation engine experiment and operate with the external exhaust gas recirculation loop reforming strategy. (Daw, report II.19)
- Oak Ridge National Laboratory is improving engine efficiency through better combustion uniformity, developing and applying diagnostics to resolve combustion-uniformity drivers, understanding origins of combustion non-uniformity and develop mitigation strategies, and addressing critical barriers to engine efficiency and market penetration. In FY 2015 they plan to, (1) Develop methodologies to monitor net cylinder-charge composition, temperature, and fluctuations; (2) Modify the exhaust gas recirculation probe to incorporate additional functions for driving engine efficiency advances; (3) Apply improved EGR probe with Cooperative Research and Development Agreement partners to development of next-generation engine efficiencies; and (4) Identify and develop diagnostics for addressing efficiency barriers. (Partridge, report II.20)
- Oak Ridge National Laboratory is developing high-fidelity neutron imaging capabilities and employing the technique to aid improved design and control of complex advanced combustion systems, and help to guide model validation and input. In FY 2015 they plan to, (1) Demonstrate dynamic imaging capability with a gasoline direct injection-based system and validate whether cavitation can be observed; (2) Investigate deposits in used injectors in conjunction with injector partners; (3) Incorporate ash-laden and gasoline particulate samples into the particulate filter study and include regeneration; and (4) Become active member of the Engine Combustion Network and incorporate neutron imaging into gasoline direct injection studies. (Toops, report II.21)
- Michigan Technological University is performing a comprehensive characterization of high injection pressure dimethyl ether (DME) spray combustion under lean-burn conditions: investigate the characteristics of DME spray combustion for use in internal combustion engines and whether these characteristics affect burning rates, quenching limits, and emissions under engine-representative conditions. In FY 2015 they plan to, (1) Evaluate the high injection pressure spray combustion performance, new DME chemical kinetics mechanism and rapid compression machine autoignition; (2) Analyze the spray dynamic and combustion test for the liquid, vapor, and flame tip penetrations in the single-hole nozzle; and (3) Conduct the single-hole injector nozzle design and fabrication, the rate of injection test, spray test, and computational fluid dynamics model. (Lee, report II.22)
- The University of New Hampshire is using collaborative experiments and numerical simulations to investigate unsteady reciprocating effects on heat transfer in piston engines. In FY 2015 they plan to, (1) Conduct physical experiments to measure and characterize heat transfer in controlled experiments with similar rapid transients and boundary layer behaviors found in engines; (2) Optimize electron vacuum- and plasma-assisted chemical vapor deposition techniques to eliminate defects observed in optical window coatings; (3) Conduct engine experiments to simultaneously determine gas velocity field and surface temperature under reversing flow motored conditions; and (4) Develop and implement new modeling approaches that better capture the transport mechanisms in non-equilibrium boundary layer flows and piston engines. (White, report II.23)
- Stanford University is conducting detailed measurements and developing advanced modeling capabilities to improve current understanding about heat transfer, thermal stratification, and non-equilibrium coupling processes in the near-wall region of internal combustion engines that are operated under low-temperature combustion conditions. In FY 2015 they plan to, (1) Acquire larger collection of flow measurements; (2) Fully implement and employ temperature imaging technique; (3) Conduct measurements for range of operating conditions; (4) Perform multiple concurrent high resolution direct numeric simulation studies;

and (5) Develop dynamic non-equilibrium wall models for large-eddy simulation calculations. (Ihme, report II.24)

- The University of California-Berkeley is demonstrating extension of engine load and speed limits using partial fuel stratification (PFS) compared to homogeneous charge compression ignition (HCCI), and developing validated models of PFS. In FY 2015 they plan to, (1) Develop and validate a model of the Massachusetts Institute of Technology engine in CONVERGE™ CFD; (2) Experimentally demonstrate that HCCI with PFS allows expansion of high- and low-load limits, to allow high-efficiency operation over the full engine load and speed requirements. Further demonstrate that exhaust temperatures are high enough for an oxidation catalyst to be used for after treatment of hydrocarbons and CO; (3) Evaluate the effect of compression ratio and injection timing on low-temperature heat release and intermediate temperature heat release for a certification gasoline; (4) Quantify experimentally the memory effect of flames propagating through a step change in fuel content; and (5) Quantify the effect of fuel stratification on flame propagation velocity using a numerical model for methane-air flames. Develop an empirical correlation for the flame speed as a function of the thermochemical state and spatial derivatives in fuel content. (Dibble, report II.25)
- Michigan State University is examining the active radicals generated in the turbulent jet ignition (TJI) process through both rapid compression machine and optically accessible engine experiments and develop a new large-eddy simulation modeling technique to model the turbulent jet ignition system. In FY 2015 they plan to, (1) Conduct further testing, including imaging, of the TJI process in the Michigan State University rapid compression machine with different nozzle geometries; (2) Develop a new rapid compression machine setup that combines visible light and chemiluminescence imaging; (3) Develop the model-based closed-loop combustion system for TJI engine experiments; (4) Design and fabricate TJI system for Michigan State University optical engine testing; (5) Conduct preliminary optical engine testing of TJI system; and (6) Conduct large-eddy simulation/filtered mass density function modeling of a series of TJI configurations to study the effects of various flow/flame parameters. (Toulson, report II.26)
- The University of Connecticut is developing a predictive turbulent combustion model that is universally applicable to mixed regimes of combustion including elements of both premixed and non-premixed flames in the presence of local limit phenomena such as extinction and autoignition. In FY 2015 they plan to, (1) Development of the turbulent combustion model based on the chemical explosive mode analysis results from Sandia's direct numerical simulation data; (2) Generation of new direct numerical simulation data of lifted autoignitive jet flames at elevated pressure with multi-stage ignition (dimethyl ether and n-heptane); (3) Generation of new direct numerical simulation data of reactivity controlled compression ignition with gasoline blend of primary reference fuel with reactivity stratification; (4) Implementation of the turbulent combustion model and the scalar dissipation rate model to large-eddy simulation and Reynolds-averaged Navier-Stokes codes; (5) Validation of the turbulent combustion model and the scalar dissipation rate model against Sandia's direct numerical simulation data; (6) Three-dimensional large-eddy simulation and Reynolds-averaged Navier-Stokes for simulations of lifted diesel jet flames for n-heptane and/or dimethyl ether using the new turbulent combustion model and the scalar dissipation rate model; (7) Comparison of the large-eddy simulation and Reynolds-averaged Navier-Stokes simulations of engine combustion with experimental data; and (8) Large-eddy simulation and model validation of lifted diesel flames against direct numerical simulations in selected subdomains based on Reynolds-averaged Navier-Stokes simulations. (Lu, report II.27)
- Clemson University is elucidating the impact of thermal barrier coatings on low-temperature combustion efficiency, operating range and emissions; develop ceramic and metallic piston coatings that increase thermal and combustion efficiency without decreasing volumetric efficiency; and developing simulation tools to predict temperature gradients and coating surface temperature swings. In FY 2015 they plan to, (1) Powder spray and experimentally test a piston with yttria-stabilized zirconia (YSZ) coating, characterizing combustion and cycle efficiency over a range of loads and speeds; (2) Experimentally test an solution precursor plasma spray low-conductivity YSZ piston with inter pass boundaries; characterize the impacts on low-temperature combustion combustion and efficiency; (3) Utilize radiation chamber to characterize thermal properties of coatings; (4) Predict low-temperature combustion engine performance and efficiency improvements with a one-dimensional code co-simulating with a three-dimensional thermal model; (5) Engine experiments measuring temperatures and heat fluxes at multiple locations on the piston for validation of the three-dimensional finite element code; and (6) Utilize the three-dimensional thermal

analysis model to investigate temperature gradients and the instantaneous piston surface temperature profiles with a dense and low-conductivity YSZ coating. (Filippi, report II.28)

- The Pennsylvania State University is quantifying effects of radiative heat transfer and turbulent fluctuations in composition and temperature on combustion, emissions, and heat losses in internal combustion engines; developing computational fluid dynamics-based models to capture these effects in simulations of in-cylinder processes in internal combustion engines; and exercising models to explore advanced combustion concepts for internal combustion engines to develop next-generation high-efficiency engines. In FY 2015 they plan to, (1) Perform fully coupled simulations including radiative heat transfer for constant-volume combustion chambers under engine-relevant conditions, and for engines operating in conventional and advanced compression-ignition combustion modes; (2) Quantify radiation and turbulence-chemistry-radiation interactions effects for conventional and advanced compression-ignition combustion modes in engines; and (3) Exercise the models to explore advanced combustion concepts for internal combustion engines and to develop next-generation high-efficiency engines. (Haworth, report II.29)
- Yale University is measuring quantitative sooting tendencies for a wide range of diesel and biodiesel fuel components, and developing a mixing rule that can be used to define surrogate fuel mixtures that mimic the sooting behavior of real diesel fuels. In FY 2015 they plan to, (1) Measure soot concentrations in flames doped with the 32 mixtures and analyze them to determine the sooting tendencies of the individual components and identify any synergistic interactions between them; (2) Derive a mixing rule from this data that can be used to choose diesel surrogate mixtures that have the same sooting behavior as their target diesel fuels; and (3) Develop surrogates for reference diesel fuels that match their soot formation characteristics. (Pfefferle, report II.30)
- Argonne National Laboratory is evaluating the impacts of low-temperature combustion technology on fuel economy and engine-out emissions using vehicle simulations and engine in the loop, and comparing the fuel economy benefits of low-temperature combustion technology to port fuel injection and spark-ignited direct-injection technologies by using simulations. In FY 2015 they plan to, (1) Update the fuel economy benefits of low-temperature combustion for a mild hybrid powertrain with an updated brake specific fuel consumption map; and (2) Quantify fuel consumption and engine-out emissions for low-temperature combustion technology with engine in the loop when steady combustion at low loads is established. (Shidore, report II.31)

EMISSION CONTROL R&D

In FY 2014, work will continue on lean oxides of nitrogen traps (LNTs) and urea-selective catalytic reduction (urea-SCR) to reduce oxides of nitrogen (NOx) emissions. The focus of activities will be on making these devices more efficient, more durable, and less costly. For particulate matter control, the focus will be on more efficient methods of filter regeneration to reduce impact on engine fuel consumption.

- Oak Ridge National Laboratory is coordinating the Cross-Cut Lean Exhaust Emission Reduction Simulation (CLEERS) activity for the DOE Advanced Engine Cross-Cut Team. In FY 2015 they plan to, (1) Continue leading the CLEERS planning and database advisory committees; (2) Continue leading the Focus Groups; (3) Organize and conduct the 2015 CLEERS Workshop; (4) Continue sharing of basic data and models with DOE Vehicle Systems projects and the Advanced Combustion and Emissions Control Team from U.S. DRIVE; (5) Continue maintenance and expansion of CLEERS website; (6) Continue providing regular update reports to the DOE Advanced Combustion Engine Cross-Cut team; and (7) Conduct 2015 CLEERS Industry Priority Survey. (Daw, report III.1)
- Oak Ridge National Laboratory is collaborating with Pacific Northwest National Laboratory to support industry in the development of accurate simulation tools for the design of catalytic emissions control systems that enable advanced high-efficiency combustion engines to meet emissions regulations while maximizing fuel efficiency. In FY 2015 they plan to, (1) Complete development and publication of mechanistic pathways and associated modeling strategies that predict N_2O formation during low-temperature LNT regeneration; (2) Quantify impacts of hydrothermal aging on energetics of NH_3 adsorption for a commercial Cu-zeolite selective catalytic reduction catalyst. Identify strategies for adjusting model parameters to account for aging; and (3) Develop experimental methods and analysis

approaches for estimating the key parameters required to calibrate models of hydrocarbon traps for low-temperature exhaust applications. (Daw, report III.2)

- Pacific Northwest National Laboratory is promoting the development of improved computational tools for simulating realistic full-system performance of lean-burn engines and the associated emissions control systems, and providing the practical and scientific understanding and analytical base required to enable the development of efficient, commercially viable emissions control solutions for ultra-high efficiency vehicles. In FY 2015 they plan to, (1) Experimentally address the continuing fundamental issues being identified in modeling studies; (2) Continue studies of the reaction mechanism for Cu-chabhazite zeolite relative to Fe-chabhazite zeolite catalysts; (3) In collaboration with partners on a new National Science Foundation/DOE-funded project, probe the nature and stability of the active Cu species in the chabhazite zeolite-based catalysts, especially for SAPO-34 zeolite-based catalysts; (4) Cooperate with Oak Ridge National Laboratory to improve selective catalytic reduction characterization protocols and experiments with fresh and aged samples for model development; (5) Recalibrate two-site selective catalytic reduction model with updated high-temperature data and publish results; (6) LNT studies will now focus on low-temperature NO adsorption (passive NOx adsorbers). Studies this next year will probe mechanisms of NO adsorption and desorption; and (7) Extend analysis of X-ray computed tomography data to samples with intermediate catalyst loadings to clarify the effect of catalyst loading on catalyst location and backpressure. (Stewart, report III.3)
- Pacific Northwest National Laboratory is identifying approaches to significantly improve both the high- and low-temperature performance, and the stability of the catalytic NOx reduction technologies via a pursuit of a more fundamental understanding. In FY 2015, (1) The primary activities will be focused on the mechanisms for low- and high-temperature performance loss as a function of operation conditions of new generation chabhazite zeolite-based NH_3 selective catalytic reduction catalysts. For these studies, we will utilize the model catalysts prepared via methods studied in the past two FYs (FY 2013 and FY 2014). These fundamental studies will be carried out in conjunction with baseline performance and stability experiments on fully formulated catalysts; and (2) Having completed the studies of K-based high temperature NOx storage and reduction materials this past year, we will initiate studies of the low-temperature performance of promising candidate passive NOx adsorber materials. (Peden, report III.4)
- Pacific Northwest National Laboratory is developing and demonstrating mixed metal oxide-based catalysts as a low-cost replacement for platinum in the oxidation of NO to NO_2 in lean engine exhaust, an essential first step in controlling oxides of nitrogen emissions. This project was completed in September, 2014.
- Pacific Northwest National Laboratory is developing an improved understanding of SCR and diesel particulate filter integration for application to on-road heavy-duty diesel emission reduction. No additional work is planned under this project in FY 2015. (Rappe, report III.6)
- Oak Ridge National Laboratory is developing emission control technologies that perform at low temperatures (<150ºC) to enable fuel-efficient engines with low exhaust temperatures to meet emission regulations, and identifying advancements in technologies that will enable commercialization of advanced combustion engine vehicles. In FY 2015 they plan to, (1) Continue to investigate pathways to take advantage of the improved Pd/Zr reactivity to CO and hydrocarbon oxidation; (2) Investigate durability of Cu-Ce-Co catalysts and how it interacts with the platinum-grade metal-based systems for hydrocarbon conversion; (3) Investigate synergy of release kinetics of low-temperature oxides of nitrogen and hydrocarbon trap materials with other technologies being studied; (4) Identify low-temperature NOx reduction strategies that can be used at 150°C; and (5) Begin exploring how the technologies discussed above can work together to achieve 90% conversion of all exhaust constituents at 150°C. (Toops, report III.7)
- Oak Ridge National Laboratory is assessing and characterizing catalytic emission control technologies for lean-gasoline engines, and identifying strategies for reducing the costs, improving the performance, and minimizing the fuel penalty associated with emission controls for lean-gasoline engines. In FY 2015 they plan to, (1) Determine the effect of thermal aging on NH_3 production by three-way catalysts; and (2) Measure the fuel penalty of the passive selective catalytic reduction approach for programmed load-step engine operation that simulates mode switching operation (between lean and rich) in transient drive cycles. (Parks, report III.8)

- Oak Ridge National Laboratory is researching the fundamental chemistry of automotive catalysts, identifying strategies for enabling self-diagnosing catalyst systems, and addressing critical barriers to market penetration. In FY 2015 they plan to quantify spatiotemporal performance of commercial Cummins selective catalytic reduction catalyst under lab- and field-aged conditions. (Partridge, report III.9)
- Argonne National Laboratory is determining detailed mechanisms of gasoline particulate filter filtration/regeneration processes, and evaluating filter performance in consideration of back pressure increase, particulate matter mass, and number emission reduction efficiencies to suggest an optimized filter substrate structure for gasoline direct-injection engines. In FY 2015 they plan to, (1) Define the role of ash components in soot oxidation; and (2) Suggest filter types appropriate for gasoline direct injection engines. (Seong, report III.10)
- Pacific Northwest National Laboratory is seeking to shorten development time of filtration technologies for future engines and developing modeling approaches relevant to the likely key challenge for gasoline particulate filtration—high number efficiency at high exhaust temperatures. In FY 2015 they plan to, (1) Complete analysis of data collected during third round of cooperative experiments at the University of Wisconsin Engine Research Center; (2) Explore the use of new techniques, such as maximal inscribed sphere analysis, to characterize three-dimensional filter microstructure and quantify features tied to pressure drop and filtration performance; (3) Extend exhaust filtration analysis experiments to multiple filter substrates from many manufacturers spanning a wide range of properties; and (4) Re-design of the University of Wisconsin exhaust filtration analysis system, including features to allow experiments with spark-ignited, direct-injection exhaust at temperatures representing close-coupled filter placement. (Stewart, report III.11)
- Pacific Northwest National Laboratory is investigating a number of candidate low-temperature oxidation catalysts as fresh materials, and after realistic laboratory- and engine-aging; obtaining a better understanding of fundamental characteristics and various aging factors in both thermal and chemical aspects that impact the long-term performance of these candidate low-temperature oxidation catalysts. In FY 2015 they plan to, (1) Conduct additional physical and chemical characterization studies to understand the activity variation patterns observed in CO oxidation over a home-made and commercial CeO_2-ZrO_2 (GMR5 & 6) supported Cu catalysts; (2) Prepare model Cu/CeO_2 catalysts with well-defined CeO_2 crystal facets (cubes, rods, polyhedral). Investigate the reactivities of these model catalysts in the oxidation of both CO and hydrocarbons. These studies will focus on understanding the effect of the different crystal facets on the overall catalyst performances of Cu/CeO_2-ZrO_2 catalysts; and (3) Conduct physicochemical characterization studies on sulfur poisoned Cu/CeO_2-ZrO_2 catalysts to understand the deactivation mechanism caused by sulfation. Try to develop methods for efficient sulfur removal. (Peden, report III.12)
- Purdue University is synthesizing Cu-SSZ-13 catalysts that are exceptionally well defined at the microscopic level, including control of number and type of active sites. In FY 2015 they plan to, (1) Develop synthesis procedures that control or optimize the SSZ-13 microstructure, specifically the Al and Cu active site type and density; (2) Develop spectroscopies (X-ray, vibrational, and ultraviolet visible near–infrared), titrations (NH_3, H/D exchange) and probe reactions (NO oxidation, NH_3 adsorption) that provide decisive information about selective catalytic reduction active site structures, before and during SCR redox cycles; (3) Develop first principles models that correlate with experiment and that predict reaction mechanism and rate as a function of site type; and (4) Use experiment and computation to characterize sulfur impact on catalyst state and performance. (Ribeiro, report III.13)
- The University of Houston is predicting binary and ternary metal alloy catalyst compositions for enhanced CO, NO and hydrocarbon oxidation from first principles density functional theory and verify through kinetic and mechanistic studies, and developing enhanced low-temperature CO, hydrocarbon and NO oxidation catalysts through zoning and profiling of metal and ceria components. In FY 2015 they plan to, (1) Improve the descriptor-based model by refining the included elementary reaction steps and tune the reaction energetics to match experimental data; (2) Calculate activation barriers for propylene oxidation and derive the corresponding scaling relationships that are needed as input for the descriptor-based microkinetic model; (3) Develop a microkinetic model of CO and C_3H_6 oxidation, while incorporating the impact of different Pt/Pd ratios; and (4) Predict NH_3 generation on an LNT at low temperature and impact on zoned or layered selective catalytic reduction. (Epling, report III.14)

- The University of Kentucky Center for Applied Energy Research is improving the low-temperature performance of catalyst-based NOx mitigation systems by designing materials which can function as either passive NOx adsorbers or low-temperature LNT catalysts. In FY 2015 they plan to, (1) Study the benefits of using Pd as a promoter in passive NOx adsorber applications (as opposed to Pt), particularly for ceria-based materials; (2) Vary the Ce-Zr ratio in MnFeOx/$CeZrO_2$ and $CeZrO_2$ materials in order to assess how increasing the Zr content affects NOx uptake and release; (3) Examine the effect on low-temperature NOx storage capacity of fine tuning the M:Ce ratio in M_2O_3-CeO_2 mixed oxides; and (4) Initiate diffuse reflectance infrared Fourier transform spectroscopy studies on the most promising materials identified above in order to elucidate the mechanism of NOx adsorption. (Crocker, report III.15)

HIGH-EFFICIENCY ENGINE TECHNOLOGIES

The objective of these projects is to increase engine and vehicle efficiency of both light- and heavy-duty vehicles using advanced technology engines and advanced drivetrains. The following describe what is planned for completion in FY 2015.

- Cummins Inc. is engaged in developing and demonstrating advanced diesel engine technologies to significantly improve the engine thermal efficiency while meeting U.S. Environmental Protection Agency 2010 emissions. In FY 2054 they plan to conduct analysis and targeted testing of technologies for achievement of a 55% thermal efficient engine, and develop the technology roadmap for a 55% thermal efficient engine with supporting analysis and test results.(Koeberlein, report IV.1)
- Detroit Diesel Corporation is conducting a demonstration of a 50% total increase in vehicle freight efficiency measured in ton-miles per gallon, with at least 20% improvement through the development of a heavy-duty diesel engine; and development of a heavy-duty diesel engine capable of achieving 50% brake thermal efficiency on a dynamometer under a load representative of a level road at 65 mph. In FY 2015, (1) While the 50% brake thermal efficiency project goal has been achieved, further refinements will continue to be tested to further improve the efficiency of both engine and waste heat recovery systems; (2) Refinement of various engine systems will continue to help fine tune their operating characteristics in support of final demonstrator testing on selected SuperTruck routes; (3) Development of mechanical expanders for the waste heat recovery system to improve its performance characteristics by eliminating the inefficiencies of energy form conversion; and (4) Complete the pilot testing of advanced combustion regimes on a stock engine in collaboration with Oak Ridge National Laboratory. (Singh, report IV.2)
- Volvo is identifying concepts and technologies that have potential to achieve 55% brake thermal efficiency (BTE) on a heavy-duty diesel engine and demonstrate a heavy-duty diesel engine capable of achieving 50% BTE at the end of the SuperTruck project. In FY 2015 they plan to, (1) Continue development of the combustion computational fluid dynamics tool to be able to simulate partially premixed combustion, with focus on kinetic mechanisms and ways to speed them up; (2) Continue to use the transported computational fluid dynamics tool for 55% BTE concept engine combustion simulation; (3) Integrate closed-cycle computational fluid dynamics result into complete GT-POWER engine models; and (4) Verify more sub-systems including waste heat recovery to reach 50% BTE. (Amar, report IV.3)
- Navistar, Inc. is using advanced engine technologies, develop a heavy-duty diesel engine capable of achieving 50% or better brake thermal efficiency on a dynamometer under a load representative of a level road at 65 mph; In FY 2015 they plan to, (1) Evaluate the implications of a downsized engine (10.5 L from 12.4 L); (2) Continue investigation and development of high-efficiency solutions focusing on the impact of premixed fuel reactivity and the assessment of variable valve actuation technologies under dual-fuel combustion; (3) Conduct three-dimensional computational fluid dynamics to analyze and develop the advanced combustion solution for high-efficiency combustion, both dual-fuel and conventional single-fuel combustion will be included under this study; (4) Investigate and evaluate the feasible technology of waste heat recover system for maximum net brake thermal efficiency gain to be applied on an engine and on the vehicle; and (5) Conduct evaluation and optimization of aftertreatment system to optimize engine brake thermal efficiency. (Zukouski, report IV.4)
- Delphi is developing, implementing, and demonstrating fuel consumption reduction technologies using a new low-temperature combustion process: gasoline direct-injection compression ignition. Future development work should concentrate on combustion control during vehicle transient operation and on

improved exhaust aftertreatment targeted for the lower temperatures resulting from this low-temperature combustion scheme. (Confer, report IV.5)

- Ford Motor Company is demonstrating 25% fuel economy improvement in a mid-sized sedan using a downsized, advanced gasoline turbocharged direct injection engine capable of meeting Tier 3 Super Ultra-Low Emissions Vehicle 30 emissions on the Federal Test Procedure 75 cycle. In FY 2015 they plan to demonstrate greater than 25% weighted city/highway fuel economy improvement and Tier 3 Super Ultra-Low Emissions Vehicle 30 emissions on the Federal Test Procedure 75 test cycle. (Wagner, report IV.6)
- Cummins Inc. is demonstrating 40% fuel economy improvement over a baseline gasoline V-8 pickup truck with Tier 2 Bin 2 tailpipe emissions compliance. In FY 2015 they plan to develop and optimize the ATLAS engine Tier 2 Bin 2 ATLAS engine-out emission demonstration in a test cell and vehicle environment. (Ruth, report IV.7)
- Robert Bosch LLC is improving light-duty vehicle fuel economy by 25% with minimum performance penalties while achieving Super Ultra-Low Emission Vehicle level emissions with gasoline. In FY 2015 they plan to, (1) Evaluate drive-cycle fuel economy and emissions performance of multi-mode combustion on prototype vehicles; (2) Improve real-world driving performance on prototype vehicles for demonstration; and (3) Analyze fuel efficiency and emission results from vehicle, identifying commercial potentials of the proposed technology solutions. (Yilmaz, report IV.8)
- Chrysler Group LLC is demonstrating 25% improvement in combined Federal Test Procedure City and Highway fuel economy for the Chrysler minivan, and accelerating the development of highly efficient engine and powertrain systems for light-duty vehicles, while meeting future emissions standards. This project is complete. (Reese, report IV.9)
- Filter Sensing Technologies, Inc. is demonstrating and quantifying improvements in efficiency and greenhouse gas reductions through improved diesel particulate filter sensing, controls, and low-pressure drop components. In FY 2015 they plan to, (1) Quantify radio frequency sensor performance and efficiency gains with a wide range of light-duty and heavy-duty engines with cordierite and aluminum titanate particulate filters; (2) Confirm on-road durability and quantify fuel savings through an additional 12-month fleet test on model year 2010+ heavy-duty vehicles; testing initiated ahead of schedule; (3) Investigate additional efficiency gains possible through the use of advanced combustion modes with real-time feedback control enabled by fast radio frequency sensor response; and (4) Develop production sensor designs and commercialization plans on the scale required to significantly impact reduction in greenhouse gas emissions and fuel consumption. (Sappok, report IV.10)
- General Motors is applying and evaluating the enabling technologies of hydrogen-augmented exhaust gas recirculation, two spark plugs per cylinder, increased compression ratio with a low surface area to volume ratio combustion chamber, increased charge motion (tumble and/or swirl), dual gasoline direct injection/port fuel injection fuel system and a variable geometry turbocharger system to a current GM-boosted spark ignition engine. In FY 2015 they will evaluate results of testing to determine performance to objectives. (Keating, report IV.11)
- Eaton Corporation is demonstrating fuel economy improvement and emissions reduction through organic Rankine cycle waste heat recovery systems utilizing a roots expander on heavy-duty diesel engines. In FY 2015 they will demonstrate roots expander capability of meeting DOE project objective utilizing the developed heavy-duty diesel engine organic Rankine cycle system. (Subramanian, report IV.12)
- MAHLE Powertrain is demonstrating thermal efficiency of 45% on a light-duty gasoline engine platform while demonstrating potential to meet U.S. Environmental Protection Agency emissions regulations, and a 30% predicted vehicle drive cycle fuel economy improvement over an equivalent conventional port-fuel-injected gasoline engine with variable cam phasing. In FY 2015 they plan to, (1) Identify optimal Turbulent Jet Ignition pre-chamber and nozzle geometry for peak thermal efficiency, drive cycle fuel consumption, and lean limit extension; (2) Identify optimal Turbulent Jet Ignition operating strategy across engine operating map for peak thermal efficiency, drive cycle fuel consumption, and lean limit extension; (3) Complete boosted multi-cylinder Turbulent Jet Ignition engine testing and analysis; (4) Complete one-dimensional Turbulent Jet Ignition drive cycle analysis utilizing multi-cylinder engine data; and (5) Utilize correlated computational fluid dynamics model to increase understanding of and optimize the pre-chamber mixture preparation process. (Blaxill, report IV.13)

- ENVERA LLC is developing a high-efficiency variable compression ratio (VCR) engine having variable valve actuation and an advanced high-efficiency supercharger to obtain up to a 40% improvement in fuel economy when replacing current production V-8 engines with the new small displacement VCR engine. In FY 2015 they plan to do, (1) Engine tuning using GT-POWER modeling; (2) VCR boosting system down-selection; (3) Advanced supercharger development—to be determined based on down-selected system; (4) Camshaft development as needed based on GT-POWER modeling; and (5) VCR engine design/build. (Mendler, report IV.14)
- Robert Bosch LLC is developing an intake air oxygen (IAO2) sensor which directly and accurately measures the oxygen concentration in the intake manifold. In FY 2015 they plan to, (1) Engine dynamometer testing of sensors and control algorithm to validate the fuel economy, emissions, and durability performance of the IAO2 sensor and control algorithm; and (2) Develop concept for second generation IAO2 sensor. (Schnabel, report IV.15)
- Los Alamos National Laboratory is developing oxides of nitrogen (NOx) and ammonia (NH_3) sensors for diesel emission control systems. In FY 2015 they plan to, (1) Validate NH_3 sensor in an engine environment for the first time; (2) Extend validation of hydrocarbon and NOx sensors to a lean-burn gasoline engine environment; (3) Evaluate sulfur tolerance of both NOx and NH_3 sensor; (4) Demonstrate improved sensor selectivity/sensitivity through use of catalyst over coat and electrode composition optimization; and (5) Explore commercialization partners for unique sensing technology. (Mukundan, report IV.16)

SOLID STATE ENERGY CONVERSION

Research will continue in FY 2015 on thermoelectrics (TEs) for converting waste heat from advanced combustion engines directly to electricity. Research will focus on development of practical systems that are suitable for future production.

- Gentherm Inc. is preparing a detailed production cost analysis for a thermoelectric generator (TEG) for passenger vehicle volumes of 100,000 units per year and a discussion of how costs will be reduced in manufacturing. In FY 2015 they plan to produce light-duty vehicle TEGs for installation in Ford and BMW vehicles, test vehicles and measure fuel efficiency improvement at vehicle manufacturer sites, perform independent testing at the National Renewable Energy Laboratory, analyze vehicle level test results and compare test and model data, and deliver TEG system for the Bradley Fighting Vehicle. (Jovovic, report V.1)
- General Motors is overcoming major obstacles to the commercialization of automotive TEG systems, developing an overall TEG system including all necessary vehicle controls and electrical systems and fully integrated onto a light-duty vehicle, and demonstrating fuel economy improvement of 5% over the US06 drive cycle. In FY 2015 they plan to, (1) Complete fabrication, assembly, and testing of initial TEG; (2) Evaluate initial TEG performance and durability; identify and address the root causes of component failures; (3) Evaluate feasibility of modified TE module architecture to reduce clamp load requirements for the Phase 2 TEG; (4) Continue to develop strategies for skutterudite oxidation suppression; and (5) Design, fabricate, and test a Phase 2 TEG that incorporates improvements based on initial TEG results. (Salvador, report V.2)
- GMZ Energy is demonstrating a robust, thermally cyclable TE exhaust waste heat recovery system that will provide approximately a 5% fuel efficiency improvement for a light-duty vehicle platform, and developing an initial design/concept for a 1-kW TEG in the exhaust stream of a Bradley Fighting Vehicle. In FY 2015 they, (1) The TEG will be subjected to extensive thermal and mechanical reliability testing; and (2) The automotive TEG currently under fabrication will be installed onboard a Honda Accord vehicle platform, and the vehicle fuel economy will be compared with the baseline data in order to establish the improvement in fuel economy due to the TEG installation. (Cleary, report V.3)
- Argonne National Laboratory is establishing requirements for a TEG to provide cost-effective power for hybrid electric vehicles when subjected to U.S. Environmental Protection Agency standard test procedures, quantifying fuel economy benefits from the EPA two-cycle procedure, developing a TEG model based on published information that can simulate the effect of exhaust flow interruptions, and estimating the net present value of the fuel savings. In FY 2015 the TEG model can be improved if more

module test data are made available from the original equipment manufacturers, and more advanced models to factor detailed material and cost data will be used for optimization studies involving cost. (Vijayagopal, report V.4)

II. COMBUSTION RESEARCH

II.1 Low-Temperature Automotive Diesel Combustion

Paul Miles
Sandia National Laboratories
P.O. Box 969
Livermore, CA 94551-0969

DOE Technology Development Manager
Leo Breton

Subcontractor
University of Wisconsin Engine Research Center, Madison, WI

Overall Objectives

- Provide the physical understanding of the in-cylinder combustion processes needed to minimize the fuel consumption and the carbon footprint of automotive diesel engines while maintaining compliance with emissions standards
- Develop efficient, accurate computational models that enable numerical optimization and design of fuel-efficient, clean engines
- Provide accurate data obtained under well-controlled and characterized conditions to validate new models and to guide optimization efforts

Fiscal Year (FY) 2014 Objectives

- Extend laboratory capabilities to permit stable, repeatable multiple injections
- Develop a capability to measure injection quantity and rate quantitatively and apply to characterize rate shaping effects associated with multiple injection strategies
- Examine the evolution of the in-cylinder flow field throughout the intake and compression strokes, with an emphasis on developing an understanding of how flow asymmetries develop and how they can be mitigated
- Improve and extend the capabilities of research computational fluid dynamics (CFD) codes and test their ability to capture flow asymmetry

FY 2014 Accomplishments

The accomplishments below target the barriers of 1) lack of fundamental knowledge, and 2) lack of a predictive modeling capability identified in the Vehicle Technologies 2011-2015 Multi-Year Program Plan.

- Upgraded fuel injection capabilities to allow several closely spaced injection events within a single cycle
- Acquired and installed a state-of-the-art injection quantity and rate bench and applied it to determine the effects of both fuel properties and operating parameters on the fuel injection rate
- Examined the evolution of the in-cylinder flow for three different swirl ratios and characterized the evolution of flow asymmetry throughout the compression stroke
- Extended CFD code capabilities to allow efficient use of parallel computing capabilities
- Examined the impact of a full-engine grid on calculations of fuel spray asymmetries and near-top-dead center (TDC) turbulence levels

Future Directions

- Examine the impact of "stepped-lip" piston bowl geometries on the in-cylinder flow development and the mixture preparation process and compare with conventional bowl geometries
- Investigate benefits of close-coupled pilot injections on mixture formation, combustion noise, and emissions and identify the physical processes dominating this behavior
- Identify and investigate multiple injection strategies suitable for limiting cold-start hydrocarbon and CO emissions

✧ ✧ ✧ ✧ ✧

INTRODUCTION

Direct-injection diesel engines have the highest proven brake fuel efficiency of any reciprocating internal combustion engine technology. Further improvements of this technology will require the ability to fully optimize the mixture formation, combustion and emissions formation processes using accurate, predictive CFD codes. Variations in the mixture formation process associated with the individual fuel jets is one source of non-optimal combustion events. These variations can be caused by both hole-to-hole differences in the fuel injector nozzle, or by asymmetries in the in-cylinder flow field. Such asymmetries can be especially problematic under conditions of small injected quantities, such as occur with pilot injections.

This year, the project has focused on resolving discrepancies between measured and predicted fuel-air mixture fields that were observed in FY 2012 and 2013. These discrepancies include an over-sensitivity of jet penetration and deflection to flow swirl ratio and an under-prediction of the turbulent diffusion of the fuel jets. Three potential causes of this behavior have been examined this year. First, the initial injection rates have been accurately measured with a new injection rate measurement capability, thus providing improved estimates of the boundary conditions for the CFD simulations. Second, the in-cylinder flow field has been measured for three different swirl ratios. Detailed comparisons with the simulations are currently in progress. Third, we have extended the computations to include the full engine, rather than a single sector. As will be seen in the following, this latter change resulted in significant increases in the simulated turbulence levels and is expected to have a marked impact on the turbulent diffusion of the fuel.

APPROACH

The overall research approach involves carefully coordinated experimental, modeling, and simulation efforts. Detailed measurements of in-cylinder flows, fuel and pollutant spatial distributions, and other thermo-chemical properties are made in an optical engine facility based on a General Motors 1.9-liter automotive diesel engine. Careful attention is also paid to obtaining accurate boundary conditions to facilitate comparisons with simulations, including intake flow rate and thermodynamic properties, fuel injection rate, and wall temperatures. Close geometric and thermodynamic correspondence between the optical engine and a traditional, all-metal test engine allow the combustion and engine-out emissions behavior of the test engine to be closely matched. These measurements are closely coordinated and compared with the predictions of numerical simulations.

The experimental and numerical efforts are mutually complementary. Detailed measurements of the in-cylinder variables permit the evaluation and refinement of the models used in the computer simulations, while the simulation results can be used to obtain a more detailed understanding of the in-cylinder flow and combustion physics—a process that is difficult if only limited measurements are available. Jointly, this approach addresses both of the principal goals of this project: 1) development of the physical understanding to guide, and 2) the simulation tools to refine the design of optimal, clean, high-efficiency diesel combustion systems.

RESULTS

Table 1 illustrates the capabilities of the Moehwald HDA (*Hydraulischer Druckanstieg* or hydraulic pressure increase) injection quantity and rate analyzer that was installed in the laboratory this year. This state-of-the-art device has a resolution and repeatability of approximately 0.01 mg, making it well suited for application to light-duty multiple injection studies, where injection quantities of 1 mg or less are not uncommon. Our initial work focused on clarifying the impact of injector temperature, axial clamping force, energizing current waveform, and high-pressure line length on the injection rate. Each of these parameters was expected to impact the accuracy with which rate measurements made with the HDA can be transferred to the operating engine environment. However, only the high-pressure line length was found to be significant. Injector-to-injector variations were also examined and found to be relatively minor.

TABLE 1. Specifications of the Moehwald HDA

Measurement resolution [mg]	~ 0.01 mg	
Measurement repeatability [mg]	~ 0.075 mg ~ 0.1 mg ~ 0.2 mg	(< 16 mg) (< 60 mg) (< 200 mg)
Number of injections per cycle	1–10	
Back pressure	5–95 bar	

More importantly, fuel type was found to have a large impact on the injection rate when multiple injections are employed. Figure 1 shows a comparison between the injection rates measured when mixtures of 25% *iso*-octane and 75% *n*-heptane (primary reference fuel-25, PRF25) and 58% *iso*-cetane and 42% *n*-cetane (diesel primary reference fuel-58, DPRF58) are employed. Both of these fuel blends approximate the combustion behavior of a certification diesel fuel well. For the single-injection case, the fuel type has very little effect on the injection rate. In this case, the use of PRF blends to examine the diesel fuel mixture formation process is justified. However, when multiple injections are used the quantity and rate shape of the main injection is significantly impacted by fuel type. Under these conditions, the amplitude of dynamic pressure waves, which is 33% higher for DPRF58, is thought to cause the considerable difference in the main injection quantity. This difference is seen for all pilot-main injection dwells investigated from 100-1,200 μs. It is clear that mixture formation studies must be conducted with a fuel having a density and bulk modulus (both of which impact the sound speed) similar to that of diesel fuel when multiple injection strategies are used.

As noted previously, we have also invested significant effort this fiscal year examining the evolution

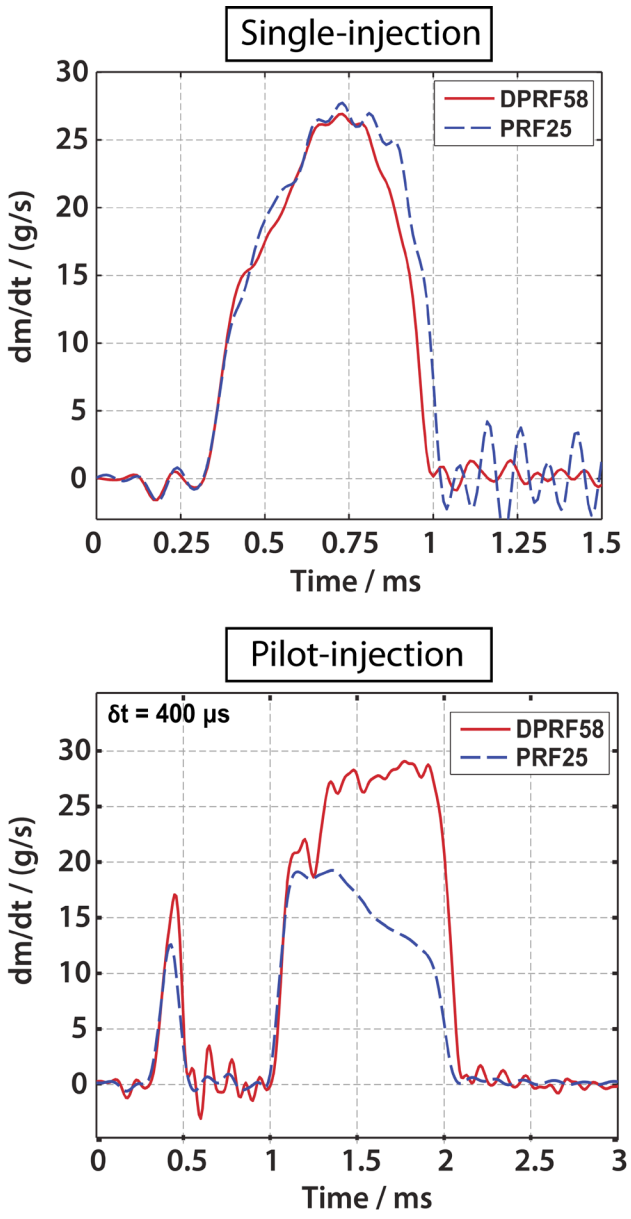

FIGURE 1. Comparison of the injection rate shape for two different fuels. The PRF25 fuel has physical properties typical of gasoline-like fuels, while the DPRF58 fuel has properties more typical of diesel fuels

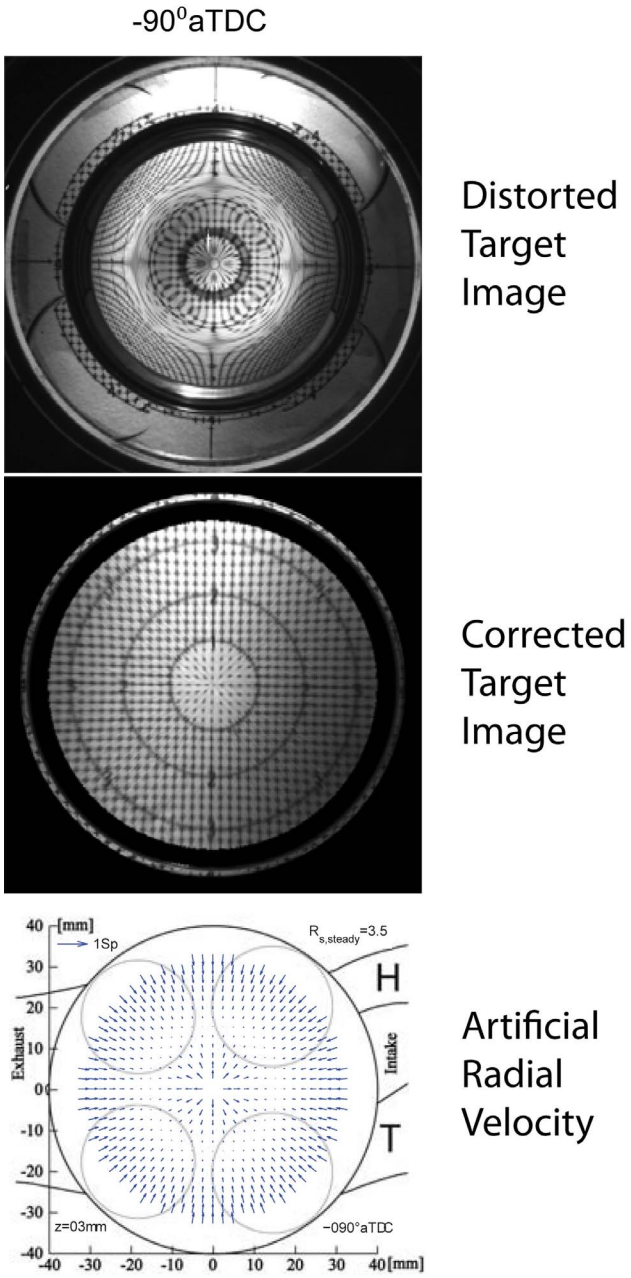

FIGURE 2. Examples of a distorted target image, a distortion corrected image, and the artificial radial velocity that results if the change in image distortion is neglected between the two PIV image pairs.

of the in-cylinder flow using particle image velocimetry (PIV) throughout the intake and compression stroke. Because the intake valve jets have been shown to interact strongly with the piston top [1,2], it is essential that a realistic piston geometry be used while obtaining these measurements. However, optical distortions induced by the piston geometry greatly complicate the measurements, especially when the piston is far from the measurement plane or when the piston is moving rapidly. Figure 2 shows the piston-induced distortion of an optical target at a measurement plane 3 mm below the head when the piston is at -90° after top-dead center (aTDC). Although the distortion is severe, the images can be corrected with sufficient resolution to allow the bulk flow structure to be determined. Due to the high piston speed at this crank angle, however, each of the two PIV images obtained must be distortion corrected with a different transformation, even if the time between images is only ~10 μs. Failure to do so leads to an artificial radial velocity that can be a significant fraction of the mean piston speed—as seen in the lower part of Figure 2. We

have also found that it can be advantageous to cross-correlate the two distorted PIV images, and to apply the transformation and artificial velocity correction to the resulting vector field, rather than to the raw images.

With careful attention to signal-to-noise ratio, we have succeeded in obtaining the evolution of the vector fields throughout the intake and compression stroke, as shown in Figure 3. Notice that throughout much of the intake stroke, the jets from the two intake ports create flows with opposing directions that prevent the development of a coherent swirling motion. By bottom-dead center (-180° aTDC), however, when the intake flows have lost much of their momentum, the flow is dominated by a single rotational structure. As the compression stroke proceeds, this structure becomes more uniform and begins to resemble a solid-body-like rotation, although with a swirl center (denoted by the red dots) that is not aligned with the cylinder centerline.

There are several global metrics that can be defined to quantify the magnitude and asymmetry of the swirl structure. The most common is the swirl ratio R_s, which is a measure of the total angular momentum and thus the magnitude of the swirl. Here we are interested more in the evolution of the flow asymmetry, which can be characterized by the location of the swirl center. The local "tilt" of the swirl axis, which can be determined from the swirl center location in multiple planes, is a second metric of interest. Figure 4 depicts the motion of the swirl center and the evolution of the swirl center tilt measured in the upper portion of the cylinder between planes 3 mm and 18 mm below the cylinder head. There is a clear clockwise motion of the swirl center between -150° and -60° aTDC, after which the swirl center remains close to the cylinder centerline. The lower portion of the figure shows that during this time, the tilt of the swirl structure initially decreases, but then increases beyond approximately -120 to -90° aTDC. Notice that a similar evolution is observed for both of the swirl ratios seen in Figure 4. A detailed comparison of these metrics of asymmetry with those predicted by numerical simulations is currently in progress.

Lastly, we make an important observation related to the generation and prediction of turbulence by flow asymmetries. Figure 5 shows the variation of the global flow turbulent kinetic energy computed within the cylinder using both the full engine geometry and a sector mesh equal to $1/7^{th}$ of the cylinder (as required by the 7-hole injector). Recall that such a sector mesh cannot capture aperiodic features on the piston top or head (such as valves or valve pockets), which can be expected to act as local sources of turbulence. More significantly, however, use of a sector mesh requires that the swirl center be located at the cylinder centerline, a requirement that is likely to significantly reduce the radial gradients

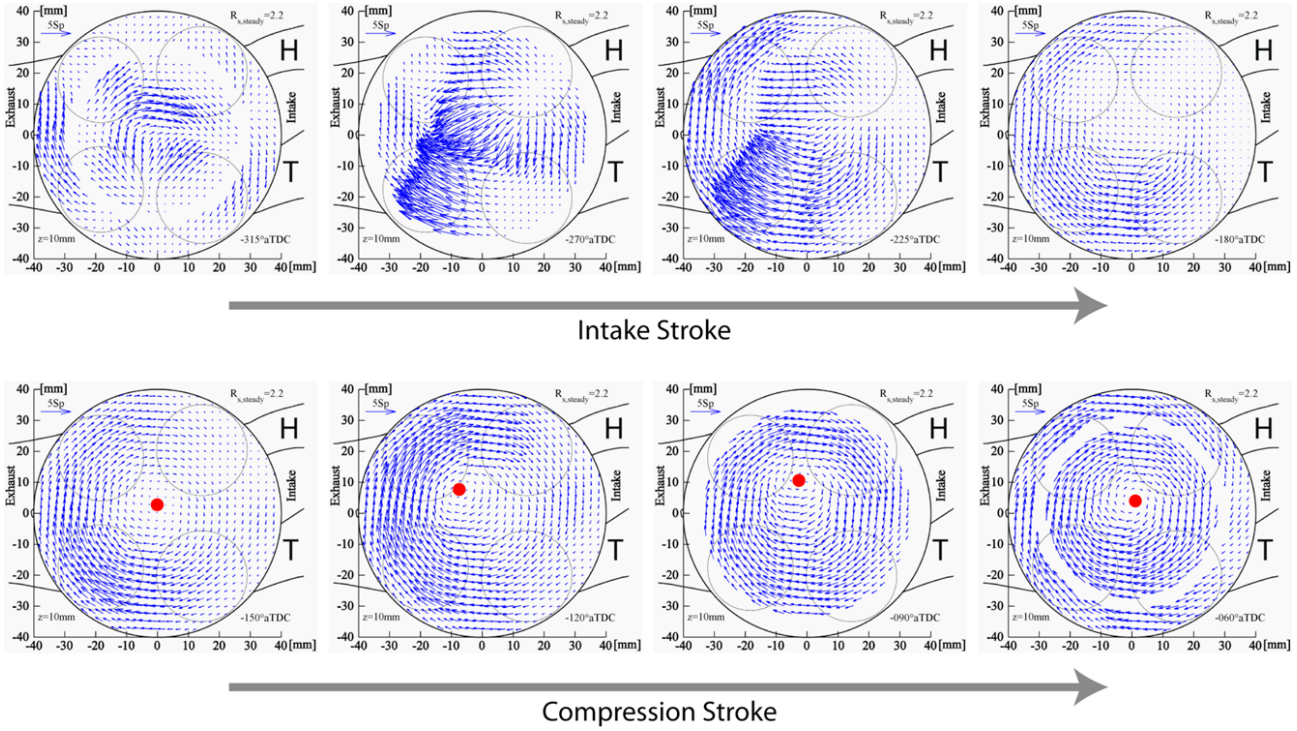

FIGURE 3. The evolution of the swirl flow in a plane 10 mm below the piston head for a swirl ratio R_s = 2.2. The red dots depict the location of the swirl center during compression.

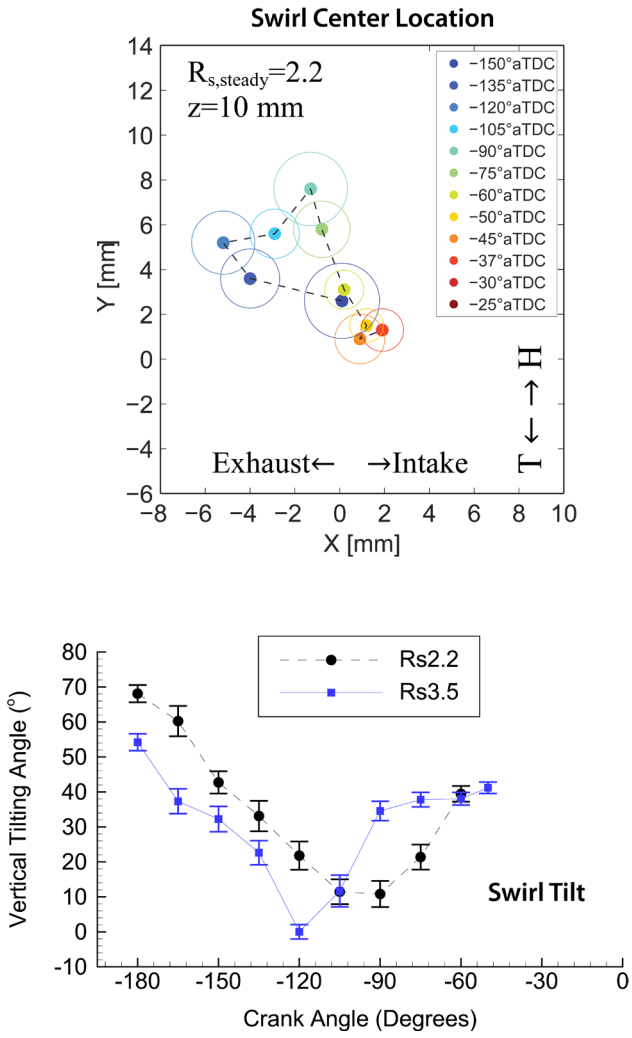

FIGURE 4. Motion of the swirl center and evolution of tilt of the swirl structure throughout the compression stroke.

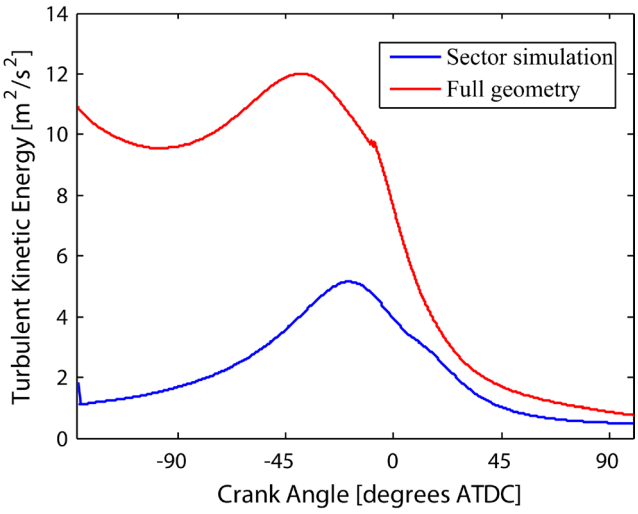

FIGURE 5. Comparison of the evolution of turbulent kinetic energy for the full engine mesh and a 1/7th sector mesh.

in the tangential velocity and to force the flow to more closely resemble solid-body rotation. Because these radial velocity gradients and departures from solid-body-like flow structures are the dominant sources of turbulence in swirling diesel engine flows [3], the two-fold reduction in near-TDC turbulence levels observed when the sector mesh is employed should not be surprising. If accurate prediction of flow turbulence is required, as well as accurate prediction of the turbulent diffusion of the injected fuel, the use of a full engine mesh is imperative.

CONCLUSIONS

- Accurate measurements of injection quantity and rate are essential for providing boundary conditions for numerical simulations, and for designating operating conditions applicable to multiple injection studies
- Fuel properties such as density and bulk modulus can significantly impact both total fuel quantity injected as well as injection rates
- Measurements of the evolution of in-cylinder flow structures can be obtained throughout the intake and compression stokes despite severe distortion caused by realistic geometry pistons
- Flow asymmetry is pronounced and evolves in a systematic manner. Establishing an ability to accurately simulate flow asymmetry (and minimize it by design) will be key to the continued improvement in efficiency and emissions of light-duty diesel engines
- Accurate prediction of flow turbulence in swirling diesel engine flows with significant amounts of flow asymmetry requires the use of a full engine mesh

REFERENCES

1. Voisine M, Thomas L, Borée J, and Rey P (2011) "Spatio-temporal structure and cycle to cycle variations of an in-cylinder tumbling flow." Exp. in Fluids 50: 1393-1407.

2. Hasse C, Sohm V, and Durst B (2010) "Numerical investigation of cyclic variations in gasoline engines using a hybrid URANS/LES modeling approach." Computers & Fluids 39: 25-48.

3. Miles PC (2009) "In-cylinder turbulent flow structure in direct-injection, swirl-supported diesel engines," Ch. 4 in Flow and Comb. in Reciprocating Engines, C. Arcoumanis and T. Kamimoto, eds. Springer-Verlag.

FY 2014 SELECTED PUBLICATIONS/ PRESENTATIONS

1. "A Comprehensive Modeling Study of In-Cylinder Fluid Flows in a High-Swirl, Light-Duty Optical Diesel Engine," Perini F, Miles PC, Reitz RD. *Computer & Fluids* **105:** 113–124, 2014.

2. "Investigations of Closely Coupled Pilot and Main Injections as a Means to Reduce Combustion Noise", Busch S, Zha K, Miles PC. *Thermo-and Fluid-Dynamic Processes in Diesel Engines: THIESEL2014,* September 9–12, 2014, Valencia, Spain. *Paper accepted for special issue of Int'l. J. of Engine Research.*

3. "Effects of In-Cylinder Non-Uniformities on Mixture Preparation in a Light-Duty Diesel Engine Operating a Light-Load Partially Premixed Combustion strategy", Perini F, Zha K, Sahoo D., Busch S., Miles PC, Reitz RD. *Thermo-and Fluid-Dynamic Processes in Diesel Engines: THIESEL2014,* September 9–12, 2014, Valencia, Spain.

4. "In-Cylinder Flow," Borée J and Miles PC. *Encyclopedia of Automotive Engineering, online © 2014 John Wiley & Sons, Ltd., DOI: 10.1002/9781118354179.auto119.*

5. "Diesel and Diesel Low-Temperature Combustion Systems," Andersson, Ö and Miles PC. *Encyclopedia of Automotive Engineering, online © 2014 John Wiley & Sons, Ltd., DOI: 10.1002/9781118354179.auto120.*

6. "Modeling the Ignitability of a Pilot Injection for a Diesel Primary Reference Fuel: Impact of Injection Pressure, Ambient Temperature and Injected Mass," Perini F, Sahoo D, Miles PC and Reitz RD. *SAE Int. J. Fuels Lubr.* 7 (1):48-64 (2014); also SAE Technical Paper 2014-01-1258, 2014.

7. "Fuel Concentration Imaging inside an Optically Accessible Diesel Engine using 1- Methylnaphthalene Planar Laser-Induced Fluorescence (PLIF)," Trost J, Zigan L, Leipertz A, Sahoo D, Miles PC. *International Journal of Engine Research, 1468087413515658, first published on February 7, 2014.*

8. "Characterization of Four Potential Laser-Induced Fluorescence Tracers for Diesel Engine Applications," Trost J, Zigan L, Leipertz A, Sahoo D, Miles PC. *Applied Optics,* 52 (33): 8001-8007, 2013.

9. "Pilot Injection Ignition Properties under Low-Temperature, Dilute In-Cylinder Conditions," Miles PC, Sahoo D, Busch S, Trost J, Leipertz A. *2013 Joint SAE/KSAE Intl. Powertrain, Fuels, and Lubricants Meeting*, SAE Technical Paper 2013-01-2531, *SAE Int J Engines.* 6: 1888-1907.

SPECIAL RECOGNITIONS

1. Invited speaker "In-Cylinder Measurements of Mixture Formation: Linkage to HC/CO Emissions from Light-Duty Diesel Engines," Miles PC. *13th Hyundai · Kia International Powertrain Conference*, Gyeongi, S. Korea, Oct. 24–25, 2013.

2. Invited seminar "Physical Fluid Dynamics in Reciprocating Engines," Miles PC. *John Deere.* Waterloo, IA, May 5, 2014.

II.2 Heavy-Duty Low-Temperature and Diesel Combustion and Heavy-Duty Combustion Modeling

Mark P.B. Musculus
Combustion Research Facility
Sandia National Laboratories
P.O. Box 969, MS9053
Livermore, CA 94551-0969

DOE Technology Development Manager
Leo Breton

Overall Objectives

This project includes diesel combustion research at Sandia National Laboratories (SNL) and combustion modeling at the University of Wisconsin (UW). The overall objectives are:

- Develop fundamental understanding of how in-cylinder controls can improve efficiency and reduce pollutant emissions of advanced low-temperature combustion (LTC) technologies
- Quantify the effects of fuel injection, mixing, and combustion processes on thermodynamic losses and pollutant emission formation
- Improve computer modeling capabilities to accurately simulate these processes

Fiscal Year (FY) 2014 Objectives

The objectives for FY 2014 are all tied to fuel injection effects on in-cylinder processes affecting fuel efficiency and pollutant formation.

- Quantify the spatial and temporal evolution of in-cylinder soot precursors under LTC conditions (SNL)
- Use high-speed imaging to generate a taxonomy of fuel injector dribble phenomena that affect fuel efficiency and unburned hydrocarbon emissions (SNL)
- Analyze diesel-jet ambient-gas velocimetry data to quantify how the end-of-injection ramp-down transient affects entrainment and mixing (SNL)
- Begin exploration of piston-bowl geometry effects on multiple injections (SNL)
- Install and use Engine Combustion Network (ECN) "spray-B" fuel injector in optical engine (SNL)
- Develop new heavy-duty high-precision fuel injection system for the optical engine (SNL)
- Analyze in-cylinder soot evolution predicted by multi-dimensional models to augment experimental insight into the processes affecting fuel efficiency and pollutant emissions with multiple injections (UW)

FY 2014 Accomplishments

- Tracked the spatial and temporal soot precursor evolution, which aided LTC computer model validation for codes used by industry (Cummins, Convergent Science)
- Identified the key features and dependencies of injector dribble throughout the engine cycle, which point to areas for further injector development
- Experimentally verified the existence and magnitude of the end-of-injection entrainment wave that was previously predicted by computer models of various complexities, which helps to justify further development of injection rate-shaping to tailor mixing
- Completed design and started fabrication of contoured bowl for multiple injections coupling with bowl shape which will allow future work with realistic in-cylinder geometries
- Implemented Engine Combustion Network (ECN) "spray-B" fuel injector in optical engine and gathered fuel dribble and combustion data for ECN database which expands the database to more engine-relevant geometry
- Started cylinder head design/modifications for installation of Delphi DFI-21 heavy-duty injector which will allow precision multiple injections at higher loads than previously achievable
- Computer models predict that a prime mechanism of post-injection soot-reduction without a fuel economy penalty is the increased rate of consumption of fuel, which reduces soot precursor concentrations

Future Directions

- Continue building a conceptual model understanding of multiple injection processes for both conventional diesel and LTC
  - Multi-injection schedules (pilot, post, split) deployed by industry
  - Use optical geometry more similar to metal engines (expense limit)

  - Compare with metal engine data where possible (industry partners)
  - Identify mechanisms and critical requirements (injector rate-shaping, dwell, duration, etc.) to improve emissions and efficiency
- Determine how combustion design affects heat transfer and efficiency
  - Measure spatial and temporal evolution of heat transfer across range of combustion modes; correlate to progression of in-cylinder combustion processes
- Continue to explore and upgrade fuel-injection technologies
  - Injection rate-shaping is very important for performance, and higher load than our current injector capability is of interest as well

INTRODUCTION

Regulatory drivers and market demands for lower pollutant emissions, lower carbon dioxide emissions, and lower fuel consumption motivate the development of clean and fuel-efficient engine operating strategies. Most current production engines use a combination of both in-cylinder and exhaust aftertreatment strategies to achieve these goals. One class of in-cylinder strategies of current interest is multiple fuel injections.

With multiple fuel injections, processes that occur after the ends of individual injections are of critical importance due to the interactions between the injections. Mixing processes occurring after the end of injection can affect the mixtures where soot is formed. Injector dribble, which is unscheduled fuel emerging from the injector after the end of injection, can affect fuel efficiency and unburned hydrocarbon emissions. The coupling of multiple injections with the in-cylinder geometry can also be important. In addition to experimental studies of these factors, computer modeling is becoming more important both for engine design as well as through analysis of the computer predictions to augment understanding gained from experiments.

APPROACH

This project uses an optically-accessible, heavy-duty, direct-injection diesel engine (Figure 1). A large window in the piston crown provides primary imaging access to the piston bowl, and other windows at the cylinder wall provide cross-optical access for laser diagnostics or imaging.

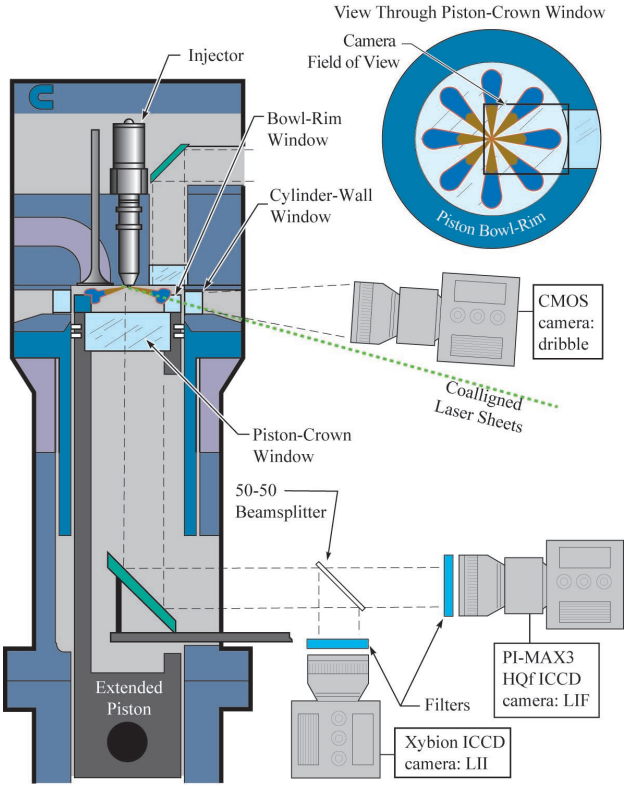

CMOS - complementary metal-oxide semiconductor; ICCD - intensified charge-coupled device

FIGURE 1. Schematic diagram of the optically accessible heavy-duty direct-injection diesel engine and optical setup.

The experiments use several of in-cylinder optical measurements. For illustrative purposes, Figure 1 shows a combination of imaging setups, with elements of different diagnostics superimposed on the same schematic, i.e., all elements in Figure 1 are not employed simultaneously. To image soot and its precursors, a laser beam in one of three wavelengths, 266, 532, or 633 nm, is formed into a sheet and co-aligned with a second laser sheet at 1,064 nm. The shorter-wavelength beam excites planar laser-induced fluorescence (PLIF) of polycyclic aromatic hydrocarbon (PAH) soot precursors of different size classes, while the 1,064-nm beam yields a simultaneous measurement of planar laser-induced incandescence (PLII) of soot. Two intensified cameras record the two signals using a beam splitter and appropriate spectral filters. For the dribble experiments, a pulsed light-emitting diode (not shown) illuminates the liquid sprays through one of the cylinder-wall windows, and two complementary metal oxide semiconductor cameras record the liquid-scattering signal simultaneously through a cylinder wall window and through the piston crown window.

RESULTS

Figure 2 shows three series of composite false-color representative images of PAH PLIF (green) and soot PLII (red) from 1,064-nm excitation over a series of crank angles at each of three PAH PLIF laser wavelengths: 266 nm (top), 532 nm (middle), and 633 nm (bottom). The images show a partial view of the combustion chamber through the piston crown window (see top right of Figure 1), with the injector on the left (white dot) and the piston bowl-wall on the right (curved dashed line). The boundaries of the laser sheets are indicated by straight dashed lines, and the crank angle is indicated in the top right. The operating condition has a compressed gas density of 16.6 kg/m^3 and temperature of 975 K at top-dead center (TDC), with an intake oxygen concentration of 10.5%, which is equivalent to operating with approximately 60% exhaust gas recirculation in a continuously fired engine. A Cummins XPI injector with eight equally spaced 0.140-mm orifices injects neat n-heptane fuel from 355 crank angle degrees (CAD, with TDC of compression at 360 CAD) to 383 CAD at a rail pressure of 1,000 bar to achieve a load of approximately 6-bar gross indicated mean effective pressure (gIMEP) at 1,200 crankshaft rotations per minute (RPM).

In the top series of images, the very first indication of PAH PLIF at 266 nm (green) first appears near the bowl rim at 368 CAD. Thereafter, the 266-nm PAH PLIF appears in other locations and grows spatially. In the other two series, PAH PLIF does not appear until 370 CAD (532-nm PAH PLIF, middle) and 371 CAD (633 nm PAH PLIF, bottom). In all three series, soot PLII (red) appears after the PAH-PLIF, in small bright pockets on the right side of the images, starting from 372-374 CAD (note some background red-colored interference, especially on the left side of images, is not indicative of soot).

These images together show the temporal progression of PAH-PLIF with increasing laser wavelength, which is consistent with increasing PAH precursor molecule size. Laser light should excite fluorescence in PAH with one to two rings at 266 nm, more than 6 rings at 532 nm, and even larger at 633 nm [1,2]. Hence, the images in Figure 2 provide semi-quantitative information about the spatial and temporal location of PAH of various size ranges, as well as the spatial and temporal location of the conversion of PAH into soot particles. Such data are useful to industry for validating chemical reaction mechanisms for the prediction of soot emissions from practical engines.

Shown in Figure 3 are three pairs of liquid-fuel elastic-scattering images at three different crank angles during and after a fuel injection event. Each image shows two simultaneous views, one from below (top) and one from the side (bottom), using both upper and lower cameras positions shown in Figure 1. The scene is illuminated with a pulsed high-power light-emitting

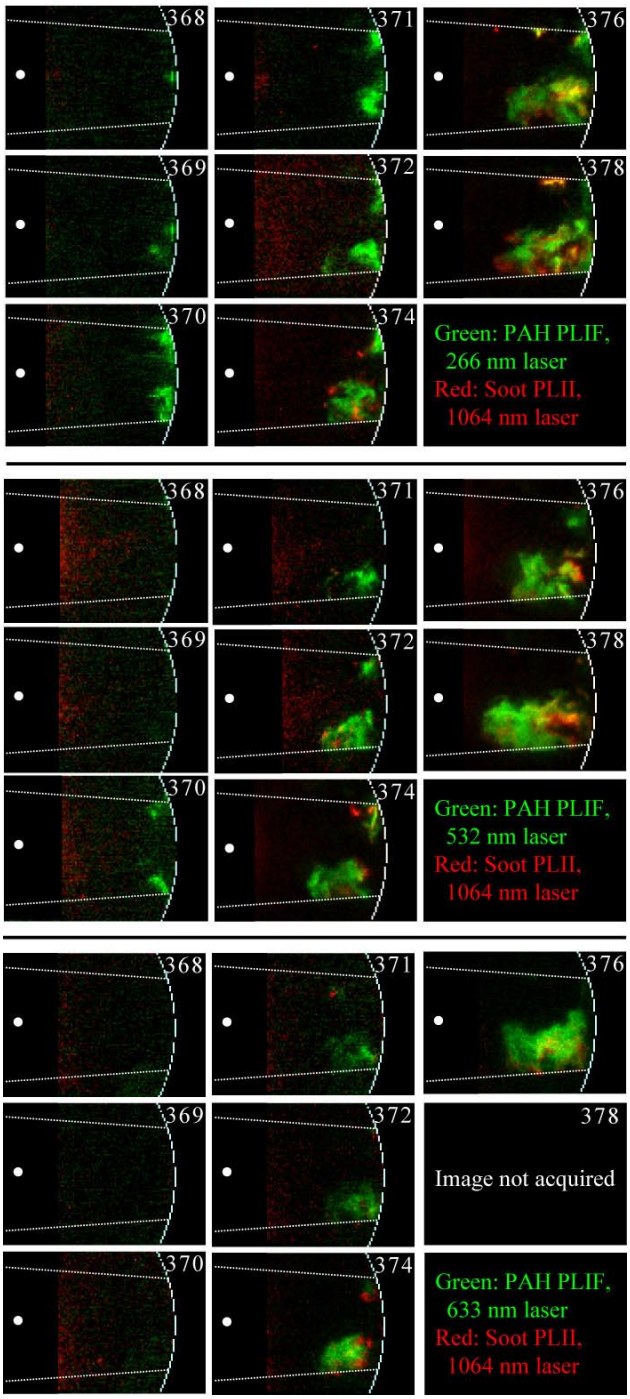

FIGURE 2. Composite false-color representative images of PAH PLIF (green) and soot PLII (red). Crank angle is in upper right corner, injector is on the left (white dot), piston bowl-wall is on the right (curved dashed line), and laser-sheet boundaries are straight dashed lines. TDC conditions are 16.6 kg/m^3 and 975 K with 10.5% O_2. Cummins XPI injector with eight equally spaced 0.140-mm orifices, neat n-heptane fuel injected from 355 to 383 CAD at a 1,000 bar rail pressure, 6-bar gIMEP at 1,200 RPM.

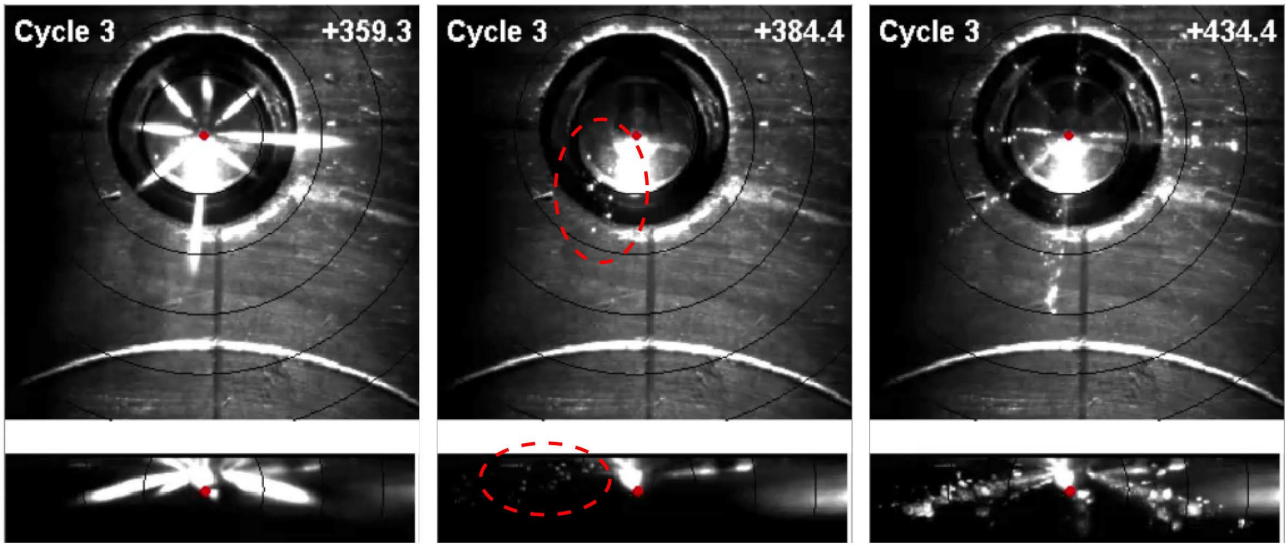

FIGURE 3. Simultaneous pairs of elastic scattering images viewed from below (top) and from the side (bottom), n-heptane fuel under non-combusting conditions (100% nitrogen intake). Crank angle is indicated in top right of images pairs.

diode, and the images show scattering from both in-cylinder features (injector and bore) and liquid fuel sprays/droplets. The injector is operated with n-heptane under non-combusting conditions (100% nitrogen intake).

The leftmost image pair at 359.3 CAD provides a reference during the intended fuel injection event. The sprays show some variation in liquid length, which is not uncommon with low viscosity n-heptane fuel. Shortly after the end of injection, the image at 384.4 CAD shows several droplets that have dribbled out of the injector, circled in the red dashed line. The dynamic movies available online [3] clearly show that these dribble droplets are not residual from the main spray event, but that rather they emerge from the injector after the end of the intended injection. Much later in the cycle at 434.4 CAD, when in-cylinder pressures drop below 20 bar, a second dribble event occurs. The second event is even more dramatic than the first, resembling a second injection. Other imaging [4] shows that similar behavior occurs with all injector variations tested, with each of multiple injections, under combusting conditions, and with other fuels including certification diesel, though the second dribble event is much more dramatic with n-heptane fuel than with diesel fuel. Such dribble would increase both fuel consumption and pollutant emissions. These data provide the first taxonomy of imaged dribble phenomena, which will be useful for developing further understanding and mitigation strategies.

In addition to dribble after the end of injection, changes in jet mixing behavior resulting from the end-of-injection transient can also affect fuel consumption and pollutant emissions. Previous work [5] has shown the rapid formation of overly lean fuel mixtures after the end of injection, which can contribute to incomplete combustion and unburned hydrocarbon emissions. Computer models of the transient jet predict that an increase in entrainment after the end of injection, termed an "entrainment wave," is responsible for the rapid formation of fuel-lean regions, but until now, the fluid mechanics had not been experimentally confirmed. As part of the data exchange associated with the ECN [6], ambient flow velocimetry during a diesel injection transient became available, and these data were analyzed for direct evidence of the entrainment wave.

The image on the top of Figure 4 shows one snapshot of the ambient flow-field surrounding a diesel jet, which is represented by the white trapezoid. The color contours indicated the magnitude of the radial velocity into the jet, from which entrainment can be quantified. The plot in the bottom of Figure 4 shows the measured (solid lines) and one-dimensional model-predicted (dashed) transient entrainment coefficient (C_e) at three instants relative to the start of the 4,100-microsecond injection event. The horizontal dashed lines show the classic steady-state entrainment coefficient near 0.32, which was confirmed by experiments during the steady part of the injection. After the end of injection, both the predictions and measurements show a propagating wave of temporarily increased entrainment. The simple one-dimensional model does not match the experimental measurements exactly, but they show the same trend and the same integral behavior (area under the curves is similar). This experimental confirmation and quantification of the entrainment wave effect helps to validate the model predictions that in-cylinder mixing can be tailored by controlling the injection rate transient and/or by using

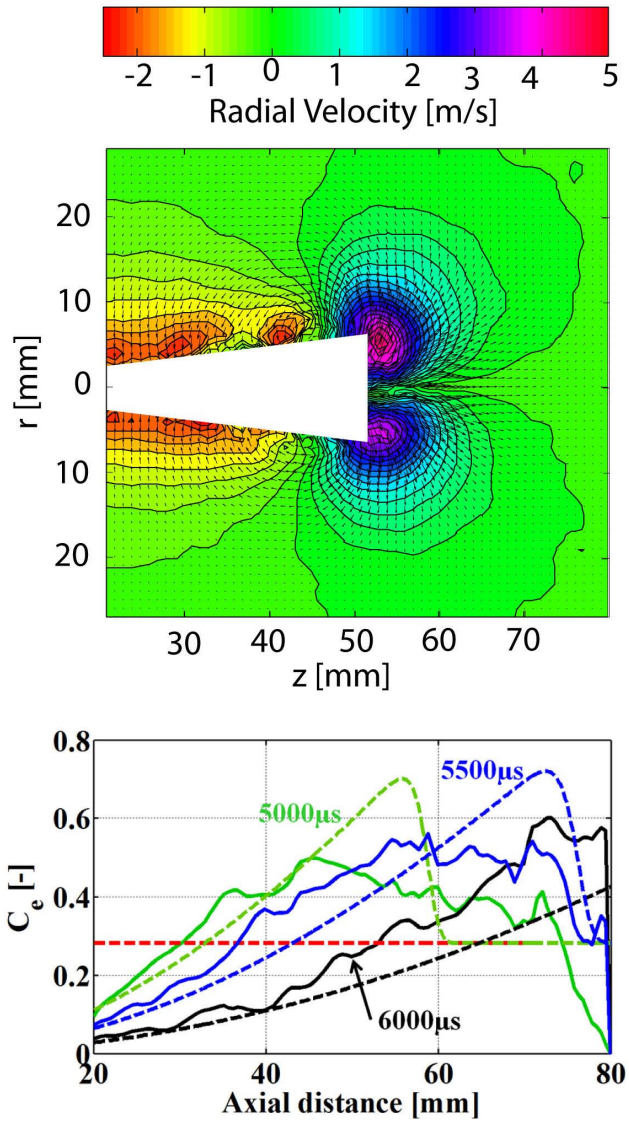

FIGURE 4. Top: ambient velocity field vectors (arrows) surrounding a diesel jet (white trapezoid). Color contours indicate radial velocity magnitude. Bottom: measured (solid lines) and predicted (dashed) transient entrainment coefficient (C_e), injection ends at 4,100 microseconds.

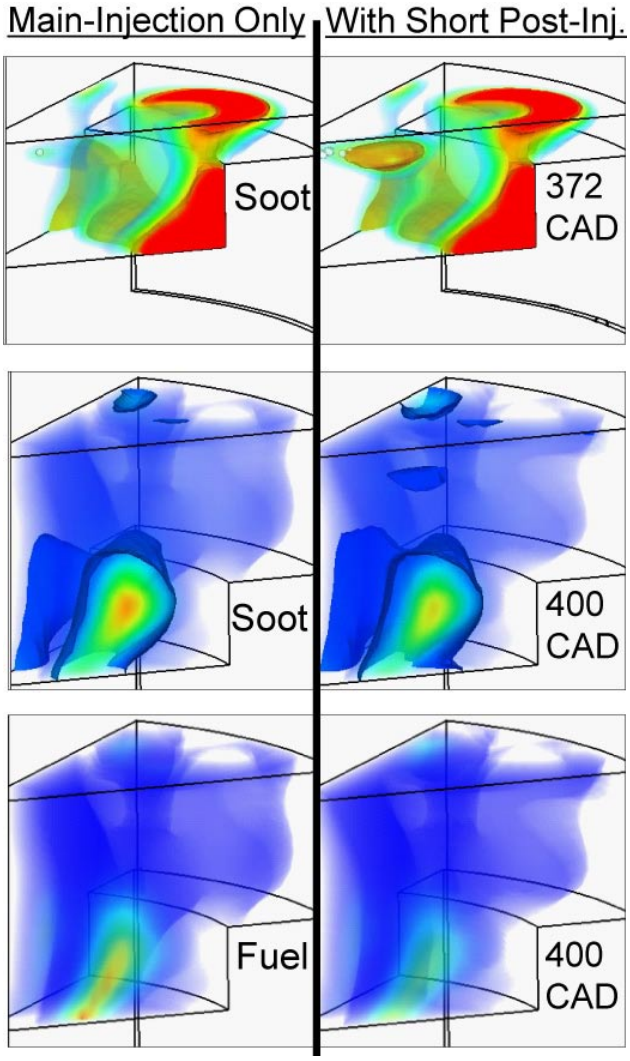

FIGURE 5. Sector renderings of three-dimensional simulations of in-cylinder soot and fuel concentration with (right) and without (left) a post injection.

multiple injections, which also motivates engine/injector development in this area.

In addition to experiments and one-dimensional modeling of in-cylinder processes related to multiple injections, full three-dimensional computer simulations of previous multiple-injection experiments are also analyzed to augment understanding of in-cylinder processes gleaned from experiments. Previous experiments [7] showed that post-injections could reduce exhaust soot, and more importantly that the post-injection conclusively reduced soot originating from the main injection. The potential explanations, which include displacement, oxidation, or disruption of soot formation, are not revealed by the experiments. The new modeling work captures the decrease in engine-out soot with a post-injection, and with analysis of the predicted in-cylinder distributions, the model helps to explain how post-injections can affect main-injection soot.

Figure 5 shows visualizations of the model-predicted in-cylinder soot and fuel in a sector of the combustion chamber centered on one of the fuel jets. The left side is for a predicted condition with main injection only, and the right side is with a short post-injection added. The top row, at 372 CAD, shows the soot field generated by the main injection (left), as well as some additional soot created by the post injection (right). Later in the cycle, at 400 CAD (middle row), the soot concentration is somewhat lower on the right than on the left (less red color). Analysis of the magnitudes of the soot formation

and oxidation terms in the model shows that formation is affected more than oxidation through reduction of the fuel concentration by action of the post injection. The bottom row shows lower fuel concentration, which is the ultimate source for the soot, and the model predicts that the fuel concentration is reduced by faster combustion induced by the post-injection. Hence, the simulations help by augmenting insight gained from experiments, predicting that the soot reduction with post-injections is mostly due to reduced soot formation rather than increased soot oxidation [8].

Finally, three notable engine hardware upgrades were also initiated in FY 2014. The first two are modifications to the cylinder head and fuel system to allow operation with two new injectors. The Bosch "spray-B" injector will allow acquisition of engine data to contribute to the ECN [6], and a Delphi DFI-21 heavy-duty injector will allow higher load operation with precision delivery of multiple injections. The third modification is a contoured optical piston for exploring the effects combustion chamber geometry on in-cylinder processes with multiple injections. The existing optical-piston has a flat-bottomed piston bowl that is sufficient for general fundamental studies, but it does not allow examination of the spray/wall coupling with realistic geometries. The first contoured optical piston design, a rendering of which is in Figure 6, will allow imaging through the large contoured piston crown window as well as cross-optical access for laser diagnostics through a small contoured piston bowl-rim window. All elements have been designed and fabricated, and will be assembled into the extended piston and used for future experiments.

CONCLUSIONS

The recent research efforts described in this report provide improved understanding of in-cylinder processes involved with post-injections required by industry to build cleaner, more efficient, heavy-duty engines. Specific conclusions include:

- Measurements of the spatial and temporal soot precursor evolution aided LTC computer model validation for codes used by industry (Cummins, Convergent Science)
- Key features and dependencies of injector dribble throughout the engine cycle point to areas for further injector development
- Experimental verification of the existence and magnitude of the end-of-injection entrainment wave helps to justify further development of injection rate-shaping to tailor mixing

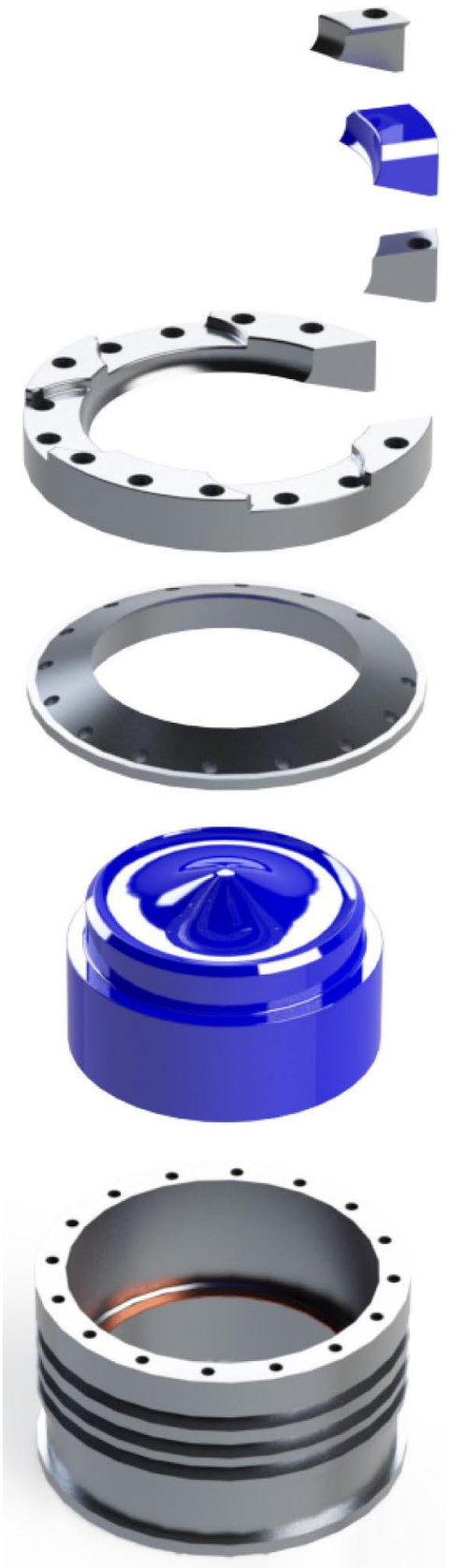

FIGURE 6. Renderings of the contoured optical piston crown and bowl-rim assembly.

- Contoured optical piston bowl will allow future work on multiple injections with realistic in-cylinder geometries
- ECN "spary-B" fuel dribble and combustion data expands the ECN database to more engine-relevant geometry
- Delphi DFI-21 heavy-duty injector capability will allow precision multiple injections at higher loads than previously achievable
- Analysis of computer models predictions augments experimental data, providing a soot formation disruption explanation for reduced exhaust soot with post-injections

REFERENCES

1. Berlman IB, Handbook Of Fluorescence Spectra of Aromatic Molecules, Academic Press, New York (1971).

2. Clar E and Schoental R, Polycyclic Hydrocarbons, Academic Press, New York (1964).

3. http://www.sandia.gov/ecn/pub-links/cdl/ThieselMovies/Fig6-n-Heptane-EnsembleAverage-Processed.mp4

4. http://www.sandia.gov/ecn/pub-links/cdl/Thiesel2014.php, "Figure 10" links

5. FY2007 Progress Report for Advanced Combustion Engine Technologies, Department of Energy, Washington D.C. http://www1.eere.energy.gov/vehiclesandfuels/pdfs/adv_engine_2007/2007_advanced_engine.pdf (2007)

6. Engine Combustion Network, http://www.sandia.gov/ecn/

7. FY2013 Progress Report for Advanced Combustion Engine Research and Development, Department of Energy, Washington, D.C. http://energy.gov/sites/prod/files/2014/04/f14/fy13advancedcombustionprogressreport.pdf (2013)

8. Hessel RP, Reitz RD, Musculus MPB, O'Connor J and Flowers DL "A CFD Study of Post Injection Influences on Soot Formation and Oxidation Under Diesel-Like Operating Conditions" SAE Technical Paper 2014-01-1256, SAE Int. J. Engines 7:694-713 (2014).

FY 2014 PUBLICATIONS/PRESENTATIONS

1. "Measuring Transient Entrainment Rates of a Confined Vaporizing Diesel Jet," W.E. Eagle, M.P.B. Musculus, L-M.C. Malbec, G. Bruneaux, ILASS Americas 26th Annual Conference on Liquid Atomization and Spray Systems, May 2014.

2. "A CFD Study of Post Injection Influences on Soot Formation and Oxidation under Diesel-like Operating Conditions," R.P. Hessel, R.D. Reitz, M.P.B. Musculus, J.A. O'Connor, D.L. Flowers, SAE Technical Paper 2014-01-1256, SAE Journal of Engines 7(2):694-713, April 2014.

3. "In-Cylinder Mechanisms of Soot Reduction by Close-Coupled Post-Injections as Revealed by Imaging of Soot Luminosity and Planar Laser-Induced Soot Incandescence in a Heavy-Duty Diesel Engine," J.A. O'Connor and M.P.B. Musculus, SAE Technical Paper 2014-01-1255, SAE Int. J. Engines 7(2):673-693, April 2014.

4. "Effect of Load on Close-Coupled Post-Injection Efficacy for Soot Reduction in an Optical, Heavy-Duty Diesel Research Engine," J.A. O'Connor and M.P.B. Musculus, paper ICEF2013-19037, ASME Internal Combustion Engine Fall Technical Conference, October 2013.

5. Encyclopedia article: "Experimental Facilities and Measurements – Fundamentals," M.P.B. Musculus, L.M. Pickett, S.A. Kaiser, to appear in "Encyclopedia of Automotive Engineering," accepted June 2013.

6. "Post Injections for Soot Reduction in Diesel Engines: A Review of Current Understanding," J. A. O'Connor and M.P.B. Musculus, SAE Technical Paper 2013-01-0917, SAE Int. J. Engines 6:400-4219, May 2013.

7. "Optical Investigation of the Reduction of Unburned Hydrocarbons Using Close-Coupled Post Injections at LTC Conditions in a Heavy-Duty Diesel Engine," J.A. O'Connor and M.P.B. Musculus, SAE Technical Paper 2013-01-0910, SAE Int. J. Engines 6:379-399, May 2013.

8. "Optical Investigation of Multiple Injections for Unburned Hydrocarbon Emissions Reduction with Low-Temperature Combustion in a Heavy-Duty Diesel Engine," J.A. O'Connor and M.P.B. Musculus, Paper # 0701IC-0033, 8th US National Meeting of the Combustion Institute, Park City, UT, May 2013.

9. "Effects of EGR and Load on Soot in a Heavy-Duty Optical Diesel Engine with Close-Coupled Post-Injections for High Efficiency Combustion Phasing," J.A. O'Connor and M.P.B. Musculus, Int. J. Eng. Res. 15(4):421-443, 2014.

10. "Sandia Maps Multiple Paths to Cleaner, Low-Temp Diesels," SAE Truck and Bus Engineering Online, http://www.sae.org/mags/TBE/12411, September 2013.

11. Invited presentation: "Thinking into the Box: Solving Engineering Problems Using Lasers and Cameras in Optical Engines," M.P.B. Musculus, Institute for Sustainable Energy seminar series, University of Alabama, Tuscaloosa, Alabama, April 2013.

12. Invited presentation: "Optical Diagnostics for Diesel Engine Combustion and Recent Post-Injection Optical Engine Research," M.P.B. Musculus, presentation to technical staff at John Deere, Waterloo, IA, July 2013.

13. Invited presentation: "A Conceptual Model for Low-Temperature Diesel Combustion," M.P.B. Musculus, SAE 11th International Conference on Engines & Vehicles, Capri, Italy, September 2013.

II.3 Spray Combustion Cross-Cut Engine Research

Lyle M. Pickett
Sandia National Laboratories
P.O. Box 969, MS 9053
Livermore, CA 94551-9053

DOE Technology Development Manager
Leo Breton

Overall Objectives

Facilitate improvement of engine spray combustion modeling, accelerating the development of cleaner, more efficient engines.

Fiscal Year (FY) 2014 Objectives

- Lead a multi-institution, international, research effort on engine spray combustion called the Engine Combustion Network (ECN), with focus on diesel and gasoline sprays.
- Provide indicators for low- and high-temperature ignition to aid deficiencies in ignition prediction in current modeling.
- Quantify the temporal evolution of fuel jet soot and radiation with impact on engine efficiency.

FY 2014 Accomplishments

- Organized ECN3, the third workshop of the Engine Combustion Network, with over 150 Web and in-person attendees focused on experimental and modeling advancement. Led the year-long experimental/modeling exchange on targets to identify the state of art and in-spray combustion modeling and remedying known weaknesses.
- Quantified the formaldehyde formation on plane with simultaneous high-speed schlieren along a line of sight to reveal the ignition location and timing for diesel sprays.
- Developed quantitative soot and soot radiation datasets for diesel Spray A and variants.

Future Directions

- Characterize multi-hole sprays compared to axial-hole sprays.
- Quantify gasoline spray mixing over a range of conditions extending from flash boiling to late injection.
- Evaluate internal flows within transparent injectors, transitioning to near-field mixing and dispersion at the exit of the nozzle.

INTRODUCTION

All future high-efficiency engines will have fuel directly sprayed into the engine cylinder. Engine developers agree that a major barrier to the rapid development and design of these high-efficiency, clean engines is the lack of accurate fuel spray computational fluid dynamics (CFD) models. The spray injection process largely determines the fuel-air mixture processes in the engine, which subsequently drives combustion and emissions in both direct-injection gasoline and diesel systems. More predictive spray combustion models will enable rapid design and optimization of future high-efficiency engines, providing more affordable vehicles and also saving fuel.

APPROACH

To address this barrier, we have established a multi-institution collaboration, called the ECN, to both improve spray understanding and develop predictive spray models. By providing highly leveraged, quantitative datasets (made available online [1]) CFD models may be evaluated more critically and in a manner that has not happened to date. Productive CFD evaluation requires new experimental data for the spray and the relevant boundary conditions, but it also includes a working methodology to evaluate the capabilities of current modeling practices. This year we organized the third ECN workshop, where workshop organizers interacted for the entire year to gather experimental and modeling results at target conditions to allow a side-by-side comparison and expert review of the current state of the art for diagnostics and engine modeling.

Experimental research in our facility this year has focused on critical topics in both diesel and gasoline spray combustion. For brevity, we will highlight a few of the key areas with regards to diesel combustion, but a more complete summary of this year's work is found in the ECN3 proceedings at [1]. The ignition characteristics, flame stabilization, and soot production are critical factors the design and operation of compression ignition engines, but they are known weaknesses in current CFD modeling efforts seeking to find design optima for the engine [2]. We developed a series of high-speed

diagnostics in a constant-volume combustion chamber to provide needed details of the ignition and soot formation processes, all at the ECN Spray A conditions [1]. We applied simultaneous schlieren and formaldehyde (CH_2O) planar laser-induced fluorescence (PLIF) imaging to investigate the low- and high-temperature auto-ignition events. High-speed (150 kHz) schlieren imaging allowed visualization of the temporal progression of the fuel vapor penetration as well as the low- and high-temperature ignition events, while formaldehyde fluorescence was induced by a pulsed laser sheet at a select time during the same injection to provide information about the planar distribution of ignition. High-speed, multi-color extinction imaging was applied to quantify the transient soot distribution.

RESULTS

Previous research has shown that a "softening" of the schlieren effect begins prior to the onset of high-temperature ignition. To confirm that the softening of the schlieren effect is associated with low-temperature reactions, schlieren imaging was performed under both non-reacting and reacting conditions as shown in Figure 1.

The images at the left represent the schlieren of cold fuel vapor in refractive index contrast to the hot ambient without any reaction. Note that the appearance is similar to the reacting case at the right until approximately 300 µs after start of injection (ASOI), at which point the reacting case begins to show a "softening" effect near the head of the spray. More specifically, at the previous timing (260 µs ASOI), the lower portion of the "reacting" spray head is characterized by a dark semi-circular region. In the following frame (280 µs ASOI), this same structure is visible, however, the region appears lighter. This is a consequence of reduced gradients in the local refractive index, which result from a rise in the local temperature to values closer to the temperature of the ambient gases. This temperature rise can be attributed to heat release from the low-temperature auto-ignition reactions. At later timings (380 µs), high-temperature ignition has ensued in the reacting case, as confirmed by the associated pressure trace and high-speed chemiluminescence imaging under identical conditions, and the axial penetration boundary of the reactive species defined by the flame is consistent once again with the non-reacting vapor penetration. The bottom right panel at 680 µs shows that the quasi-steady lift-off length has been established in the reacting spray and can be identified by the abrupt radial expansion of the schlieren boundary near 17 mm. This radial expansion of the high-temperature products near the lift-off length has been emphasized by overlaying the non-reacting vapor boundary at this same timing as a white border.

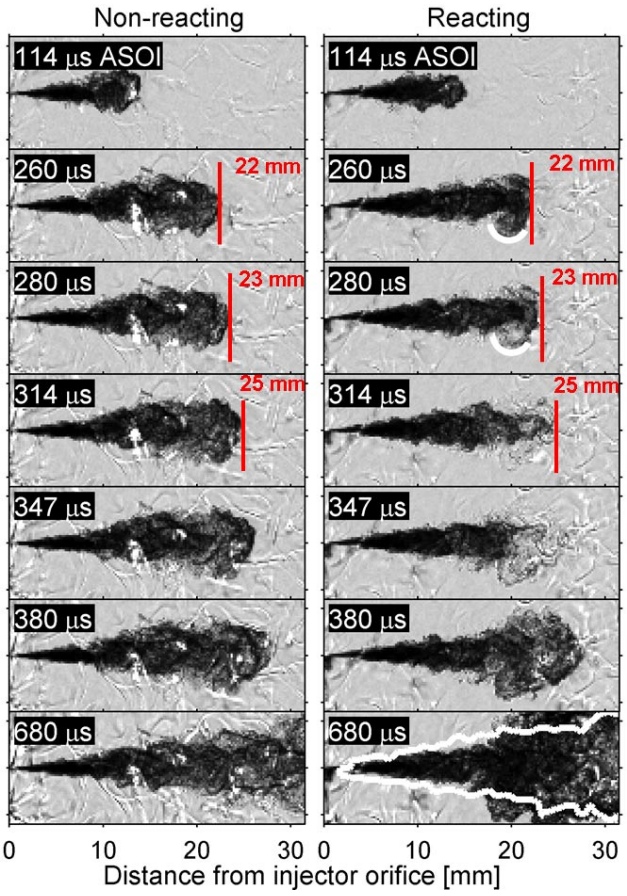

FIGURE 1. Time sequence of schlieren images resolving vapor penetration (for the non-reacting spray, left panels) and the low- and high-temperature ignition events (for the reacting spray, right panels). Spray A conditions [1].

The images in Figure 2 represent a time sequence of paired formaldehyde PLIF and schlieren images, resolving the low- and high-temperature ignition events for the very same injection. False color images of the formaldehyde PLIF are presented in the left column. High-speed movies and LIF images acquired are also available on the ECN website [3]. The general conclusion from the analysis of the planar images in comparison to the schlieren at the same timing is that the schlieren imaging softening of refractive index gradients is indeed related to low-temperature heat release. Pockets of formaldehyde PLIF are found in the same regions indicated by the schlieren but the PLIF is more sensitive to the earliest appearance, highlighting the advantage of the planar technique. The transition to high-temperature ignition corresponds to a reappearance of the schlieren border at the edge of the jet and a decrease in formaldehyde in the same region. Overall, the experiments show that valuable information about low- and high-temperature ignition location and timing can be captured with the combined diagnostic, providing much needed details for CFD model validation.

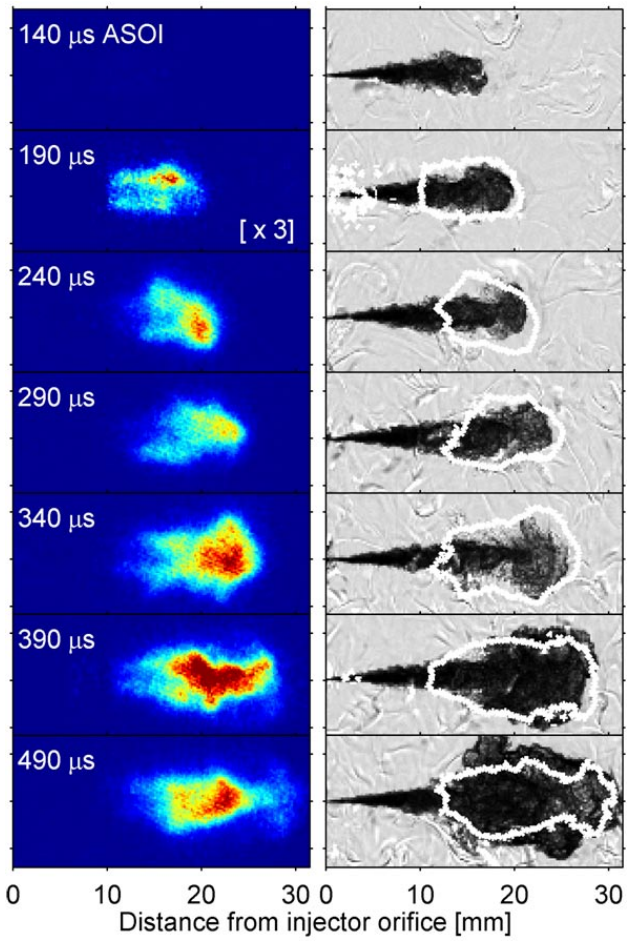

FIGURE 2. Time sequence of formaldehyde PLIF (left panels) and schlieren images (right panels) for Spray A.

The ignition sequences precede the formation of soot, which also undergoes transients associated with jet development and soot precursor growth. We developed a high-speed extinction imaging diagnostic to quantify the location and level of soot formation and oxidation. A summary of the total soot mass measured in the jet is given in Figure 3. Soot forms after high-temperature ignition, and the timing of soot onset given in the legend is compared between IFP Energies nouvelles experiments (with shorter injection duration) using laser-induced incandescence and Sandia using extinction imaging. The maximum total soot mass is attained shortly before 2 ms, well after the start of combustion. Analysis of the soot spatial distribution shows a large amount of soot in the head of the jet, which eventually dissipates when the head of the jet is oxidized and a quasi-steady distribution is established. Comparison to CFD models used by ECN participants shows that they do not capture the transient dynamic with more soot found in the head of the jet [1].

Finally, we show measurements of the spatially resolved total soot radiation emitted from fuel jets at the same conditions [4] in Figure 4. Radiation heat transfer affects engine efficiency, and it also creates temperature redistribution affecting both soot and nitrogen oxide formation. The figure shows the evolution of soot radiation with ambient temperature. At low ambient temperature, there is little soot and the spectrum is dominated by chemiluminescence. But as ambient temperature increases, there is progressively more soot radiation, as shown at the bottom panel. Currently most CFD models do not address radiation heat transfer and its impacts on combustion performance.

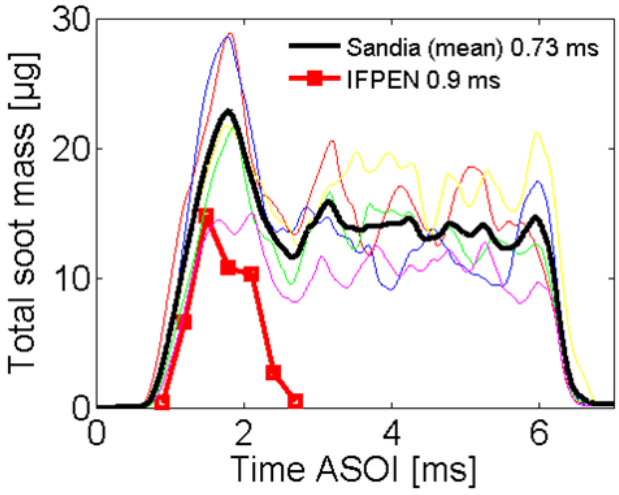

FIGURE 3. Total mass of soot measured by extinction imaging at Spray A conditions.

CONCLUSIONS

Research this year has shown significant advances with respect to modeling and experimental coordination as a part of the ECN. Overall, the coupling of high-speed and planar diagnostics provide improved information about the dynamics of low- and high-temperature ignition, resolved even for individual injection events. The quantitative soot and soot radiation data also provides useful information about the evolution of soot formation and oxidation and heat transfer. Collectively, this spray combustion research program provides unique information needed for the development of high-fidelity CFD models that will be used to optimize future engine designs.

REFERENCES

1. Engine Combustion Network, http://www.sandia.gov/ECN.

2. "Simultaneous formaldehyde PLIF and high-speed schlieren imaging for ignition visualization in high-pressure spray flames." Skeen, S.A., Manin, J., and Pickett, L.M., Proceedings of the Combustion Institute, in press, 2014.

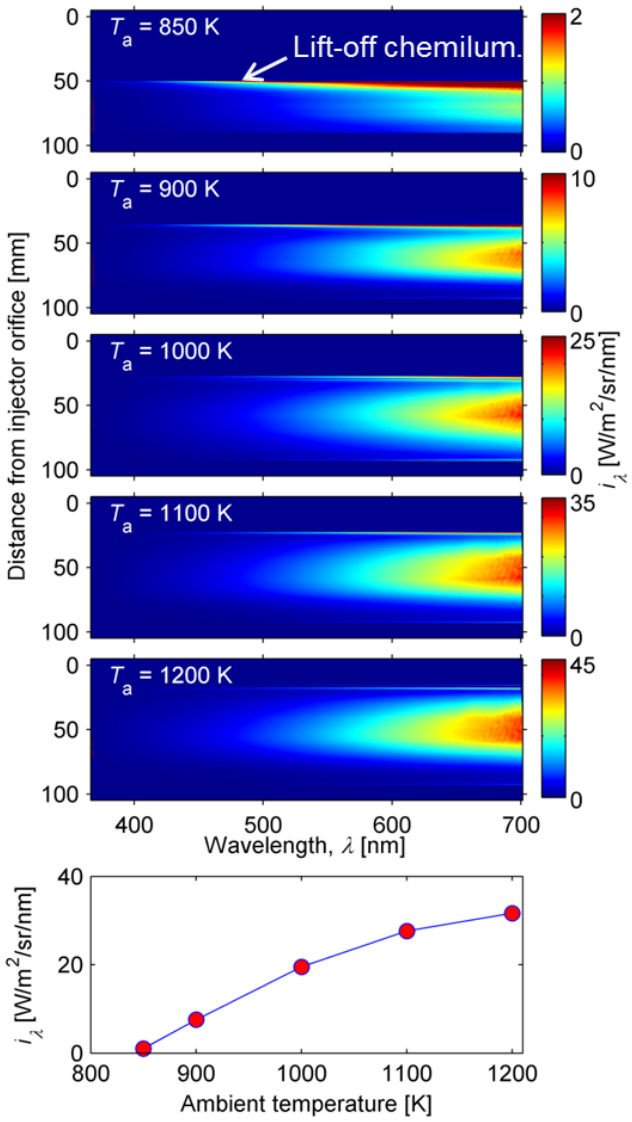

FIGURE 4. False color images of the quantitative spectral intensity along the flame centerline at five different ambient temperatures during quasi-steady combustion. The color scale changes in each panel. The peak spectral intensity observed in the soot region is shown in the bottom panel.

3. Engine Combustion Network <www.sandia.gov/ecn/pub-links/sas001/schlif.php> .

4. "Quantitative Spatially Resolved Measurements of Total Radiation in High-Pressure Spray Flames," Skeen, S., Manin, J., Pickett, L.M., Dalen, K., and Ivarsson., A., SAE 2014-01-1252, 2014.

FY 2014 PUBLICATIONS

1. "Simultaneous formaldehyde PLIF and high-speed schlieren imaging for ignition visualization in high-pressure spray flames." Skeen, S.A., Manin, J., and Pickett, L.M., Proceedings of the Combustion Institute, in press, 2014.

2. "Microscopic investigation of the atomization and mixing processes of diesel sprays injected into high pressure and temperature environments," Manin, J., Bardi, M., Pickett, L.M., Dahms, R.N., and Oefelein, J.C. Fuel 134:531-543, 2014.

3. "Quantitative Spatially Resolved Measurements of Total Radiation in High-Pressure Spray Flames," Skeen, S., Manin, J., Pickett, L.M., Dalen, K., and Ivarsson., A., SAE 2014-01-1252, 2014.

4. "Comparison of Near-Field Structure and Growth of a Diesel Spray Using Light-Based Optical Microscopy and X-Ray Radiography," Pickett, L.M., Manin, J., Kastengren, A., and Powell, C., SAE Int.J.Engines 7 (2), 2014, doi:10.4271/2014-01-1412.

5. "Numerical Simulations of Supersonic Diesel Spray Injection and the Induced Shock Waves," Quan, S., Dai, M., Pomraning, E., Senecal, P.K., Richards, K., Som, S., Skeen, S., Manin, J., and Pickett, L.M., SAE Int.J.Engines 7 (2), 2014, doi:10.4271/2014-01-1423.

6. "Quantitative Mixing Measurements and Stochastic Variability of a Vaporizing Gasoline Direct-Injection Spray. International Journal of Engine Research, Blessinger, M., Manin, J., Skeen, S.A., Meijer, M., Parrish, S., Pickett, L.M., doi:10.1177/1468087414531971, 2014.

SPECIAL AWARDS AND RECOGNITION

1. SAE International Excellence in Oral Presentation Award (2014), Lyle Pickett

II.4 Low-Temperature Gasoline Combustion (LTGC) Engine Research

John E. Dec
Sandia National Laboratories
MS 9053, P.O. Box 969
Livermore, CA 94551-0969

DOE Technology Development Manager
Leo Breton

Overall Objectives

Provide the fundamental understanding (science-base) required to overcome the technical barriers to the development of practical LTGC engines by industry.

Fiscal Year (FY) 2014 Objectives

- Determine the high-load limits for LTGC with a compression ratio (CR) of 16:1 over a range of intake-boost pressures (P_{in}) and engine speeds.
- Conduct an analysis of the potential of a Miller cycle to allow higher loads with CR = 16:1.
- Conduct a comprehensive noise analysis of LTGC to investigate combustion noise level (CNL) and ringing intensity (RI) over a wide range of operating conditions.
- Examine factors affecting measurement of thermal efficiency (TE), and clarify differences in peak TE between LTGC, reactivity-controlled compression ignition (RCCI), and conventional diesel combustion (CDC).
- Evaluate the potential for improving TE over load range by optimizing the gasoline direct injection (GDI) fuel-injection strategies used for partial fuel stratification (PFS) (multi-year task).
- Support new CFD modeling efforts for LTGC operation with PFS at the University of California, Berkeley (UC-Berkeley) and General Motors (GM), and chemical-kinetic mechanism development at Lawrence Livermore National Laboratory (LLNL).

FY 2014 Accomplishments

- Determined high-load limits for CR = 16:1 over range of P_{in}s and engine speeds, compared results with data for CR = 14:1, and investigated the effects on TE.
- Analyzed how a Miller cycle would affect maximum load over a range of P_{in} for both premixed and PFS fueling strategies.
- Conducted extensive study of CNL and RI over a range of loads, P_{in}s, combustion phasings, speeds, and pressure-rise rates. Explained reasons for differences between these two metrics.
- Conducted an in-depth investigation of all potential factors affecting measurement of TE and developed methods to correct for errors and eliminate uncertainties.
  - Compared TE of LTGC with that of RCCI and CDC.
- Evaluated the potential for improving TE over the load range by better optimizing PFS fuel distributions.
  - Evaluated the effect of GDI timing for a single-injection PFS.
  - Initial investigation of potential for further improvements with multiple injections.
- Collaborated with UC-Berkeley and GM on CFD modeling of PFS operation in our LTGC engine, and made comparisons of CFD and experimental results.
- Supported development of chemical-kinetic mechanisms at LLNL for LTGC operation with ethanol-gasoline blends.

Future Directions

- Conduct a comprehensive investigation of the use of multiple injections to better optimize fuel distributions with direct-injection PFS (DI PFS) for LTGC (multi-year task).
  - Initial work will be based on double injections, but more injections may also be used.
  - Work to improve TEs over the load range, particularly at higher loads.
  - Determine factors affecting the ability to increase the high-load limit with DI PFS, as well as improving the TE.
- Image fuel distributions in the optical engine to guide selection of fuel-injection strategies for multiple-injection DI PFS to be applied in the metal engine (multi-year task).
- Conduct multi-zone kinetic modeling to determine desired fuel distributions.

  - Combine results with fuel-distribution imaging to further optimize performance with multiple-injection DI PFS in the metal engine.
- Full evaluation of performance with new low-swirl, spark-plug capable cylinder head.
  - Determine TE, load range, heat transfer losses, etc., and compare with data using the previous cylinder head.
  - Investigate potential of new 300 bar GDI injectors for improving DI PFS operation.
  - Initial testing of spark-assisted LTGC.
- Apply turbocharger and friction models from GM to investigate how these real-engine effects would affect LTGC performance.
- Continue to provide data, analysis, and discussions to support 1) CFD modeling at UC-Berkeley and GM and 2) kinetic modeling at LLNL.

INTRODUCTION

Improving the efficiency of internal combustion engines is critical for meeting global needs to reduce petroleum consumption and CO_2 emissions. LTGC engines, including homogeneous charge compression ignition (HCCI) and partially stratified variants of HCCI, have a strong potential for contributing to these goals since they have high thermal efficiencies and ultra-low emissions of oxides of nitrogen (NO_X) and particulates. Furthermore, with intake-pressure boost, LTGC can achieve loads comparable to turbocharged diesel engines. Perhaps most importantly, LTGC provides a means for producing high-efficiency engines that operate on light distillates, thus complementing diesel engines which use middle distillates, for more effective overall utilization of crude-oil supplies and lower total CO_2 production.

Results during FY 2014 have contributed to overcoming three of DOE's technical barriers to the practical implementation of LTGC/HCCI combustion in production engines: 1) extending operation to higher loads, 2) increasing TE, and 3) providing an improved understanding of in-cylinder processes. First, the effect of increasing the CR from 14:1 to 16:1 on the high-load limits for a wide range of intake-boost pressures has been investigated for both premixed and early DI PFS fueling strategies. Second, the potential of using a Miller cycle to improve performance with a geometric CR of 16:1 has been analyzed. Third, a comprehensive analysis of LTGC-engine combustion noise, including knock has been conducted. Fourth, methods for improving the TE of LTGC have been investigated, including both an analysis of the accuracy of methods used to determine the TE and an initial study of a new approach based on double fuel injections to increase the TE-improving benefits of PFS. Additionally, collaborative CFD modeling efforts have been established with UC-Berkeley and GM, and collaborations with LLNL for chemical-kinetic mechanism development have continued.

APPROACH

Studies were conducted in our dual-engine LTGC laboratory which is equipped with both an all-metal and a matching optically accessible LTGC research engine (displacement = 0.98 liters). This facility allows operation over a wide range of conditions, and it can provide precise control of operating parameters such as combustion phasing, injection timing, intake temperature (T_{in}), intake pressure (P_{in}), engine speed, and mass flow rates of supplied fuel and air. The facility also allows the use of cooled exhaust gas recirculation (EGR) and is equipped with a full emissions bench (hydrocarbons, CO, CO_2, O_2, NO_X, and smoke).

The all-metal engine was used for the majority of our research in FY 2014, which required high-quality performance measurements under well-controlled conditions. For the high-load studies, combustion phasing (CA50, the crank angle at which 50% of the combustion heat release has occurred) was adjusted by controlling T_{in} or the amount of cooled EGR to prevent engine knock while maintaining good stability as the fueling was incrementally increased to the maximum load for each intake-boost pressure. Intake pressures were systematically increased from naturally aspirated conditions (P_{in} = 1 bar) up to the P_{in} for which the maximum fueling rate was limited by the cylinder-head pressure limit of 155–160 bar (a P_{in} of 3.0 to 3.4 bar). TE measurements required similar precise control of engine operation, combined with the ability accurately measure the amount of fuel supplied. These studies of TE were facilitated by the design of the all-metal engine, which has a low crevice-volume for high combustion efficiencies and is equipped with a centrally mounted GDI injector. Previous work has shown that PFS produced by 100% DI fueling early in the intake stroke (early-DI PFS) has significant advantages for increasing the TE [1,2], so this technique was used for most investigations of TE. Additionally, a study was initiated to investigate the potential for improving PFS by using double-injection fueling for further increases in TE. For all TE studies, the engine was operated at the maximum RI without engine knock (taken to be RI = 5 MW/m^2 [1]), which allows CA50 to be as advanced as possible, resulting in the highest TE for a given operating condition.

Collaborations have been established with UC-Berkeley and with GM to apply CFD modeling to our engine. This modeling complements the experimental work and will help provide an improved understanding of the effects of PFS and its potential to increase LTGC efficiencies and load range.

RESULTS

Selection of the CR for an LTGC engine can affect many aspects of engine operation and performance. Raising the CR from 14:1 to 16:1 has provided a consistent increase in the TE [3], but the effect on the load range at various boost levels is less clear. Higher CRs are often considered to decrease the maximum load because they drive the charge into autoignition more quickly, which can lead to overly advanced combustion phasing and engine knock. However, by carefully controlling CA50 with T_{in} adjustments or the addition of cooled EGR, this problem of CA50 advancement can be overcome. As shown Figure 1, CR = 16:1 actually allows slightly higher loads (up to 13% higher) for premixed fueling at naturally aspirated and low-boost conditions (P_{in} = 1.0 and 1.3 bar). This is because less intake heating (or retained hot residuals) is required with CR = 16:1 so a greater charge mass is inducted, while the fuel/air ratio at the knock/stability limit remains similar. This advantage for CR = 16:1 with premixed fueling disappears for higher P_{in} as the T_{in} for both CRs is reduced to 60°C (the minimum value without fuel condensation in the intake system) to partially compensate for the autoignition enhancement with boost. However, using early-DI PFS, CR = 16:1 can also give higher loads for P_{in} from 1.6 to 2.5 bars, because the PFS combustion appears to be more stable with the higher CR at these P_{in}, for reasons that are not fully understood.

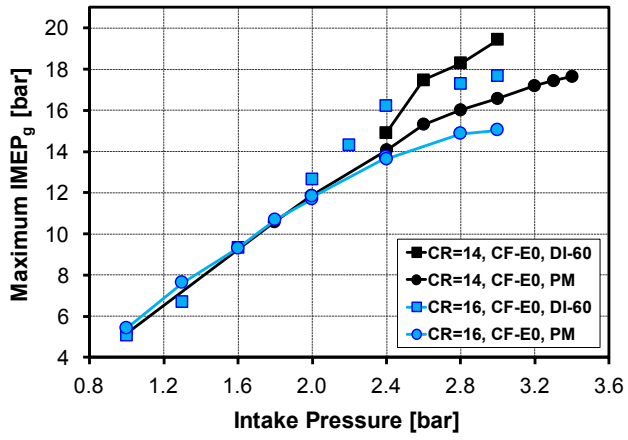

FIGURE 1. High-load limits as a function of intake pressure for premixed (PM) and early-DI PFS (DI-60) fueling. Fuel is certification gasoline (CF-E0, AKI = 93). All data points are at 1,200 rpm, have no knock (RI ≈5 MW/m^2), and NOx and particulate emissions are well below U.S.-2010 standards.

Despite these load advantages for CR = 16:1 at low- to mid-range intake pressures, Figure 1 shows that CR = 14:1 provides higher loads for P_{in} > 2.4–2.5 bar. This is because more EGR is required with CR = 16:1 to prevent overly advanced combustion, and above these boost pressures, all the excess air has been replaced with EGR, so increasing the EGR fraction to control CA50 at higher P_{in} requires reducing the fuel-air fraction of the charge. As a result, the load increase with P_{in} is less with CR = 16:1 above 2.4–2.5 bar, and CR = 14:1 gives higher loads. Also, the combustion stability for early-DI PFS with CR = 14:1 increases substantially as P_{in} is increased from 2.4 bar to 2.6 bar, allowing proportionally more fuel to be added to the charge, as evident from the relatively large increase in the maximum indicated mean effective pressure, gross, ($IMEP_g$) between these two P_{in} (see Figure 1). Thus, CR = 14:1 can reach $IMEP_g$ = 19.4 bar at P_{in} = 3.0 bar, while the maximum load for CR = 16:1 is a lower, but still very respectable, $IMEP_g$ = 17.7 bar at P_{in} = 3.0 bar. CR = 16:1 also gives higher TEs than CR = 14:1 at the high-load limits over the P_{in} range in Figure 1.

A Miller cycle is often suggested as a means of taking advantage of the higher TEs with a higher geometric CR, while avoiding the problem of overly rapid autoignition. To accomplish this, a Miller cycle closes the intake valve either earlier or later than with a standard cycle. In either case, the change in valve timing reduces the effective CR, but the expansion ratio is preserved, so the TE is still essentially the same as for a standard cycle with the same geometric CR. For example, with late intake-valve closure, part of the inducted charge is pushed back into the intake system, and compression does not begin until the valve closes after the piston has already moved partway toward top-dead center, so the amount of charge compression is reduced. To determine the potential benefits of a Miller cycle for LTGC with a geometric CR = 16:1, an analysis was conducted for both premixed and early-DI PFS fueling. Figure 2 presents the analysis for early-DI PFS, with the blue and red data points corresponding to the higher-load points from Figure 1 for CR = 16:1 and 14:1, respectively. The corresponding TEs are shown in Figure 2b. For a Miller cycle with the valve timing adjusted to reduce the effective CR to 14:1, the charge mass would be reduced by about 12.5%, which a commensurate reduction in $IMEP_g$ as indicated by the light brown data points in Figure 2. However, the TE would be the same as for CR = 16:1, which would increase the load ~2% as shown by the darker brown open symbols in Figure 2. The net result is that the Miller cycle gives a lower maximum load than could be obtained with a standard cycle using additional EGR to control CA50 (blue data points), except for the highest boost pressure. At this P_{in} = 3.0 bar condition, the

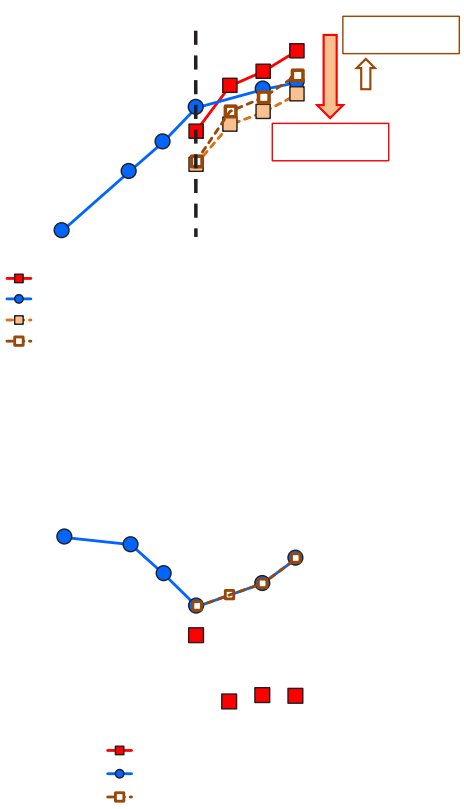

FIGURE 2. Evaluation of the performance of a Miller cycle over a range of P_{in}s for a geometric CR = 16:1 with late intake valve closure reducing the effective CR to 14:1 while maintaining an expansion ratio = 16:1. The data used as a basis for the analysis (blue and red data points) are the higher-load early-DI PFS data points from Figure 1.

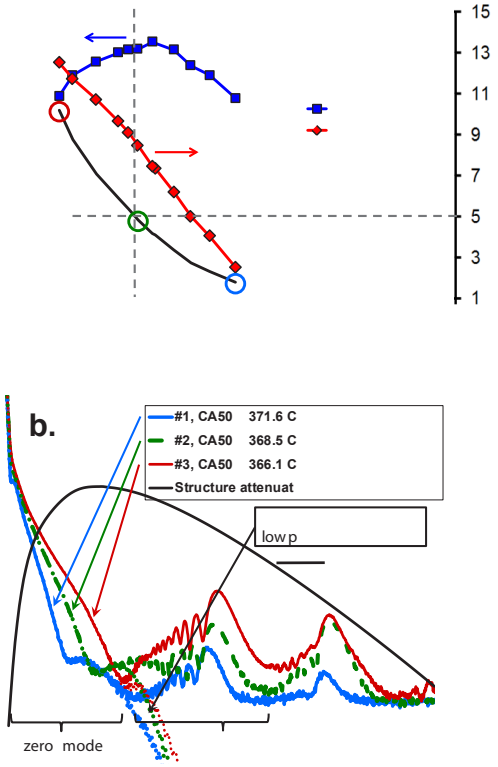

FIGURE 3. (a) Changes in RI, CNL, and TE for a combustion timing (CA50) sweep at constant fueling (ϕ_m = 0.32). (b) Power spectral density plots for the three circled points on the RI curve in the top plot.

Miller cycle gives a slightly higher maximum load, but the increase is so small it would not be worth the penalty of reduced load at lower boost pressures. It is noteworthy, however, that the trend indicates a greater advantage to the Miller cycle if the engine was to be operated at higher boost, as would be possible for an LTGC engine with higher cylinder-head pressure limits. A Miller cycle might also be more attractive if it was combined with a variable intake-valve timing mechanism that allowed the engine to switch between standard and Miller cycles as P_{in} was increased.

Figure 3 presents an example of some results from the comprehensive noise-analysis study [4]. These data show how the two commonly used metrics, RI and CNL vary as CA50 is swept from being very retarded (372° crank angle, CA) to very advanced (366° CA) for a fixed fueling rate corresponding to a charge-mass equivalence ratio (ϕ_m) = 0.32. As can be seen in Figure 3a, both RI and CNL vary from small to large values as CA50 is advanced, while the TE goes through a maximum. Figure 3b shows the power spectral densities for the three points denoted by the colored circles on the RI curve in Figure 3a. As CA50 is advanced from 372°CA, the TE increases because the effective expansion ratio after combustion increases, increasing the work extracted. This trend continues to about the point where the RI is ~5 MW/m^2 (see dashed guide lines), which is typically taken to be the point where acoustic oscillations become sufficiently strong to be considered knock [1,4]. As CA50 is advanced beyond the point of maximum TE, the increased heat transfer losses resulting from the velocities associated with the increasingly strong acoustic oscillations (knock) exceeds the diminishing gains from advancing CA50, and the TE begins to decrease.

The RI was designed to be a measure of the intensity of the acoustic oscillations [5]. Although there is not a sharp transition between non-knocking and knocking operation, RI ≈5 MW/m^2 has been found to correspond to the limit of acceptable oscillations (i.e., no knock) over a wide range of operating conditions as noted above. The acoustic oscillations are evident as the 1,0 and 2,0 modes in the power spectral density (PSD) plots in Figure 3b.

Noting the logarithmic scale, it can be seen that the magnitude of the 1,0 mode, which dominates LTGC knock, shows a much greater increase from the middle curve to the strongly knocking curve (top) than from the weak oscillation curve (bottom) to the middle curve. The CNL, on the other hand, was found to be only a measure of the zero mode (see Figure 3b), which corresponds to the noise from the main pressure rise with combustion. It is completely insensitive to the magnitude of the acoustic oscillations. The CNL analysis gives almost the same value when the PSD is truncated with a high-frequency reject filter that removes the acoustic modes, as indicated by the dotted PSD lines in Figure 3b, as it does for the unfiltered PSD, even for the case with the strongest 1,0 mode. Thus, the CNL was found to be good measure of the noise for non-knocking combustion, but not for the additional irritating noise of engine knock. The RI was found to be a good indicator of knock and for avoiding knocking combustion, but it does not always correspond to well to variations in the noise generated by the main pressure rise with combustion.

High TEs are one of the main advantages of LTGC over conventional spark-ignition gasoline combustion. Therefore, it is important that experimental measurements of the TE be accurate, and it is desirable to have as high of a TE as possible over the load range. With respect to the first point, an in-depth investigation has been conducted of all potential factors affecting TE measurements in our laboratory. Several improvements were made, including installation of a new high-resolution fuel flow meter, development of an improved technique for calibrating the meter to account for compressibility differences between fuels which were found to be important, development of a system to monitor variations in fuel temperature and correct for them, and improved seals in the high-pressure fuel supply. With these changes, a peak gross indicated TE of 49.7% was achieved with a CR = 16:1. Considering differences in engine size, this value is very comparable to those achieved with RCCI and partially premixed compression ignition with similar CRs, and it is well above typical values for CDC.

Early-DI PFS provides significant improvements in TE and high-load limits compared to premixed fueling. As a means of retaining the advantages of early-DI PFS, but adding the capability of tuning the fuel distribution for more optimal PFS performance, an investigation into double-injection DI PFS was initiated. Figure 4 presents some initial results from this work. The many square data points show the load-TE tradeoff for early-DI PFS at a mid-range boost level of P_{in} = 2.4 bar. As can be seen, the peak TE is 49.6%, but the TE falls to as low as about 46% at the highest load presented, mostly due to the increased CA50 retard required to prevent knock with increased load. First, a double injection with 92.5% of the

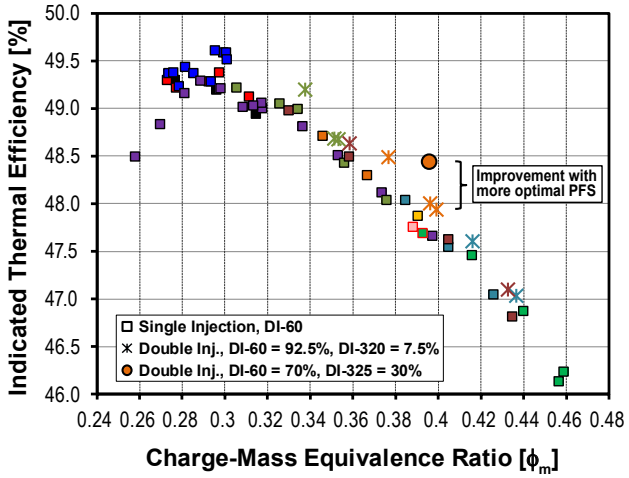

FIGURE 4. Thermal efficiency as a function of fueling rate (ϕ_m) for early-DI PFS using a single injection (squares), and for double-injection DI PFS with both 92.5% early-DI and 7.5% late-DI fueling (asterisk-like symbols) and with 70% early-DI and 30% late-DI fueling (circle). Fuel = CF-E0, RI ≈5 MW/m^2, P_{in} = 2.4 bar, 1,200 rpm.

fuel injected early in the intake stroke and 7.5% injected at 320° CA (40° before top-dead center compression) was tried, and it increased the TE by about 0.2–0.3 %-units over most of the load range as shown by the asterisk-like symbols. Next, much higher levels of stratification were investigated at a single fueling rate near the middle of the load range (ϕ_m = 0.396), resulting in a TE improvement of more than 0.7 %-units with 70% early-DI and 30% late-DI fueling, as shown by the single circle-symbol data point. This preliminary work indicates that multiple-injections have considerable potential for improving PFS mixtures, and additional work in planned as indicated previously under "Future Directions."

CONCLUSIONS

- An investigation of the high-load limits for CR = 16:1 for both premixed and early-DI PFS fueling showed that changes in the high-load limit compared to CR = 14:1 depend on the boost pressure.
  - For P_{in} < 2.5 bar, CR = 16:1 can provide higher loads than CR =14:1.
  - With CR = 16:1, a load of $IMEP_g$ = 16 bar was achieved with only 2.4 bar boost.
  - For P_{in} > 2.5 bar, CR = 16:1 gave lower loads, with a maximum load of $IMEP_g$ = 17.7 bar at P_{in} = 3.0 bars, compared to a maximum $IMEP_g$ = 19.4 bar at this P_{in} for CR = 14:1.
- Analysis of expected performance with a Miller cycle shows that it offers little potential benefit over a standard cycle that uses increased EGR to control CA50. The Miller cycle gives lower loads at

all P_{in}s except for a slight increase at the highest P_{in} investigated, 3.0 bar.

- A comprehensive study of LTGC-engine noise with a comparison of CNL and RI over a wide range of loads, CA50s, P_{in}s, engine speeds, and pressure-rise rates showed the following:
  - RI tracks the resonant acoustic modes and provides a metric for the onset of unacceptable acoustic oscillations, i.e., knock.
  - The CNL is not sensitive to knock, but provides a good measure of noise from the combustion event itself.
  - CNL can be reduced by CA50 retard with only a modest reduction in TE, with $\Delta TE/\Delta CNL \approx 0.8\%$-units/5 dB
- Evaluation of all factors affecting our TE measurements, with improvements as necessary and more optimized operating conditions yielded a peak TE of 49.7%.
- Initial investigation of double-injection DI-fueling showed that it can significantly improve PFS to increase the TE over the load range.
- Collaborations with UC-Berkeldy and GM to apply CFD modeling for an improved understanding of PFS are underway.
- Collaborations with LLNL have helped the development of a chemical-kinetic mechanism for gasoline/ethanol blends.

REFERENCES

1. Dec, J.E., Yang, Y., and Dronniou, N., "Improving Efficiency and using E10 for Higher Loads in Boosted HCCI Engines," *SAE Int. J. Engines* 5(3):1009-1032, 2012, doi:10.4271/2012-01-1107.

2. Dec, J.E., Yang, Y., Ji, C., and Dernotte, J., "Effects of Gasoline Reactivity and Ethanol Content on Boosted, Premixed and Partially Stratified Low-Temperature Gasoline Combustion (LTGC)," SAE paper offer number 15PFL-0299, submitted for the 2015 SAE International Congress.

3. Dec, J.E., "HCCI and Stratified-Charge CI Engine Combustion Research," DOE-OVT FY 2013 Annual Progress Report, Advanced Engine Combustion R&D, II.8.

4. Dernotte, J., Dec, J., and Ji, C., "Investigation of the Sources of Combustion Noise in HCCI Engines," *SAE Int. J. Engines* 7(2), 2014, doi:10.4271/2014-01-1272.

5. Eng, J.A, "Characterization of Pressure Waves in HCCI Combustion," SAE Technical Paper 2002-01-2859, 2002, doi:10.4271/2002-01-2859.

FY 2014 PUBLICATIONS/PRESENTATIONS

1. Dec, J.E., Yang, Y., Ji, C., and Dernotte, J., "Effects of Gasoline Reactivity and Ethanol Content on Boosted, Premixed and Partially Stratified Low-Temperature Gasoline Combustion (LTGC)," SAE paper offer number 15PFL-0299, submitted for the 2015 SAE International Congress.

2. Dernotte, J., Dec, J., and Ji, C. "Energy Distribution Analysis in Boosted HCCI-like / LTGC Engines," DOE Advanced Engine Combustion Working Group Meeting, August 2014.

3. Wolk, B., Chen, J.-Y., and Dec, J.E., "Computational Study of the Pressure Dependence of Sequential Autoignition for Partial Fuel Stratification with Gasoline," accepted for publication in the *Proceedings of the Combustion Institute,* **35**, 2015.

4. Dernotte, J., Dec, J., and Ji, C., "Investigation of the Sources of Combustion Noise in HCCI Engines," *SAE Int. J. Engines* 7(2), 2014, doi:10.4271/2014-01-1272.

5. Ji, C., Dec, J., Dernotte, J. and Cannella, W., "Effect of Ignition Improvers on the Combustion Performance of Regular Gasoline in an HCCI Engine," *SAE Int. J. Engines* **7**(2), 2014, doi:10.4271/2014-01-1282.

6. Lawler, B., Lacey, J., Dronniou, N. Dernotte, J., Dec, J., Gurlap, O., Najt, P. and Filipi, Z., "Refinement and Validation of the Thermal Stratification Analysis: A Post-processing Methodology for Determining Temperature Distributions in an Experimental HCCI Engine," SAE Technical Paper 2014-01-1276, SAE International Congress, Detroit MI, April 2014.

7. Dec, J.E., Ji, C., and Dernotte, J., "Increasing the Load Range and Efficiency of Low-Temperature Gasoline Combustion (LTGC)," DOE Advanced Engine Combustion Working Group Meeting, February 2014.

8. Ji, C., Dec, J.E., Dernotte, J, and Cannella, W., "Effect of Ignition Improvers on the Combustion Performance of Regular Gasoline in an HCCI Engine," DOE Advanced Engine Combustion Working Group Meeting, February 2014.

9. Invited Presentation: Dec, J.E., "Achieving High Loads with HCCI & Partially Stratified Low-Temperature Gasoline Combustion (LTGC)," Coordinating Research Council (CRC) Advanced Fuels and Engines Efficiency Workshop, Baltimore, MD, February, 2014.

10. Dec, J.E., Encyclopedia of Automotive Engineering, Section on "Advanced Compression-Ignition Combustion Systems for High Efficiency and Ultra-Low NOx and Soot Emissions," Wiley and Sons, published on-line November 2014.

11. Yang, Y. and Dec, J.E., "Bio-Ketones: Autoignition Characteristics and Their Potential as Fuels for HCCI Engines," *SAE Int. J. Fuels Lubr.*, **6**(3): 713-728, 2013, doi:10.4271/2013-01-2627.

SPECIAL RECOGNITIONS & AWARDS/ PATENTS ISSUED

1. U.S. Patent Issued, No. 8,689,767 B1: Dec, J.E., Yang, Y., and Dronniou, N. "A Method for Operating Homogeneous Charge Compression Ignition Engines Using Conventional Gasoline," April 2014.

2. Provisional U.S. Patent Filed: Yang, Y. and Dec, J.E., "Bio-Ketones: Autoignition Characteristics and Their Potential as Fuels for HCCI Engines," Application number 61,981,389, April 2014.

II.5 Automotive Low-Temperature Gasoline Combustion Engine Research

Isaac W. Ekoto (Primary Contact),
Richard R. Steeper
Sandia National Laboratories (SNL)
7011 East Ave.
Livermore, CA 94551

DOE Technology Development Manager
Leo Breton

Overall Objectives

- Develop robust automotive low-temperature gasoline combustion (LTGC) strategies that improve fuel economy and reduce pollutant emissions.
- Research technologies such as negative valve overlap (NVO) fueling or advanced ignition that extend the LTGC operation envelope.
- Work closely with manufacturers to address crucial mid- to long-range research challenges and accelerate advanced engine technology deployment.

Fiscal Year (FY) 2014 Objectives

- Characterize NVO reaction chemistry via a custom cylinder-dump sampling system.
- Quantify extent of local rich combustion from late NVO injection via gas chromatography (GC) measurements of dump samples.
- Apply computational models that use the GC measurements as boundary conditions to understand NVO fueling chemical enhancement effects on main combustion.
- Initiate new research to elucidate fundamental processes of innovative ignition technologies that enable advanced LTGC strategies.

FY 2014 Accomplishments

- Quantified NVO period species that influence main-cycle ignition through dump sampling and GC measurements.
- Clarified importance of select hydrocarbon species on main-cycle ignition through the application of CHEMKIN-PRO models.
- Performed exploratory vacuum ultraviolet mass spectroscopy experiments at the Lawrence Berkeley National Laboratory synchrotron to obtain detailed information about NVO sample speciation.
- Published a report that details advanced gasoline ignition system challenges and opportunities, and started lab facility upgrades to enable future ignition research.

Future Directions

- Evaluate potential advanced ignition technologies to widen LTGC operating envelopes.
- Develop/apply diagnostics to measure fundamental ignition system processes.
- Develop phenomenological models for novel ignition hardware and operating strategies.
- Collaborate with combustion chemistry modeling groups to improve kinetics mechanisms used for LTGC simulations.

✧ ✧ ✧ ✧ ✧

INTRODUCTION

The current project focuses on the development of automotive LTGC strategies that help achieve DOE Vehicle Technologies Office goals for fuel economy and pollutant emissions. To be successful, LTGC strategies must achieve a wide operating range through the use of technologies such as NVO fueling and enhanced ignition. Sandia's optically accessible engine capabilities and diagnostic expertise are leveraged to acquire high-value measurements at realistic conditions—often within challenging environments—to generate new phenomenological understanding of relevant combustion processes. For FY 2014, there were two primary tasks:

- **Task 1:** Use custom sampling hardware and novel diagnostics to characterize NVO period reaction chemistry, with computational modeling used to elucidate the impact on main combustion. Work was performed in collaboration with Jim Szybist (Oak Ridge National Laboratory, ORNL) and Lee Davisson (Lawrence Livermore National Laboratory), with technical feedback provided by GM Research.
- **Task 2:** Start retrofit of a vacated automotive engine lab for high-value research into fundamental processes of various advanced ignition technologies. Guidance and technical feedback provided by automotive manufacturers.

APPROACH

The relevance of each task and the approach applied is as follows:

Task 1: The most recent Advanced Combustion and Emissions Control Tech Team roadmap calls for low-cost, efficient, onboard means of tailoring LTGC fuel properties. In response, we have focused on NVO strategies that facilitate auto-ignition control through modified valve timings to retain and recompress residual burned gases along with a small quantity of injected fuel that is both oxidized and reformed; a representative NVO cycle is given in Figure 1. While the thermal effects of NVO fueling on main combustion are well understood, less is known about the impact of fuel reforming on main charge reactivity. We previously characterized NVO products from fuel-lean operation—where large residual gas oxygen concentrations are available to oxidize NVO injected fuel—via laser diagnostics and from a custom dump-sampling apparatus and GC illustrated in Figure 2. Recently we have investigated oxygen deficient NVO periods with little heat release but large intermediate hydrocarbon concentrations from parent fuel reformation.

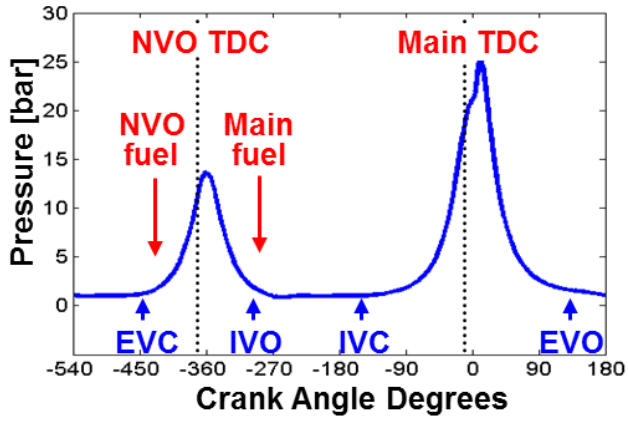

TDC - top-dead center

FIGURE 1. Typical pressure trace for NVO LTGC with approximate valve and injection timings.

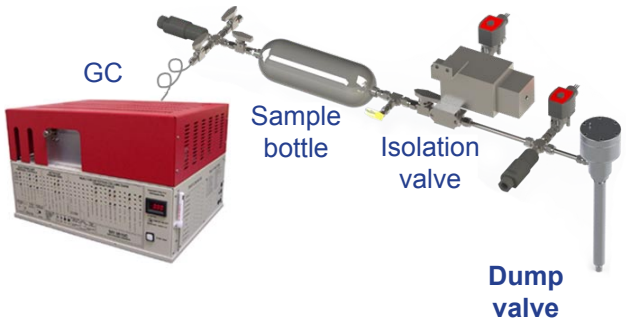

FIGURE 2. Dump valve assembly arrangement including the gas chromatograph.

Complementary combustion modeling has been used to isolate the effects of added thermal energy and change in charge reactivity.

Task 2: A new advanced ignition initiative is motivated by the Advanced Combustion and Emissions Control Tech Team call for more robust systems suitable for high-efficiency dilute gasoline combustion regimes. Conventional transistor coil igniters that feature a short-duration breakdown followed by a longer discharge period are unsuitable for next-generation lean-burn engines due to: 1) intermittently combustible spark gap mixtures that reduce engine stability, 2) high required breakdown voltages and large electrode gaps that lead to durability and energy use concerns, and 3) large charge motions that alter ignition characteristics through spark deflection. To investigate performance characteristics and underlying physical processes of next-generation ignition systems, a retrofit of an inactive engine laboratory is underway. Guidance on engine geometry and operating conditions has been solicited from automotive manufacturers, while relevant research groups developing advanced ignition technologies (e.g., low-temperature plasma, microwave, jet ignition) have been engaged. Relevant diagnostics needed to characterize ignition phenomena have also been identified.

RESULTS

Major findings for each task are as follows:

Task 1: In FY 2014, GC measurements from a high excess-oxygen (7%) NVO operating condition revealed that intermediate hydrocarbon production trended up as NVO injection timing was retarded and piston-top spray impingement increased. Figure 3 illustrates single-zone CHEMKIN-PRO model heat release profiles for an early and late NVO start-of-injection (SOI) condition. Late NVO SOI operation increased intermediate hydrocarbon production, which led to a clear auto-ignition phasing advance relative to the early NVO SOI condition. A sensitivity analysis indicated it was mainly acetylene that accounted for the phasing advance. Recently, Jim Szybist (ORNL) demonstrated enhanced charge reactivity can also be achieved in low-oxygen NVO environments. A select ORNL low excess-oxygen (4%) NVO operating condition was reproduced in the SNL LTGC engine—small hydrocarbon concentration trends from each engine were well matched as can be seen in Figure 4. Despite little NVO period heat release, intermediate hydrocarbon formation increased with NVO SOI advance, which suggests production was driven by kinetics limited bulk-gas reformation.

To investigate other species that could influence main-cycle charge reactivity, NVO dump samples from select operating conditions were transported to the

Measured species concentrations:

Species	Early NVO	Late NVO	
Hydrogen	61.1	528	ppm
Methane	70.4	304	ppm
Acetylene	11.8	128	ppm
Ethylene	47.1	128	ppm
DME	21.6	49.2	ppm

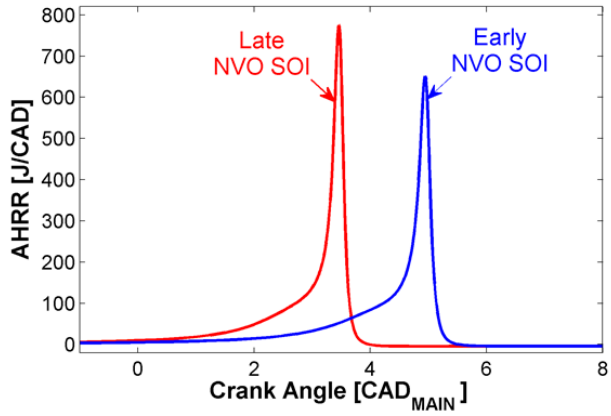

FIGURE 3. CHEMKIN-PRO single-zone simulation prediction of main combustion heat release for early and late NVO SOI, with initial hydrocarbon and hydrogen species concentrations for each condition.

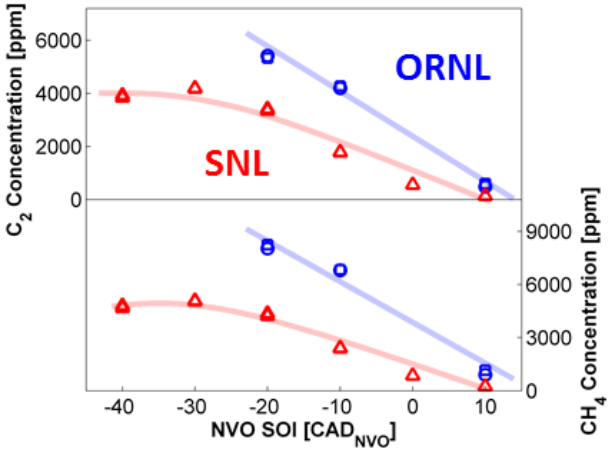

FIGURE 4. Sandia vacuum ultraviolet molecular beam mass spectroscopy schematic adapted to accept engine NVO sample bottles.

Lawrence Berkeley National Laboratory synchrotron and analyzed by a vacuum ultraviolet mass spectrometer; a schematic is provided in Figure 5. Data analysis will continue into FY 2015 with results expected to provide detailed GC calibration points, validate NVO chemistry modeling, and elucidate key species responsible for enhanced main combustion.

Task 2: In FY 2014, we published a report that summarizes the opportunities and challenges for

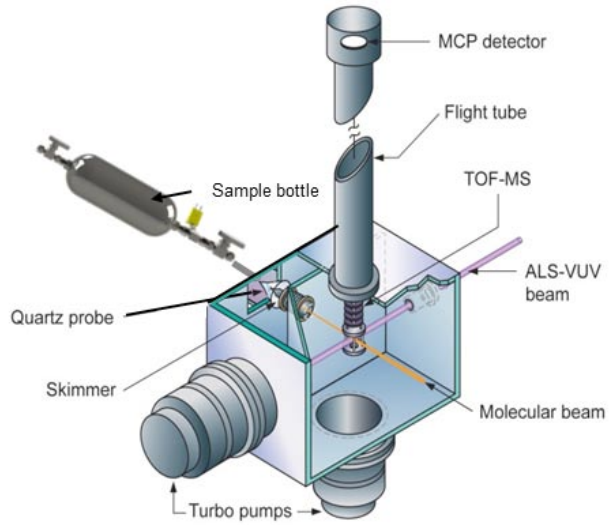

MCP - multichannel plate; TOF-MS - time-of-flight mass spectrometer; ALS-VUV: advanced light source vacuum ultraviolet

FIGURE 5. End-cycle methane and combined ethylene/acetylene measurements from a low excess-oxygen (4%) NVO SOI sweep from similar Sandia and ORNL engines.

advanced ignition technologies. It is known for example that large ignition volumes with long durations increase ignition probability and subsequent flame sustainment for stratified charges, while enhanced flame propagation can overcome slow flame speeds at elevated pressures and lean mixtures. From this review and based on industry feedback, we identified a downsized boost engine head with direct injection as the best platform to explore advanced igniter characteristics. Custom optical engine component fabrication will continue into FY 2015. A low-temperature plasma igniter developed by Transient Plasma Systems Inc., which shows promise for extending dilution limits through the production of highly reactive species, is currently being explored. Laser diagnostic development is underway to enable quantitative in situ atomic oxygen measurements, which is produced in large quantities by high-energy plasmas for atmospheric flames. A tunable high-power laser needed to excite fluorescence is already available, and a custom intensified camera with high quantum efficiency in the near infrared needed to image atomic oxygen fluorescence was purchased. Exploratory plasma igniter measurements are planned for FY 2015, with results to inform complementary simulations by Riccardo Scarcelli (Argonne National Laboratory).

CONCLUSIONS

Industry focus on automotive LTGC strategies has driven our research project to develop new tools and improved understanding for enabling approaches.

Detailed NVO product speciation and heat release characterization is expected to enable optimal control strategies that minimize combustion instabilities and associated fuel economy penalties during the NVO period. Future advanced ignition experiments will improve system designs and clarify key physical processes.

FY 2014 PUBLICATIONS

1. Ekoto IW, Steeper RR, Advanced Ignition Challenges and Strategies for Lean-Burn Gasoline Engines. SAND2014-1240P, Sandia National Laboratories, Feb, 2014.

2. Steeper RR, Davisson ML, Analysis of Gasoline Negative-Valve-Overlap Fueling via Dump Sampling. SAE Int J Engines, 2014;7:762-71, 10.4271/2014-01-1273.

3. Szybist JP, Steeper RR, Splitter D, Kalaskar VB, Pihl J, Daw C, Negative Valve Overlap Reforming Chemistry in Low-Oxygen Environments. SAE Int J Engines, 2014;7:418-33, 10.4271/2014-01-1188.

II.6 Spray and Combustion Modeling using High-Performance Computing

Sibendu Som (Primary Contact), Qingluan Xue, Michele Battistoni, Yuanjiang Pei
Argonne National Laboratory
9700 S Cass Ave.
Argonne, IL 60439

DOE Technology Development Manager
Leo Breton

Overall Objectives

- Development of physics-based nozzle flow and spray models. Develop capability to perform coupled nozzle flow and spray simulations.
- Development and validation of high-fidelity turbulence models for diesel engine applications.
- Development and validation of reduced chemical-kinetic models for realistic diesel fuel surrogates.
- High-performance computing (HPC) tool development on codes used by the industry for internal combustion engine (ICE) applications.

Fiscal Year (FY) 2014 Objectives

- Implement in-nozzle flow models in CONVERGE™ code [1] followed by extensive validation against experimental data accounting for needle transients and off-axis motion.
- Develop strategies to simulate the start of injection (SOI) and end of injection (EOI) transients, and together with X-ray measurements at Argonne, improve our understanding of the injection transients.
- Develop a coupled nozzle flow and spray simulation approach using the Eulerian-Eulerian (EE) methodology and validate against X-ray radiography data from Argonne.
- Develop and validate a reduced chemical kinetic mechanism for a multi-component diesel surrogate mixture consisting of n-dodecane and m-xylene.
- Demonstrate grid-converged engine simulations using HPC resources.

FY 2014 Accomplishments

- Three-dimensional, transient, turbulent in-nozzle flow simulations have been performed. For the first time, needle off-axis (wobble) motion has been accounted for in multi-hole injectors. The needle wobble is shown to have a profound influence on cavitation characteristics and mass flow rate from each orifice.
- Lagrangian-Eulerian (LE) droplet models are widely used for engine simulations, however, in the near-nozzle dense spray regime we demonstrated that an EE approach is more suitable to mimic the spray distribution.
- For the first time ever, the effect of SOI transients was well predicted by simulations. These simulations together with X-ray experiments at Argonne provided unique insights about the processes governing the initial injection of ingested gas and liquid spray.
- We developed and validated a 163-species-based reduced reaction mechanism for a mixture of n-dodecane and m-xylene as surrogate for diesel fuel. This mechanism is validated through the Engine Combustion Network data [2]. Usually n-heptane is used as a diesel fuel surrogate and it is not a truly representative surrogate.
- Typical production type engine simulations in the industry are performed on 32-64 processors. We have performed engine simulations on 1,024 processors in a scalable fashion. These simulations were performed with a peak cell count of 50 million cells, which is the largest diesel engine simulation run to date. These simulations enabled grid-convergent engine simulations, thus enhancing predictive capabilities.

Future Directions

- Nozzle flow simulations with production multi-hole injectors using the best-available geometry information and needle lift profiles. Coupling the nozzle flow simulations with classical spray simulations to understand the influence of in-nozzle flows on spray and combustion processes.
- Implement the best-practices developed for large-eddy simulation calculations on engine simulations with different engine geometries available in literature. This will provide a clear path for

manufacturers to take advantage of our high-fidelity computational studies.

- Developing a near-nozzle Eulerian spray modeling approach which in principle is significantly different from a classical spray modeling approach which is Lagrangian in nature [3]. Dynamically couple the nozzle flow simulations with the Eulerian approach for near-nozzle spray simulations.
- Develop a multi-component surrogate (with four or five components) mechanism for diesel fuel and validate against experimental data in constant volume chamber [2] and single-cylinder engine.
- Systematically improve the fidelity of the simulations by improving the nozzle flow, spray, turbulence, and combustion models. The computational cost is likely to increase significantly due to the use of these robust models. Develop HPC capabilities to ensure reasonable wall-clock times with these higher-fidelity models.

INTRODUCTION

ICE processes are multi-scale and highly coupled in nature and characterized by turbulence, two-phase flows, and complicated spray physics. Furthermore, the complex combustion chemistry of fuel oxidation and emission formation makes engine simulations a computationally daunting task. Given the cost for performing detailed experiments spanning a wide range of operating conditions and fuels, computational fluid dynamics modeling aided by HPC has the potential to result in considerable cost savings. Development of physics-based computational fluid dynamics models for nozzle flow, spray, turbulence, and combustion are necessary for predictive simulations of the ICE. HPC can play an important role in ICE development by reducing the cost for design and optimization studies. This is largely accomplished by being able to conduct detailed simulations of complex geometries and moving boundaries with high-fidelity models describing the relevant physical and chemical interactions, and by resolving the relevant temporal and spatial scales. These simulations provide unprecedented physical insights into the complex processes taking place in these engines, thus aiding designers in making judicious choices. The major focus of our research in FY 2014 has been towards the development and validation of robust and predictive nozzle flow, spray and turbulent combustion models for ICE applications aided by HPC tools.

APPROACH

During the past year, we have focused on improving the fidelity of nozzle flow simulations and couple it with a new EE spray model [4]. Our approach to improved modeling capability is highlighted here:

- In-nozzle flow simulations are performed by implementing a Homogeneous Relaxation Model-based two-phase flow model within a volume of fluid approach [5]. The boundary conditions for the simulations are obtained from X-ray phase-contrast imaging at Argonne which includes the needle-lift and wobble profiles [6]. The multi-hole geometry information is obtained from a previous study [7]. The SOI and EOI transients were captured using very small spatial resolutions to ensure grid convergence and correspondingly small temporal resolutions to ensure code stability.
- An Eulerian single-fluid (mixture) approach by Vallet et al. [8] is implemented for the coupled nozzle flow and spray simulations. The large scale flow features dominate rather than the small scale structures under the high Reynolds and Weber number conditions. The liquid mass fraction is transported with a model for the turbulent liquid diffusion flux into the gas. Closure for the liquid mass transport is based on a turbulent gradient flux model.
- In order to improve the load-balancing capability, METIS [9] was chosen to replace the original algorithm. METIS is widely known for its efficiency in partitioning complex geometries and its capabilities to minimize the connectivity and to enforce contiguousness between partitions. The METIS algorithm enabled significantly improved load-balance so that the simulations would not run out of memory and crash.
- A two-component mixture of n-dodecane and m-xylene (called SR23) was considered as a surrogate to represent diesel fuel. A detailed mechanism (2,885 species, 11,754 reactions) from Lawrence Livermore National Laboratory [10] was reduced for three-dimensional simulations to obtain a mechanism consisting of 163 species and 887 reactions. A multiple representative interactive flamelet (mRIF) advanced turbulent combustion model was also developed [11] and coupled together with the reduced chemical kinetic mechanism. The reduced mechanism together with the mRIF model was extensively validated against Engine Combustion Network data available in the literature.

RESULTS

Some critical findings associated with the five different objectives for FY 2014 highlighted before are discussed here. Further details can be obtained from authors' publications in FY 2014. Figure 1 plots the mass flow rate through each orifice for a five-hole injector [7] (only three orifices are shown) with needle off-axis motion along the +x direction and lift profile. It should be noted that the peak needle-off axis motion occurs during low lifts i.e., at 0.4 ms and 1.5 ms (approximately) and at ~0.9 ms which coincides with the peak needle lift of ~225 µm. Large hole-to-hole differences in the velocity stream lines (and hence mass flow rates) are observed at low needle lift positions. At 0.9 ms, the needle lift is high; hence it does not influence the flow development in the sac and orifice entry region. The above analysis shows that if the needle is lifted more than 100 µm, the off-axis motion does not influence the flow development. It should also be noted that hole # 2 is mostly affected by the needle off-axis motion and the flow enters the orifice in a toroidal fashion. Grid convergence was observed with about 5 µm resolution for in-nozzle flow simulations.

Figure 2 plots void fraction through a single-hole injector during the EOI process at about 2.147 ms from SOI. The simulation conditions mimic experiments done at the Advanced Photon Source (APS) using a diesel surrogate fuel at high injection and back pressures. The figure shows that once the needle closes, the liquid fuel still has momentum which results in cavitation inception at the needle seat region. At the same time-instant in the orifice region, due to the low pressures, the dissolved gases in the liquid fuel expand still resulting in voids. In the next time instant (not shown here), the ambient gas is ingested back to the orifice. The simulations were performed with a minimum cell size of 5 µm and time

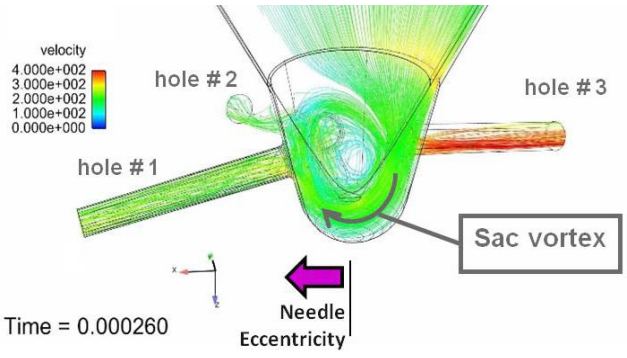

FIGURE 1. Three-dimensional transient simulation of a multi-hole injector with specified needle lift and wobble profile. The differences in mass flow rates between different orifices are clearly observed, especially during the needle transients.

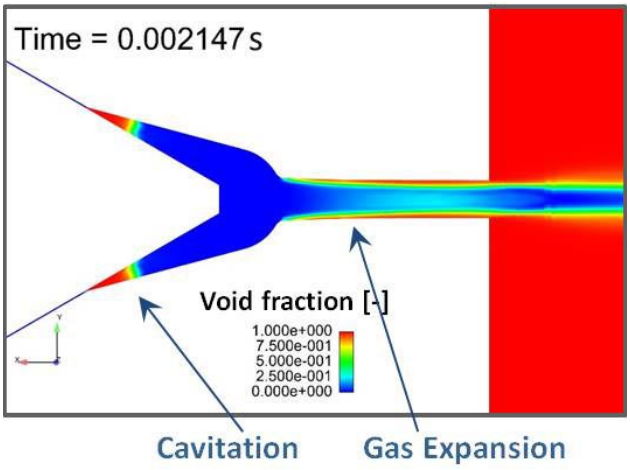

FIGURE 2. The voids generated inside an injector during end of injection transients for a single-hole injector simulation done by mimicking the experiments at the APS. The simulations show distinct regions of void due to cavitation and air expansion.

step size of $1x10^{-9}$. The simulations took about three weeks on 128 processors.

Figure 3 shows validation of the coupled EE model against X-ray radiography data at 0.022 ms by plotting the projected density in $\mu g/mm^2$ units. The EE model captures the near-field fuel distribution very well in terms of penetration and dispersion. Further details about the experiments and simulations can be found in Ref. [4]. The projected density vs. transverse distance at 2 mm from the injector exit shows that grid convergence is observed with about 10 µm resolution in the dense spray regime.

The comparison of ignition delay for SR23 and n-dodecane from both experiments and computations is reported in Figure 4 (top) at different ambient temperatures. In the simulation, ignition delay was defined from the SOI to the time of maximum rate of peak temperature rise. Excellent predictions for ignition delay were obtained for both SR23 and n-dodecane compared to the available experimental results at different ambient temperatures. Addition of m-xylene slows down the reactivity and delays ignition, and the simulations captured this trend very well at all the ambient temperatures. The higher ignition delay of the SR23 mixture compared to that of neat n-dodecane allows more time for fuel-air mixing before the start of combustion. The lift-off length was defined as the distance from the nozzle exit to the point where the OH mass fraction reaches 14% of its maximum in the quasi steady-state portion of the simulation. In Figure 4 (bottom), it can be seen that the lift-off lengths of neat n-dodecane at different ambient temperatures can be predicted well. However, under-predictions were observed for SR23, especially at lower ambient temperatures.

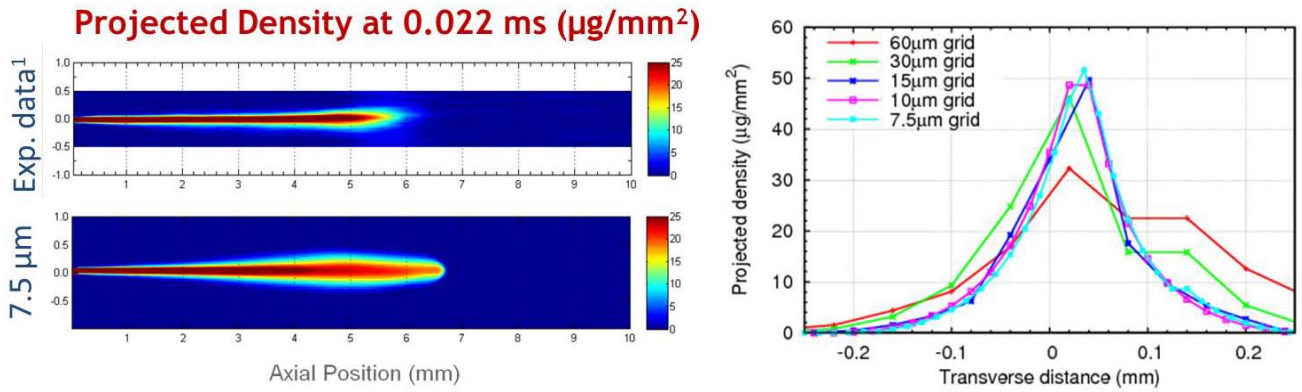

FIGURE 3. (Left) Projected density contours from the coupled EE simulations compared against the experimental data from APS. (Right) Projected density vs. transverse distance at an axial location of 2 mm from the nozzle exit for different minimum grid sizes.

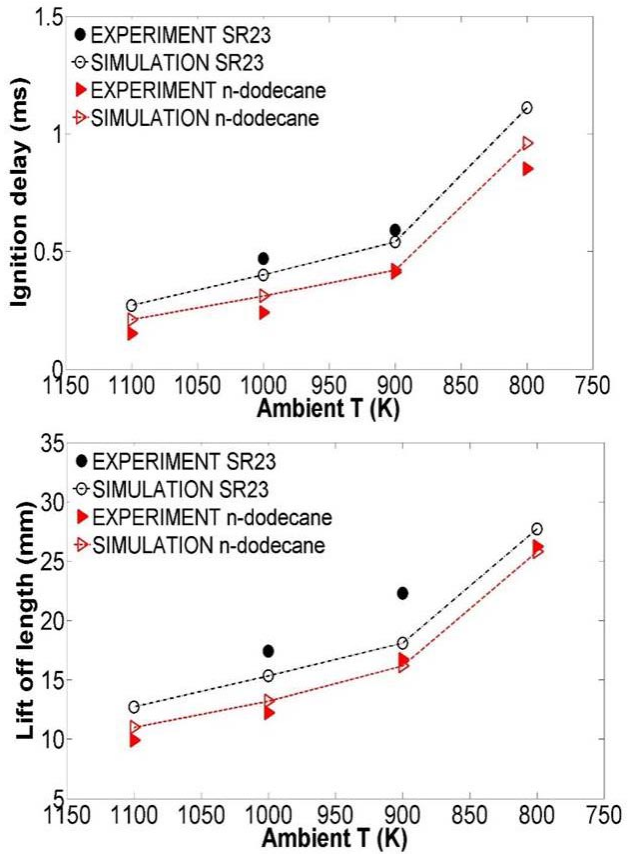

FIGURE 4. Ignition delay and flame lift-off length vs. ambient temperature for simulations using a multi-component mixture of n-dodecane and m-xylene compared against experimental data from the Engine Combustion Network. For reference the corresponding results for n-dodecane are also plotted.

The use of higher fidelity nozzle flow, spray, and turbulence models along with grid convergent resolutions significantly increases the computational cost for simulations. While these simulation approaches provide a path forward for predictive ICE simulations, the computational cost could be prohibitive for engine design and optimization applications. We are also focusing towards developing HPC tools to effective load balance the simulations so that the benefits of multi-processor simulations can be fully realized. Towards this, in FY 2012 a load balancing approach was implemented in which enabled HPC simulations up to 256 processors [9]. Figure 5 presents simulations on 128–1,024 processors showing grid-convergence of pressure and emissions. The simulations were performed for a single-cylinder Caterpillar engine. The simulations show global parameters like pressure grid convergences at a coarser resolution, compared to emissions which grid convergence at 0.125 mm for Reynolds-averaged Navier-Stokes calculations.

CONCLUSIONS

- In-nozzle flow simulations performed can capture the mass flow and cavitation trends very well. For the first time, the simulations accounted for needle transients including the wobble. Differences in mass flow rates between different plumes were observed especially during the needle transients.
- The high-fidelity nozzle flow simulations provide unprecedented insights into the EOI transients and together with APS measurements, enhanced the understanding of the true physics during the EOI. At least 5-μm resolution was necessary to capture in-nozzle flow trends.
- Coupled EE simulations were performed to capture the near-nozzle dense spray region and were validated against X-ray radiography data from Argonne. The coupled EE model was able to predict the spray penetration and dispersion quite well, especially in the near nozzle region and during the initial transients.

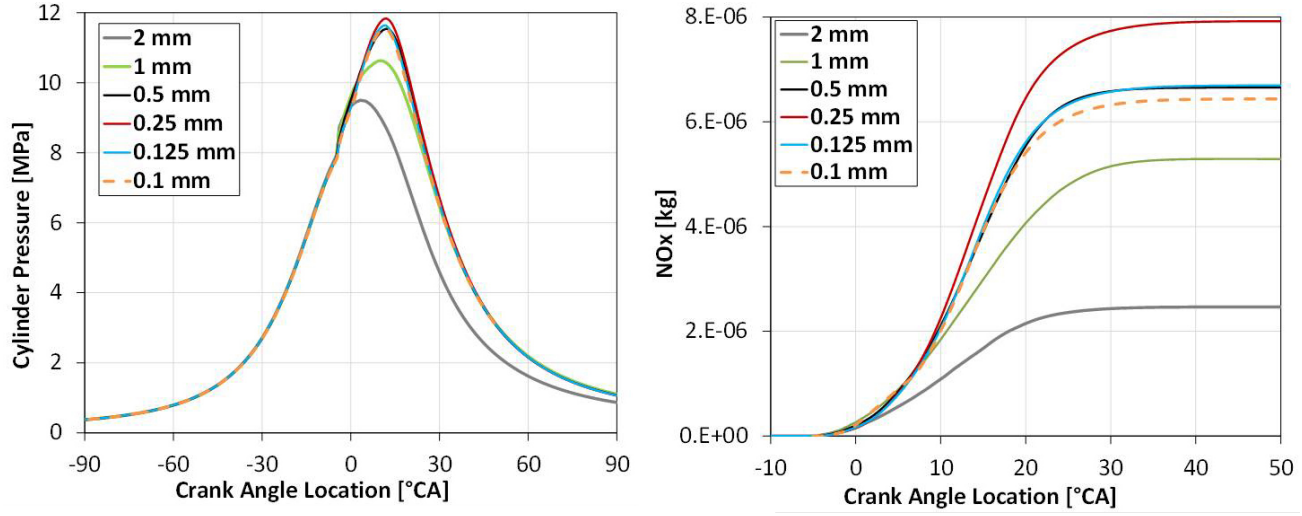

FIGURE 5. (Left) Cylinder pressure and (Right) oxides of nitrogen emissions for different minimum grid sizes, for simulations performed on a Caterpillar single-cylinder engine.

- SR23 chemical kinetic model along with an mRIF turbulent combustion model was able to capture the ignition delay and flame lift-off length characteristics quite well. The reduced mechanism is available from Argonne for other researchers to download and test.
- Load-balancing in engine simulations was significantly improved by the implementation of METIS algorithm thus enhancing the computational speedup [9]. Significant speedup was demonstrated up to 1,000 processors for a typical engine simulation. Global parameters were observed to grid converge at a coarser resolution compared to the local parameters such as emissions.

REFERENCES

1. Richards, K.J., Senecal, P.K., Pomraning, E., CONVERGE (Version 2.1.0) Manual, Convergent Science, Inc., Middleton, WI, 2013.

2. http://www.sandia.gov/ecn/

3. Som, S., Aggarwal, S.K., 2010, *Combustion and Flame*, Vol. 157, pp.1179-1193.

4. Q. Xue, M. Battistoni, S. Som, S. Quan, P.K. Senecal, E. Pomraning, D. Schmidt, "Eulerian CFD modeling of coupled nozzle flow and spray with validation against x-ray radiography data," *SAE International Journal of Fuels and Lubricants,* 7(2):2014, doi:10.4271/2014-01-1425.

5. S. Quan, H. Zhao, M. Dai, E. Pomraning, P.K. Senecal, Q. Xue, M. Battistoni, S. Som, "Validation of a three-dimensional internal nozzle flow model including automatic mesh generation and cavitation effects," *Journal of Engineering for Gas Turbine and Power* 136 (9), 092603: 1-10, 2014.

6. Kastengren, A.L., Tilocco, F.Z., Powell, C.F., Manin, J., Pickett, L.M., Payri, R., and Bazyn, T., Accepted in *Atomization and Sprays* (2013).

7. Payri, R., Gil, A., Plazas, A.H., and Gimenez, B., *SAE World Congress* Paper No. 2004-01-2010 (2004).

8. Vallet, A., Burluka, A.A., & Borghi, R. "Development of a Eulerian Model for the Atomization of a Liquid Jet," *Atomization and Sprays* 11, 619-642, 2001.

9. S. Som, D.E. Longman, S.M. Aithal, R. Bair, M. Garcia, S.P. Quan, K.J. Richards, P.K. Senecal, *SAE Paper No.* 2013-01-1095, 2013.

10. M. Mehl, W.J. Pitz, C.K. Westbrook, S.M. Sarathy, Fifth European Combustion Meeting (ECM2011), Cardiff University, Wales, UK, June 28 – July 1, 2011.

11. P. Kundu, Y. Pei, S. Som, M. Wang, R. Mandhapati, "Evaluation of Turbulence Chemistry Interactions under Diesel Engine conditions with a Multi-Flamelet RIF model," *Atomization and Sprays*, 24 (9): 779-800, 2014.

SELECTED FY 2014 PUBLICATIONS

1. M. Battistoni, D.J. Duke, A.L. Kastengren, A.B. Swantek, F.Z. Tilocco, C.F. Powell, S. Som, "Effect of Non-Condensable Gas on Cavitating Fuel Nozzles," accepted *Atomization and Sprays*, 2014.

2. A.I. Ramirez, S.K. Aggarwal, S. Som, T. Rutter, D.E. Longman, "Effects of blending a heavy alcohol ($C_{20}H_{40}O$) with diesel in a heavy-duty compression ignition engine," *Fuel*, 10.1016/j.fuel.2014.06.039, 2014.

3. P. Kundu, Y. Pei, S. Som, M. Wang, R. Mandhapati, "Evaluation of Turbulence Chemistry Interactions under Diesel Engine conditions with a Multi-Flamelet RIF model," *Atomization and Sprays*, 24 (9): 779-800, 2014.

4. P.K. Senecal, E. Pomraning, Q. Xue, S. Som, S. Banerjee, B. Hu, K. Liu, J. Deur, "Large Eddy simulation of vaporizing sprays considering multi-injection averaging and grid-convergent mesh resolution," *Journal of Engineering for Gas Turbine and Power* 136 (11), 111504: 1-13, 2014.

5. S. Quan, H. Zhao, M. Dai, E. Pomraning, P.K. Senecal, Q. Xue, M. Battistoni, S. Som, "Validation of a three-dimensional internal nozzle flow model including automatic mesh generation and cavitation effects," *Journal of Engineering for Gas Turbine and Power* 136 (9), 092603: 1-10, 2014.

6. Q. Xue, M. Battistoni, S. Som, S. Quan, P.K. Senecal, E. Pomraning, D. Schmidt, "Eulerian CFD modeling of coupled nozzle flow and spray with validation against x-ray radiography data," *SAE International Journal of Fuels and Lubricants,* 7(2):2014, doi:10.4271/2014-01-1425.

7. M. Battistoni, Q. Xue, S. Som, E. Pomraning, "Effect of off-axis needle motion on internal nozzle and near exit flow in a multi-hole diesel injector," *SAE International Journal of Fuels and Lubricants,* 7(1):2014, doi:10.4271/2014-01-1426.

8. S. Quan, M. Dai, E. Pomraning, P.K. Senecal, K. Richards, S. Som, S. Skeen, J. Manin, L.M. Pickett, "Numerical simulations of supersonic diesel spray injection and the induced shock," *SAE International Journal of Fuels and Lubricants,* 7(1):2014, doi:10.4271/2014-01-1423.

9. Z. Luo, S. Som, S.M. Sarathy, M. Plomer, W.J. Pitz, D.E. Longman, T. Lu, "Development and validation of an n-Dodecane skeletal mechanism for diesel spray-combustion applications," *Combustion Theory and Modeling*, doi:10.1080/13647830.2013.872807, 2014.

10. M. Battistoni, S. Som, D.E. Longman, "Comparison of mixture and multi-fluid models for in-nozzle cavitation prediction," *Journal of Engineering for Gas Turbine and Power* 136 (6), 061506: 1-12, 2014.

11. M. Wang, M. Raju, E. Pomraning, P. Kundu, Y. Pei, S. Som, "Comparison of Representative Interactive Flamelet and Detailed Chemistry based combustion models for internal combustion engines," *Proceedings of the ASME 2014 Internal Combustion Engine Division Fall Technical Conference*, ICEF2014-5522, Columbus, IN, October 2014.

12. P.K. Senecal, S. Mitra, E. Pomraning, Q. Xue, S. Som, S. Banerjee, B. Hu, K. Liu, D. Rajamohan, J.M. Deur, "Modeling fuel spray vapor distribution with large eddy simulation of multiple realizations," *Proceedings of the ASME 2014 Internal Combustion Engine Division Fall Technical Conference*, ICEF2014-5488, Columbus, IN, October 2014.

13. J. Kodavasal, C. Kolodziej, S. Ciatti, S. Som, "CFD Simulation of Gasoline Compression Ignition," *Proceedings of the ASME 2014 Internal Combustion Engine Division Fall Technical Conference*, ICEF2014-5591, Columbus, IN, October 2014.

14. Y. Pei, W. Liu, M. Mehl, T. Lu, W.J. Pitz, S. Som, "A multi-component blend as a diesel fuel surrogate for compression ignition engine applications," *Proceedings of the ASME 2014 Internal Combustion Engine Division Fall Technical Conference*, ICEF2014-5625, Columbus, IN, October 2014.

15. Y. Pei, R. Shan, S. Som, T. Lu, D.E. Longman, M.J. Davis, "Global sensitivity analysis of a diesel engine simulation with multi-target functions," SAE Paper No. 2014-01-1117, *SAE 2014 World Congress,* Detroit, MI, April 2014.

16. M. Battistoni, A.L. Kastengren, C.F. Powell, S. Som, "Fluid Dynamics modeling of End-of-Injection Process," *ILASS Americas 26th Annual Conference on Liquid Atomization and Spray Systems*, Portland, OR, May 2014.

17. S.P. Quan, M. Dai, K. Richards, P.K. Senecal, E. Pomraning, S. Som, "Compressible VOF-Based simulations of high pressure fuel spray injection," *ILASS Americas 26th Annual Conference on Liquid Atomization and Spray Systems*, Portland, OR, May 2014.

18. Q. Xue, M. Battistoni, S.P. Quan, P.K. Senecal, E. Pomraning, D.P. Schmidt, S. Som, "Eulerian Modeling of Fully-Coupled Diesel Injector Flow and Sprays," *ILASS Americas 26th Annual Conference on Liquid Atomization and Spray Systems*, Portland, OR, May 2014.

19. P. Kundu, Y. Pei, S. Som, "Combustion modeling under diesel engine conditions with multi-flamelet RIF model," *Spring Technical Meeting of the Central States Section of the Combustion Institute*, Tulsa, OK, March 2014.

20. Y. Pei, W. Liu, M. Mehl, S. Som, T. Lu, W.J. Pitz, "A multi-component blend as a diesel fuel surrogate for compression ignition engine applications," *Spring Technical Meeting of the Central States Section of the Combustion Institute*, Tulsa, OK, March 2014.

21. Y. Pei, E.R. Hawkes, S. Kook, G.M. Goldin, S. Som, "An analysis of the structure of Spray A flame using TPDF modelling," *Spring Technical Meeting of the Central States Section of the Combustion Institute*, Tulsa, OK, March 2014.

SPECIAL RECOGNITIONS & AWARDS/ PATENTS ISSUED

1. High Performance Computing Innovation Excellence Award from International Data Corporation, June 2014

2. Invitee to US-Frontiers of Engineering workshop organized by National Academy of Sciences (only 100 people under the age of 45 were invited)

II.7 Fuel Injection and Spray Research Using X-Ray Diagnostics

Christopher F. Powell (Primary Contact),
Alan Kastengren
Argonne National Laboratory
9700 S. Cass Ave.
Argonne, IL 60439

DOE Technology Development Manager
Leo Breton

Overall Objectives

- Study the mechanisms of spray atomization by performing detailed, quantitative measurements in the near-nozzle region of sprays from fuel injectors.
- Make the measurements under conditions as near as possible to those in modern engines.
- Utilize the results of our unique measurements in order to advance the state of the art in spray modeling.
- Provide industrial partners in the spray and engine community with access to a unique and powerful diagnostic of fuel injection and sprays.

Fiscal Year (FY) 2014 Objectives

- Perform measurements of fuel density, needle life, and nozzle geometry using the hardware and conditions of the Engine Combustion Network (ECN). Share this data with computational modelers for validation and improvement of spray modeling.
- Develop diagnostics for fuel flow inside injectors, including measurements of cavitation and gas ingestion at the end of injection.
- Explore the use of X-ray diagnostics for other advanced combustion applications, such as droplet sizing, fluid dynamics of sprays, and chemical kinetics.

FY 2014 Accomplishments

- Completed measurements of the internal geometry of all 12 samples of the ECN "Spray G" gasoline injectors.
- Organized the Internal Geometry and Nozzle Flow topic at the ECN3 Workshop.
- In collaboration with University of Massachusetts Amherst, completed simulations of cavitating nozzle flows and compared them to X-ray measurements.
- Completed the fabrication of a new spray chamber which was used to perform three-dimensional tomography of sprays at elevated pressure and temperature.
- Performed measurements of near-nozzle droplet size for the ECN "Spray A" diesel injection conditions.
- Completed measurements of shot-to-shot variation of the density of diesel sprays.

Future Directions

- The ECN has begun to distribute the "Spray G" gasoline direct-injection injectors. The needle motion and fuel distribution from the injectors will be measured using X-ray diagnostics, and will be made available to experimental and modeling partners in the ECN.
- Spray measurements will be done in conjunction with Argonne's Engine and Emissions Research group. We will measure the fuel/air mixing in a gasoline direct-injection system that is being used in engine tests of advanced combustion strategies. The high precision spray measurements will be used to validate simulations of the engine's combustion process, providing these research programs with the data that is needed for high-fidelity modeling.
- Further studies of cavitation will be done to improve the community's understanding of this phenomenon and its impact on fuel/air mixing and injector internal flows. Cavitation will be studied in an improved X-ray transparent nozzle, enabling unprecedented accuracy of the results.
- Studies of injector dribble will be performed. Dribble is the undesirable ejection of fuel after the nominal end of the injection event; the fuel is slow-moving, poorly atomized, and likely to generate particulate matter emissions. Measurements will be performed under conditions similar to those in an optical engine at Sandia National Laboratories; the results from the two labs will be combined to get a comprehensive measurement of the phenomenon. With quantification of the causes of dribble, injector manufacturers may be able to minimize its impact.

INTRODUCTION

Fuel injection systems are one of the most important components in the design of combustion engines

with high efficiency and low emissions. A detailed understanding of the fuel-injection process and the mechanisms of spray atomization can enable better engine performance. The limitations of visible light diagnostics in the near-nozzle region of the spray have spurred the development of X-ray diagnostics for the study of fuel sprays. X-rays are highly penetrative, and measurements are not complicated by the effects of scattering. The technique is non-intrusive, quantitative, highly time-resolved, and allows detailed measurements of the spray, even in the optically opaque region very near the nozzle.

APPROACH

The aim of this project is to develop and perform high-precision measurements of fuel injection and sprays to further the development of accurate computational spray models. These measurements are primarily performed at the Advanced Photon Source at Argonne National Laboratory. This source provides a very high flux beam of X-rays, enabling quantitative, time-resolved measurements of sprays with very high spatial resolution. A schematic of the experimental setup for X-ray radiography is shown in Figure 1; detailed descriptions of the experimental methods are given in [1] and [2]. X-ray radiography has a significant advantage over optical techniques in the measurement of sprays. Because the measurement is not complicated by the effects of scattering, there is a simple relation between the measured X-ray intensity and the mass of fuel in the path of the X-ray beam. This allows direct determination of the mass of fuel at any position in the spray as a function of time. The parameters of injection pressure, ambient pressure, and nozzle geometry are explored in detail, allowing the quantification of how each of these variables affects the structure of the spray.

In the process of making these measurements, we collaborate with industrial partners including engine and fuel-injection system manufacturers so that they have access to these diagnostics for improvement of their products. We also collaborate with spray modelers to incorporate this previously unknown information about the spray formation region into new models. This leads to an increased understanding of the mechanisms of spray atomization and facilitates the development of fuel injection systems designed to improve efficiency and reduce pollutants.

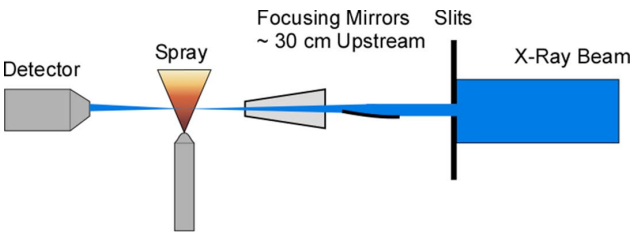

FIGURE 1. Schematic of the Experimental Setup

A significant amount of effort over the last few years has been spent performing experiments in collaboration with the ECN. This collaboration is led by Sandia National Laboratories, who has defined a specific set of operating conditions and procured a set of shared identical hardware. Argonne uses its full suite of unique injector and spray diagnostics to contribute to the ECN community. This partnership gets Argonne's data in the hands of simulation groups worldwide, and maximizes the impact of the work on improving computational simulations of sprays, combustion, and engines.

In addition to measurements of sprays, we explore other applications of X-ray diagnostics for combustion research. This includes X-ray imaging of the internal components of fuel injectors while they are in operation; this diagnostic allows injector manufacturers to develop and optimize injector designs. Measurements of cavitating flows provides unique data to improve the fundamental understanding of this internal fuel flow and its role in spray atomization, as well as the relationship between injector geometry, cavitation, and nozzle damage. Recent measurements have also evaluated the use of X-rays as a diagnostic for shock tubes, enabling better measurements of combustion kinetics to improve engine modeling. We also continue to develop X-ray measurements of droplet sizing. These measurements can determine the Sauter mean diameter of the fuel parcels in the near-nozzle region, a parameter that has never before been available for validation of primary breakup models.

RESULTS

Argonne's has continued its work studying the ECN "Spray A" and "Spray B" diesel operating conditions [3], and the data are now being used for validation of injector and spray models, including models that incorporate the eccentric needle motion when calculating fuel flow [4]. At the ECN3 Workshop in FY 2014, Argonne's data was used for validation by at least six different spray modeling groups [5], see Figure 2. Through this involvement in ECN, the data are being actively used to improve spray models and simplify the development of clean, efficient engines.

In FY 2014, measurements of the internal geometry of all 12 samples of the ECN "Spray G" gasoline injectors were completed. The measurement results are being analyzed and will be used to generate extremely precise three-dimensional models of these injectors. These models will be shared with partners in the ECN, giving the ECN simulation groups precise models of the

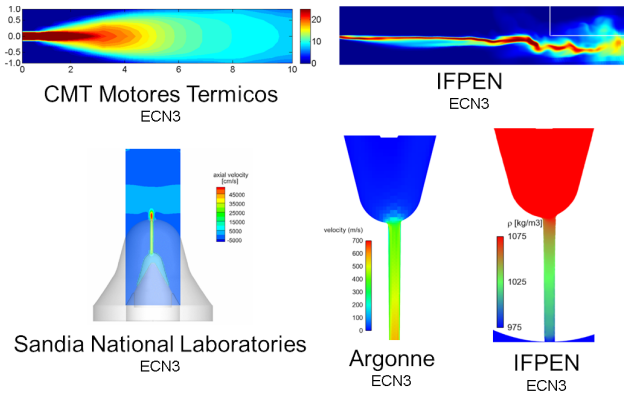

FIGURE 2. A collection of figures from the ECN3 Workshop, showing Argonne's X-ray measurements of nozzle geometry and fuel distribution being used for model development and validation.

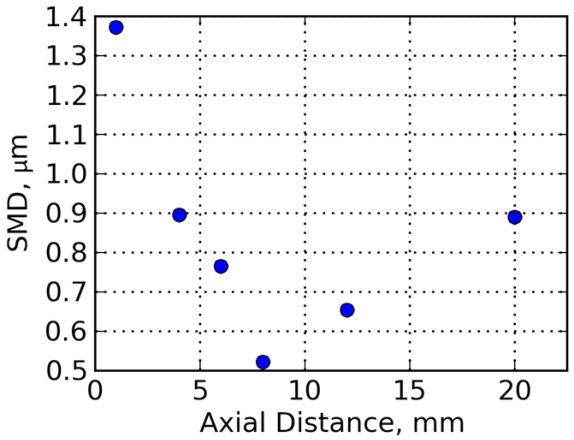

FIGURE 3. Sauter mean diameter (SMD) of fuel parcels in the spray versus distance from the nozzle for the ECN "Spray A" test condition. These measurements were performed using X-ray small angle scattering, a new diagnostic for measuring particle size in the near-nozzle region.

internal flow passages for predictions of injector internal flows.

The fabrication of a new spray chamber was completed in FY 2014. This chamber enables three-dimensional tomography measurements of sprays at elevated pressure and temperature for the first time. The first use of the chamber was to make three-dimensional measurements of sprays from a gasoline injector used in Argonne's engine research group. This device will significantly expand the capability to study modern fuel injection hardware, and will provide computational modelers with high precision data on multi-hole nozzles for model development and validation.

Also in FY 2014, measurements of the near-nozzle droplet size were performed at the ECN Spray A diesel injection conditions using ultra small-angle X-ray scattering. The results are shown in Figure 3, and were used for comparison with simulation predictions at the ECN3 Workshop [5]. This diagnostic is unique for measurements of droplet size in the region very close to the injection model, where spray models have very limited data for validation. With further development, this new diagnostic will become a valuable tool for measuring spray morphology, and provide another constraint to drive the development of accurate spray simulations.

A new method for measuring the shot-to-shot variation in sprays was developed in FY 2014. Improvements to X-ray optics and data acquisition have allowed quantitative measurements of the fuel mass without averaging multiple spray events. This has enabled the measurement of the fluctuation in the amount of fuel from one shot to another as a function of position and time [6]. In Figure 4, two-dimensional plots show the spatial distribution of the standard deviation during the steady-state portion of the spray. Note that at the higher ambient pressure, large fluctuations in fuel mass from one shot to the next develop closer to the nozzle than at 1 bar ambient. This method is the first to quantify shot to shot variations in absolute units of mass. The measurement allows testing of the repeatability of various injectors in terms of the local fuel density, as well as comparison to predictions of models that include shot-to-shot variations, such as large-eddy simulation.

Cavitation is an important problem in high-pressure fuel injection systems, such as those found in modern direct-injection diesel engines. Cavitation—where fuel in the injector vaporizes due to a drop in pressure—can cause mechanical damage to injector components and affect fuel/air mixing and thus efficiency and pollutant formation. State-of-the-art computer models for cavitation are now being incorporated into engine modeling software to account for these factors. However, there is little information available on the accuracy of these models because cavitation is very difficult to measure experimentally. In FY 2014, four papers were published in which Argonne's unique measurements of cavitating flow were used for the development and validation of computational models of internal nozzle flow [4,7-9]. These collaborations with modelers from both Argonne and the University of Massachusetts Amherst (Figure 5) have resulted in improvements to computational fluid dynamics solvers and cavitation models that are widely used in the U.S. auto industry. Improvements to those models will lead to a broader understanding of this complex physical phenomenon, as well as better and more accurate engine modeling software.

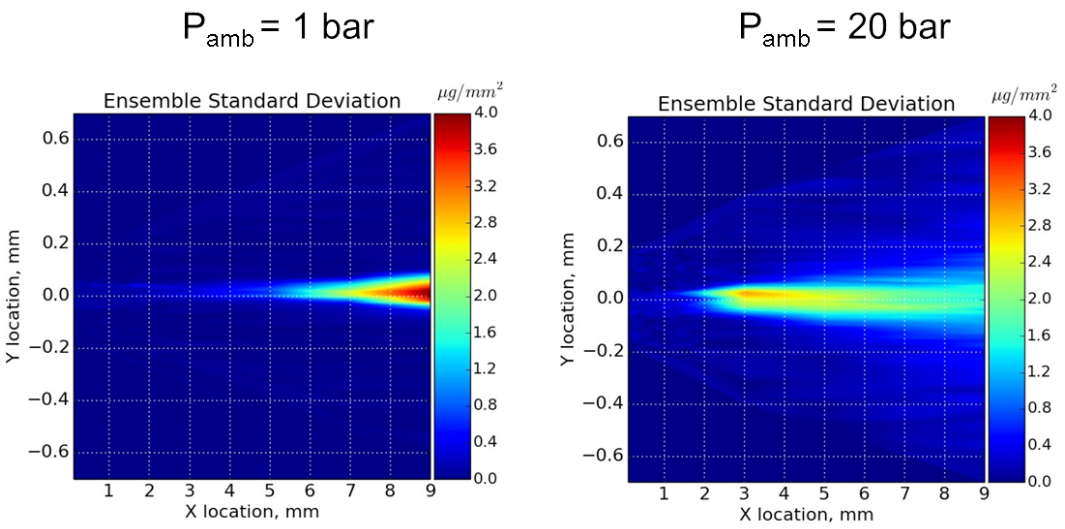

FIGURE 4. Two-dimensional maps of the standard deviation of the mass from sprays measured at 1 bar and 20 bar ambient pressure.

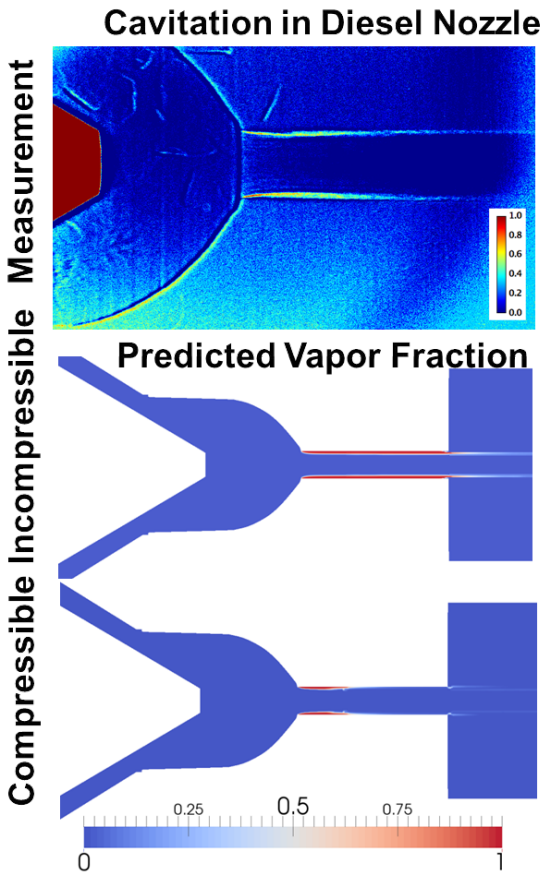

FIGURE 5. A comparison of X-ray measurements of cavitation in a steel nozzle (top) versus computational fluid dynamics simulations using incompressible (middle) and compressible (bottom) flow.

CONCLUSIONS

X-ray diagnostics can be used to help understand the flows inside the injector as well as the mixing of fuel and air in the engine. Such measurements are not possible using other imaging techniques, and represent a powerful data set for validating computational models of fuel flow. This data is crucial for the development of accurate spray models and for the detailed understanding of spray behavior. Improvements to these models will speed the development of cleaner, more efficient engines.

REFERENCES

1. "Time-Resolved Measurements of Supersonic Fuel Sprays using Synchrotron X-rays", C.F. Powell, Y. Yue, R. Poola, and J. Wang, *J. Synchrotron Rad.* 7:356-360 (2000).

2. "Spray Density Measurements Using X-Ray Radiography" A.L. Kastengren, C.F. Powell, *Journal of Automobile Engineering*, Volume 221, Number 6, 2007, pp 653-662.

3. "Engine Combustion Network (ECN): Measurements of Nozzle Geometry and Hydraulic Behavior", A.L. Kastengren, F.Z. Tilocco, C.F. Powell, J. Manin, L.M. Pickett, R. Payri, T. Bazyn. Atomization & Sprays 22 (12), pp 1011-1052 (2012).

4. Q. Xue, M. Battistoni, S. Som, D.E. Longman, H. Zhao, P.K. Senecal, E. Pomraning, "Three-dimensional Simulations of the Transient Internal Flow in a Diesel Injector: Effects of Needle Movement," 25th Annual Conference on Liquid Atomization and Spray Systems, Pittsburg, PA, May 2013.

5. http://www.ca.sandia.gov/ecn/workshop/ECN3.php

6. "End of injection, mass expulsion behaviors in single hole diesel fuel injectors", A.B. Swantek, D. Duke, F.Z. Tilocco, N. Sovis, C. F. Powell, A.L. Kastengren. 26th Annual Conference on Liquid Atomization and Spray Systems, Portland, OR, May 2014.

7. "X-ray Imaging of Cavitation in Diesel Injectors", D.J. Duke, A.B. Swantek, F.Z. Tilocco, C.F. Powell, A.L. Kastengren, K. Fezzaa, K. Neroorkar, M. Moulai, D.P. Schmidt. SAE International Journal of Engines 7 no. 2 pp. 1003-1016, July 2014.

8. "High Resolution Large Eddy Simulations of Cavitating Gasoline-Ethanol Blends", D.J. Duke, D. Schmidt, K. Neroorkar, A.L. Kastengren, C.F. Powell, International Journal of Engine Research 14: 578-589, October 2013.

9. "Comparing Simulations and X-ray Measurements of a Cavitating Nozzle", D. Duke, A.L. Kastengren, A. Swantek, N. Sovis, K. Fezzaa, K. Neroorkar, M. Moulai, C. Powell, D. Schmidt. 26th Annual Conference on Liquid Atomization and Spray Systems, Portland, OR, May 2014.

FY 2014 PUBLICATIONS

1. "X-ray Imaging of Cavitation in Diesel Injectors", D.J. Duke, A.B. Swantek, F.Z. Tilocco, C.F. Powell, A.L. Kastengren, K. Fezzaa, K. Neroorkar, M. Moulai, D.P. Schmidt. SAE International Journal of Engines 7 no. 2 pp. 1003-1016, July 2014.

2. "Time-Resolved X-Ray Radiography of Sprays from Engine Combustion Network Spray A Diesel Injectors", A.L. Kastengren, F.Z. Tilocco, D.J. Duke, C.F. Powell, S. Moon, X. Zhang, Atomization & Sprays 24 (3), pp 251-272, February 2014.

3. "Synchrotron X-Ray Techniques for Fluid Dynamics", A.L. Kastengren, C.F. Powell. Experiments in Fluids 55:1686, February 2014.

4. "High Resolution Large Eddy Simulations of Cavitating Gasoline-Ethanol Blends", D.J. Duke, D. Schmidt, K. Neroorkar, A.L. Kastengren, C.F. Powell, International Journal of Engine Research 14: 578-589, October 2013.

5. "X-ray Imaging of Cavitation in Diesel Injectors", D.J. Duke, A.B. Swantek, F.Z. Tilocco, C.F. Powell, A.L. Kastengren, K. Fezzaa, K. Neroorkar, M. Moulai, D.P. Schmidt. Society of Automotive Engineers, Paper 2014-01-1404 (2014).

6. "Comparison of Near-Field Structure and Growth of a Diesel Spray Using Light-Based Optical Microscopy and X-Ray Radiography", L.M. Pickett, J. Manin, A.L. Kastengren, C.F. Powell. Society of Automotive Engineers, Paper 2014-01-1412 (2014).

7. "Fluid Dynamics Modeling of the End-of-Injection Process", M. Battistoni, S. Som, C.F. Powell, A.L. Kastengren, 26th Annual Conference on Liquid Atomization and Spray Systems, Portland, May 2014.

8. "Comparing Simulations and X-ray Measurements of a Cavitating Nozzle", D. Duke, A.L. Kastengren, A. Swantek, N. Sovis, K. Fezzaa, K. Neroorkar, M. Moulai, C. Powell, D. Schmidt. 26th Annual Conference on Liquid Atomization and Spray Systems, Portland, OR, May 2014.

9. "End of injection, mass expulsion behaviors in single hole diesel fuel injectors", A.B. Swantek, D. Duke, F.Z. Tilocco, N. Sovis, C.F. Powell, A.L. Kastengren. 26th Annual Conference on Liquid Atomization and Spray Systems, Portland, OR, May 2014.

II.8 Large Eddy Simulation Applied to Advanced Engine Combustion Research

Joseph C. Oefelein (Primary Contact), Guilhem Lacaze, Layal Hakim
Sandia National Laboratories
7011 East Avenue, Mail Stop 9051
Livermore, CA 94551-0969

DOE Technology Development Manager
Leo Breton

Overall Objectives

- Combine unique state-of-the-art simulation capability based on the large-eddy simulation (LES) technique with DOE Advanced Engine Combustion R&D activities.
- Perform companion simulations that directly complement optical engine and supporting experiments being conducted at the Sandia Combustion Research Facility and elsewhere.
- Maximize benefits of high-performance massively-parallel computing for advanced engine combustion research using DOE leadership-class computer platforms.
- Apply high-resolution LES and first-principles models at conditions unattainable using direct numerical simulation to complement key experiments and bridge gap between basic/applied research:
  - Perform detailed simulations that match operating conditions (e.g., high Re).
  - Retain full system coupling and incorporate detailed physics and geometry.
  - Establish validated correspondence between available data and LES.
  - Extract high-fidelity data from validated LES not available from experiments.
  - Use these data to understand and develop affordable models for engineering.

Fiscal Year (FY) 2014 Objectives

- Implement real-fluid thermodynamics and transport model designed to handle high-pressure supercritical injection processes.
- Perform LES of the Engine Combustion Network (ECN) Spray-A case in collaboration with Pickett et al. and present results at the 3rd ECN Workshop, SAE International, and AEC meetings.
- Demonstrate fully-coupled first-principles LES of ECN Spray-A and pathway for development of reduced order models for engineering.

FY 2014 Accomplishments

- An improved understanding of the transient structure of reacting diesel jets was established that demonstrated the effects of real-fluid thermodynamics and transport.
- Using these data, a systematic study of high-pressure transient mixing processes served to quantify the envelope of relevant physical conditions just prior to auto-ignition.
- This provided a detailed framework for simultaneous development of advanced combustion closures with optimized chemical mechanisms that efficiently capture turbulence-chemistry interactions and cool/hot flame ignition with equal fidelity.

Future Directions

- Continue to extend development of models and corresponding benchmark simulations to high-Reynolds-number, direct-injection processes for both diesel and gasoline direct injection engine applications over a wide range of pressures and temperatures.
- Perform detailed calculations and analysis of internal injector flow physics and heat transfer and extend treatment of complex geometry to optical engine configurations.

✧ ✧ ✧ ✧ ✧

INTRODUCTION

Imaging has long shown that under some high-pressure conditions, the presence of discrete two-phase flow processes becomes diminished. Under such conditions, liquid injection processes transition from classical sprays to dense-fluid jets, with no drops present. Using the insights gained from past theoretical studies that have quantified when and how this transition occurs. We have summarized a new theoretical

description that quantifies the effects of real fluid thermodynamics on liquid fuel injection processes as a function of pressure at typical diesel engine operating conditions. We then focused on the effects of real fluid thermodynamics and transport using the LES technique. Analysis was performed using the ECN (www.sandia.gov/ECN) Spray-A case. LES was performed by identically matching the operating conditions used in the experiments. Results were analyzed with emphasis placed on the state of the transient mixing field prior to auto-ignition and using this information to develop an optimal combination of models that simultaneously treat both the effects of turbulence and chemistry in a robust and efficient manner.

APPROACH

To enhance our understanding of the supercritical fuel injection at high pressures in the context of diesel engines, new theoretical findings reported last year that quantify when supercritical mixing is prevalent have been combined with high-fidelity LES to gain a more detailed view into transient mixing processes. Detailed LES calculations have been synchronized with the experiments performed by Pickett et al. as part of the ECN (www.ca.sandia.gov/ECN). The LES is performed using a single unified code framework called RAPTOR. Unlike conventional LES codes, RAPTOR is a direct numerical simulation solver that has been optimized to meet the strict algorithmic requirements imposed by the LES formalism. The theoretical framework solves the fully-coupled conservation equations of mass, momentum, total energy, and species for a chemically reacting flow. It is designed to handle high Reynolds number, high-pressure, real-gas and/or liquid conditions over a wide Mach operating range. It also accounts for detailed thermodynamics and transport processes at the molecular level, and is sophisticated in its ability to handle a generalized model framework in both the Eulerian and Lagrangian frames. A noteworthy aspect of RAPTOR is it was designed specifically for LES using non-dissipative, discretely conservative, staggered, finite-volume differencing. This eliminates numerical contamination of the subgrid-scale models due to artificial dissipation and provides discrete conservation of mass, momentum, energy, and species, which is an imperative requirement for high quality LES.

RESULTS

Using LES with real-fluid thermodynamics and transport, we have performed a series of studies aimed at understanding the transient turbulent mixing phenomena that dominates at high-pressure supercritical conditions. We focus on the Spray-A experiment, where liquid n-dodecane at 363 K is injected through a 0.09 mm diameter injector nozzle into a gaseous mixture at 900 K and 60 bar. The peak injection velocity is 620 m/s, which was selected to provide the same injected mass flow rate as the experiment. A synthetic turbulent signal with a turbulent intensity of 5% is superimposed on the bulk profile. Measurements have shown that the vessel temperature is almost uniform in space, which justifies the use of adiabatic walls in the simulation. The grid spacing in the vicinity of the injector exit is approximately 4 μm, and the grid stretched optimally in the downstream and radial directions. The integration time step is 2.3 ns.

Figure 1 shows a qualitative comparison of the injection sequence. The experimental images (left side) were obtained using a diffuser back illumination method, with the dense region highlighted using an arbitrary cut-off value in the gray scale. Based on recommendations from Picket et al., instantaneous shots of the LES temperature field (right side) were chosen for comparisons. Comparisons between respective images show qualitatively good agreement between the experiment and LES. Large structures present in the back-illumination images are also observed in the numerical results. The density of the n-dodecane jet is slightly above 700 kg/m^3 at the injector nozzle exit whereas the density of the ambient gas is 23 kg/m^3. The presence of strong density gradients is known to have a stabilization effect on hydrodynamic instabilities, which delays the destabilization of the jet. Once destabilization occurs, parcels of dense fluid detach from the compressed liquid jet. The presence of these fast-moving structures enhances local turbulence, which significantly affects mixing.

The vapor and liquid penetration trajectories are shown in Figure 2. In the LES, vapor penetration is detected by the most upstream point of the iso-surface characterized by a mixture fraction of Z = 0.01. The sensitivity of this value has been tested and penetration curves have less than 2% variation between Z = 0.01 and Z = 0.1. The time-resolved liquid core length was determined from high-speed Mie-scatter imaging using a 3% threshold of maximum intensity, which to some degree is an arbitrary value. Given the current premise that a distinct gas-liquid interface does not exist in this flow, defining the threshold associated with the compressed-liquid core requires additional analysis. Two liquid penetration curves are extracted from the LES to investigate. The first is based on a threshold of Z = 0.79, which is the value where the density changes the most with respect to Z. The second was based on a threshold of Z = 0.6, which is simply the value that provides the best match with the experimental data. Both thresholds lead to the same trend as in the experiment. A plateau is observed in the temporal evolution with differing

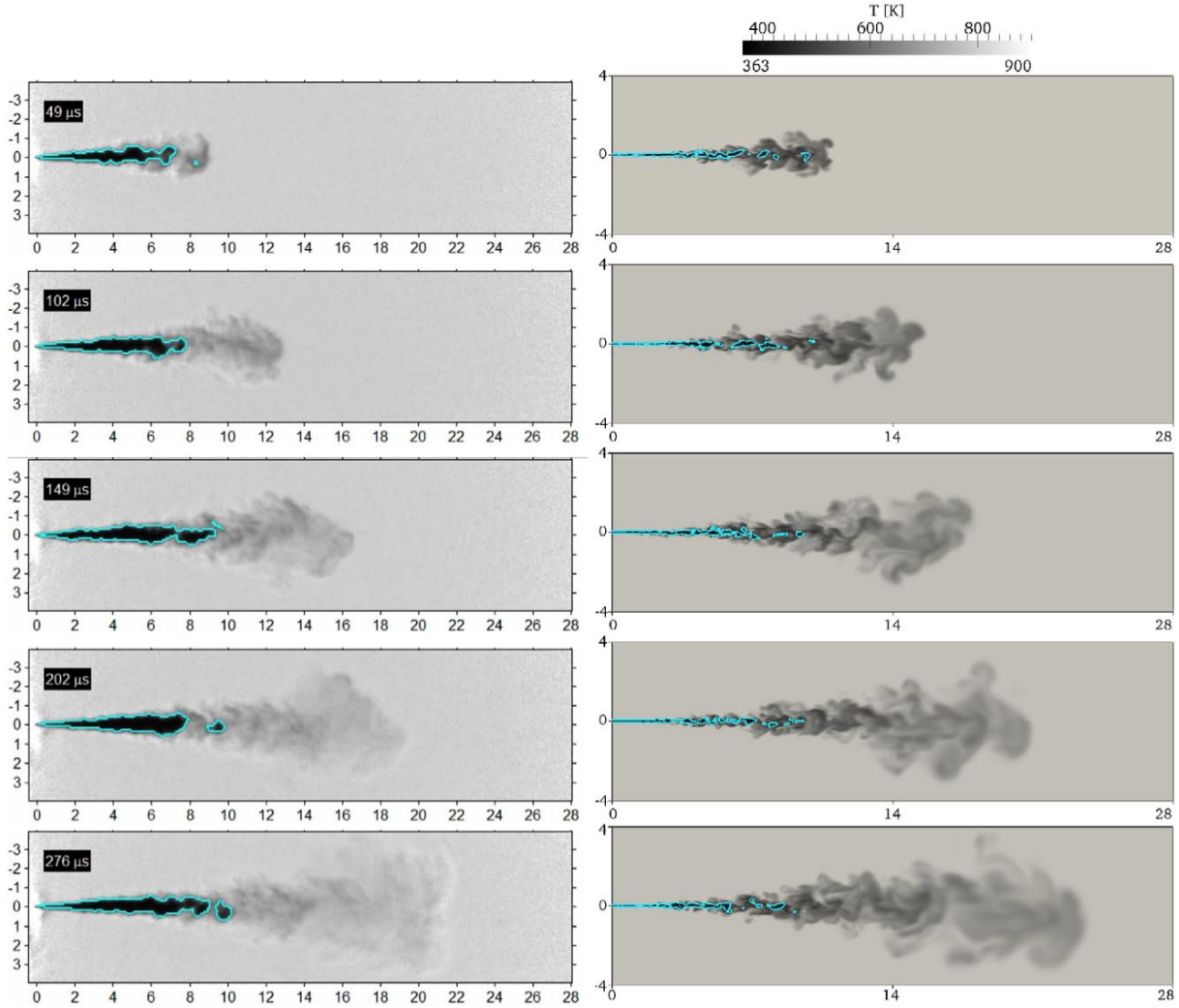

FIGURE 1. Injection sequence showing (a) shadowgraphs from Pickett et al. (www.sandia.gov/ECN) and (b) corresponding LES fields.

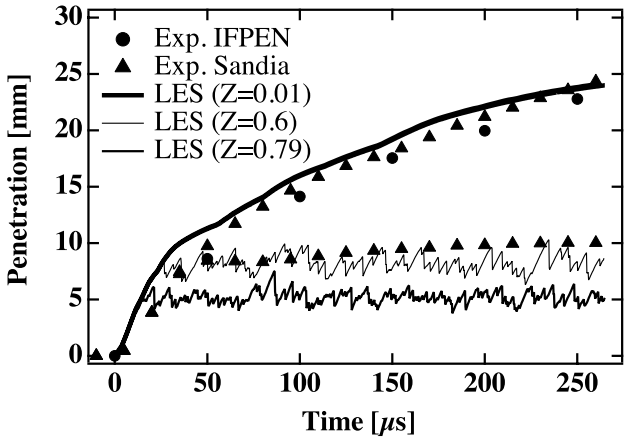

FIGURE 2. Vapor and liquid penetration trajectories of the jet. The time-resolved liquid core length was determined from high-speed Mie-scatter imaging using a 3% threshold of maximum intensity.

constant values of penetration depending on the mixture fraction value chosen.

A key focal point of this study is to better understand the local instantaneous mixture state of the jet immediately prior to auto-ignition, which occurs at approximately t = 260 µs after the start of injection. To better understand the state of the transient mixing field just prior to auto-ignition, a parameterization was performed to approximate local ignition delay times in the mixture. The adiabatic mixing temperature is discretized in mixture fraction space. Then a set of perfectly stirred reactor simulations were performed at each of these points using detailed chemical kinetics. As is consistent with experimental studies of diesel combustion, a two-stage ignition process is observed. The auto-ignition time is defined as that needed for the perfectly stirred reactor to reach 90% of its equilibrium

temperature. Using these results provides a way to quantify regions where auto-ignition is most likely to occur. Figure 3(a) shows the ignition delay time, (b) the magnitude of the mixture fraction gradient, (c) the magnitude of the axial-component of velocity, and (d) the typical location where the first ignition kernels are observed in the experiment. Analysis of the temporal evolution of these fields reveals that regions of the flow that are both flammable and have low values of scalar dissipation rate only appear after approximately 200 μs after the start of injection. Thus, the instantaneous flow structure at 260 μs was selected to highlight where the ignition delay time is less than 2.5 ms. This allows one to focus on the structure of the chemically active regions, which in turn now allow one to understand the envelop of pressure, temperature, and equivalence ratio that the detailed chemical mechanism must be reduced and optimized over. The current analysis reveals that there are many favorable locations that trigger chemical reactions within the mixing layer. Upstream locations before 200 diameters (18 mm) are where small pockets of flammable mixture appear first. However, Figures 3(b) and (c) show that strong velocity and mixture fraction gradients in these regions will prohibit the formation of the first flame kernels due to high stretch and scalar dissipation rate. Low gradients and larger flammable pockets are present between 200 and 250 diameters (18-22.5 mm) downstream of the injector, which is in qualitative agreement with the location of the initial kernels observed in the experiment. Current research in now focused on development of advanced combustion closures with an optimized chemical mechanism that efficiently captures turbulence-chemistry interactions and cool/hot flame ignition with equal fidelity and minimal computational overhead.

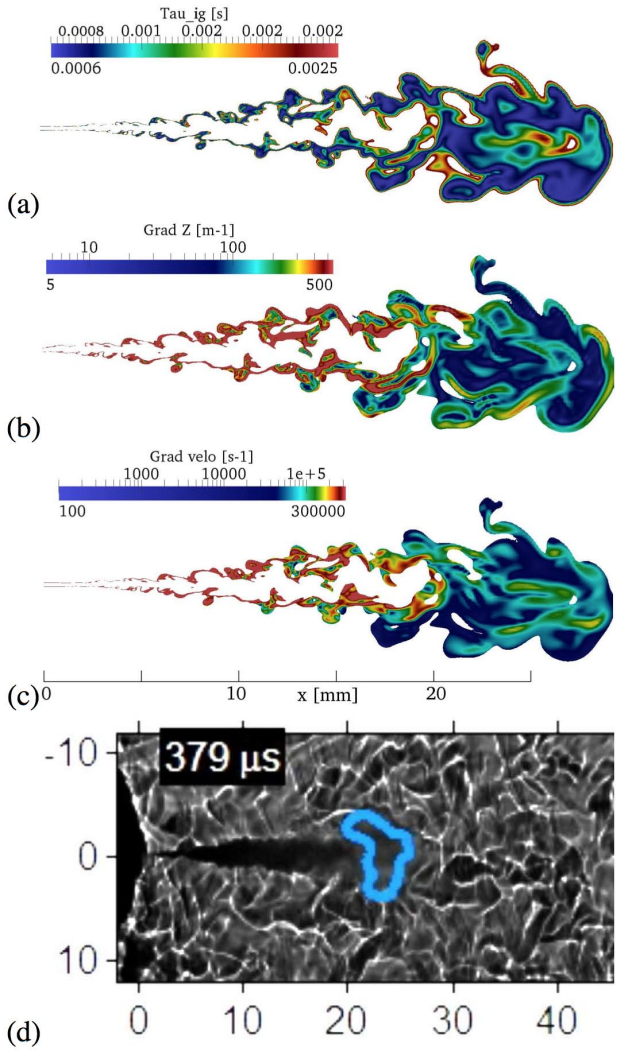

FIGURE 3. Instantaneous flow structure close to the ignition time (260 ms) where the ignition delay is less than 2.5 ms; (a) ignition delay time, (b) magnitude of mixture fraction gradient, (c) magnitude of axial-component of velocity, and (d) typical location of first ignition kernels in the experiment.

CONCLUSIONS

Current LES results have revealed the instantaneous three-dimensional structure of injected fuel jets with a degree of resolution that is not accessible by current experimental diagnostics or engineering computational fluid dynamics codes. Corresponding mixture fraction, temperature, density, Mach number, and speed of sound distributions were analyzed. Large density gradients associated with the compressed liquid core triggers a cascade of processes characteristic of supercritical flows, where high-pressure non-linear mixing and diffusion profoundly modify turbulent mixing. Once the destabilization of the dense core occurs, parcels of dense fluid detach. The presence of these fast-moving dense structures enhances local turbulence, which has a profound effect on local transient mixing of fuel and oxidizer and thus combustion. The present work also focused on the identification of the flammable regions resulting from non-ideal mixing. Using the observation that the scatter of temperature in mixture fraction space is small, a series of perfectly stirred reactors were computed to generate a mapping of ignition delay time as a function of mixture fraction. This provided an accurate way to localize potentially reactive mixtures. Analysis of the gradients of mixture fraction and velocity showed that a large region of flammable mixture with low gradients forms between 200 and 250 diameters downstream of the injector. In this region, any initial kernel would experience minimum heat losses and stretching. It is in this zone that ignition is observed experimentally. These findings represent a logical step toward advanced development of a robust ignition model and advanced combustion closures that use optimized

chemical mechanisms that simultaneously and efficiently capture turbulence-chemistry interactions and cool/hot flame ignition with equal levels of fidelity.

FY 2014 PUBLICATIONS/PRESENTATIONS

1. G. Lacaze, A. Misdariis, A. Ruiz, and J.C. Oefelein. Analysis of high-pressure diesel fuel injection processes using LES with real-fluid thermodynamics and transport. Proceedings of the Combustion Institute, 2015. Accepted.

2. M. Khalil, G. Lacaze, J.C. Oefelein, and H.N. Najm. Uncertainty quantification in LES of a turbulent bluff-body stabilized flame. Proceedings of the Combustion Institute, 2015. Accepted.

3. R.N. Dahms and J.C. Oefelein. Non-equilibrium gas-liquid interface dynamics in high-pressure liquid injection systems. Proceedings of the Combustion Institute, 2015. Accepted.

4. J. Manin, M. Bardi, L.M. Pickett, R.N. Dahms, and J.C. Oefelein. Microscopic investigation of the atomization and mixing processes of diesel sprays injected into high pressure and temperature environments. Fuel, 134:531–543, 2014. doi: 10.1016/j.fuel.2014.05.060.

5. J. Oefelein, G. Lacaze, R. Dahms, A. Ruiz, and A. Misdariis. Effects of real-fluid thermodynamics on high-pressure fuel injection processes. SAE International Journal of Engines, 7(3):1–12, 2014. doi: 10.4271/2014-01-1429.

6. R.N. Dahms and J.C. Oefelein. On the transition between two-phase and single-phase interface dynamics in multicomponent fluids at supercritical pressures. Physics of Fluids, 25(092103):1–24, 2013. doi: 10.1063/1.4820346.

7. J. Oefelein, "Effects of Real Fluid Thermodynamics on High-Pressure Fuel Injection Processes," invited speaker, Stanford University, October 8, 2013.

8. J. Oefelein, "Toward Predictive Simulations of Turbulent Multiphase Combustion Processes in Advanced Combustion Systems," invited speaker, Princeton University, October 11, 2013.

9. J. Oefelein, "Numerical Simulation of Turbulent Combustion," invited speaker, University of the Pacific, November 8, 2013.

10. J. Oefelein, "Needs Related to Development of LES for Propulsion Applications," invited speaker, United Technologies Research Center, East Hartford, Connecticut, December 9, 2013.

11. J. Oefelein, R. Dahms, G. Lacaze, A. Ruiz, "High-Fidelity Large Eddy Simulation of Direct Injection Processes in IC-Engines," Toyota, January 20, 2014.

12. J. Oefelein, G. Lacaze, A. Ruiz, R. Dahms, "Toward Detailed Simulations of Direct Injection Processes in IC-Engines, DOE Advanced Engine Combustion Meeting, February 11, 2014.

13. J. Oefelein, S. Skeen, L. Pickett, R. Dahms, G. Lacaze, A. Ruiz, "Synergy between Experiments and Simulations for Advanced Research and Development of Propulsion and Power Systems," presentation to Deputy Assistant Secretary for Transportation Reuben Sarkar, April 14, 2014.

14. J. Oefelein, R. Dahms, G. Lacaze, A. Ruiz, "New Discoveries from LES of Liquid Fuel Injection at High Pressures," invited speaker, NSF-AFOSR Turbulent Combustion Workshop, University of Michigan, June 9, 2014.

15. J. Oefelein, G. Lacaze, L. Hakim, "Large Eddy Simulation (LES) Applied to Advanced Engine Combustion Research," DOE Advanced Engine Combustion Annual Merit Review, Washington, DC, June 17, 2014.

16. J. Oefelein, "Obstacles to the efficient advancement of engineering codes, how they can be overcome, and how an effective program can be established," invited speaker, DOE Vehicle Technologies CFD Workshop," USCAR, Detroit, Michigan, August 18, 2014.

17. J. Oefelein, G. de Bord, G. Lacaze, R. Dahms, A. Ruiz, L. Hakim, F. Doisneau, "Progress and Needs in Modeling and Simulation of Engine Relevant Flows," DOE Advanced Engine Combustion Meeting, Detroit, Michigan, August 19, 2014.

SPECIAL RECOGNITIONS AND AWARDS/ PATENTS ISSUED

1. Excellence in Oral Presentation Award, SAE World Congress, 2014.

II.9 Collaborative Combustion Research with Basic Energy Sciences

S. Scott Goldsborough
Argonne National Laboratory (ANL)
9700 S. Cass Avenue
Bldg. 362
Argonne, IL 60439

DOE Technology Development Manager
Leo Breton

Overall Objectives

- Collaborate with combustion researchers within DOE's Offices of Basic Energy Sciences and Vehicle Technologies Office programs to develop and validate predictive chemical kinetic models for a range of transportation-relevant fuels.
- Acquire ignition time delay, and other necessary combustion data using ANL's rapid compression machine (RCM) at conditions representative of today's and future internal combustion engines, including high pressure (p = 15-80 bar) and low to intermediate temperatures (T = 650-1,100 K).

Fiscal Year (FY) 2014 Objectives

- Acquire ignition delay measurements for gasoline surrogate blends and a full-boiling range gasoline, with these also doped using small quantities of reactivity modifiers; assemble and validate detailed chemical kinetic models to describe the autoignition processes.
- Develop new targets to be used for kinetic mechanism improvement, e.g., heat release based metrics for low- and intermediate-temperature ignition chemistry.
- Implement advanced tools, such as global sensitivity analysis, in order to better understand predictions of chemical kinetic mechanisms and facilitate improvements in predictive capabilities.

FY 2014 Accomplishments

- Acquired new measurements for a research grade gasoline, multi-component surrogate blends, and measurements of these fuels doped with a reactivity modifier, 2-ethylhexyl nitrate (2EHN). Developed chemical kinetic models for these fuels and compared predictions with experimental data, highlighting sensitive reaction pathways which should be further investigated in order to improve the chemical kinetic model predictions.
- Developed an approach to quantify, from RCM data, extents of low- and intermediate-temperature heat release (LTHR, ITHR) which occur prior to the main ignition event.

Future Directions

- Acquire measurements for gasoline/diesel surrogates and multi-component surrogate blends, as well as full-boiling range fuels, and mixtures of these with reactivity modifiers, including ethanol.
- Improve methods to formulate surrogate fuel blends which can represent the autoignition behavior of real transportation fuels.
- Further develop and utilize novel approaches for kinetic mechanism validation/improvement, including global sensitivity analysis, along with new targets such as rate of heat release and extents of LTHR and ITHR.
- Test and validate the operational characteristics of a new, single-piston RCM.

✧ ✧ ✧ ✧ ✧

INTRODUCTION

Accurate, predictive combustion models are necessary in order to reliably design and control next-generation fuels and future engines which can meet mandated fuel economy and emissions standards, while achieving reductions in development times and costs for new configurations [1]. The imprecision of available models prevents the adoption of detailed simulation techniques within current design processes. Existing engineering-scale models can achieve satisfactory performance at some operating points, however they are not sufficiently robust to cover complete ranges of conventional engine operation, or when novel or advanced combustion concepts are utilized. Towards this, there is a critical need to improve the understanding of the multiple physical and chemical processes that occur within combustion engines, some of which include chemical ignition, fluid-chemistry interactions and pollutant formation/decomposition. To advance these understandings collaborations are necessary across multiple disciplines, for example between combustion engineers within DOE's Vehicle Technologies Office and scientists who are supported through DOE's

Basic Energy Sciences. Through these interactions fundamental, engine-relevant data can be acquired with low experimental uncertainties, while predictive models can be developed and validated based on these datasets.

APPROACH

RCMs are highly sophisticated, experimental tools that can be employed to acquire fundamental insight into fuel ignition and pollutant formation chemistry, as well as fluid-chemistry interactions, especially at conditions that are relevant to advanced, low-temperature combustion (LTC) concepts [2]. They are capable of creating and maintaining well-controlled, elevated temperature and pressure environments (e.g., T = 600 to 1,100 K, P = 5 to 80 bar) where the chemically-active period preceding autoignition can be monitored and probed via advanced in situ and ex situ diagnostics. The ability to utilize wide ranges of fuel and oxygen concentrations within RCMs, from ultra-lean to over-rich (e.g., ϕ = 0.2 to 2.0+), and spanning dilute to oxyen-rich regimes (e.g., O_2 = 5 to >21%), offers specific advantages relative to other laboratory apparatuses such as shock tubes and flow reactors, where complications can arise under such conditions. The understanding of interdependent chemicophysical phenomena that can occur at some conditions within RCMs is a topic of ongoing investigation within the combustion community, while interpretation of facility influences on datasets is also being addressed [2]. Approaches to implement novel diagnostics which can provide more rigorous constraints for model validation compared to integrated metrics such as ignition delay times, e.g., quantification of important radical and stable intermediates such as H_2O_2 and C_2H_4 [3,4], are under development by many combustion researchers.

Argonne's twin-piston RCM is utilized in this project to acquire data necessary for chemical kinetic model development and validation, while improvements to the facility's hardware and data analysis protocol are performed to extend its capabilities and fidelity. Collaborations are undertaken with Basic Energy Sciences-funded scientists at ANL and other U.S. laboratories, as well as with researchers at national and international institutions, including complementary RCM facilities.

RESULTS

Experiments were conducted to improve the capability to represent full-boiling range gasoline fuels with multi-component surrogates, and to be able to accurately model the chemical kinetic processes leading to ignition at combustion engine conditions. Blends of four, three-component surrogates were formulated where n-heptane and iso-octane were used as the blending feedstock (primary reference fuel, PRF) with toluene, 2-hexene, and methyl cyclohexane added in portions of 20% (toluene reference fuel [TRF], olefin reference fuel [ORF], and cycloalkane reference fuel [CRF], respectively), where these molecules were used as surrogates for the chemical classes of aromatics, olefins and naphthenes, respectively, which are contained within today's and future commercial gasolines. The fraction of n-heptane and iso-octane were adjusted in order to achieve similar levels of overall reactivity, e.g., anti-knock index (AKI) = 91, between the fuels. Tests were conducted at stoichiometric conditions with oxygen fractions of 11.4% and pressures near 20 bar. A range of compressed temperatures was covered (Tc = 675 to 1,050 K). Representative results are presented in Figure 1 where ignition delay times are plotted as a function of inverse temperature. Results for a full-boiling range gasoline, in this case Fuels for Advanced Combustion Engines (FACE)-F, are also shown for comparison, while typical temperature ranges for Research Octane Number (RON) and Motor Octane Number (MON) tests are included for reference. It can be seen here that measured ignition delay times are different for each of the surrogate blends, and that none of these closely match the behavior for the FACE-F gasoline, though the FACE-F times mostly fall between the surrogate test times. It is interesting to note that the FACE-F has a fairly steep negative temperature coefficient curve even though its RON and MON are substantially different (S = 5.6). Simulation results are also presented here where the Lawrence Livermore National Laboratory (LLNL)-detailed gasoline surrogate model is used [5-7], and it can

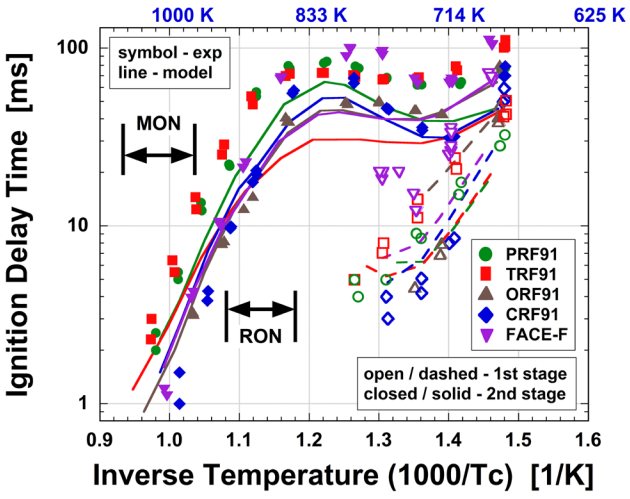

FIGURE 1. Measured ignition delay times as a function of temperature for five undoped fuels, PRF91, TRF91, ORF91, CRF91 and FACE-F at 21 bar and stoichiometric conditions with 11.4% oxygen. Simulated ignition delay times are shown as lines with colors corresponding to the symbols.

be seen that the predicted times are generally faster than the experimentally measured ones, especially at lower temperatures, e.g., below Tc = 870 K.

Additional tests were conducted in order to better understand the influence and effectiveness of fuel additives for gasoline-relevant fuels. There is interest in applying fuel additives to advanced, LTC concepts, such as homogeneous-charge compression-ignition or gasoline compression ignition in order to enable a means to dynamically control fuel reactivity during engine operation and thus cover a wide range of combustion modes, including conventional and LTC modes [8-16]. Additives are chemicals that contain a weak intramolecular bond where this leads to rapid decomposition at modest temperatures, so that in the combustion chamber they break down early in the combustion process, substantially before the fuel. The decomposition process yields active chemical species, such as alkyl radicals and nitrogen dioxide, which can stimulate or suppress fuel reactivity, e.g., through the formation or scavenging of OH. Though a number of studies have been conducted with fuel additives in fundamental laboratory experiments [17-24], as well as within internal combustion engines, important questions remain regarding how additives interact with various fuel components (e.g., parffins, branched alkanes, aromatics) across a range of conditions; what influences alter exothermicity and kinetic pathway acceleration; how interactions and influences can be reliably predicted, along with impacts to pollutant formation, e.g., oxides of nitrogen; and if are there optimal additives that can be used across a range of engine operating modes.

The four surrogates and the FACE-F gasoline were doped with 2EHN at levels of 0.1, 1.0 and 3.0% liquid volume, with tests conducted near 21 bar covering temperatures from 675 to 1,050 K. Doping levels covered the range of typical applications (0.1%) to reactivity controlled compression ignition-type application (3%). Stoichiometric fuel/oxygen ratios were used with the experimental are results plotted in Figure 2. Here an effectiveness ratio (R_{eff}) is utilized for the presentation where this is defined as the ratio of the doped to undoped ignition delay times. For conditions where R_{eff} is greater than 1.0, the additive extends the ignition times, or reduces the overall reactivity. For conditions where R_{eff} is less than 1.0, the reactivity is enhanced. In Figure 2, it can be seen that at intermediate temperatures, e.g., Tc > 800 K the fuel surrogates do a fair job in tracking the behavior of the FACE-F, particularly at doping levels of 1.0% and less, though there are some significant differences, while R_{eff} can be seen to be a non-linear function of the doping level, as has been observed in operating engines. At lower temperatures, the surrogate blend results indicate that R_{eff} peaks close to 1.0 (e.g., near Tc = 740 K), whereas R_{eff} is never greater than

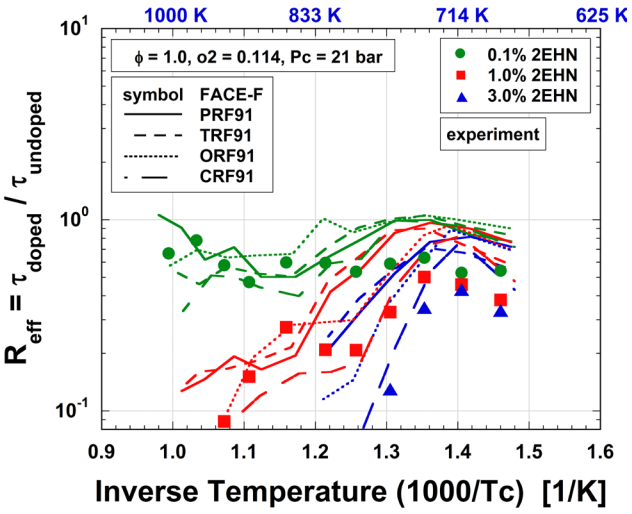

FIGURE 2. Measured effectiveness of 2EHN doped into a full-boiling range gasoline (FACE-F) and four three-component surrogates at various doping levels.

0.7 for the FACE-F gasoline. At the lowest temperatures, the 2EHN is much more effective when doped into FACE-F gasoline than into any of the surrogates utilized.

Simulation results for the experimental conditions are presented in Figure 3 where again the LLNL gasoline surrogate model is used along with sub-mechanisms to describe the 2EHN decomposition, as well as detailed nitrogen chemistry. The FACE-F fuel is represented using a five-component surrogate. Here it can be seen that while the general experimental trends are followed by the model over the range of doping levels, the effectiveness ratios are typically much smaller compared to the experiments indicating that the predicted reactivity enhancements are much more significant than are observed in the data. This is especially true at temperatures greater than 800 K. To better understand the discrepancies in the model predictions, a local sensitivity study was conducted for the PRF91 and TRF91 blends at two representative temperatures (Tc = 684 and 836 K) and across the three doping levels whereby the pre-exponential factors for each rate constants in the mechanism were perturbed by a factor of 2.0. These results indicated that the CH_2O and CH_3O_2 chemistry are very sensitive to the fuel doping at all conditions, while 2EHN decomposition only seems to be sensitive at the lower temperature where its decomposition rate is slower due to the high activation energy of the reaction (~40 kcal/mole). At higher temperatures, dopant-derived 3-heptyl radicals are predicted to play an important role stimulating ignition, while the detailed nitrogen chemistry becomes important only at the highest doping levels, primarily through the formation of methyl nitrite and nitric acid. The formation of methyl and ethyl nitrite, as well as nitric acid are

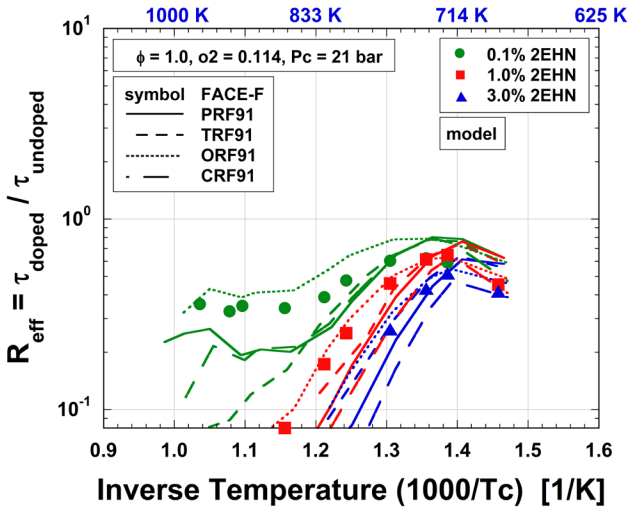

FIGURE 3. Simulated effectiveness of 2EHN doped into a full-boiling range gasoline (FACE-F) and four three-component surrogates at various doping levels.

predicted to compete with the 'NO–NO_2 loop' where this reduces the production of OH, and thereby constrains the effectiveness of 2EHN.

A new approach was also devised this year to quantify the extents of pre-ignition heat release from RCM data. The methodology employs an energy balance formulation which tracks the energy flows into and out of the reacting system, including volumetric compression due to piston motion, mass transfer to the piston crevices and heat loss to the walls of the reaction chamber. A high-fidelity, reduced-order model of the system is utilized in order to accurately represent the various dynamics that affect the thermodynamic state of the reacting mixture. Since the piston position is not directly measured in the ANL RCM, which is typical of most existing rapid compression machines, a sub-model was formulated to calculate the piston motion during the test. This is based on a dynamical analysis that accounts for all of the forces on the shaft, including the pneumatic driving force, the resistive force in the reaction chamber due to gas compression, the forces due to the hydraulic fluid flow around the hydraulic piston, and the friction due to the various seals in the system. The gas flow from the reaction chamber into the piston crevice volume and heat loss to the walls are taken into account via a multi-zone model that was developed and validated previously [25-26]. Representative results are presented in Figure 4 where data for iso-octane/'air' mixtures at the RCM Workshop conditions [2] are shown. In addition to the main ignition delay times, the calculated LTHR and ITHR data are indicated. Simulated results are based on the LLNL gasoline surrogate model. It can be seen in this figure that for these conditions fairly good agreement is

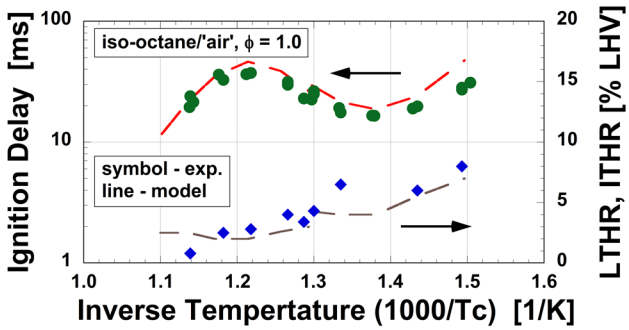

FIGURE 4. Measured and simulated ignition delay times and extents of low- and intermediate-temperature heat release as a function of inverse temperature for stoichiometric iso-octane/'air' mixtures at 20 bar.

observed between the measurements and the predictions. Refinements are ongoing in order to reduce the scatter seen in the experimental values.

Finally, work was initiated this year to utilize global sensitivity analysis tools [27-28] in order to better understand predictions from detailed chemical kinetic mechanisms and facilitate improvements in predictive capabilities. In this approach, which differs from typical local, or one-at-a-time sensitivity studies, all of the reaction rate parameters, i.e., the A-factors, are perturbed simultaneously, and within specified uncertainty bounds. This allows interactions between reactions to be better captured, and for large mechanisms, can reduce the number of cases that must be simulated. Furthermore, sensitive reactions with large uncertainties are better highlighted, where these can be targeted for more detailed study, using experimental or computational approaches. Challenges with utilizing these tools with the LLNL gasoline surrogate model include: realistic uncertainty bounds need to be specified for each of the thousands of reactions in the model, and thousands of simulations must to be conducted at each simulated condition. Efforts were undertaken this year to address these two challenges, and the first results are expected to be presented in FY 2015.

CONCLUSIONS

- ANL's RCM has been used to acquire autoignition data for a range of multi-component gasoline surrogate blends, a full-boiling range gasoline and mixutres of these fuels doped with a reactivity modifier, 2EHN. Chemical kinetic models have been assembled for these fuels with predictions compared against experimental measurements. Improvements are necessary in order to formulate better surrogates for real fuels, and to be able to more reliably predict the ignition characteristics of the fuels, and how they behave in the presence of fuel additives.

- A methodology has been developed to extract pre-ignition heat release information from RCM measurements where fairly good agreement has been observed compared to predictions against the LLNL-detailed gasoline model for iso-octane/'air' mixtures at the RCM Workshop conditions, while improvements are underway to reduce the scatter in the measurement calculations.
- Work is ongoing to implement GSA tools with the large, detailed LLNL mechanism in order to facilitate improvements to the chemical kinetic predictions.

REFERENCES

1. Basic Research Needs for Clean and Efficiency Combustion of 21st Century Transportation Fuels. (http://science.energy.gov/~/media/bes/pdf/reports/files/ctf_rpt.pdf)

2. S.S. Goldsborough, D. Longman, M.S. Wooldridge, R.S. Tranter and S. Pratt, "1st International RCM Workshop Meeting Report," August 28–29, 2012. (http://www.transportation.anl.gov/rcmworkshop)

3. C. Bahrini, O. Herbinet, P.-A. Glaude, C. Schoemaecker, C. Fittschen and F. Battin-Leclerc, J. Am. Chem. Soc. (139) 11944-11947, 2012.

4. I. Stranic, S.H. Pyun, D.F. Davidson, R.K. Hanson, Combust. Flame (159) 3242-3250, 2012.

5. M. Mehl, W.J. Pitz, C.K. Westbrook, H.J. Curran, Proc. Comb. Inst. 33:193-200, 2011.

6. G. Kukkadapu, K. Kumar, C.-J. Sung, M. Mehl, W.J. Pitz, Combust. Flame 159:3066-3078, 2012.

7. G. Kukkadapu, K. Kumar, C.-J. Sung, M. Mehl, W.J. Pitz, Proc. Comb. Inst. 34:345-352, 2013.

8. A.M. Ickes, S.V. Bohac and D.N. Assanis, Energy Fuels 23:4943-4948, 2009.

9. J.A. Eng, W.R. Leppard and T.M. Sloane, SAE Paper 2003-01-3179, 2003.

10. X. Gong, R. Johnson, D.L. Miller and N.P. Cernansky, SAE Paper 2005-01-3740, 2005.

11. A. Gupta, D.L. Miller and N.P. Cernansky, SAE Paper 2007-01-2002, 2007.

12. J.H. Mack, R.W. Dibble, B.A. Buchholz and D.L. Flowers, SAE Paper 2005-01-2135, 2005.

13. D. Splitter, R. Reitz and R. Hanson, SAE Paper 2010-01-2167, 2010, 2010.

14. R. Hanson, S. Kokjohn, D. Splitter, R. Reitz, SAE Paper 2011-01-0361, 2011.

14. J. Kaddatz, M. Andrie, R. Reitz, S. Kokjohn, SAE Paper 2012-01-1110, 2012.

15. A.B. Dempsey, N.R. Walker, R. Reitz, SAE Paper 2013-01-1678, 2013.

16. B. Higgins, D. Siebers and C. Mueller, Sandia Report SAND98-8243, 1998.

17. G.J. Suppes, Y. Rui, A.C. Rome and Z. Chen, Ind. Eng. Chem. Res. 36:4397-4404, 1997.

18. T. Inomata, J.F. Griffiths, A.J. Pappin, 23rd Symp. (Int.) Combust. 1759-1766, 1990.

19. J.F. Griffiths, Q. Jiao, W. Kordylewski, M. Schreiber, J. Meyer, and K.F. Knoche, Combust. Flame 93:303-315, 1993.

20. S. Tanaka, F. Ayala, J.C. Keck and J.B. Heywood, Combust. Flame 132:219-239, 2003.

21. A. Toland, J.M. Simmie, Combust. Flame 132:556-564, 2003.

22. M. Hartmann, K. Tian, C. Hofrath, M. Fikri, A. Schubert, R. Schiessl, R. Starke, B. Atakan, C. Schulz, U. Maas, F. Kleine Jäger and K. Kühling, Proc. Comb. Inst. 32:197-204, 2009.

23. Y. Stein, R.A. Yetter, F.L. Dryer and A. Aradi, SAE Paper 1999-01-1504, 1999.

24. S.S. Goldsborough, C. Banyon, G. Mittal, Combust. Flame (159) 3476-3492, 2012.

25. S.S. Goldsborough, G. Mittal, C. Banyon, Proc. Comb. Inst. (34) 685-693, 2013.

26. D.D.Y. Zhou, M.J. Davis, R.T. Skodje, J. Phys. Chem. A (117) 3569-3584, 2013.

27. E. Hebrard, A.S. Tomlin, R. Bounaceur, R. Battin-Leclerc, Proc. Comb. Inst. (in press).

FY 2014 PUBLICATIONS/PRESENTATIONS

1. S.S. Goldsborough, "RCM studies to enable predictive design of gasoline-relevant LTC," AEC Meeting, Sandia National Laboratory, 2014.

2. C. Banyon and S.S. Goldsborough, "An investigation of phase-change behavior in RCM experiments with large molecular weight fuels," Spring Technical Meeting of the Central States Section of the Combustion Institute, 2014.

3. S.S. Goldsborough, M.V. Johnson, C. Banyon, W.J. Pitz, M.J. McNenly, "Experimental and modeling study of fuel interactions with an alkyl nitrate cetane enhancer, 2-ethyl-hexyl nitrate," Proc. Comb. Inst. (in press).

4. A. Fridlyand, S.S. Goldsborough, K. Brezinsky, S.S. Merchant and W.H. Green, "Influence of the double bond position on the oxidation of decene isomers at high pressures and temperatures," Proc. Comb. Inst. (in press).

5. G. Vanhove, S.S. Goldsborough, C.J. Sung, H. Curran, M. Wooldridge, "RCM Characterization Initiative: Towards Haromonizing Ignition Data," 35th Combustion Symposium, 2014.

6. C. Banyon and S.S. Goldsborough, "An investigation of phase-change behavior in RCM experiments with large molecular weight fuels," 35th Combustion Symposium, 2014.

II.10 Chemical Kinetic Models for Advanced Engine Combustion

William J. Pitz (Primary Contact), Marco Mehl, Charles K. Westbrook
Lawrence Livermore National Laboratory (LLNL)
P.O. Box 808, L-288
Livermore, CA 94551

DOE Technology Development Manager
Leo Breton

Overall Objectives

- Develop detailed chemical kinetic models for fuel components used in surrogate fuels for compression ignition (CI), homogeneous charge compression ignition (HCCI) and reactivity-controlled compression-ignition (RCCI) engines.
- Combine component models into surrogate fuel models to represent real transportation fuels. Use them to model low-temperature combustion strategies in HCCI, RCCI, and CI engines that lead to low emissions and high efficiency.

Fiscal Year (FY) 2014 Objectives

- Develop detailed chemical kinetic models for larger alkyl aromatics relevant to diesel fuels
- Develop more accurate surrogate kinetics models for gasoline surrogate fuels
- Develop chemical kinetic model for a large alkyl-cyclohexane as a diesel surrogate component
- Develop chemical kinetic model for a naphtho-aromatic as a diesel surrogate component
- Develop a preliminary model for a large polycyclic aromatic hydrocarbon as a soot precursor

FY 2014 Accomplishments

- Developed a chemical kinetic model for tri-methylbenzene, a surrogate component surrogate diesel fuel
- Developed a chemical kinetic model for n-butyl-cyclohexane, a surrogate component for diesel fuel
- Developed a chemical kinetic model for tetralin, a surrogate component for diesel fuel
- Performed detailed chemical kinetic modeling of surrogates of gasoline fuels

Future Directions

- Continue to develop detailed chemical kinetic models for additional cycloalkanes for gasoline and diesel fuel
- Develop gasoline surrogate fuels for additional Fuels for Advanced Combustion Engines (FACE) fuels
- Develop improved models for incipient soot

✧ ✧ ✧ ✧ ✧

INTRODUCTION

Predictive engine simulation models are needed to make rapid progress towards DOE's goals of increasing combustion engine efficiency and reducing pollutant emissions. In order to assess the effect of fuel composition on engine performance and emissions, these engine simulations need to couple fluid dynamic and fuel chemistry submodels. Reliable chemical kinetic submodels representative of conventional and next-generation transportation fuels need to be developed to fulfill these requirements.

APPROACH

Gasoline and diesel fuels consist of complex mixtures of hundreds of different components. These components can be grouped into chemical classes including n-alkanes, iso-alkanes, cycloalkanes, alkenes, oxygenates, and aromatics. Since it is not practicable to develop chemical kinetic models for hundreds of components, specific components need to be identified to represent each of these chemical classes. Then detailed chemical kinetic models can be developed for these selected components. These component models are subsequently merged together to produce a "surrogate" fuel model for gasoline, diesel, and next-generation transportation fuels. This approach creates realistic surrogates for gasoline or diesel fuels that can reproduce experimental behavior of the practical real fuels that they represent. Detailed kinetic models for surrogate fuels can then be simplified as needed for inclusion in multidimensional computational fluid dynamic models of engine combustion.

RESULTS

Mueller et al. [1] have proposed a nine-component surrogate to represent the ignition behavior of representative diesel fuels in terms of distillation

characteristics, density, and chemical composition. In previous years at LLNL, chemical kinetic models for five of these components were developed. In FY 2014, new chemical kinetic models were developed to represent three of the remaining four components. These models were for 1,2,4-tri-methylbenzene to represent alkyl-aromatics, tetralin to represent naphtha-aromatics, and n-butyl-cyclohexane to represent alkyl-cyclohexanes in diesel fuel. These new chemical kinetic models were validated by comparison of results from the model to measurements of ignition delay times in shock tubes and rapid compression machines (RCMs). The agreement between the model and experiment was generally good (e.g. Figures 1-3). Only one model for the remaining component needs to be developed to complete the nine-component surrogate model for diesel fuel.

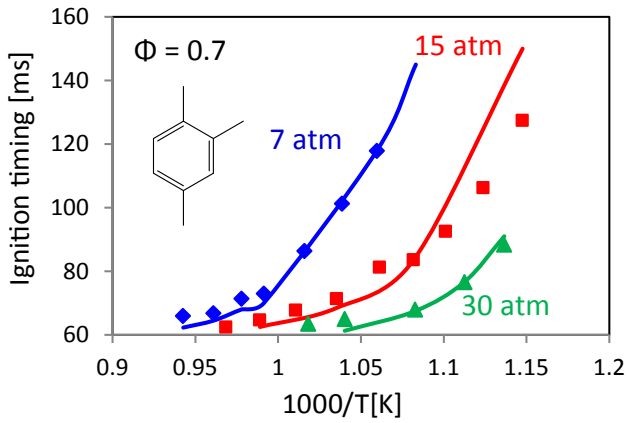

FIGURE 1. A comparison of ignition behavior computed from the chemical kinetic model (curves) and measured in the experiments (symbols) for 1,2,4-trimethylbenzene in the RCM. Times are referred to the start of the compression. The experimental measurements are from Prof. Sung's group at the University of Connecticut.

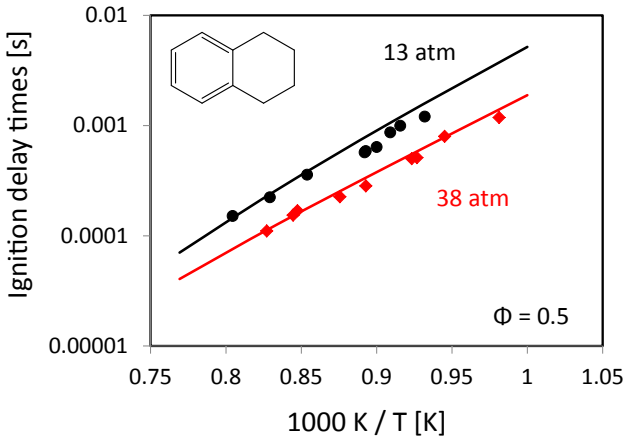

FIGURE 2. Comparison of ignition delay times for tetralin in a shock tube at an equivalence ratio of 0.5. Lines are from the LLNL model and symbols from the experiments [7].

FACE fuels for gasoline have been developed to provide researchers with controlled compositions that can be used to assess the fuel effects on advanced engine combustion [2]. In FY 2014 at LLNL, a 10-component gasoline surrogate palette was developed to represent the properties of FACE gasoline fuels. Subsequently, a gasoline surrogate model based on components in this palette was used to simulate the ignition behavior of FACE A and C. Ignition delay times from the model were compared to those measured in shock tubes and RCMs for FACE A and C at pressure and temperature conditions found in engines. Good agreement was found between the predictions and experimental measurements (Figure 4) [3].

To simulate combustion in direct-injection spark-ignition engines, chemical kinetic models need to accurately predict flame speeds. In FY 2014, flame speeds for a series of alkyl-benzenes were simulated including LLNL chemical kinetic models for toluene, ethyl-benzene, n-propyl-benzene and n-butyl-benzene. Comparisons of these model calculations were made to measurements performed at the National Center for Scientific Research, France [4]. The experimentally observed behavior was reproduced both qualitatively and quantitatively (Figure 5). After the effect of adiabatic flame temperature was accounted for, it was found that the observed behavior of the alkyl-benzenes could be explained by their relative propensity to form benzyl radicals: A higher formation rate of benzyl radicals corresponds to a relatively lower flame speed.

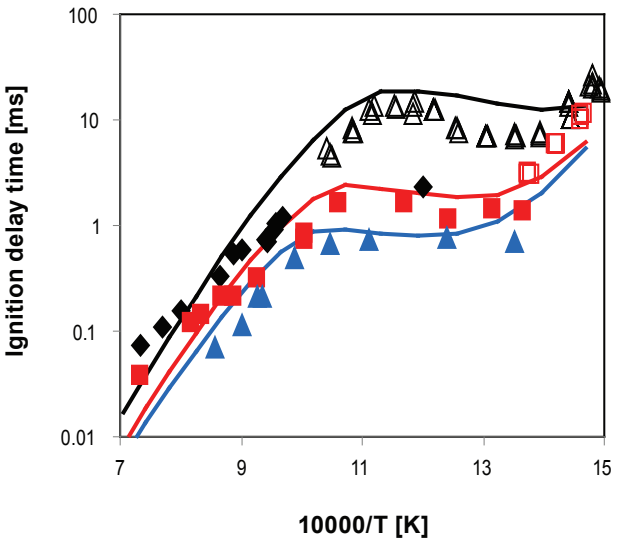

FIGURE 3. A comparison of ignition behavior from the chemical kinetic model (curves) and the experiments (symbols) for a stoichiometric mixture of n-butyl cyclohexane in air. The closed symbols are results from the shock tube and the open symbols are from the RCM. Experiments were performed by Prof. Curran's group at the National University of Ireland, Galway.

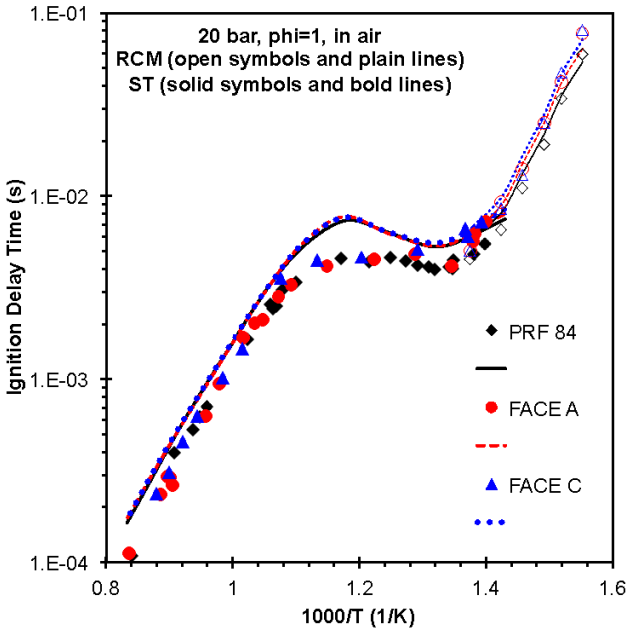

FIGURE 4. Comparison of the gasoline surrogate model (curves) with shock tube (filled symbols) and RCM (open symbols) ignition experiments for FACE gasoline fuels A and C. Comparisons are also made to PRF84, a primary reference fuel mixture of 84% isooctane and 16% n-heptane with similar ignition characteristics. Experimental data from the shock tube were taken by Prof. Oehlschlaeger's group at Rensselaer Polytechnic Institute and from the RCM by Dr. Sarathy's group at the King Abdullah University of Science and Technology [3].

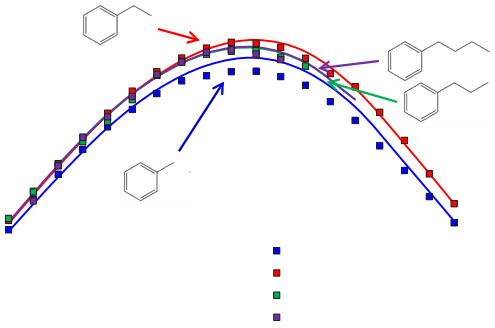

FIGURE 5. Comparison of laminar flame velocities (symbols: experiments, lines: calculations) as a function of equivalence ratio for alkyl-benzenes from toluene up to n-butyl-benzene at 358 K [4]. The lines for n-propyl-benzene and n-butyl-benzene overlap.

In collaboration with Argonne National Laboratory and University of Connecticut, a two-component diesel surrogate model was developed for use in a multidimensional engine simulation code. First, a two-component detailed chemical kinetic model of

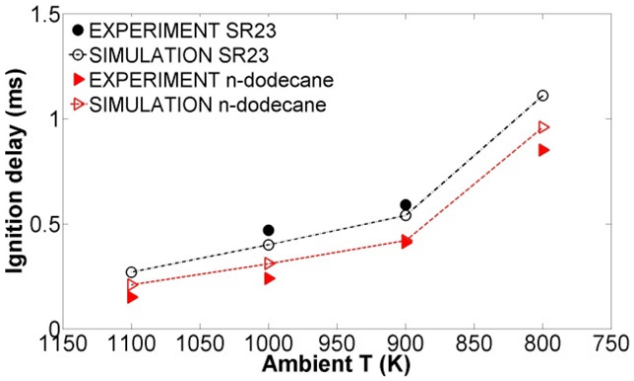

FIGURE 6. Simulated [5] and experimentally-measured [6] ignition delays for n-dodecane and an n-dodecane/m-xylene mixture in a spray chamber of Dr. Pickett at Sandia National Laboratories.

n-dodecane and m-xylene was assembled at LLNL and validated by comparison to shock tube and flow reactor data for the neat components and their mixture. These components were chosen because they can represent the alkane and aromatic fractions in diesel and the resulting mechanism is computationally manageable in the engine simulation code. The detailed chemical kinetic model was reduced at the University of Connecticut and used at Argonne National Laboratory to simulate diesel reacting sprays in a constant volume vessel [5]. The reduced mechanism was able to simulate the experimentally measured ignition delays [6] in a spray chamber (Figure 6).

CONCLUSIONS

- New mechanisms have been developed for three of the four remaining components in a nine-component surrogate for diesel fuel.
- A reduced, two-component mechanism for diesel has been developed in collaboration with Argonne National Laboratory and the University of Connecticut.
- A surrogate palette to represent FACE gasoline fuels has been developed and used to develop a chemical kinetic model for FACE A and C.
- A mechanism for alkyl-benzenes was validated for prediction of flame speeds important for direct-injection spark ignition engines.
- This work was performed under the auspices of the U.S. Department of Energy by Lawrence Livermore National Laboratory under Contract DE-AC52-07NA27344.

REFERENCES

1. C.J. Mueller, W.J. Cannella, T.J. Bruno, B. Bunting, H.D. Dettman, J.A. Franz, M.L. Huber, M. Natarajan, W.J. Pitz, M.A. Ratcliff and K. Wright, "Methodology for Formulating Diesel Surrogate Fuels with Accurate Compositional, Ignition-Quality, and Volatility Characteristics," *Energy & Fuels* 26 (6) (2012) 3284–3303.

2. "FACE gasoline fuels," http://www.crcao.org/Publications/advancedVehiclesFuelsLubricants/FACE/index.html, 2013.

3. S.M. Sarathy, G. Kukkadapu, M. Mehl, W. Wang, T. Javed, S. Park, M.A. Oehlschlaeger, A. Farooq, W.J. Pitz and C.-J. Sung, "Ignition of alkane-rich FACE gasoline fuels and their surrogate mixtures," *Proc. Combust. Inst.* (2015).

4. M. Mehl, O. Herbinet, P. Dirrenberger, R. Bounaceur, P.-A. Glaude, F. Battin-Leclerc and W.J. Pitz, "Experimental and Modeling Study of Burning Velocities for Alkyl Aromatic Components Relevant to Diesel Fuels," *Proc. Combust. Inst.* (2015).

5. Y. Pei, W. Liu, M. Mehl, S. Som, T. Lu and W.J. Pitz, "A Multi-Component Blend as a Diesel Fuel Surrogate for Compression Ignition Engine Applications," ICEF2014-5625, (2014).

6. "Engine Combustion Network," http://www.sandia.gov/ecn/, 2014.

7. H. Wang, W.J. Gerken, W. Wang and M.A. Oehlschlaeger, "Experimental Study of the High-Temperature Autoignition of Tetralin," *Energy & Fuels* 27 (9) (2013) 5483–5487.

FY 2014 PUBLICATIONS/PRESENTATIONS

1. Mehl, M., Herbinet, O., Dirrenberger, P., Bounaceur, R., Glaude, P.-A., Battin-Leclerc, F. and Pitz, W.J., "Experimental and Modeling Study of Burning Velocities for Alkyl Aromatic Components Relevant to Diesel Fuels," Proceedings of the Combustion Institute (2015).

2. Sarathy et al., Reference 3 above.

3. Goldsborough, S.S., Johnson, M.V., Banyon, C., Pitz, W.J. and McNenly, M.J., "Experimental and Modeling Study of Fuel Interactions with an Alkyl Nitrate Cetane Enhancer, 2-Ethyl-Hexyl Nitrate," Proceedings of the Combustion Institute (2015).

4. Pei et al., Reference 5 above.

5. Allen, J. C., Pitz, W. J. and Fisher, B. T., "Experimental and Computational Study of n-Heptane Autoignition in a Direct-Injection Constant-Volume Combustion Chamber," Journal of Engineering for Gas Turbines and Power 136(9) (2014).

6. Weber, B.W., W.J. Pitz, M. Mehl, E.J. Silke, A.C. Davis and C.-J. Sung (2014). "Experiments and Modeling of the Autoignition of Methylcyclohexane at High Pressure." Combustion and Flame 161 (8) (2014) 1972-1983.

7. C.K. Westbrook and W.J. Pitz, "Fundamental Chemical Kinetics," in Encyclopedia of Automotive Engineering (David Crolla; David E. Foster; Toshio Kobayashi; Nicholas Vaughan, Eds.), Wiley Online Library (2014).

8. Vuilleumier, D., Kozarac, D., Mehl, M., Saxena, S., Pitz, W.J., Dibble, R., Chen, J. and Sarathy, M., "Intermediate Temperature Heat Release in an HCCI Engine Fueled by Ethanol / N-Heptane Mixtures: An Experimental and Modeling Study," Combustion and Flame 161 (3) (2014).

9. Sarathy, S.M., Javed, T., Karsenty, F., Heufer, A., Wang, W., Park, S., Elwardany, A., Farooq, A., Westbrook, C.K., Pitz, W.J., Oehlschlaeger, M.A., Dayma, G., Curran, H.J. and Dagaut, P., "A Comprehensive Combustion Chemistry Study of 2,5-Dimethylhexane," Combustion and Flame 161 (6) (2014) 1444–1459.

10. Darcy, D., Nakamura, H., Tobin, C.J., Mehl, M., Metcalfe, W.K., Pitz, W.J., Westbrook, C.K. and Curran, H.J., (2013). "An Experimental and Modeling Study of a Surrogate Mixtures of n-Propyl- and n-Butylbenzene in n-Heptane to Simulate n-Decylbenzene Ignition," Combustion and Flame 161 (6) (2014) 1460-1473.

SPECIAL RECOGNITIONS & AWARDS/ PATENTS ISSUED

1. Charles Westbrook and William Pitz recognized on the Thomson Reuters' list of The World's Most Influential Scientific Minds.

II.11 Computationally Efficient Modeling of High Efficiency Clean Combustion Engines

Russell Whitesides (Primary Contact), Salvador Aceves, Nick Killingsworth, Guillaume Petitpas, and Matthew McNenly
Lawrence Livermore National Laboratory (LLNL)
P.O. Box 808, L-792
Livermore, CA 94551

DOE Technology Development Manager
Leo Breton

Overall Objectives

- Gain fundamental and practical insight into high efficiency clean combustion (HECC) regimes through numerical simulations and experiments.
- Develop and apply numerical tools to simulate HECC by combining multidimensional fluid mechanics with chemical kinetics.
- Reduce computational expense for HECC simulations.
- Democratize high fidelity engine simulation by bringing computational tools to the desktop computer for use by engine designers and researchers.

Fiscal Year (FY) 2014 Objectives

- Improve availability of advanced kinetic solvers to industry computational fluid dynamics (CFD) users.
- Enhance performance and robustness of interface between advanced kinetics solvers and CFD codes.
- Implement fast chemistry solutions on state-of-the-art massively parallel architectures.
- Conduct detailed analysis of premixed charge compression ignition (PCCI) engine experiments to assess fuel kinetic effects and model parameter sensitivities.

FY 2014 Accomplishments

- Implemented algorithms for fast chemical solutions of small to moderate mechanism sizes enabling faster engine simulations.
- Made improvements and generalizations to the chemistry solver interface to CFD codes, making it more widely applicable/available to engine researchers and designers.
- Continued interaction with Convergent Science Inc., the leading distributor of engine CFD software.
- Further developed chemical integration algorithms for graphical processing units (GPUs) to enable use of massively parallel architectures for engine simulations.
- Exploration of parameter sensitivities in PCCI engine simulations.

Future Directions

- Continue solver development and licensing to improve robustness and availability.
- Complete key features for practical use of GPU chemistry solvers for engine CFD.
- Continue full-engine simulations identifying key issues in simulation setup and analysis.

INTRODUCTION

This project focuses on the development and application of computationally efficient and accurate simulation tools for prediction of engine combustion phenomena. Simulations of combustion processes aid in the development of high-efficiency and low-emissions engines by providing detailed characterization of in-cylinder engine processes that are difficult to measure directly. Simulations also inform design of new engines through numerical evaluation of the effects of engine parameters, allowing valuable and limited experimental resources to be focused on the most promising strategies.

Combustion simulations are computationally demanding because of the combined need to resolve three-dimensional turbulent fluid flow and highly exothermic chemical reactions proceeding at rates that span several orders of magnitude. As such, simulations of engines commonly sacrifice simulation detail to make run-times tractable based on the availability of computing resources and necessary simulation turn-around time. One major motivation of this research is to use physical and mathematical methods to reduce computational expense of combustion simulation with minimal loss of accuracy. These computationally efficient tools are applied to understand the fundamental physical

processes occurring in engines operating with high efficiency clean combustion strategies.

APPROACH

The physical processes endemic to internal combustion engines, thermo-chemical kinetics and turbulent fluid flows, are challenging to simulate because of the large gradients present and the wide range of time scales over which these processes occur, from picoseconds to milliseconds. This project seeks to maximize the computational performance of high-fidelity internal combustion engine simulations by taking advantage of physical discretization strategies, numerical methods, and new computer architectures. Specifically, chemical kinetics software is being developed that interfaces to CFD codes and provides accurate solution to chemical source terms at much lower computation cost than previously available methods. The software takes advantage of the work done in a related project at LLNL headed by Matthew McNenly [1], as well as extending that work in developing chemical algorithms for GPU architectures. The software packages being developed are intended for broad use by the engine research and design community and so significant effort is being put into making them generally applicable and available. The software tools are also being employed to investigate fundamental questions in advanced engine combustion physics. This project is also closely coupled to the project on Chemical Kinetics Models for Advanced Engine Combustion led by William Pitz [2], which provides better physical models of fuel ignition.

RESULTS

Improvements have been made to the interface between the fast chemical integrators and CFD codes in three major areas in the current FY.

The code has been made more general for easier integration into any CFD software that relies on operator splitting for chemistry source terms. Figure 1 provides a diagram of the code organization and the possible interfaces supported by these improvements. These updates bring fast chemistry algorithms to a wider group of engine researchers regardless of their preferred analysis software.

Improvements were also made to the chemistry solver routines to improve the efficiency of solving mechanisms that are commonly used in “engineering” engine simulations, i.e. from tens to one hundred species. Previously, the focus of the fast integrator development has been on very large mechanisms, hundreds to thousands of species. The large mechanism regime is vital to the workflow for detailed mechanism development and for prediction of ignition dynamics in kinetically controlled engine designs such as PCCI and other low-temperature combustion modes. However, at the engine design level, reduced and skeletal mechanisms are more commonly employed in design of experiment simulations and other parameter investigation/optimization studies. For this class of simulations, fast chemistry solvers with a direct matrix solution using dense matrix factorization have been developed that provide a significant speedup in simulation time. In Figure 2, simulation times for a range of chemical mechanism sizes are compared using the CONVERGE™ detailed chemistry integrator and the new integrator with direct dense solution. The results show between 1.5x and 2x speed-up over the whole range of mechanisms with increasing speed-up as the mechanism size grows. This means that an engine designer can perform twice

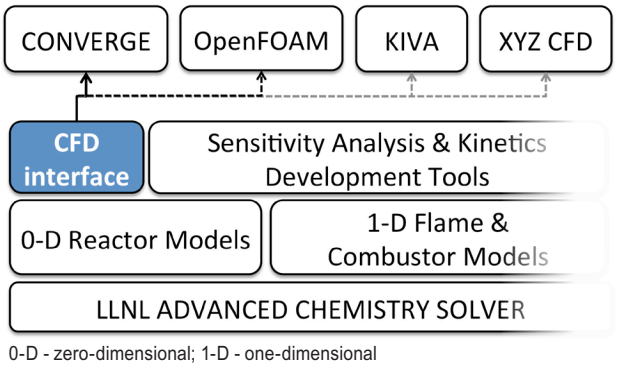

FIGURE 1. Structure of chemistry software highlighting the CFD interface. Advanced chemistry solver work primarily developed in an associated project [1].

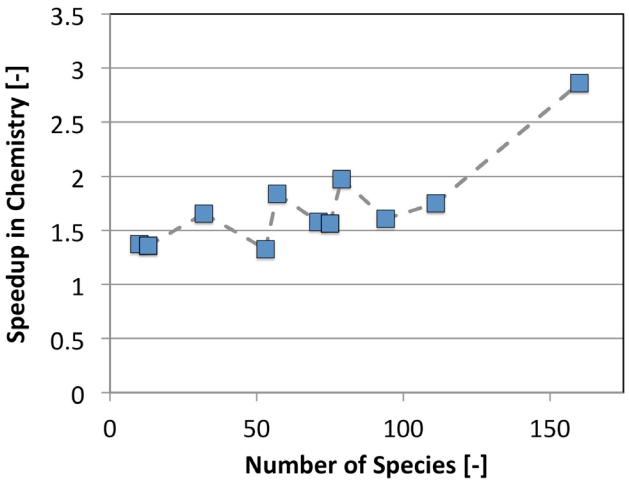

FIGURE 2. Speed-up of solution time for chemistry integration of small to moderate mechanism sizes comparing best algorithm in standard CONVERGE™ with best algorithm developed in this project.

as many simulations in the same period to survey a larger parameter space or can halve the time necessary to perform the current level of study, reducing the engine design turnaround time.

Significant effort has also been put into implementing the fast chemistry integrators on massively parallel architectures known as GPUs. This work takes advantage of recent trends in computing hardware towards many-core platforms. In the current FY the previously developed proof of principle work has been brought much closer to practicality. Figure 3 shows the speed-up over the best CPU implementations as the ideal case. The GPU calculations were performed on the Big Red 2 supercomputer at Indiana University through a collaboration with Cummins Inc. Further development will make this work practical for speeding up engine simulations.

Finally, a study on the sensitivity of engine simulations to the various algorithmic tolerances that are commonly employed in them was performed. For a PCCI simulation it was found that the typical tolerances on the species concentrations, internal energies, and for the chemical integrators lead to high errors in the calculated quantities of interest. Figure 4 shows the dependence of the indicated mean effective pressure (IMEP), crank angle of 50% burn (CA50), and ringing intensity on the simulation solver tolerances applied. These quantities are directly linked to the power output, the ignition timing, and the engine noise, respectively. The results indicate that much tighter tolerances should be employed than are typically used when performing simulations that include kinetically controlled ignition. The modest increase in cost associated with the tighter tolerances is more than offset by the significant speedup in the chemistry calculations achieved by LLNL.

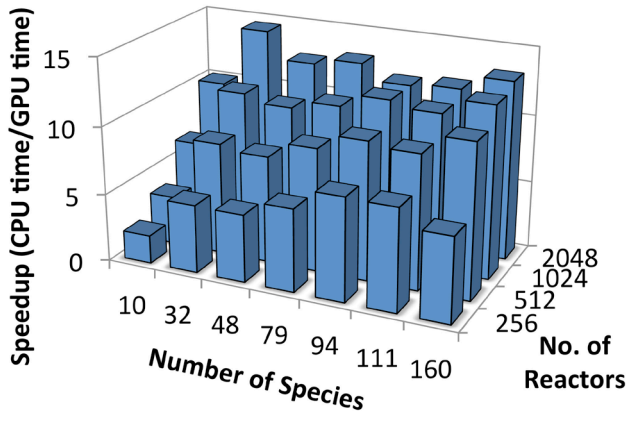

FIGURE 3. Speed-up of solution time for chemistry comparing GPU to CPU algorithms in ideal case as a function of chemical mechanism size and number of simultaneously solved reactors.

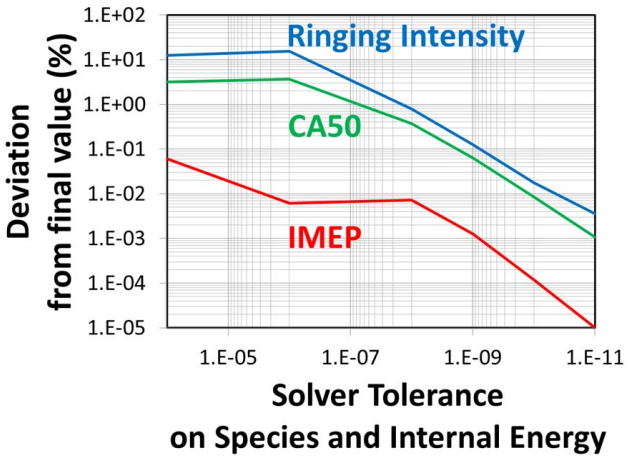

FIGURE 4. Relative deviation from converged solution of IMEP, CA50, and ringing intensity as a function of species and internal energy solver tolerances.

CONCLUSIONS

The performance of chemical calculations in CFD have been improved significantly. The key developments are in improving and generalizing the solver interfaces, applying previous techniques in fast solvers to smaller mechanisms, and further development of algorithms for massively parallel architectures. In addition, fundamental aspects of engine simulations continue to be investigated for practical results in the interest of informing the wider engine research and design community.

REFERENCES

1. McNenly, M.J., Improved solvers for advanced engine combustion simulation," II.22 in Advanced Combustion Engine Research and Development 2014 Annual Progress Report, U.S. Department of Energy, 2014.

2. Pitz, W.J., "Chemical Kinetics Models for Advanced Engine Combustion," II.12 in Advanced Combustion Engine Research and Development 2014 Annual Progress Report, U.S. Department of Energy, 2014.

FY 2014 PUBLICATIONS/PRESENTATIONS

1. Whitesides, R.A. "Accelerating Combustion Kinetics in CONVERGE CFD with GPUs," Converge Users Group Meeting, Madison, Wisconsin, September 24, 2014.

2. McNenly, M.J., Whitesides R.A., and Flowers D.L., "Faster solvers for large kinetic mechanisms using adaptive preconditioners," Proceedings of the Combustion Institute, Available online 20 August 2014, ISSN 1540-7489.

3. Whitesides, R.A. "LLNL Engine Modeling Update," Advanced Engine Combustion Program Review, Livermore, California, February 13, 2014.

SPECIAL RECOGNITION

1. McNenly, M.J. and Whitesides, R.A., LLNL Director's Science and Technology Award for "Adaptive preconditioner solver for internal combustion engine computational fluid dynamics."

Auspices Statement

This work was performed under the auspices of the U.S. Department of Energy by Lawrence Livermore National Laboratory under Contract DE-AC52-07NA27344.

LLNL Document Number: LLNL-AR-663183

II.12 Improved Solvers for Advanced Combustion Engine Simulation

Matthew McNenly (Primary Contact),
Salvador Aceves, Daniel Flowers,
Nick Killingsworth, Guillaume Petitpas,
W. Thomas Piggott, and Russell Whitesides
Lawrence Livermore National Laboratory (LLNL)
7000 East Ave. (L-140)
Livermore, CA 94550

DOE Technology Development Manager
Leo Breton

Overall Objectives

- Accelerate development and deployment of high-efficiency clean combustion (HECC) engine concepts through deeper understanding of complex fluid and chemistry interactions.
- Improve physical accuracy of combustion simulations by enabling the use of large chemistry mechanisms representing real transportation fuels.
- Reduce the time and resource cost for combustion simulations by designing efficient algorithms guided by applied mathematics and physics.
- Develop truly predictive combustion models and software that are fast enough to impact the engine design cycle.

Fiscal Year (FY) 2014 Objectives

- Measure the cost of the multispecies transport algorithms that are coupled with the chemically reacting flow solvers used for HECC engine design.
- Develop new tools to aid in the fuel mechanism development process.
- Increase the number of algorithms in the LLNL chemistry solver that are accelerated on a general-purpose graphics processing unit (GPU).

FY 2014 Accomplishments

- Completed a detailed code profile that identifies when the multispecies transport algorithms dominate the simulation cost for kinetically controlled engine design.
- Created a suite of mechanism development tools for reaction analysis and error detection.
- Accelerated the design of a new gasoline mechanism to study the impact of cetane enhancers on oxides of nitrogen (NOx) using the new suite of tools.
- Adapted all major algorithms in the LLNL chemistry solver to the GPU.

Future Directions

- Continue efforts to distribute the project's new software to industrial and academic partners, and to the multidimensional computational fluid dynamics (CFD) software packages they use.
- Improve the fluid transport calculation and other simulation bottlenecks that occur now that the chemistry solver is substantially faster.
- Continue to create new combustion algorithms for the GPU.
- Explore more robust error theory for physical models in engine simulations to ensure that accuracy is maintained in a rigorous manner transparent to all users.

INTRODUCTION

This project aims to fill the present knowledge gap through substantial improvements in the performance and accuracy of combustion models and software. The project is focused largely on the applied mathematics underpinning efficient algorithms, and the development of combustion software on new computing architectures. It is a natural complement to the other LLNL projects in the quest to gain fundamental understanding of the new engine modes investigated under the Advanced Combustion Engine R&D Program. Other LLNL projects include the multidimensional engine modeling project led by Whitesides (see II.11) and the high-fidelity chemistry mechanisms developed for real transportation fuels by Pitz (see II.10). The long-term goal of this project is to develop predictive combustion software that is computationally fast enough to impact the design cycle and reduce the deployment time for new high-efficiency, low-emissions engine concepts. Toward this goal, the project developed a new thermochemistry library and chemistry solver [1-3] that achieves multiple orders of magnitude speedup over the traditional approaches found in CFD (e.g. OpenFOAM®) without any loss of accuracy. Further, the LLNL library and solver are 5-15 times faster than sophisticated commercial solvers

like CHEMKIN-PRO. As a consequence of this project, it is now possible to model high fidelity fuel mechanisms (on the order of a thousand species) in multidimensional engine simulations that run in a day on industry-scale computational resources.

APPROACH

The project is focused on creating combustion software capable of producing accurate solutions in a short time relative to the engineering design cycle on commodity computing architectures. The approach advances engine simulations along several fronts simultaneously. Major bottlenecks in the software are found through detailed code profiling, while bottlenecks in the general computational-aided analysis are identified through engagements with manufacturers, universities, and national laboratories. New algorithms are created for the slowest code sections and existing algorithms are adapted to new applications that can accelerate the overall analysis workflow for HECC design. The new algorithms seek performance gains by implementing new theories from applied mathematics and/or by exploiting the new low-cost, massively parallel computing architectures like the GPU.

RESULTS

The project completed three tasks in FY 2014 in support of the overall goals of the Advanced Combustion Engine R&D Program:

- **Task 1.** Analyzed the computational cost solving the multispecies transport equations
- **Task 2.** Created a suite of tools to aid in the development of new fuel mechanisms
- **Task 3.** Adapted all major algorithms in the LLNL chemistry solver to the GPU

Task 1: The code performance analysis suite HPCToolkit [4] was used to measure the cost of all the algorithms in a representative HECC simulation with detailed fuel chemistry models in FY 2014. It is important to measure the algorithms in an HECC engine simulation that have the highest relative cost in order to prioritize future research directions in this project. The significant reduction in the computational cost for the integration of detailed fuel mechanism achieved in past years by this project makes the new performance study necessary. Specifically, CONVERGE^{TM} CFD [5] was used to simulate Dec's homogeneous charge compression ignition (HCCI) engine at Sandia National Laboratories [6] using six large fuel mechanisms ranging in size from 160 species (skeletal heptane mechanism) to more than 2,100 species (detailed hexadecane). The closed-cycle simulation of the lean (ϕ = 0.4), highly dilute (exhaust gas recirculation = 50% v/v) charge was performed using LLNL's multi-zone model with 35 fluid cells per chemical reactor on average to improve the measurement fidelity. The initial charge temperature was varied to match the combustion phasing between fuels to assess the relative computational cost of the multi-species transport algorithms and the chemistry solver algorithms. The cost breakdown of these algorithms is given in Figure 1 for the standard CONVERGE^{TM} CFD simulation (ver. 2.1 using the large mechanism options) and using LLNL's new chemistry solver. Using the chemistry solver as a plug-in for CONVERGE^{TM} CFD resulted in an overall speedup of five for the 2,100 species mechanism. To help prioritize the future algorithm developments, the code performance measurements were used to determine the point at which the multi-species transport and chemistry solver algorithms are the same cost. This break-even curve is plotted as a function of mechanism size in Figure 2. The code performance measurements indicate that multi-species transport algorithms become the dominant cost for coarser multi-zone models (more than 250 fluid cells per reactor), and that the chemistry solver costs dominate the finer multi-zone models (less than 75 fluid cells per reactor).

Task 2: The new algorithms in the LLNL chemistry solver were leveraged to create a suite of mechanism development tools in FY 2014 that help to identify erroneous kinetic rates, thermodynamic functions and reaction pathways. This is an example of the project removing a key bottleneck in the overall workflow for HECC design. The most successful fuel models for resolving kinetically controlled ignition processes

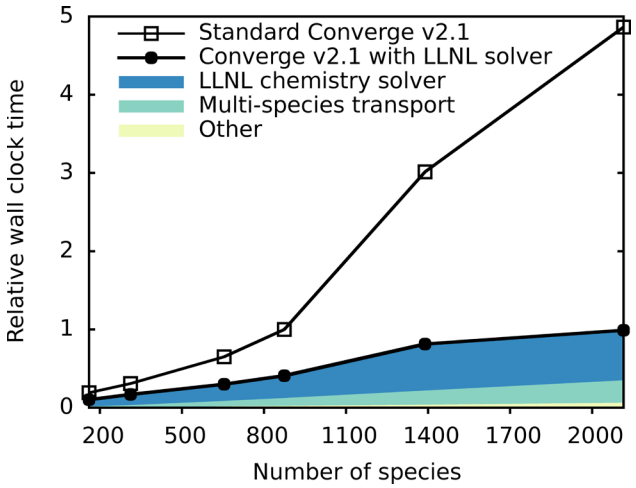

FIGURE 1. Computational cost breakdown for the algorithms used to simulate a lean-burn, high exhaust gas recirculation HCCI operation using detailed fuel mechanisms in CONVERGE^{TM} CFD. The LLNL chemistry solver delivers a five-fold speedup for the mechanisms larger than 2,000 species using a multi-zone resolution with 35 fluid cells per reactor on average.

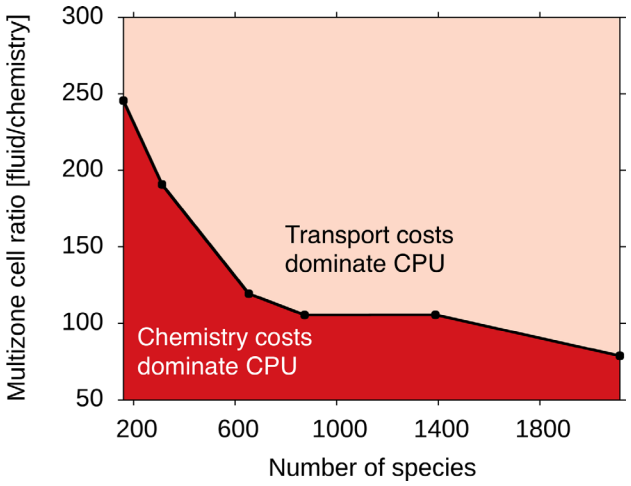

FIGURE 2. The mechanism sizes and multi-zone resolutions where either the multi-species transport algorithms or the chemistry solver algorithms dominate the computational cost.

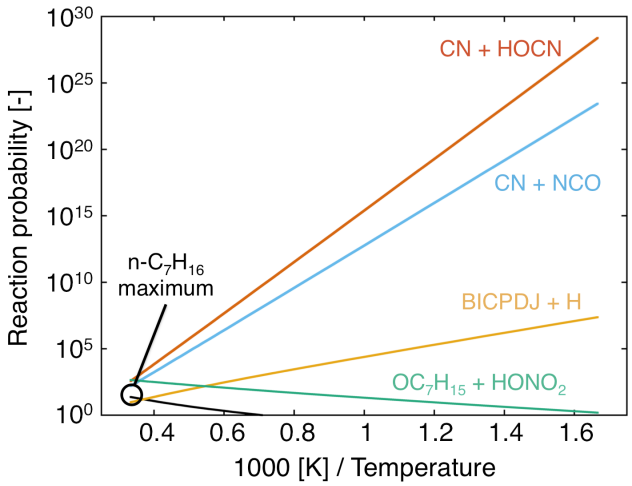

FIGURE 3. The new LLNL suite of tools identifies four unphysical binary reactions during the development of a new gasoline mechanism to study the impact of cetane enhancers on NOx production.

(e.g. HCCI, premixed charge compression ignition, reactivity-controlled compression ignition, and spark-assisted compression ignition) are built using the detailed mechanisms developed by Pitz and colleagues (see II.10), which typically containing several thousand species and tens of thousands of reactions. Updating and debugging these mechanisms is similar to editing a 4,000-page document for typos. To aid fuel researchers and accelerate new mechanism development, a suite of tools was built to identify potential errors based on algorithm performance metrics and other physical information used to construct the adaptive pre-conditioners that are at the foundation of the LLNL chemistry solver. One example from this suite is the analysis of the reaction probability for binary collisions. Reaction probabilities significantly larger than one are most likely unphysical and indicate a potentially erroneous rate definition in the mechanism. The tool was used in the development of a gasoline mechanism that could be used to explore the impact of cetane enhancers on the production of NOx [7]. Specifically, the new tool quickly identified four erroneous reactions with unphysical rates shown in Figure 3, which saved another project in the same subprogram considerable time (see Goldsborough, II.9).

Task 3: Porting all major chemistry solver algorithms to the GPU was completed in FY 2104. The thermo-chemistry functions and the ordinary differential equations vector data had been successfully ported to the GPU in FY 2013 and achieved an order of magnitude speedup over their serial CPU counterpart. The remaining algorithms on the GPU involved the sparse matrix functions used in LLNL's adaptive pre-conditioner approach, which represented 25% to 75% of the total solver cost on the CPU. In order to attain an

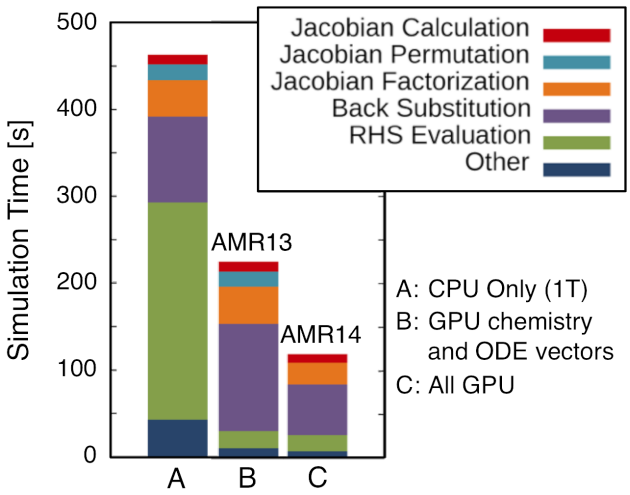

FIGURE 4. The sparse Jacobian matrix operations are ported to the GPU using the GPU library from NVIDIA, which delivers a four-fold speedup for 256 simultaneous reactor calculations using LLNL's detailed iso-octane mechanism (874 species).

appreciable overall speedup, these matrix functions were ported to the GPU with support from NVIDIA using their GPU library [8-9]. The all-GPU version is found to have a factor of four or more speedup over a single CPU as illustrated in Figure 4 for 256 simultaneous chemical reactor calculations using the detailed iso-octane mechanism from LLNL (874 species). Further development of combustion algorithms for the GPU at LLNL is covered in the multi-dimensional, HECC engine modeling project led by Whitesides (see II.11).

CONCLUSIONS

In FY 2014, this project progressed toward the goal of bringing truly predictive combustion software to the computational level needed to impact the engine design cycle for new HECC operating modes. Key achievements included:

1. Completed a detailed code analysis that identifies when the multispecies transport algorithms dominate the simulation cost for kinetically controlled engine design
2. Created a suite of mechanism development tools for reaction analysis and error detection
3. Adapted all major algorithms in the LLNL chemistry solver to the GPU

As result of the measurements in Task 1, this project will start focusing more on the computational bottlenecks in the multispecies transport algorithms in order to accelerate the HECC simulations used by manufactures, which typically use much coarser multi-zone models than tested here. In FY 2015, the project will continue its efforts to distribute the high-performance solvers and libraries developed here to industrial and academic partners, and explore new algorithms to further accelerate the software and new applications to accelerate the workflow of the advanced combustion engine community.

REFERENCES

1. M.J. McNenly, R.A. Whitesides and D.L. Flowers, "Fast solvers for large kinetic mechanisms," *Proc Combust Inst*, 2014.

2. McNenly, M.J., Whitesides, R.A., Flowers, D.L, "Adaptive preconditioning strategies for integrating large kinetic mechanisms," The 8th US National Combustion Meeting, Park City, Utah, May 19–22, 2013.

3. Whitesides, R.A., McNenly, M.J., Flowers, D.L., "Optimizing time integration of chemical-kinetic networks for speed and accuracy," The 8th US National Combustion Meeting, Park City, Utah, May 19–22, 2013.

4. L. Adhianto, *et al*., "HPCToolkit: tools for performance analysis of optimized parallel programs," *Concurrency Computat.: Pract. Exper.* **22**(6), 2010.

5. Raju, M.P. *et al*.,"Acceleration of Detailed Chemical Kinetics Using Multi-zone Modeling for CFD in Internal Combustion Engine Simulations," SAE Paper 2012-01-0135.

6. J. Dec *et. al*., "The Effects of Gasoline Reactivity and Ethanol Content on Boosted HCCI Performance", AEC Working Group Meeting, Livermore, CA, Feb. 2013.

7. S. Goldsborough, *et. al*., "Experimental and modeling study of fuel interactions with an alkyl nitrate cetane enhancer, 2-ethyl-hexyl nitrate," *Proc Combust Inst*, 2014.

8. M.J. McNenly and R.A. Whitesides, "Challenges simulating real fuel combustion: the role of GPUs," GPU Technology Conference, San Jose, CA, Mar. 2014.

9. Whitesides, R.A. "Accelerating Combustion Kinetics in CONVERGE CFD with GPUs", Converge Users Group Meeting, Madison, Wisconsin, September 24, 2014.

FY 2014 PUBLICATIONS/PRESENTATIONS

1. M.J. McNenly, "Progress on advanced combustion numerics and multidimensional engine simulation," AEC Working Group Meeting, Southfield, MI, Aug., 2014.

2. M.J. McNenly, R.A. Whitesides and D.L. Flowers, "Fast solvers for large kinetic mechanisms," *Proc Combust Inst*, 2014.

3. S.S. Goldsborough, *et. al*., "Experimental and modeling study of fuel interactions with an alkyl nitrate cetane enhancer, 2-ethyl-hexyl nitrate," *Proc Combust Inst*, 2014.

4. "Chemistry in motion: solving big problems with an ultrafast code," LLNL Science & Technology Review, Apr/May, 2014.

5. M.J. McNenly and R.A. Whitesides, "Challenges simulating real fuel combustion: the role of GPUs," GPU Technology Conference, San Jose, CA, Mar. 2014.

6. M.J. McNenly, "Progress in combustion modeling software," AEC Working Group Meeting, Livermore, CA, Feb., 2014.

SPECIAL RECOGNITIONS AND AWARDS/ PATENTS ISSUED

1. M.J. McNenly and R.A. Whitesides, "Adaptive preconditioner solver for internal combustion engine computational fluid dynamics," 2014 Director's Science and Technology Award, LLNL.

II.13 KIVA Development 2014

David B. Carrington
Los Alamos National Laboratory
P.O. Box 1663
Los Alamos, NM 87545

DOE Technology Development Manager
Leo Breton

Subcontractors
- Dr. Juan Heinrich, University of New Mexico, Albuquerque, NM
- Dr. Xiuling Wang, Purdue University, Calumet, Hammond, IN
- Dr. Darrell W. Pepper and Dr. Jiajia Waters, University of Nevada, Las Vegas, Las Vegas, NV

Objectives

- Develop algorithms and software for the advancement of speed, accuracy, robustness, and range of applicability of the KIVA internal engine combustion modeling—to be more predictive. This to be accomplished by employing higher-order spatially accurate methods for reactive turbulent flow, and spray injection, combined with robust and accurate actuated parts simulation and more appropriate turbulence modeling.
- To provide KIVA software that is easier to maintain and is easier to add models to than the current KIVA. To reduce code development costs into the future via more modern code architecture. The new code is KIVA-hpFE, an *hp*-adaptive finite-element method (FEM).

Fiscal Year (FY) 2014 Objectives

- Continue developing code and algorithms for the advancement of speed, accuracy, robustness, and range of applicability of the KIVA combustion modeling software to higher-order spatial accuracy with a minimal computational effort.
- Finish developing underlying discretization to an *hp*-adaptive predictor-corrector split (PCS) using a Petrov-Galerkin (P-G) FEM for multi-species flow, fluids with multiple components.
- Develop a plasma kernel spark model to supply heat at a single node based on engine manufacturer-specified spark current.
- Validate KIVA chemistry in the KIVA-hpFE solver to lower heating values (LHV) of fuel based on exact amount of fuel burned.
- Continue developing the three-dimensional (3-D) overset grid system to quickly utilized ‘stl’ file type from grid generator for quick/automatic overset parts surface generation.
  - Simulate 3-D flow with immersed actuated parts of valves and scalloped bowled piston.
- Finish developing dynamic large-eddy simulation (LES) for the PCS FEM system
- Continue developing the Message Passing Interface (MPI) parallel solution methods for the domain-decomposed geometry that has nest OpenMP threaded for maximal use of multi-core processors.

FY 2014 Accomplishments

- Finished developing underlying discretization to an *hp*-adaptive PCS using a P-G FEM for multi-species flow inclusive the chemistry input system and setup.
- Validated 3-D local-Arbitrary Lagrangian-Eulerian (ALE) moving parts algorithm/code with extensive error and convergence analysis. The method demonstrates near-zero error as determined by comparison to a moving surface problem that has a closed form or analytic solution.
  - Simulated 3-D flow with immersed actuated parts, a scalloped bowled piston.
- Developed a plasma kernel spark model, to supply heat at a single node based on engine manufacturer-specified spark current.
- Installed and validated KIVA chemistry package into the PCS FEM solver. Chemistry and burn model validated in the FEM system showing less than 1% error in LHV. The spark model does not supply significant heat to the energy in the domain.
- Developed a dynamic LES turbulence modeling for wall-bounded flows, and will be especially applicable to internal combustion engine modeling.
- Merged the grid formats, KIVA chemistry and spray along with multi-species component fluids into *hp*-adaptive FEM framework. Validation continues on this effort.
- Parallel global pressure solver system completed, wrappers for MPI installed with algorithms and coding for the solution of the primitive variables being completed and testing debugging continuing.

Future Directions

- Continue developing the parallel system in the *hp*-adaptive FEM. Continue implementing this method to perform modeling of internal combustion engines, other engines, and general combustion. Parallel structure is MPI (MPICH2, portable implementation of MPI) with nested OpenMP system that has a maximum efficiency on clusters with multi-core processors.
- Continue developing comprehensive comparative results to benchmark problems and to commercial software as part of the verification and validation of the algorithms.
- Continue developing the implicit solver system for the PCS FEM system, for no error 3-D moving parts method.
- Validate the KIVA chemistry and spray with *hp*-adaptive scheme.
- Continue developing the parallel solution method for the *hp*-adaptive PCS algorithm. Continue developing more appropriate turbulence models for more predictive modeling.
- Continue to verify and validate combustion and spray models, and the local ALE in 3-D.
- Incorporate volume of fluid method in spray modeling for more predictive modeling capability. Incorporate the Kelvin-Helmholtz Rayleigh-Taylor, spray in the KIVA multicomponent spray model.

INTRODUCTION

Los Alamos National Laboratory and its collaborators are facilitating engine modeling by improving accuracy and robustness of the modeling, and improving the robustness of software. We also continue to improve the physical modeling methods. We are developing and implementing new mathematical algorithms, those that represent the physics within an engine. We provide software that others may use directly or that they may alter with various models e.g., sophisticated chemical kinetics, different turbulent closure methods, or other fuel injection and spray systems.

APPROACH

Development of computational fluid dynamics models and algorithms relies on basic conservation laws and various mathematical and thermodynamic concepts and statements. The process encompasses a great many requirements including:

- Expertise in turbulence and turbulent modeling for multiphase/multispecies fluid dynamics.
- Expertise in combustion dynamics, modeling, and spray dynamics modeling.
- Skill at developing and implementing numerical methods for multi-physics computational fluid dynamics on complex domains with moving parts using variational methods.
- Careful validation and error analysis of the developed code and algorithms.

RESULTS

When considering the development of algorithms and the significant effort involved producing reliable software, it is often best to create algorithms that are more accurate at a given resolution and then resolve the system more accurately only where and when it is required. We began developing a new KIVA engine/combustion code with this idea in mind [1]. This new construction is a Galerkin FEM approach that utilizes conservative momentum, species, and energy transport. The FEM system is P-G and pressure stabilized [2].

A projection method is combined with higher order polynomial approximation for model dependent physical variables (*p*-adaptive) along with grid enrichment (locally higher grid resolution – *h*-adaptive). Overset grids are used for actuated and immersed moving parts to provide more accurate and robust solutions in the next generation of KIVA. The scheme is particularly effective for complex domains, such as engines.

The *hp*-adaptive FEM is at a minimum second-order accurate in space and third-order for advection terms, but becomes higher-order where required as prescribed by the adaptive procedures that is determined by the mathematical analysis of solution's error as the solution proceeds or error measures [2]. The *hp*-adaptive method employs hierarchical basis functions, constructed on the fly as determined by a stress-error measure [3].

A dynamic LES method was developed for the PCS FEM system that spans from laminar to highly turbulent flow without needed special damping such wall functions. This dynamic LES is based on a scheme developed by Vreman [4]. The model removes assumptions about the laminar sublayer and allows modeling non-equilibrium turbulent flows. The method allows backscatter, a natural process that is inherent turbulent flow. The results for Mach 2.25 flow over an 18 degree inclined ramp are shown in Figure 1. Figure 2 demonstrates reasonable accuracy compared to

experimental data [5]. Note though, the experimental data is the magnitude of the mean velocity, so we show the absolute value of the velocity from the simulation for comparison. The recirculation zones caused by the adverse pressure gradients create the detached shocks are the correct size and location compared to experiment.

Using the FEM method with the spray models provides a more accurate representation of the droplets interaction with the conveying fluid and with walls than the original finite volume method of KIVA. Because the FEM method allows for a continuous representation of phase-space, grid-scale accuracy can be applied everywhere. Problems with coarse grids influencing the spray are only related to the solution accuracy—the spatial representation of the spray model is therefore grid convergent, something that has not been true in the past. This nodal valued primitive variables system, allows for better accuracy of the species and heat distribution within a cell/element. The new plasma kernel model takes advantage of those nodal values, allowing the spark heat to be supplied at a single node, and mimics the solution to the plasma kernel equation. The spark model is based on the solution of the plasma kernel equations. These equations are solved as shown in a paper by K. Eisazadeh-Far et al. [6] and J. Song and M. Sunwoo solve the radius and temperature of the kernel [7]. The plasma kernel equation terms are as follows, *Tk* is the spark kernel's temperature, *dWspark/dt* is the change in spark current over time, *h* is enthalpy of the kernel *Vk* is the kernel's volume, *Ak* kernel's surface area, *Seff* is the effective flame speed, *P* is the pressure, *rk* the radius of the spark kernel and *dQloss/dt* is the change in heat loss in the kernel over time.

$$\frac{dT_k}{dt} = \frac{1}{m_k c_{p,k}}\left(\frac{dW_{spark}}{dt} + \left(h_{chem} - h_k\right)\rho\ A_k S_{eff} - \frac{dQ_{loss}}{dt} + V_k \frac{dP}{dt}\right)$$

$$\frac{dV_k}{dt} = \frac{\rho_f}{\rho_k} A_k S_{eff} + V_k\left(\frac{1}{T_k}\frac{dT_k}{dt} - \frac{1}{P}\frac{dP}{dt}\right)$$

$$\frac{dr_k}{dt} = \frac{\rho_f}{\rho_k} S_{eff} + \frac{V_k}{A_k}\left(\frac{1}{T_k}\frac{dT_k}{dt} - \frac{1}{P}\frac{dP}{dt}\right)$$

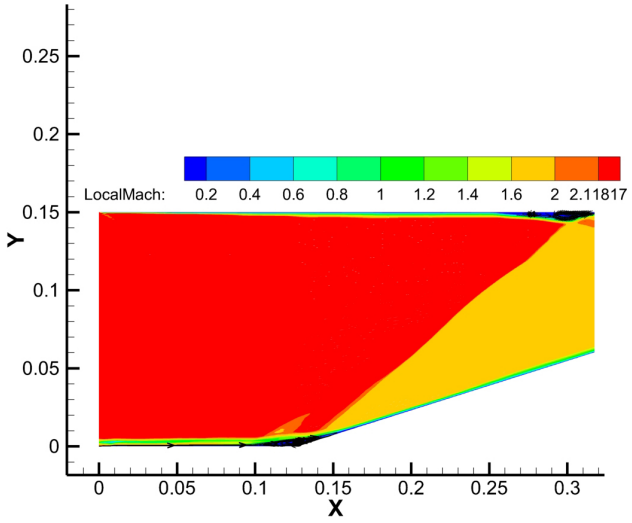

FIGURE 1. Supersonic Compression Ramp, Mach 2.25 Inlet Flow over 18 Degree Incline

A collimator test shown in Figure 3 is for near-engine operating temperatures and pressure. Gasoline is injected at 325 K at 15.8 atm and 525 K°. The results show less than 1% error in the LHV for the mass of gasoline burned in the collimator.

In 2014, we completed the 3-D local ALE method as shown in Figure 4 for a bowled piston moving in a cylinder. The local ALE scheme uses overset grids for immersed parts described by points on their boundaries which overlays the fluid grid. The moving parts within the fluid are not taken into account during the grid generation process. Hence, ports and cylinder portions of the grid are continuously represented. The overset grid method allows for computer aided design-to-grid in nearly a single step, providing nearly automatic grid generation.

The ALE system adjusts the grid locally as the parts move through the fluid, and maintains second-

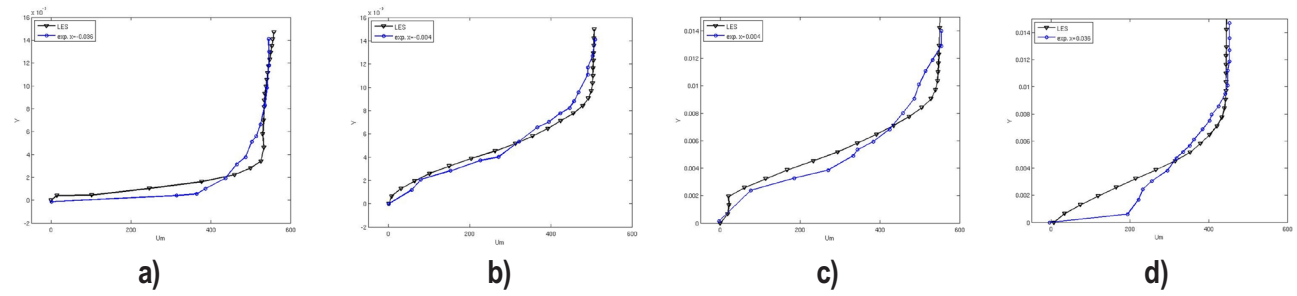

FIGURE 2. U (Mean Velocity) in Bottom Boundary Layer Using a Dynamic LES Model
Comparison to data at various locations: u upstream(-) and downstream(+) of the ramp a) -0.036 m , b) -0.004 m, c) +0.004 m, and d) +0.036 m.

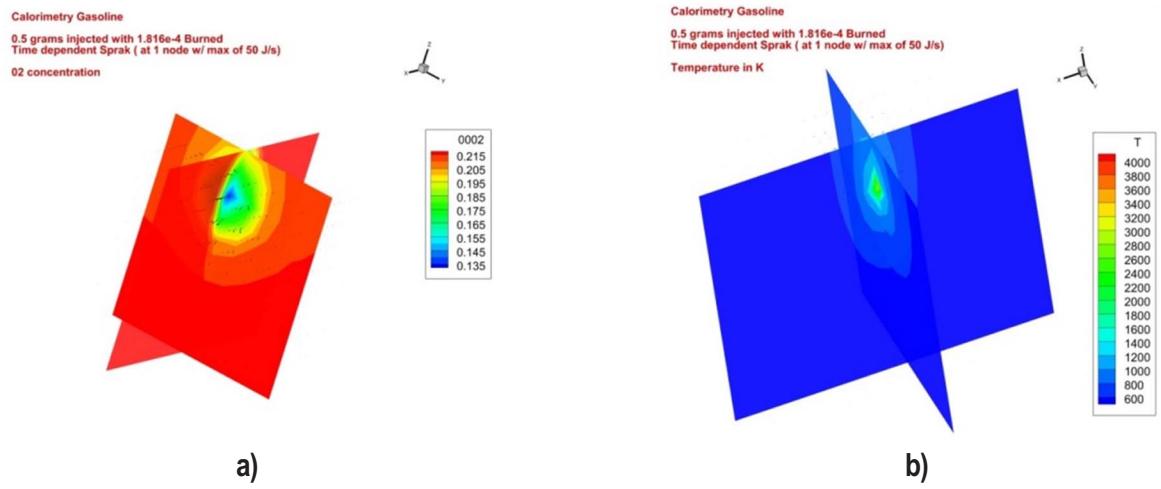

FIGURE 3. Gasoline being ignited by the plasma kernel model: a) oxygen concentration during burn and b) temperature of the fluid and also showing the temperature in the plasma kernel a short time after ignition.

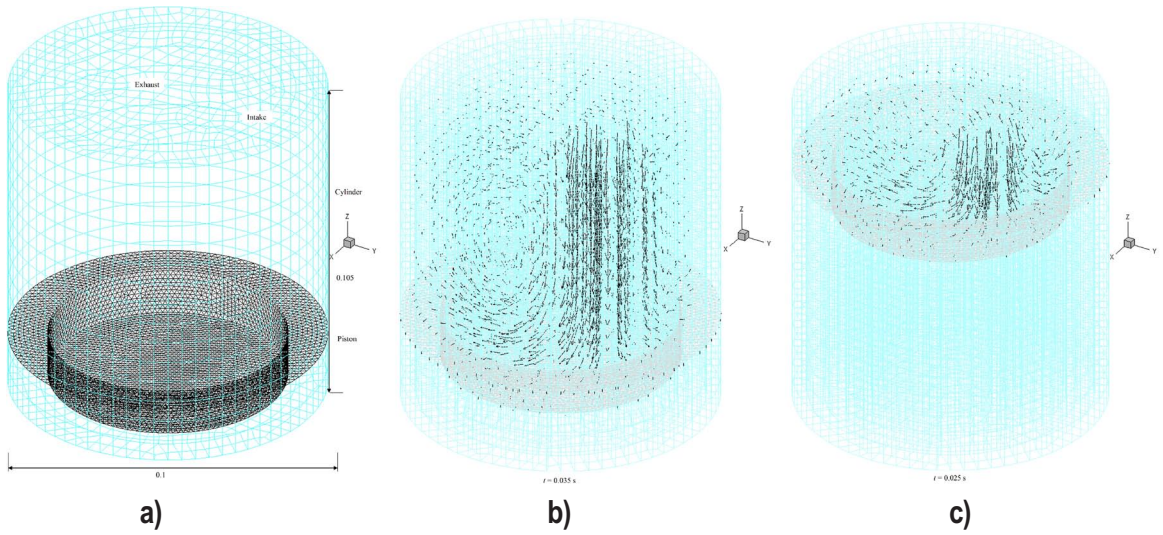

FIGURE 4. Cylinder with moving piston showing: a) piston surface of markers and triangles, b) and c) velocity vectors, piston location, and cylinder grid as piston moves.

order spatial accuracy while never allowing the grid to tangle or producing an element that cannot be integrated accurately [8]. Since the fluid is represented continuously, fluxing of material through the grid, as it is moves is not required. This need to flux through the grid is just one portion of the error when the usual ALE method is employed with finite volumes. Here the fluid solver remains Eulerian and the moving grid portions are no longer entwined with fluid solution. Figure 5 shows error and convergence compared to an analytic solution for the moving parts algorithm. The method demonstrates second-order spatial accuracy in Figure 5a and near zero error in Figure 5b. The method is robust, the grid will never tangle and the parts can move in any way desired through the cylinder's grid.

CONCLUSIONS

In FY 2014, we continued advancing the accuracy, robustness, and range of applicability internal combustion engine modeling algorithms and coding for engine simulation. We have performed the following to advance the state of the art:

- Development of an *hp*-adaptive PCS FEM for all for multi-component fluids

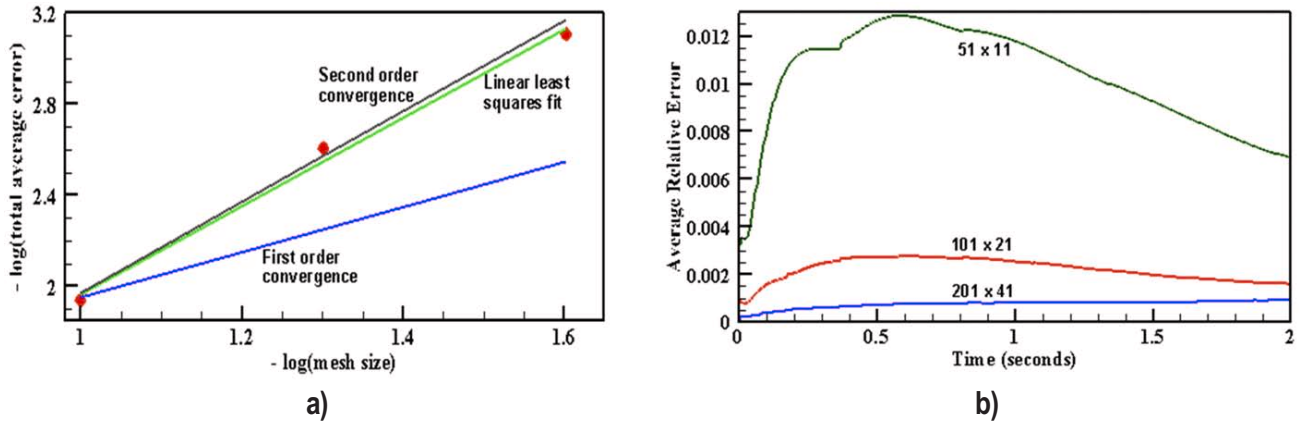

FIGURE 5. Convergence rates a) and solution error b) compared to the analytic solution for flow between moving parallel plates with inlet on one open side.

- Validated the immersed moving parts method in 3-D with extensive error analysis and comparisons to analytic solution.
- Developed a plasma kernel spark model for spark ignition that mimics the energy transport and timing of true spark, is applied as a single nodal source, and is a function of engine manufacturer-specified spark current.
- Validated the KIVA reactive chemistry model into PCS FEM solver.
- Developing the rest of MPI parallel system that will contain OpenMP threading to in the *hp*-adaptive FEM.
- Developed LES turbulence modeling for wall-bounded flows.

REFERENCES

1. Carrington, D.B., Wang, X. and Pepper, D.W. (2013) A predictor-corrector split projection method for turbulent reactive flow, Journal of Computational Thermal Sciences, Begell House Inc., vol 5, no. 4, pp.333-352.

2. Carrington, D.B., (2011) A Fractional step hp-adaptive finite element method for turbulent reactive flow, Los Alamos National Laboratory Report, LA-UR-11-00466.

3. Wang, X., Carrington, D. B., Pepper, D.W. (2009) An adaptive FEM model for unsteady turbulent convective flow over a backward-facing step, Journal of Computational Thermal Sciences, vol 1, no. 2, Begell House Inc., pp. 121-135.

4. Vreman, A.W., (2004) "An eddy-viscosity subgrid-scale model for turbulent shear flow: Algebraic theory and applications," *Physics of Fluids*, 16, pp. 3670-81.

5. Vallet, I. (2008), "Reynolds-stress modeling of M=2.25 shock-wave/turbulent boundary-layer interaction," International Journal of Numerical Methods in Fluids, vol. 56, Wiley, pp. 525-555.

6. K. Eisazadeh-Far, F. Parsinejad, H. Metghalchi, J. Keck, (2010) "On Flame kernel formation and propagation in premixed gases," Combustion and Flame, vol. 157, Elsevier, pp. 2211-2221

7. J. Song and M. Sunwoo, (2001) "Flame kernel formation and propagation modeling in spark ignition engines," Proceeding of the Institution of Mechanical Engineers, vol. 215, no. 1, pp. 105-114.

8. Carrington, D.B., Munzo, D.A., Heinrich, J.C (2014), "A local ALE for flow calculations in physical domains containing moving interfaces," "A local ALE for flow calculations in physical domains containing moving interfaces," Progress in Computational Fluid Dynamics, an Int. Jour. vol 14, no, 3, pp. 139-150.

FY 2014 PUBLICATIONS/PRESENTATIONS

1. Wang, X., Carrington, D. B. and Pepper, D. W. (2014) An *hp*-adaptive Predictor-Corrector Split Projection Method for Turbulent Compressible Flow, *Proceedings of the 15th International Heat Transfer Conference, IHTC-15,* Kyoto, Japan, August 10-15.

2. Carrington, D.B., Munzo, D.A., Heinrich, J.C (2014), "A local ALE for flow calculations in physical domains containing moving interfaces," "A local ALE for flow calculations in physical domains containing moving interfaces," Progress in Computational Fluid Dynamics, an Int. Jour. vol 14, no, 3, pp. 139-150.

3. Carrington, D.B., Wang, X. and Pepper, D.W. (2013), A predictor-corrector split projection method for turbulent reactive flow, Journal of Computational Thermal Sciences, Begell House Inc., vol 5, no. 4, pp.333-352.

II.14 Engine Efficiency Fundamentals – Accelerating Predictive Simulation of Internal Combustion Engines with High Performance Computing

K. Dean Edwards (Primary Contact), Charles E.A. Finney, Sreekanth Pannala, Wael R. Elwasif, Miroslav K. Stoyanov, Clayton G. Webster, Robert M. Wagner, C. Stuart Daw

Oak Ridge National Laboratory (ORNL)
National Transportation Research Center
2360 Cherahala Blvd.
Knoxville, TN 37932

DOE Technology Development Manager
Leo Breton

Overall Objectives

- Develop and apply innovative strategies that maximize the benefit of high-performance computing (HPC) resources and predictive simulation to support accelerated design and development of advanced engines to meet future fuel economy and emissions goals.
- Demonstrate potential of HPC to provide unprecedented new information on the development of combustion instabilities for advanced combustion engines.
- Development and validation of multi-processor simulation tools to accelerate design and optimization of fuel-injector design for direct-injection gasoline applications.

Fiscal Year (FY) 2014 Objectives

- Develop and demonstrate novel approach to investigate cyclic variability in highly dilute and dual-fuel applications.
- Couple computational fluid dynamics (CFD) injector and engine models to enable simulation of in-cylinder spray development.

FY 2014 Accomplishments

- Supported three ongoing efforts with direct industry collaboration.
- Developed and demonstrated computational frameworks for managing massively parallel simulation and optimization jobs on ORNL's Titan supercomputer.
- Observed significant variation in predicted combustion performance at highly dilute conditions due to stochastic variability in initial spray conditions.

Future Directions

- Collaborating with industry and Lawrence Livermore National Laboratory to enable graphical processing unit implementation of Converge™ flow solvers and evaluate the resulting speed-up on Titan.
- Continued effort to couple injector and engine models to include in-cylinder spray development and combustion into the injector design optimization process.

INTRODUCTION

This project supports rapid advancements in engine design, optimization, and control required to meet increasingly stringent fuel economy and emissions regulations through the development of advanced simulation tools and novel techniques to best utilize HPC resources such as ORNL's Titan. This effort couples ORNL's leadership role in HPC with experimental and modeling expertise with engine and emissions-control technologies. Specific project tasks evolve to support the needs of industry and DOE. Three tasks were supported during FY 2014:

- **Task 1:** Use of highly parallelized engine simulations to understand the stochastic and deterministic processes driving cyclic variability in dilute combustion systems. Collaborative effort with Ford Motor Company and Convergent Science.
- **Task 2:** Use of detailed CFD simulations to understand and optimize the design of gasoline direct-injection fuel injectors for improved engine efficiency. Collaborative effort with General Motors.
- **Task 3:** Use of highly parallelized, detailed CFD simulations to investigate stability of dual-fuel operations for locomotive applications. Collaborative effort with General Electric and Convergent Science.

APPROACH

The aim of this project is to develop and apply innovative approaches which use HPC resources for simulation of engine systems to address specific issues of interest to industry and DOE. The specific issues addressed and approaches applied for the three current tasks are described below.

Task 1: Dilute combustion provides a potential pathway to simultaneous improvement of engine efficiency and emissions. However, at sufficiently high dilution levels, flame propagation becomes unstable, and small changes in initial cylinder conditions can produce complex cycle-to-cycle combustion variability, forcing the adoption of wide safety margins and failure to achieve the full potential benefits of charge dilution. The use of computational simulations to understand the physics and chemistry behind the combustion stability limit has the potential to facilitate control of the instabilities allowing operation at the 'edge of stability.' A major challenge is that many of the associated dynamical features are very subtle and/or infrequent, requiring simulation of hundreds or thousands of sequential engine cycles in order to observe the important unstable events with any statistical significance. Complex CFD simulations can require days of computational time for a single engine cycle making serial simulation of thousands of cycles time-prohibitive. In this task, we are partnering with Ford and Convergent Science to address these computational challenges. Our approach uses uncertainty quantification and sparse-grid sampling of the parameter space to replace simulation of many successive engine cycles with multiple, concurrent, single-cycle simulations which exhibit statistically similar behavior. Results from these simulations are then used to generate lower-order metamodels which retain the key dynamic features of the complex model but computationally are simple enough to allow simulation of serial combustion events and detailed studies of the parameters that promote combustion instability.

Task 2: Multi-hole injectors utilized by gasoline direct-injection engines offer the flexibility of manufacturing the nozzle holes at various orientations to engineer a variety of spray patterns. The challenge is to determine the optimal design to maximize efficiency and emissions benefits for a given application. Detailed analytical tools, such as CFD, can provide a cost-effective approach to reduce the number of potential injector concepts for a given combustion system. However, each CFD simulation requires substantial run time and conducting a thorough investigation of the design and operating parameter space to optimize injector design remains tedious and labor intensive. In this task, we are working with General Motors to develop and validate a high-fidelity, multi-processor simulation tool to accelerate design and optimization of fuel injector hole patterns for direct-injection gasoline applications. Our approach involves the use of an optimization routine to coordinate parallel fuel-spray and combustion simulations with different injector geometries to hasten convergence on an optimal design.

Task 3: The growing availability and lower sustained price of natural gas versus diesel fuel has led to a growing interest in natural gas as a substitute fuel for traditional diesel applications. However, with increasing substitution of natural gas comes increasing combustion instability resulting in reduced fuel economy benefits and rough engine performance thus limiting the practical range of operation in real-world applications. In this new task for FY 2014, we are partnering with General Electric and Convergent Science to adapt tools and approaches developed for Task 1 to enable detailed study of the parameters promoting instabilities in dual-fuel locomotive applications.

RESULTS

Efforts in FY 2014 have focused on development and application of the tools and methodologies required for each task and transfer of those tools and capabilities to our industry partners.

Task 1: Efforts for this task during FY 2014 were focused on demonstration of our metamodel approach on a detailed CFD model of a spark-ignition engine with high dilution due to external and internal exhaust gas recirculation. To accurately capture the deterministic trends associated with variations in key operating parameters with a single-cycle simulation approach, each CFD simulation must produce a unique, repeatable result. However, simulation results from our initial sparse-grid sampling were found to exhibit strong stochastic variability which masks the underlying deterministic dynamics. The source of this variability was traced to the Lagrangian spray model which introduces uncontrolled, stochastic variability to the initial conditions of the direct-injection fuel spray. At the highly dilute conditions in this study, these small variations produce highly variable combustion performance as shown in Figure 1. In lieu of a predictive spray model to provide repeatable spray initialization, we have modified our approach by simulating multiple cycles at each sample point and averaging the results. Initial grid sampling results with this modified approach have shown promise. Additional efforts which will continue into FY 2015 include adapting the engine model for large-eddy simulation turbulent modeling and collaborating with Convergent Science, NVIDIA, and Lawrence Livermore National Laboratory to adapt the Converge™ flow solvers for

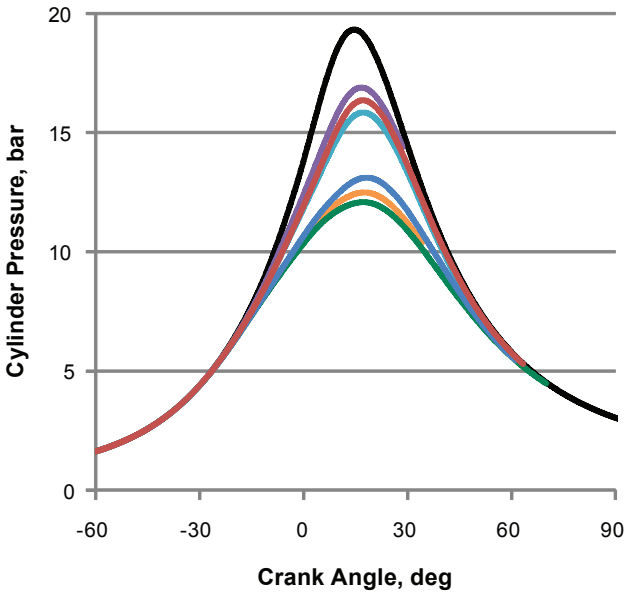

FIGURE 1. Stochastic variability in initial spray conditions (generated by changing the random seed for the Lagrangian spray model while maintaining all other parameters constant) was observed to produce significant variation in predicted combustion performance at highly dilute conditions.

graphical processing unit implementation and evaluate the resulting speed-up on Titan.

Task 2: Efforts for this task in FY 2014 were focused on continued development of the computational framework to manage the design optimization tasks and coupling of the OpenFOAM® injector model with a Converge™ engine model. The computational framework was used to perform a large-scale sweep of injector geometric and operating parameters consisting of seven candidate injector designs, each evaluated at 42 reference operating points. Simulation results were validated against experimental spray visualization measurements provided by General Motors. A user-defined function was created to couple the validated injector model with a Converge™ engine model to enable simulation of in-cylinder spray development, fuel-air mixing, and combustion. Predictive results from the OpenFOAM® injector model provide initial and boundary conditions to the traditional Lagrangian spray model in Converge™ eliminating the introduction of stochastic variation to the initial conditions as in Task 1. Initial testing of the coupled model (without combustion) was completed this FY with full implementation set for early FY 2015.

Task 3: Efforts for this task began in FY 2014 with General Electric and Convergent Science developing and calibrating a Converge™ CFD engine model for dual-fuel operation and ORNL adapting the metamodel approach to this application. An initial sparse-grid sampling of the parameter space was set up on Titan and evaluated on a limited basis. Evaluation of these results and refinement of the engine model continue into FY 2015.

CONCLUSIONS

Increasing industry interest in utilizing HPC resources to hasten advancements in engine design has led to collaborative efforts with industry stakeholders in the important areas of understanding and controlling cycle-to-cycle variability in highly dilute and dual-fuel combustion applications and optimization of fuel injector design. Progress on these tasks is on track and showing great promise.

FY 2014 PUBLICATIONS/PRESENTATIONS

1. KD Edwards, *et al.* (2014). *Accelerating advanced engine development with high-performance computing.* **AEC Program Review Meeting**. Southfield, MI, USA; Aug 2014.

2. KD Edwards (2014). *Overview of predictive simulation and high performance computing activities at ORNL*. **DOE CFD Workshop**. Southfield, MI, USA; Aug 2014.

3. CEA Finney, *et al.* (2014). *Exploring the dynamics of cycle-to-cycle variability using many high-dimensional single-cycle simulation*. **35th International Symposium on Combustion**. San Francisco, CA, USA; Aug 2014.

4. KD Edwards, *et al.* (2014). *Accelerating predictive simulation of IC engines with high performance computing.* **2014 DOE Vehicle Technologies Office Annual Merit Review**. Washington, D.C., USA; June 2014.

5. CEA Finney, *et al.* (2014). *Application of high performance computing for simulating the unstable dynamics of dilute spark-ignited combustion*. **Understanding Complex Systems: Proceedings of 2012 International Conference on Theory and Applications of Nonlinear Dynamics (ICAND)**. ISBN 978-3-319-02924-5. pp. 259-270.

6. MK Stoyanov (2014). *High dimensional multiphysics metamodeling for combustion engine stability.* **SIAM Conference on Uncertainty Quantification 2014**. Savannah, GA, USA; April 2014.

7. MK Stoyanov (2014). *High dimensional multiphysics metamodeling for combustion engine stability.* **2014 SIAM Southeastern Atlantic Section Annual Meeting**. Melbourne, FL, USA; March 2014.

8. KD Edwards, *et al.* (2014). *Accelerating advanced engine development with high-performance computing.* **AEC Program Review Meeting**. Livermore, CA, USA; Feb 2014.

SPECIAL RECOGNITIONS AND AWARDS/ PATENTS ISSUED

1. Awarded two of the 42 DOE Office of Science 2014 ASCR Leadership Computing Challenge (ALCC) awards including 17.5Mhrs and 15Mhrs allocated on Titan to support Tasks 1 and 2, respectively

II.15 Use of Low-Cetane Fuel to Enable Low-Temperature Combustion

Stephen Ciatti
Argonne National Laboratory
9700 S. Cass Ave.
Bldg. 362
Argonne, IL 60439

DOE Technology Development Manager
Leo Breton

Subcontractor
University of Wisconsin-Madison Engine Research Center, Madison, WI

Overall Objectives

- Optimize the operating conditions to use low-cetane fuel to achieve clean, high-efficiency engine operation.
- Demonstrate the use of low-temperature combustion (LTC) as an enabling technology for high-efficiency vehicles.

Fiscal Year (FY) 2014 Objectives

- Optimize the engine control parameters (injection strategy, exhaust gas recirculation [EGR], intake temperature) for 87 anti-knock index (AKI) gasoline fuel to achieve wide range (low load/idle to full load) performance using pump gasoline.
- Demonstrate the efficiency benefits of LTC using an Autonomie simulation to validate higher efficiency vehicles.
- Demonstrate collaboration with Argonne's engine simulation team to provide further insight into gasoline compression ignition enhanced operation.

FY 2014 Accomplishments

- Achieved idle (-0.2 bar brake mean effective pressure, BMEP) to 20-bar BMEP using only 87 AKI fuel.
- Attained a 30% fuel economy improvement using LTC in a conventional powertrain vehicle over a similar port-fuel-injected (PFI) vehicle on the combined Urban Dynamometer Driving Schedule and Highway Fuel Economy Test cycles in a 2007 Cadillac BES vehicle.
- Utilized high-fidelity simulations at Argonne to explore three-dimensional assessments of in-cylinder reactivity.

Future Directions

- Continue to improve low-load operation using low-pressure diesel injection, reduced injector umbrella angles and reduced swirl to enhance local richness in the combustion chamber.
- Use 10% ethanol-based 87 AKI fuel to insure success using a more representative U.S. pump gasoline.
- Explore the opportunity to utilize a turbo/supercharger combination to enhance intermediate temperature heat release (results from John Dec's work at Sandia National Laboratories) to further enhance low-load operation.
- Conduct additional engine performance tests for Autonomie simulations to support LTC development as applied to vehicles.

INTRODUCTION

Current diesel engines already take advantage of the most important factors for efficiency—no throttling, high compression ratio and low heat rejection. However, diesel combustion creates a significant emissions problem. Mixing or diffusion combustion creates very steep gradients in the combustion chamber because the ignition delay of diesel fuel is extremely short. Particulate matter PM and oxides of nitrogen (NO_x) are the result of this type of combustion, requiring expensive after-treatment solutions to meet emissions regulations.

The current work seeks to overcome the mixing controlled combustion dilemma by taking advantage of the long ignition delay of gasoline to provide much more premixing of fuel and air before ignition occurs. This premixing allows for the gradients of fuel and air to be much less steep, drastically reducing the PM-NO_x tradeoff relationship of mixing-controlled combustion.

APPROACH

The intent of this project is to utilize the long ignition delays of low-cetane fuels to create an advanced combustion system that generates premixed (but not homogeneous!) mixtures of fuel and air in the

combustion chamber. As reported in several articles, if the local equivalence ratio is below 2 (meaning at most, twice as much fuel as oxidizer) and the peak combustion temperature is below 2,000 K (using EGR to drop the oxygen concentration below ambient 21%, thereby slowing the peak reaction rates and dropping the peak combustion temperature), a combustion regime that is very clean and yet retains reasonably high power density is achieved.

The challenge to this type of combustion system is the metering of fuel into the combustion chamber needs to be precise, both in timing and amount. If too much fuel is added too early, a very loud, ringing type of combustion occurs, which creates unacceptably high combustion noise or worse. If not enough fuel is added, ignition may not occur at all and raw hydrocarbon exits the exhaust. Control over the relevant operating parameters is very important—fuel properties, injection strategy, compression ratio and intake temperature all have large influence upon ignition propensity.

Different-injection strategies were employed this year to extend low-load operation operating on only 87 AKI fuel and lower injection pressures (500 bar and 250 bar) along with a narrow inclusion angle nozzle (120 degree as opposed to the 148 degree stock), along with uncooled EGR and swirl effects.

RESULTS

Injection strategy was altered in an effort to determine how much premixing is necessary to achieve the low-load goals. First, one injection was used, with injection timing swept from -9 deg after top-dead center (ATDC) to -42 deg ATDC. Rail pressure was held constant at 500 bar and 250 bar during these sweeps. Fuel rate was adjusted at each injection timing/pressure to the minimum allowed while maintaining a 3% coefficient of variance of indicated mean effective pressure or better for combustion stability for all points above 1 bar BMEP. A metric of 15 kPa standard deviation was used for loads below 1 bar BMEP. No EGR was used for these tests. Results showed that for 850 RPM, the optimal injection timing for maximum reactivity was -18 deg ATDC, while for 1,500 RPM the optimal injection timing was -30 deg ATDC – see Figure 1.

The engine simulations conducted by both the University of Wisconsin-Madison Engine Research Center and by Argonne showed a three-dimensional profile in reactivity (Phi-T) to characterize the distribution in-cylinder—see Figure 2. The significant part of this result is that the reactivity of the gasoline in each cell showed the areas where ignition occurred first—areas that were lean (Phi between 0.45 and 0.8, with local temperatures around 900 K) because this

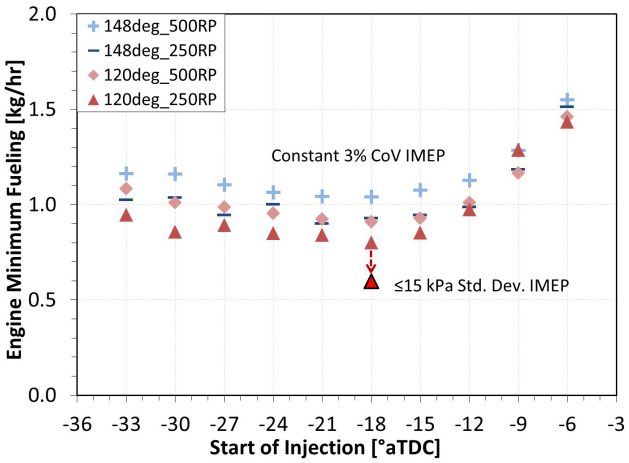

FIGURE 1. Minimum Fueling Rates for 500 Bar and 250 Bar Injection Pressure for 148 and 120 degree Inclusion Angles

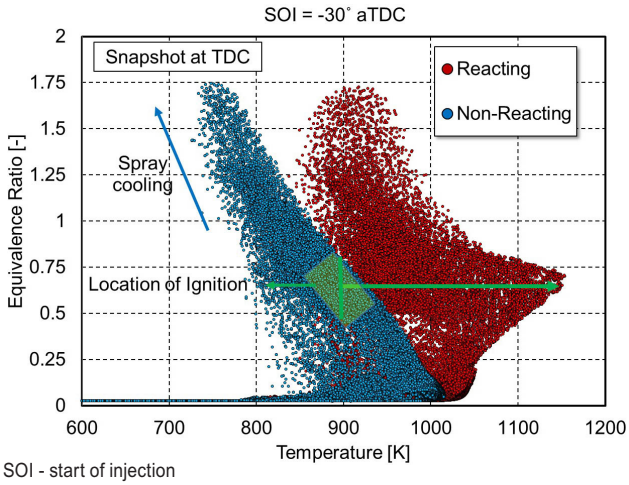

SOI - start of injection

FIGURE 2. Reactivity Phi-T Plot for Unreacting and Reacting Simulation for Gasoline Compression Ignition Engine

combination produced the maximum reactivity for this fuel.

In addition, additional points were run for the Autonomie simulations (building upon FY 2012's work) to refine the vehicle potential for fuel economy improvement. A 2007 Cadillac BES was chosen as the example vehicle because it can be purchased with a PFI engine or the General Motors diesel engine upon which the LTC engine is based. With the additional points and a further refined vehicle simulation, the fuel economy improvement was found to be 30% based upon the combined drive cycles for the Urban Dynamometer Driving Schedule and Highway Fuel Economy Test—see Figure 3.

LTC Engine Shows Significant Fuel Economy Improvement over PFI and DI

Fuel Consumption

Fuel Consumption [l/100km]	PFI	SIDI	LTC	LTC with new map
UDDS	8.1	7.3	6.3	6.22
HWFET	6.0	5.6	4.9	4.6
Combined [55/45]	7.1	6.6	5.7	5.5
Improvement over PFI		8%	21%	23%
Improvement over SIDI			13%	16%

Fuel Economy

Fuel Economy [MPG]	PFI	SIDI	LTC	LTC with new map
UDDS	29.2	32.2	37.5	37.8
HWFET	39.0	41.9	47.6	50.7
Combined [55/45]	32.9	35.9	41.4	42.7
Improvement over PFI		9%	26%	29.6%
Improvement over SIDI			15%	19%

FIGURE 3. Cadillac BES Fuel Economy Comparisons—LTC vs. PFI

CONCLUSIONS

- A specific study was performed with the aim of extending the low-load limit toward idle. -0.2 bar BMEP was achieved using 87 AKI fuel, which is significantly lower than the FY 2013 accomplishment of 1.5 bar BMEP—while maintaining 3% coefficient of variance of indicated mean effective pressure or 15 kPa standard deviation—in each cylinder independently.
- Injection timing sweeps at two injection pressures (500 bar and 250 bar) were done, using both the 148 degree inclusion angle and the modified 120 deg inclusion angle. Single injections around -18 deg ATDC provided idle load at 850 RPM, while -30 deg ATDC provided 1.0 bar BMEP at 1,500 RPM.
- Using 250 bar rail pressure extended the low-load limit beyond the ability of 500 bar rail pressure; probably due to decreased mixing and enhanced local richness for ignition.
- Using the 120 deg inclusion angle provided even further enhancement to low-load operation, allowing the engine to idle at -0.2 bar BMEP.

FY 2014 PUBLICATIONS/PRESENTATIONS

1. Kolodziej, C.P., Ciatti, S.A., Vuilleumier, D., Das Adhikary, B., Reitz, R., (April 2014), SAE 2014-01-1302, "Extension of the Lower Load Limit of Gasoline Compression Ignition with 87 AKI Gasoline by Injection Timing and Pressure", SAE World Congress, Detroit, MI.

2. Das Adhikary, B., Reitz, R., Ciatti, S.A., Kolodziej, C.P., (April 2014), SAE 2014-01-01297 "Computational Investigation of Low Load Operation in a Light-Duty Gasoline Direct Injection Compression Ignition [GDICI] Engine Using Single-Injection Strategy", SAE World Congress, Detroit, MI.

3. Presentation for workshop on future fuels and future engines (September 2014), hosted by Tsinghua University, Beijing, China and funded by Saudi Aramco.

4. Invited keynote speaker for THIESEL 2014 (September 2014), hosted by CMT Motores Termico, Valencia, Spain.

II.16 High Efficiency GDI Engine Research

Thomas Wallner (Primary Contact), Riccardo Scarcelli, James Sevik
Argonne National Laboratory
9700 S. Cass Avenue
Lemont, IL 60439

DOE Technology Development Manager
Leo Breton

Overall Objectives

- Quantify efficiency potential and combustion stability limitations of advanced gasoline direct injection (GDI) engines operating under lean and exhaust gas recirculation (EGR) dilute conditions.
- Extend lean and EGR dilution tolerance of light-duty GDI engines through the implementation of advanced coil-based and non-coil-based ignition systems.
- Develop a three-dimensional computational fluid dynamics (3D-CFD) methodology to analyze and predict cyclic variability in GDI engines using conventional as well as advanced ignition systems.

Fiscal Year (FY) 2014 Objectives

- Quantify potential of high-energy spark plug and multi-spark operation.
- Initiate quantification of potential of laser ignition for dilute and lean combustion.
- Identify key partners for assessment of further advanced ignition systems.
- Establish correlation between the characteristics of the proposed ignition systems and flame propagation in a dilute environment using 3D-CFD.

FY 2014 Accomplishments

- Completed evaluation of spark-based ignition systems under dilute operation with focus on ignition energy and release profile.
- Collaboration with a research project on advanced ignition systems led by Isaac Ekoto from Sandia National Laboratories planned in detail for improving numerical modeling of conventional as well as alternative ignition systems.
- Successfully validated Reynolds-averaged Navier-Stokes (RANS) modeling characterized by low numerical diffusion as a tool to analyze cyclic variability for dilute operation.
- Free-air delivered laser system successfully implemented on the existing engine hardware and tested yielding improved combustion stability for dilute operation.

Future Directions

- Improve the understanding of engine cyclic variability and contrast RANS against large-eddy simulation engine multi-cycle results in terms of accuracy and computational requirements.
- Perform experiments and simulations to further the understanding of the basic interaction between ignition source and in-cylinder flow with the goal to improve flame propagation under dilute conditions.
- Develop and evaluate comprehensive numerical models for advanced ignition systems and validate with targeted experiments.

INTRODUCTION

Due to the U.S. heavy reliance on gasoline engines for automotive transportation, efficiency improvements of advanced gasoline combustion concepts have the potential to dramatically reduce foreign oil consumption. While downsized, turbocharged GDI engines currently penetrating the market already show significant improvements in fuel economy, advanced gasoline combustion concepts could enable further significant efficiency gains [1]. However, combustion strategies such as stratified, lean-burn, high EGR, and boosted operation present challenging conditions for conventional ignition systems thereby limiting the attainable benefits of these advanced combustion concepts [2]. When comparing dilute combustion against stoichiometric operation, the engine exhibits increased cyclic variability which negatively affects combustion stability and thermal efficiency.

This project is designed to identify the fundamental limitations of lean, boosted, and EGR-dilute combustion through experimental R&D combined with advanced 3D-CFD simulation to extend the lean and dilute limits by combining fundamental findings with benefits offered by advanced ignition systems.

APPROACH

Main thrust areas of this project are (1) expanding the fundamental understanding of characteristics and limitations of lean, boosted and EGR-dilute combustion, (2) performing a technology evaluation of advanced coil-based, and assessing the potential of non-coil-based, ignition systems on a consistent state-of-the-art automotive engine platform, and (3) developing robust modeling tools for the analysis of dilute combustion and advanced ignition systems.

The project includes experimental, as well as simulation-focused components. 3D-CFD simulation is adapted and applied to broaden the understanding of current limitations of lean, boosted, and EGR-dilute combustion with a focus on developing a best practice with reasonable computational requirements. Another main component of the project focuses on expanding simulation capabilities to allow (1) the evaluation of the effect of ignition properties on cyclic variability under dilute operation as well as (2) realistic simulation of advanced and non-coil-based ignition systems.

RESULTS

Comprehensive Evaluation of Spark-Based Systems with Programmable Discharge Profile

By using a programmable spark-based ignition system, the spark event can be altered to include multiple pulses of energy in rapid succession and variable pulses of energy. Figure 1 shows the examined ignition profiles, at a nominal energy level of 75 mJ. In addition to a conventional spark profile the ignition system was configured to deliver a sustained spark as well as multi-pulse spark. The duration of the spark delivery changes significantly with the conventional spark exhibiting the shortest delivery time of approximately 0.5 ms compared to the multi-pulse configuration at a total delivery in excess of 1 ms.

Results shown in Figure 2 highlight the effect of the total amount of delivered energy (75 mJ and 150 mJ tested) and delivery profile (conventional, sustained arc, multi-pulse) on combustion stability for both EGR dilute and lean operations. It can be seen that the increase of total energy only slightly reduces cyclic variability (coefficient of variation of indicated mean effective pressure, COV_{IMEP}). Conversely, delivering the same amount of energy with multiple pulses in a rapid succession greatly improves combustion stability for both dilute and lean operations. At 1,500 RPM and 3.2 bar IMEP, doubling the total energy and using a multi-pulse spark leads to 20% relative increase of EGR dilution (EGR = 18% vs. 15% baseline) and 10% relative increase in the lean limit (λ = 1.58 vs. 1.44 baseline, results not shown in Figure 2) with the combustion stability limit defined by a COV_{IMEP} value of 5%.

Validation of RANS Multi-Cycle Simulations for the Analysis of Combustion Stability

RANS modeling using fine mesh and detailed chemistry has shown potential not only to properly describe flame propagation under dilute conditions but also to capture typical combustion stability features. Figure 3 shows 10 consecutive cycles simulated at 2,000 RPM and 6 bar IMEP by using the baseline single-pulse 75 mJ ignition as well as the advanced multi-pulse 150 mJ profiles. The fluctuation of the numerical pressure traces, which is not damped out due to the low numerical viscosity, correlates well with the experimental data.

Using multiple pulses in a rapid succession reduces the amplitude of variation in the pressure traces due

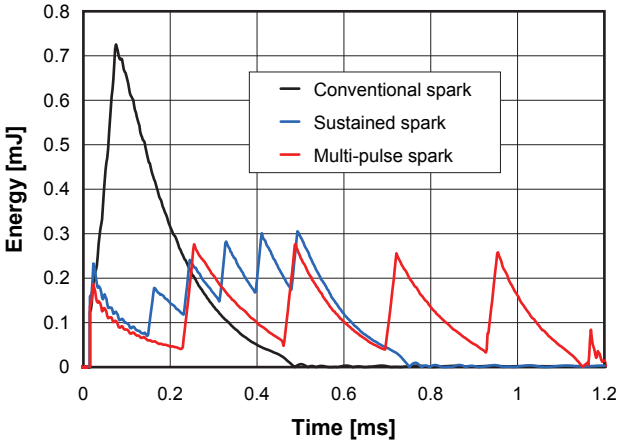

FIGURE 1. Characterization of Tested Ignition Profiles

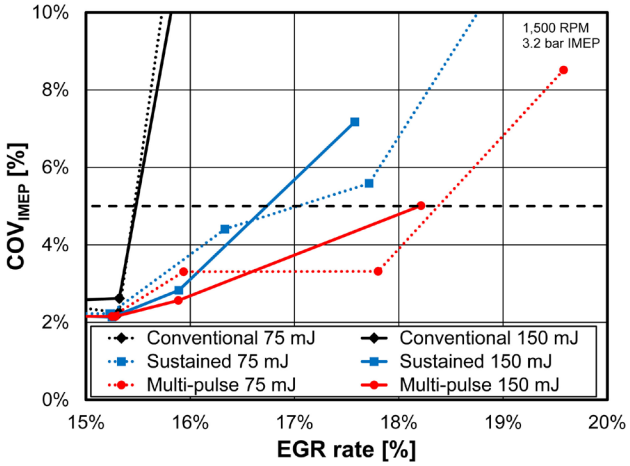

FIGURE 2. Influence of Ignition Profile and Energy Level on Combustion Stability in EGR Dilute (top) and Lean (bottom) Operation

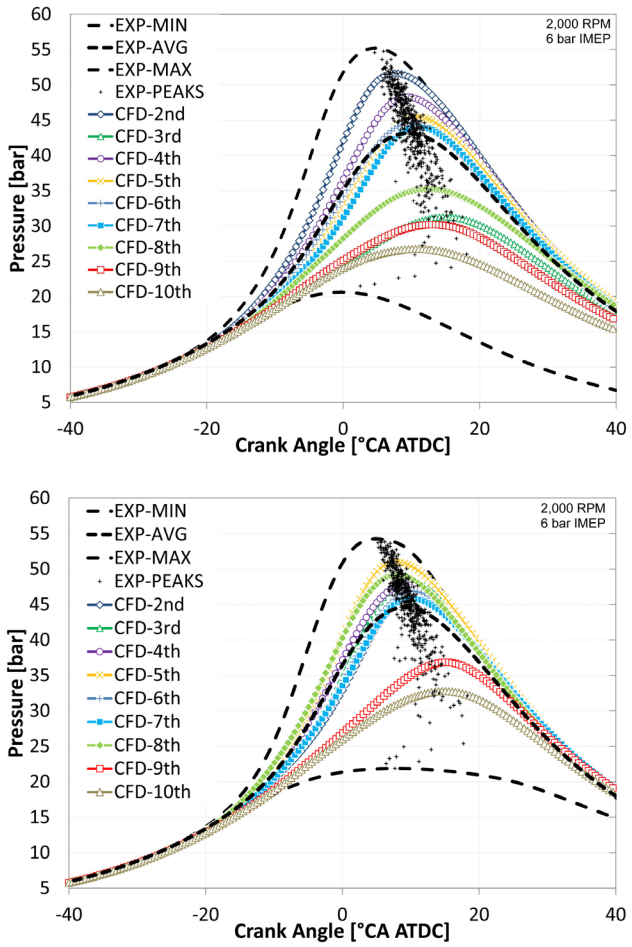

FIGURE 3. Effect of the Ignition Profile on Experimental and Numerical Cyclic Variability Conventional Spark 75 mJ (top) Vs. Multi-Pulse Spark 150 mJ (bottom)

to reduced sensitivity of the ignition event to localized charge motion variances. Figure 4 shows that increasing the delivered energy during the spark event while maintaining a single pulse has only a slight impact on the cycle-to-cycle variation phenomena since combustion varies greatly resulting in fast and slow cycles due to the near-spark flow structures at the ignition time. Indeed, increasing the energy magnifies the difference between fast and slow combustion cycles. Conversely, when the spark event is extended, as in the case of sustained arc and multi-pulse spark, there is a reduced dependency of the early flame development on in-cylinder flow. This is the effect of extending the duration of the spark event and potentially delivering re-strike events, characterized by locally high temperature values (order of magnitude of tens of thousands of K) that lead to the formation of active radical species that promote combustion. Therefore, the multi-pulse spark system delivers improved COV_{IMEP} due to stabilized flame kernel during the ignition event. As a result, poor combustion and misfire events are significantly reduced.

Key Partners Identified for Collaboration on Advanced Ignition Systems

The quality of numerical predictions can be further improved through the development of comprehensive ignition models for spark-based as well as alternative (laser) ignition systems. For this purpose, a technical collaboration between Argonne and Sandia National Laboratories has been defined with the goal of improving the basic understanding of the ignition process and developing advanced models for simulating the ignition event in high efficiency GDI engines. A research

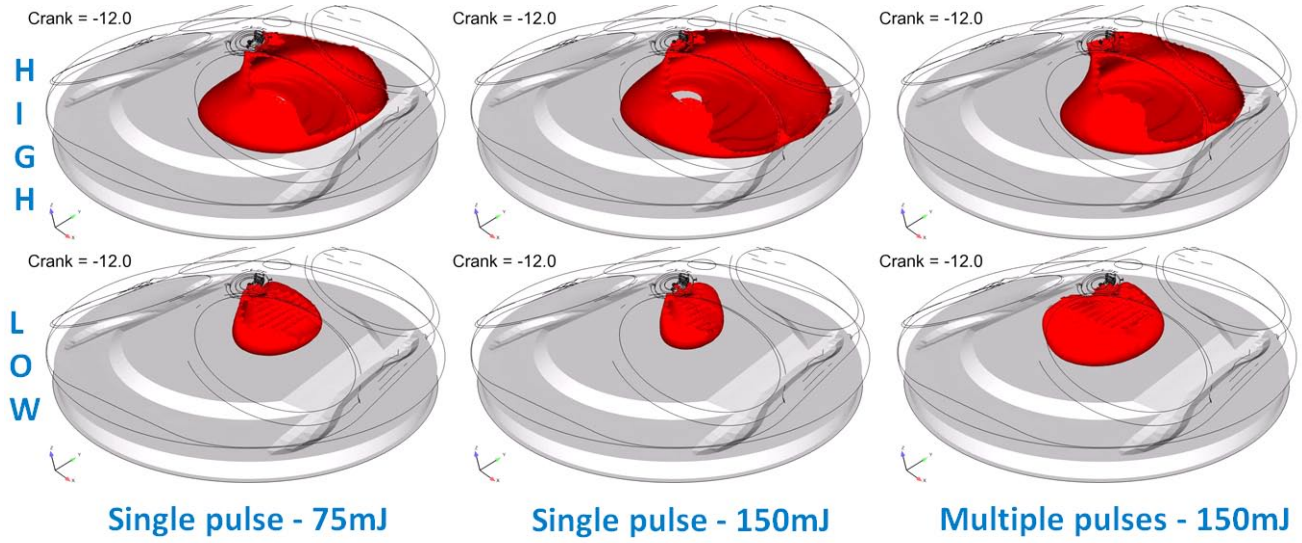

FIGURE 4. Effect of Ignition Profile on Flame Propagation in Case of Fast (HIGH) and Slow (LOW) Combustion Event

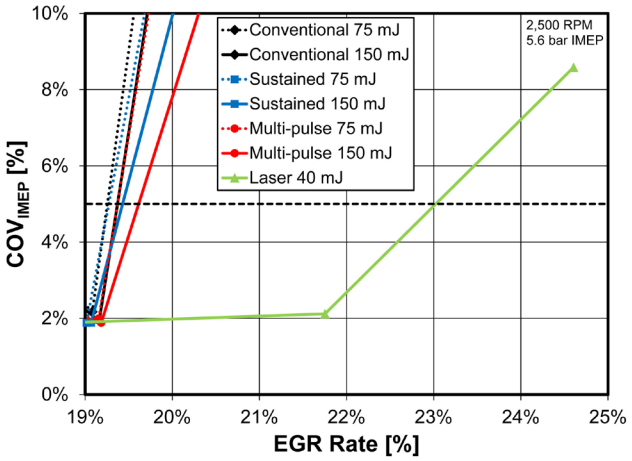

FIGURE 5. Preliminary Results Comparing Laser Ignition to Advanced Spark-Based Options

project on advanced ignition systems led by Isaac Ekoto at Sandia is expected to deliver optical data for the development and validation of advanced ignition models during FY 2015.

Successful Implementation of Laser Technology on a Single-Cylinder Light-Duty Platform

A free-air delivered laser system was successfully implemented on the existing engine hardware and was initially tested and compared against baseline and advanced ignition spark-based profiles. Figure 5 shows preliminary laser ignition results. In particular, laser ignition was effective under EGR dilute conditions, showing significant potential to extend the dilution tolerance compared to spark-based systems. At 2,500 RPM and 5.6 bar IMEP, laser ignition led to 18% relative increase of EGR dilution compared to the spark-based ignition system.

CONCLUSIONS

- The evaluation of a programmable spark-based system was completed and the benefit of using higher energy and sustained as well as multi-spark modes was assessed showing a maximum 20% relative increase of EGR dilution and maximum 10% relative increase in the lean limit.
- A promising approach to qualitatively analyze and predict cyclic variability and combustion stability using multi-cycle RANS simulations was identified. Fine mesh RANS simulations characterized by low numerical viscosity delivered fluctuations in the numerical pressure traces that well correlated to the experimental stability trend and provided insight into the fundamental interaction of the ignition source and the in-cylinder flow.
- The collaboration with a research project on advanced ignition systems carried out at Sandia was planned in detail to provide further understanding of the in-cylinder ignition process and deliver data for development and validation of advanced ignition models.
- A free-air delivered laser ignition system was successfully implemented on the single-cylinder research engine platform and demonstrated the potential to further extend dilution tolerance and improve the indicated thermal efficiency.

REFERENCES

1. Alger, T. and Mangold, B., "Dedicated EGR: A New Concept in High Efficiency Engines", SAE Int. J. Engines 2(1):620-631, 2009.

2. Kaul, B., Wagner, R., and Green, J., "Analysis of Cyclic Variability of Heat Release for High-EGR GDI Engine Operation with Observations on Implications for Effective Control", SAE Int. J. Engines 6(1):132-141, 2013.

FY 2014 PUBLICATIONS/PRESENTATIONS

1. Matthias, N.S., Wallner, T., Scarcelli, R., Analysis of Cyclic Variability and the Effect of Dilute Combustion in a Gasoline Direct Injection Engine. SAE Int. J. Eng. 7(2), 2014.

2. Scarcelli, R., "RANS Cycle-to-Cycle Variations in SI Engine Simulations," Converge User Group Meeting, Madison, WI, 2–24 September 2014.

3. Scarcelli, R., Matthias, N.S., Wallner, T., "Numerical and Experimental Analysis of Ignition and Combustion Stability in EGR Dilute GDI Operation," ASME Paper ICEF2014-5607, 2014.

4. Richards, K.J., Scarcelli, R., et al., "The Observation of Cyclic Variation in Engine Simulations when using RANS Turbulence Modeling," ASME Paper ICEF2014-5605, 2014.

5. Wallner, T., Sevik, J., Scarcelli, R., "Extending the Lean and EGR Dilute Operating Limits of a Light-Duty GDI Engine using Alternative Spark-Based Ignition," scheduled for publication in the proceedings of 2nd International Conference on Ignition Systems for Gasoline Engines (IAV), 24–25 November, 2014.

6. Scarcelli, R., Sevik. J., Wallner, T., et al. "Capturing Numerical Cyclic Variability in the RANS Simulation of Dilute SI Combustion," SAE Technical Paper 15PFL-0357. Scheduled for publication at the SAE 2015 World Congress.

7. Sevik, J.M., Wallner, T., Scarcelli, R., et al., "Effects of Ignition and Injection Perturbation under Lean and Dilute GDI Engine Operation," Scheduled for publication at the JSAE 2015/ SAE PFL2015 conference.

II.17 High Dilution Stoichiometric Gasoline Direct-Injection (GDI) Combustion Control Development

Brian C. Kaul
Fuels, Engines, and Emissions Research Center
Oak Ridge National Laboratory (ORNL)
2360 Cherahala Boulevard
Knoxville, TN 37932

DOE Technology Development Manager
Gurpreet Singh

Overall Objectives

- Characterize dynamics of cyclic variability that limits dilution levels in spark-ignition (SI) engines
- Evaluate potential engine efficiency gains resulting from effective control of cyclic variations
- Demonstrate dilution limit extension through active control to reduce cyclic variability

Fiscal Year (FY) 2014 Objectives

- Characterize sensitivity of control parameters to data sampling quality
  - Production-grade sensors and engine control units (ECUs) do not provide the same resolution of data acquisition as laboratory-grade equipment
  - Results will determine the necessary resolution and accuracy of data to apply these control strategies in the market
- Evaluate potential of next-cycle control strategies for combustion stability and efficiency improvements

FY 2014 Accomplishments

- Commissioned new engine control system and implemented initial next-cycle control strategy based on symbol-sequence-statistics analysis of prior-cycle events
- Characterized sensitivity of control parameters to data sampling quality and determined that symbolic analysis approach is robust for reduced-quality data
- Determined that dual-timescale control is necessary for high-EGR control strategies to be effective
- Determined that effective dual-timescale next-cycle control strategies have the potential to yield an additional three point reduction in coefficient of variation relative to single-timescale control with a 5% overall fuel efficiency improvement at a high exhaust gas recirculation (EGR), 2,000 rpm/4-bar brake mean effective pressure operating condition, based on available deterministic information

Future Directions

- FY 2015: Demonstrate impact of dual-timescale control strategies on EGR dilution limit extension
- FY 2015: Demonstrate applicability of short-timescale next-cycle control strategy to homogeneous lean combustion
- FY 2016: Develop model-based control strategies and integrate with symbol-sequence-based strategies
- FY 2017: Evaluate potential same-cycle control applications (e.g. misfire avoidance)

INTRODUCTION

Operation of SI engines with high levels of charge dilution through EGR achieves significant efficiency gains while maintaining stoichiometric operation for compatibility with three-way catalysts. At high engine loads, efficiency gains of 10-15% are achievable with current technology. Dilution levels, however, are limited by cyclic variability—including significant numbers of misfires—that increases in frequency with dilution, especially at low engine loads typical of operation on standard light-duty drive cycles. The cyclic variability encountered at the dilution limit is not random, but has been shown to be influenced by the events of prior engine cycles. This determinism offers an opportunity for dilution limit extension through active engine control, thus enabling significant efficiency gains by extending practically achievable dilution levels to the edge of combustion stability.

This project is focused on gaining and utilizing knowledge of the recurring patterns that occur in cyclic variability to predict and correct for low-energy cycles such as misfires that reduce engine efficiency at the dilution limit. In particular, the dynamics of systems using cooled EGR loops have been elucidated for the first time, and are somewhat different from those of lean combustion systems for which similar background work has been carried out in the past. This knowledge will

be utilized to develop and implement next-cycle active control strategies for extending the dilution limit.

APPROACH

A modern, turbocharged 2.0-L GDI engine, modified with a higher-than-stock compression ratio, has been installed in an engine test facility at ORNL. An external cooled EGR loop has been installed on the engine to allow operation with external EGR, as illustrated in Figure 1. An open, LabVIEW-based engine controller with next-cycle control capabilities is used to operate the engine and evaluate control strategies.

Experiments have been conducted operating the engine at steady-state EGR levels beyond the practical dilution limit imposed by cyclic variability limits. The dynamics of cycle-to-cycle variations at these conditions were observed and analyzed using tools derived from chaos theory to identify recurring patterns that indicate non-random structure. Knowledge of these patterns is being used to implement control strategies based on the events of prior cycles, to stabilize combustion near the dilution limit.

RESULTS

Symbol-sequence analysis of the time series of heat release data is a useful method for identifying recurring patterns in the cyclic variations. In this method, the data are binned and each bin is assigned a symbol; these symbols can be thought of as "letters" and sequences of these letters can be compiled into "words." Examination of these symbolic words will often elucidate patterns that were obstructed by noise (i.e. stochastic variations) in the raw data. This method is described in detail by Finney et al. [1] and by Daw et al. [2]. Using these symbolic words, undesirable trajectories in the cycle-to-cycle variations can be detected, enabling control decisions to push the system back to the desired fixed point. To this end, a fully open, programmable control system that is capable of next-cycle controls was installed and commissioned on the engine, and an initial symbol-sequence-based strategy for controlling cyclic variability at the dilute limit was implemented.

Experiments performed in the previous FY and published this year in the SAE Journal of Engines (listed publication number 1) elucidated previously unknown long-timescale dynamics for external EGR systems

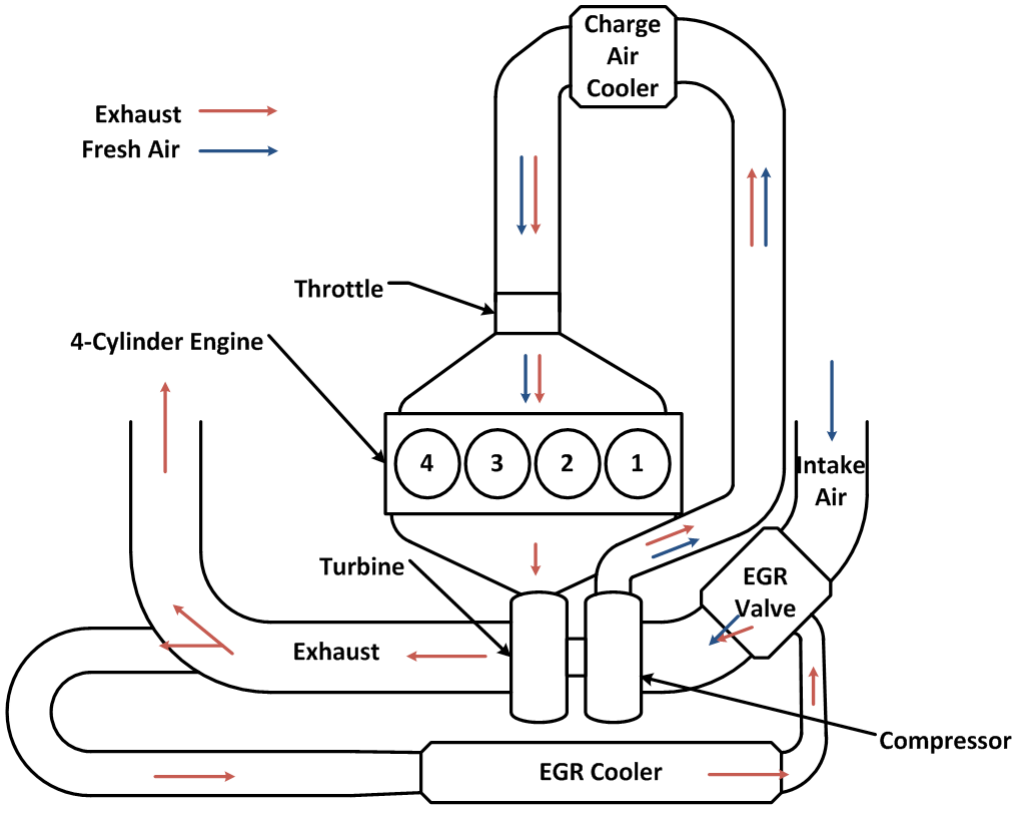

FIGURE 1. EGR System Diagram

caused by the recirculated exhaust gas composition. This long-timescale feedback effect is superimposed on the short-timescale (prior-cycle) feedback effects from the internal residual gases that have been previously noted for lean and dilute combustion [3,4], and evaluations of the initial symbol-sequence-based strategy indicate that it will be necessary to combine both in a dual-timescale control approach in order to achieve effective dilute limit extension. A method for constructing symbolic words that will give the necessary information about the system has been devised and will be evaluated and refined in the upcoming FY. Analysis of engine data indicates that the additional deterministic information available to a dual-timescale controller gives the potential for an additional three point reduction in coefficient of variation relative to a single-timescale controller, and could yield an overall 5% fuel efficiency improvement.

One concern about the practical implications of the nonlinear dynamics-based control approaches pursued in this project is the use of laboratory-quality in-cylinder pressure data and combustion analysis as feedback. In production, cylinder pressure is rarely available, and laboratory-grade data acquisition and analysis would not be practical on an automotive ECU. To this end, analysis of the sensitivity of the combustion metrics and symbol sequence response to reduced-quality data was performed. The effects of data quality on combustion metrics were examined by introducing phase shifts (top-dead center [TDC] location errors), reducing data resolution, introducing pressure pegging errors, and adding random noise in postprocessing. For example, Figure 2 shows the baseline cylinder pressure trace, which was collected with a 0.2° (1,800 pulse per revolution) crankshaft encoder, as well as a 6° resolution trace. This has a significant impact on combustion metrics including indicated mean effective pressure (IMEP) and heat release, as illustrated in Figure 3, where it can be seen that even for 1° resolution, there is a 2% error in IMEP and a 4% error in cumulative heat release, relative to the baseline condition. Other reductions in data quality also had notable impacts, including a 4.5% error in IMEP per crankangle degree of TDC offset.

Symbol-sequence analysis proved to be robust despite the errors imposed by reduced data quality. Figure 4 shows a histogram of the frequency of occurrence of observed symbolic words in the sample data set. Note that the structure is largely preserved, with the same words occurring frequently and infrequently. The horizontal red line in this figure indicates the frequency of occurrence that would be expected for stochastic variations, if no deterministic effects were present. From the similarity of the histograms, it is apparent that the symbol sequence analysis method

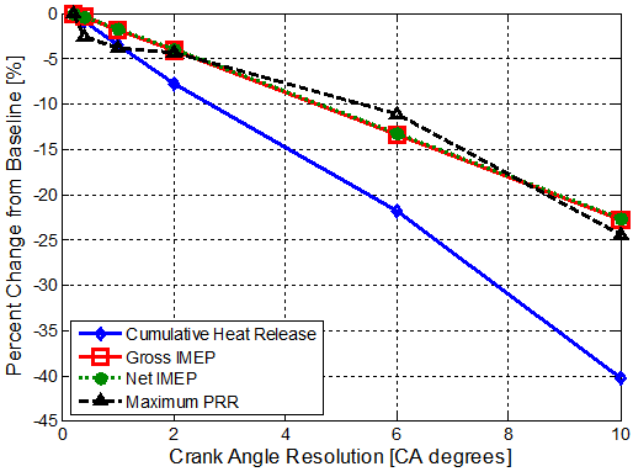

FIGURE 3. Effect of Reduced Encoder Resolution on Combustion Metrics

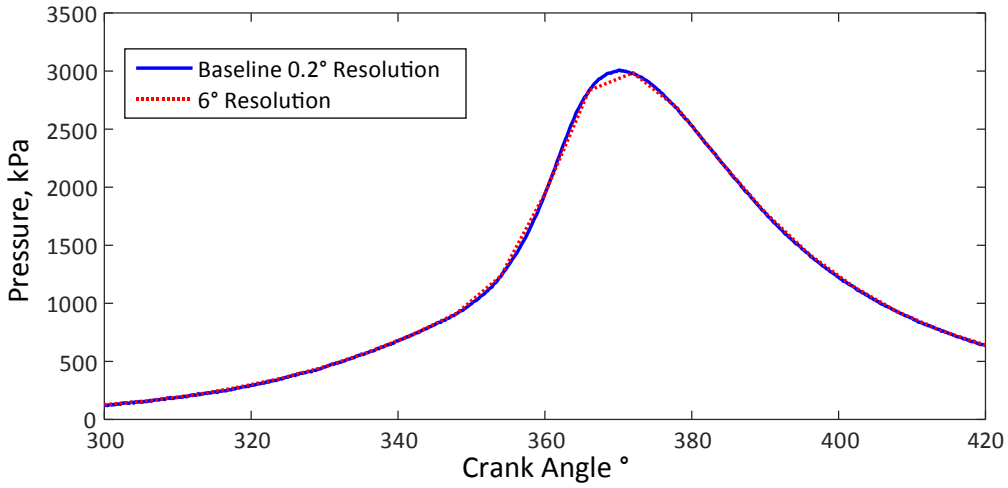

FIGURE 2. Baseline and Reduced-Resolution Pressure Traces

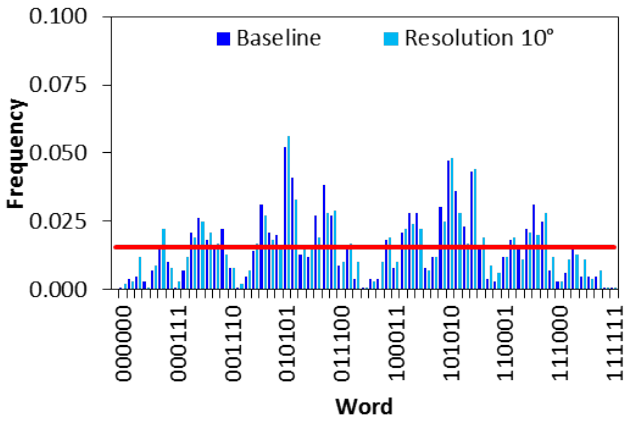

FIGURE 4. Symbol Sequence Histograms for Baseline Aad Reduced-Resolution Data

detects the same deterministic patterns in the data despite errors in the combustion feedback metrics. This is typical of what was observed for other reductions in data quality as well, and indicates that controllers using this approach would be robust even without laboratory-grade sensors and data acquisition hardware. Results from this study have been compiled into a paper and will be presented at the 2014 SAE International Powertrain, Fuels, and Lubricants conference.

CONCLUSIONS

- Symbol-sequence analysis was shown to be robust for detecting deterministic patterns even with low quality data
- Next-cycle capable controller has been commissioned, and initial symbolic strategies implemented on the engine
- Dual-timescale control will be necessary to achieve effective dilution limit extension with external EGR

REFERENCES

1. Finney CEA, Green JB, Daw CS. "Symbolic time-series analysis of engine combustion measurements," SAE Technical Paper 980624: 1998, doi: 10.4271/980624.

2. Daw C, Finney C, Tracy E. "A review of symbolic analysis of experimental data," Review of Scientific Instruments 74(2): 2003 February: p. 915-930, doi: 10.1063/1.1531823.

3. Wagner RM, Drallmeier JA, Daw CS. "Characterization of lean combustion instability in premixed charge spark ignition engines," International Journal of Engine Research 1(4): 2000: p. 301-320.

4. Sutton RW, Drallmeier JA. "Development of nonlinear cyclic dispersion in spark ignition engines under the influence of high levels of EGR," In Proceedings of the 2000 Technical meeting of the Central States Section of the Combustion Institute; 2000.

FY 2014 PUBLICATIONS/PRESENTATIONS

1. Kaul, BC, Finney, CEA, Wagner, RM, and Edwards, ML, "Effects of External EGR Loop on Cycle-to-Cycle Dynamics of Dilute SI Combustion," SAE Int. J. Engines 7(2):2014, doi: 10.4271/2014-01-1236.

2. Finney, CEA, Kaul, BC, Splitter, DA, Daw, CS, and Wagner, RM, "Long-Timescale Combustion Instabilities in Spark-Ignited Engines," 2014 Spring Technical Meeting of the Central States Section of the Combustion Institute, (March 16–18, 2014, Tulsa, OK).

3. Finney CEA, Kaul BC, Splitter DA, Daw CS, and Wagner RM, "Engines on the Edge: Long Memory and Mode Switching in Internal Combustion Engines," Poster, XXXIII Dynamics Days US (January 2–5, 2014, Atlanta, GA).

II.18 High-Efficiency Clean Combustion in Light-Duty Multi-Cylinder Diesel Engines

Scott J. Curran (Primary Contact), Zhiming Gao, Vitaly Y. Prikhodko, Adam B. Dempsey, John M. Storey, James E. Parks, and Robert M. Wagner
Oak Ridge National Laboratory (ORNL)
2360 Cherahala Blvd.
Knoxville, TN 37830

DOE Technology Development Manager
Leo Breton

Subcontractor
The University of Wisconsin, Madison, WI

Overall Objectives

- Develop and evaluate the potential of high-efficiency clean combustion (HECC) strategies with production viable hardware and aftertreatment on multi-cylinder engines.
- Expand the HECC operational range for conditions consistent with real-world drive cycles in a variety of driveline configurations (conventional, down-sized, and hybrid electric vehicle/plug-in hybrid electric vehicles).
- Improve the fundamental thermodynamic understanding of HECC in order to better identify the opportunities, barriers, and tradeoffs associated with higher efficiency combustion concepts.
- Characterize the controls challenges including transient operation and fundamental instability mechanisms which may limit the operational range of HECC. This includes the development of low-order models for prediction and avoidance of abnormal combustion events.
- Understand the interdependent emissions and efficiency challenges including integration of exhaust aftertreatments for HECC and multi-mode operation.
- Support demonstration of DOE and U.S. DRIVE efficiency and emissions milestones for light-duty diesel engines.

Fiscal Year (FY) 2014 Objectives

- Develop a Reactivity-Controlled Compression Ignition (RCCI) combustion map on a multi-cylinder engine suitable for light-duty drive cycle simulations. The map will be developed to maximize efficiency with lowest possible emissions with production viable hardware and conventional fuels.
- Demonstrate improvements in modeled fuel economy of 25% for passenger vehicles solely from improvements in powertrain efficiency relative to a 2009 port fuel injected (PFI) gasoline baseline.
- Quantify the effectiveness of diesel oxidation catalysts on particulate matter (PM) destruction with RCCI for steady-state operation.
- Characterize the challenge of emissions control at low temperatures associated with high-efficiency combustion concepts.

FY 2014 Accomplishments

- Attained the 2014 technical target of developing an RCCI engine map suitable for use in vehicle system drive cycle simulations.
- Attained the 2014 technical target of demonstrating greater than 25% improvement in modeled fuel economy with multi-mode RCCI operation as compared to a 2009 PFI gasoline baseline.
- Performed drive cycle estimations of fuel economy and emissions using vehicle systems modeling with experimental data with multi-mode RCCI/conventional diesel combustion (CDC) operation.
- Collaboration with University of Minnesota on an RCCI PM characterization campaign.
- Collaboration with Los Alamos National Laboratory on evaluation of mixed potential hydrocarbons (HCs)/oxides of nitrogen (NOx) sensor.
- Completed RCCI PM study with paper published at 2014 SAE World Congress.
- RCCI hybrid vehicle collaboration with University of Wisconsin, Madison.

Future Directions

- Evaluate the role of advanced air handling and hybrid exhaust gas recirculation systems for RCCI load expansion and potential efficiency increases.
- Conduct transient dual- and single-fuel low-temperature combustion experiments in conjunction with exhaust aftertreatments including experiments investigating the effectiveness of a selective catalytic reduction/diesel oxidation catalyst (DOC) system

to store/oxidize high levels of CO/HC from RCCI operation.

- Analyze RCCI PM data to determine composition and nature of RCCI PM.
- Conduct heavy-duty RCCI experiments in collaboration with Cummins.

INTRODUCTION

Advanced combustion concepts have shown promise in achieving high thermal efficiencies with ultra-low NOx and PM emissions. RCCI makes use of in-cylinder blending of two fuels with differing reactivity for improved control of the combustion process. Previous research and development at ORNL has demonstrated successful implementation of RCCI on a light-duty multi-cylinder engine over a wide range of operating conditions with a focus on identifying the translational effects of going from a combustion concept to a multi-cylinder engine with production viable hardware. The scope of the project focuses on the challenges of implementing advanced combustion concepts on production-viable multi-cylinder engines and includes addressing emissions with advanced emission control technologies (aftertreatment). More specifically, this effort includes investigating high-efficiency concepts developed on single-cylinder engines and addressing challenges related to dilution levels, heat rejection, boosting, thermal management, adaptive controls, and aftertreatment requirements. This activity helps to characterize the interdependency of fuel economy and emissions performance including the performance of exhaust aftertreatments focuses on understanding the synergies between aftertreatment and combustion modes with the expectation that engines may operate in both conventional and advanced combustion modes (referred to as "multi-mode").

APPROACH

A 4-cylinder General Motors (GM) 1.9-L diesel engine installed at ORNL was modified to include a port fuel injection system using conventional gasoline injectors and pistons that were designed for RCCI operation. A flexible microprocessor-based control system allowed for full authority of both fueling systems and other engine operating parameters. Experimental steady-state RCCI operating points on the modified RCCI engine using an in-house methodology for RCCI combustion were used to develop a speed/load map consistent with a light-duty drive cycle with sufficient detail to support vehicle simulations. The potential fuel economy of RCCI operation was evaluated using vehicle systems simulations with experimental steady-state engine maps compared to a representative 2009 gasoline PFI engine. Figure 1 illustrates the concept of moving from experimental engine mapping to drive cycle simulations. The ORNL engine test cell, shown in Figure 2, is well suited for detailed HC speciation and low-temperature combustion particle studies. Collaborations with industry, university and national laboratory partners leverage expertise at ORNL to meet the project objectives.

RESULTS

An improved modeled fuel economy of 25% for a passenger vehicle solely from improvements in powertrain efficiency relative to a 2009 PFI gasoline baseline was demonstrated. ORNL made use of the gasoline and diesel fuel RCCI engine map completed for the Advanced Combustion Engine third quarter Joule milestone in vehicle systems simulations to

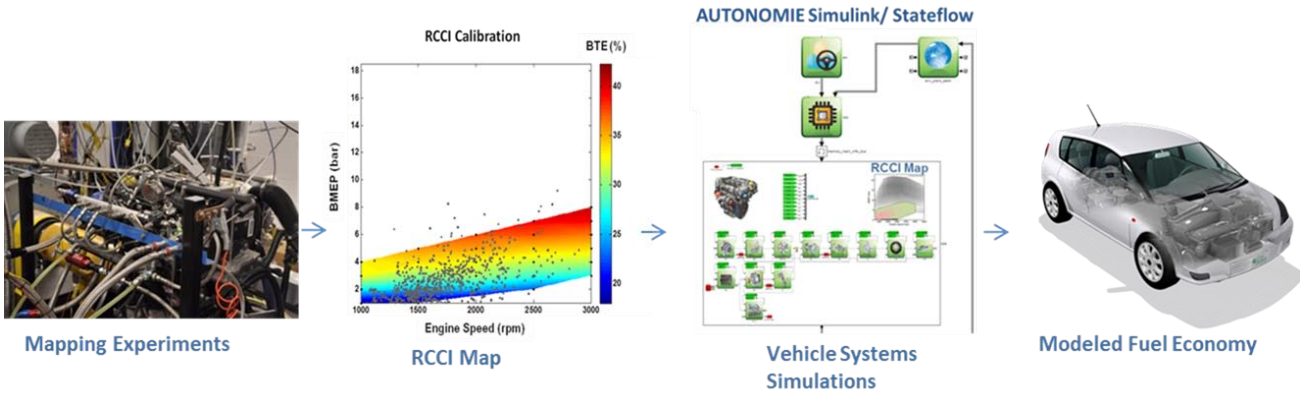

FIGURE 1. Experimental RCCI Mapping Leading to Modeled Fuel Economy using Vehicle Systems Simulations

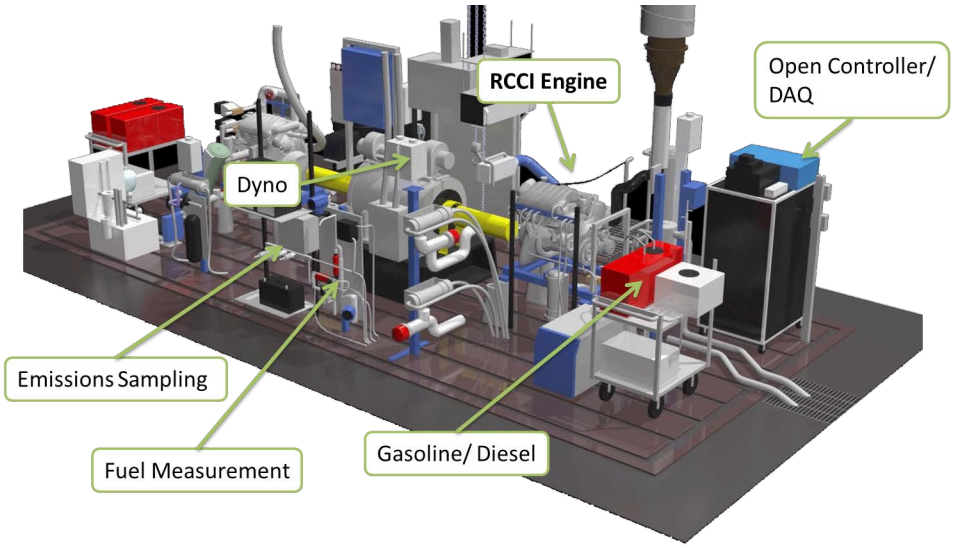

FIGURE 2. ORNL Multi-Cylinder Low-Temperature Combustion Research and Development Test Cell

model the potential fuel economy improvements with RCCI compared to a 2009 PFI gasoline engine on the same vehicle platform. All simulations were carried out in Autonomie using a 1,580 kg passenger vehicle over numerous U.S. federal light-duty drive cycles. Representative 2009 PFI engine maps ranging from 1.8-L to 4.0-L were obtained from a manufacturer partner for use in the vehicle simulations. The RCCI map used 96 research octane number gasoline for the PFI low-reactivity fuel and certification grade diesel for the high-reactivity direct-injection fuel. The simulations used a multi-mode RCCI/diesel operating strategy where the engine would operate in RCCI mode whenever possible, and would switch to diesel mode for conditions outside of the RCCI operating window. The results in Figure 3 show the RCCI multi-mode fuel economy results compared to the PFI engine baselines as well as a CDC baseline on the same vehicle.

The University of Wisconsin RCCI hybrid vehicle was evaluated at the ORNL chassis dynamometer laboratory. An aftertreatment-train consisting of a three-way catalyst, DOC and diesel particulate filter was installed. Experiments at ORNL focused on evaluating fuel economy and emissions over the highway fuel economy test at the different RCCI power points for the charge sustaining series-hybrid powertrain control strategy. Figure 4 shows the University of Wisconsin vehicle being evaluated on the ORNL chassis dynamometer laboratory.

A study focusing on the PM emissions from RCCI with and without a DOC was completed and published. It was found that while RCCI yields a near-zero smoke number (i.e., black carbon soot), there is a significant amount of particle mass being produced. RCCI PM is

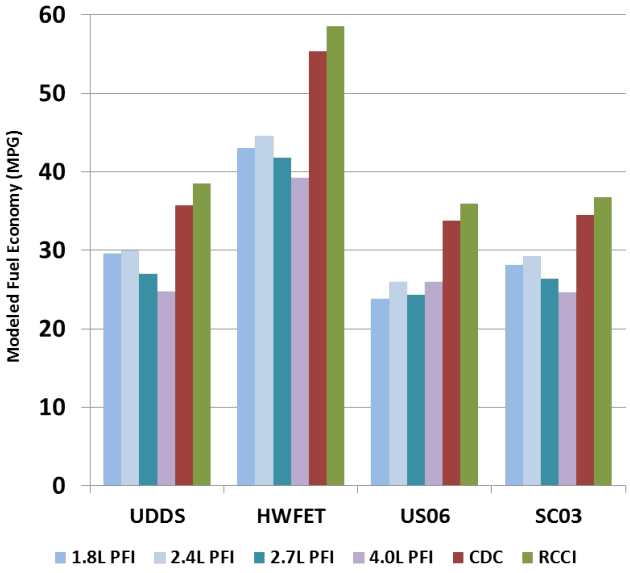

FIGURE 3. Fourth Quarter JOULE Milestone Fuel Economy Modeling demonstrating at least a 25% Fuel Economy Improvement with RCCI over 2009 Gasoline PFI Baselines

unique in having almost 0% elemental carbon (soot) yet still having other characteristics that are typical of exhaust PM. These particles appear to be partially composed of volatiles because they are reduced by a second-stage of heating and dilution. Interesting results showing a small increase of NOx emissions over the DOC during low-temperature combustion were also reported. In collaboration with the University of Minnesota, a follow-up RCCI PM study was conducted to further understand the makeup of RCCI PM. The advanced combustion engine capabilities, analytical

FIGURE 4. University of Wisconsin RCCI Hybrid Vehicle on the ORNL Chassis Dynamometer undergoing Drive Cycle Evaluations

chemistry and PM expertise at ORNL provided an opportunity for the University of Minnesota researchers to collect PM from a multi-cylinder RCCI engine using specialized prototype particulate sampling equipment from TSI to help identify and characterize the nature of RCCI PM. At the time this report was written, results were being analyzed for an upcoming joint publication with the University of Minnesota.

Collaborations with Los Alamos National Laboratory on mixed-potential sensors took place on a multi-cylinder engine at ORNL. The results of these experiments were presented to the Cross-Cut Lean Exhaust Emissions Reduction Simulations community and a draft manuscript is being led by researchers at the Los Alamos National Laboratory. Other collaborations included multi-cylinder RCCI combustion data with the stock GM 1.9-L piston were shared with Convergent Science for model validation. Planning for an exhaust thermal management study collaboration with 3M was completed in the fourth quarter. Experiments are planned for the first quarter of FY 2015 and will include investigation of thermal management of exhaust temperature for advanced combustion modes enabled by a novel exhaust insulation material developed by 3M.

These results were highlighted in a number of papers and presentations. Highlights included invited talks to the 2014 CRC workshop on Advanced Fuels and Engine Efficiency discussing fuel effects on RCCI, the 2014 SAE High Efficiency Symposium to present initial findings of RCCI/gasoline compression ignition comparison and the selection of the SAE paper documented 2013 JOULE milestones for SAE journals.

CONCLUSIONS

Advanced combustion techniques such as RCCI can increase engine efficiency and lower NOx and soot emissions over the engine map. Furthermore, an RCCI/CDC multi-mode approach has been shown to allow greater than 20% fuel economy improvement over a 2009 PFI gasoline baseline in a mid-size passenger vehicle. The ability for an RCCI-enabled engine was demonstrated with the collaboration with the University of Wisconsin RCCI hybrid vehicle team. This activity has shown the importance of taking a comprehensive engine systems approach to help meet Vehicle Technologies Office goals and milestone.

- Multi-mode RCCI operation can allow greater than a 25% improvement in modeled fuel economy as compared to a 2009 PFI gasoline baseline.
- In-cylinder blending of two fuels with different fuel reactivity (octane/cetane) allows increased control over combustion compared to single fuel advanced combustion techniques.
- Increased HC/CO emissions will be a challenge and will require progress in low-temperature aftertreatment.

FY 2014 PUBLICATIONS/PRESENTATIONS

1. Curran, S.J., "Emission Challenges and Opportunities for Multi-Cylinder RCCI on a Light-Duty Diesel Engine", Presentation, 5th International CTI Conference: Emissions Challenges Troy, MI: Sept 2014) [Invited].

2. Curran, S.J.," Fuel Economy Estimates of RCCI/Diesel Multi-Mode Operation Using Vehicle System Simulations", Presentation, Advanced Engine Combustion Program Review (Southfield, MI: Aug 2014).

3. Curran, S.J., "Emission Challenges and Opportunities for Multi-Cylinder RCCI on a Light-Duty Diesel Engine ", Presentation, 5th International CTI Conference: Emissions Challenges Troy, MI: Sept 2014) [Invited].

4. Curran, S.J., "Efficiency and Emissions Comparison of Single and Dual-Fuel Low Temperature Combustion on a Light Duty Multi-Cylinder Diesel Engine, SAE 2014 High Efficiency Engine Symposium, April 6, 2014, Detroit, MI.

5. Dempsey, A., Curran, S., Storey, J., Eibl, M. et al., "Particulate Matter Characterization of Reactivity Controlled Compression Ignition (RCCI) on a Light Duty Engine," SAE Technical Paper 2014-01-1596, 2014.

6. Curran, S.J., Gao, Z., Szybist, J., Smith, D., and Wagner, R., "Fuel Effects on RCCI Combustion: Performance and Drive Cycle Considerations", 2014 CRC Workshop on Advanced Fuels and Engine Efficiency, Baltimore, Md, Feb 25, 2014 [invited].

7. Curran, S., Gao, Z., and Wagner, R., "Reactivity Controlled Compression Ignition Drive Cycle Emissions and Fuel Economy Estimations Using Vehicle Systems Simulations with E30 and ULSD," SAE Int. J. Engines 7(2):2014.

8. Curran, S.J, Gao, Z., Daw, S., Prikhodko, V., Smith, D., Parks, J., and Wagner, R., "Opportunities and Challenges

for Integrating Future Engine Concepts into Hybrid Electric Vehicle Powertrains, "SAE 2014 Hybrid and Electric Vehicle Technologies Symposium, Feb 11, 2014 San Diego, Ca [invited].

9. Wagner, R.M., Curran, S.J., "ORNL Advanced Combustion Research and Future Fuel Opportunities", Saudi Aramco Workshop "Future of Transport Fuels", March 24–26, 2014.

10. Dempsey, A.B., Curran, S.J., Wagner, R.M., and Cannella, W., "Effect of premixed fuel preparation for partially premixed combustion with a low octane gasoline on a light-duty multi-cylinder compression ignition engine", 2014 ASME Internal Combustion Engine Division Fall Technical Conference ICEF2014, ICEF2014-5561.

11. Hanson, R.M., Spannbauer, S., Bower, G., and Rolf Reitz, R., "Preliminary Drive Cycle Performance Measurements of the UW RCCI Hybrid Vehicle", AEC/HCCI Group Meeting, Livermore, Ca, Feb, 2014.

II.19 Stretch Efficiency – Exploiting New Combustion Regimes

C. Stuart Daw (Primary Contact),
James P. Szybist, Josh A. Pihl, Derek A. Splitter, and Chao Xie
Oak Ridge National Laboratory (ORNL)
NTRC Site
2360 Cherahala Blvd.
Knoxville, TN 37932

DOE Technology Development Manager
Leo Breton

Subcontractor
Galen Fisher, University of Michigan, Ann Arbor, MI

Overall Objectives

- Define and analyze specific advanced pathways to improve the energy conversion efficiency of internal combustion engines with emphasis on thermodynamic opportunities afforded by new approaches to combustion.
- Implement critical measurements and proof of principle experiments for the identified pathways to stretch efficiency.

Fiscal Year (FY) 2014 Objectives

- Build a new flexible experimental laboratory platform for thermochemical recuperation (TCR) investigations on a multi-cylinder engine.
- Demonstrate that the TCR engine is capable of operation with the ORNL in-cylinder reforming strategy.
- Characterize the thermodynamics and reforming performance of a rhodium-based catalyst under engine-relevant conditions.

FY 2014 Accomplishments

- Published a collaborative study with Sandia National Laboratories on the chemistry of in-cylinder reforming.
- Commissioned a new flexible multi-cylinder engine experiment capable of two reforming strategies: an internal in-cylinder reforming strategy and an external exhaust gas recirculation (EGR)-loop reforming strategy.
- Characterized performance, temperature dependency, and sulfur tolerance of a rhodium reforming catalyst.

Future Directions

- Characterize in-cylinder reforming chemistry through speciation of reformate for parametric investigations of engine operating conditions.
- Determine the in-cylinder reforming chemistry for multiple fuel types differing in H/C ratio.
- Develop an engine operating strategy for EGR-loop reforming based on flow-reactor results of catalyst performance.
- Acquire a full-sized reforming catalyst for the TCR engine experiment and operate with the external EGR-loop reforming strategy.

INTRODUCTION

In conventional internal combustion engines, unutilized fuel energy ends up in the form of waste heat. Waste heat cannot be utilized directly by the piston, but it can be converted into other forms which can be recycled and used to boost piston output. The goal of this project is to identify and demonstrate strategies that enable waste heat recuperation and transformation into forms that can boost the thermodynamic efficiency of single-stage engines.

Our approach to improving internal combustion engine efficiency is based on developing a better understanding of thermodynamic losses on both a First and Second Law of Thermodynamics basis in current engines and then developing ways to mitigate them. Previous studies of internal combustion engine thermodynamics conducted in collaboration with Professors Jerald Caton (Texas A&M University) and David Foster (University of Wisconsin) identified combustion irreversibility as the largest single contributor to fuel exergy loss. In addition, these studies revealed that thermal exhaust exergy is not directly usable by the piston unless it is first transformed into a more suitable state. As a result, our efforts have focused on novel concepts that transform and recuperate thermal exhaust exergy and improve dilute combustion. We are guided by combined input from industry, academia, and national labs, such as that summarized in the report from the Colloquium on Transportation Engine Efficiency

held in March 2010 at USCAR [1]. In previous years we identified three promising approaches for improving engine efficiency: counterflow preheating of inlet fuel and air with exhaust heat [2]; TCR [3]; and chemical looping combustion [4]. Of these, TCR appears to have the greatest near-term potential, and in 2011 we developed a multi-year path to pursue TCR through fuel reforming. In addition to offering a potential pathway for recovering thermal exhaust exergy, TCR has the added benefit of generating an H_2-rich reformate stream, which can enable more efficient engine operation by extending dilute combustion limits.

APPROACH

We are actively pursuing TCR through (1) a non-catalytic in-cylinder reforming approach that thermally reforms the fuel in a hot, oxygen-deficient negative valve overlap (NVO) portion of an engine cycle, and (2) a catalytic reforming of fuel in an oxygen-deficient EGR stream. Both approaches aim to use waste exhaust heat to drive endothermic reforming reactions to produce a mixed reformate and EGR stream that is rich in H_2 and CO. The reformate can then be used to extend the EGR dilution limit of spark-ignited (SI) combustion for a more thermodynamically favorable engine cycle.

The activities in FY 2014 built on the results from FY 2013 where a novel 6-stroke engine experiment was used to parametrically investigate the effect of operating conditions and parent fuel composition on the extent of reforming and reformate composition. The in-cylinder reforming approach has been transitioned to a multi-cylinder engine experiment that uses a unique 4-stroke strategy where reformate is produced in one cylinder and consumed in the three other cylinders. This flexible multi-cylinder TCR engine is a new, highly modified engine platform, and much of the effort over the past year was spent on getting the engine platform installed and commissioned.

A rhodium-based catalyst was selected as the most promising formulation for reforming at the relatively low-temperatures available from engine exhaust. A series of flow reactor experiments were used to characterize the reforming activity and sulfur tolerance of this catalyst. Then, the flow reactor experiments were used to validate thermodynamic modeling of the catalyst to identify the most thermodynamically-favorable conditions for reforming. A combination of flow reactor performance measurements, thermodynamic modeling, and measured engine exhaust properties will be used to develop the reformer catalyst system architecture and operating conditions for use in the engine EGR loop.

RESULTS

In-Cylinder Reforming

A significant portion of the FY 2014 effort was focused on designing, building, and installing a flexible multi-cylinder TCR engine. Simply by changing the intake and exhaust manifolds, the engine is capable of operating under a conventional SI combustion strategy, the ORNL in-cylinder reforming strategy, and an external EGR-loop fuel reforming strategy. Schematics of the latter two strategies are shown in Figure 1.

Much of the flexibility of the system is due to the Sturman hydraulic valve actuation (HVA) system for cylinder 4. The HVA system allows the intake and exhaust valves to be opened or closed at any time during the engine cycle, while cylinders 1-3 are driven by the original engine camshaft. Simply by changing controller settings, this system allows the user to choose from conventional SI operation or the ORNL in-cylinder reforming strategy where the engine breathes in from the exhaust manifold and exhausts into the intake system. Within each of these strategies, parametric sweeps of valve timing can be conducted readily without hardware changes. Installing the HVA system on a multi-cylinder engine required modification of the engine head, fabrication of a custom valve cover with three-dimensional printing at the ORNL manufacturing demonstration facility, and construction of a high-pressure fuel cart to supply fuel rail pressure to the engine. A timeline illustrating the buildup of the experimental facility in FY 2014 is shown in Figure 2.

The engine is currently functional in both the conventional SI combustion strategy, as shown in Figure 3, and in the in-cylinder reforming strategy, as shown in Figure 4. At the time the in-cylinder reforming data was collected, temperature in the reforming cylinder was lower than anticipated, causing the H_2 production to be very low. Ongoing efforts are focused on insulating and/or redesigning the exhaust manifold to preserve as much thermal energy as possible for the in-cylinder reforming event before proceeding to a large set of parametric investigations in FY 2015.

EGR-Loop Reforming

Onboard an engine, the reformer catalyst inlet temperature is limited to an exhaust temperature of about 550-650°C at cruise conditions. Steam reforming catalysts are typically operated at significantly higher temperatures to achieve high fuel conversion efficiencies. One strategy for boosting catalyst temperature and increasing reformate production is to include some O_2 in the catalyst feed gas. The residual O_2 partially oxidizes some of the fuel fed to the catalyst, resulting in increased

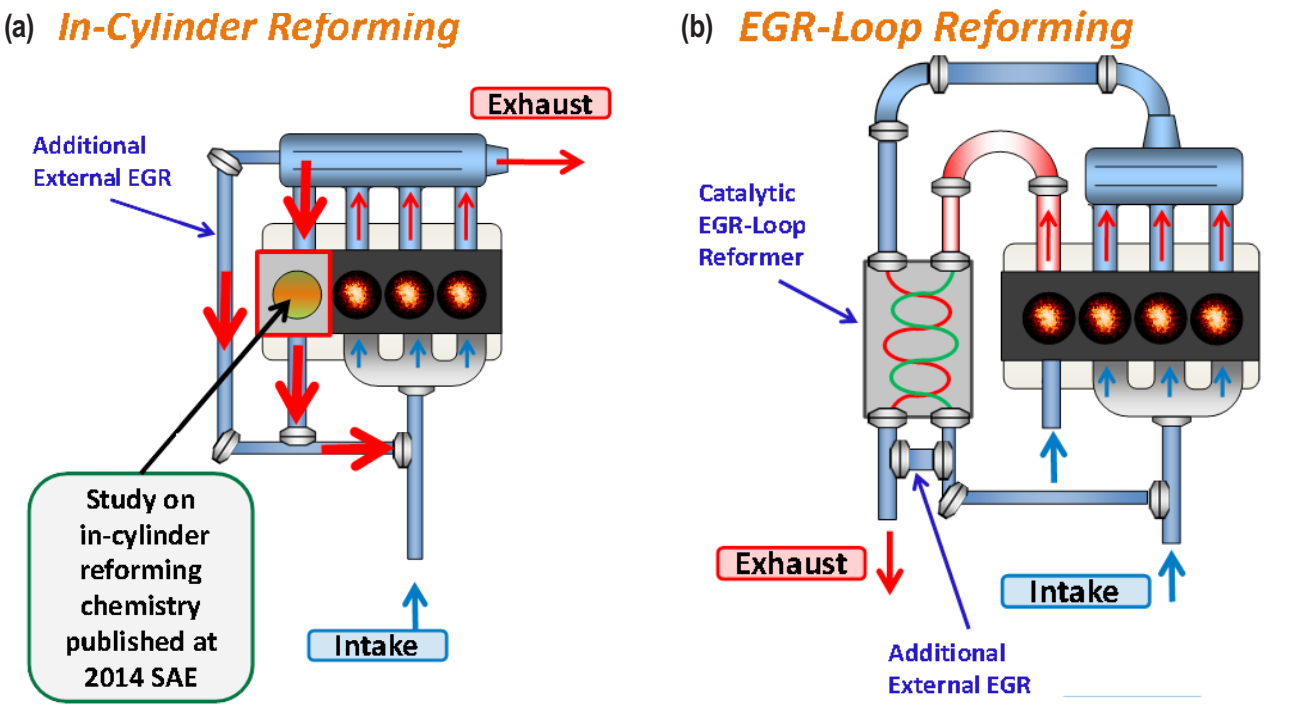

FIGURE 1. Schematics of the reforming strategies that can be investigated by the ORNL multi-cylinder TCR engine: a) In-cylinder reforming, and b) EGR loop reforming.

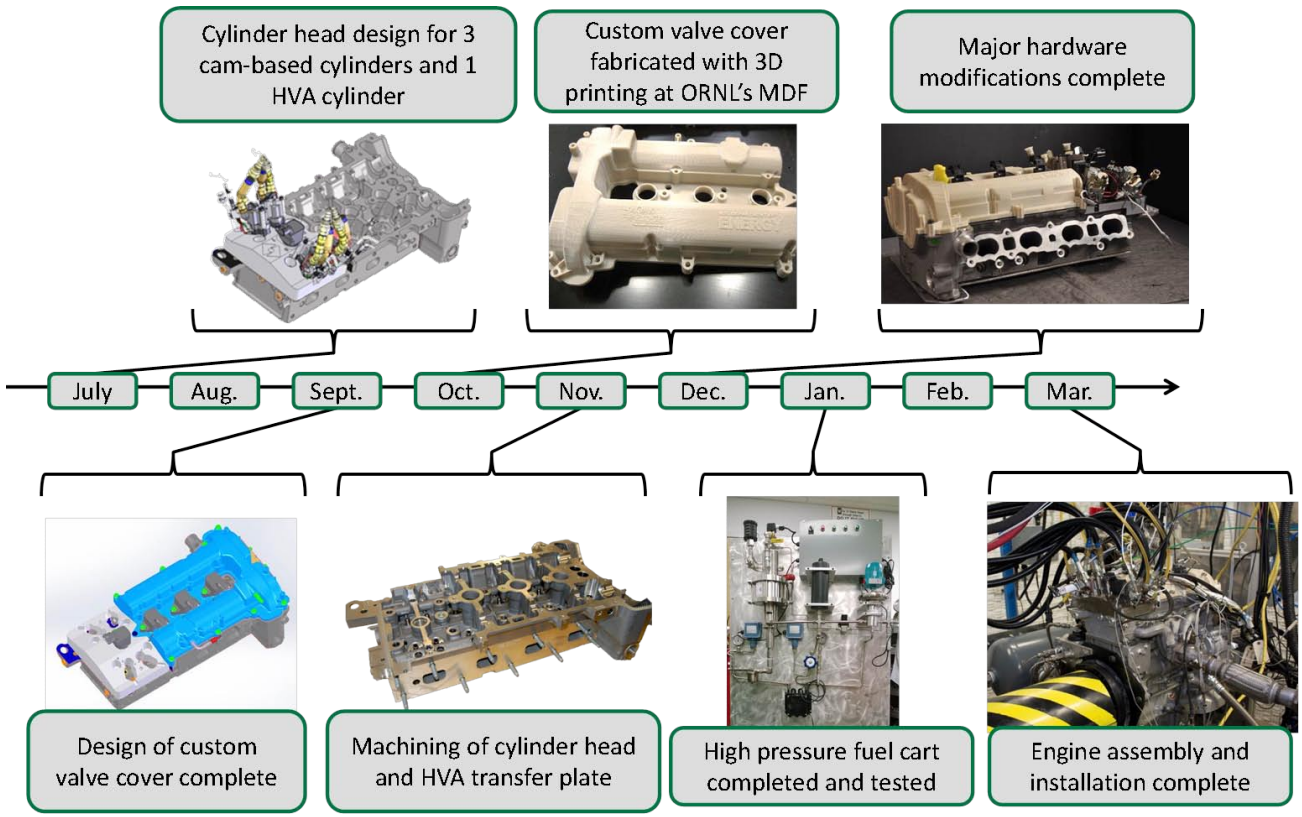

FIGURE 2. Timeline showing the progression of the ORNL multi-cylinder TCR engine assembly and commissioning.

catalyst temperature and higher fuel conversion, but also loss of fuel energy as some of the fuel hydrogen is fully oxidized to H_2O. Figure 5(a) demonstrates the potential benefits of O_2 in the reformer feed: increasing the O_2 concentration from 1 to 4% nearly doubles the H_2 yield. The increased H_2 yield is due to much higher fuel conversion efficiency, but comes at the expense of lower H_2 selectivity, as shown in Figure 5(b). The flow reactor experiments also showed that the catalyst is more sulfur tolerant with O_2 in the feed. Thus, identifying the optimal O_2 concentration in the reformer feed is one of the critical steps in developing the EGR-loop reforming system.

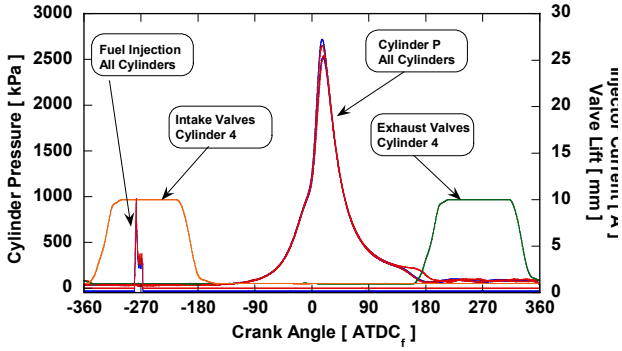

FIGURE 3. Cylinder pressure traces for all four cylinders under conventional SI operation at 1,500 rpm, 5.4 bar indicated mean effective pressure, gross.

To better understand the tradeoffs between higher H_2 yields and reduced reformate energy retention, thermodynamic modeling was conducted. The modeling was done as a function of inlet temperature using three different O_2 levels: 0%, 1.5%, and 3%. Figure 6 shows the First and Second Laws of Thermodynamics evaluation of the fuel energy recovered from the reforming process. In both cases, a value of unity means that the fuel energy is fully recovered as chemical energy in the reformate, lower values represent an energy penalty, and higher values represent a fuel energy benefit through thermochemical recuperation. A thermodynamic benefit

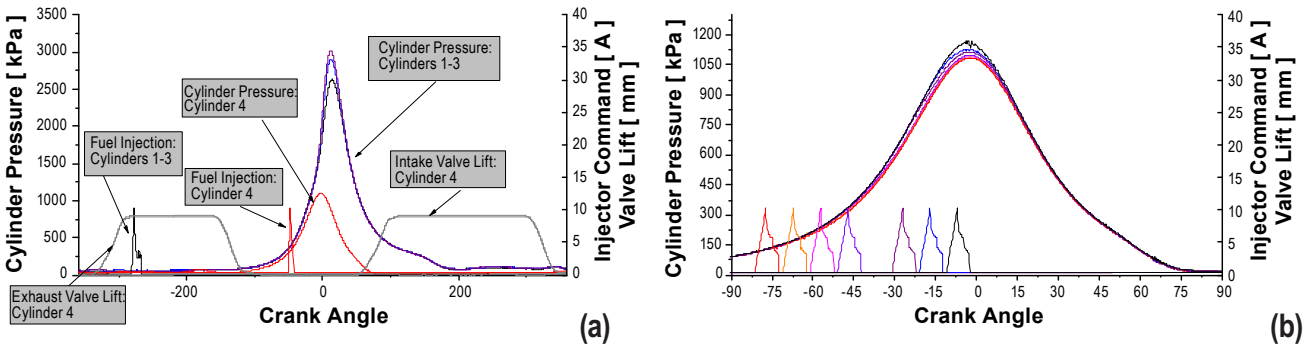

FIGURE 4. Cylinder pressure traces while operating under the in-cylinder pressure strategy for a) single operating condition for all four cylinders, and b) a sweep of injection timing for the reforming cylinder (cylinder 4).

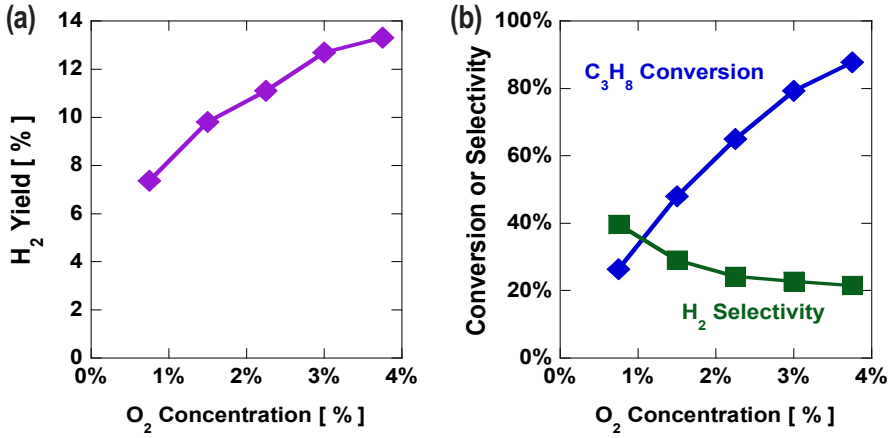

FIGURE 5. Results from the bench flow reactor experiments with the Rh-based reforming catalyst showing a) H_2 yield as a function of oxygen, and b) fuel conversion and H_2 selectivity as a function of oxygen content at a constant catalyst inlet temperature of 600°C.

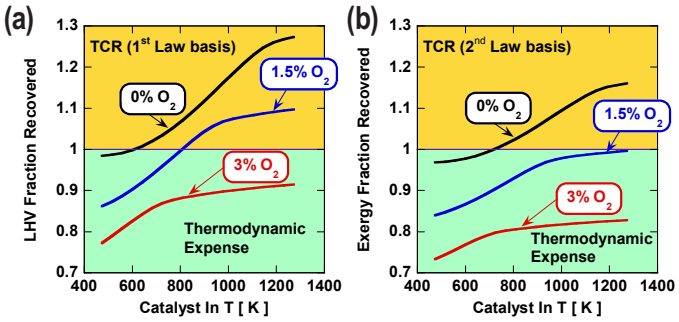

FIGURE 6. Thermodynamic modeling results of the equilibrium reforming energy benefit or penalty as a function of catalyst inlet temperature for three different oxygen concentrations on a) a First Law basis, and b) a Second Law basis.

can occur only when little or no O_2 is present, and with high catalyst temperatures, but a thermodynamic penalty is encountered as O_2 content increases and the initial temperature decreases.

From a practical standpoint, some level of O_2 may be necessary at the catalyst inlet to provide high H_2 yield and sulfur tolerance at the available engine exhaust temperatures, despite a thermodynamic penalty tradeoff. Because the H_2 can enable more efficient combustion through highly dilute conditions, the system may be able to tolerate a thermodynamic penalty in the reformer and still increase the overall efficiency. These tradeoffs will be a key focus of future flow reactor and engine experiments.

CONCLUSIONS

Two pathways are being pursued to boost efficiency through TCR pathways. The first, non-catalytic in-cylinder reforming, was shown to be thermodynamically inexpensive in FY 2013, and efforts in FY 2014 were focused on developing a flexible experimental platform on which to conduct experiments. The flexible TCR engine is now complete and operation of the TCR reforming strategy has been demonstrated. With the engine experiment now fully functional, we will proceed with a series of parametric engine experiments in FY 2015 to quantify the feasibility of this strategy on a multi-cylinder platform.

Significant progress was made towards understanding the operating conditions that lead to thermodynamic benefits and penalties with EGR-loop catalytic reforming. Due to practical limitations, though, it may be necessary to operate under non-ideal thermodynamic conditions to achieve the necessary catalyst performance, specifically H_2 yield and sulfur tolerance. We will continue to develop our understanding of these tradeoffs while working to move the catalytic EGR-loop reforming strategy to the multi-cylinder engine experiment.

REFERENCES

1. C.S. Daw, R.L. Graves, R.M. Wagner, and J.A. Caton, "Report on the Transportation Combustion Engine Efficiency Colloquium Held at USCAR, March 3-4, 2010," ORNL/TM-2010/265, October 2010.

2. C.S. Daw, K. Chakravarthy, J.C. Conklin and R.L. Graves, "Minimizing destruction of thermodynamic availability in hydrogen combustion," International Journal of Hydrogen Energy, 31, (2006), pp 728-736.

3. V.K. Chakravarthy, C. S. Daw, J.A. Pihl, J.C. Conklin, "A Study of the Theoretical Potential of Thermochemical Exhaust Heat Recuperation in Internal Combustion Engines," Energy & Fuels, 2010, 24 (3), pp 1529-1537.

4. V.K. Chakravarthy, C.S. Daw, and J.A. Pihl, "A thermodynamic analysis of alternative approaches to chemical looping combustion," Energy & Fuels, 25 (2011), pp 656–669.

FY 2014 PUBLICATIONS/PRESENTATIONS

1. Daw, C.S., Szybist, J.P., Pihl, J.A., Splitter, D.A., Kalaskar, V.B., Xie, C., Fisher, G.B., and Chiangmai, C.N., "Stretch Efficiency for Combustion Engines: Exploiting New Combustion Regimes," Presented at the 2014 DOE Annual Merit Review, Project ID: ACE015, June 18, 2014.

1. Szybist, J.P., Steeper, R.R., Splitter, D.A., Kalaskar, V.B., Pihl, J.A., and Daw, C.S., "Negative Valve Overlap Reforming Chemistry in Low-Oxygen Environments," *SAE Int J. Engines* 7(1):2014, doi:10.4271/2014-01-1188.

II.20 Cummins-ORNL Combustion CRADA: Characterization and Reduction of Combustion Variations

Bill Partridge[1] (Primary Contact), Sam Geckler[2], Gurneesh Jatana[1], Anthony Perfetto[2], Vitaly Prikhodko[1], David Koeberlein[2], Lyle Kocher[2], Rick Booth[2], Kevin Augustin[2], Suk-min Moon[2], Sriram Popuri[2], Rajkumar Subramanian[2], Alex Woods[2], Karthik Kameshwaran[2], Ryan Green[2], Brian Reed[2], Adam Wade[2], John Helt[2], Feng Tao[2], Yifeng Wu[2]

[1]Oak Ridge National Laboratory (ORNL)
[2]Cummins Inc.
2360 Cherahala Blvd.
Knoxville, TN 37932

DOE Technology Development Manager
Ken Howden

Overall Objectives

- Improve engine efficiency through better combustion uniformity
- Develop and apply diagnostics to resolve combustion uniformity drivers
- Understand origins of combustion non-uniformity and develop mitigation strategies
- Address critical barriers to engine efficiency and market penetration

Fiscal Year (FY) 2014 Objectives

- Develop multi-color multi-species exhaust gas recirculation (EGR) probe for simultaneous CO_2, H_2O, temperature (T) and pressure (P) measurements
- Apply multi-color multi-species EGR probe to Cooperative Research and Development Agreement (CRADA) and SuperTruck projects to assess specific hardware, validate and improve numerical design tools, and gain fundamental insights into performance drivers

FY 2014 Accomplishments

- Multi-color multi-species EGR probe developed and demonstrated
  - Simultaneous measurements from four EGR probes
  - Faster, linear and more sensitive response
  - Improved analysis for better accuracy
  - Simultaneous CO_2, H_20, T and P measurements
  - Quantifies hot and cool combustion charge components
- EGR probe applied to CRADA and SuperTruck measurement campaigns in Columbus, IN
- U.S. patent granted on DOE-sponsored CRADA-developed fuel-in-oil technology based on optically stimulated differential impedance spectroscopy
- One patent; two invited presentations; three oral presentations; one poster

Future Directions

- Develop methodologies to monitor net cylinder-charge composition, temperature, and fluctuations
- Modify EGR probe to incorporate additional functions for driving engine efficiency advances
  - Exhaust-side measurements
  - CH_4 measurements for compressed natural gas applications
  - CO measurements for assessing combustion completion and extent of fuel reforming
- Apply improved EGR probe with CRADA partners to development of next-generation engine efficiencies
  - Assess hardware performance
  - Assess performance of numerical design tools
  - Assess advanced control strategies
- Identify and develop diagnostics for addressing efficiency barriers

INTRODUCTION

A combination of improved engine and aftertreatment technologies are required to meet increased efficiency and emissions goals. This CRADA section focuses on engine and combustion uniformity technologies, while a parallel section (NO_x Control and Measurement Technology for Heavy-Duty Diesel Engines) focuses on emissions and catalyst technologies. Improved efficiency, durability and cost can be realized via combustion uniformity improvements which enable reduction of engineering margins required by non-

uniformities; specifically, these margins limit efficiency. Specific needs exist in terms of reducing cylinder-to-cylinder and cycle-to-cycle combustion variations. For instance, combustion variations mandate system-calibration tradeoffs which move operation away from optimum efficiency points. Combustion variations are amplified at high EGR conditions which are expected in advanced engine systems. Advanced efficiency engine systems require understanding and reducing combustion variations. Development and application of enhanced diagnostic tools is required to realize these technology improvements, and is a major focus of this CRADA.

APPROACH

The CRADA applies the historically successful approach of developing and applying minimally invasive advanced diagnostic tools to resolve spatial and temporal variations within operating engines and catalysts. Diagnostics are developed and demonstrated on bench reactors and engine systems (as appropriate) at ORNL prior to field application at Cummins.

Diagnostics are applied at ORNL and Cummins to study the nature and origins of performance variations. For example, this may be manifested in cylinder-to-cylinder CO_2 variations due to non-uniform fueling, air and/or EGR charge, fuel spray, component tolerance stacking, or other variations. Detailed measurements are used to assess the performance of specific hardware designs and numerical design tools, and identify non-uniformity origins and mitigation strategies, e.g., hardware and control changes.

RESULTS

Development of an Advanced Multi-Color Multi-Species Multiplex Laser-Based EGR Probe

A major accomplishment for FY 2014 was development and application of an improved multi-color multi-species EGR probe in partnership with the separate DOE-funded Cummins SuperTruck project. This new probe expanded on and preserved the capabilities of the multiplex laser-based EGR probe; specifically, capabilities for simultaneous measurements from four multiplexed probes, and the enhanced sensitivity, wide dynamic range and linearity of laser-based absorption measurements. The improved probe allows for simultaneous fast (5-kHz rate, 200 us, 1.2 crank angle degrees [CAD] at 1,000 revolutions per minute [RPM]) measurements of CO_2, H_2O, T and P from four separate locations. It uses the same probe body, and thus allows for single-point access, which broadens the applications compared to line-of-sight and other more invasive diagnostics, and enables spatial mapping via probe translation. A major motivation for development of this advanced probe was to enable temperature measurements and quantification of both high- and low-temperature CO_2 for applications in measuring cylinder charge components. Specifically, the cylinder charge is composed of combustion residual from the previous combustion event which never left the cylinder, re-breathed combustion residual which flows backwards into the intake runner during valve overlap, and new external-EGR-air charge, as shown in Figure 1. The improved probe can quantify the parameters of both the hot and cool backflow and external-EGR-air charges, which can

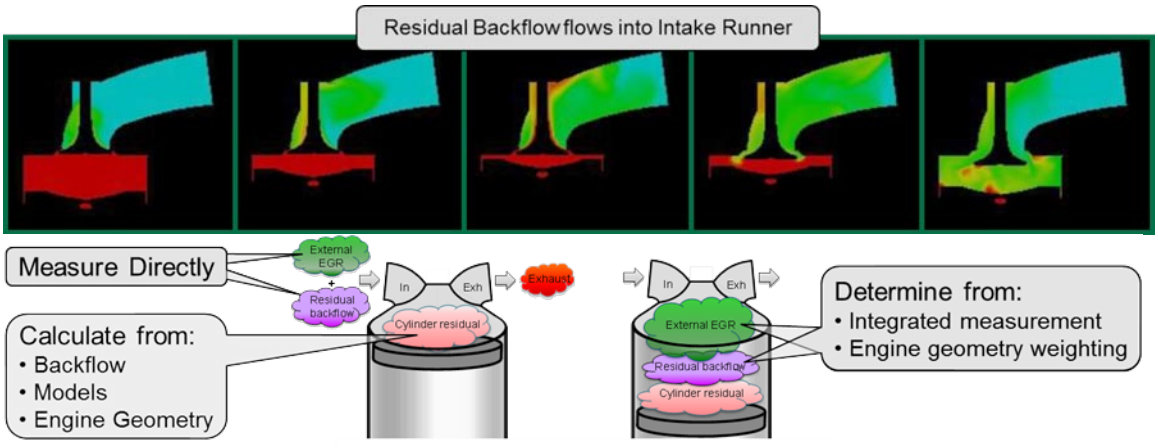

FIGURE 1. Cylinder charge components: combustion residual, residual backflow and external EGR-air. (top) Computational fluid dynamics model results showing cylinder charge components and combustion residual backflowing into the intake runner. (bottom) schematic of cylinder charge components.

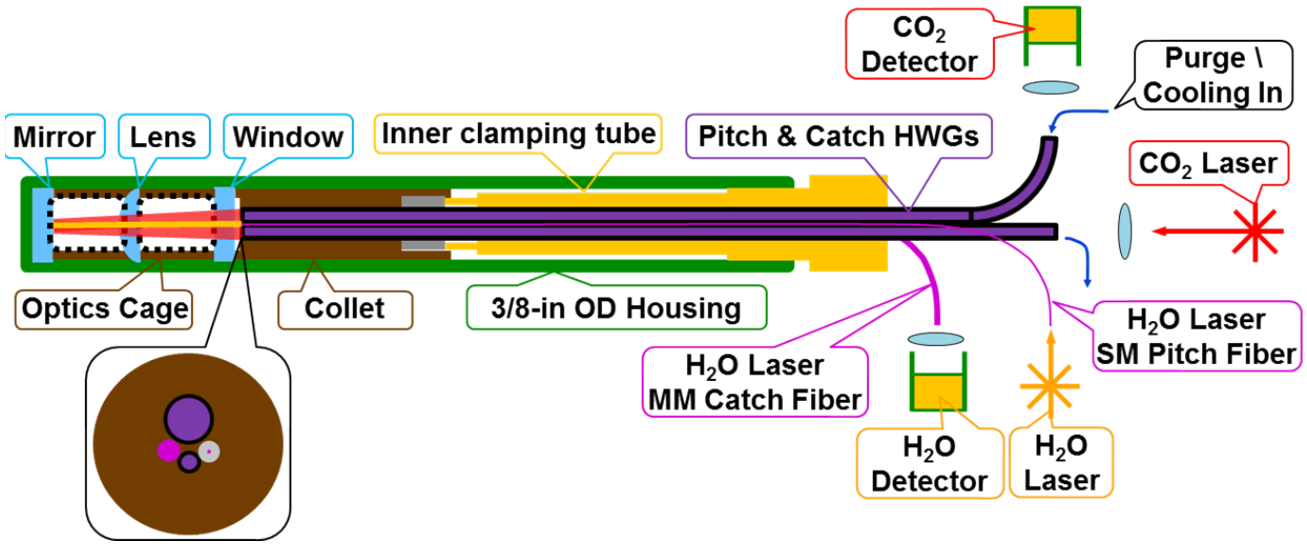

FIGURE 2. Schematic of the multi-color multi-species EGR probe.

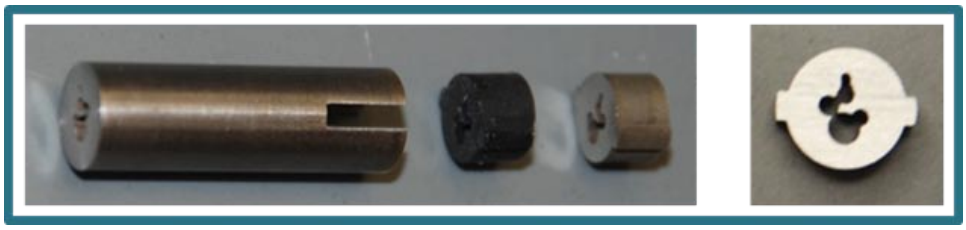

FIGURE 3. Collet and collet inserts for positioning the two HWGs and two optical fibers in the multi-color multi-species EGR probe.

then be used to characterize the cylinder charge on a cylinder- and cycle-specific basis.

The multi-color EGR probe uses two separate lasers to probe five H_2O transitions around 1,388 nm, and the same single CO_2 transition around 2.7 µm used in the earlier probe and campaigns. The multiple H_2O transitions allow T, P and H_2O concentration to be measured simultaneously, and leverages separate DOE-sponsored SuperTruck work [1]. This measured temperature is used along with separately quantified CO_2 temperature sensitivity factors to correct the simultaneously measured CO_2 concentration for temperature effects. The resulting independent H_2O and CO_2 dynamic measurements provide redundant and self-checking of the EGR level based on the two combustion constituents, and increase the number of parameters available for model tuning and assessment. The EGR probe was modified to accommodate optical fibers for guiding the 1,388 nm light for probing the H_2O transitions in addition to the hollow waveguides (HWGs) used in the earlier EGR probe.

Figure 2 shows a schematic of the multi-color EGR probe, which uses the 3/8-in outside diameter outer tube, inner tube and optics assembly of the previous probe. Three optics, secured in an optics cage assembly, form two measurement ducts through which the gas sample flows for light interaction and absorption-based measurements. Figure 3 details the collet and collet inserts for orienting and securing the two HWGs and two optical fibers; 500-µm inside diameter and 1-mm inside diameter HWGs are used to pitch and catch the ca. 2.7 -m laser for CO_2 measurements, while a single mode and 600-µm core multi-mode optical fibers were used to pitch and catch the ca. 1,388-nm laser for H_2O and temperature measurements. Compared to the earlier probe version, the pitch HWG diameter was reduced to open space in the collet for positing the two optical fibers. The four collet channels orient the four optics, while the keyed rubber and stainless steel collet inserts secure the optics when the probe is assembled. The collet and stainless steel insert were fabricated (by the Cummins Technical Center machine shop) using fine-wire electric discharge machining, while the rubber inserts were cast in various

durometer materials using molds fabricated based on the stainless steel inserts (Mid America Prototyping Inc.).

Figure 4 shows the multi-color multi-species EGR probe instrument housed in an enclosure for protection and N_2 purging to eliminate CO_2 background interference in the free-space 2.7-µm 1:4 multiplex unit. The instrument contains two lasers, two 1:4 multiplex splitters and four detectors each for both the H_2O and CO_2 spectroscopy. In addition to the Scanning Fabry Perot Interferometer, apparent in Figure 3 (left) as the horizontally oriented cylindrical unit in the lower center of the left side figure and used for wavelength calibration of the 1,388-nm (H_2O) laser, a solid silicon etalon was applied for wavelength calibration of the 2.7-µm (CO_2) laser. The 2.7-µm laser is the box with the orange stripe in the upper right of Figure 4 (left), and is coupled into the multiplex unit which sits below the four 2.7-µm detectors; three of these are blue and one is grey in Figure 4 (left). The single-mode fiber-coupled 1,388-nm laser (situated below the etalon and not visible in Figure 4, left) is coupled into the fiber-based multiplex unit mounted on the housing wall (c.f. lower left of Figure 4, left image), and the four output fibers are mounted to the housing wall (c.f. lower right of Figure 4 pictures). A manifold of critical-flow orifices is positioned along the housing back wall (c.f. top of Figure 4, left image) which supplies purge N_2 to the HWGs and the four H_2O detectors. Antireflection coatings were added (via Lattice Electro Optics) to the probe window and lens optics; these reduced reflections by over one half, and significantly reduced unwanted etalon signals which interfere with the absorption signals and analysis. Certain sapphire windows in the CO_2 free-space multiplex unit, which were required for purging the hollow waveguides, were also antireflection coated to reduce interfering etalons. In applications, the pitch and catch optics were connected to the instrument with the EGR probes mounted on the engine; in Figure 4 (right), the four EGR probes are positioned at various locations on the engine, which is off picture to the left, and Dr. Jatana is shown connecting the corresponding probe HWGs and optical fibers to the instrument.

In addition to the hardware improvements described above, several advances in the control, analysis and data acquisition were implemented with the multi-color EGR probe, many of which were developed in the previous DOE-sponsored SuperTruck project [1]. Baseline fitting is an initial critical step in determining absorption spectra, and any error in this baseline will propagate through, producing errors in the measured parameters. An iterative fitting routine was implemented in each spectral scan resulting in significant improvements to the baseline fit. In the past we have used the typical approach of spectrally sweeping the lasers via saw-tooth current-time, I(t), functions; in this mode, the laser wavelength sweeps in time proportionally to the driving current. In the improved control, a shifted-saw-tooth function was used, which contains a low-and-constant-current temporal region before each current ramp; because the driving current is below the laser threshold in this region, the laser does not emit and detector signals are indicative of thermal background emission. Thus, the shifted-saw-tooth driving function allows a background measurement for each absorption measurement; i.e., both are occurring at 5 kHz. This allows real-time correction for variations in the background thermal emission, such as occur during many engine transients. Better wavelength calibration was implemented for

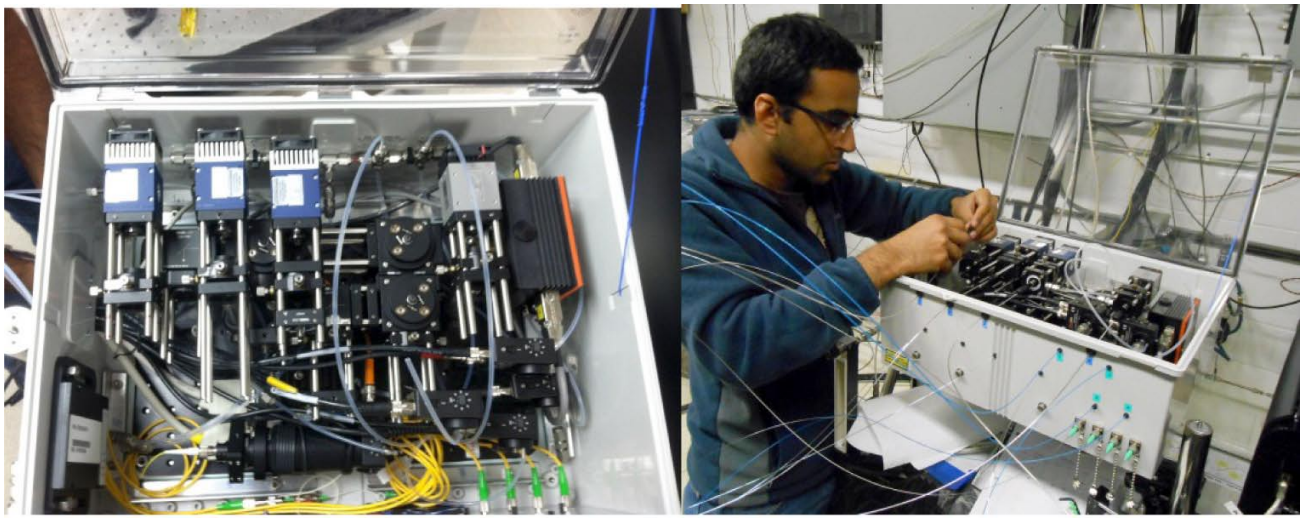

FIGURE 4. Multi-Color Multi-Species EGR Probe Instrument (left) view of components in the purged instrument housing. (right) view of Dr. Gurneesh Jatana connecting the probe pitch and catch optics to the instrument.

both the 1,388-nm and 2.7-μm lasers by using etalons to characterize their unique nonlinear wavelength response to the driving current ramp. Both the CO_2 and H_2O analysis are based on fitting the full spectra to absorption theory (in effect full-spectrum chemometric analysis), which provides for more accurate and robust analysis vs. the previous approach which used spectral integration and calibration factors. The data acquisition and analysis codes were improved and implemented on a high-speed gaming-based computer platform, allowing for real-time T, P, CO_2 and H_2O concentration output at 100 Hz, and higher-speed post-analysis resolution at 5 kHz (200 μs, or 1.2 CAD at 1,000 RPM).

In collaboration with and primary leadership from the Cummins SuperTruck project, a modified EGR probe tip was designed for use in applications with end-on flow orientations, such as when the probe is positioned down the intake runner and behind the intake valve for sampling residual backflow. The tip is shown in Figure 5, and has forward- and rear-facing external ducts to direct the axial flow into and through the two measurement ducts at the probe tip, where the laser light interacts with the gas sample for measurement. This modified tip was designed based on extensive flow analysis using computational fluid dynamics models. Based on the complex geometry of these probe tips, three-dimensional metal printing technology was used to fabricate these end-on-flow probe tips from 316 stainless steel (Mid American Prototyping Inc., Anderson, IN). In addition to the end-on flow tip, Figure 5 shows a stiffened probe for application to residual backflow measurements requiring longer probe cantilever lengths to reach the intake valve region. Frequency analysis was applied to a base probe and the probe with stiffening jacket shown in Figure 5 to insure it would not resonate with engine harmonics. In the application discussed in the following, some vibrations were detected at the longest cantilever length, and created dynamic etalon signals reducing the measurement signal-to-noise ratio. A tuned damper may provide a solution for mitigating such vibrations in future applications.

EGR Probe Applications to Assess Design Tools, Hardware, Combustion and Mixing Fundamentals

The improved multi-color multi-species EGR probe was applied to both the CRADA and SuperTruck projects. A SuperTruck measurement campaign September 22-26, 2014 in Columbus, Indiana focused on characterizing the spatiotemporal nature of cylinder- and cycle-specific combustion residual backflow and external EGR-air charge. A separate application focused on assessing detailed spatial and temporal EGR mixing in an advanced intake architecture during a CRADA measurement campaign October 27-31, 2014 at the Cummins Technical Center.

Figure 6 shows measurements of combustion residual backflow at varying external EGR levels measured during the SuperTruck campaign, and which are applicable to the CRADA objective of realizing cycle- and cylinder-specific measures of combustion charge nature (CO_2, H_2O and T). The blue trace pulses are residual backflow flooding the probe at the measurement location in the intake runner, and the Figure 6 curves correspond to a cylinder with intake starting around 360 CAD. The magnitude and duration of these dynamic signals give insights regarding the nature of the combustion residual and intake dynamics; and can be used to assess spatial distribution and uniformity. The base level of the blue curves outside the backflow pulses corresponds to the initial intake runner charge prior to, during and after the intake event; it is clear that this EGR-air charge is temporally uniform throughout the engine cycle, and increases with increasing external EGR. The red curves indicate crank angle-resolved cycle-to-cycle uniformity of the measured charge components, and it is apparent that this uniformity is similar for the re-breathed backflow and external

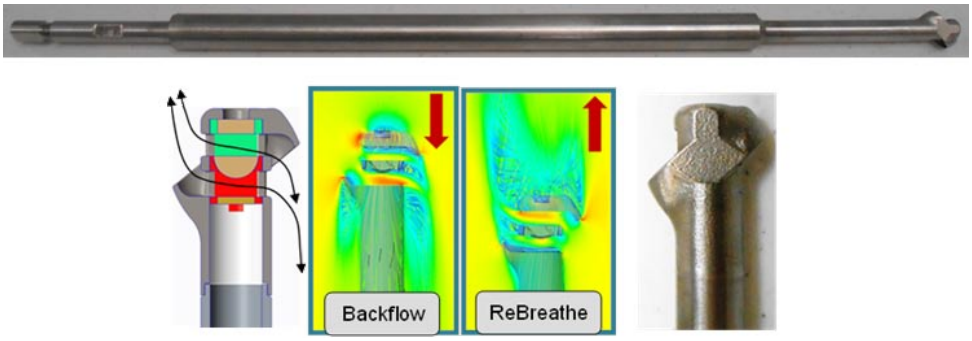

FIGURE 5. EGR probe with three-dimensional-printed tip for end-on flow orientations and stiffing jacket to avoid resonance with engine harmonics. For applications down the intake runner for sampling residual backflow, and requiring longer cantilever lengths.

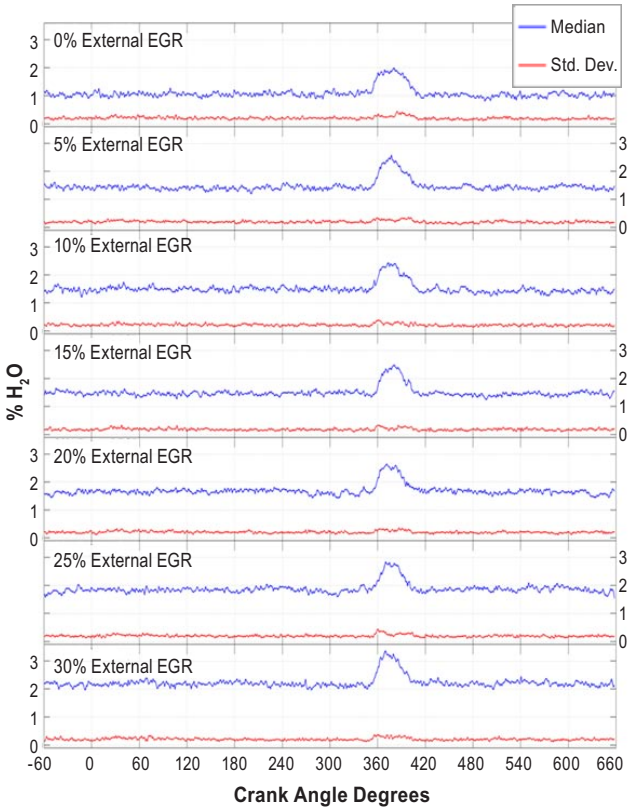

FIGURE 6. Crank angle-resolved median and standard deviation of the residual backflow and external EGR-air charge based on 30 cycles.

EGR-air charge components; the main deviations occur at the leading and tailing edges of the backflow event, which are more sensitive to cycle-to-cycle variations. Through this and similar data we were able to show that the external EGR-air charge is very uniform from cylinder-to-cylinder, assess cylinder-specific mixing dynamics, and acquire spatiotemporal measurements for assessing the computational fluid dynamics design tools (e.g., as produced the results shown in Figure 1, top). The CO_2 measurements gave similar results. This demonstrates application of the advanced EGR Probe for directly measuring two of the three combustion charge components. The backflow measurement can be used with heat transfer models to characterize the temperature of the cylinder residual; the CO_2 and H_2O concentrations are equivalent as the backflow occurs at the end of the exhaust stroke when the cylinder charge should be well mixed. In future CRADA work we will develop strategies to use such measurements to characterize the cylinder- and cycle-specific nature of the combustion charge, to which advanced combustion methods such as reactivity-controlled compression ignition are uniquely sensitive.

In the CRADA measurement campaign, the multi-color EGR probe was applied to assess spatial and temporal effectiveness of two EGR mixer designs in an advanced intake architecture. The measurements were able to clearly quantify impacts of design changes, and through ongoing work, the results are being applied to assess the design models used for system development.

CONCLUSIONS

- Improved multi-color multi-species EGR probe provides advanced insights via off-site engine measurement campaigns
  - Improved speed, linearity and sensitivity
  - Faster mapping with four simultaneous probes
  - Simultaneous pressure measurements used to distinguish EGR concentration dynamics from pressure dynamics
  - Distinguishing hot and cool cylinder-charge components
- Improved EGR probe applied in CRADA to:
  - Improve numerical design tools
  - Assess spatial and temporal mixing, hardware and mixing fundamentals
- Improved EGR probe applied to Cummins SuperTruck project
- Residual backflow and external-loop EGR measured and distinguished by EGR probe
  - Demonstrates components of cylinder charge can be measured
  - Provides pathway for quantify cylinder charge composition, temperature and fluctuations

REFERENCES

1. Gurneesh S. Jatana, Sameer V. Naik, Gregory M. Shaver, Robert P. Lucht (2014). "High-speed diode laser measurements of temperature and water vapor concentration in the intake manifold of a diesel engine" International Journal Of Engine Research 15773-788.

FY 2014 PUBLICATIONS/PRESENTATIONS

Oral Presentations

1. Kyle Thurmond, Emmanuel Duenas, Subith S. Vasu, William P. Partridge Jr. "Development of a LED-based sensor for simultaneous, time-resolved measurements of CO and CO_2 from combustion exhausts," The Combustion Institute, Eastern States Section, Fall 2013 Technical Meeting, Clemson, South Carolina, October 14, 2013.

2. Bill Partridge, Jae-Soon Choi, Jim Parks, Maggie Connatser, Jon Yoo, Rodrigo Sanchez, Vitaly Prikhodko, Neal Currier, Sam Geckler, Mike Ruth, Rick Booth, David Koeberlein,

Alex Yezerets. "Diagnostic Developments & Applications for Enabling Advanced-Efficiency Automotive Systems," Arnold Air Force Base, Arnold Engineering Development Complex, Manchester, Tennessee, November 21, 2013. ***Invited Presentation***

3. Bill Partridge, Jae-Soon Choi, Jim Parks, Maggie Connatser, Jon Yoo, Rodrigo Sanchez, Vitaly Prikhodko, Neal Currier, Sam Geckler, Mike Ruth, Rick Booth, David Koeberlein, Alex Yezerets. "Diagnostic Developments & Applications for Enabling Advanced-Efficiency Automotive Systems," Mechanical and Aerospace Engineering Department, University of Central Florida, Orlando, Florida, March 28, 2014. ***Invited Presentation***

4. Jihyung Yoo, Derek Splitter, James Szybist, William Partridge. "Cycle-resolved intake residual backflow measurement using an optical Probe," SAE World Congress, Diagnostic Development session, Detroit, Michigan, April 8, 2014.

5. W.P. Partridge, S.C. Geckler, J. Yoo, D.A. Splitter, J.P. Szybist, V. Prikhodko, R.S.-Gonzalez, R.M. Connatser, J.E. Parks, A. Perfetto, R.A. Booth, D.E. Koeberlein, K. Augustin, S.-m. Moon, S.S. Popuri, F. Tao, L.E. Kocher, "Cummins/ORNL FEERC Combustion CRADA: Characterization & Reduction of Combustion Variations," 2014 DOE Vehicle Technologies Program Annual Merit Review, Washington, D.C., June 18, 2014.

Poster Presentation

1. Kyle Thurmond, Zachary Loparo, Raynella Connatser, William Partridge, Subith Vasu, "Design and Validation of LED-Based Absorption Sensor for Simultaneous Detection of CO & CO2," 35th International Symposium on Combustion, San Francisco, California, August 7, 2014.

PATENTS

1. L.C. Maxey, W.P. Partridge, S.A. Lewis, J.E. Parks "Optically Stimulated Differential Impedance Spectroscopy," United States Patent, Patent No. US 8,653,830, Date of Patent February 18, 2014.

II.21 Neutron Imaging of Advanced Transportation Technologies

Todd J. Toops (Primary Contact),
Charles E.A. Finney, Eric J. Nafziger,
Derek Splitter, Hassina Bilheux
Oak Ridge National Laboratory (ORNL)
2360 Cherahala Boulevard
Knoxville, TN 37932

DOE Technology Development Manager
Leo Breton

Subcontractor
Professor Jens Gregor, University of Tennessee,
Knoxville, TN

Overall Objectives

- Develop high-fidelity neutron imaging capabilities using the High Flux Isotope Reactor (HFIR) and Spallation Neutron Source at ORNL
  - Once fully developed, this advanced capability will allow the imaging of a range of processes that occur in advanced vehicle systems
- Employ technique to aid improved design and control of complex advanced combustion systems and help to guide model validation and input
- Report findings to research community and work with industrial partners to ensure research is focused on the most critical topics

Fiscal Year (FY) 2014 Objectives

- Obtain computed tomography (CT) scans of particulate filters filled with gasoline direct-injection engine particulate (12/31/2013).
- Complete and submit manuscript on particulate filter regeneration studies (3/31/2014).
- Complete reconfiguration of spray chamber to enable evacuation and heating for outer injector condensation control (6/30/2014).
- Image internal fluid during injection using a gasoline direct injection component (9/30/2014).

FY 2014 Accomplishments

- Awarded ORNL-funded project to fully develop the dynamic imaging capability for fuel injector study
  - Demonstration with new micro-channel plate (MCP) detector
  - Higher resolution stroboscopic capability
- Recorded higher resolution CT scan of commercial gasoline direct injector (GDI)
  - Including new fly-through movie
- Acquired or modified one- and two-hole GDIs
  - One designed for off axis one-hole operation
  - Others were modified six-hole injectors that were sealed for one- or two-hole operation
- Initiated gasoline particulate filter (GPF)-focused study
  - Obtained particulate profile for four GPFs using non-destructive technique
- In collaboration with the Massachusetts Institute of Technology (MIT), used technique to quantify ash loading density profiles in a series of ash-filled samples

Future Directions

- Demonstrate dynamic imaging capability with a GDI-based system and validate whether cavitation can be observed
  - Currently focusing on cyclopentane as the injection fluid and spraying into a vacuum
  - Will move to more realistic systems once we validate the technique
- Investigate deposits in used injectors in conjunction with injector partners
  - Working with both fuel injectors and urea injectors
- Incorporate ash-laden and gasoline particulate samples into PF study and include regeneration
  - Working with partners to obtain parts as possible
  - Quantify density using standards
- Become active member of the Engine Combustion Network and incorporate neutron imaging into GDI studies

INTRODUCTION

Unlike X-rays, neutrons are very sensitive to light elements such as hydrogen (H) atoms and can penetrate through thick layers of metals (Figure 1a) [1]. These

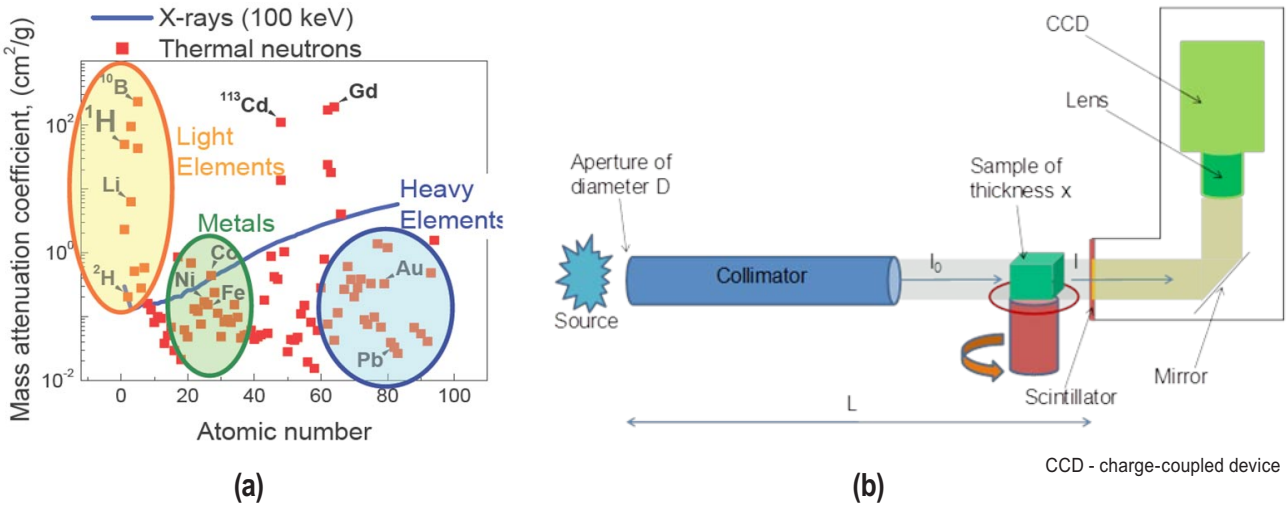

FIGURE 1. (a) Mass attenuation coefficients of a range of elements as a function of atomic number. Comparison given between neutron (squares) and X-rays (line). (b) Schematic of a neutron imaging facility at ORNL.

two properties suggest neutrons are well suited to probe engine parts such as diesel particulate filters, exhaust gas recirculation coolers, fuel injectors, oil in engines, oil residues in filters, etc. Neutron imaging is based on the interactions of a sample with a neutron beam. The interactions are dependent on sample thickness/density and elemental make-up and result in absorption and scattering of neutrons within the sample. A two-dimensional position-sensitive detector placed behind the sample can measure the transmitted neutron flux, as illustrated in Figure 1b. When combined with a well-controlled rotational stage it is possible to perform CT scans and thus generate three-dimensional images of working fluids inside real devices. Samples can be analyzed at one cross-section or a complete reconstruction can provide a cross-section of the entire sample at a resolution of the detector; the detector resolution is currently at ~50 microns.

APPROACH

This project is focused on using this unique neutron imaging capability to advance the understanding of two components being employed in modern vehicles: the particulate filter (PF) and the in-cylinder fuel injector. Recent efforts are aimed at investigating intra-nozzle fuel injector fluid properties and cavitation events during dynamic spraying. These efforts are designed at improving understanding of how external conditions influence internal dynamics, especially as it relates to advanced combustion regimes and injector durability. PFs are a key component of the emissions control system for modern diesel engines, and possibly gasoline engines in the future, yet there remain significant questions about the basic behavior of the filters. In particular, understanding how ash, or non-regenerable metal oxide-based particulate, fills the PF and interacts with the wall. The results of these measurements will provide important data to the aftertreatment modeling community on the soot and ash profiles, which change over the course of the vehicle's lifetime. In carrying out these studies, we work closely with industrial partners to obtain relevant systems and devices. The proximity of our research facility to the neutron beam allows for iterative studies when appropriate.

RESULTS

ORNL has invested internal funds to upgrade the neutron imaging capabilities being used on this project and to demonstrate the potential of this activity. The first improvement that was recently installed is an MCP detector. This critical piece of equipment was developed by Anton Tremsin at the University of California, Berkeley and although the field of view has decreased to 4-cm x 4-cm, the resolution has increased such that we can easily see down to 40 microns with the possibility to get down to 20 microns. Another key feature of the MCP detector is the ability to synchronize image capture with the injector operation. This allows a binning or stroboscopic technique to be used to accurately capture injection events, i.e. we can operate the injector in a normal mode of operation and repeatedly record small portions of the injection event. It can do this at timing intervals as small as 5 microseconds (μs). Thus, during a typical 1 ms injection, up to 200 frames can be recorded. The current neutron flux does not allow for this image to be captured in a single shot, but relies on repeated injections to capture the image with enough neutron interactions. The image is thus a composite of

the injection and illustrates where areas of low density are expected to occur over thousands or even millions of injections, and when combined will allow the reconstruction of the injection with time resolution on the order of 5-20 μs.

This capability was demonstrated during FY 2014 with the results captured in Figure 2. The GDI that is the focus of this work can be seen in Figure 2a and it was placed in front of the MCP detector. To demonstrate the functionality and the synchronization capability, the injector was operated without fluid spraying but with only a small amount of lubricating oil inside and a significant amount of cooling to keep the injector from overheating. Figure 2b shows how the injector is being opened and closed. The injector drive unit triggers off of the falling edge of a transistor–transistor logic signal (yellow line), followed by a short delay, then a peak current spike associated with the opening of the pintle (purple line). The hold current settles down and stays open for the remaining duration and is then closed. We recorded these events for 20 hours and over 1 million injections and were able to capture a video that showed each of these subtleties. The difference of the position of the pintle between the opening and closed positions is shown in Figure 2c. It clearly shows the movement of the pintle and interestingly we can also see the injector holes where the fluid would be ejected into the chamber. Although this experiment did not employ fuel, the residual lubrication fluid was moving in and out of the holes as the injector was being opened and closed. This is the discoloration that is captured at the bottom of the image.

After this campaign, a new pumping system was fully developed and commissioned that included a closed-loop fuel injection system. The sophisticated system was designed to operate with commercial and prototype injectors and deliver fuel to the injectors at pressures up to 150 bar. The spray chamber can be operated at absolute pressures as low as 0.2 bar, i.e. sub-ambient, and currently has a maximum pressure just slightly over 1 bar. The vacuum pumps pull the injected fuel, which is primarily in the vapor phase at these pressures, out of the spray chamber and exhaust it into a large vessel that is chilled to ~0°C. This condenses the majority of the fuel, and any residual fuel in the argon sweep gas is filtered through a charcoal trap or commercial filtration system. Figure 3 shows the system installed at HFIR and in operation with spray being emitted from the injector. Analysis and reporting of the dynamic imaging during fuel injection will be discussed next FY.

Another area of this project is focused on non-destructive characterization of PF deposition properties. This year we started a collaboration with another project that is looking at particulate formed from GDI-based operation and is thus a GPF study. The deposition was performed using a GDI stoichiometric engine that was operated periodically with a rich "tip-in" to accentuate particulate formation. The particulate was collected using a holder with four 1-inch x 3-inch GPFs and filled to a nominal density of 4 g/L. The samples were then analyzed at HFIR using the standard charge-coupled device-based neutron detector. The resulting CT scans are shown in Figure 4 at a representative distance down the length of the channel. Although it is subtle, the inlet channels in the filled GPF have rounded edges and illustrate the deposition. By subtracting the dark area in the filled GPF from the dark area in the empty GPF it is then possible to calculate an average soot cake thickness for each channel and for each position down the channel. Figure 5c is the average thickness for 20 analyzed channels and it clearly shows how this layer builds up depth going from the inlet to the outlet of the GPF. In comparing this to our previous work with diesel PFs [2,3], we noted that the packing density of this layer

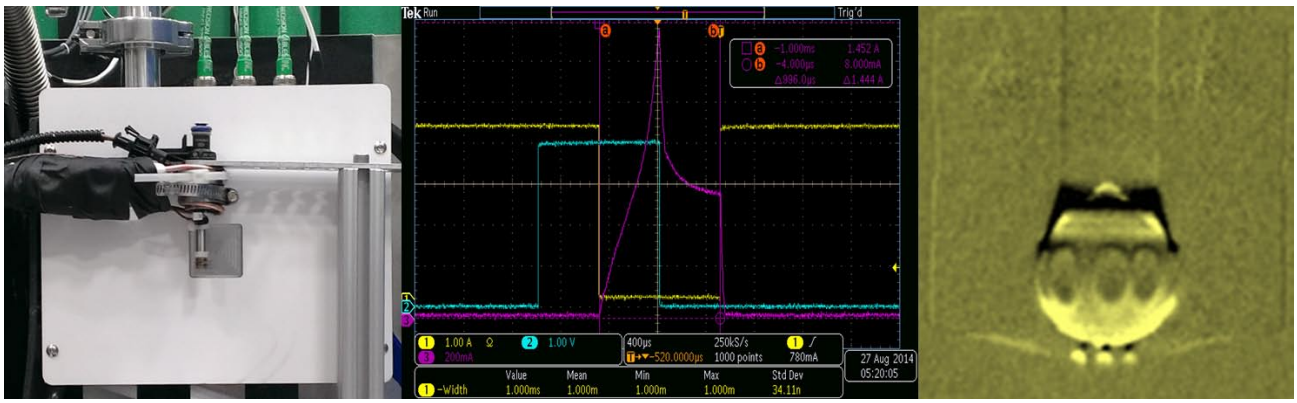

(a) (b) (c)

FIGURE 2. (a) GDI in position at HFIR in front of the MCP detector. (b) Control signals being sent to the injector, recorded with an oscilloscope. (c) Difference image of the injector on the open and closed position showing the maximum movement of the pintle and residual fluid in the nozzles.

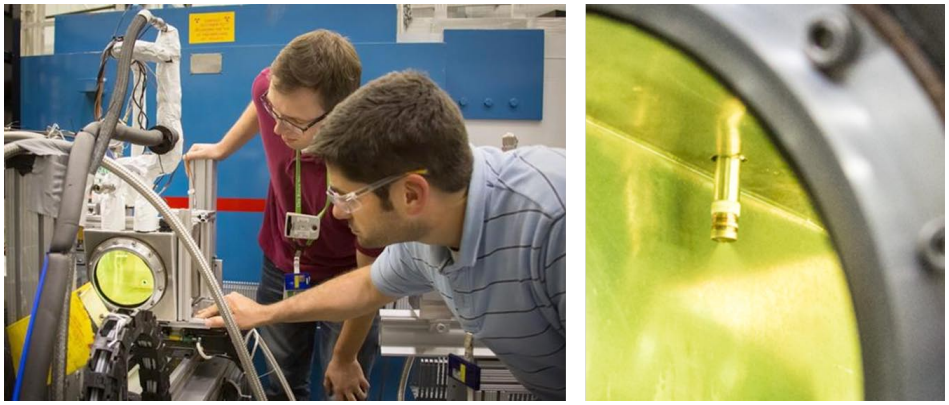

(a) (b)

FIGURE 3. (a) Spray chamber installed at HFIR being prepared for neutron imaging. (b) Fluid injection with spray apparent coming from 6-hole commercial GDI.

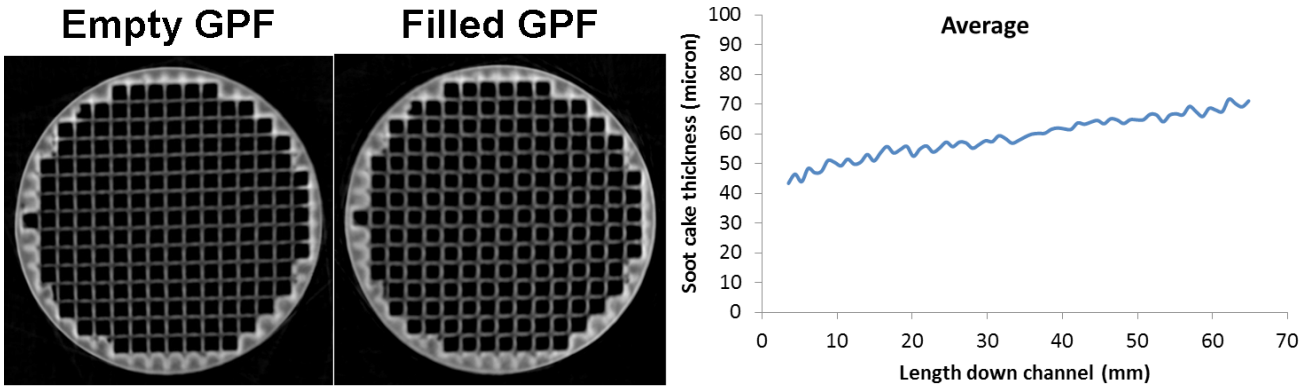

(a) (b) (c)

FIGURE 4. Neutron computed tomography scans of an (a) empty and (b) filled GPFs. (c) Average soot cake thickness is calculated through the subtracted analysis of the two images on a channel by channel basis.

is 20% denser than diesel particulate. This observation is a consistent theme that GDI-generated particulate has significantly different characteristics than diesel generated particulate. One of the noted differences is the variability in particulate size in gasoline particulate—diesel particulate is on average 25-30 nm with a little variability [4].

In FY 2014, we continued our collaboration with MIT with the non-destructive analysis of ash distributions in particulate filters. We performed a CT-scan of nine samples that were operated in MIT's accelerated ash loading system. Figure 5 shows the group of samples in place at the HFIR as well as one of the slices of the nine samples. The samples had the following characteristics (sample label: ash origination, ash loading, regeneration protocol)

- A1: CJ4, 25.2 g/L, continuous/passive
- B1: CJ4, 25 g/L, periodic/passive

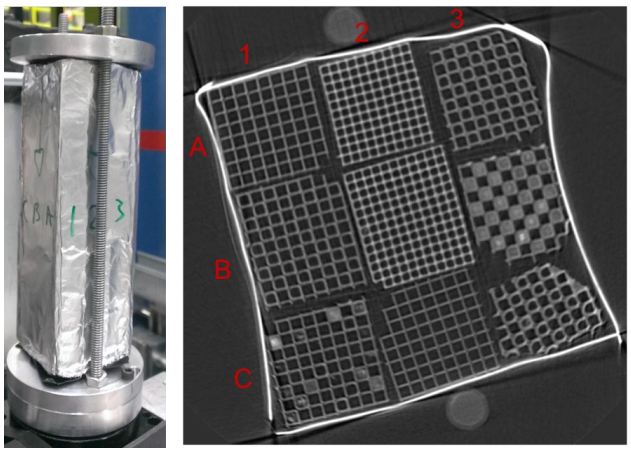

(a) (b)

FIGURE 5. (a) Ash loaded samples from MIT in a 3x3 matrix in the rotation stage for a CT scan at HFIR. (b) Processed images from the CT scan showing one slice of the nine samples.

- C1: CJ4, 24.6g/L, periodic/passive
- A2: DOC-A
- B2: DOC-B
- C2: Blank-DPF
- A3: CJ4, 12.5 g/L, periodic/active
- B3: CJ4, 42 g/L, periodic/active
- C3: CJ4, 33 g/L, continuous/active

In addition to these nine samples, MIT provided a sample of the ash that is generated when using the CJ-4 lubricant. We then turned this into a standard that allowed us to quantify the ash profiles from the CT scans. The ash standard was packed to a density of 0.52 g/cc, and a CT scan was performed. This allowed us to estimate what the density of the ash plugs will be in the PFs based on the number of "counts" that the neutron detector assigns to the plug. The normalization factor was determined to be $12.9(g/cc)_{ash}/(counts)_{neutron}$. With this in mind we performed a detailed analysis of samples A3 and B3 and quantified the density of the ash plugs observed (Figure 6). In the current analysis we did not focus on the thin layers of ash on the wall of the samples, just the plugs found at the end of the PF. Figure 6a lists the profiles calculated for each of the 10 channels analyzed. There is significant channel to channel variability observed, but this clearly shows the PF that was loaded to 12.5 g/L has ash plugs that are approximately 4-mm long with a density between 0.4 and 1.2 g/cc. Figure 6b shows the profiles of 10 channels in the PF filled to 43 g/L, and once again there is significant variability in the channels with the plug density varying from 12-18 mm long with a density between 0.2 and 0.8 g/cc. Figure 6c shows the average density for the 10 channels analyzed in both samples. This more clearly illustrates the length of the ash plugs in the samples, and that the ash density is significantly higher on average in the A3 sample. Verification of the process and continued analysis will commence in FY 2015.

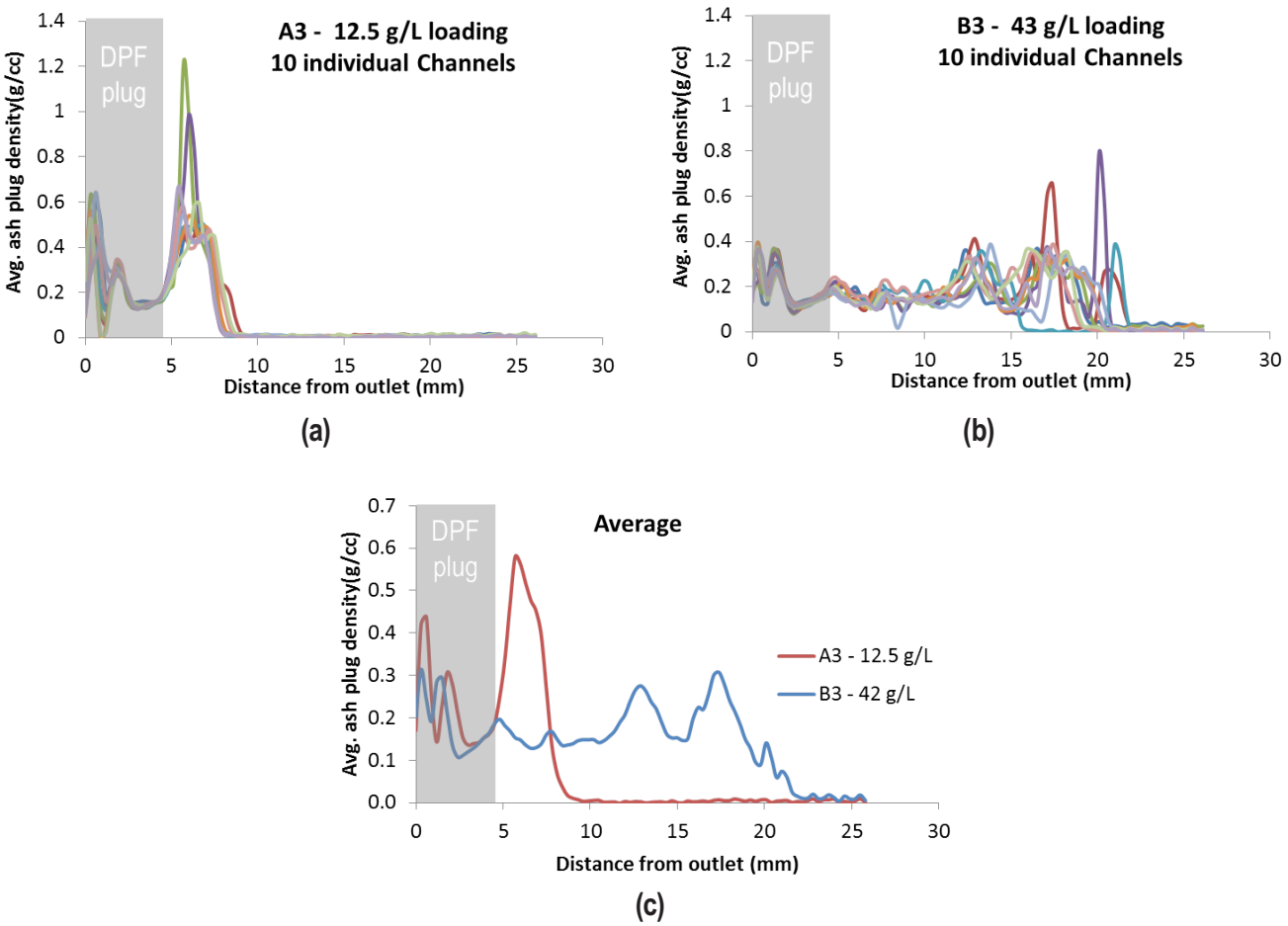

FIGURE 6. Quantified ash profiles for (a) 10 individual channels from sample A3, (b) 10 individual channels from B3, and (c) the average density profile for both samples.

CONCLUSIONS

- To help facilitate the findings in this project, internal ORNL funds were invested in the hardware and experimental effort that will enable dynamic neutron imaging of advanced transportation technologies
  - Improved resolution and stroboscopic imaging capability
- Using dynamic neutron imaging capabilities internal pintle movement was captured in a GDI that demonstrated the potential of the technique
  - Captured with ~40 µm resolution and 5-20 µs time resolution
  - Efforts moving towards fluid dynamics in FY 2015
- Analysis of GDI-based particulate captured in PFs illustrate a soot cake layer that grows in thickness from inlet to outlet of the PF and is 20% denser than diesel-based particulate
- Using ash standards a quantification routine was demonstrated on ash-filled GPFs
  - Ash plugs show significant variability in density: 0.2-1.2g/cc

REFERENCES

1. N. Kardjilov, "Absorption and phase contrast neutron imaging", Imaging and Neutrons 2006, Oak Ridge, TN, October 23-25, 2006; http://neutrons.ornl.gov/workshops/ian2006/MO1/IAN2006oct_Kardjilov_02.pdf

2. Todd J. Toops, Hassina Bilheux, Sophie Voisin, Jens Gregor, Lakeisha Walker, Andrea Strzelec, Charles E.A. Finney, and Josh A. Pihl, "Neutron Tomography of Particulate Filters: a non-destructive investigation tool for applied and industrial research", Nuclear Instruments and Methods in Physics Research Section A 729 (2013) 581-588.

3. Todd J. Toops, Josh A. Pihl, Charles E.A. Finney, Jens Gregor, Hassina Bilheux, "Progression of soot cake layer properties during the systematic regeneration of diesel particulate filters measured with neutron tomography," Emission Control Science and Technology, submitted for review.

4. Storey, J.M. "Changing Urban Particulate Matter: The Convergence of Diesel PM Removal and Increasing Gasoline PM," Presentation to the 2014 Transportation Planning, Land Use, and Air Quality Meeting. Transportation Research Board. Charlotte, NC 2014.

FY 2014 PUBLICATIONS/PRESENTATIONS

1. Todd J. Toops, Josh A. Pihl, Charles E.A. Finney, Jens Gregor, Hassina Bilheux, "Progression of soot cake layer properties during the systematic regeneration of diesel particulate filters measured with neutron tomography," Emission Control Science and Technology, submitted for review.

2. Todd J. Toops, Charles E.A. Finney, Eric J. Nafziger, "Neutron Imaging of Advanced Transportation Technologies," presentation to the U.S. DOE Vehicle Technologies Office 2014 Annual Merit Review and Peer Evaluation Meeting, Washington D.C., June 18, 2014.

3. Todd J. Toops, Eric Nafziger, Charles E.A. Finney, Hassina Bilheux, Jean-Christophe Bilheux, "Neutron Imaging of Diesel and Gasoline Fuel Injectors", 2014 SAE World Congress, Detroit, Michigan, April 10, 2014.

4. Todd J. Toops, Charles E.A. Finney, Eric J. Nafziger, Josh A. Pihl, "Neutron Imaging of Advanced Transportation Technologies", DOE 2013 Annual Progress Report.

5. Todd J. Toops, Charles E.A. Finney, Josh A. Pihl "Neutron Imaging of DPFs and a Path Towards Quantification of Ash Distributions," Massachusetts Institute of Technology Consortium to Optimize Lubricant and Diesel Engines for Robust Aftertreatment Systems, Fall Review Meeting, Cambridge, MA, October 10, 2013.

II.22 Ignition and Combustion Characteristics of Transportation Fuels under Lean-Burn Conditions for Advanced Engine Concepts

Seong-Young Lee (Primary Contact), Jaclyn Johnson, Sreenath Gupta, Gregory Siuchta, William de Ojeda, James Cigler, Gaurav Mittal
Michigan Technological University (MTU)
815 R.L. Smith Bldg.
1400 Townsend Drive
Houghton, MI 49931

DOE Technology Development Manager
Leo Breton

Subcontractors
- Argonne National Laboratory, Chicago, IL
- Navistar, Chicago, IL

Overall Objectives

- A comprehensive characterization of high injection pressure dimethyl ether (DME) spray combustion under lean-burn conditions: investigate the characteristics of DME spray combustion for use in internal combustion engines and whether these characteristics affect burning rates, quenching limits, and emissions under engine-representative conditions.
- A comprehensive determination of highly dilute reaction at autoignition conditions with substantial exhaust gas recirculation (EGR) levels: investigate DME ignition process by changing air-fuel mixing strength, amount of EGR, ambient pressure and ambient temperature to characterize whether high-temperature DME autoignition is similar to that under low-temperature conditions.
- Development of computational fluid dynamics (CFD) predictive tools for emissions and combustion efficiency: validate the predictive CFD model of spray and combustion under vaporizing and combusting conditions by introducing the key controlling parameters including ambient temperature, pressure, density, etc.
- Optimization of high-pressure DME fuel injection system: characterize DME injection as a function of several parameters including injection pressure, nozzle diameter, and injection duration to obtain better spray performance, achieve same amount of energy comparable to diesel combustion, and avoid issues associated with low viscosity and high compressibility.

Fiscal Year (FY) 2014 Objectives

- Design and fabricate the DME injector window, DME fuel delivery system and its interface controller system for the spray combustion test in the combustion vessel at MTU.
- Develop the rapid compression machine (RCM) autoignition test for dilute DME ignition characteristics at Argonne National Laboratory along with the University of Akron.
- Initiate the development and validation of DME chemical kinetics mechanism for ignition delay prediction and select the optimized DME chemistry for CFD model.
- Establish the CFD model of DME spray combustion.

FY 2014 Accomplishments

- Designed and fabricated the DME injector window mounted in the combustion vessel test facility.
- Fabricated the fuel delivery system of hydraulically activated electronic unit injector (HEUI) operated by oil-intensified system along with interface controller.
- Measured the rate of injection (ROI) for DME and diesel fuels with various injection pressures.
- Conducted experiment of non-vaporizing, vaporizing, and combusting spray in the MTU combustion vessel and autoignition test using an RCM.
- Developed various DME detailed and reduced chemistries for the predictive tool modeling development.

Future Directions

- Evaluate the high injection pressure spray combustion performance, new DME chemical kinetics mechanism and RCM autoignition.
- Analyze the spray dynamic and combustion test for the liquid, vapor and flame tip penetrations in the single-hole nozzle.
- Conduct the single-hole injector nozzle design and fabrication, the rate of injection test, spray test, and CFD model.

INTRODUCTION

This project is an extensive numerical and experimental characterization of the spray and combustion characteristics of DME, which is an attractive alternative to conventional diesel fuel for compression ignition engines. DME produces no soot and has a higher combustion quality due to higher cetane number relative to diesel fuel. Additionally, fast evaporation and good atomization are superior characteristics of DME relative to diesel, resulting in improved combustion performance. The overall work of this project includes: (a) the design and fabrication of fuel injection and control systems; (b) rate of injection measurement for spray characterization; (c) performance and visualization of DME spray and combustion experiment in a combustion vessel (CV) and corresponding analysis; (d) auto-ignition study in an RCM for chemical mechanism development; and (e) numerical work including CFD analysis with experimental validation. The significance of performance of various DME tests and their CFD model is to achieve low-temperature combustion for higher engine combustion efficiency and reduction in harmful emissions.

APPROACH

- The application of the HEUI system including the HEUI injector requires a specific enclosure (DME injector window) that can be integrated into the current CV system. A completed design of the injector window is fully functional with current CV design for various experiment and diagnostics of spray and combustion. The non-intrusive visualization diagnostic of spray combustion is the direct high-speed flame luminosity and schlieren imaging to track spray evolution. Estimation of the momentum flux and mass flow rate of the injector were acquired from an ROI measurement. The rate of injection is estimated by measuring the pressure wave following the injector opening into the fluid contained in a measuring cup and a long coiled tube, similar to the Bosch tube technique.
- Also, RCM is used for investigating homogeneous gas phase chemical kinetics at conditions of elevated pressures and low-to-intermediate temperatures. The ignition characteristic is determined by the pressure wave measured by the pressure transducer in the RCM. Homogeneous closed-reactor, two-stage Lagrangian, and CONVERGE™ modeling were utilized for the emissions predictions and basic flame properties.

RESULTS

With good collaborative work among MTU, Navistar, Argonne National Laboratory, and WMI, each of our tasks provides preliminary data for study of ignition and combustion characteristics of DME. The results from each task are described in the following.

- Task 1: The present work employed an intensified injector that uses high oil pressure to intensify the fuel pressure with ratio of 1:9.9. The injector is based on the current 2014 model year Navistar injector utilized in the medium-duty diesel market sector with injection pressure capability to 2,900 bar. Much of the DME studies have been reported at injection pressures ranging from 300-500 bar, with literature studies showing improved fuel economy with increased injection pressure due to better mixing and atomization [1]. This type of injector is referred to as a HEUI system as shown in Figure 1 (top left) with the advantage of limiting the fuel (DME) exposure to the injector nozzle alone. The oil pressure is built up on a common rail to amplify the piston hydraulically and provide high pressure at the fuel injector outlet. This provides for the activation of the injector while DME fuel supply pressure is kept to 0.8 MPa for liquefaction. According to the injector design and speed of the switching valve, the injector is fully electronically controlled and can accommodate several injection events. The unit injector was used successfully in the work of [2] based on a jerk-type pump but to injection pressures of only 300 bar. The overall fuel injection system is shown in Figure 1 with fuel supply for DME and diesel separately, DME injector window, and hydraulic oil system for high pressure before intensification of fuel.
- Task 2: The HEUI fuel injection was successfully used for both diesel and DME fuels. Oil inlet to the injector was precisely controlled for nearly stabilized oil pressure. The injection pulse width was controlled through developed software with accuracy of +/- 10 µsec from the input value. No leakage was observed on the oil side as well as the fuel side. The system was handled with ease when switching fuel between diesel and DME. Additionally, DME in the system was safely purged out at completion of the test with nitrogen. Procedures were also developed for each process.
- Task 3: The ROI setup schematic is shown in Figure 2, and the system is similar to the Bosch measurement [3]. ROI profiles at 1,024 bar injection pressure for DME and diesel can be seen in Figure 3. The ROI profile shows a delay from start of injection (electronically) and the actual flow rate signal. This is likely due to the significant amount of time

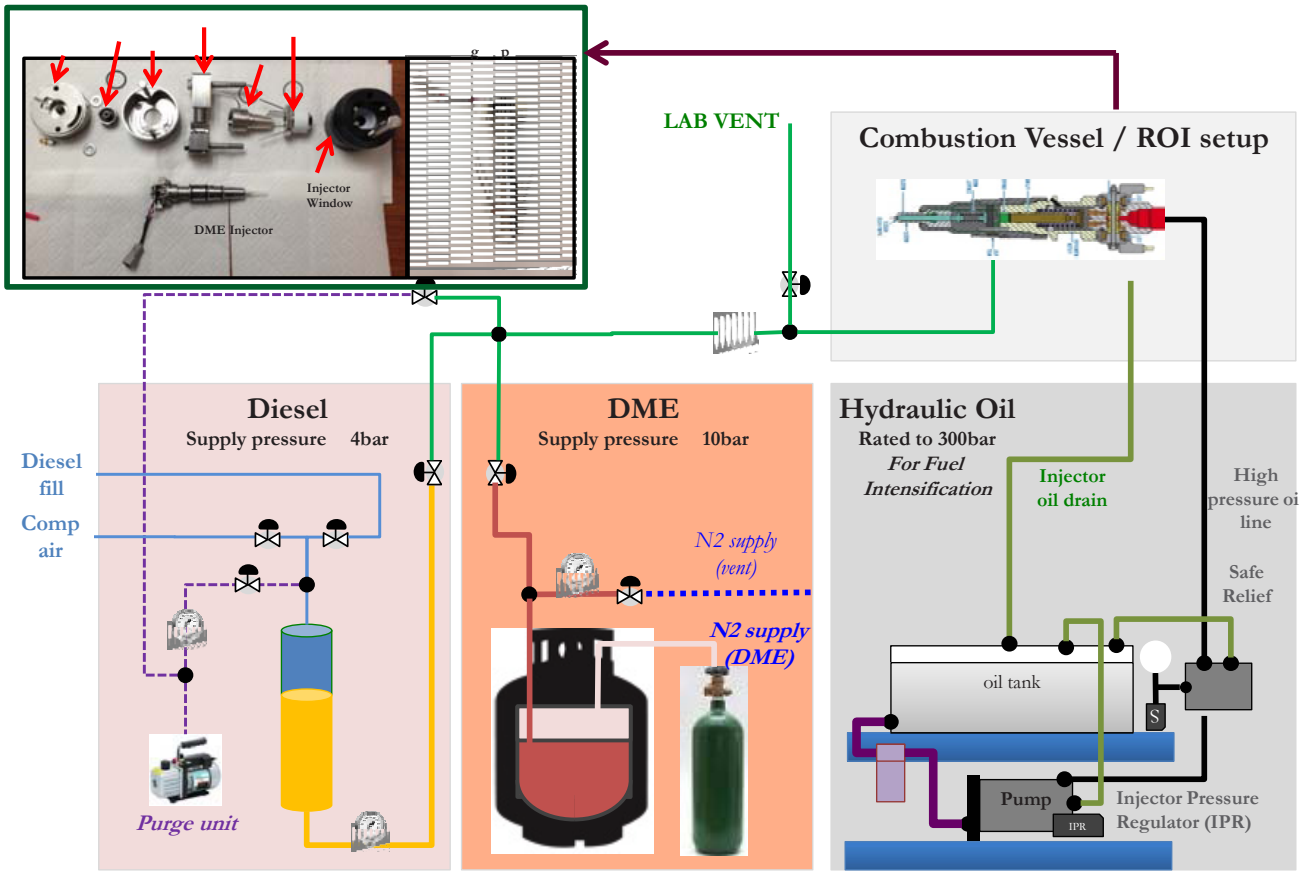

FIGURE 1. Fuel injection system of DME and diesel combination for integration to combustion vessel at MTU using the fabricated DME injector window.

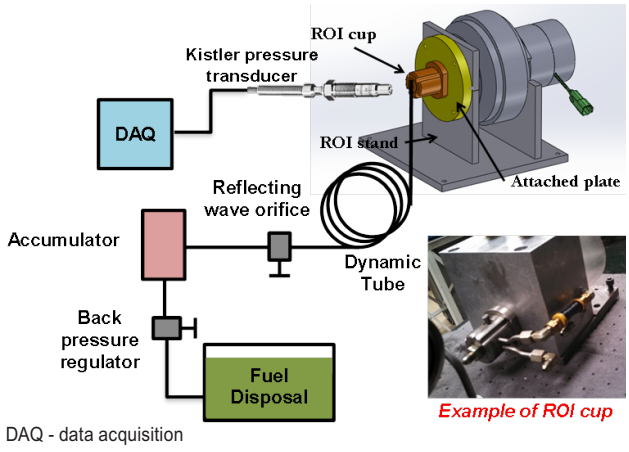

FIGURE 2. Diagram of rate of injection measurement using the Bosch tube method.

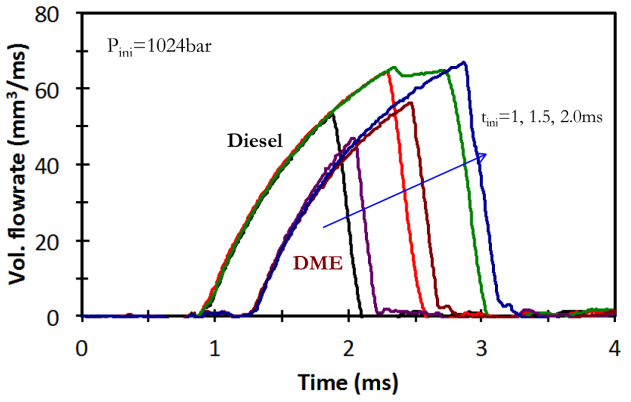

FIGURE 3. ROI profiles at the injection pressure of 1,024 bar for DME and diesel under different injection dwells of 1.0, 1.5, and 2.0 ms.

required to compress the two internal springs of the HUEI system: one spring for the piston at the pressurized oil side, then fuel sprays out from the lift of the needle pushing the second spring by the high pressure built in the fuel line. ROI measurement of DME showed that it was injected later compared to diesel at the same injection pressure. This is expected due to the higher compressibility of DME than diesel fuel. These results were published in the DME6 conference as listed in the FY 2014 Publications/Presentations section.

- Task 4: Different mixtures of DME with oxidizer and exhaust gas recirculation (EGR) including O_2,

CO_2, N_2, and Ar were selected for auto-ignition measurement in the RCM test. Almost no effect of CO_2 on the combustion chemistry was observed. The mixture that represents rich local equivalence ratio (ψ=4) gives a shorter ignition delay compared to leaner mixture (ψ=1). The ambient temperature effect on DME auto-ignition is shown in Figure 4.

- Task 5: Spray and combustion of DME and diesel were successfully characterized using a newly developed fuel injection system in the MTU combustion vessel [4]. Spray penetration and ignition delay were analyzed for comparison of two fuels. Several important findings are described in the following. DME liquid penetration is longer compared to diesel at the later stage of injection, but shows little or no difference at the early time of the injection for the same test condition. Ambient density can greatly affect the DME penetration that shows shorter penetration as seen in Figure 5 with increasing ambient density. In addition, the initial fuel temperature plays a key role in the liquid penetration of DME with higher fuel temperature, fuel penetration decreases. However, at higher ambient pressure, the effect of fuel temperature is also believed to be insignificant. Flame luminosity images show that DME has weaker and less combustion intensity compared to diesel as shown in Figure 6. The spray combustion results were submitted to the 2015 SAE World Congress as listed in the FY 2014 Publications/Presentations section.
- Task 6: The developed mechanism of DME with soot and oxides of nitrogen (NOx) chemistry was validated successfully with several mechanisms and reduced mechanism for a wide range of pressures (13-40 bar). The result was proven to be useful for use in other computational models with detailed chemistry of DME capable of soot and emissions prediction. The ϕ-T diagram in the closed reactor model shows soot precursor (acetylene and benzene) and soot indicator (pyrene) and NOx regions for a wide range of temperatures (1,000-3,000 K) and equivalence ratios (ϕ = 0.1-8). Pyrene is formed in the region with a similar range of ϕ > 3 and temperature range of 1,500-2,000 K compared to n-heptane and JP-8 surrogate, but forms only a

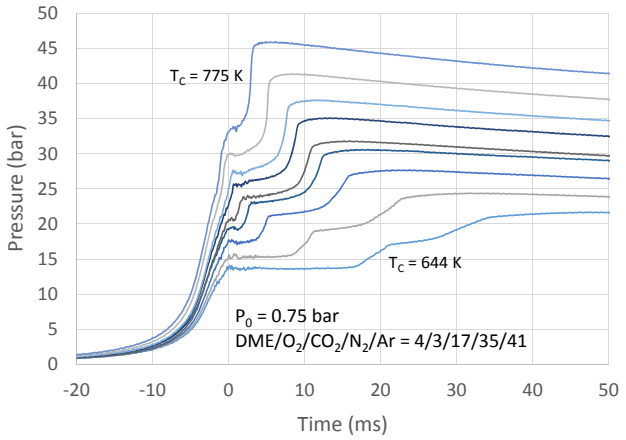

FIGURE 4. Pressure traces from the RCM experiment of DME auto-ignition over the temperature range of 644-775 K, end compression pressure of 9 bar, and rich local equivalence ratio of 4.

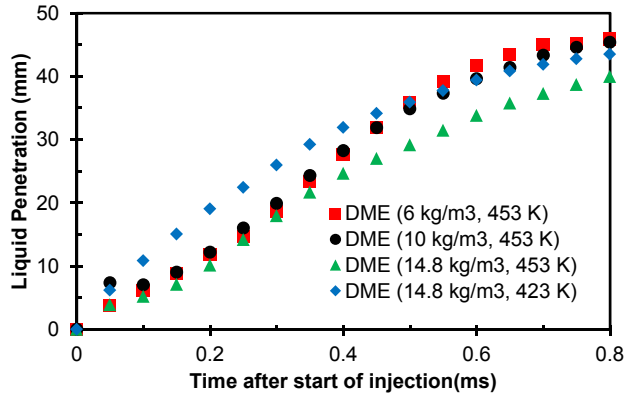

FIGURE 5. Spray penetration of DME at different ambient densities (6, 10, and 14.8 kg/m^3) and temperatures (423 and 453 K) in a nitrogen environment, injection pressure of 500 bar, 1 ms injection duration.

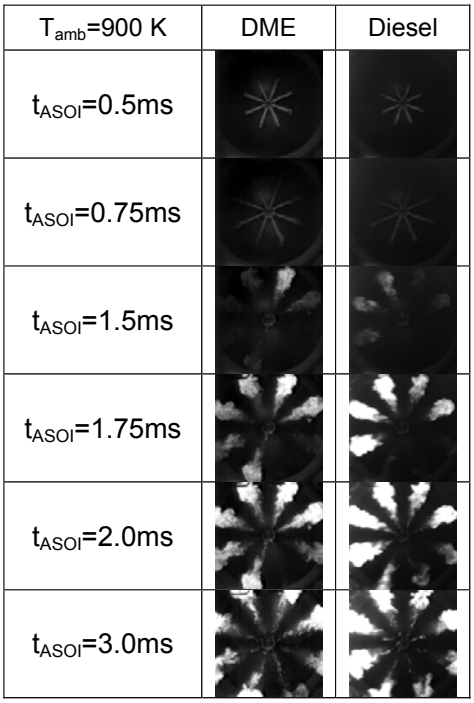

FIGURE 6. Snap shot image of DME and diesel spray combustion: ambient temperature 900 K, ambient gas 15% O_2, injection pressure 500 bar, and transistor-transitor logic injection duration of 1 ms.

relatively small yield. C_2H_2 formation region in the DME reaction is available in the high temperature region as comparing to other fuels and therefore DME combustion limits the formation of higher aromatics such as pyrene. The effects of ambient temperature and injection pressure were investigated through the two-stage Lagrangian model. The results show that soot and NO tend to increase as ambient temperature and injection pressure increases. In the two-stage Lagrangian simulation, the lowest amount of pyrene was produced in DME reaction when compared to other fuels such as diesel surrogate (n-heptane) and JP-8 surrogate fuel, which is in agreement with the closed-reactor simulation of the ϕ-T plot as well. Vaporizing spray formation characterization has also been conducted and its results will be prepared for publication.

CONCLUSIONS

The current developed fuel injection system provides great potential for the study of ignition and combustion of DME with the benefit of running diesel fuel for direct comparison. The overall progress of the project contributes to the development of spray and combustion modeling for DME using validated chemical kinetic models from RCM data. Further optimization is underway for the fuel injection system and injection strategies.

REFERENCES

1. C Arcoumanis, C Bae, R Crookes, E Kinoshita, *The potential of di-methyl ether (DME) as an alternative fuel for compression-ignition engines: A review,* Fuel, 2008. **87**(7):1014-1030.

2. Y Sato, S Nozaki, T Noda, *The Performance of a Diesel Engine for Light Duty Truck Using a Jerk Type In-Line DME Injection System,* 2004.

3. W Bosch, *The fuel rate indicator: a new measuring instrument for display of the characteristics of individual injection,* 1966, SAE Technical Paper.

4. K Cung, A Moiz, J Johnson, S.-Y. Lee, C-B Kweon, A Montanaro, *Spray–combustion interaction mechanism of multiple-injection under diesel engine conditions, Proc. Combust. Inst.* (2014), http://dx.doi.org/10.1016/ j.proci.2014.07.054, 2014.

FY 2014 PUBLICATIONS/PRESENTATIONS

1. Khanh Cung, Ahmed Moiz, Jaclyn Johnson, Seong-Young Lee, Chol-Bum Kweon, Luigi Allocca, "Spray-Combustion Interaction of Multiple Injections under Diesel Engine Condition," Proc. Combust. Inst. (2014), http://dx.doi.org/10.1016/ j.proci.2014.07.054, 2014.

2. Abdul Moiz, Seong-Young Lee, "15PFL-0251: Experimental and Numerical Studies on Combustion Model Selection for Split Injection Spray Combustion," 2015 SAE World Congress, 2014.

3. Khanh Cung, Jaclyn Johnson, Seong-Young Lee, William De Ojeda "15PFL-0596: Experimental Comparison of Spray and Combustion Characteristic Dimethyl Ether (DME) and Diesel under Different Ambient Conditions and Fuel Temperature," 2015 SAE World Congress, 2014.

4. Sreenath Gupta, Bikash Parajuli, Gaurav Mittal, Khanh Cung, Jaclyn Johnson, Seong-Young Lee, Grzegorz Siuchta, "RCM studies of DME ignition and combustion under highly diluent conditions," 6th International DME Conference, 2014.

5. Khanh Cung, Chunqiu Guo, Jaclyn Johnson, Seong-Young Lee, Willy de Ojeda, "High-pressure Oil Intensified DME Fuel Injection System Development for Engine-Condition Spray Combustion," 6th International DME Conference, 2014.

6. Khanh Cung, Jaclyn Johnson, Seong-Young Lee, Sreenath Gupta, Gregory Siuchta, "Experimental and Numerical Study of High Pressure DME Injection under Diesel Engine Conditions," 6th International DME Conference, 2014.

7. Khanh Cung, Jaclyn Johnson, Seong-Young Lee, Sreenath Gupta, Gregory Siuchta, "Numerical simulation of High Pressure Dimethyl Ether (DME) Injection under Diesel Engine Conditions," 248th ACS DME Symposium American Chemical Society National Meeting, 2014.

8. Seong-Young Lee, "NSF-DOE Partnership on Advanced Engine Combustion: Ignition and combustion characteristics of transport fuels under lean-burn conditions for advanced engine concepts: Dimethyl Ether (EMD)," 2014 Advanced Engine Combustion Program Review Meeting at Sandia National Laboratories- Livermore, February 2014.

9. Seong-Young Lee, "NSF-DOE Partnership on Advanced Engine Combustion: High injection pressure DME spray and combustion characteristics: Development of FI system and RCM autoignition," 2014 Advanced Engine Combustion Program Review Meeting at USCAR – Southfields, August 2014.

II.23 A Comprehensive Investigation of Unsteady Reciprocating Effects on Near-Wall Heat Transfer in Engines

Christopher White[1] (Primary Contact), Marcis Jansons[2], Yves Dubief[3]
[1]University of New Hampshire, [2]Wayne State University, [3]University of Vermont
[1]Kingsbury Hall Room W101, 33 Academic Way
Durham, NH 03824

DOE Technology Development Manager
Leo Breton

Overall Objectives

- Use collaborative experiments and numerical simulations to investigate unsteady reciprocating effects on heat transfer in piston engines.
- Develop a two-wavelength infrared (IR) temperature diagnostic capable of acquiring surface temperature measurements and wall heat flux in piston engines at high frequency.
- Formulate the foundations for the modeling of heat transfer in piston engines that account for the effects of rapid transients and non-equilibrium boundary layer behaviors.

Fiscal Year (FY) 2014 Objectives

- Establish the experimental facilities, measurement diagnostics, and the simulation and analytical tools needed to study and quantify the effects of unsteady reciprocating effects on heat transfer in piston engines.
- Evaluate the performance of existing Reynolds-averaged Navier-Stokes (RANS) heat transfer wall models in non-equilibrium boundary layer flow by direct comparison with direct numerical simulation (DNS).

FY 2014 Accomplishments

- Designed, built, and tested a constant temperature wall-plate to study heat transfer in controlled experiments with simulated conditions found in engines.
- Validated a two-wavelength IR surface temperature measurement technique against simultaneous thermocouple and thermographic phosphor measurements.
- Demonstrated a four-layer thin-film optical coating design to extend the two-wavelength IR surface temperature measurement technique to fired engine conditions.
- Performed DNS of reciprocal channel flow with heat transfer for flow regimes with strong non-equilibrium behaviors and compared the results to RANS models.
- Developed an exact integral method to evaluate wall heat flux suitable for experimental data. The method also provides a means to connect wall heat flux to bulk flow dynamics.

Future Directions

- Conduct physical experiments to measure and characterize heat transfer in controlled experiments with similar rapid transients and boundary layer behaviors found in engines.
- Optimize electron vacuum and plasma assisted chemical vapor deposition techniques to eliminate defects observed in optical window coatings.
- Conduct engine experiments to simultaneously determine gas velocity field and surface temperature under reversing flow motored conditions.
- Develop and implement new modeling approaches that better capture the transport mechanisms in non-equilibrium boundary layer flows and piston engines.

INTRODUCTION

This research project investigates the effects of rapid transients on heat transfer in piston engines. The capacity to understand and predict heat transfer in reciprocating piston engines is critically important for optimizing fuel efficiency, reducing harmful engine-out emissions, and furthering advanced combustion strategies. The proposed research is motivated by the fact that engine simulations almost exclusively use heat transfer models that cannot accurately capture the effects of rapid transients, and in turn cannot accurately predict heat transfer over a typical drive cycle. The modeling difficulty is owed to nonlinear interactions between in-cylinder turbulence, fuel injection, combustion, piston geometry, and piston motion that produce complex non-equilibrium boundary layers along the cylinder walls. Combining analytical,

numerical simulation and experimental approaches, the project work is to conduct a systematic scientific investigation focused on understanding how these nonlinear interactions affect in-cylinder heat transfer. The overarching goal of the project is to use the results from these scientific investigations to improve upon the robustness of engine heat transfer models so that they can be used for engineering design of low-emission, high-efficiency engines.

APPROACH

Laboratory and numerical experiments of increasing complexity are being conducted to elucidate the fundamental thermal transport processes found in piston engines. In parallel, a two-wavelength IR temperature diagnostic capable of acquiring surface temperature and wall heat flux measurements in a fired engine is being developed. Following the development and validation of the IR temperature diagnostic, it will be used in conjunction and simultaneously with other techniques measuring in-cylinder gas velocity (with particle image velocimetry) and in-cylinder gas temperature (two-color method) to provide both fundamental knowledge of heat transfer in piston engines and validation data to evaluate heat transfer wall models.

Informed by the experimental and numerical results described above, a first-principles modeling approach will be used to develop new heat transfer models that better capture the transport mechanisms in non-equilibrium boundary layers and piston engines. The approach will aim to exploit scale separation associated with either coherent turbulent flow structures or distinct turbulence regimes identified through existing but newly emerging data analysis techniques.

RESULTS

FY 2014 (first year of project) results primarily relate to the establishment of the experimental facilities, measurement diagnostics, and the simulation and analytical tools needed to study and quantify the effects of rapid transients on near-wall heat transfer.

Development of a two-wavelength IR temperature diagnostic: The optics-based IR technique developed is a dual-wavelength IR pyrometric technique in which the temperature dependency of the ratio of emission intensity over two discrete wavebands is determined by calibration experiments and then exploited to measure surface temperature. The experimental setup designed and fabricated to perform IR surface temperature measurements in a piston engine is shown in Figure 1. Validation experiments were conducted by focusing the IR system onto a fast-response thermocouple mounted

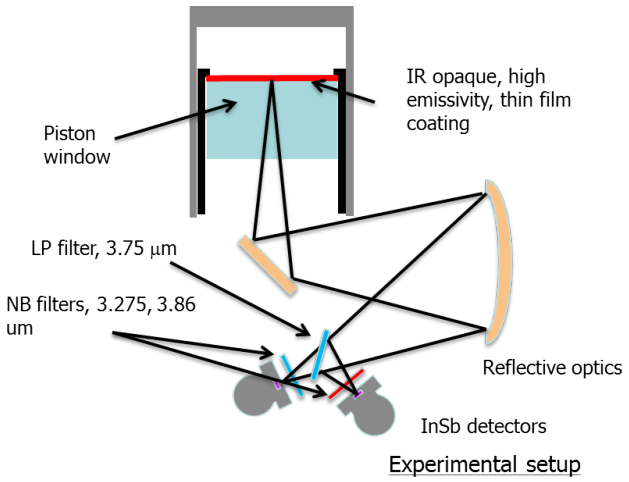

FIGURE 1. Experimental setup to measure in-cylinder surface temperature using the two-wavelength IR temperature diagnostic.

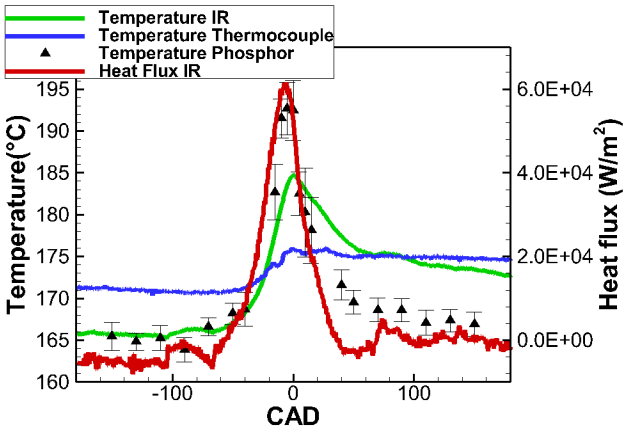

FIGURE 2. Simultaneously measured surface temperatures using three techniques and IR-based heat flux under motored engine conditions.

on the tip of a dummy fuel injector, which was also painted with a thermographic phosphor. This allowed simultaneous surface temperature measurement using three independent techniques, which agreed to better than 15 Kelvin (see Figure 2). Local heat flux was determined from the measured IR temperature history.

A major effort was to develop coatings and coating processes to satisfy the requirements of the IR diagnostic when used under fired engine conditions when combustion luminosity interferes with infrared emission from the lower temperature surfaces. Electron vapor, sputtering, and plasma-assisted chemical vapor deposition techniques have been used to form single- and multi-layer coatings of titanium, titanium dioxide, silicon dioxide, and silicon nitride in layers from 500 Angstrom to 1 micron thicknesses. Desirable properties are for a thin, IR-opaque coating, which itself has high emissivity

and can withstand combustion chamber environments. Coatings have been produced and evaluated using Wayne State University's nano-fabrication, white-light interferometry, scanning electron microscopy, and energy-dispersive X-ray spectroscopy facilities. High-emissivity coatings that have withstood repeated fired cycles have been produced, and current efforts are being devoted to limit defects observed in the coatings.

Controlled experiments simulating non-equilibrium engine boundary layer behaviors: The flow configuration is boundary layer flow over a constant temperature wall. Experiments will be conducted with systematically increasing boundary layer perturbations to generate non-equilibrium boundary layer flows of increasing complexity that simulate boundary layer behaviors found in piston engines. The FY 2014 activities have been the design, build, and test of a constant temperature wall-plate. The wall-plate shown in Figure 3 is a sectioned wall design where each section is independently heated and controlled. The ability of the plate design to maintain the wall at a pre-selected fixed temperature has been validated by wind tunnel studies in which the mean plate temperature can be held within 0.3% of the set temperature.

The experimental study of non-equilibrium thermal boundary layer flow is difficult since determination of the wall heat flux is challenging. The primary difficulty is that the wall heat flux is typically determined by indirect methods such as empirical correlations or employing Reynolds analogy between the wall shear stress and the wall heat flux. In non-equilibrium boundary layers, however, both these methods fail and the wall-heat flux must be measured directly. Extending the framework of the University of New Hampshire principal investigator's work on shear stress measurements, a mathematically exact, integral method to evaluate wall heat flux in turbulent wall-bounded flows has been developed. The method is amenable to experimental studies and provides a mean to connect transport properties at the wall to the bulk flow dynamics. The latter is important for heat transfer model development in non-equilibrium boundary layers.

Numerical simulations of non-equilibrium boundary layer flows: The work in FY 2014 has focused on the simplest representation of reciprocal non-equilibrium boundary layer flow: a channel flow with an oscillating pressure gradient and zero mean flow. This simple flow is illustrated with three different simulations of the same flow (1) a finite volume DNS code (exact solution), (2) unsteady RANS using a v2-f model, and (3) unsteady RANS using a k-ε model. The simulations were performed over a range of flow Reynolds number and pulsation periods with turbulence levels typical of those observed in piston engines. Flow statistics are phase-averaged over sufficient flow duration to achieve convergence.

The results of this first campaign of simulation have highlighted the fragility of the equilibrium hypothesis presently used in existing heat transfer models. This fragility is illustrated in Figure 4 where the mean velocity and temperature profiles, when scaled with the so-called wall units, should follow the green line in equilibrium boundary layers. For clarity, only three phases of the cycle are plotted. The three phases are representative of the modeling shortcomings of current RANS simulations, and also show that the flow is mostly "out-of-equilibrium", as illustrated by the DNS. Moreover, the discrepancy between the DNS and RANS prediction is quite staggering and model dependent. The latter is easily observed in the temperature profiles where the v2-f and k-ε models consistently over and under-predict the mean flow temperature respectively.

CONCLUSIONS

- Intermediate project objectives have been met, current work shows promise, and is on schedule.

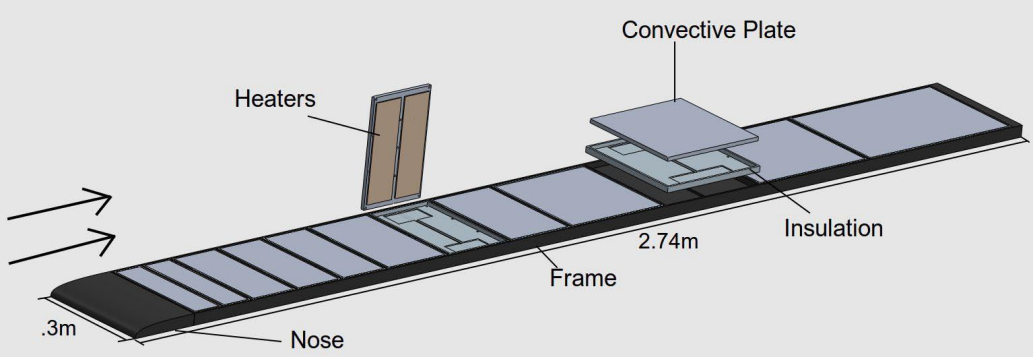

FIGURE 3. Schematic of the sectioned wall-plate design. The sectioned convective plates are made from aluminum 6061, are independently heated and controlled, and sit in an insulated frame for thermal isolation.

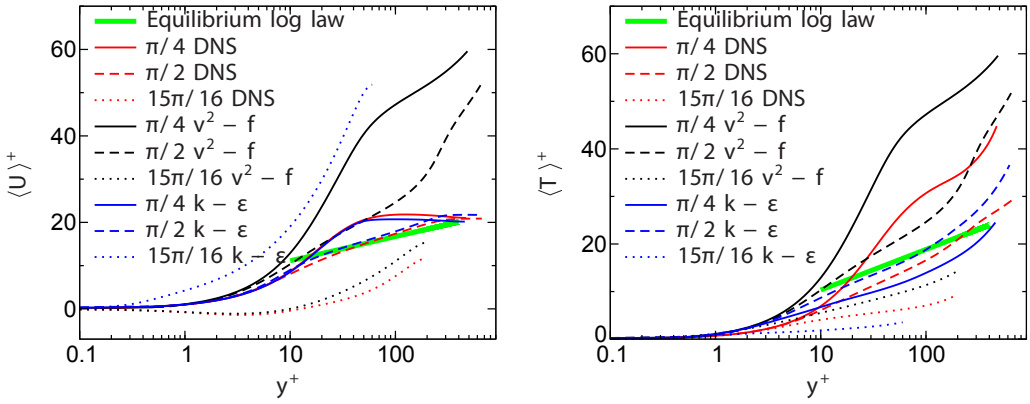

FIGURE 4. Comparison between DNS and unsteady RANS simulations. Plots of mean velocity (left) and temperature (right) profiles in a channel flow subjected to an oscillatory pressure gradient of the form: -dP/dx = cos(2πt/T), where t is time and T is the period of oscillation. The thick green line corresponds to the expected profiles for equilibrium boundary layer behavior. The superscript + denotes normalization by τ_w, q_w, ρ, and ν, where τ_w and q_w are the wall shear stress and heat flux, respectively, and ρ and ν are the fluid density and kinematic viscosity, respectively.

- The experimental facilities, measurement diagnostics, and the simulation and analytical tools needed to study and quantify the effects of rapid transients and non-equilibrium boundary layer behaviors on heat transfer are in place.
- The breakdown of equilibrium flow behaviors in a simple reciprocating flow and the failure of RANS models to accurately predict mean flow behaviors has been demonstrated.

FY 2014 PUBLICATIONS/PRESENTATIONS

1. C.M. White, M. Jansons and Y. Dubief. Heat Transfer in Non-Equilibrium Boundary Layers and Piston Engines", Ford Research and Innovations, Dearborn, Michigan (2014).

2. C.M. White, M. Jansons and Y. Dubief. NSF/DOE Partnership On Advanced Combustion Engines: Unsteady Reciprocating Effects On Near-Wall Heat Transfer In Engines", Advanced Engine Combustion Program Review Meeting, Southfield, Michigan (2014).

3. Luo, X., Yu, X., Zha, K., Jansons, M., Soloiu, V., "In-Cylinder Wall Temperature Influence on Unburned Hydrocarbon Emissions During Transitional Period in an Optical Engine Using a Laser-Induced Phosphorescence Technique," Technical Paper 2014-01-1373, presented SAE World Congress, Detroit, MI April 2014.

4. Luo, X., Yu, X., Zha, K., Jansons, M., Soloiu, V., "In-Cylinder Wall Temperature Influence on Unburned Hydrocarbon Emissions During Transitional Period in an Optical Engine Using a Laser-Induced Phosphorescence Technique," SAE Int. J. Engines 7(2):995-1002, 2014.

5. C.M. White, M. Jansons and Y. Dubief. NSF/DOE Partnership On Advanced Combustion Engines: Unsteady Reciprocating Effects On Near-Wall Heat Transfer In Engines", Advanced Engine Combustion Program Review Meeting, Livermore, CA (2014).

II.24 Development of a Dynamic Wall Layer Model for LES of Internal Combustion Engines

Matthias Ihme
Stanford University
488 Escondido Mall
Building 500, Room 500A
Stanford, CA 94304

DOE Technology Development Manager
Leo Breton

Subcontractors
- Volker Sick, University of Michigan, Ann Arbor, MI
- Claudia Fajardo, Western Michigan University, Kalamazoo, MI

Overall Objectives

Conduct detailed measurements and develop advanced modeling capabilities to improve current understanding about heat transfer, thermal stratification, and non-equilibrium coupling processes in the near-wall region of internal combustion engines that are operated under low-temperature combustion (LTC) conditions.

Fiscal Year (FY) 2014 Objectives

- Optimize microscopic particle image velocimetry (micro-PIV) for dynamic boundary layer measurements
- Demonstrate temperature imaging strategy in engine
- Develop initialization method for direct numeric simulation (DNS) that uses mean flow properties gained from large-eddy simulation (LES)
- Perform a priori analysis of experimental near-wall measurements and develop non-equilibrium near wall model

FY 2014 Accomplishments

- Achieved high frame-rate micro-PIV measurements in operating engine with spatial accuracy for surface position of 30 ±0.5 μm.
- Demonstrated the potential of 3-pentanone laser-induced-fluorescence measurements to identify structures of local temperature variations in optical engine
- Created several post-processing tools to examine near-wall region and transient boundary-layer effects in DNS
- Developed non-equilibrium wall models and demonstrated the significance of pressure gradients near top-dead center that are induced by large in-cylinder vortical structure

Future Directions

- Acquire larger collection of flow measurements
- Fully implement and employ temperature imaging technique
- Conduct measurements for range of operating conditions
- Perform multiple concurrent high resolution DNS studies
- Develop dynamic non-equilibrium wall models for LES calculations

✧ ✧ ✧ ✧ ✧

INTRODUCTION

This project supports the advancement of in-cylinder LES wall-layer models to improve engine simulation accuracy thereby facilitating computational engine design from high-accuracy predictive simulations. In-cylinder heat transfer significantly impacts combustion processes and governs near-wall pollutant formation and cycle efficiency. Therefore, accurate wall-layer models are crucial to the development of predictive engine simulations. The following tasks were conducted during FY 2014:

- Task 1: Advancement of near-wall velocity and temperature measurements in canonic transparent combustion chamber (TCC) engine. This task provides enhanced physical understanding and experimental validation data for model development.
- Task 2: Development of LES wall model. Using the data from experimental and computational studies, develop a non-equilibrium wall model that accounts for local and transient effects by momentum and energy transfer.

APPROACH

The aim of the project is to develop wall-layer models with predictive accuracy to facilitate high-fidelity engine simulations for computational design leading to faster and less costly development of high-efficiency,

low-emission engines. The specific approaches used for each task are described in the following.

- **Task 1:** The current engine optimization process is severely hampered by the lack of accurate predictive simulations. Current simulations fail to predict engine operation largely due to grossly inadequate wall models. In-cylinder near-wall processes are not nearly as well understood as for the canonical boundary layer flows. Our research aims to characterize and increase the physical understanding of the processes governing these highly turbulent, transient, low Mach number, compressible, near-wall flows. Micro-PIV is applied to a region below the engine head to measure planar velocity fields in the near wall region. Coherent flow structures are identified and their interactions with the wall observed. A fluorescent tracer seeding system was designed and implemented to facilitate laser-induced fluorescence measurements of temperature. Exploratory studies of in-cylinder temperature fields have been undertaken.
- **Task 2:** The near wall region is the most computationally expensive portion to simulate in a flow because of the small scales. To develop an appropriate wall model it is essential to have an understanding of processes in the near-wall region. High resolution DNS studies can provide more information than is currently available from experiments. The DNS will be used to examine the complicated local and transient effects found in the boundary layers of in-cylinder flows. This data can then be used to compare to our LES model and experimental measurements.
- **Task 3:** Wall-resolved LES is still not practical for in-cylinder engine simulations and wall models are needed to resolve the computational cost issue. As a first step towards the development of dynamic LES wall models for in-cylinder flow, the experimental measurements are used to conduct a priori analysis on different wall models, including the classical equilibrium wall-function model and two other non-equilibrium wall models with two different turbulence closure models. The results of this study can be used to assess the performance of the commonly used wall-function models and potential advantage of non-equilibrium wall models.

RESULTS

Our efforts in FY 2014 have focused on building experimental systems and computational fluid dynamics techniques to facilitate the development of dynamic wall-models for LES of engines.

- **Task 1:** Efforts at the University of Michigan in FY 2014 focused on building optical diagnostic systems to measure planar velocity and temperature fields below the engine head of our TCC engine (Figure 1). Experimental challenges unique to this engine compared to those used previously for similar experiments are optical aberrations introduced by imaging at high magnification through the curved quartz cylinder of this engine, and by the head surface occluding half of a conventional imaging system. These issues were largely corrected through several generations of experimental setups and the use of nonconventional imaging systems. New results for velocimetry measurements (Figure 2) indicate the ability to track coherent structures in the flow and observe their interactions with the wall. Phenomenological processes analogous to those observed in the literature of impinging jet wall flows were also visualized in the near-wall region of this engine. Work to implement gas temperature measurements in the near-wall region is progressing on schedule.
- **Task 2:** Efforts at Stanford in FY 2014 were focused on preparing to run a high-resolution DNS study, developing several post-processing tools, and performing preliminary analysis on wall models. In preparation of a large-scale DNS many small cases were initially run to determine the best methods to initialize flow and ensure proper resolution of the boundary layer. Using the low-resolution test cases, several post-processing tools were created to aid in the visualization of various flow features.
- **Task 3:** Complementing the DNS-effort, a priori analyses of different wall models based on experimental measurements were conducted. Data analysis is performed to assess the inner structure of

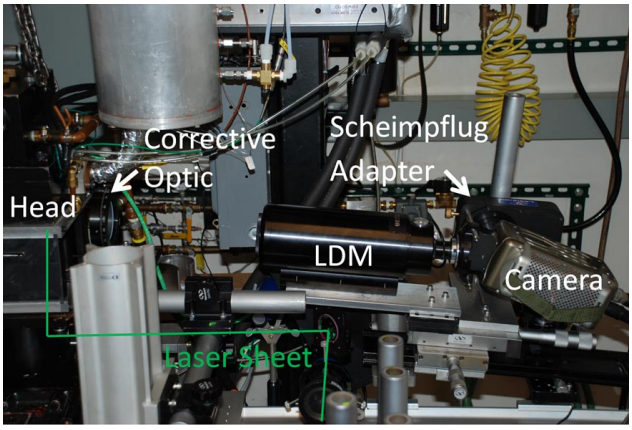

FIGURE 1. Current Unconventional Imaging System showing Scheimpflug Arrangement of Image Sensor, Lens, Long-Distance Microscope (LDM), and Object Plane

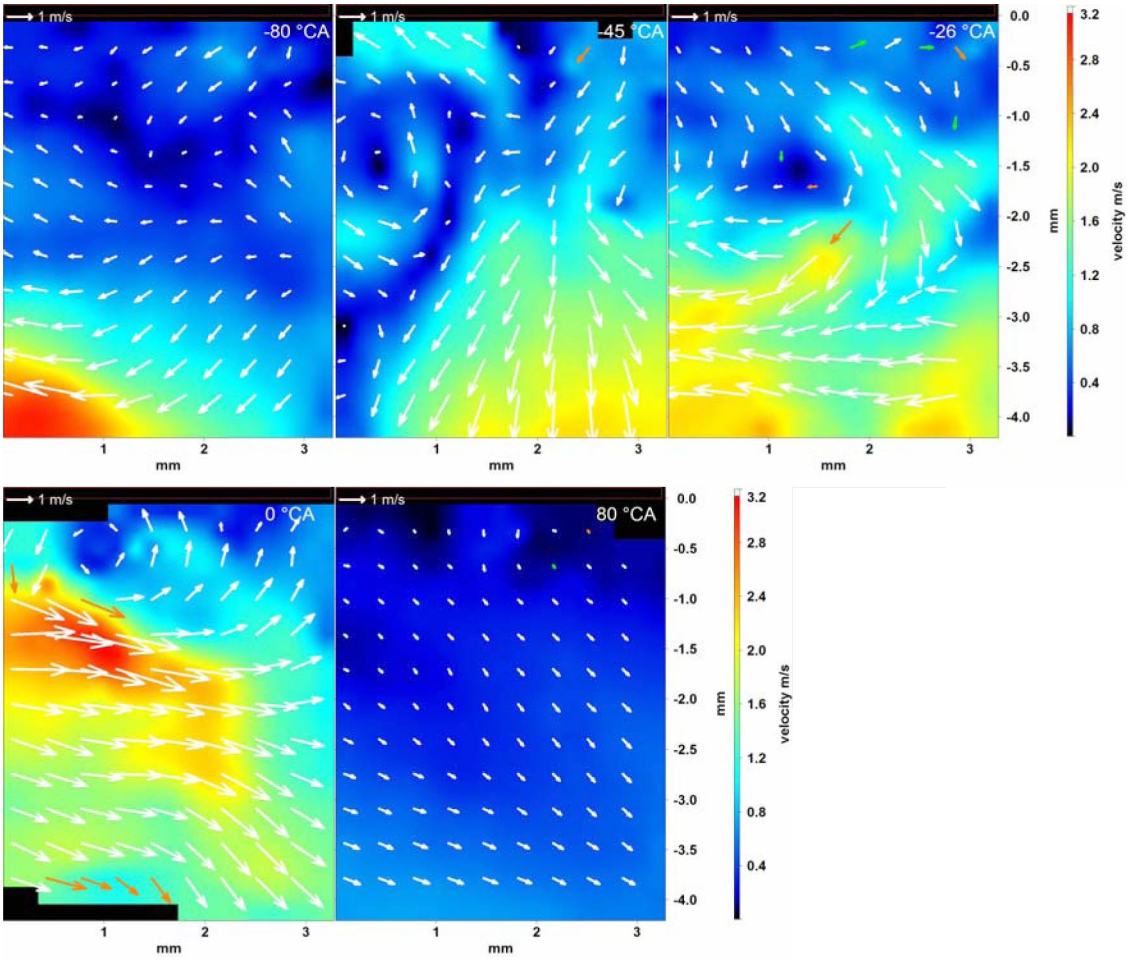

FIGURE 2. Flow field evolution through a single engine cycle. Only every fourth vector shown in 5 of 181 measured crank angles. Note the change in flow direction from predominantly left to right as the cycle progresses past 0 crank angle (CA) degrees.

the boundary layer. Using the experimental data, the performance of a hierarchy of wall models, including the algebraic equilibrium wall-function model commonly used in Reynolds-averaged Navier-Stokes and LES internal combustion engine simulations, and two non-equilibrium differential wall models with different near-wall turbulence modeling are investigated. It is shown that all three wall models provide adequate predictions of the shear velocity if the first grid point is located in the viscous sublayer. However, it was shown that algebraic wall function models consistently underpredict the shear velocity if the first grid point is located outside the viscous sublayer. By considering non-equilibrium effects, the other two models provide improved predictions of the near-wall region and shear velocity irrespective of the wall distance. By utilizing the experimental data, significant adverse pressure gradients due to the large vortical motion inside the cylinder are observed and applied to the non-equilibrium wall model to further improve the model performance.

CONCLUSIONS

Joint experimental work at the University of Michigan and computational studies at Stanford University are progressing on schedule and show progress to deliver advanced wall-models for engine LES.

- Near-wall velocity measurement system built up on the TCC engine using nonconventional imaging systems to improve image quality.
- Preliminary findings demonstrate ability to track coherent structures through near-wall region and observe interactions with wall. This shows promise in leading to a better understanding of these physical processes.
- Fluorescent tracer seeding system installed on TCC engine and preliminary in-cylinder temperature fields recorded.
- The equilibrium wall-function model is not adequate for description of in-cylinder near-wall region and

relative error of underprediction of shear velocity can be as high as 60%.

- Description of near-wall regions requires consideration of non-equilibrium effects.
- Large in-cylinder vortical structure (tumble, swirl, turbulence) introduces substantial pressure gradients near top-dead center compression conditions, which needs consideration in non-equilibrium wall models.

FY 2014 PUBLICATIONS/PRESENTATIONS

1. Annual Report: NSF/DOE Advanced Combustion Engines: Development of a Dynamic Wall Layer Model for LES of Internal Combustion Engines, NSF, 2014.

II.25 Advancing Low-Temperature Combustion and Lean Burning Engines for Light- and Heavy-Duty Vehicles with Microwave-Assisted Spark Plugs and Fuel Stratification

Robert W. Dibble (Primary Contact),
Jyh-Yuan Chen
University of California-Berkeley
6159 Etcheverry Hall, Mailstop 1740
Berkeley, CA 94720-1740

Wai Cheng
Massachusetts Institute of Technology (MIT)

DOE Technology Development Manager
Leo Breton

Subcontractor
Ricardo North America, Burr Ridge, IL

Overall Objectives

- Demonstrate extension of engine load and speed limits using partial fuel stratification (PFS) compared to homogeneous charge compression ignition (HCCI), understand fuel chemistry and improve fuel chemical mechanisms, and develop validated models of PFS.
- Demonstrate extension of ignition limits to high pressure and exhaust gas recirculation (EGR) using advanced ignition systems and PFS, optimize ignition strategies, and optimize injection strategies.
- Develop an improved understanding of the fundamental physics governing advanced ignition and flame propagation in stratified charges.

Fiscal Year (FY) 2014 Objectives

- Develop and validate numerical models of HCCI with PFS that allow fundamental understanding of interacting chemistry and fluid dynamics, specifically of the Sandia and MIT engines.
- Demonstrate the effect of intake pressure boost and ethanol addition to the fuel on low-temperature heat release (LTHR) and intermediate temperature heat release (ITHR) for various gasoline fuels in an HCCI engine.
- Provide fundamental understanding of the chemical reactions that lead to ITHR and φ-sensitivity in gasoline at high intake pressures, and demonstrate how ITHR and φ-sensitivity can be used to achieve high efficiency over the full load range.
- Experimentally demonstrate extension of ignition limits using advanced ignition systems for a range of pressures, air and EGR dilution, and PFS. Quantify the influence of the ignition systems on flame kernel development with respect to pressure and turbulence.
- Quantify the effect of fuel stratification on local flame speed and develop an empirical model for use in spark-ignited engines.

FY 2014 Accomplishments

- Demonstrated that LTHR and ITHR increase with intake pressure boost for gasoline, becoming active above about 1.3-1.4 bar for 0% ethanol, above about 1.7-1.8 bar for 10% ethanol, and above about 2.2 bar for 20% ethanol.
- Quantified the effect of start-of-injection timing on PFS with a certification gasoline.
- Developed and validated a model of the Sandia engine in CONVERGE™ CFD [1].
- Quantified the ability of available chemical kinetic mechanisms to predict the pressure-boost onset of LTHR and ITHR for gasoline and the effect of ethanol addition to gasoline on LTHR/ITHR.
- Quantified the effect of fuel stratification on flame propagation velocity using a numerical model for hydrogen-air flames.

Future Directions

- Develop and validate a model of the MIT engine in CONVERGE™ CFD.
- Experimentally demonstrate that HCCI with PFS allows expansion of high- and low-load limits, to allow high efficiency operation over the full engine load and speed requirements. Further demonstrate that exhaust temperatures are high enough for an oxidation catalyst to be used for after treatment of hydrocarbons and CO.
- Evaluate the effect of compression ratio and injection timing on LTHR and ITHR for a certification gasoline.
- Quantify experimentally the memory effect of flames propagating through a step change in fuel content.

- Quantify the effect of fuel stratification on flame propagation velocity using a numerical model for methane-air flames. Develop an empirical correlation for the flame speed as a function of the thermochemical state and spatial derivatives in fuel content.

INTRODUCTION

This project set out to help achieve the 54 mile per gallon target (year 2025) for vehicle mileage by providing experimental data, simulation tools and understanding of fundamental phenomena to develop the next generation of high-efficiency engines for vehicles. The main objective is the extension of clean and efficient low-temperature combustion (LTC) technology to operate over the full load and speed range required of an engine. Two main technology paths were proposed: 1) PFS in LTC compression ignition engines, and 2) advance ignition systems combined with PFS in spark-ignited engines.

On a fundamental level, this project set out to provide detailed understanding of the chemical kinetics that cause pressure-sensitive ITHR and equivalence ratio sensitivity in gasoline, phenomena that enable high load boosted LTC with PFS. For the advanced ignition system technology, this project set out to provide understanding of the interactions between the spark discharge, the electric field and the stratified mixture in the flame kernel formation process. Additionally, the fundamental physics behind flame propagation through a stratified charge will be studied to obtain a comprehensive description of the PFS ignition process. These scientific insights will be applied, through fundamentally based phenomenological models, to engines for improving engine efficiency and lowering emissions.

APPROACH

The approach used to conduct the research under this project involves close collaboration between experimental and numerical efforts. The experimental approach is to collect high-quality data at a wide range of relevant conditions to understand the response of the system to a range of external inputs. The computational approach is to use multiple levels of numerical tools, from simplified to detailed models, to complement the experimental results and elucidate the physical processes governing observed trends. In short, experiments are used to guide simulations and simulations are used to guide experiments.

RESULTS

Extend Engine Load and Speed Limits of HCCI with PFS

An injection timing span conducted at φ = 0.33, 1,200 rpm, 10 bar nominal gross mean effective pressure, port fuel injection/direct injection 60/40 split, and 15% EGR shows three distinct regimes, as seen in Figure 1. In Regime A, delay in the direct injection timing (increasing stratification) delays the combustion phasing as measured by crankangle (CA)10. This is because the decrease in the physical delay times (evaporation, mixing, chemical) from injecting into a hotter environment does not compensate for the delay in the start of injection (SOI). Additionally, the higher equivalence ratio regions are not sufficiently more reactive than the premixed charge. However, in Regime B, delaying SOI (increasing stratification) advances the CA10. Here, the increased reactivity of the higher equivalence ratio regions advances the combustion phasing. Regime B is the desired regime for PFS. In Regime C, the physical delay times are too long compared to the SOI delay, such that the combustion phasing is delayed.

Simulations of the PFS in the Sandia engine using a validated model in CONVERGE™ CFD indicate that LTHR, present for gasoline only at sufficiently boosted intake pressures, compensates for evaporative cooling from the liquid fuel spray and decreased compression heating from reduced values of the ratio of specific heats. The sequential auto-ignition event is dictated by the fuel content and temperature stratification/distribution, which is influence by LTHR.

Understand Fuel Chemistry and Improve Fuel Mechanisms

It has been found that gasoline feedstock, typically with an anti-knock index (AKI) of 84, will transition from burning with single-stage heat release to dual-

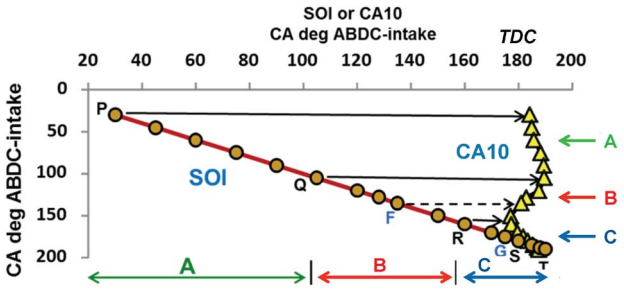

ABDC – after bottom-dead center; TDC – top-dead center

FIGURE 1. Effect of SOI Timing on Combustion Phasing as Measured by the 10% Burn Point (CA10)

stage heat release between approximately 1.3-1.4 bar intake pressure in a high compression ratio engine (CR = 16.5:1) in a lean mixture (φ = 0.4). The addition of 10% ethanol to the feedstock, resulting in approximately 87 AKI, delays the transition to dual-stage heat release until intake pressure is increased to 1.7-1.8 bar. The addition of a further 10% ethanol, resulting in 20% ethanol in total, further delays dual-stage heat release until intake pressure is increased to 2.2-2.3 bar intake pressure.

More specific to experimental results, smaller differences were noticed between different fuel blends. Primary reference fuel (PRF) 84, which has the same AKI as the two gasolines, was found to be slightly more reactive. The two gasolines, FACE A and FACE C, which differ significantly in formulation, were very similar in their behavior during these experiments.

Initial findings suggest that many mechanisms predict the correct trends of pre-ignition heat release propensity with pressure boost and ethanol addition, however, the surveyed mechanisms do not predict the true behavior accurately. An efficient way to compare pre-ignition heat release among many cases is to plot the intake temperature required for a constant combustion phasing (here 6 deg after top-dead center) versus intake pressure. As the intake pressure is increased, the intake temperature requirement begins to drop as the reactions proceed at faster rates. At a certain intake pressure, the pre-ignition heat release chemistry "turns on," and a rapid reduction in intake temperature is required with increasing intake pressure. In other words, rapidly decreasing intake temperatures with increasing intake pressure are indicative of increasing pre-ignition heat release. Comparison between predictions from mechanisms using a single-zone model and engine experiments are presented in Figure 2 for PRF85 [2] (top) and PRF84 and PRF84 with 10% ethanol (bottom).

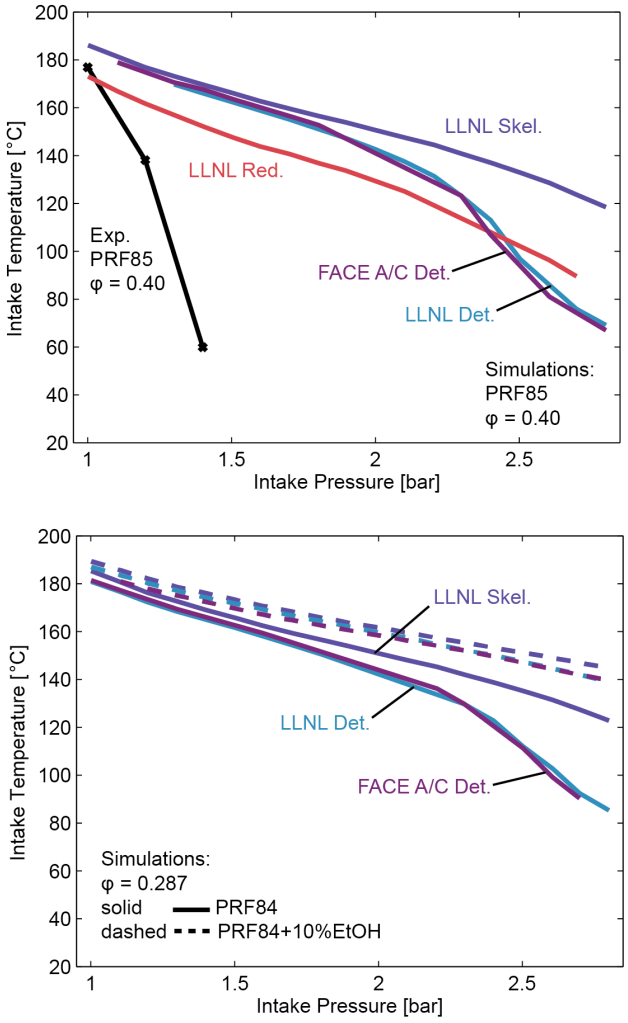

FIGURE 2. Intake temperature versus intake pressure for single-zone simulations and HCCI engine experiments for PRF85 (top) and single zone simulations for PRF85 with 0% and 10% ethanol (bottom). The mechanisms presented are based on the gasoline surrogate mechanism from Lawrence Livermore National Laboratory (LLNL).

CONCLUSIONS

- Ethanol inhibits the pressure boost onset of LTHR for gasoline-like fuels, increasing the required pressure boost by about 0.4 bar for each 10% ethanol added to the fuel in a CR = 16.5 HCCI engine.
- Many available mechanisms do not adequately predict the pressure boost onset of LTHR, but do predict the correct trends with ethanol addition to the fuel.
- Increased mixture stratification through a delay in the start of injection does not necessarily increase mixture reactivity. Mixing limited combustion can occur at overly delayed injection timings, with the same maximum pressure rise rate as earlier injection timings.
- For PFS with gasoline at sufficiently boosted intake pressures, LTHR compensates for evaporative cooling from the liquid fuel spray and decreased compression heating from lower values of the ratio of specific heats, leading to sequential auto-ignition in order of decreasing fuel content.

REFERENCES

1. Richards, K.J., Senecal, P.K., Pomraning, E., "CONVERGE (Version 2.1.0)", (Middleton, WI, Convergent Science Inc.), 2013.

2. Vuilleumier, D., Selim, H., Dibble, R., and Sarathy, M., "Exploration of Heat Release in a Homogeneous Charge Compression Ignition Engine with Primary Reference Fuels," SAE Technical Paper 2013-01-2622, 2013, doi:10.4271/2013-01-2622.

FY 2014 PUBLICATIONS/PRESENTATIONS

1. B. Wolk, J.Y. Chen, J.E. Dec, "Computational study of the pressure dependence of sequential auto-ignition for partial fuel stratification with gasoline," *Proceedings of the Combustion Institute* 35 (2014) in-press.

2. W. Sang, W. Cheng, A. Maria, "The nature of heat release in gasoline PPCI engines," SAE Technical Paper 2014-01-1295 (2014).

II.26 Modeling and Experiments of a Novel Controllable Cavity Turbulent Jet Ignition System

Elisa Toulson (Primary Contact), Harold Schock, George Zhu, Farhad Jaberi, Indrek Wichman, Giles Brereton
Michigan State University (MSU)
1497 Engineering Research Crt.
East Lansing, MI 48824

DOE Technology Development Manager
Leo Breton

Overall Objectives

- Examine the active radicals generated in the turbulent jet ignition (TJI) process through both rapid compression machine and optically accessible engine experiments
- Develop a new large-eddy simulation (LES) modeling technique to model the TJI system, as both turbulence and active species from the pre-chamber play a role in TJI combustion
- Demonstrate the controllable cavity TJI system's performance in engine tests

Fiscal Year (FY) 2014 Objectives

- Design and fabricate TJI hardware
- Develop TJI control system
- Initiate experimental testing of fabricated turbulent jet igniter and control system in a rapid compression machine (RCM)
- Develop hybrid LES/filtered mass density function (FMDF) model of the TJI process

FY 2014 Accomplishments

- Designed, fabricated and tested generation 3 TJI system in an RCM
- Developed TJI control system for a RCM and preliminary model-based closed-loop combustion control system based on a 2.0-L 4-cylinder engine with TJI
- Demonstrated lean limit extension capability of TJI in the RCM
- Conducted LES/FMDF modeling of propane in a closed chamber and preliminary LES/FMDF simulations of TJI in a coupled prechamber RCM

Future Directions

- Conduct further testing, including imaging, of the TJI process in the MSU RCM with different nozzle geometries
- Develop a new RCM setup that combines visible light and chemiluminescence imaging
- Develop the model-based closed-loop combustion system for TJI engine experiments
- Design and fabricate TJI system for MSU optical engine testing
- Conduct preliminary optical engine testing of TJI system
- Conduct LES/FMDF modeling of a series of TJI configurations to study the effects of various flow/flame parameters

✧ ✧ ✧ ✧ ✧

INTRODUCTION

TJI is an advanced pre-chamber-initiated combustion system that enables very fast burn rates due to the ignition system producing multiple, distributed ignition sites, that consume the main charge rapidly and with minimal combustion variability. The fast burn rates allow for increased levels of dilution (lean burn and/or exhaust gas recirculation) when compared to conventional spark-ignition combustion. The TJI process permits a wide range of lean operating conditions and the distributed ignition sites enable small flame travel distances rapid burn rates. The purpose of this research project is to conduct a thorough study of the TJI process. To fulfill this purpose, a novel TJI system with variable pressure control of the pre-chamber will be studied numerically and experimentally in MSU's RCM, and MSU's optical and metal engines. The major goals of the project are 1) to experimentally examine the active radicals generated in the TJI process through both RCM and optically accessible engine experiments, 2) to develop a new LES modeling technique to model the TJI system, as both turbulence and active species from the pre-chamber play a role in TJI combustion, and 3) to experimentally examine the controllable cavity TJI system's performance and efficiency in metal engine tests.

The main project tasks that were supported during FY 2014 include:

- **Task 1:** Design, fabrication and preliminary testing of the RCM TJI system and development of a control system for pressure and mixture control of the pre-chamber
- **Task 2:** LES/FMDF modeling of propane TJI in closed chambers and preliminary simulations of TJI in coupled pre-chamber-RCM

APPROACH

The aim of this project is to gain a better understanding of the contributions of thermal, turbulence, and active radical influences on ignition enhancement through both experimental testing and modeling of the TJI process. The approaches taken to address this aim with each of the two aforementioned tasks is described in the following.

Task 1: In this project the TJI method is used to achieve overall very lean combustion control by providing properly timed, distributed ignition sites in the main combustion chamber via turbulent mixing. Advances in microelectronics and control systems during the past decade make it possible to reconsider TJI systems, which have the potential to operate at low to high engine rotational speeds. The unique features of the system designed and fabricated for this project include the ability to maintain the pressure in the pre-chamber at nearly that of the main combustion chamber during the compression stroke thereby inhibiting residual main-chamber gases from entering the TJI assembly. Secondly, independent control of the stoichiometry of the pre-chamber for each cycle is possible, depending on engine operating conditions, important for operating over a range of power outputs

Task 2: The high fidelity computational model used in this project was developed by the computational team at MSU and is based on the hybrid LES/FMDF methodology [1]. The LES/FMDF is used for TJI and flows/combustion in three configurations: (1) three-dimensional planar jet, (2) round hot product jet injected into a closed square chamber, and (3) a pre-chamber coupled with an RCM.

RESULTS

Our progress during FY 2014 on the hardware development, experimental testing and LES modeling is described in each of the following tasks.

Task 1

TJI Design and Testing: A TJI system was designed and fabricated and preliminary testing was commenced in the RCM during FY 2014. A schematic of the TJI system implemented in the RCM is shown in Figure 1. A high-speed color camera coupled with an objective lens was used to image the TJI process in the RCM. Preliminary visualization results comparing TJI combustion with no nozzle installed (similar to spark ignition), a non-fueled prechamber case, and a fueled pre-chamber TJI case are shown in Figure 2 (λ=1.75). The figure clearly shows the increased rate of combustion initiation and propagation with the fueled TJI system. In addition, RCM pressure traces showing the lean limit extension provided by the fueled pre-chamber TJI system are shown in Figure 3. During FY 2014, a second TJI system was designed for use in the MSU optical engine, with fabrication and preliminary testing expected in FY 2015.

TJI Control: The jet-ignition combustion process needs to be accurately controlled to ensure high thermal efficiency with low oxides of nitrogen emissions. For model-based closed-loop combustion control, a precise control-oriented combustion model is a necessity. A crank-resolved one-zone combustion model was developed to simulate the gas exchange and combustion processes in the pre-combustion chamber. The main-combustion chamber was modeled by an existing control-oriented two-zone charge mixing and combustion model [2,3]. The jet-ignition engine model is based on a 2.0-L 4-cylinder engine equipped with one turbulent jet igniter per cylinder. The simulation of the jet-ignition system is performed with a hardware-in-the-loop simulation environment incorporating a dSPACE-based real-time engine simulator that interacts with a host computer, which is used for displaying the simulation results and setting the simulation parameters. The RCM TJI experimental data were used to validate the developed model. The simulation results of the developed jet-ignition model are compared with the RCM data at three different air-to-fuel ratios. Figure 4 shows the simulation and RCM results when λ=1.25. Since the pressure in the pre-chamber was not measured in the preliminary

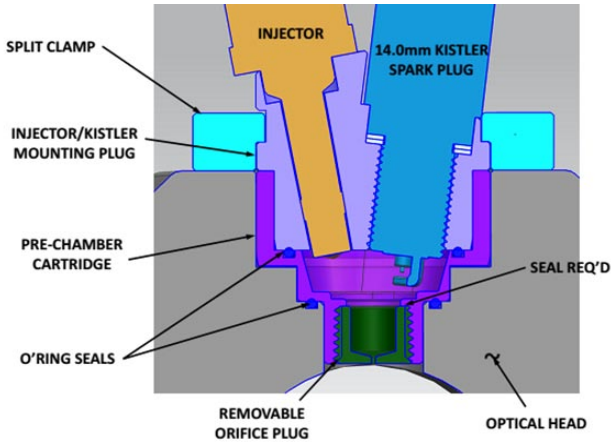

FIGURE 1. Schematic of TJI System Installed in an RCM Cylinder Head

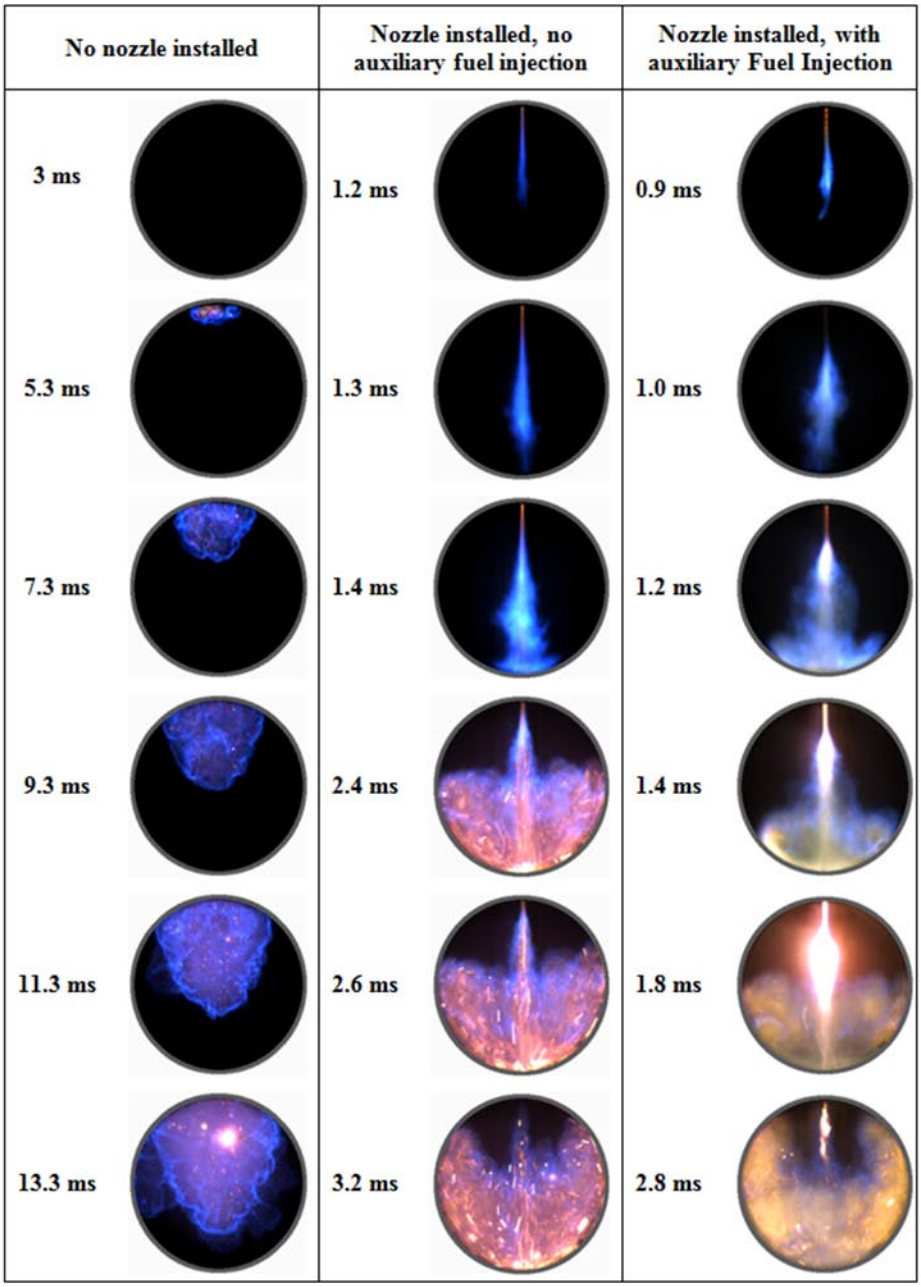

FIGURE 2. Combustion Visualization at λ=1.75 of RCM Combustion with No Nozzle Installed in the TJI System (left), Nozzle Installed with No Pre-Chamber Fuel Injection (center), and the Nozzle Installed with Pre-Chamber Fuel Injection (right)

experiments, the pre-chamber pressure simulation results were not compared. However, we believe that the model provides a reasonable pre-chamber pressure that is similar to the GT-POWER simulation result provided in Ref. [4]. For the main-combustion chamber pressure, the simulation result matches the RCM experiment data very well under all conditions with different air-to-fuel ratios.

Task 2

LES/FMDF modeling of the TJI system was completed for three configurations including (1) three-dimensional planar jet, (2) round hot product jet injected into a closed square chamber, and (3) a pre-chamber coupled with a RCM. Figure 5 shows the temperature contours in one of the simulations recently conducted for configuration 3. The results in this figure (and those not

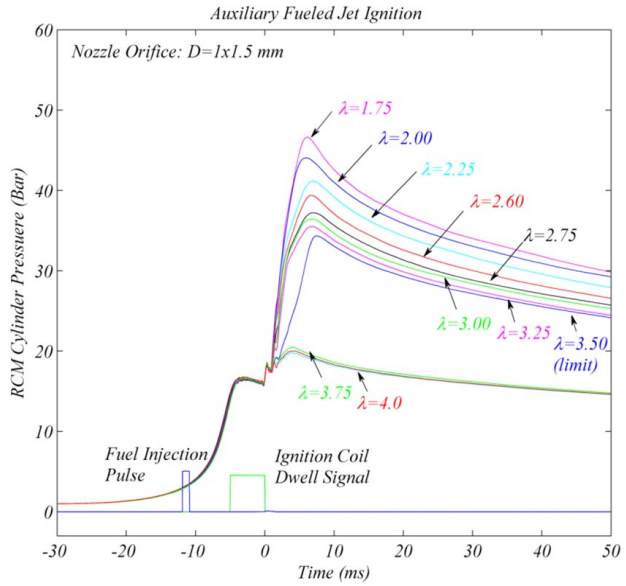

FIGURE 3. RCM Pressure Traces Showing Lean Limit Extension Provided by the Fueled TJI System

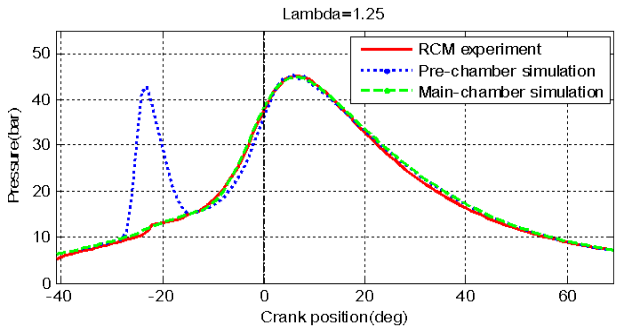

FIGURE 4. Comparison of Simulation and Experimental RCM Results at λ=1.25

shown here) indicate that the LES/FMDF methodology is a robust methodology for complex turbulent combustion problems and can be used for TJI in various configurations and conditions. For hydrogen, a fast detailed explicit chemical kinetics mechanism is used. For propane, only a global mechanism has been used thus far. To be able to conduct the above simulations, the following steps have been taken in FY 2014 (1) the LES/FMDF model has been extended and used for propane combustion in closed chambers, (2) LES/FMDF of TJI of propane in a closed rectangular chamber was conducted, (3) finite difference and Monte Carlo solvers of LES/FMDF have been modified for simulations of flows in a relatively complex geometry involving a prechamber combustor, a nozzle and an RCM main-combustion chamber, and (4) preliminary simulations of TJI in a coupled pre-chamber-RCM were conducted via LES/FMDF.

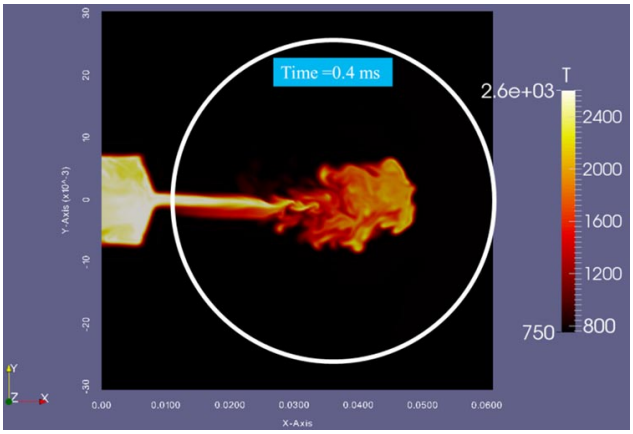

FIGURE 5. Contours of Temperature in a Three-Dimensional Pre-Chamber-RCM Configuration

CONCLUSIONS

During FY 2014 a TJI system was designed and preliminary testing was completed in the MSU RCM, which showed the potential for lean limit extension with the TJI system. In addition, a model-based closed-loop combustion control system based on a 2.0-L 4-cylinder engine with TJI was developed. LES/FMDF modeling of propane in a closed chamber was also completed and preliminary LES/FMDF simulations of TJI in a coupled pre-chamber RCM were commenced.

REFERENCES

1. A. Banaeizadeh, A. Afshari, H. Schock, F. Jaberi, Int. J. of Heat and Mass Transfer, 60 (2013) 781-796.

2. S. Zhang, G. Zhu and Z. Sun, "A Control-Oriented Charge Mixing and Two-Zone HCCI Combustion Model," *Vehicular Technology, IEEE Transactions on* , vol.63, no.3, pp.1079,1090, March 2014.

3. X. Yang, and G. Zhu, "A control-oriented hybrid combustion model of a homogeneous charge compression ignition capable spark ignition engine," *Proceedings of the Institution of Mechanical Engineers, Part D: Journal of Automobile Engineering* 226.10 (2012): 1380-1395.

4. O. Vítek, J. Macek, and M. Polášek, "Simulation of Pre-Chambers in an Engine Combustion Chamber Using Available Software," *SAE Technical Paper* 2003-01-0373, 2003.

FY 2014 PUBLICATIONS/PRESENTATIONS

1. H. Schock, E. Toulson, F. Jaberi, G. Zhu, G. Brereton, I. Wichman, AEC Program Review Meeting, February 2014.

2. H. Schock, E. Toulson, F. Jaberi, G. Zhu, G. Brereton, I. Wichman, AEC Program Review Meeting, August 2014.

II.27 A Universal Combustion Model to Predict Premixed and Non-Premixed Turbulent Flames in Compression Ignition Engines

Tianfeng Lu (Primary Contact), Zhuyin Ren
University of Connecticut (UConn)
191 Auditorium Rd., U-3139
Storrs, CT 06269-3139

DOE Technology Development Manager
Leo Breton

Subcontractors
- Sibendu Som, Argonne National Laboratory, Argonne, IL
- Jacqueline H. Chen, Sandia National Laboratories, Livermore, CA

Overall Objectives

The primary objective of the proposed research is to develop a predictive turbulent combustion model that is universally applicable to mixed regimes of combustion including elements of both premixed and non-premixed flames in the presence of local limit phenomena such as extinction and auto-ignition.

Fiscal Year (FY) 2014 Objectives

Objectives for FY 2014 include:

- Update the reduced mechanism for n-heptane to reflect the recent changes in C1-C4 chemistry in the detailed Lawrence Livermore National Laboratory (LLNL) mechanism
- Perform chemical explosive mode analysis (CEMA) on Sandia's direct numerical simulation (DNS) datasets to extract critical flame features and prepare for the turbulent combustion model creation
- Development of the scalar dissipation rate model based on Sandia's three-dimensional (3-D) DNS datasets
- Implementation of the reduced mechanisms to the large-eddy simulation (LES) and Reynolds-averaged Navier-Stokes (RANS) codes for engine simulations

FY 2014 Accomplishments

During the reporting period, progress has been made in the following areas:

- Developed and validated reduced mechanisms for gasoline and diesel surrogates
- Implemented the reduced mechanisms into Argonne's LES and RANS codes for engine simulations
- Performed CEMA-based computational diagnostics of Sandia's DNS datasets to extract critical flame features
- Performed DNS-based scalar dissipation rate modeling for a premixed hydrogen flame

Future Directions

Future directions of the research include:

- Turbulent combustion model development based on the CEMA results from Sandia's DNS data
- Generation of new DNS data of lifted autoignitive jet flames at elevated pressure with multi-stage ignition (dimethyl ether and n-heptane)
- Generation of new DNS data of reactivity controlled compression ignition with gasoline blend of primary reference fuel with reactivity stratification
- Implementation of the turbulent combustion model and the scalar dissipation rate model to LES and RANS codes
- Validation of the turbulent combustion model and the scalar dissipation rate model against Sandia's DNS data
- 3-D LES and RANS for simulations of lifted diesel jet flames for n-heptane and/or dimethyl ether using the new turbulent combustion model and the scalar dissipation rate model
- Comparison of the LES and RANS simulations of engine combustion with experimental data
- LES and model validation of lifted diesel flames against DNS simulations in selected subdomains based on RANS simulations

INTRODUCTION

Predictive simulation of turbulent combustion is of paramount importance to enable computational design and optimization of advanced combustion engines while there is a dearth of regime-independent turbulent combustion models that are required in device-level engine simulations. The primary objective of the

proposed research is to develop a predictive turbulent combustion model that is universally applicable to mixed regimes of combustion including elements of both premixed and non-premixed flames in the presence of local limit phenomena, such as extinction and auto-ignition. LES and RANS of engine combustion with the new combustion model can be used to address many long-standing questions on fuel efficiency, combustion control, and emissions reduction.

APPROACH

The research is a collaborative effort between UConn, Sandia, and Argonne based on DNS with systematically reduced non-stiff chemistry for practical engine fuels at diesel and gasoline engine conditions. The model development will be based on CEMA that can rigorously detect critical flame features, e.g. local ignition, extinction, and premixed and non-premixed flamelets, from highly complex turbulent flames, by further utilizing the low-dimensional manifold induced by exhausted fast chemistry and thin spatial structures in turbulent flames. The new model will then be implemented into LES and RANS and validated against DNS results and experimental data at engine conditions.

RESULTS

A 54-species skeletal mechanism was developed for n-dodecane as a diesel fuel surrogate based on the detailed JetSurF mechanism developed at the University of Southern California, which consists of elementary reactions for C1-C4 species and lumped semi-global reactions for low-temperature (low-T) reaction pathways for n-dodecane. The skeletal reduction was performed based on reaction states sampled from auto-ignition and perfectly stirred reactors. The rate parameters of the high-T reactions for C1-C4 species are kept unchanged such that high-T flame behaviors, such as premixed flame speed and flame extinction, can be correctly predicted. The rate parameters of the semi-global low-T reactions involving the negative temperature coefficient behaviors are optimized against the detailed mechanism for n-alkanes by LLNL, over a wide range of parameters: pressure from 1 to 50 bar, initial temperature (T) from 800 K to 1,100 K, and equivalence ratio from 0.3 to 2.0, such that the skeletal mechanism can accurately predict both low-T and high-T ignition relevant to lifted diesel jet flames. The mechanism was further reduced using quasi steady-state approximation. Seventeen species were identified as quasi-steady state species and a 37-species reduced mechanism was eventually obtained. The mechanism was extensively validated against the detailed LLNL mechanism and experimental data. The present reduced mechanism is significantly smaller, and thus more efficient for 3-D flame simulations than our previous reduced mechanisms obtained directly from the detailed LLNL mechanisms, which typically consist of more than 100 species at similar accuracy. Selected validation is shown in Figure 1 for the tuned skeletal mechanism in comparison with the detailed LLNL mechanism.

The skeletal mechanism has been implemented into the CONVERGE engine modeling code used by Argonne for LES and RANS simulations of lifted diesel jet flames. Ignition delays and lifted-off length are calculated using the skeletal mechanism at diesel engine conditions as shown in Figure 2. Good agreement was observed compared with experimental measurement obtained through the Engine Combustion Network. Figure 3 further shows the calculated flame structures using a RANS approach at different ambient temperatures.

In addition, a 28-species non-stiff reduced mechanism was developed for ethanol which is typically used as a gasoline fuel substitute. A sub-mechanism for NO formation was also included. The reduction was based on a detailed mechanism consisting of 145 species and 839 reactions, using the methods of directed relation graph, directed relation graph-aided sensitivity analysis, linearized quasi steady-state approximation, and dynamic stiffness removal. The mechanism was validated for ethanol/air mixtures with equivalence ratio from 0.3 to 1.1, temperature from 700 to 1,600 K and pressure from 1 to 150 atm. The mechanism has been employed at Sandia for 3-D DNS of spark-assisted homogeneous charge compression ignition combustion.

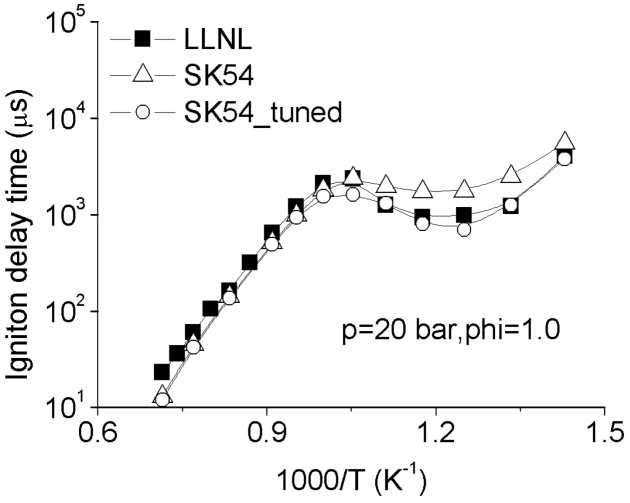

FIGURE 1. Ignition delay time of constant-pressure auto-ignition of stoichiometric n-dodecane/air as a function of the initial temperature, calculated with the detailed LLNL mechanism and 54-species skeletal mechanism, respectively.

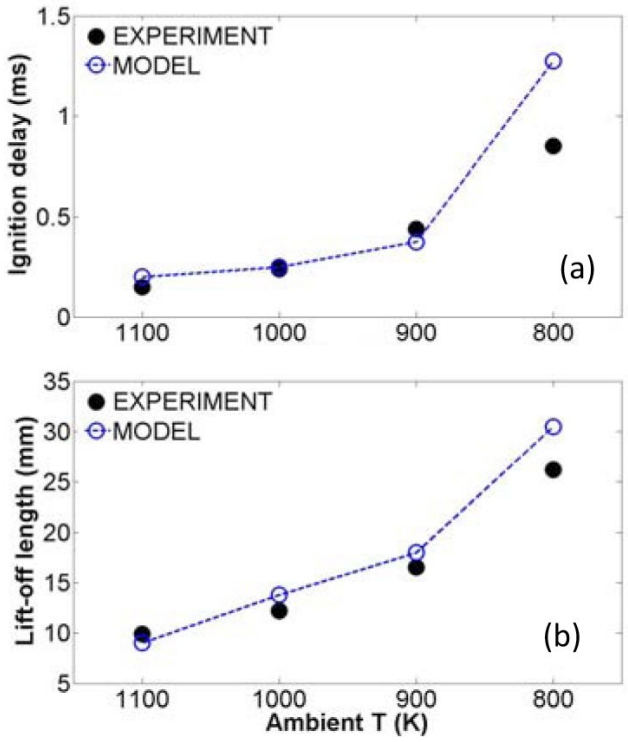

FIGURE 2. (a) Ignition delay, and (b) lift-off length predictions, at different ambient temperatures from 900 K to 1,100 K, for a lifted diesel jet flame calculated with a 54-species skeletal mechanism for n-dodecane, compared with experimental measurement from the Engine Combustion Network.

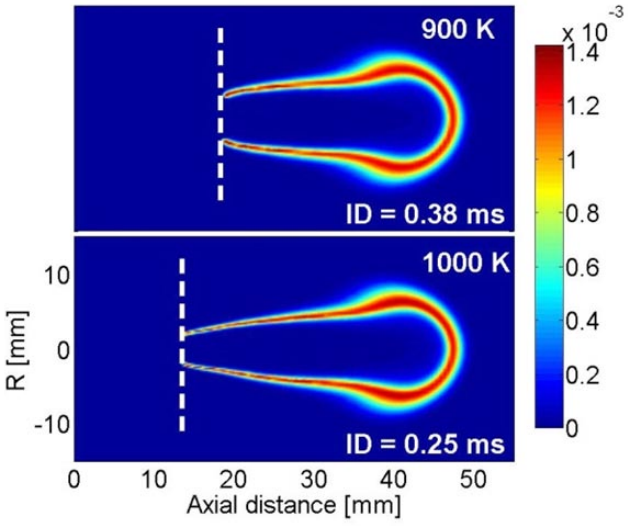

FIGURE 3. Flame shapes indicated by OH mass fraction at 900 K and 1,000 K ambient conditions, respectively, calculated with the 54-species skeletal mechanism. The white line is the lift-off locations and the ignition delays are also shown.

Scalar dissipation rate is a quantity of fundamental importance in turbulent combustion as it appears either

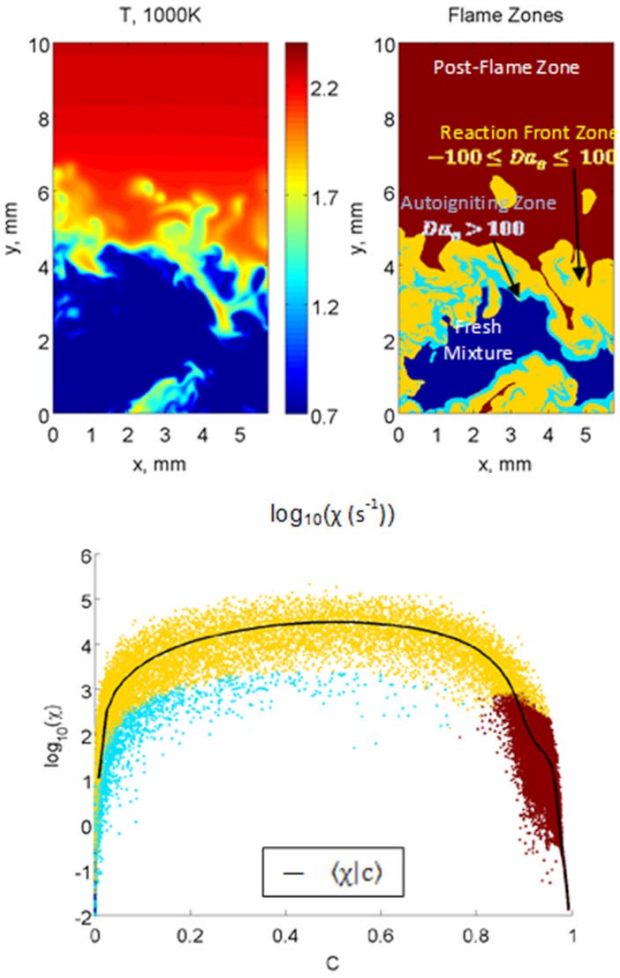

FIGURE 4. Temperature field (top-left panel), flame zones identified by CEMA (top-right), and zone-dependent scalar dissipation rate scattering (bottom) for a turbulent premixed hydrogen/air flame simulated by DNS.

directly or indirectly in most modeling approaches. To model scalar dissipation rate at complex flow conditions, CEMA was used to determine the degree of scatter in the instantaneous scalar dissipation rate in a turbulent premixed flame of lean hydrogen/air simulated with DNS using Sandia's S3D code and a detailed chemical kinetic model. The flame is in a temporally evolving slot jet flame configuration at different Damköhler numbers and fixed Reynolds number. CEMA was applied to 3-D chunks of the DNS data to systematically divide the flow field to different zones, where chemistry and transport play vastly different roles. In Figure 4, the scatter plot in the lower panel shows the instantaneous scalar dissipation rate in different flame zones, with the same color scheme as that used in the top-right panel. The overlaid black line represents the global conditional mean of scalar dissipation rate, which is calculated based on all of the points in the DNS data chunk. The CEMA results demonstrate that the scalar dissipation rate in the reaction front zone spans an order of magnitude above or below

the global conditional mean. The scalar dissipation rate in the auto-ignition zone, however, is an order of magnitude or more lower than the global conditional mean. Zone-dependent modeling of the scalar dissipation rate is therefore needed and performed to improve the modeling accuracy.

CONCLUSIONS

- Reduced mechanisms for engine fuels were developed and validated
- The reduced mechanisms were implemented to Argonne's LES and RANS codes and used for diesel engine simulations
- Sandia's DNS data was systematically diagnosed with CEMA, and the results show significantly different behaviors of scalar dissipation rate in different flame zones, which are considered in the modeling work

FY 2014 PUBLICATIONS/PRESENTATIONS

1. Zhang H., Hawkes E.R., Kook S., Luo Z., Lu T.F., "Computational investigations of the effects of thermal stratification in an ethanol-fuelled HCCI engine," *Fuel*, submitted.

2. Zhou L., Lu Z., Ren Z., Lu T.F., Luo K.H., "Numerical analysis of ignition and flame stabilization in an n-heptane spray flame," *Int. J. Heat Mass Transfer*, submitted.

3. Payri, R., Viera, J.P., Pei, Y. and Som, S., "Experimental and numerical study of lift-off length and ignition delay of a two-component diesel surrogate," *Fuel*, 2014, submitted.

4. Pei Y., Mehl M., Liu W., Lu T.F., Som S., "A multi-component blend as a diesel fuel surrogate for compression ignition engine applications," *Proceedings of the ASME 2014 Internal Combustion Engine Division Fall Technical Conference*, ICEF2014, October 19–22, 2014, Columbus, IN, USA, accepted.

5. Kuron M., Ren Z., Chen J.H., Lu T., "A Study of Conditional Scalar Dissipation Rate In A Premixed Hydrogen Flame Using Chemical Explosive Mode Analysis," poster presentation at *the 35th International Symposium on Combustion*, San Francisco, California, August 3–8, 2014.

II.28 Thermal Barrier Coatings for the LTC Engine – Heat Loss, Combustion, Thermal vs. Catalytic Effect, Emissions and Exhaust Heat

Zoran Filipi (Primary Contact), Mark Hoffman, Robert Prucka, Eric Jordan (University of Connecticut), Nick Killingsworth (Lawrence Livermore National Laboratory)

Clemson University
Department of Automotive Engineering
4 Research Drive
Greenville, SC 29607

DOE Technology Development Manager
Leo Breton

Subcontractors
- University of Connecticut, Storrs, CT
- Lawrence Livermore National Laboratory (LLNL), Livermore, CA

Overall Objectives

- Elucidate the impact of thermal barrier coatings (TBCs) on low-temperature combustion (LTC) efficiency, operating range and emissions
- Develop ceramic and metallic piston coatings that increase thermal and combustion efficiency without decreasing volumetric efficiency
- Develop simulation tools to predict temperature gradients and coating surface temperature swings; extrapolate experimental results and quantify the benefits of the preferred TBC over a range of operating conditions expected in a practical engine

Fiscal Year (FY) 2014 Objectives

- Set up a single-cylinder research engine, including fast response thermocouples and custom telemetry systems which enable crank angle resolved temperature measurements on the piston surface and cylinder head
- Modify the ex situ radiation chamber to provide a controlled environment for TBC thermal property characterization
- Develop effective solution precursor plasma spray (SPPS) method and parameters for applying TBC to the surface of the aluminum piston; carry out initial work with yttria-stabilized zirconia (YSZ)
- Develop the three-dimensional (3-D) finite element analysis (FEA) code for predicting TBC temperature swings on the surface and temperature gradients in the coating

FY 2014 Accomplishments

- Engine test cell was constructed: enclosure, bedplate, air handling, infrastructure modifications, dynamometer, drive, data acquisition and subsystems have been installed and commissioned
- Instrumentation allowing simultaneous crank angle resolved measurement of eight fast response temperature and heat flux probes on the piston has been fabricated and assembled
- Temperature limits of the piston aluminum alloy were determined through the investigation of surface hardness variations with temperature; SPPS process parameters were adjusted based on findings
- Successful use of SPPS to spray YSZ on aluminum piston material
- Process parameters developed for spraying both a dense YSZ coating and a coating with inter-pass boundaries reducing the thermal conductivity by a factor of two (0.62 W/mK)
- ANSYS was used to create an FEA model of a TBC-coated piston and determine the flow of heat through the barrier coating layers and the metal piston

Future Directions

- Powder spray and experimentally test a piston with YSZ coating, characterizing combustion and cycle efficiency over a range of loads and speeds
- Experimentally test an SPPS low-conductivity YSZ piston with inter pass boundaries; characterize the impacts on LTC combustion and efficiency
- Utilize radiation chamber to characterize thermal properties of coatings
- Predict LTC engine performance and efficiency improvements with a one-dimensional code co-simulating with a 3-D thermal model
- Engine experiments measuring temperatures and heat fluxes at multiple locations on the piston for validation of the 3-D finite element code
- Utilize the 3-D thermal analysis model to investigate temperature gradients and the instantaneous piston surface temperature profiles with a dense and low-conductivity YSZ coating

INTRODUCTION

This research focuses on the impact of TBC on LTC engines, and the design of engineered coatings that will produce the most desirable effects on combustion, efficiency, and emissions. The project is designed to increase the fundamental understanding of the mechanisms responsible for the effects of coatings on LTC, making coating design less empirical. To achieve these goals, this multi-disciplinary team brings together expertise in: (a) LTC engine combustion, heat transfer, emissions, (b) ceramic and metallic coatings, and (c) modeling of heat transfer and thermal stresses in thin coatings.

APPROACH

The investigation uses TBC to achieve the desired swing of instantaneous piston surface temperature and reduce heat losses during combustion while minimally impacting the rest of the cycle, Figure 1. Increasing the surface temperature swing during combustion will reduce the temperature difference between the charge and the wall and reduce heat loss, improving LTC thermal efficiency. This is fundamentally different from "adiabatic engines", which implied complete insulation and elevation of the overall surface temperature level, creating adverse effects on the volumetric efficiency and control of combustion.

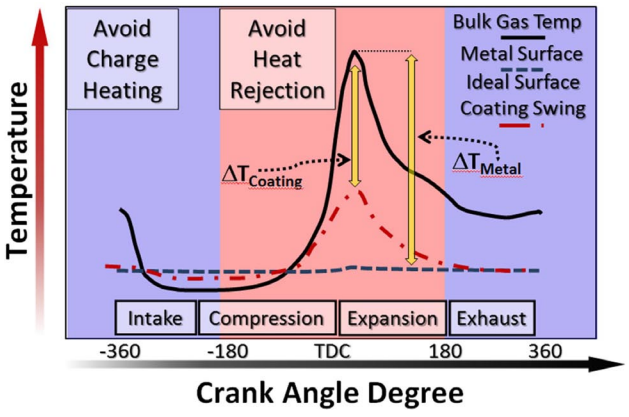

FIGURE 1. Conceptual illustration of the thermal effect achieved with the low thermal-capacity coating on the piston surface. Temperature swing on the surface of a coating illustrated with a red line reduces the temperature difference between the bulk gas and the wall during combustion, thus improving thermal and combustion efficiency of an LTC engine. Temperature returns to normal levels by the next intake event, thus avoiding adverse effects on volumetric efficiency and combustion control

Engine experimentation will correlate coating properties with their impacts on LTC burn rates, resulting in increased fundamental understanding of the mechanisms responsible for the effects of coatings on LTC and making coating design less empirical. Additionally, piston coating methods will be developed which allow for the rapid screening of materials, and systematic manipulation of material formulation, thermal properties, porosity and roughness.

Experiments will also validate a detailed physics-based model capable of predicting multi-dimensional temperature gradients in the coating, and the instantaneous temperature swing in the surface during combustion. The 3-D finite element heat transfer code will be coupled to a GT-POWER one-dimensional engine system simulation and predict the piston heat transfer rate over the expected operational map. This tool can then expand the coating design space, and quantify the benefits of a preferred coating over the speed load range of LTC engines.

RESULTS

Experimental Instrumentation Advancements

A single-cylinder engine and dynamometer were set up. Building infrastructure modifications were completed to allow full test cell functionality. Installation of the data acquisition system and commissioning of the relevant sensors on the engine, dynamometer, and subsystems has been completed, Figure 2.

Specialized instrumentation was prepared which enables fast response probes to measure crank angle resolved temperature and heat fluxes on the cylinder head and piston. The telemetry linkages manage the motion and stress of piston probe signal wires. To eliminate repeated bending stress and increase the life of the wires,

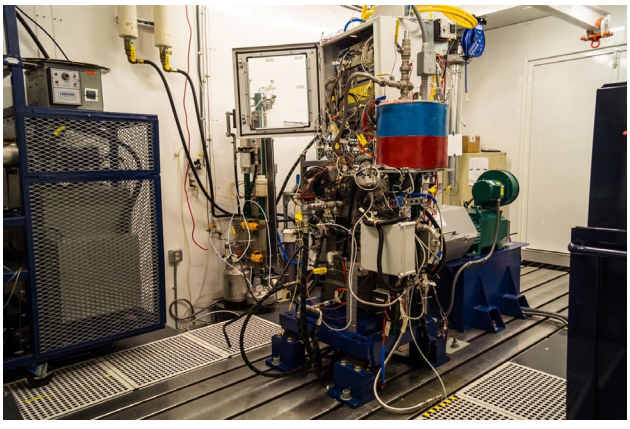

FIGURE 2. LTC Testing Facility

the telemetry systems have been designed to put wires in twisting rather than bending.

Detailed characterization of TBC thermo-physical properties is essential to accurately model/calculate heat transfer in these materials. A purpose-built radiation chamber is utilized to conduct ex situ conductivity and diffusivity testing. The device provides a non-reactive environment for temperature and heat flux measurements with the ability to produce constant or periodic heat flux boundary conditions. Due to the partial transparency of TBC to radiation sources, the angle of incidence between the infrared probe and the sample surface must be known during conductivity determination. Additional instrumentation has been designed and fabricated to enable such control, Figure 3.

A finite element representation of the TBC was constructed and used within a sequential function specification method (SFSM) to calculate TBC surface temperature and heat flux profiles utilizing experimental temperature and heat flux measurements from beneath the TBC. Surface temperature results from the SFSM code were validated by direct comparison to Fourier reconstruction heat flux calculation methodologies from [1-3], Figure 4. The ex situ radiation chamber provided a known heat flux to the surface of both uncoated and TBC-treated probes, enabling the comparison of SFSM and direct numerical techniques.

TBC Development

TBCs in this project are made by both air plasma spray and the unique SPPS process. Aluminum disks (alloy 2018) have been sprayed with an air plasma spray YSZ coating and an SPPS coating containing inter-pass boundaries, as shown in Figure 5. The inter-pass boundaries allow thermal conductivity to be independently lowered by a factor of two, minimizing coating thermal inertia and cost by realizing the same thermal protection with half the material thickness.

Hardness measurements were taken in a stand-alone experiment to determine appropriate coating process conditions such that the aluminum mechanical properties were not degraded. A representative piston was also coated, demonstrating that realistic combustion chamber geometries can be accommodated.

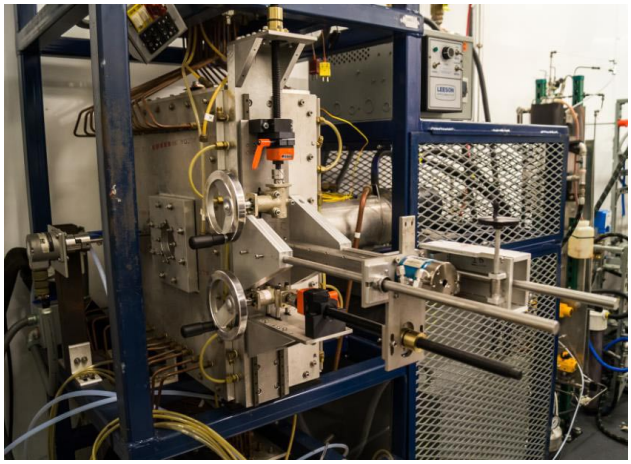

FIGURE 3. Radiation chamber instrumentation developed to enable the non-destructive determination of conductivity for insulative coatings, accounting for the impact of radiation transparency.

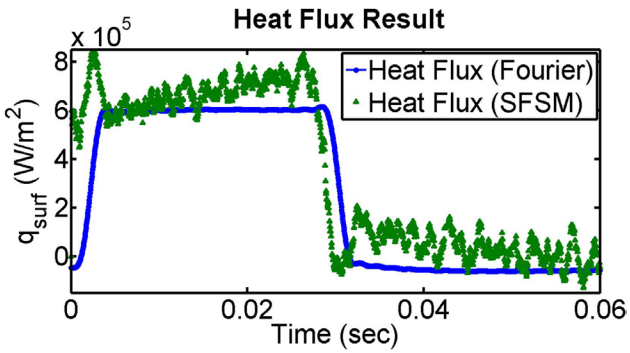

FIGURE 4. Reconstruction of surface heat flux profile using sub-surface temperature trace. 'Temperature Result' again shows convergence of modeled and observed temperature profiles. 'Heat Flux Result' shows reasonable convergence of analytic (Fourier) and estimation (SFSM) routines for sub-surface temperature data. More accurate measurement of material properties (thickness, conductivity, diffusivity, etc.) will further minimized error within the estimation routine.

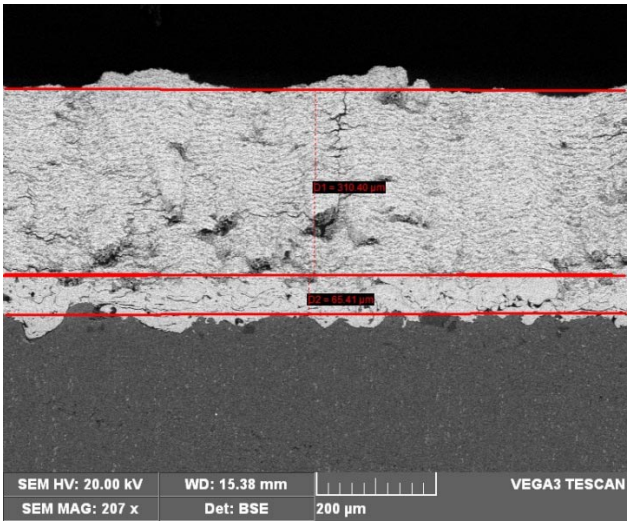

FIGURE 5. An SPPS coating with conductivity lowering inter pass boundaries on a 2018 aluminum disk. Having succeeded to create the desired coatings on aluminum disks, we then have coated a piston crown from a General Motors 4-cylinder engine that has a more complex bowl shape than the Clemson test engine piston. Figure 3 shows that a nice uniform coating is achieved on a realistic piston crown shape.

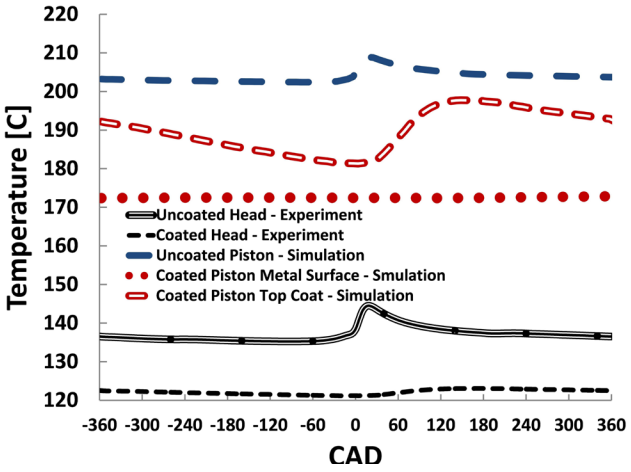

FIGURE 6. Temperature versus crank angle degree (CAD) for experimental coated and uncoated heat flux probe in head of engine and for simulations of coated and uncoated piston. For simulations, temperature given at both top surface of top coat and at metal.

Heat Transfer Simulation

An FEA model of the experimental piston (Al-Si eutectic aluminum alloy) coated with a 50-µm NiCrAl stress-relief layer and a 150-µm $MgZrO_3$ TBC has been developed in ANSYS. Heat flux data obtained from cylinder head probes during HCCI operation [1,2] were used as the boundary condition of the piston crown surface within the model.

Temperature histories from the cylinder head heat flux probes of the experimental engine are shown in Figure 6. The uncoated probe is in direct contact with the hot in-cylinder gases while the coated probe has a TBC separating it from the hot gas, accounting for the decreased temperature of the coated probe. The simulated piston temperature predictions have similar trends to that of the experimental data, but at a higher temperature due to less effective cooling of the piston compared to the head. The coated piston stays at a relatively constant temperature whereas the TBC surface undergoes a 20°C temperature swing. These simulations serve as a useful tool to better understand the experimental data and to quickly explore new thermal barrier coating materials and thicknesses.

CONCLUSIONS

Significant strides have been made toward the overall project goals, and progress continues on schedule. A summary of FY 2014 is as follows:

- The single-cylinder LTC experimental facility has been constructed and commissioned; collection of baseline HCCI combustion data is in progress
- Telemetry systems enabling crank angle resolved heat transfer have been fabricated
- Capability of the radiation chamber has been expanded, facilitating the non-destructive determination of TBC conductivity and thermal diffusivity
- SFSM has been applied toward prediction of TBC surface temperatures based on sub-insulator temperature and heat flux measurements, establishing a methodology for attainment of simulation boundary conditions
- SPPS technique was successfully modified for application of TBC with inter-pass boundaries on aluminum piston surrogates
- A 3-D FEA model of the piston and TBC was constructed and validation with experimental data has begun

REFERENCES

1. Chang, J., Güralp, O., Filipi, Z., Assanis, D. et al., "New Heat Transfer Correlation for an HCCI Engine Derived from Measurements of Instantaneous Surface Heat Flux," SAE Technical Paper 2004-01-2996, 2004.

2. Güralp, O., Hoffman, M., Assanis, D., Filipi, Z. et al., "Characterizing the Effect of Combustion Chamber Deposits on a Gasoline HCCI Engine," SAE Technical Paper 2006-01-3277, 2006.

3. Hoffman, M., Lawler, B., Filipi, Z., Guralp, O., and Najt, P., "Development of a Device for the Nondestructive Thermal Diffusivity Determination of Combustion Chamber Deposits and Thin Coatings" J. of Heat Transfer 136(7), 071601, March 17, 2014, doi: 10.1115/1.4026908.

FY 2014 PUBLICATIONS/PRESENTATIONS

1. Filipi, Z., "Efficient Small Engines for CHP: Opportunities and Research Needs, from Combustion and Heat Transfer to System Integration," ARPA-E Workshop, Chicago, May, 2014.

2. Filipi, Z., "Thermal Barrier Coatings for the LTC Engine – Heat Loss, Combustion, Thermal vs. Catalytic Effects, Emissions and Exhaust Heat," Stuttgart, July 3, 2014.

3. Filipi, Z., "Thermal Barrier Coatings for the Low Temperature Combustion Engine," presented at the AEC Review Meeting, Sandia National Lab, February 12th, 2014.

4. Filipi, Z and Jordan, E., "Thermal Barrier Coatings for the Low Temperature Combustion Engine – SPPS Technique Applied to Aluminum", presented at the AEC Review Meeting, USCAR, August 21st, 2014.

5. Hoffman, M., Lawler, B., Filipi, Z., Guralp, O., and Najt, P., "Development of a Device for the Nondestructive Thermal Diffusivity Determination of Combustion Chamber Deposits and Thin Coatings" J. of Heat Transfer 136(7), 071601, March 17, 2014, doi: 10.1115/1.4026908.

6. Hoffman, M., Lawler, B., Filipi, Z., Guralp, O., and Najt, P., "The Impact of a Magnesium Zirconate Thermal Barrier Coating on Homogeneous Charge Compression Ignition Operational Variability and the Formation of Combustion Chamber Deposits," Journal of Engine Research, IJER-14-0105, accepted.

II.29 Radiative Heat Transfer and Turbulent Fluctuations in IC Engines – Toward Predictive Models to Enable High Efficiency

Daniel C. Haworth[1] (Primary Contact),
Michael F. Modest[2]
[1]The Pennsylvania State University
240 Research Building East
State College, PA 16802
[2]University of California, Merced
Science & Engineering Building, Room 392
Merced, CA 95343

DOE Technology Development Manager
Leo Breton

Overall Objectives

- Quantify effects of radiative heat transfer and turbulent fluctuations in composition and temperature on combustion, emissions, and heat losses in internal combustion (IC) engines.
- Develop computational fluid dynamics (CFD)-based models to capture these effects in simulations of in-cylinder processes in IC engines.
- Exercise the models to explore advanced combustion concepts for IC engines and to develop next-generation high-efficiency engines.

Fiscal Year (FY) 2014 Objectives

- Extend deterministic radiation models that have been used for earlier modeling studies of radiative heat transfer and turbulence-chemistry-radiation interactions (TCRI) in laboratory turbulent flames to engine-relevant environments and configurations.
- Initiate simulations of radiative heat transfer and TCRI for constant-volume configurations under engine-relevant conditions.
- Initiate simulations of radiative heat transfer and TCRI for simplified engine configurations.

2014 Accomplishments

- Implemented radiative transfer equation solvers in OpenFOAM®, and coupled the radiation calculations with liquid fuel-spray models.
- Mapped out a "radiation state space" to identify engine-relevant conditions where radiative heat transfer and TCRI are expected to be most prominent. These are conditions where the optical thickness of the in-cylinder mixture is neither optically thin nor excessively optically thick at engine-relevant length scales (~1-10 cm), and where radiation can be expected to significantly change the temperature distribution of the in-cylinder mixture on engine-relevant time scales (~10's of ms).
- Quantified radiative emission in a heavy-duty diesel engine by post-processing earlier simulation results.

Future Directions

- Perform fully coupled simulations including radiative heat transfer for constant-volume combustion chambers under engine-relevant conditions, and for engines operating in conventional and advanced compression-ignition combustion modes.
- Quantify radiation and TCRI effects for conventional and advanced compression-ignition combustion modes in engines.
- Exercise the models to explore advanced combustion concepts for IC engines and to develop next-generation high-efficiency engines.

INTRODUCTION

It is increasingly recognized that radiative heat transfer plays an important role in virtually all practical combustion systems, and may in fact dominate heat-transfer rates in many applications. While radiation in IC engines has received relatively little attention up until now, advanced high-efficiency engines are expected to function close to the limits of stable operation, where even small perturbations to the energy balance can have a large influence on system behavior. The premise of this research is that radiative heat transfer and complex TCRI may be particularly important in the "non-robust" combustion environments that will characterize advanced high-efficiency IC engines. These effects warrant thorough investigation under engine-relevant conditions, and predictive models that account for them will be required to realize the ambitious efficiency targets that have been established for next-generation engines and vehicles.

APPROACH

CFD tools for radiative heat transfer and TCRI are being developed using the open-source CFD toolkit, OpenFOAM®. The research is organized into four tasks: 1) extend multiphase radiation models to engine-relevant conditions; 2) explore radiation and turbulence-chemistry-radiation interactions in engine-relevant environments; 3) perform quantitative comparisons with experiment for constant-volume combustion chambers; and 4) perform quantitative comparisons with experiment for compression-ignition engines. Through collaboration with the Combustion Research Facility at Sandia National Laboratories (Joseph C. Oefelein), the models and tools also will be implemented in a high-fidelity large-eddy simulation code. Ongoing active participation in the Engine Combustion Network provides access to experimental data for high-pressure, constant-volume turbulent spray combustion under engine-relevant conditions. And through collaboration with Volvo (Samuel L. McLaughlin), engine data for model validation are available for heavy-duty compression-ignition engines operating in conventional diesel combustion modes and in advanced combustion modes.

RESULTS

A radiation "phase space" has been mapped out to identify engine-relevant thermochemical conditions (mass fractions of radiatively participating gas-phase species—mainly CO_2 and H_2O, soot volume fraction, temperature and pressure) where radiation effects are expected to be prominent. These are conditions of intermediate optical thickness (neither optically thin nor excessively optically thick) over engine-relevant length scales (~1-10 cm), and where radiative transfer can be expected to change the in-cylinder temperature distribution appreciably over engine-relevant time scales (~10's of ms). It has been found that there are, in fact, conditions in both conventional and advanced compression-ignition engines where radiation and TCRI can be expected to significantly influence heat losses, efficiency, and emissions. Examples are shown in Figures 1 and 2.

Spectral radiation property databases have been extended to higher pressures, several radiative transfer equation solvers that had been developed for earlier simulation studies of laboratory turbulent flames have been implemented in OpenFOAM®, the radiation models have been coupled with the liquid-fuel-spray models in OpenFOAM®, and OpenFOAM®-compatible computational meshes have been generated for simplified constant-volume configurations and engine configurations.

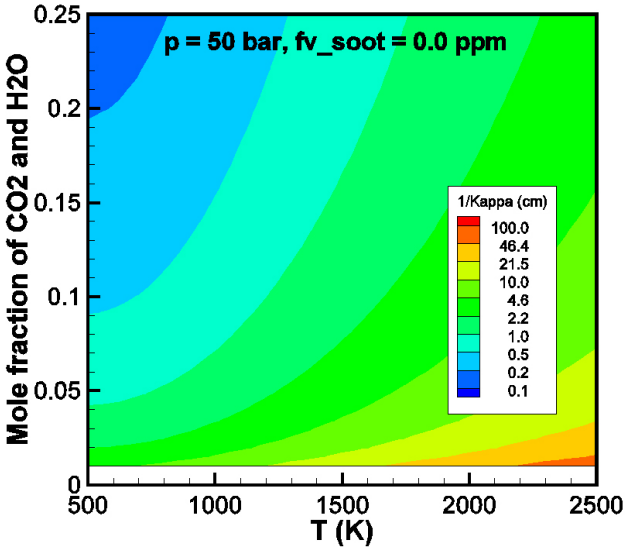

FIGURE 1. Length scale (cm) at which the optical thickness is equal to unity as a function of temperature and mole fraction of CO_2 (= mole fraction of H_2O) for a homogeneous mixture at 50 bar with no soot.

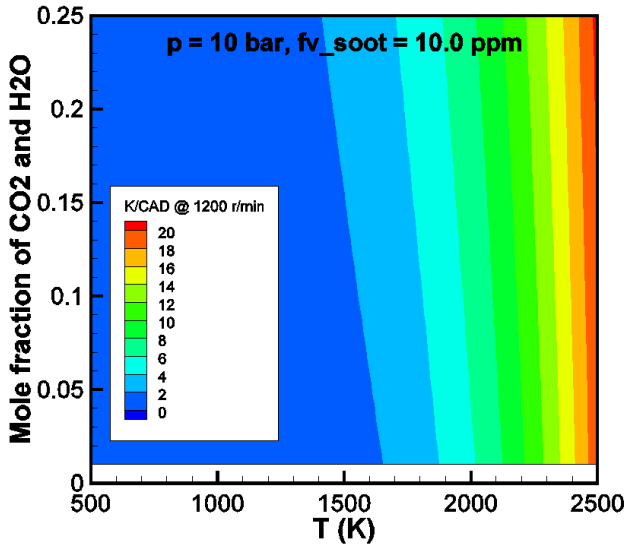

FIGURE 2. Cooling rate due to radiative emission (Kelvin per crank-angle-degree of rotation) at an engine speed of 1,200 r/min as a function of temperature and mole fraction of CO_2 (= mole fraction of H_2O) for a homogeneous mixture at 10 bar with 10 ppm soot.

Earlier CFD simulations of in-cylinder combustion in a conventional heavy-duty diesel engine at four different operating conditions (including soot formation and oxidation [1]) have been post-processed to explore the extent to which radiation effects might be important. It was found that radiative emission corresponds to as high as 40% of the total heat losses (Figure 3), and that for high levels of exhaust gas recirculation, the emission

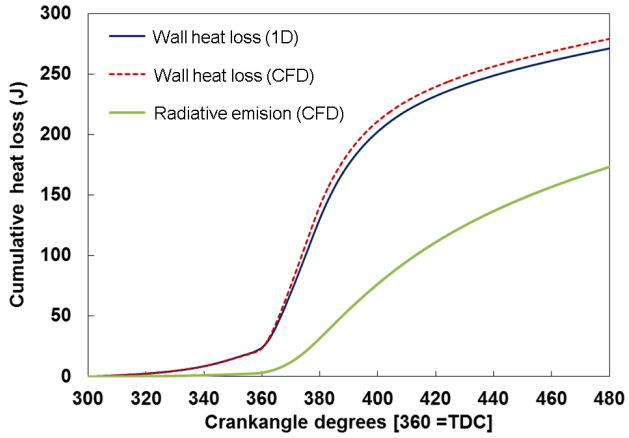

FIGURE 3. CFD-computed cumulative wall heat loss and radiative emission for a heavy-duty diesel engine with exhaust gas recirculation [1]. Computed wall heat loss from a tuned one-dimensional engine model also is shown.

is dominated by gas-phase radiation from CO_2 and H_2O rather than from soot particles.

CONCLUSIONS

There are engine-relevant conditions where radiation and TCRI are expected to be important. For the high-pressure, high- exhaust gas recirculation combustion systems that characterize some advanced high-efficiency engine concepts, gas-phase radiation dominates soot radiation. OpenFOAM®-based tools are in place for in-cylinder CFD simulations, including fully coupled radiative heat transfer.

REFERENCES

1. V. Raj Mohan and D.C. Haworth, Turbulence-chemistry interactions in a heavy-duty compression-ignition engine, Proc. Combust. Inst. 35 (2014). In press.

FY 2014 PUBLICATIONS/PRESENTATIONS

1. S.P. Roy, Aerosol-dynamics-based soot modeling of flames, Ph.D. thesis, The Pennsylvania State University, University Park, PA, 2014.

2. M.F. Modest, J. Cai, W. Ge and E. Lee, Elliptic formulation of the simplified spherical harmonics method in radiative heat transfer, Intern'l. J. Heat Mass Transfer (2014). In press.

3. W. Ge, R. Marquez, M.F. Modest and S.P. Roy, Implementation of high-order spherical harmonics methods for radiative heat transfer in OpenFOAM, J. Heat Transfer (2014). Submitted for publication.

4. W. Ge, M.F. Modest and R. Marquez, Two-dimensional axisymmetric formulation of high-order spherical harmonics methods for radiative heat transfer, J. Quant. Spectrosc. Radiat. Transfer (2014). Submitted for publication.

5. R. Marquez and M.F. Modest, Two-cimensional axisymmetric formulation of higher-order P_N Approximations, 22nd National and 11th International ISHMT–ASME Heat and Mass Transfer Conference 2013, Kharagpur, India 2013. To appear in ASME J. of Heat Transfer.

6. D.C. Haworth, Radiative heat transfer in engine-relevant environments, Advanced Engine Combustion Review Meeting, Livermore, CA (11–13 February 2014).

7. D.C. Haworth, Radiative heat transfer in engine-relevant environments, Advanced Engine Combustion Review Meeting, Southfield, MI (19–21 August 2014).

II.30 Sooting Behavior of Conventional and Renewable Diesel-Fuel Compounds and Mixtures

Lisa Pfefferle (Primary Contact) and
Charles McEnally
Yale University
New Haven, CT 06520

Collaborators
- Charles Mueller, Sandia National Laboratories
- William Canella, Program Manager of Advanced Liquid Transportation Fuels R&D, Chevron Corp.

DOE Technology Development Manager
Leo Breton

Overall Objectives

- Measure quantitative sooting tendencies for a wide range of diesel and biodiesel fuel components
- Develop a mixing rule that can be used to define surrogate fuel mixtures that mimic the sooting behavior of real diesel fuels

Fiscal Year (FY) 2014 Objectives

- Develop a fuel delivery system that can dope diesel fuel and diesel surrogate compounds into the reactant stream of our nonpremixed burner.
- Construct an experimental system capable of making laser-induced incandescence (LII) measurements of soot volume fraction in fuel-doped flames.
- Define a series of diesel surrogate mixtures suitable for determining the sooting tendencies of the individual surrogate components and a mixing rule for combining them.

FY 2014 Accomplishments

- Rebuilt the burner and fuel system and verified with time-resolved measurements that flames could be doped with diesel fuels without condensation.
- Validated the LII quantitative sooting tendencies for several diesel and biodiesel components.
- Prepared 32 diesel surrogate component mixtures that follow an optimized scheme for determining properties of the individual components and measured sooting tendencies.

Future Directions

- Measure soot concentrations in flames doped with the 32 mixtures and analyze them to determine the sooting tendencies of the individual components and identify any synergistic interactions between them.
- Derive a mixing rule from this data that can be used to choose diesel surrogate mixtures that have the same sooting behavior as their target diesel fuels.
- Develop surrogates for reference diesel fuels that match their soot formation characteristics.

INTRODUCTION

The best way for engine manufacturers to optimize the efficiency of their designs while minimizing pollutant emissions is by performing extensive computer simulations before building physical prototypes. Unfortunately, real fuels such as diesel and gasoline are complex mixtures containing hundreds or more of separate chemicals; computer models that can describe the kinetics of such fuels are too computationally expensive to be run in real engine geometries. The most promising solution to this problem is to identify surrogate fuels which are mixtures of only a few hydrocarbons, but which mimic the behavior of real fuels. These surrogate mixtures can then be used as the fuels in computer studies to optimize engine design and achieve the DOE technical targets.

Surrogate diesel fuels have been developed that can reproduce the density, ignition, and volatility characteristics of real diesel fuels. However, another critical fuel-specific aspect of diesel engine performance is emissions of carbonaceous particles known as soot. Soot particles are the second most important source of global warming and they directly harm the health of people in urban areas who breathe them. The goal of this project is to develop surrogate diesel fuels that have similar soot formation characteristics to real diesel fuels.

APPROACH

The main requirements for developing diesel fuel surrogates are to have (1) a laboratory technique for measuring the sooting propensity of a fuel that corresponds to sooting behavior in a real diesel engine, and (2) a procedure for estimating the sooting tendency.

In recent years we have developed a new procedure for measuring sooting tendency which is easier to perform and more accurate than the traditional procedures. It involves adding a small amount of the test substance to the fuel of a methane/air flame and measuring the soot particle concentration in the resulting flame. The basic idea is that if the test substance has a greater propensity to form soot, then the doped flame will contain more soot and we will measure a larger concentration. As part of a collaboration with researchers at Sandia National Laboratories we will compare the results of our procedure with particle emission measurements from actual diesel engines.

RESULTS

The main results for the first year of this project were to set up and validate the equipment for measuring sooting tendencies of diesel fuel and diesel fuel surrogates. These results provide a foundation for high quality measurements during the subsequent years of this project.

The fuel supply system and burner were rebuilt with stronger heating tapes; these allow all of the fuel passages to be heated to high enough temperatures that diesel fuel will rapidly evaporate when injected into them and not subsequently condense. The performance of this system was verified through time resolved measurements of soot concentrations in flames where the fuel was doped with diesel fuel and its components.

An LII system was built to measure soot concentrations in the doped flames. This diagnostic is able to measure soot concentrations without insertion of physical probes into the flame, or sampling particles from the flame. It provides highly accurate, sensitive, rapid measurements. Preliminary measurements in a flame doped with 32 mixtures formulated to span diesel surrogates were used to verify all of these performance attributes.

CONCLUSIONS

Quantitative sooting tendencies for real diesel fuels and diesel surrogate mixtures can be measured in laboratory-scale flames by doping them into the fuel of methane/air flames and measuring the resulting soot concentrations with the technique of laser-induced incandescence. This will provide the basis for developing mixture rules to predict sooting tendencies of mixtures.

FY 2014 PUBLICATIONS/PRESENTATIONS

1. Dhrubajyoti D. Das, Charles S. McEnally, Lisa D. Pfefferle. "Sooting Tendencies of Unsaturated Esters in Nonpremixed Flames." *Combustion and Flame* (submitted).

2. Charles S. McEnally, Dhrubajyoti D. Das, Lisa D. Pfefferle. *Fuel-Doped Flames as Model Systems for Studying Soot Formation from Liquid Fuels*. 2014 International Sooting Flame (ISF) Workshop. Pleasanton, CA; 2-3 August 2014.

II.31 Evaluation of the Fuel Economy Impact of Low-Temperature Combustion (LTC) using Simulation and Engine in the Loop

Neeraj Shidore
Argonne National Laboratory
9700 South Cass Avenue
Argonne, IL 60439

DOE Technology Development Manager
David Anderson

Overall Objectives

- Evaluate the impacts of LTC technology on fuel economy and engine-out emissions using vehicle simulations and engine in the loop (EIL)
- Quantify the fuel economy benefits of LTC on standard drive cycles using EIL
- Evaluate test-to-test variability with LTC compared to diesel
- Assess the transient behavior of LTC
- Compare the fuel economy benefits of LTC technology to port fuel injection (PFI) and spark-ignited direct-injection (SIDI) technologies by using simulations

Fiscal Year 2014 Accomplishments

- Completed EIL setup; demonstrated EIL operation with diesel (baseline) fuel
- Established baseline fuel consumption and engine-out emission numbers with diesel fuel using EIL
- Quantified the fuel economy benefits of LTC for a mild hybrid powertrain, belt-integrated starter-generator (BISG)
- Updated the fuel economy benefits of LTC for a conventional powertrain with improved low-load steady-state brake specific fuel consumption (bsfc) data on LTC from the Argonne Engine Research Group

Future Directions

- Update the fuel economy benefits of LTC for a mild hybrid powertrain with an updated bsfc map
- Quantify fuel consumption and engine-out emissions for LTC technology with EIL when steady combustion at low loads is established

INTRODUCTION

LTC technology research is being conducted by Argonne's Advanced Combustion Engines research group to improve the engine efficiency of light-duty passenger vehicles. One of the goals of the vehicle systems research at DOE is to rapidly evaluate components and systems through model-based design and component in the loop. This project evaluates DOE-developed strategies for LTC of 87 anti-knock index (AKI) gasoline in a systems context by using transient vehicle drive cycles. A 1.9-L turbo direct injection (TDI) engine, with diesel as the default fuel, is used for the LTC study with 87 AKI gasoline.

LTC research performed by the Engine Research Group at Argonne National Laboratory (Argonne) with 87 AKI gasoline has shown lower fuel consumption and oxides of nitrogen (NO_x) emissions as compared to gasoline spark-ignition engines [1] (Figure 1).

This project evaluates the fuel consumption and emissions benefits of LTC over transient cycles at a vehicle system level.

APPROACH

The design of the experiment for the project is shown in Figure 2. The PFI and SIDI engine technologies,

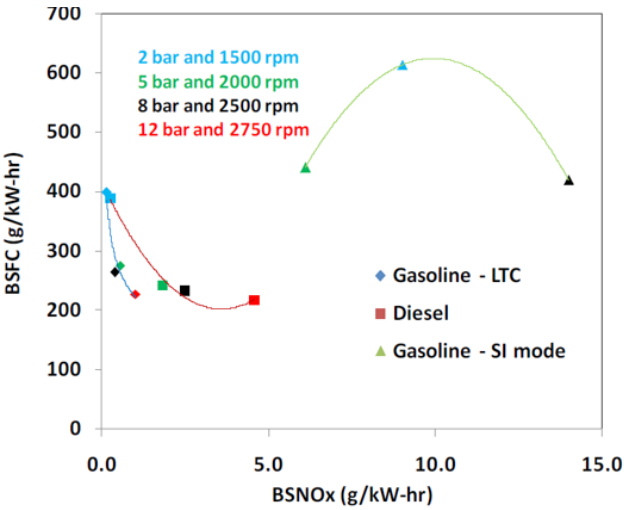

FIGURE 1. BSFC and Engine-Out NO_x for LTC compared to Gasoline Spark-Ignition and Diesel Engines

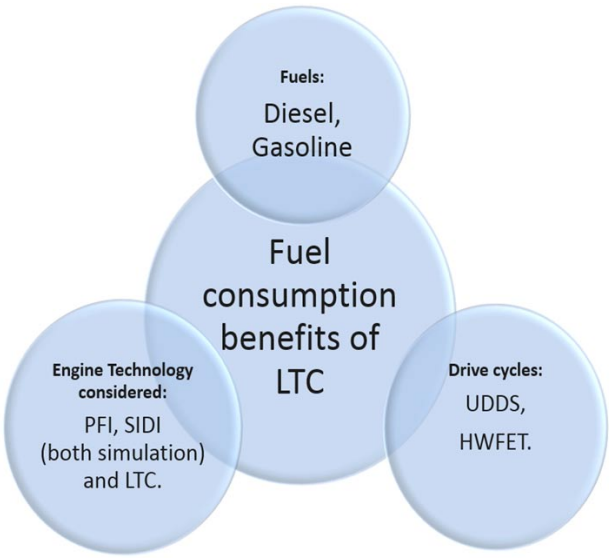

FIGURE 2. Design of Experiment

which act as a baseline to which LTC will be compared, are evaluated via simulation. Fuel consumption and engine-out emissions with LTC of gasoline will be measured from EIL tests. Before the EIL tests with LTC, a simulation study was conducted to compare LTC to SIDI and PFI, and EIL tests were conducted with diesel fuel to validate the system approach to reduce engine-out emissions and improve fuel consumption. For these fuels and combustion technologies, the comparison between fuel consumption and emissions is performed for a midsize sedan (conventional powertrain) over the Urban Dynamometer Drive Cycle (UDDS) and the highway drive cycle (HWFET).

In order to compare the LTC technology to PFI and SIDI in simulation, a fuel rate map of LTC gasoline was generated from measured steady-state points. This was done by creating efficiency lines (willans) proportional to available efficiency curves from the steady-state data [2].

The specifications for the conventional vehicle used for the study are listed in Table 1. The specifications are those of a model year 2007 Cadillac BLS Wagon [3], which has the same diesel engine as the one used at Argonne for the LTC research.

TABLE 1. Vehicle Specifications

Vehicle	Cadillac BLS Wagon
Vehicle Mass	1,560 kg
Engine	1.9-L TDI, 110 kW, 320 Nm peak torque, I-4
Transmission	Manual, 6-speed

For a fair comparison among SIDI, PFI, and LTC technologies, the SIDI and PFI engines were scaled in power in order to meet the vehicle technical specifications of the model year 2007 Cadillac BLS Wagon. Different transmission ratios and final drives were selected for the PFI, SIDI, and LTC engines, on the basis of each engine's peak torque and maximum speed characteristics. The fuel consumption map for the SIDI engine was generated from a 2.2-L ECOTEC SIDI engine. The fuel consumption map for the PFI engine was generated from a 1.8-L Peugeot engine.

Figure 3 shows the powertrain specifications for the conventional and the BISG powertrain with the different engines. It should be noted that the battery and electric

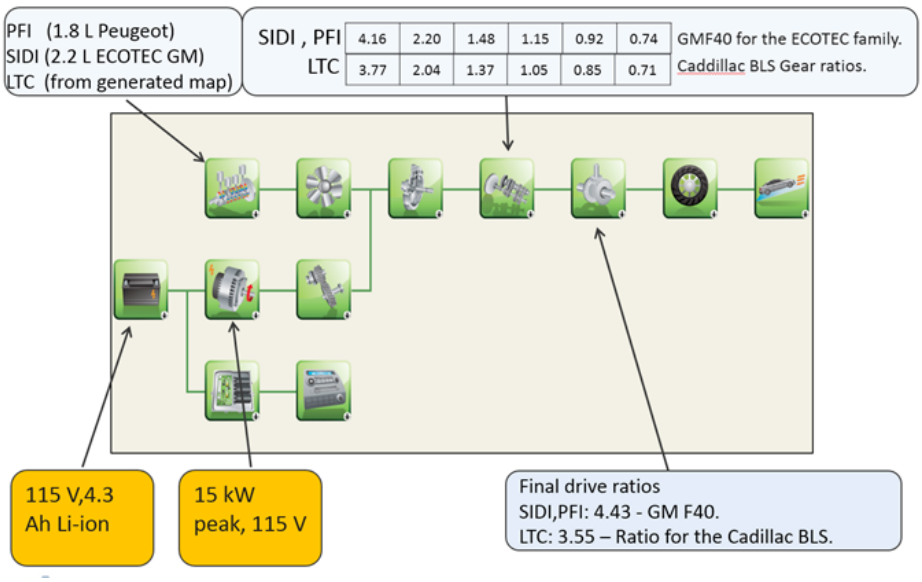

FIGURE 3. Specifications of the Conventional and BISG Powertrains

machine specifications are valid only for the BISG configuration.

Figure 4 shows a conceptual representation of the EIL setup for the GM 1.9-L engine.

In the fourth quarter of FY 2014, the baseline bsfc maps for the LTC mode were updated in accordance with new results at low loads. Figure 5 compares the fuel consumption curves for the previous and updated fuel rates at 2,500 RPM. The fuel rate improvement at low

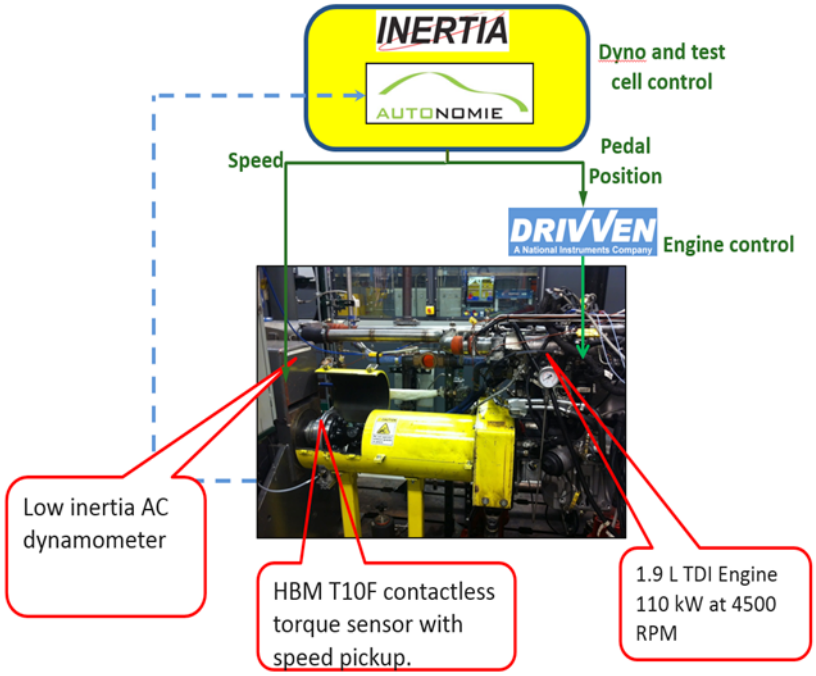

FIGURE 4. EIL Setup with the 1.9-L TDI Engine used for the LTC Tests

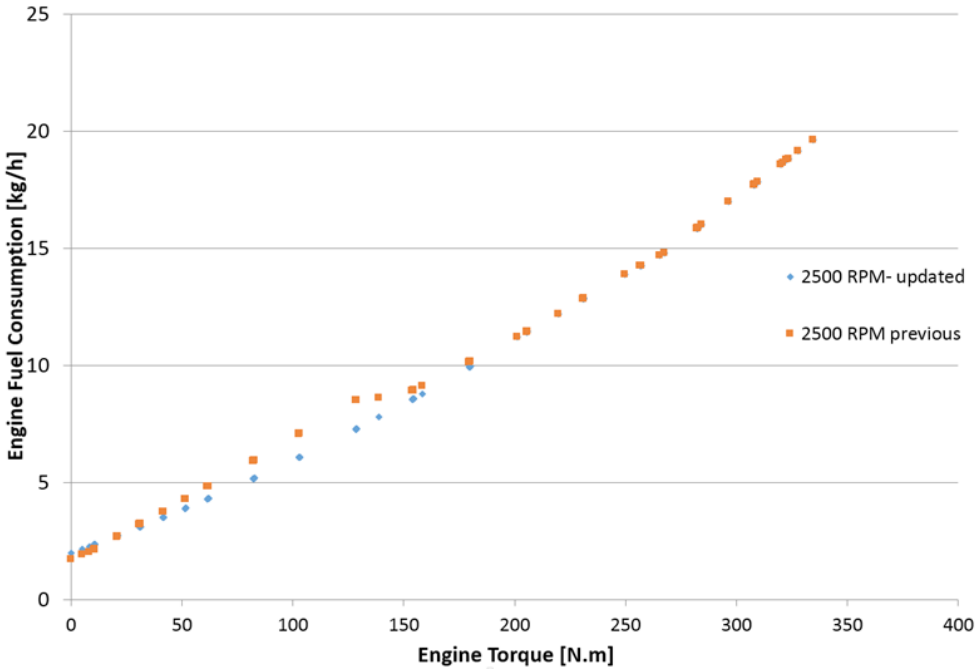

FIGURE 5. Improvement in Fuel Consumption with Updated Fuel Rate at Low and Medium Loads at 2,500 RPM

and medium loads can be seen. The bsfc map used for the Autonomie simulation was updated for a speed range from 800 RPM to 2,500 RPM.

The conventional baseline simulations were therefore updated to account for the improvements seen at low and medium loads.

RESULTS

EIL Results with Baseline Diesel Engine

EIL capability was established with the default diesel fuel on the GM 1.9-L TDI engine. With the EIL capability established with diesel fuel, performing transient analysis on the LTC technology would require a much shorter lead time.

Table 2 lists the mean fuel consumption and emissions (engine-out) values for the baseline diesel engine. The emissions data were recorded in ppm, and converted to a per-mile basis on the basis of published calculations [4].

TABLE 2. Fuel Consumption and Emissions with Diesel Fuel for the GM 1.9-L TDI Engine, from EIL data

Drive Cycle	Fuel Consumption L/100 km	NOx g/mi	HC g/mi	CO g/mi
UDDS	5.72	1.11	0.12	1.72
HWFET	4.02	0.40	0.05	0.88

Gear ratio selection and shift parameter optimization, for particular cycles, has a significant impact on fuel consumption and emissions. In FY 2013, a simulation study, based on steady-state emission maps for the 1.9-L TDI engine with diesel fuel, was conducted to evaluate the impact of shift parameters on fuel consumption and emissions [5]. In FY 2014, with the EIL setup functional with diesel fuel, the same study was repeated on hardware to validate the trends observed in simulation. Figure 6 shows a plot of engine speed with the default and updated shift parameters. It can be seen that with the updated shift parameters, the engine operates at lower speeds, and therefore higher torque, in the time interval between 230 and 300 s.

Figure 7 shows the measured fuel rate (kg/hr) for the segment of the drive cycle between 230 and 300 s. The impact of downspeeding can be clearly seen, as the fuel rate with the updated shift parameters is lower than the default case.

Figure 8 shows the impact of downspeeding on instantaneous NOx emissions. As stated in last year's annual report, simulations with steady-state NOx maps suggested a trade-off between fuel consumption and

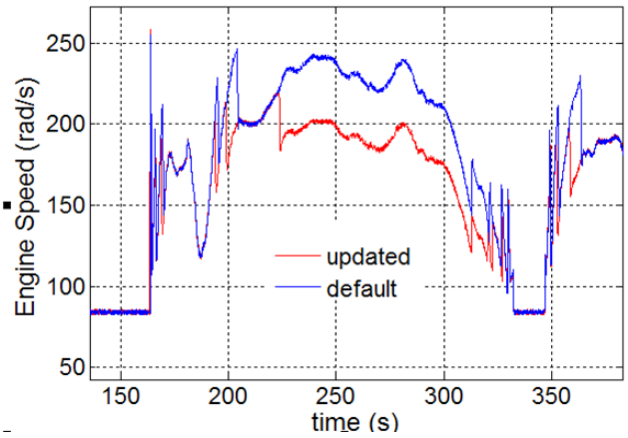

FIGURE 6. Engine Downspeeding via Updated Shift Parameters during a Section of the UDDS Cycle

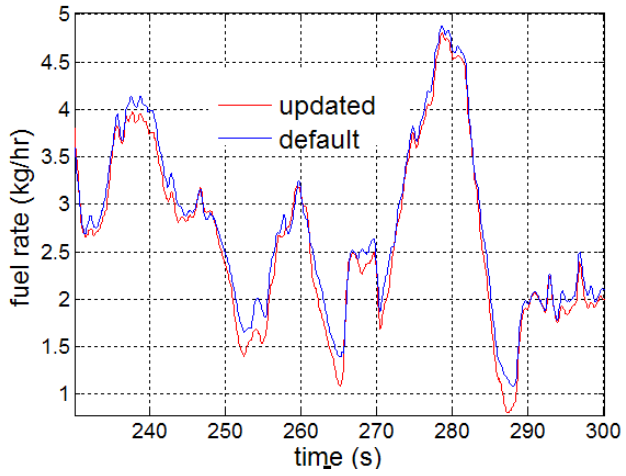

FIGURE 7. Reduction in Engine Fuel Consumption due to Downspeeding

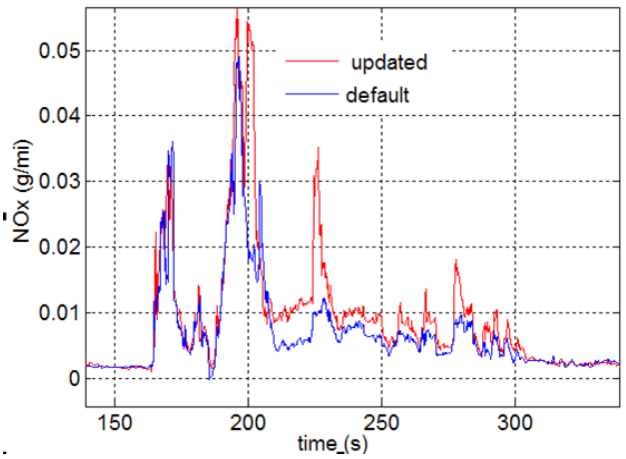

FIGURE 8. Increase in NOx due to Downspeeding

NOx due to downspeeding. As Figure 8 shows, NOx does increase due to downspeeding and the resulting higher torque operation of the engine. It should be noted that early in the shift regime, when the engine is in the same gear (i.e., engine speed and torque are the same) for both sets of shift parameters, the NOx emissions are very similar to each other.

Table 3 summarizes the impact of downspeeding on fuel consumption and emissions for the UDDS cycle. The mean values indicated in Table 2 and Table 3 are over five cycles (five with default shifting and five with shift parameters updated for downspeeding).

TABLE 3. Impact of Downspeeding on Fuel Consumption and Emissions (mean values)

Shift parameters	Fuel Consumption L/100 km	NOx g/mi	HC g/mi
Default	5.81	0.9	0.13
Updated (downspeeding)	5.72	1.11	0.12

Fuel Consumption Benefits of LTC for a Mild Hybrid Powertrain Using Simulation (based on earlier version of bsfc maps)

As stated in the approach section, the fuel consumption benefits of LTC with gasoline were evaluated for a BISG. The BISG enables engine stop at idle and provides slight torque assist at low vehicle speeds. Therefore, the three engines were resized in order to have the same 0-60 mph performance. Table 4 shows the original engine peak power, the engine peak power after resizing for the conventional powertrain, and the engine peak power after resizing for the BISG powertrain.

TABLE 4. Engine Resizing for the Conventional and the BISG Powertrain to Match the IVM-60 MPH Performance for the Three Engines

Engine Type	Original (unsized) Peak Power (kW)	Engine Peak Power (resized) for Conventional Powertrain (kW)	Engine Peak Power (resized) for BISG Powertrain (kW)
PFI	90	147	110
SIDI	104	135	107
LTC (gasoline)	110	115	92

For reference, the fuel economy benefit for a conventional powertrain with LTC compared to the PFI engine, based on earlier versions of the bsfc map, is 25% over the combined cycle.

Table 5 lists the fuel economy benefits for the BISG configuration. As seen in Table 5, for the BISG configuration, LTC technology offers a 23% improvement in fuel economy over PFI and a 7% improvement over SIDI over the combined cycle.

TABLE 5. Fuel Economy Benefits of LTC Compared to PFI and SIDI (simulation study results) for BISG Powertrain with Earlier-Generation bsfc Map

Drive Cycle	Fuel Economy (mpg, unadjusted)		
	PFI	SIDI	LTC
UDDS	30	35.6	38
HWFET	34	42	46
Combined (55/45)	31.6	38.22	41.2
Improvement over PFI		17%	23%
Improvement over SIDI			7%

Fuel Consumption Benefits of LTC for a Conventional Powertrain with Updated Versions of the BSFC Map

In the fourth quarter of FY 2014, updated bsfc maps were generated which reflected decreased low-load fuel consumption. Figure 5 shows the improvement in fuel consumption at low and medium loads for an engine speed of 2,500 RPM. Table 6 shows the fuel economy improvements with the conventional powertrain with the updated bsfc map.

TABLE 6. Fuel Economy Benefits of LTC Compared to PFI and SIDI (simulation study results) for Conventional Powertrain with Updated bsfc Map

Drive Cycle	Fuel Economy (mpg, unadjusted)		
	PFI	SIDI	LTC
UDDS	29.1	32.6	37.6
HWFET	39.6	42.1	50.7
Combined (55/45)	33.1	36.3	42.5
Improvement over PFI		10%	28.7%
Improvement over SIDI			17%

It should be re-emphasized that the conventional fuel economy results in Table 6 look comparable to the BISG results in Table 5 because of the updated bsfc maps based on the latest steady-state combustion results.

CONCLUSIONS AND FUTURE DIRECTIONS

This project evaluates a DOE-developed combustion technology (LTC with generic gasoline) in a vehicle systems context through the use of simulation and EIL.

The fuel consumption of a midsize sedan (conventional powertrain) with LTC was compared to the same vehicle with SIDI and PFI engines (the SIDI and PFI engines are scaled in power such that the vehicle 0-60 mph performance is the same in each case) via simulation. In addition, fuel consumption and engine-out emissions for the said technology will be quantified by using EIL. Shift parameters will be optimized to minimize the fuel consumption and/or engine-out NO_x emissions of the LTC engine.

The updated simulation study on the conventional powertrain has shown that with LTC, a 28.7% improvement in fuel consumption over a PFI engine and a 10% improvement over SIDI engine technology are possible.

EIL has been implemented on the engine dyno test cell with the 1.9-L TDI engine. Fuel consumption and emissions with diesel fuel have been quantified with EIL.

The trends in the impact of shift parameters on fuel consumption and engine-out emissions, predicted through a simulation study in FY 2013, have been confirmed through EIL in FY 2014 for the baseline (diesel) fuel.

The improvement in fuel economy due to LTC for a mild hybrid powertrain (BISG configuration) has been quantified.

Once engine hardware upgrades are complete and steady engine combustion has been established across the entire engine operating map, transient evaluation with LTC will be performed using EIL.

The impact of LTC on the fuel consumption and emissions of an electrified powertrain will be updated in FY 2015 by using the updated bsfc map.

REFERENCES

1. Stephen Ciatti, Christopher Kolodziej, "Use of Low Cetane Fuel to Enable Low Temperature Combustion," DOE Annual Merit Review, June 18, 2014.

2. Phillipe Abiven, Steve Ciatti, Aymeric Rousseau, "Fuel Consumption Benefit of Low Temperature Combustion Engine for Conventional Vehicle," presentation to DOE, August 29, 2012.

3. http://www.carinf.com/en/9220414062.html

4. SAE J1003: Diesel Engine Emission Measurement Procedure.

5. Neeraj Shidore, Stephen Ciatti, Chris Kolodziej, Daehung Lee, Namdoo Kim, "Impact of Shift Parameter Turning on Fuel Consumption and NOx for the 1.9 L TDI Engine," presentation to DOE, June 12, 2013.

FY 2014 PRESENTATIONS

1. N. Shidore, A.Rouseau, S. Ciatti, "Evaluation of the Fuel Economy Impacts of Low Temperature Combustion."

2. (LTC) Using Engine in the Loop: Status Update to DOE Sponsors," demo and presentation to Ken Howden and Leo Breton.

III. EMISSION CONTROL R&D

III.1 Cross-Cut Lean Exhaust Emission Reduction Simulation (CLEERS): Administrative Support

Stuart Daw (Primary Contact),
Vitaly Prikhodko, Charles Finney, Zhiming Gao, Josh Pihl
Oak Ridge National Laboratory (ORNL)
National Transportation Research Center
2360 Cherahala Blvd.
Knoxville, TN 37932

DOE Technology Development Manager
Ken Howden

Subcontractor
Richard Blint, N2Kinetics Research,
Shelby Township, MI

Overall Objectives

Coordinate the CLEERS activity for the DOE Advanced Engine Cross-Cut Team to accomplish the following:

- Promote development of improved computational tools for simulating realistic full-system performance of lean-burn engines and associated emissions controls.
- Promote development of performance models for emissions control components such as exhaust manifolds, catalytic reactors, and sensors.
- Provide consistent framework for sharing information about emissions control technologies.
- Help identify emissions control R&D needs and priorities.

Fiscal Year (FY) 2014 Objectives

- Facilitate monthly CLEERS Focus Group teleconferences.
- Organize and conduct the 2014 DOE Cross-Cut Workshop on Lean Emissions Reduction Simulation (CLEERS Workshop).
- Maintain CLEERS website and bibliographic database.

FY 2014 Accomplishments

- Continued leadership of the CLEERS Planning Committee.
- Facilitated CLEERS Focus teleconferences, which continue to have strong domestic and international participation (typically 30-50 participants).
- Provided regular update reports to DOE Advanced Combustion Engine Cross-Cut Team.
- Organized the 2014 DOE Cross-Cut Workshop on Lean Emissions Reduction Simulation (CLEERS Workshop) at University of Michigan, Dearborn on April 29-May 1, 2014.
- Maintained the CLEERS website (www.cleers.org), including the CLEERS bibliographic database.
- Supported the Advanced Combustion and Emissions Control (ACEC) Low Temperature Aftertreatment Team in developing an evaluation protocol for low-temperature oxidation catalysts.

Future Directions

- Continue leading the CLEERS planning and database advisory committees.
- Continue leading the Focus Groups.
- Organize and conduct the 2015 CLEERS Workshop.
- Continue sharing of basic data and models with DOE Vehicle Systems projects and the ACEC Team from U.S. DRIVE.
- Continue maintenance and expansion of CLEERS website.
- Continue providing regular update reports to the DOE Advanced Combustion Engine Cross-Cut team.
- Conduct 2015 CLEERS Industry Priority Survey.

INTRODUCTION

Improved catalytic emissions controls will be essential for utilizing high-efficiency lean-burn engines without jeopardizing the attainment of much stricter U.S. Environmental Protection Agency emission standards that will begin taking effect after 2013. Simulation and modeling are recognized by the Advanced Engine Cross-Cut Team as essential capabilities needed to address the continually evolving regulatory environment and advances in combustion engine and emissions control technology. In response to this need, the CLEERS activity was initiated several years ago to promote

improved computational tools and data for simulating realistic full-system performance of lean-burn engines and the associated emissions control systems. Specific activities supported under CLEERS include:

- Public workshops on emissions control topics.
- Pre-competitive collaborative interactions among Cross-Cut Team members, emissions control suppliers, universities, and national labs under a limited access focus group.
- Development of experimental data, analytical procedures, and computational tools for understanding performance and durability of catalytic materials.
- Establishment of consistent frameworks for sharing information about emissions control technologies.
- Recommendations to DOE and the DOE Cross-Cut Team regarding the most critical emissions control R&D needs and priorities.

ORNL is involved in two separate DOE-funded tasks supporting CLEERS:

- Overall administrative support; and
- Joint development of benchmark emissions control catalyst kinetics in collaboration with other national labs and university and industry partners.

APPROACH

In the administrative task, ORNL coordinates the CLEERS Planning Committee, the CLEERS Database Advisory Team, the CLEERS Focus groups, CLEERS public workshops, the biannual CLEERS industry survey, and the CLEERS website (http://www.cleers.org). ORNL acts as a communication hub and scheduling coordinator among these groups and as the spokesperson and documentation source for CLEERS information and reports. The latter includes preparation and presentation of status reports to the Advanced Engine Cross-Cut Team, responses to requests and inquiries about CLEERS from the public, and summary reports from the biannual industry surveys.

RESULTS

CLEERS technical teleconferences continued this year on roughly a monthly basis. The presentations covered a wide range of research results in emissions control experimentation, modeling, and simulation by members of the CLEERS Focus Group as well as outside experts including: Xavier Auvray (Chalmers University), Xiaobo Song (Michigan Technological University), Chuck Peden (Pacific Northwest National Laboratory, PNNL), Eric Brosha (Los Alamos National Laboratory), George Muntean (PNNL), Mario Trujillo (University of Wisconsin), Alex Sappok (Filter Sensing Technologies), and Ty Caudle (BASF). As previously, we have continued to restrict teleconference attendance to members of the Advanced Engine Cross-Cut Team and their direct collaborators, because these teleconferences sometimes include unpublished or sensitive information. In some cases, presentations include pre-publication or sensitive information and are made only via live weblink without distributing electronic copies of slides to the participants. Attendance is now typically between 30 and 50 participants. International participation continues to be good and is mostly from Europe.

The 2014 (17th) CLEERS Workshop was held April 29 – May 1, 2014 at the Institute of Advanced Vehicle Studies on the Dearborn campus of the University of Michigan. As has been the tradition, the workshop was a fully public event and open to participants from any organization or institution. The workshop program included four invited speakers:

- Bob McCabe (Ford): "Cold-start and low-temperature emissions challenges."
- Raj Gounder (Purdue University): "New insights into the properties of and mechanistic roles of Brønsted acid sites."
- Martin Votsmeier (Umicore): "Reversible deactivation effects: A challenge for catalyst simulation."
- Cary Henry (Southwest Research Institute®): "Implications of Advanced Combustion Strategies on Emission Control System Design."

Besides the invited speakers, there were also 35 contributed talks and 13 posters by researchers from industry, universities, and national labs. As illustrated in Figure 1, the oral presentations included a wide range of technical topics, including particulate matter, lean-NOx (oxides of nitrogen) traps, selective catalytic reduction (SCR) NOx reduction, and a significant emphasis on catalysts for low-temperature and/or advanced combustion applications. Additional details can be found on the CLEERS website (www.cleers.org) under the 2014 Workshop heading [1].

The industry panel discussion at the CLEERS Workshop was "Expected impacts of advanced combustion regimes and alternate fuels on emissions controls." Panel members included: Neal Currier (Cummins), Craig Dimaggio (Chrysler), Tim Johnson (Corning), Stuart Johnson (Volkswagen), Chang Kim (General Motors), and Will Ruona (Ford Motor). One of the themes that emerged from the panel discussion centered on the complex interplay between regulations for greenhouse gases (GHG) and criteria pollutants

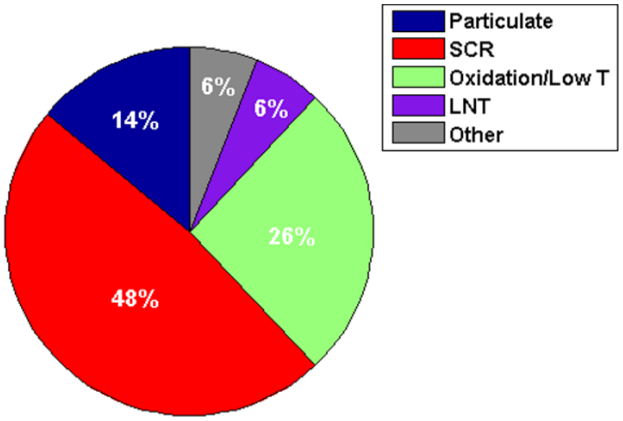

FIGURE 1. Distribution of emission control topics for the 2014 CLEERS Workshop oral presentations. Abbreviations: SCR: urea or NH_3 selective catalytic reduction; LNT: lean-NOx trap; Particulate: particulate matter; Oxidation/low T: catalysts for low temperature and/or advanced combustion applications.

(particulate matter, NOx + hydrocarbons [HCs], CO), and the key role aftertreatment systems will continue to play in future vehicles. Many of the technologies being deployed or developed to improve efficiency and reduce GHG emissions (such as gasoline direct injection, lean gasoline engines, turbocharging, and low-temperature combustion modes) create new challenges in meeting emissions regulations by reducing exhaust temperatures and/or increasing pollutant concentrations. Furthermore, there are efficiency (and GHG emissions) benefits that can be derived simply by improving the performance of the emissions control system. For example, a catalyst that lights off at lower temperature reduces the fuel penalty associated with cold start emissions control. The panelists also discussed how alternate fuels will introduce new aftertreatment challenges. Different HC species have different reactivities, so changes in fuel formulation could impact catalyst performance. The extreme example of this is natural gas, since methane is highly unreactive compared to other HC species and will pose a challenge in meeting GHG emissions regulations. Finally, the panelists emphasized the continuing importance of catalyst durability and onboard diagnostics in meeting full-useful-life emissions regulations.

ORNL continues to work with other DOE national laboratories to support collaboration and coordination of emissions control related research. ORNL's collaboration with PNNL has continued to center on the characterization and modeling of commercial chabazite copper-zeolite SCR catalysts, with a particular emphasis on modeling NH_3 storage and release. This focus is driven by experimental and modeling observations at ORNL and PNNL and feedback from our industry partners regarding their concerns for urea-SCR diagnostics and controls. Additional details about the measurement and quantification of NH_3 storage are described in the 2014 annual report for the other ORNL CLEERS activity ("Joint Development of Emissions Control Data and Models"). ORNL has also worked with researchers Los Alamos National Laboratory to help evaluate their NOx, HC, and NH_3 sensors in realistic exhaust environments and to make the larger CLEERS community aware of their work. Finally, ORNL has worked closely with PNNL and the industry members of the ACEC Tech Team Low Temperature Aftertreatment Working Group to support the development of a new low-temperature oxidation catalyst laboratory evaluation protocol. The protocol was discussed during a CLEERS focus group teleconference and at the 2014 CLEERS Workshop, and the final draft version of the protocol will be posted on the CLEERS website for the emissions control community to review and provide feedback.

Collaborations with university and industry partners in both the U.S. and Europe continue to be very active. European university partners include Prof. Petr Koci at the Institute for Chemical Technology in Prague, Prof. Louise Olsson at Chalmers University of Technology, and Professors Isabella Nova and Enrico Tronconi at Politecnico di Milano. This year, ORNL hosted a student researcher from Prague, who conducted laboratory experiments in the Fuels, Engines, and Emissions Research Center to develop improved kinetic mechanisms for N_2O formation over lean-NOx trap catalysts. ORNL also established a new collaboration with Prof. Raj Gounder at Purdue University on characterization of chabazite SCR catalysts. ORNL has provided commercial SCR catalyst samples to Purdue, and Purdue has provided model SSZ-13 samples to ORNL; both institutions will apply their specialized characterization techniques on the commercial and model materials and will compare the results. ORNL has also continued close interactions with Gamma Technologies via sharing of detailed experimental reactor and engine dynamometer data. Gamma is sharing the results of their analyses with us to help improve estimates of key model parameters and also make improvements to the CLEERS catalyst characterization protocols. Both the improved model parameter estimates and modified protocols are being shared with the CLEERS community in the expanded CLEERS database.

CONCLUSIONS

Industry feedback to CLEERS researchers at national labs is providing a critical, fast-response mechanism to help redirect activities and maximize the commercial relevance of R&D efforts at DOE labs. CLEERS is also providing DOE with key information

needed for strategic planning. The important role for CLEERS in facilitating new directions has been exemplified by CLEERS' support of the U.S. DRIVE ACEC Team in identifying and prioritizing new R&D directions for emissions controls of advanced, high-efficiency combustion engines with low-temperature exhaust. Participation by industry, labs, and universities in the CLEERS public workshops and technical focus meetings continues to be very high.

REFERENCES

1. 2014 (17th) CLEERS Workshop agenda and presentations at http://www.cleers.org.

FY 2014 PUBLICATIONS/PRESENTATIONS

1. Šárka Bártová, Petr Kočí, David Mráček, Miloš Marek, Josh A. Pihl, Jae-Soon Choi, Todd J. Toops, William P. Partridge, "New Insights on N_2O Formation Pathways during Lean/Rich Cycling of a Commercial Lean NOx Trap Catalyst," Catalysis Today 231 (2014) 145-154.

2. J.A. Pihl, C.S. Daw, "NH_3 storage isotherms: a path toward better models of NH_3 storage on zeolite SCR catalysts," presentation to the U.S. DRIVE Advanced Combustion and Emission Control Tech Team, Southfield, MI, January 9, 2014.

2. J.A. Pihl, C.S. Daw, "NH_3 storage isotherms: a path toward better models of NH_3 storage on zeolite SCR catalysts," presentation to the 2014 DOE Crosscut Workshop on Lean Emissions Reduction Simulation, Dearborn, MI, April 29, 2014.

3. D. Mráček, P. Kočí, M. Marek, J.-S. Choi, J.A. Pihl, T.J. Toops, W.P. Partridge, "Kinetics of N_2O and N_2 Peaks During and After the Regeneration of Lean NOx Trap," presentation to the 2014 DOE Crosscut Workshop on Lean Emissions Reduction Simulation, Dearborn, MI, April 30, 2014.

4. C.S. Daw, J.A. Pihl, J.-S. Choi, M.-Y. Kim, W.P. Partridge, T.J. Toops, V.Y. Prikhodko, C.E.A. Finney, "Joint Development and Coordination of Emissions Control Data and Models (CLEERS Analysis and Coordination)," presentation to the 2014 DOE Vehicle Technologies Office Annual Merit Review and Peer Evaluation Meeting, Washington, DC, June 18, 2014.

5. Š. Bártová, D. Mráček, P. Kočí, M. Marek, J.-S. Choi, "Ammonia reactions with the stored oxygen in a commercial lean NOx trap catalyst," poster to the 23rd International Symposium on Chemical Reaction Engineering, Bangkok, Thailand, September 7–10, 2014.

6. P. Kočí, D. Mráček, M. Marek, J.-S. Choi, J.A. Pihl, T.J. Toops, W.P. Partridge, "N_2O and N_2 formation dynamics during and after the regeneration of lean NOx trap," presentation to the the 8th International Conference on Environmental Catalysis, Asheville, NC, August 24–27, 2014.

7. J.A. Pihl, C.S. Daw, "NH_3 storage isotherms: a path toward better models of NH_3 storage on zeolite SCR catalysts," presentation to the 8th International Conference on Environmental Catalysis, Asheville, NC, August 24–27, 2014.

8. C.S. Daw, J.A. Pihl, J.-S. Choi, W.P. Partridge, T.J. Toops, V.Y. Prikhodko, C.E.A Finney, "Joint Development and Coordination of Emissions Control Data and Models (CLEERS Analysis and Coordination)," presentation to U.S. DOE Advanced Engine Crosscut Team, Southfield, MI, September 11, 2014.

III.2 Cross-Cut Lean Exhaust Emissions Reduction Simulations (CLEERS): Joint Development of Emissions Control Data and Models

Stuart Daw (Primary Contact), Josh Pihl, Jae-Soon Choi, Bill Partridge, Mi-Young Kim, Todd Toops
Oak Ridge National Laboratory (ORNL)
2360 Cherahala Blvd.
Knoxville, TN 37932-1563

DOE Technology Development Manager
Ken Howden

Overall Objectives

- Collaborate with Pacific Northwest National Laboratory (PNNL) to support industry in the development of accurate simulation tools for the design of catalytic emissions control systems that enable advanced high efficiency combustion engines to meet emissions regulations while maximizing fuel efficiency; specifically:
  - Identify reaction mechanisms occurring over catalytic devices under relevant operating conditions
  - Develop modeling strategies that represent key catalyst processes in a computationally efficient manner
  - Generate benchmark data sets for use in model calibration and validation
  - Measure critical device parameters needed for model development
- Disseminate mechanistic insights, modeling strategies, benchmark data sets, and representative device parameters through the CLEERS website, CLEERS focus group teleconferences, and CLEERS workshop.
- Utilize results from fundamental research to develop new approaches for advanced emissions control systems (e.g., with enhanced low-temperature function).

Fiscal Year (FY) 2014 Objectives

- Identify chemical processes leading to N_2O formation during low-temperature lean-NOx trap (LNT) regeneration (collaboration with Institute of Chemical Technology, Prague).
- Investigate reaction mechanisms for NO selective catalytic reduction (SCR) by NH_3 and NO oxidation over small pore copper zeolite catalysts (collaboration with Politecnico di Milano).
- Develop measurement and modeling strategies that capture the impacts of hydrothermal aging on the NH_3 storage capacity of a commercial zeolite SCR catalyst (collaboration with PNNL).

FY 2014 Accomplishments

- Conducted detailed measurements of N_2O formation as a function of time and catalyst location during LNT regeneration. Identified the chemical pathways leading to N_2O formation upon the switch from rich regeneration back to lean trapping conditions.
- Proposed new mechanisms for NO oxidation and NO SCR over a small pore copper zeolite that are consistent with measured reaction rates and observed surface intermediates.
- Refined measurement and analysis techniques for quantifying NH_3 adsorption enthalpies on zeolite SCR catalysts. Measured impacts of catalyst state on NH_3 adsorption enthalpy as a function of coverage on a commercial small pore copper zeolite.

Future Directions

- Complete development and publication of mechanistic pathways and associated modeling strategies that predict N_2O formation during low-temperature LNT regeneration.
- Quantify impacts of hydrothermal aging on energetics of NH_3 adsorption for a commercial Cu-zeolite SCR catalyst. Identify strategies for adjusting model parameters to account for aging.
- Develop experimental methods and analysis approaches for estimating the key parameters required to calibrate models of hydrocarbon traps for low-temperature exhaust applications.

INTRODUCTION

Catalytic emissions control devices will play a critical role in deployment of advanced high-efficiency engine systems by enabling compliance with increasingly stringent emissions regulations. High-efficiency diesel

and lean gasoline engines, for example, will require NOx reduction catalysts with very high conversion efficiencies to meet the Environmental Protection Agency Tier 3 NOx emissions standard. Low-temperature combustion strategies, on the other hand, significantly reduce engine-out NOx, but they generate a challenging combination of high hydrocarbon and carbon monoxide concentrations at low exhaust temperatures that will likely demand novel approaches to emissions control. Design of progressively more complex engine/aftertreatment systems will increasingly rely on advanced simulation tools to ensure that next-generation vehicles maximize efficiency while still meeting emissions standards. These simulation tools will, in turn, require accurate, robust, and computationally efficient component models for emissions control devices. Recognizing this need, the DOE Diesel Cross-Cut Team initiated the CLEERS activity to support the development of improved computational tools and data for simulating realistic full-system performance of high efficiency engines and associated emissions control systems.

APPROACH

ORNL is involved in two separate DOE-funded tasks supporting CLEERS: overall administrative support and joint development of emissions control data sets and models. Under the second activity, which is covered by this report, ORNL works closely with PNNL to support the development of accurate simulation tools for the design of catalytic emissions control systems that enable advanced high-efficiency combustion engines to meet emissions regulations while maximizing fuel efficiency. Specific activities include: identification of reaction mechanisms occurring over catalytic devices under relevant operating conditions; development of modeling strategies that represent key catalyst processes in a computationally efficient manner; generation of benchmark data sets for model calibration and validation; and measurement of critical device parameters needed for model development. The resulting mechanistic insights, modeling strategies, benchmark data sets, and representative device parameters are disseminated through the CLEERS website, during monthly CLEERS focus group teleconferences, at the annual CLEERS workshop, and through publications and presentations. Research directions are guided by the DOE Advanced Engine Cross-Cut Team, which collectively oversees CLEERS, and by regular CLEERS industry participant priority surveys. ORNL's CLEERS research activities have historically focused on approaches to NOx reduction in lean exhaust such as LNTs and urea SCR.

RESULTS

Due to its potency as a greenhouse gas, N_2O will be included in upcoming emissions regulations. One of the challenges facing designers of emissions control systems is to develop component architectures and control strategies that can minimize N_2O formation while maintaining high NOx reduction activity. This is particularly true for LNTs, which can generate significant N_2O quantities (Figures 1 and 2). Therefore, it is critical that LNT simulation tools accurately capture N_2O formation. ORNL has been working closely with collaborators at the Institute of Chemical Technology, Prague to unravel the complex surface chemistry that drives N_2O selectivity. Detailed flow reactor investigations using specialized techniques, including spatially resolved capillary inlet mass spectrometry with isotopically labeled ^{15}NO, have revealed two distinct N_2O production processes (Figure 2). The primary N_2O peak

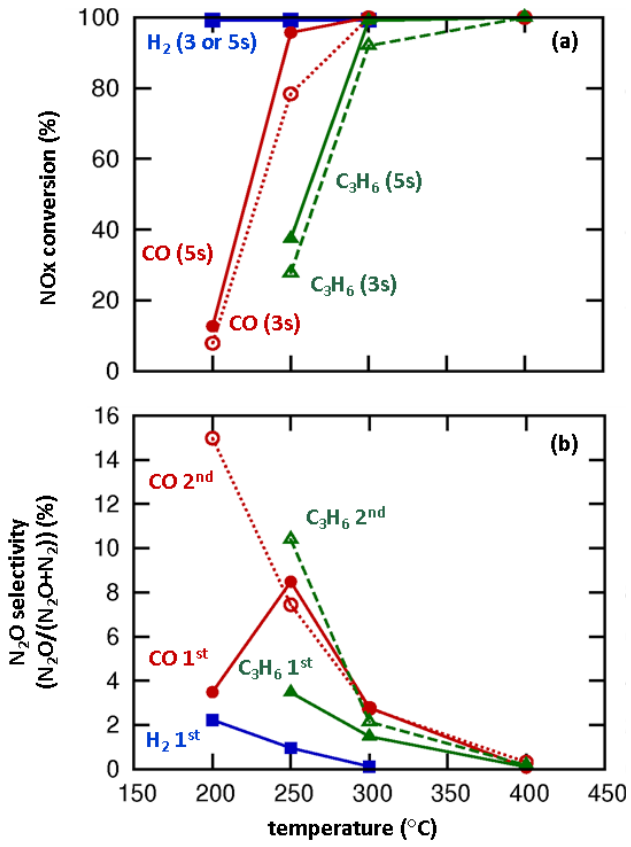

FIGURE 1. (a) NOx conversion for two different regeneration times (3 s and 5 s) and (b) N_2O selectivity at beginning (data series marked 1st) and end (data series marked 2nd) of a 5 s regeneration as a function of temperature for a commercial LNT catalyst (removed from a BMW 120i lean gasoline vehicle) operated at a gas hourly space velocity of 30,000 h^{-1} under lean/rich cycles with 60 s lean (300 ppm NO, 10% O_2, 5% H_2O, 5% CO_2, balance N_2) and 3 or 5 s rich (3.4% CO or 0.38% C_3H_6, 5% H_2O, 5% CO_2, balance N_2).

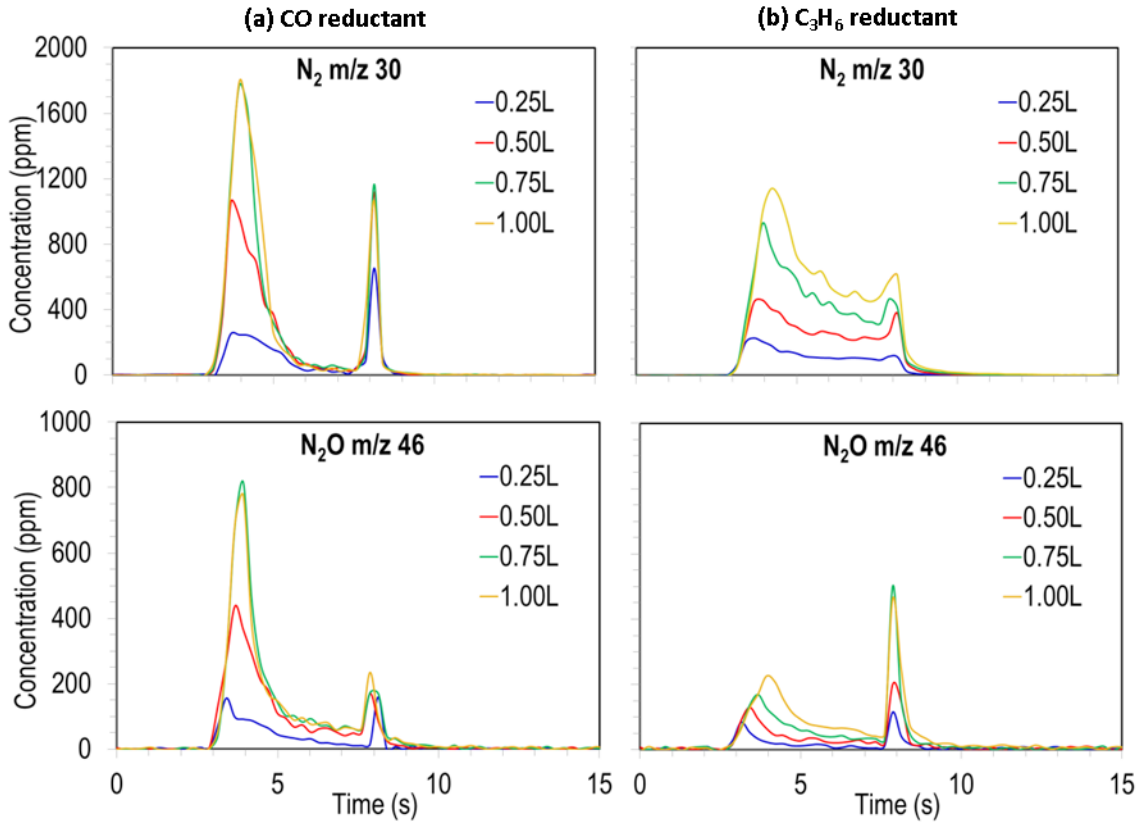

FIGURE 2. N_2 and N_2O concentrations as a function of time and catalyst position (0.0 L = catalyst inlet, 1.0 L = catalyst outlet) during regeneration of a commercial LNT catalyst (removed from a BMW 120i lean gasoline vehicle) operated at 250°C and a gas hourly space velocity of 30,000 h^{-1} under lean/rich cycles with 60 s lean (300 ppm NO, 10% O_2, 5% H_2O, 5% CO_2, balance N_2) and 5 s rich ((a) 3.4% CO or (b) 0.38% C_3H_6, 5% H_2O, 5% CO_2, balance N_2).

occurs near the transition from lean to rich operating conditions at the beginning of the catalyst regeneration process and is largest at temperatures near the light off for a given formulation and reductant species (Figure 1). The secondary N_2O peak occurs immediately after the transition from rich back to lean conditions at the end of the regeneration period. Prior work indicated that the N_2O generated at the beginning of regeneration correlates with relative rates of reduction of the platinum group metal (PGM) LNT components [1]. Fully reduced PGM surfaces are very effective at generating N_2 and NH_3 from stored NOx species. However, if the PGM surfaces are not fully reduced, such as at very early regeneration times or at low temperatures near catalyst light off, there is a higher probability that an adsorbed N adatom will combine with an adsorbed NO, forming N_2O.

The FY 2013 annual progress report included results from our collaborators at the Institute of Chemical Technology, Prague, who incorporated PGM redox state into their LNT model, resulting in good agreement between predicted and measured product selectivities over a wide temperature range for multiple reductant species. Efforts during FY 2014 focused on experiments designed to isolate the chemical processes that generate the secondary N_2O spike during the switch from rich to lean conditions. Results from these experiments showed that the N_2O released at the switch from rich to lean is formed by reactions involving residual stored NOx, reductants or reduction intermediates (such as isocyanates) adsorbed on the catalyst surface, and incoming O_2. Since all three components must be present to form N_2O, the surface state of the PGM sites plays a critical role in controlling N_2O formation at the end of regeneration, much as for the primary N_2O peak. Thus, inclusion of PGM oxidation/reduction kinetics in global LNT mechanisms, such as the one developed by the Institute of Chemical Technology, Prague, will provide more accurate predictions of N_2O formation. More accurate simulation tools will, in turn, enable design of system architectures and operating strategies that minimize N_2O emissions.

In addition to improved simulation tools, the results of this work point to several strategies for reducing N_2O produced by LNTs. For both the primary and secondary peaks, more reactive PGM surfaces minimize N_2O formation. Increasing the activity at the PGM sites

can be achieved through increasing the LNT operating temperature or shifting the reductant composition to include more H_2 and less hydrocarbons. For the secondary N_2O peak, introducing a short stoichiometric purge between rich and lean conditions allows the reductants and reaction intermediates on the catalyst to desorb or react before O_2 introduction, resulting in significantly lower N_2O formation.

As the LNT N_2O work demonstrates, a more thorough understanding of the fundamental surface chemistry occurring on a catalyst enables development of higher fidelity simulation tools and reveals opportunities for improving performance. While small pore copper zeolites have already found commercial application in urea SCR systems, the reaction mechanisms that control their performance are not well understood. To overcome this challenge, ORNL is collaborating with researchers at Politecnico di Milano to investigate the detailed chemistry during NH_3 SCR of NO and to propose revised reaction mechanisms that account for experimental observations. The annual report for FY 2013 discussed kinetic evidence that the pathway for NO SCR by NH_3 does not proceed through NO oxidation to NO_2 followed by the "fast SCR" reaction, as previously thought.

Efforts during FY 2014 focused on detailed analysis and interpretation of surface spectroscopy experiments designed to identify reaction intermediates on the SCR catalyst surface. The resulting spectra, some of which are shown in Figure 3(a), revealed several key findings. First, nitrates were formed in the absence of O_2 by flowing NO over a pre-oxidized catalyst, demonstrating the ability of the Cu sites to directly participate in oxidation/reduction reactions. Second, the spectra revealed the formation of NO^+ species prior to nitrates (Figure 3b). This observation is consistent with NO^+ being an intermediate in the NO oxidation process. ORNL worked with Politecnico di Milano to develop detailed mechanisms for NO oxidation and NO SCR by NH_3 that include these features. Models built from these mechanisms will yield better predictions of SCR catalyst performance, particularly under the low-temperature operating conditions critical for control of emissions from next-generation high-efficiency engine systems.

Another key knowledge gap on small pore copper zeolites revolves around modeling of NH_3 storage and release. Respondents to a 2013 survey of CLEERS industry participants indicated that this issue should be the highest priority focus of CLEERS research activities related to catalytic NOx control. ORNL has been working closely with partners at PNNL to determine how urea SCR model parameters can be adjusted to reflect changes in catalyst properties over the vehicle lifetime, with a particular emphasis on the impact of aging on NH_3 storage. These efforts revealed that the standard

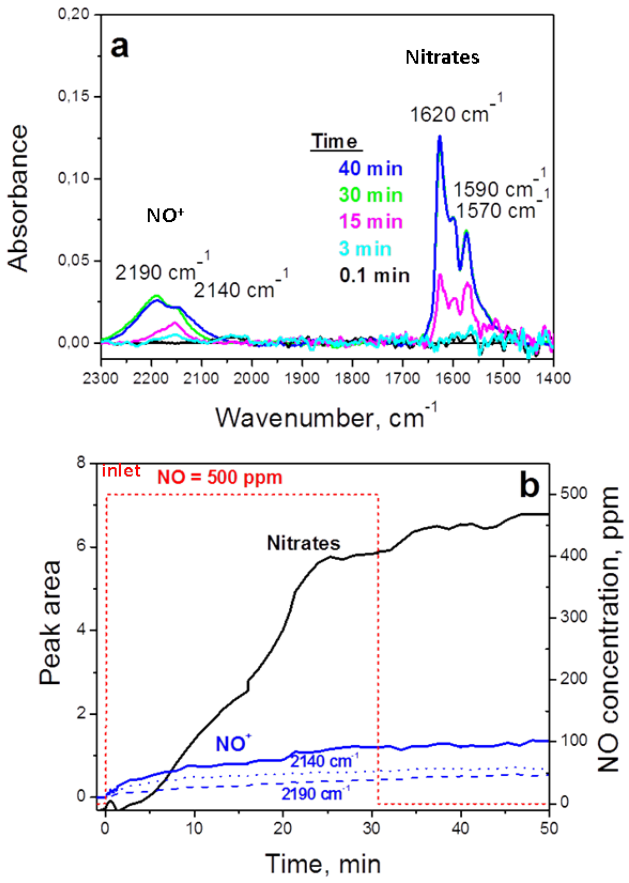

FIGURE 3. (a) DRIFT spectra and (b) peak area as a function of time during and after exposure of a commercial small pore copper zeolite (from a General Motors vehicle) to 500 ppm NO, balance Ar at 120°C after a pretreatment under 8% O_2, balance Ar at 500°C.

experimental methods for characterizing NH_3 storage over zeolite SCR catalysts generate data sets in which the thermodynamics of the NH_3 adsorption/desorption processes are intertwined with reaction rates and mass transport. Calibrating models to these data sets results in non-unique parameter estimates that are not robust to changes in operating conditions.

To avoid these complications, ORNL developed a new strategy for measuring the energetics of the NH_3 adsorption process that relies on equilibrium isotherm measurements, thereby eliminating kinetic and mass transport effects. Through straightforward thermodynamic analysis, these isotherms can be used to calculate the NH_3 adsorption enthalpy as a function of NH_3 coverage. During FY 2014, these measurement and analysis techniques were refined and applied to catalyst materials under different operating conditions to establish correlations between NH_3 storage behavior and catalyst state; parameters of interest include oxidation state, humidification, and hydrothermal aging. In addition, the analysis techniques were further developed to better

access the information generated through the NH_3 isotherm approach. For example, Figure 4 demonstrates that, in addition to providing key parameters for NH_3 storage models, a measurement of how NH_3 adsorption enthalpy changes as more NH_3 is added to the surface yields insights that can direct the development of appropriate modeling strategies. Figure 4(a-d) shows calculations of how adsorption enthalpy changes as a function of coverage for four different commonly used models of adsorption, while figure 4(e) shows the NH_3 adsorption enthalpy measured for a commercial small pore copper zeolite used in General Motors vehicles. For this particular material, a 2-site Langmuir adsorption model gives a much better representation of the adsorption energetics than any of the single site models. Findings such as this provide valuable guidance in the development of more accurate simulation tools, which will be needed to design the next generation of high NOx conversion efficiency aftertreatment systems for lean-burn engines.

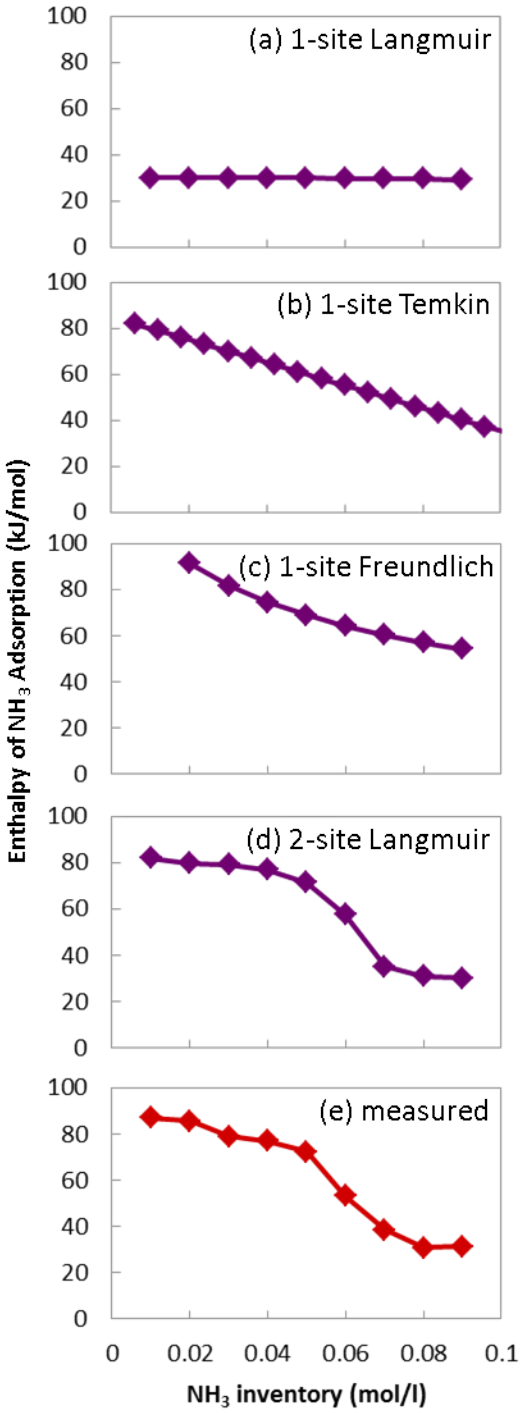

FIGURE 4. NH_3 adsorption enthalpy as a function of NH_3 inventory calculated from (a) 1-site Langmuir, (b) 1-site Temkin, (c) 1-site Freundlich, and (d) 2-site Langmuir model isotherms and (e) measured over a commercial small pore copper zeolite in the presence of 5% H_2O under 12-1,000 ppm NH_3 and at temperatures between 150 and 400°C.

CONCLUSIONS

- During LNT regeneration, the secondary N_2O peak produced upon the switch from rich to lean conditions is formed by reactions involving residual stored NOx, adsorbed reductants or reduction intermediates, and incoming O_2. Secondary N_2O can be minimized by operating at higher temperatures, by generating a more reactive reductant mixture (with more H_2 and less HCs), or by introducing a stoichiometric phase before transitioning to lean conditions to allow time for adsorbed reductants and reductant intermediates to dissipate.
- On a commercial small pore copper zeolite, the Cu sites can participate in oxidation/reduction reactions, and NO^+ appears to be an intermediate in the NO oxidation process. New mechanisms including these findings will be published in the coming year.
- Measurements of NH_3 adsorption enthalpy as a function of NH_3 coverage on a zeolite SCR catalyst surface can be used to guide the selection of appropriate NH_3 storage modeling approaches.
- Humidification, oxidation state, and hydrothermal aging can all impact NH_3 storage energetics on zeolite SCR catalysts.

REFERENCES

1. Šárka Bártová, Petr Kočí, David Mráček, Miloš Marek, Josh A. Pihl, Jae-Soon Choi, Todd J. Toops, William P. Partridge, "New Insights on N_2O Formation Pathways during Lean/Rich Cycling of a Commercial Lean NOx Trap Catalyst", Catalysis Today 231 (2014) 145-154.

FY 2014 PUBLICATIONS/PRESENTATIONS

1. Šárka Bártová, Petr Kočí, David Mráček, Miloš Marek, Josh A. Pihl, Jae-Soon Choi, Todd J. Toops, William P. Partridge, "New Insights on N_2O Formation Pathways during Lean/Rich Cycling of a Commercial Lean NOx Trap Catalyst", Catalysis Today 231 (2014) 145-154.

2. J.A. Pihl, C.S. Daw, "NH_3 storage isotherms: a path toward better models of NH_3 storage on zeolite SCR catalysts," presentation to the U.S. DRIVE Advanced Combustion and Emission Control Tech Team, Southfield, MI, January 9, 2014.

3. J.A. Pihl, C.S. Daw, "NH_3 storage isotherms: a path toward better models of NH_3 storage on zeolite SCR catalysts," presentation to the 2014 DOE Crosscut Workshop on Lean Emissions Reduction Simulation, Dearborn, MI, April 29, 2014.

4. D. Mráček, P. Kočí, M. Marek, J.-S. Choi, J.A. Pihl, T.J. Toops, W.P. Partridge, "Kinetics of N_2O and N_2 Peaks During and After the Regeneration of Lean NOx Trap," presentation to the 2014 DOE Crosscut Workshop on Lean Emissions Reduction Simulation, Dearborn, MI, April 30, 2014.

5. C.S. Daw, J.A. Pihl, J.-S. Choi, M.-Y. Kim, W.P. Partridge, T.J. Toops, V.Y. Prikhodko, C.E.A. Finney, "Joint Development and Coordination of Emissions Control Data and Models (CLEERS Analysis and Coordination)," presentation to the 2014 DOE Vehicle Technologies Office Annual Merit Review and Peer Evaluation Meeting, Washington, DC, June 18, 2014.

6. Š. Bártová, D. Mráček, P. Kočí, M. Marek, J.-S. Choi, "Ammonia reactions with the stored oxygen in a commercial lean NOx trap catalyst", poster to the 23rd International Symposium on Chemical Reaction Engineering, Bangkok, Thailand, September 7-10, 2014.

7. P. Kočí, D. Mráček, M. Marek, J.-S. Choi, J.A. Pihl, T.J. Toops, W.P. Partridge, "N_2O and N_2 formation dynamics during and after the regeneration of lean NOx trap", presentation to the the 8th International Conference on Environmental Catalysis, Asheville, NC, August 24–27, 2014.

8. J.A. Pihl, C.S. Daw, "NH_3 storage isotherms: a path toward better models of NH_3 storage on zeolite SCR catalysts," presentation to the 8th International Conference on Environmental Catalysis, Asheville, NC, August 24–27, 2014.

9. C.S. Daw, J.A. Pihl, J.-S. Choi, W.P. Partridge, T.J. Toops, V.Y. Prikhodko, C.E.A Finney, "Joint Development and Coordination of Emissions Control Data and Models (CLEERS Analysis and Coordination)," presentation to U.S. DOE Advanced Engine Crosscut Team, Southfield, MI, September 11, 2014.

III.3 CLEERS Aftertreatment Modeling and Analysis

Mark Stewart (Primary Contact),
Alla Zelenyuk-Imre, Feng Gao,
George Muntean, Chuck Peden, Ken Rappe,
Janos Szanyi
Institute for Integrated Catalysis
Pacific Northwest National Laboratory (PNNL)
P.O. Box 999, MS K7-15
Richland, WA 99354

DOE Technology Development Manager
Ken Howden

Overall Objectives

- Promote the development of improved computational tools for simulating realistic full-system performance of lean-burn engines and the associated emissions control systems
- Provide the practical and scientific understanding and analytical base required to enable the development of efficient, commercially viable emissions control solutions for ultra-high efficiency vehicles

Fiscal Year (FY) 2014 Objectives

- Lead and contribute to Cross-Cut Lean Exhaust Emissions Reduction Simulations (CLEERS) activities, e.g. lead technical discussions, invite distinguished speakers, and maintain an open dialogue on modeling issues.
- Continue detailed kinetic and mechanistic studies for NO reduction over the state-of-the-art small-pore zeolite-based Cu selective catalytic reduction (SCR) catalysts. A new focus for these studies will be small-pore Fe SCR catalysts, which provide considerable advantages for high-temperature performance over Cu-based catalysts.
- Complete studies of K-based lean-oxides of nitrogen (NOx) trap (LNT) catalysts in this coming year with a focus on properties of spinel magnesium aluminate supports.
- Characterize current production and advanced diesel particulate filter (DPF) substrates through advanced image and statistical analysis of high resolution computed tomography data and extend these studies to include DPFs coated with SCR catalysts for integrated DPF/SCR systems.
- Begin preliminary investigations of novel passive NOx adsorber formulations.
- Characterize particulates produced by advanced, lean-burn spark-ignited direct-injection (SIDI) engines.
- Analyze commercial multi-function SCR filters to determine physical placement of the SCR catalyst within the porous substrate microstructure and the effect it has on flow and backpressure.

FY 2014 Accomplishments

- Seven journal publications, one provisional patent application, two invention reports, and 15 presentations (11 invited).
- Analysis of data previously collected in cooperative experiments with Oak Ridge National Laboratory (ORNL) revealed important differences between particulate populations produced by stoichiometric and lean stratified combustion.
- Continued to obtain highly relevant fundamental insights into the properties of Cu-chabhazite zeolite (CHA)-based SCR catalysts that are recognized internationally as leading the research (see “Special Recognition” section).
- Micro-scale flow and filtration simulations of multi-functional exhaust filters showed how the three-dimensional location of catalysts affects backpressure during soot loading.
- Completed studies of candidate new LNT materials for high-temperature applications. Initiated new studies on passive NOx adsorbers for low-temperature aftertreatment of NOx emissions.

Future Directions

- Experimentally address the continuing fundamental issues being identified in modeling studies.
- Continue studies of the reaction mechanism for Cu-CHA relative to Fe-CHA catalysts:
  - Why differences in NO oxidation, low- and high-temperature performance, and sensitivity to NO/NO_2 ratios?
  - Are there differences in the structure and location of these metal cations?
- In collaboration with partners on a new National Science Foundation/DOE-funded project, probe the nature and stability of the active Cu species in

the CHA-based catalysts, especially for SAPO-34 zeolite-based catalysts.

- Cooperate with ORNL to improve SCR characterization protocols and experiments with fresh and aged samples for model development.
- Recalibrate two-site SCR model with updated high-temperature data and publish results.
- LNT studies will now focus on low-temperature NO adsorption (passive NOx adsorbers). Reducible oxides such as ceria and titania appear to be useful for this but likely prone to aging and sulfur poisoning. Studies this next year will probe mechanisms of NO adsorption and desorption.
- Extend analysis of X-ray computed tomography data to samples with intermediate catalyst loadings to clarify the effect of catalyst loading on catalyst location and backpressure.

INTRODUCTION

CLEERS is an R&D focus project of the Diesel Cross-Cut Team. The overall objective is to promote the development of improved computational tools for simulating realistic full-system performance of lean-burn engines and the associated emissions control systems. Three fundamental research projects are sponsored at PNNL through CLEERS: DPF, SCR, and LNT. Resources are shared between the three efforts in order to actively respond to current industrial needs.

APPROACH

SIDI Particulates: In a recent study, conducted at the ORNL's Fuels, Engines, and Emissions Research Center, we characterized the detailed properties of particulate matter (PM) emissions generated by a 2.0-L lean-burn SIDI engine (2008 BMW 1-Series) operated using different combustion strategies that include lean-homogeneous, lean-stratified, stoichiometric, and fuel-rich conditions. A three-way catalyst was installed on the engine and both engine-out and catalyst-out exhaust PM was characterized. In addition to the measurements of PM number concentrations and size distributions, we characterized the size, mass, composition, and effective density of individual exhaust particles emitted under ~20 different engine operating conditions. These measurements are used to calculate fractal dimension, average diameter of primary spherules, and number of spherules, void fraction, and dynamic shape factors as function of particle size.

Multi-Functional Exhaust Filters: We developed computer programs to analyze micro X-ray computed tomography scans of high porosity cordierite filters commercially coated with a state-of-the-art SCR catalyst. We used image processing techniques, along with mercury porosimetry data, to identify the three-dimensional locations of the zeolite catalyst with respect to the substrate microstructure. We then conducted micro-scale flow and filtration simulations using the lattice-Boltzmann method in order to examine the effect of the catalyst on flow paths through the filter walls and backpressure during filtration.

SCR: Considerable progress has been made in updating SCR kinetics models to accurately describe the performance of state-of-the-art Cu-CHA catalysts. However, a need still exists for accurate yet relatively simple global kinetics models for design of aftertreatment systems. Moreover, systems designers need a simple method to account for changes in performance due to aging over the life of an SCR unit. Investigations of SCR catalysts involve the coordinated efforts of modeling, testing and research. In FY 2013 PNNL bolstered its test capability with the development of an automated protocol reactor system. In FY 2014, this capability became available for round-robin testing of a new Low Temperature Oxidation protocol developed by the U.S. DRIVE/Advanced Combustion and Emission Control (ACEC) Tech Team.

LNT Fundamentals Research: PNNL fundamental studies of possible new LNT formulations able to function at higher temperatures than the current generation of Ba-based materials has focused on changes in the composition of both the NOx storage and support materials. In particular, substituting K for Ba as the NOx storage material, and substitution of traditional alumina supports with spinel magnesium aluminate are known to provide higher temperature performance. During FY 2014, we completed our studies of the effects of LNT catalyst supports and K-loading on the NOx reduction performance of K- and Ba-based catalysts. In FY 2015, we will initiate fundamental studies of passive NOx adsorber materials.

RESULTS

SIDI Particulates: Overall, properties of gasoline direct-injection PM were shown to vary significantly depending on engine operation condition. Figure 1 shows, as an example, distributions of vacuum aerodynamic diameters of particles emitted under lean-stratified and stoichiometric conditions (1,000 rpm, 1 bar). The data show that lean-stratified operation yielded the most diesel-like size distributions. The vast majority of these particles are fractal soot agglomerates

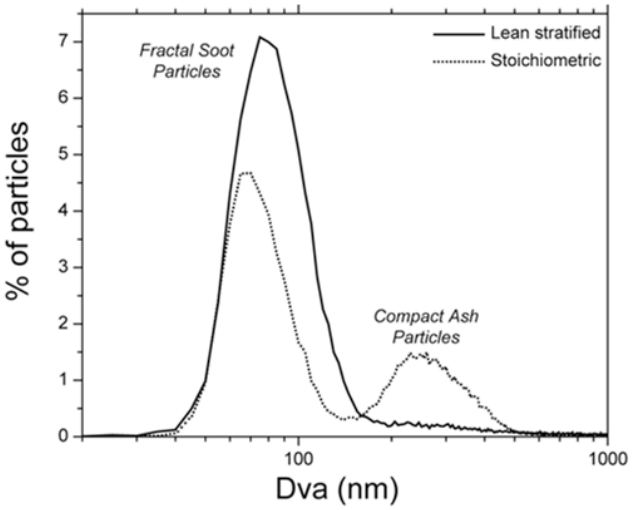

FIGURE 1. Distributions of vacuum aerodynamic diameters of particles emitted under lean-stratified and stoichiometric conditions (1,000 rpm, 1 bar).

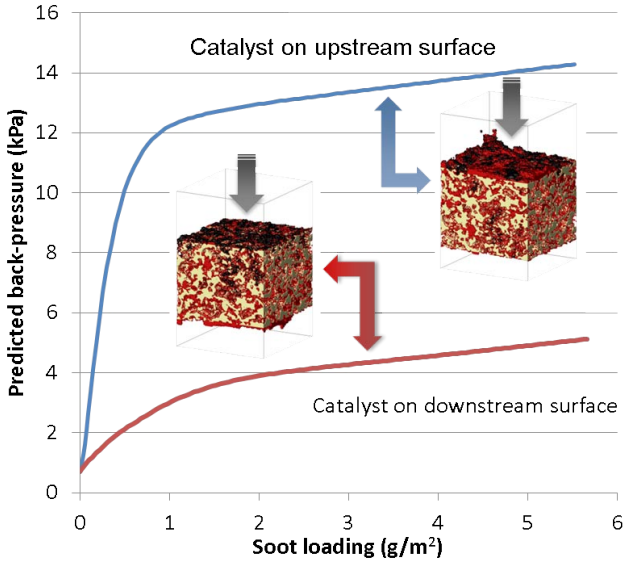

FIGURE 2. Simulation results showing dramatically different back-pressure profiles with respect to soot loading as a multi-functional filter is exposed to exhaust from different orientations.

comprising primary spherules with an average diameter of 22 nm. They have a fractal dimension of 2.18 and are composed of elemental carbon (>80%), small amounts of organics (consisting mostly of carboxylic acids with very small contributions by hydrocarbons and polycyclic aromatic hydrocarbons), and some Ca from lube detergent additives. Stoichiometric operation resulted in PM number concentrations an order of magnitude lower than those emitted under lean-stratified operation. While fractal soot particles emitted under stoichiometric operation are very similar to those emitted under lean stratified operation, stoichiometric PM contains a higher (~50%) number fraction of non-fractal ash particles. These particles represent the dominant fraction of PM mass.

Multi-Functional Exhaust Filters: The filters examined were coated primarily from one side of the filter walls, where the catalyst interacts with a relatively low porosity region at the wall surfaces, which we have found to be a common feature of extruded porous ceramic honeycombs. This appears to result in the blockage of many flow paths through the catalyzed filter wall at that surface. Lattice-Boltzmann filtration simulations were able to qualitatively duplicate behavior observed during filtration experiments with the same multi-functional filters: backpressure during soot loading was dramatically higher when the filters were oriented such that soot collected on the more heavily catalyzed filter wall. The higher backpressures were caused when soot covered the relatively sparse openings in the catalyzed wall surface. Backpressures were significantly lower when the filter was loaded from the opposite direction, since the layer of soot formed where there were more openings through the porous wall, resulting in lower local velocities through the soot layer. Simulation results are shown in Figure 2. The ability to examine where catalyst resides in multi-functional filters and how its presence affects backpressure, filtration, and NOx abatement performance will support development of future filter substrates and coating techniques for optimum performance and higher overall fuel efficiency.

SCR Fundamentals: During FY 2014, PNNL researchers continued fundamental studies of state-of-the-art small-pore Cu-CHA catalysts with a focus on both the chemical and physical nature of the active Cu site and the mechanism of the SCR reaction. Extensive kinetics studies of the performance of these catalysts and spectroscopic measurements of the Cu-CHA materials under realistic reaction conditions were performed. This work has been documented in a number of publications as listed at the end of this report. Highlighted here are results that provide important new information about the nature of the active Cu species under realistic SCR conditions.

Prior to full dehydration of the zeolite catalysts, hydrated Cu^{2+} ions are found to be very mobile as judged from electron paramagnetic resonance. NO oxidation is catalyzed by O-bridged Cu-dimer species that form at relatively high Cu loadings and in the presence of O_2. For NH_3 oxidation on samples with low to intermediate Cu loadings, transient Cu-dimers are the low-temperature (≤300°C) active centers, while these dissociate to monomers at 350°C and above and become active centers. For the much more complex standard SCR reaction, transient Cu-dimers are proposed to be the active sites for reaction temperatures <250°C at

very low Cu loadings (Cu/Al ≤0.016). Between ~250 and 350°C, these Cu-dimers become less stable, due to loss of coordinating water and/or ammonia molecules, causing SCR reaction rates to decrease. At temperatures ≥350°C, Cu^{2+} monomers that had migrated to faces of 6-membered rings are the active sites. The changing nature of the active Cu species provides a highly likely explanation for the unusual kinetics observed for SCR over Cu/CHA catalysts, the so-called "seagull-shape" performance curves, as illustrated in Figure 3. Also shown in the figure are schematic structures for the active Cu species at various temperatures.

Low-Temperature Protocol Development: Low-temperature exhaust conditions, associated with new powertrains being developed for future fuel-efficient engines, are especially challenging for any current aftertreatment technology to meet regulated standards. This new focus area of catalyst research is occurring at various institutions across the nation to address this significant challenge. Considering this, the U.S. DRIVE/ACEC Tech Team has identified the need for consistent and realistic metrics of catalyst evaluation. In response, PNNL is leading a team of researchers at General Motors, Ford, Chrysler and ORNL in the development of catalyst test protocols, or standardized test procedures that are relatively simple and efficient to execute, yet sufficiently capture the technology's performance capability. The team has completed the first step in this effort, an oxidation catalyst test protocol (Figure 4). The intent of the catalyst test protocols is to maximize the value and impact of reported data in a manner that is consistent with anticipated technologies and has industry and community consensus.

LNT Fundamentals: MgAlOx mixed oxides have been employed as support materials for potassium-based LNTs in high-temperature applications. Effects of support composition, K/Pt loadings, thermal aging and catalyst regeneration on NOx trapping capacity were systematically investigated, and the catalysts carefully characterized by X-ray diffraction, NOx-temperature programmed desorption, electron microscopy (transmission electron microscopy and high angle annular dark field scanning transmission electron microscopy), and in situ X-ray absorption spectroscopy. Combined results from these measurements indicate that Pt species in the thermally aged samples are highly dispersed in the oxide matrix as isolated atoms as shown in Figure 5. This strong metal-support interaction stabilizes Pt and minimizes the extent of sintering. However, such strong interactions result in Pt oxidation via coordination with the support so that NO oxidation activity cannot be maintained after aging. This, in turn, decreases NOx trapping ability for catalysts after thermal aging. Interestingly, a high-temperature reduction treatment remarkably regenerates the NOx trapping capability. After regeneration, the $Pt/K/MgAlO_x$ catalysts exhibit much better NOx trapping performance than the $Pt/K/Al_2O_3$ catalysts over the entire temperature range that we investigated.

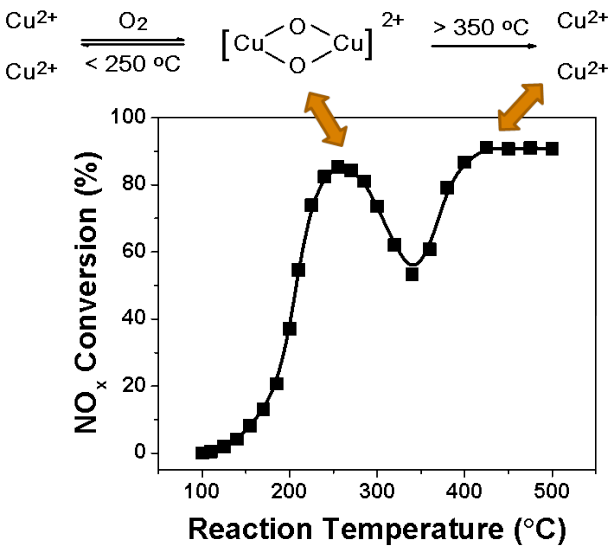

FIGURE 3. Steady-state NOx conversion during "standard" SCR over a Cu-CHA catalyst. Note the so-called "seagull shape" to the performance curve. Also shown schematically are possible active Cu species structures present under various reaction conditions, explaining the "seagull-shape."

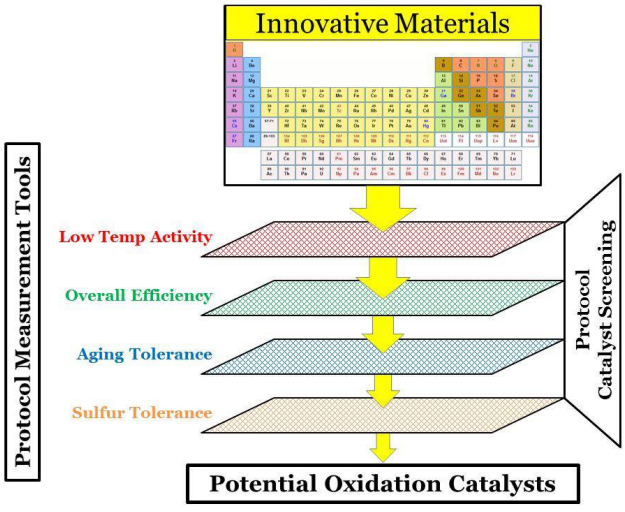

FIGURE 4. Oxidation catalyst test protocol for efficiently and reproducibly screening catalyst technologies for low-temperature activity, overall efficiency, and tolerance to thermal aging and chemical poisoning.

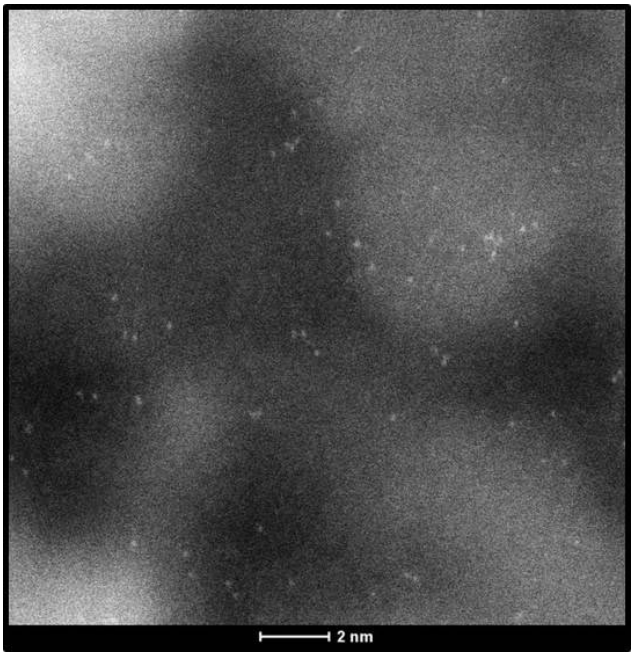

FIGURE 5. High-angle annular dark field-scanning transmission electron microscopy images of an aged 10K/Pt/MG30 sample.

CONCLUSIONS

- Diesel-like particulates are produced by a state-of-the-art European SIDI engine when operating in lean-stratified mode, along with large compact ash particles. Soot production is dramatically reduced during stoichiometric combustion, leading to a higher proportion of ash particles.
- Current commercial coating techniques for multi-functional materials efficiently use much of the pore volume inside high porosity substrate walls. However, relatively low porosities at the wall surfaces are exacerbated by the presence of the catalyst, which can have a dramatic impact on backpressures during filtration.
- In fundamental SCR studies, significant new information concerning the nature of the active Cu species in Cu-CHA-based catalysts has been obtained. These studies are providing important new insights into important phenomena observed for practical catalysts under their operating conditions. New studies have been initiated (but not discussed here) on Fe-CHA catalysts. A significant initial conclusion from this work is an explanation for why mixed Cu- and Fe-CHA catalysts can provide significant advantages by taking advantage of their individual attributes that are not shared by the other.
- We completed our studies this year on candidate high-temperature LNT materials with one conclusion being that K-based materials are not likely to be viable for vehicle applications. Studies are now focusing on the development of candidate low-temperature passive NOx adsorber materials.

FY 2014 PUBLICATIONS/PRESENTATIONS

Publications

1. Zammit, M; DiMaggio, C.L.; Kim, C.H.; Lambert, C.K.; Muntean, G.G.; Peden, C.H.F.; Parks, J.E.; Howden, K. "Future Automotive Aftertreatment Solutions: The 150°C Challenge Workshop Report." U.S. Drive Report (Southfield, MI) 2013, PNNL-22815.

2. Gao, F.; Kwak, J.H.; Szanyi, J.; Peden, C.H.F. "Current Understanding of Cu-Exchanged Chabazite Molecular Sieves for Use as Commercial Diesel Engine DeNOx Catalysts." Topics in Catal. **56** (2013) 1441-1459.

3. Kwak, J.H.; Varga, T.; Peden, C.H.F.; Gao, F.; Hanson, J.C.; Szanyi, J. "Following the Movement of Cu Ions in a SSZ-13 Zeolite During Dehydration, Reduction and Adsorption: A Combined in situ TP-XRD, XANES/DRIFTS Study." J. Catal. **314** (2014) 83-93.

4. Zelenyuk, A.; Reitz, P.; Stewart, M.; Imre, D.; Loeper, P.; Adam, C.; Foster, D.; Rothamer, D.; Andrie, M.; Krieger, R.; Narayanaswamy, K.; Najt, P.; Solomon, A. "Detailed Characterization of Particulates Emitted by Pre-commercial Single-cylinder Gasoline Direct Injection Compression Ignition Engine." Combust. Flame **161** (2014) 2151-2164.

5. Wang, D.; Gao, F.; Peden, C.H.F.; Kamasamudram, K.; Epling, W.S. "Excellent Performance in Selective Catalytic Reduction of NOx with NH_3 (NH_3-SCR) over a Cu-SSZ-13 Catalyst Prepared by a Solid State Ion Exchange Method." ChemCatChem (2014) in press.

6. Gao, F.; Walter, E.D.; Kollar, M.; Wang, Y.; Szanyi, J.; Peden, C.H.F. "Understanding Selective Catalytic Reduction Kinetics over Cu-SSZ-13 from Motion of the Cu Ions." J. Catal. (2015) in press.

7. Zhang, R.; McEwen, J.-S.; Kollar, M.; Wang, Y.; Gao, F.; Szanyi, J.; Peden, C.H.F. "NO Chemisorption on Cu/SSZ-13: a Comparative Study from Infrared Spectroscopy and DFT Calculations." ACS Catal. (2015) in press.

Invention Disclosures

1. Stewart, ML, GG Muntean. "Process for modifying ceramic exhaust filter substrates to achieve greater fuel efficiency." Invention Disclosure, June 2014; #30626-E.

2. Stewart, ML, GG Muntean. "Software and methodology for identifying catalyst distribution in multi-function ceramic exhaust filters." Invention Disclosure, June 2014; #30616-E.

Invited Presentations

1. Peden CHF. "Future Challenges for Catalytic Vehicle Emission Control." Presented by **Chuck Peden (Invited Speaker)** to the University of Toronto, Department of Chemical

Engineering and Applied Chemistry, Toronto, ON, Canada, October 2013.

2. Gao, F; J Szanyi, and CHF Peden. "Cu/CHA materials for the selective catalytic reduction of NOx with NH_3: Catalyst structure/function and mechanistic studies." Presented by **Chuck Peden (Invited Speaker)** at the 2013 AIChE National Meeting, San Francisco, CA, November 2013.

3. Gao F, J Szanyi, and CHF Peden. "Changing Nature of the Active Cu Species During NH_3 SCR over Cu/CHA Catalysts." Presented by **Chuck Peden (Invited Speaker)** for the CLEERS Conference Call, January 2014.

4. Gao, F; JH Kwak, HY Zhu, J Szanyi, and CHF Peden. "Cu-CHA Catalysts for the Selective Catalytic Reduction of NOx with NH_3: Catalyst Structure/Function and Mechanistic Studies." Presented by **Chuck Peden (Invited Speaker)** at the 247th ACS National Meeting, Dallas, TX, March 2014.

5. Zammit, M, C DiMaggio, M Smith, C Lambert, J Theis, C Kim, J Parks, J Pihl, S Daw, G Muntean, C Peden, K Rappe, K Birnbaum, D Tran, M Stewart, and K Howden. "Protocol Development Update." Presented by **George Muntean (Invited Speaker)** for the CLEERS Conference Call, April 2014.

6. Zelenyuk, A. "Detailed Characterization of Particulates Emitted by a Lean-Burn Gasoline Direct Injection Engine." Presented by **Alla Zelenyuk (Invited Speaker)** at the 18th Annual CLEERS Workshop, Dearborn, MI, April 2014.

7. Stewart, ML. "Microstructural features of catalyzed and uncatalyzed DPFs." Presented by **Mark Stewart (Invited Seminar)** at the Advanced Combustion Engine Tech Team Meeting, Southfield, MI, May 2014.

8. Gao, F, GG Muntean, CHF Peden, K Rappe, ML Stewart, J Szanyi, DN Tran, and Y Wang. "CLEERS Aftertreatment Modeling and Analysis." Presented by **George Muntean (Invited Speaker)** at Vehicle Technologies Program Annual Merit Review and Peer Evaluation Meeting, Washington, DC, June 2014.

9. Peden CHF, F Gao, J Szanyi, JH Kwak, M Kollar, and Y Wang. "Cu-CHA zeolite materials for the selective catalytic reduction of NOx with NH_3: Catalyst structure/function and mechanistic studies." Presented by **Chuck Peden (Invited Speaker)** at the Seventh Tokyo Conference on Advanced Catalytic Science and Technology (TOCAT7), Kyoto, Japan, June 2014.

10. Stewart, ML. "Microstructural features of catalyzed and uncatalyzed exhaust particulate filters." Presented by **Mark Stewart (Invited Seminar)** at Corning Incorporated Sullivan Park R&D Center, Corning, NY, July 2014.

11. Gao F, M Kollar, Y Wang, J Szanyi, and CHF Peden. "Understanding ammonia selective catalytic reduction kinetics over Cu/SSZ-13 from motion of the Cu ions." Presented by **Feng Gao (Invited Speaker)** at the 248th ACS National Meeting, San Francisco, CA, August 2014.

Contributed Presentations

1. Stewart, ML. "Microstructural features of catalyzed and uncatalyzed DPFs." Presented by Mark Stewart at the 18th Annual CLEERS Workshop, Dearborn, MI, April 2014.

2. Gao F, Y Wang, M Kollar, ED Walter, J Szanyi, and CHF Peden. "Structure/Activity Relationships in Cu-CHA-Based NH3 Selective Catalytic Reduction Catalysts." Presented by Chuck Peden at the 18th Annual CLEERS Workshop, Dearborn, MI, May 2014.

3. Kwak JH, T Varga, CHF Peden, F Gao, JC Hanson, and J Szanyi. "Following the movement of Cu ions in a SSZ-13 zeolite during dehydration, reduction and adsorption: a combined in situ TP-XRD, XANES/DRIFTS study." Presented by Janos Szanyi at the 8th International Conference on Environmental Catalysis, Asheville, NC, August 2014.

4. Gao F, M Kollar, Y Wang, ED Walter, NM Washton, J Szanyi, and CHF Peden. "Understanding NH3-SCR kinetics over Cu-SSZ-13 catalysts from motion of the Cu ions." Presented by Feng Gao at the 8th International Conference on Environmental Catalysis, Asheville, NC, August 2014.

SPECIAL RECOGNITIONS AND AWARDS/ PATENTS ISSUED

1. Stewart, ML, GG Muntean. "Process for modifying ceramic exhaust filter substrates to achieve greater fuel efficiency." Provisional Patent Application, July, 2014; #8753.

2. The Elsevier-published journal, the *Journal of Catalysis*, just released the most cited papers for 2012-2013. One of our earlier publications, from work funded by this program, made the list. The paper described how very high temperatures change the reactivity of Cu/CHA catalysts in comparison to other Cu/zeolite materials.

3. PNNL hosted Dr. Hai-Ying Chen, Scientific and Product Development Manager at Johnson Matthey's Emission Control Technologies Division, for an extended (two month) visit during the summer of 2014. Dr. Chen carried out fundamental studies of N_2O formation on zeolite-based SCR catalysts with staff in the Institute for Integrated Catalysis at PNNL.

4. Chuck Peden was named a "Wiley Research Fellow" for the Environmental Molecular Sciences Laboratory, a Department of Energy/Office of Science national scientific user facility funded by the DOE's Biological and Environmental Research (BER) program.

III.4 Enhanced High- and Low-Temperature Performance of NOx Reduction Catalyst Materials

Feng Gao, George Muntean,
Chuck Peden (Primary Contact)
Institute for Integrated Catalysis
Pacific Northwest National Laboratory (PNNL)
P.O. Box 999, MS K2-12
Richland, WA 99354

DOE Technology Development Manager
Ken Howden

Cooperative Research and Development Agreement (CRADA) Partners
- Neal Currier, Krishna Kamasamudram, Ashok Kumar, Junhui Li, Jinyong Lou, Randy Stafford, Alex Yezerets – Cummins Inc.
- Mario Castagnola, Hai-Ying Chen, Howard Hess – Johnson Matthey

Objectives

Identify approaches to significantly improve both the high- and low-temperature performance, and the stability of the catalytic oxides of nitrogen (NOx) reduction technologies via a pursuit of a more fundamental understanding of:

- the various roles for the multiple catalytic materials
- the mechanisms for these various roles
- the effects of high temperatures on the performance of these catalyst component materials in their various roles
- mechanisms for higher temperature NOx storage performance for modified and/or alternative storage materials
- the interactions between the precious metals and the storage materials in both optimum NOx storage performance and long-term stability
- modes of thermal degradation of new generation chabhazite zeolite (CHA) zeolite-based selective catalytic reduction (SCR) catalysts
- the sulfur adsorption and regeneration mechanisms for NOx reduction catalyst materials

Fiscal Year (FY) 2014 Objectives

- Complete catalyst characterization of model K/titania-based high-temperature NOx storage and reduction (NSR) catalysts with a variety of state-of-the-art methods.
- Complete comparative studies of the synthesis of model Cu-SAPO-34 CHA zeolite-based catalysts for ammonia SCR.
- Carry out performance and thermal durability studies of model Cu-SAPO-34 CHA zeolite-based catalysts.
- Initiate similar studies on Fe-based CHA zeolite catalysts.

FY 2014 Accomplishments

- Two research thrusts continued this year:
  - Mechanisms for high- and low-temperature performance stability of CHA-based zeolites (primary activity—will be focus of this report)
    - Based on prior literature reports, several synthesis efforts were carried out at PNNL to prepare model CHA-based catalysts.
    - Catalysts were characterized before and after incorporation of Fe by nuclear magnetic resonance (NMR), Mossbauer and Fourier transform infrared (FTIR) spectroscopies.
    - Baseline reactivity measurements were performed on these catalysts in preparation for mechanistic studies of high-and low-temperature performance loss.
    - New CHA-based formulations were discovered and their initial “standard” SCR performance has been assessed.
  - Fundamental studies of high-temperature NSR catalysts prepared by PNNL
    - The synthesis, characterization of stability of a variety of model K-titania catalysts were completed this year.
- Seven manuscripts, one invention report, and six public presentations (three invited) have resulted from this project this year.

Future Directions

- The primary activities will be focused on the mechanisms for low- and high-temperature performance loss as a function of operation

conditions of new generation CHA-based NH_3 SCR catalysts. For these studies, we will utilize the model catalysts prepared via methods studied in this past two FYs (FY 2013 and FY 2014). These fundamental studies will be carried out in conjunction with baseline performance and stability experiments on fully formulated catalysts.

- Having completed the studies of K-based high temperature NSR materials this past year, we will initiate studies of the low-temperature performance of promising candidate passive NOx adsorber materials.

INTRODUCTION

Two primary NOx aftertreatment technologies have been recognized as the most promising approaches for meeting stringent NOx emission standards for diesel vehicles within the Environmental Protection Agency's 2007/2010 mandated limits, NOx NSR and NH_3 SCR; both are, in fact being commercialized for this application. Small pore copper ion exchanged zeolite catalysts with a CHA structure have recently been shown to exhibit both remarkable activity and very high hydrothermal stability in the NH_3 SCR process [1]. The NSR (also known as the lean-NOx trap, LNT, or NOx absorber) technology is based upon the concept of storing NOx as nitrates over storage components, typically barium species, during a lean-burn operation cycle, and then desorbing and subsequently reducing the stored nitrates to N_2 during fuel-rich conditions over a precious metal catalyst [2]. However, in looking forward to 2015 and beyond with expected more stringent regulations, the continued viability of the NSR technology for controlling NOx emissions from lean-burn engines such as diesels will require at least two specific, significant and inter-related improvements. First, it is important to reduce system costs by, for example, minimizing the precious metal content while maintaining, even improving, performance and long-term stability. A second critical need for future NSR systems, as well as for NH_3 SCR, will be significantly improved higher and lower temperature performance and stability. Furthermore, these critically needed improvements will contribute significantly to minimizing the impacts to fuel economy of incorporating these after-treatment technologies on lean-burn vehicles. To meet these objectives will require, at a minimum an improved scientific understanding of the following things:

- the various roles for the precious and coinage metals used in these catalysts
- the mechanisms for these various roles
- the effects of high temperatures on the active metal performance in their various roles
- mechanisms for higher temperature NOx storage performance for modified and/or alternative storage materials
- the interactions between the precious metals and the storage materials in both optimum NOx storage performance and long-term stability
- the sulfur adsorption and regeneration mechanisms for NOx reduction materials
- materials degradation mechanisms in CHA-based NH_3 SCR catalysts

The objective of this CRADA project is to develop a fundamental understanding of the previously listed issues. Model catalysts that are based on literature formulations are the focus of the work being carried out at PNNL. In addition, the performance and stability of more realistic catalysts, supplied by the industrial CRADA partners, are being studied in order to provide baseline data for the model catalysts that are, again, based on formulations described in the open literature.

For this short summary, we will briefly highlight results from our recent studies of the stability of candidate K-based high-temperature NSR materials, and comparative studies of low-temperature performance of SSZ-13 and SAPO-34 CHA catalysts; in particular, recent results comparing Fe- and Cu-based CHA materials.

APPROACH

In microcatalytic reactor systems, catalyst performance is evaluated in two separate fixed bed reactors. In the NSR technology, the state of the system is constantly changing so that performance depends on when it is measured. Therefore in studies at PNNL, we obtain NOx removal efficiencies as "lean conversion (30 minutes)," which measures NOx removal efficiencies for the first 30 minutes of a lean period that follows multiple lean-rich cycles to insure consistent behavior. We have established a reaction protocol, which evaluates the performance of samples after various thermal aging and sulfation condition. In this way, we could identify optimum de-sulfation treatments to rejuvenate catalyst activities.

Based on formulations and synthesis procedures described in the literature, PNNL has prepared model NSR and NH_3 SCR catalysts. Activity and performance stability measurements were performed. State-of-the-art catalyst characterization techniques such as X-ray diffraction, X-ray photoelectron spectroscopy, FTIR, nuclear magnetic resonance (NMR), electron paramagnetic resonance, transmission electron

microscopy/energy dispersive spectroscopy, Brunauer-Emmett-Teller pore size distribution, and temperature programmed desorption/reaction (TPD/TPRX) were utilized to probe the changes in physicochemical properties of the PNNL-prepared model catalyst samples under deactivating conditions; e.g., thermal aging and SO_2 treatment.

RESULTS

High-Temperature NSR Catalysts Prepared by PNNL

K-loading and thermal stability of model Pt-K/TiO_2 NSR catalysts: To date in this project, we have studied various characteristics of PtK/Al_2O_3 and PtK/$MgAl_2O_4$ LNT catalysts including the effect of K loading on nitrate formation/decomposition, NOx storage activity, and durability [3-6]. Due to issues of K morphology stability, we initiated a number of studies on titanate-supported K NSR catalysts. In this past year, we completed our studies of these materials. Indeed, we found that the reaction of K with TiO_2 to form potassium titanates can lead to a positive increase in the stability of K. Unfortunately, however, this reaction continues to proceed after pre-calcination treatments; in particular, at increasing K contents and temperatures, continuously decreasing NO_x storage performance due to formation of potassium titanates that block K sites, rendering them unavailable for storage of NOx. For example, one of our most promising results was obtained for a K-based catalyst supported on a crystalline $K_2Ti_6O_{13}$ material. Figure 1(a) demonstrates the significantly better performance of this catalyst relative to two catalysts prepared on the $K_2Ti_6O_{13}$ material itself and by deposition K onto TiO_2 supports. However, as shown in Figure 1(b), this catalyst was still unstable under hydrothermal aging conditions likely due to K migration. On this basis, we have concluded that K-based LNTs, while promising for high temperature applications due to the increased stability of their nitrates relative to Ba-based catalysts, will not be viable commercially in vehicle applications due to their insufficient stability to aging.

Synthesis and Initial Evaluation of Model Fe/CHA Zeolite Catalysts at PNNL

Using a traditional aqueous solution ion-exchange method under a protecting atmosphere of N_2, an Fe/SSZ-13 catalyst active in NH_3-SCR was synthesized [7]. Mössbauer and FTIR spectroscopies were used to probe the nature of the Fe sites as discussed briefly in the following. NO/NH_3 oxidation reaction tests reveal that dehydrated cationic Fe are substantially more active in catalyzing oxidation reactions than the hydrated ones. For NH_3-SCR, enhancement of NO oxidation under 'dry' conditions promotes SCR rates below ~300°C. This is due mainly to contribution from the "fast" SCR channel. Above ~300°C, enhancement of NH_3 oxidation under 'dry' conditions, however, becomes detrimental to NOx conversions. The hydrothermal aging sample loses much of the SCR activity below ~300°C; however, above ~400°C much of the activity remains. This may suggest that the $FeAlO_x$ and FeO_x species become active at such elevated temperatures. Alternatively, the high-temperature activity may be maintained by the remaining extra-framework cationic species.

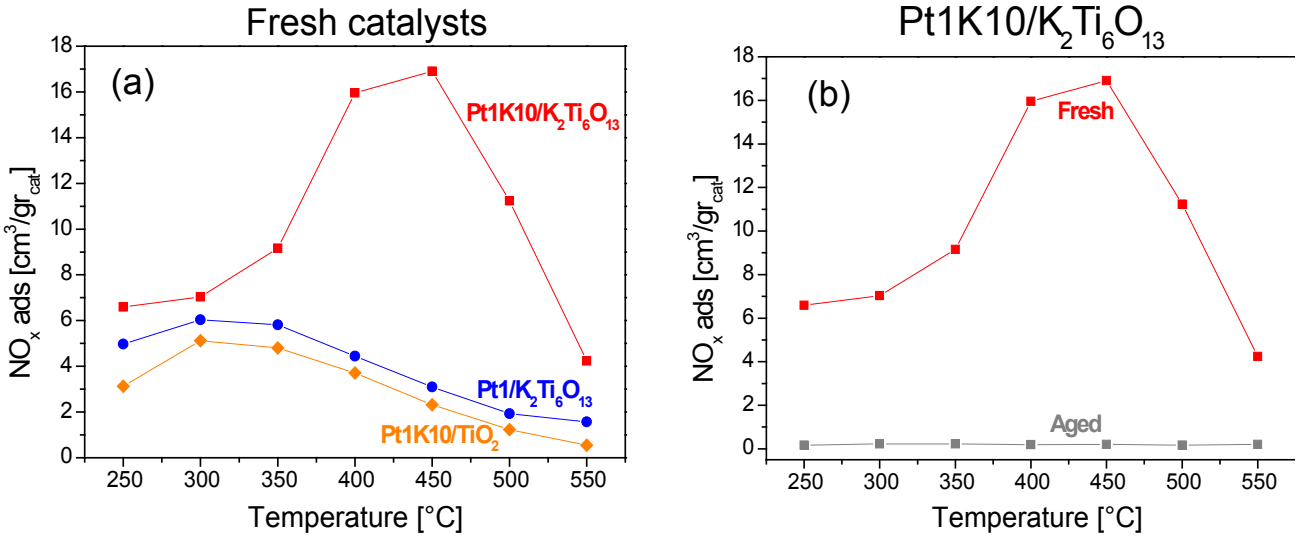

FIGURE 1. (a) Comparison of NOx stored amount over fresh PtK10/TiO_2, Pt/$K_2Ti_6O_{13}$, Pt1K10/$K_2Ti_6O_{13}$ samples; and (b) comparison of NOx stored amount over fresh and aged Pt1K10/$K_2Ti_6O_{13}$ samples. LNT test: Lean Phase: NO 150 ppm + O_2 5% v/v + CO_2 5% v/v + H_2O 5% v/v in He; Rich Phase: H_2 4% v/v + CO_2 5% v/v + H_2O 5% v/v in He.

In addition to steady-state measurements, transient SCR performance measurements were performed. In these experiments, after the reactant feed is turned on, the samples are first maintained at 100°C for 1 h, then ramped to 500°C at 2°C/min, cooled back to 100°C at 2°C/min, and maintained at 100°C for 1 h before the feed is turned off. Finally, after purging with dry N_2 at 100°C for 1 h, a TPD experiment was conducted (not shown here) at 10°C/min to desorb species that are adsorbed/deposited on the catalysts during reaction. Both standard- and fast-SCR are probed in this case. Note that these measurements are a very good supplement to steady-state measurements in studying transient kinetic behaviors, kinetic hysteresis, NH_3 and NH_4NO_3 inhibitions, etc.

Figure 2(a) presents NO outlet concentrations (in ppm, measured with an online FTIR cell) during temperature ramping for standard SCR. In two temperature ranges (i.e., 100-250°C and 450-500°C), no hysteresis is observed. However, from 250 to ~330°C, NO outlet values during heating are higher than that during cooling, while from 330 to 450°C, NO outlet concentrations during heating are lower than that during cooling. Figure 2(b) shows the corresponding NH_3 outlet values. During heating, NH_3 outlet concentrations gradually decrease and only become undetectable above 450°C. However, during the cooling step, zero NH_3 outlet values are maintained until ~290°C and then increase abruptly as the temperature further decreases.

Similar experiments, conducted under fast SCR conditions ($NO + NO_2 + 2NH_3 = N_2 + 3H_2O$), were also performed but are only briefly described here. For NO, very minor hysteresis is found between ~200 and ~280°C where outlet NO concentrations are slightly higher during heating indicative of some inhibition by NH_3 and/or NH_4NO_3. At temperatures above ~280°C, no NO in the outlet is observed. The behavior of NO_2, however, is very different. In this case, the 1 h waiting period at 100°C prior to temperature ramping is far from sufficient for the NO_2 outlet to reach the inlet concentration (175 ppm). This indicates extensive NO_2 storage. However, control experiments without co-feeding NH_3 demonstrate that the catalyst is only capable of storing much lower amounts of NO_2. Therefore, NO_2 must be storing as ammonium nitrate/nitrite in the presence of NH_3. This point is partially confirmed from the detection of N_2O between 200 and 300°C during ramping up the catalyst. Since NOx storage is not expected at temperatures where NH_4NO_3 becomes unstable, the lack of NOx in the outlet above ~300°C suggests that NO and NO_2 are completely converted to N_2. This result is fully expected since in the absence of NH_3/NH_4NO_3 inhibition (which is met at temperatures above ~300°C), fast SCR can be expected to proceed more rapidly than standard SCR for Fe-based catalysts. The corresponding NH_3 outlet concentrations during the experiment, to some extent, resemble the NOx outlet curves but with some distinct differences. During the heating step, NH_3 outlet values do not decrease to zero above ~300°C as do NOx concentrations, due to desorption of stored NH_3 at lower temperatures. During the cooling step, NH_3 outlet values remain negligible until ~220°C, much lower than ~300°C at which NOx concentrations start to be detected in the outlet. Again, this is due to the extra NH_3 storage at Brønsted acid sites.

Finally for these studies, we briefly describe some of the results of the characterization of these Fe/SSZ-13 catalysts. In fresh samples, the majority of Fe species are extra-framework cations. The likely monomeric and

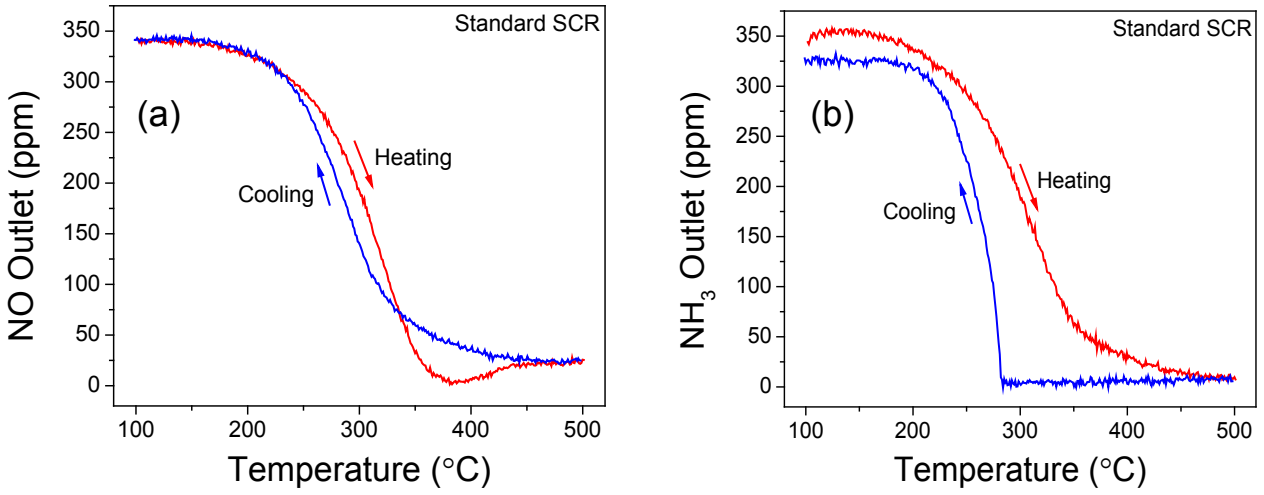

FIGURE 2. NO (a) and NH_3 (b) outlets during temperature-programmed standard NH_3–SCR reaction on the fresh Fe/SSZ-13 sample. Reactant feed contains 350 ppm NO, 350 ppm NH_3, 14% O_2, 2.5% H_2O balanced with N_2 at a gas hourly space velocity of 200,000 h^{-1}. The sample is exposed to the feed at 100°C for 1 h and ramped to 500°C at 2°C/min, and then ramped from 500 to 100°C at 2°C/min, and maintained at 100°C for 1 h before finish.

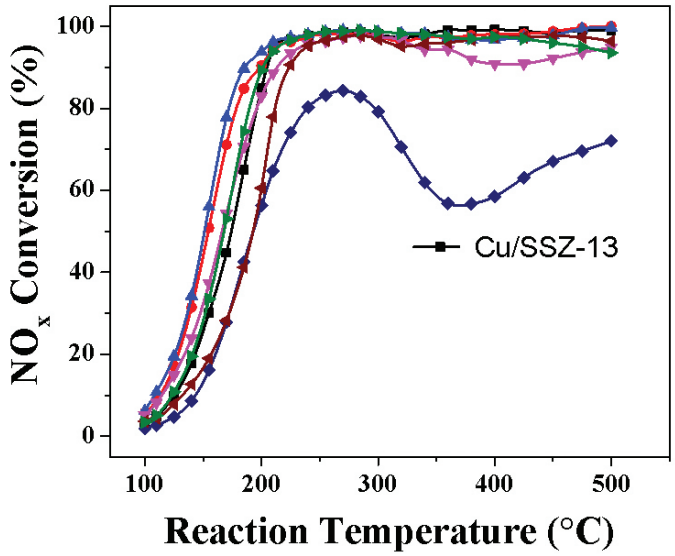

Sample	T_{50} (°C)
Cu/SSZ-13	174
Red Circles	154
Blue Triangles	151
Pink Inverted Triangles	166
Brown Triangles	193
Dark Blue Diamonds	193
Green Triangles	168

FIGURE 3. 'Light-off' curves for the "standard" SCR of NOx with NH_3 for an industry standard material (Cu-SSZ-13 – black squares) and a range of recently synthesized Cu/zeolite-based catalysts (patent currently being filed by PNNL). Note especially, the very low (~150°C) 'light-off' temperature for material indicated by the blue triangles.

dimeric ferric ions in hydrated form are $[Fe(OH)_2]^+$ and $[HOFeOFeOH]^{2+}$, based on Mössbauer measurements. During the harsh hydrothermal aging applied in this study, a majority of cationic Fe species convert to $FeAlO_x$ and clustered FeO_x species, accompanied by dealumination of the SSZ-13 framework. The clustered FeO_x species do not give a sextet Mössbauer spectrum, indicating that these are highly disordered. However, some Fe species in cationic positions remain after aging as determined from Mössbauer measurements and CO/NO FTIR titrations.

Unexpected Low-Temperature Performance in Modified CHA-Based Catalysts

PNNL's recent studies of CHA-based catalysts for NH_3 SCR recently discovered new formulations that can significantly affect the temperature at which these catalysts perform [8]. Notably, the temperature at which the catalyst 'lights off' is critical and is highly desirable for this temperature to be reduced. As demonstrated in Figure 3, a reduction in 'light-off' temperature can be as much as 25°C in these new but non-optimized catalysts. An appropriate measure of low-temperature activity is the so-called T-50, measured as part of a performance 'light-off' curve. The T-50 measures the temperature at which conversion is 50%. Thus, the T-50 is a good qualitative measure of performance and when low-temperature performance is desired, a low T-50 value is optimum. For the standard catalyst, Cu/H-SSZ-13, we measured a T-50 of ~174°C. For the new catalysts, T-50s were as low as 151°C. It is significant that T-50s near 150°C are achievable, and these represent a significant and considerable improvement to the baseline Cu/HSSZ13 catalyst.

CONCLUSIONS

PNNL and its CRADA partners from Cummins Inc. and Johnson Matthey have been carrying out a CRADA project aimed at improving the higher temperature performance and stability of candidate NOx reduction technologies.

Results obtained this year demonstrate that titania-supported K-based NSR catalysts have significant issues with respect to thermal stability even though good performance is displayed for the freshly synthesized catalysts. On this basis, it seems highly unlikely that such materials can be used for vehicle exhaust emission control applications.

Model Fe/SSZ-13 catalysts were successfully synthesized via a modified solution ion exchange method for fundamental studies of their performance and stability. These catalysts are quite active for NO oxidation, and their SCR performance is significantly improved in the presence of NO_2 due to the participation of the "fast" SCR reaction.

PNNL has invented new CHA-based catalysts that provide SCR activity at significantly lower temperatures than achieved by the industry standard Cu/SSZ-13 materials.

REFERENCES

1. J.H. Kwak, D. Tran, S.D. Burton, J. Szanyi, J.H. Lee, C.H.F. Peden, *Journal of Catalysis* 287 (2012) 203-209.

2. W.S. Epling, L.E. Campbell, A. Yezerets, A., N.W. Currier, J.E. Parks, *Catalysis. Review.–Science and Engineering* 46 (2004) 163.

3. G.G. Muntean, M. Devarakonda, F. Gao, J.H. Kwak, J.Y. Luo, C.H.F. Peden, M.L. Stewart, J. Szanyi, D.N. Tran, K. Howden, in *Advanced Combustion Engine Research and Development: FY2012 Annual Progress Report*, III-3 – III-7.

4. D.H. Kim, K. Mudiyanselage, J. Szanyi, H. Zhu, J.H. Kwak, C.H.F. Peden, *Catalysis Today* 184 (2012) 2-7.

5. D.H. Kim, K. Mudiyanselage, J. Szanyi, J.H. Kwak, H. Zhu, C.H.F. Peden, *Applied Catalysis B* 142-143 (2013) 472478.

6. J.Y. Luo, F. Gao, C.H.F. Peden, *Catalysis Today* 231 (2014) 164-172.

7. F. Gao, M. Kollar, R.K. Kukkadapu, Y. Wang, J. Szanyi, C.H.F. Peden, *Applied Catalysis B* (2015) in press.

8. Gao, F, Y Wang, M Kollar, J Szanyi, CHF Peden, Invention Disclosure, February, 2014; #30561-E.

FY 2014 PUBLICATIONS

1. Gao, F.; Muntean, G.; Peden, C.; Howden, K.; Currier, N.; Kamasamudram, K.; Kumar, A.; Li, J.; Stafford, R.; Yezerets, A.; Castagnola, M.; Chen, H.-Y.; Hess, H. "Enhanced High and Low Temperature Performance of NOx Reduction Materials." Advanced Combustion Engine Research and Development, FY2013 Progress Report (2013) III-21 – III-27.

2. J.Y. Luo, F. Gao, D.H. Kim, C.H.F. Peden, "Effects of Potassium Loading and Thermal Aging on K/Pt/Al_2O_3 High-Temperature Lean NO_x Trap Catalysts," *Catalysis Today* **231** (2014) 164-172.

3. D.H. Kim, K. Mudiyanselage, J. Szanyi, J.C. Hanson, C.H.F. Peden, "Effect of H_2O on the Morphological Changes of KNO_3 Formed on $K_2O/\gamma Al_2O_3$ NOx Storage Materials: Fourier Transform Infrared (FTIR) and Time-Resolved X-ray Diffraction (TR-XRD) Studies," *Journal of Physical Chemistry C* **118** (2014) 4189-4197.

4. F. Gao, E.D. Walter, N.M. Washton, J. Szanyi, C.H.F. Peden, "Synthesis and Evaluation of Cu-SAPO-34 Catalysts for Ammonia Selective Catalytic Reduction. 2. Solid-State Ion Exchange and One-Pot Synthesis," *Applied Catalysis B* **162** (2015) 501-514.

5. F. Gao, M. Kollar, R.K. Kukkadapu, Y. Wang, J. Szanyi, C.H.F. Peden. "Fe/SSZ-13 as an NH_3-SCR Catalyst: a Reaction Kinetics and FTIR/Mössbauer Spectroscopic Study." *Applied Catalysis B* (2015) in press.

6. J.Y. Luo, F. Gao, A. Karim, P. Xu, N. Browning, C.H.F. Peden. "Advantages of $MgAlO_x$ over γ-Al_2O_3 as supports for potassium-based high temperature lean NO_x traps." *ACS Catalysis* (2015) submitted.

7. L. Righini, L. Lietta, F. Gao, C.H.F. Peden. "Properties of K and TiO_2 based LNT catalysts." *Applied Catalysis B* (2015) submitted.

FY 2014 INVENTION REPORT

1. Gao, F, Y Wang, M Kollar, J Szanyi, CHF Peden. "Catalysts for Low Temperature Selective Catalytic Reduction of NOx with Ammonia." Invention Disclosure, February, 2014; #30561-E.

FY 2014 PRESENTATIONS

1. Luo J, F Gao, and CHF Peden. "Potassium-based lean NOx trap for high temperature application: Effect of support on the performance and thermal stability." Presented by **John Luo** at the SAE 2014 World Congress & Exhibition, Detroit, MI, March 2014.

2. Gao F, M Kollar, Y Wang, J Szanyi, and CHF Peden. "Synthesis, characterization and evaluation of Cu/Fe-Chabazite catalysts for use in selective catalytic reduction (SCR) with ammonia." Presented by **Chuck Peden (Invited Speaker)** at the 247th ACS National Meeting, Dallas, TX, April 2014.

3. Gao F, M Kollar, Y Wang, RK Kukkadapu, NM Washton, J Szanyi, and CHF Peden. "NH_3-SCR on fresh and hydrothermally aged Fe-SSZ-13 catalysts." Presented by **Feng Gao** at the 18th Annual CLEERS Workshop, Dearborn, MI, May 2014.

4. Gao, F, GG Muntean, J Szanyi, CHF Peden, N Currier, A Kumar, K Kamasamudram, J Li, J Luo, A Yezerets, M Castagnola, HY Chen, and H. Hess. "Enhanced High Temperature Performance of NOx Storage/Reduction (NSR) Materials." Presented by **Chuck Peden (Invited Speaker)** at the DOE Combustion and Emission Control Review, Washington, DC, June 2014.

5. Kollar M, F Gao, RK Kukkadapu, Y Wang, J Szanyi, and CHF Peden. "Fe/SSZ-13 as an NH3-SCR catalyst." Presented by **Marton Kollar (Invited Speaker)** at 2014 Postdoc Research Symposium, Richland, WA, July 2014.

6. Kollar M, F Gao, Y Wang, RK Kukkadapu, J Szanyi, and CHF Peden. "NH3-SCR on fresh and hydrothermally aged Fe/SSZ-13 catalysts." Presented by **Marton Kollar** at the 8th International Conference on Environmental Catalysis, Asheville, NC, August 2014.

III.5 Investigation of Mixed Oxide Catalysts for NO Oxidation

János Szanyi (Primary Contact),
Ayman M. Karim, Larry R. Pederson,
Ja Hun Kwak, Donghai Mei, Diana Tran,
Darrell R. Herling, George G. Muntean, and
Charles H.F. Peden

Pacific Northwest National Laboratory (PNNL)
902 Battelle Blvd., PO Box 999
Richland, WA 99352

DOE Technology Development Manager
Ken Howden

Cooperative Research and Development Agreement Partner
Gongshin Qi and Wei Li – General Motors Company (GM)

Overall Objectives

- Develop and demonstrate mixed metal oxide-based catalysts as a low-cost replacement for platinum in the oxidation of NO to NO_2 in lean engine exhaust, an essential first step in controlling oxides of nitrogen (NO_x) emissions.
- Improve the understanding of the nature and structure of active sites of mixed metal oxide catalysts for NO oxidation in diesel oxidation catalysts (DOCs) and lean-NO_x traps (LNTs).

Fiscal Year (FY) 2014 Objectives

- Evaluate oxygen mobility in MnO_x/CeO_2 catalysts using isotopically labelled NO.
- Determine the nature of surface species formed on MnO_x/CeO_2 catalysts upon their exposure to NO. Follow interconversion of surface NO_x species as a function of temperature, and in the presence of O_2 in the gas phase.
- Understand how MnO_x acts in NO oxidation activity enhancement of CeO_2; notably, do Mn ions need to be in the CeO_2 lattice?
- Perform density functional theory (DFT) computational studies to investigate the role of MnO_x clusters on the NO oxidation activity of CeO_2.

FY 2014 Accomplishments

- The extensive isotope exchange between MnO_x/CeO_2 and $^{15}N^{18}O$ clearly shows that the oxygen mobility in these catalysts is very high indeed.
- NO decomposition is facile on MnO_x/CeO_2 catalysts even at 300 K. In addition to N_2O, N_2 formation was also observed.
- Upon NO exposure, the initially formed hyponitrite and nitrite species on MnO_x/CeO_2 transform to nitrates. This transformation is accelerated in the presence of gas phase O_2.
- A physical mixture of MnO_x and CeO_2 exhibits comparable NO oxidation activity to the catalyst prepared by incipient wetness with the same composition.
- Using DFT we have shown that the presence of Mn^{4+} ions enhances the activity of nearby CeO_2, and NO oxidation can also proceed on Mn_2O_4 "clusters."

Future Directions

This three-year Cooperative Research and Development Agreement project was completed in September, 2014.

INTRODUCTION

The oxidation of engine-generated NO to NO_2 is an important step in the reduction of NO_x in lean engine exhaust because NO_2 is required for the performance of the LNT technology [1], and it enhances the activities of ammonia selective catalytic reduction (SCR) catalysts [2]. In particular, for SCR catalysts an NO:NO_2 ratio of 1:1 is most effective for NO_x reduction, whereas for LNT catalysts, NO must be oxidized to NO_2 before adsorption on the storage components. However, NO_2 typically constitutes less than 10% of NO_x in lean exhaust, so catalytic oxidation of NO is essential. Platinum has been found to be especially active for NO oxidation, and is widely used in DOC and LNT catalysts. However, because of the high cost and poor thermal durability of Pt-based catalysts, there is substantial interest in the development of alternatives. The objective of this project, in collaboration with partner General Motors, is to develop mixed metal oxide catalysts for NO oxidation, enabling lower precious metal usage in emission control systems.

APPROACH

This project with GM and PNNL is aimed at replacing or reducing platinum usage in DOC and LNT catalysts, and was initiated in 2012. This project

builds on success achieved recently by GM researchers, who reported excellent NO oxidation efficiency over substituted lanthanum-based mixed oxides, such as $LaCoO_3$ and $LaMnO_3$, when compared to a commercial Pt-based DOCs [1].

Well-coordinated and complementary research activities were performed at GM and PNNL. The principal focus of GM research was on catalyst formulation, evaluation of catalytic activity under conditions relevant to lean engine exhaust, and catalyst aging. State-of-the-art analytical and computational techniques were applied at PNNL to characterize the structure of the catalysts and to determine the concentration and nature of active sites. Surface and bulk properties of catalyst materials were established as a function of catalyst composition, and correlated to trends in catalytic activity. Computational analyses of active sites and possible reaction mechanisms were probed using DFT, which provides information concerning the interaction between reactants and active sites. It is anticipated that this research will lead to the development of low-cost, durable, and active catalysts for the oxidation of NO to NO_2.

RESULTS

Fast oxidation of NO requires the availability of labile oxygen on the catalyst surface. In order to shed light on the mobility of surface oxygen atoms in the MnO_x/CeO_2 systems, we have recently conducted experiments with isotopically labelled nitrogen-oxide, $^{15}N^{18}O$. In this study we exposed the annealed (under vacuum) MnO_x/CeO_2 catalysts to $^{15}N^{18}O$ and followed the nature of the surface species formed by Fourier transform infrared (FTIR) spectroscopy, and monitored the gas phase composition during $^{15}N^{18}O$ exposure by mass spectrometry. A series of FTIR spectra (obtained during the first cycle of $^{15}N^{18}O$ exposure) and selected mass fragments during five cycles of $^{15}N^{18}O$ exposure are displayed in Figure 1. The FTIR spectra revealed that the adsorbed surface species were mostly hyponitrites and nitrites. Mass spectrometry analysis of the gas phase during gas exposures showed the formation of a large number of NO_x species, from N_2 to NO_2. NO_x species with both ^{16}O and ^{18}O were observed. This study provided two main findings: 1) isotope exchange between $^{15}N^{18}O$ and MnO_x/CeO_2 is very fast; and 2) NO decomposition is extensive on these catalysts; beside N_2O, N_2 formation was also observed. The NO decomposition reaction is suppressed upon subsequent $^{15}N^{18}O$ exposures, while isotope exchange was still very facile even after four cycles of $^{15}N^{18}O$ exposure/evacuation at 300 K. Temperature programmed desorption following $^{15}N^{18}O$ exposure (Figure 2) showed that, as the sample was heated up, some of the nitrites decomposed resulting in NO evolution, but a large fraction of the nitrites converted to nitrates and, as such, decomposed at much higher sample temperatures. Interestingly, during the nitrite-to-nitrate transformation N_2 formation was observed as well.

In order to provide further insights into the structure of the active sites in MnO_x/CeO_2, we performed extended X-ray absorption fine structure measurements on selected MnO_x/CeO_2 catalysts. Table 1 shows the Mn-Mn and Mn-O bond distances determined for the 3.4 and 30.7 wt% MnO_x/CeO_2 catalysts, together with those for MnO_x standard materials. Also listed in the table are bond distances provided by DFT calculations for MnO_2(110)

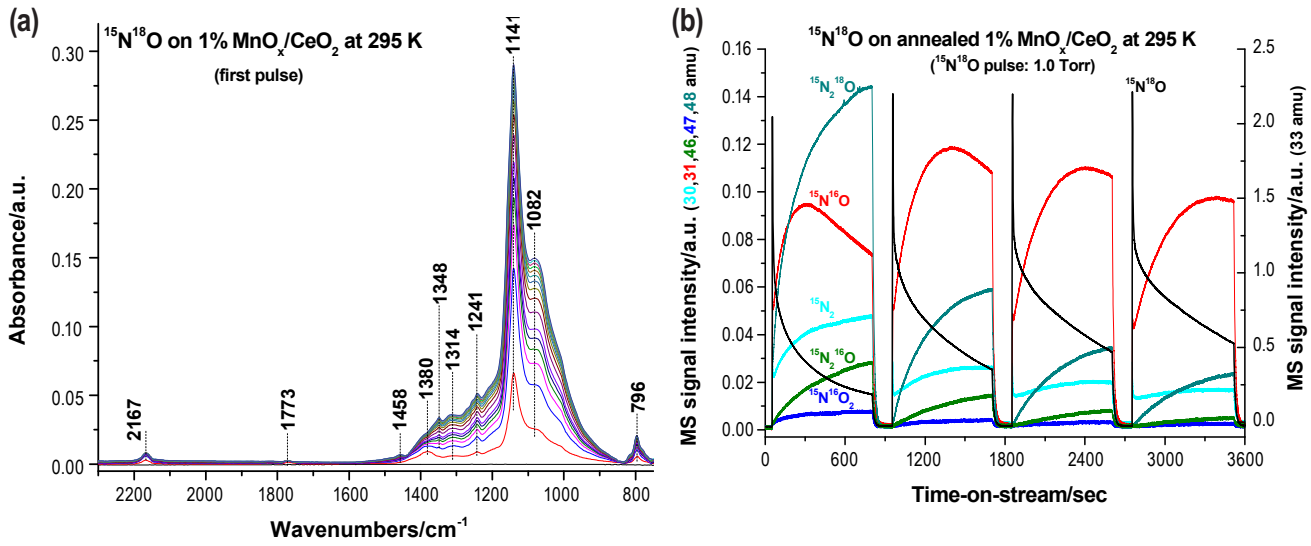

FIGURE 1. (a) Series of FTIR spectra collected during the first $^{15}N^{18}O$ pulse of an annealed 1% MnO_x/CeO_2 sample. (b) Variation of the gas phase composition during four $^{15}N^{18}O$ pulses (after each pulse the infrared cell was evacuated): selected mass signals as a function of time.

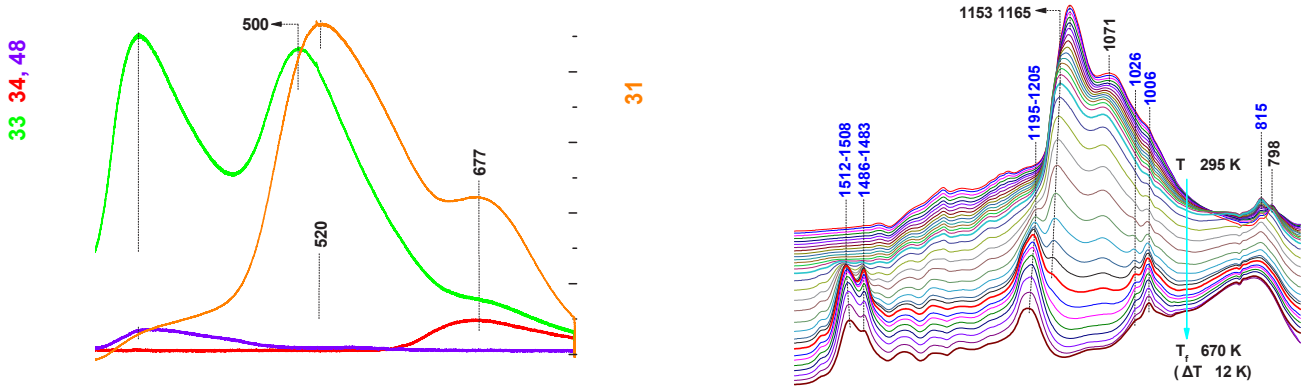

FIGURE 2. (a) Series of FTIR spectra collected during temperature programmed desorption after four pulses of $^{15}N^{18}O$ exposure of an annealed 1% MnO_x/CeO_2 catalyst, and (b) the corresponding mass spectrometry signals of selected mass fragments.

TABLE 1. Mn-O and Mn-Mn bond distances determined from extended X-ray absorption fine structure data analysis, and compared to results obtained from DFT calculations on model systems (last four rows).

	Mn–O (Å)	Mn–Mn (Å)
MnO	2.22	3.14
Mn_2O_3	1.89	3.12
MnO_2	1.86	2.87
Bulk MnO_x	1.90	3.16
3.4% MnO_x/CeO_2	1.84	2.80
30.7% MnO_x/CeO_2	1.86	2.86
Mn_2O_4 cluster/CeO_2	1.93-2.00	2.66
Mn_2O_2 cluster/CeO_2	1.90-2.1	2.67
Mn doped CeO_2	2.24-2.28	3.80 (Mn–Ce)
MnO_2(110)	1.89-1.90	2.87

and different MnO_x clusters on CeO_2(111) surfaces. These results confirm the formation of MnO_2 clusters on the ceria surface. They also reveal that, at low MnO_x loading (in this case 3.4 wt%), the Mn-O bond distance is reduced, presumably due to the strong interaction between MnO_x and CeO_2. (We believe that this effect is even more pronounced at lower MnO_x loadings.)

Our prior experimental and theoretical studies showed that, in these MnO_x/CeO_2 systems, MnO_x clusters reside on the CeO_2 surface and not in the CeO_2 lattice (Mn doping of CeO_2 is not extensive). In order to substantiate the hypothesis that Mn doping is not essential in the activity enhancement of CeO_2 in NO oxidation, we prepared a MnO_x/CeO_2 sample by physically mixing MnO_2 (30%) and CeO_2 (70%), and tested the reactivity of this physical oxide mixture in NO oxidation (under the same conditions we have done in previous work). The activity of this physically mixed oxide is compared to that of MnO_x, CeO_2, and the 30.7% MnO_x/CeO_2 sample that was prepared by incipient wetness method. Interestingly, the physical mixture of MnO_2 and CeO_2 showed comparable NO oxidation activity to that of the 30.7% MnO_x/CeO_2 sample, and was much more active than either MnO_x or CeO_2 (Figure 3). These results further supported our prior conclusion that Mn ions do not need to be incorporated into the CeO_2 lattice; however, the interface between MnO_x and CeO_2 is very important to achieve high NO oxidation activity.

First principles DFT calculations were performed to investigate the effects of defect sites on the reactivity of NO oxidation over CeO_2 supported Mn_2O_x (x=3,4) clusters. As shown in Figure 4, NO oxidation is thermodynamically favorable over the supported Mn_2O_4 cluster while it is not feasible after the cluster is reduced to Mn_2O_3. To keep the NO activity, one of the surface oxygen atoms has to migrate to the cluster. Similarly, NO oxidation easily occurs on the perfect CeO_2(111) surface when the Mn_2O_4 cluster is nearby. The reduced Mn_2O_3 is prohibitive to the surface NO oxidation. These results suggest that the Mn_2O_4 cluster with Mn^{4+} is key to the NO oxidation which could occur on both the cluster and the supporting ceria surface.

CONCLUSIONS

- The extensive isotope exchange between MnO_x/CeO_2 and $^{15}N^{18}O$ clearly shows that the oxygen mobility in these catalysts is very high indeed.
- NO decomposition is facile on MnO_x/CeO_2 catalysts even at 300 K. In addition to N_2O, N_2 formation was also observed.

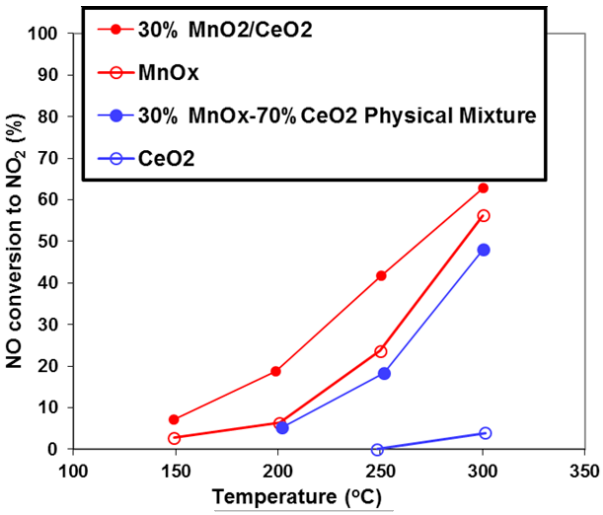

	Reaction rate x10^{-3} (mol/m^2/min)	Reaction rate (mol/Surface mol Mn min)
MnO_x	10.1	541
30% MnO_x/CeO_2 physical mixture	24.8	1332

FIGURE 3. NO oxidation activity of a physical mixture of 30% MnO_x and 70% CeO_2: activity comparison to MnO_x, CeO_2, and 30.7% MnO_x/CeO_2 catalysts.

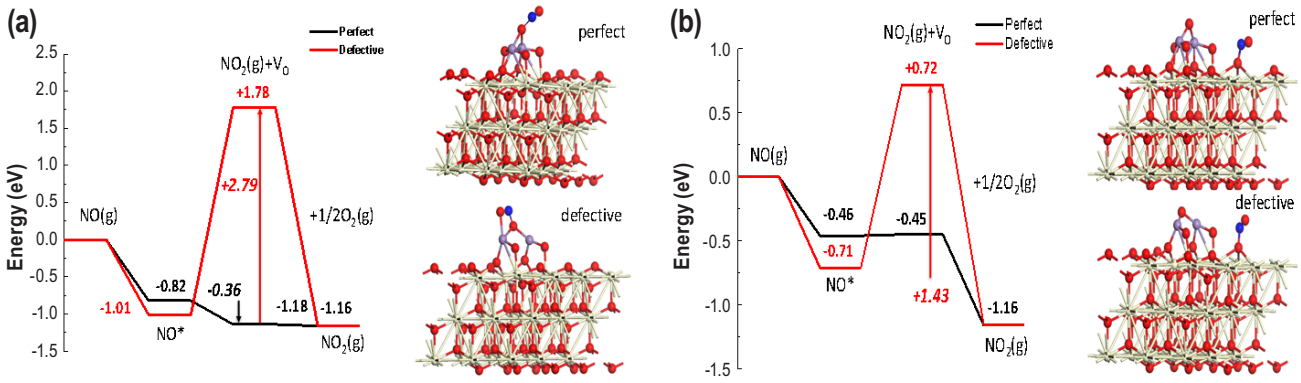

FIGURE 4. NO oxidation over a model $Mn_2O_4/CeO_2(111)$ catalyst. (a) A situation where only the Mn_2O_4 cluster is involved; and (b) where only the $CeO_2(111)$ surface is involved.

- Upon NO exposure, the initially formed hyponitrite and nitrite species on MnO_x/CeO_2 transform to nitrates. This transformation is accelerated in the presence of gas phase O_2.
- A physical mixture of MnO_x and CeO_2 exhibits comparable NO oxidation activity to the catalyst prepared by incipient wetness with the same composition.
- Using DFT we have shown that the presence of Mn^{4+} ions enhances the activity of nearby CeO_2, and NO oxidation can also proceed on Mn_2O_4 "clusters."

REFERENCES

1. C.H. Kim, G.S. Qi, K. Dahlberg, and W. Li, Science 327, 1624 (2010).

2. M. Koebel, G. Madia, and M. Elsener, Catalysis Today 73, 239 (2002).

FY 2014 PUBLICATIONS/PRESENTATIONS

1. AY Karim, LR Pederson, J Szanyi, D Mei, JH Kwak, D Tran, CHF Peden, GG Muntean, "Investigation of Mixed Oxide Catalysts for NO Oxidation," 2012 DOE Vehicle Technologies Program Annual Merit Review and Peer Evaluation Meeting, June 18, 2014, Washington, D.C.

2. AY Karim, LR Pederson, JH Kwak, D Mei, D Tran, DR Herling, GG Muntean, J Szanyi, CHF Peden, "Investigation of Mixed Oxide Catalysts for NO Oxidation," Advanced Combustion Engine Research and Development, FY2013 Progress Report (2013) III-28 – III-31.

3. J Szanyi, J.H. Kwak, "$^{15}N_2$ formation and fast oxygen isotope exchange during pulsed $^{15}N^{18}O$ exposure of MnO_x/CeO_2," Chemical Communications, 2014, 50 (95), 14998 – 15001.

4. G Qi, AM Karim, D Mei, J Szanyi, JH Kwak, W Li, D Tran, L Pederson, "Insights on the active phase and mechanism for NO oxidation on MnO_x-CeO_2 mixed oxide," International

Conference on Environmental Catalysis, August 24–27, 2014, Ashville, NC.

5. AM Karim, JH Kwak, J Szanyi, D Mei, D Tran, "Role of Ce-Mn interaction in NO oxidation," in preparation.

III.6 Integration of DPF and SCR Technologies for Combined Soot and NO_x After-Treatment

Kenneth G. Rappé (Primary Contact),
Gary D. Maupin
Pacific Northwest National Laboratory
Post Office Box 999
Richland, WA 99354

DOE Technology Development Manager
Ken Howden

Overall Objectives

- Develop an improved understanding of selective catalytic reduction (SCR) and diesel particulate filter (DPF) integration for application to on-road heavy-duty diesel emission reduction.
- Probe the DPF-SCR couple with a view towards maximum SCR conversion efficiency, optimum soot oxidation performance, and acceptable pressure drop.
- Determine performance limitations and define basic design and operating requirements for efficient integration with the engine that minimizes impact on vehicle efficiency.

Fiscal Year (FY) 2014 Objectives

- Develop the ability to qualitatively predict the effect of soot on the SCR process, and an understanding of the reactive drivers governing the observed behavior, as a pathway towards improved modeling capability of the integrated system.
- Investigate the coupling of SCR and DPF with a view towards maximizing the passive soot oxidation activity exhibited in the integrated system, while retaining the necessary SCR activity.

FY 2014 Accomplishments

- Investigating the relationship between soot loading behavior and SCR catalyst concentration and location in SCR-DPF samples has led to greater understanding of the pathway towards improved SCR-DPF integration and increased SCR catalyst loading in excess of 150 g/L.
- SCR reaction rate measurements at different NO_2/oxides of nitrogen (NO_x) ratios in the presence of soot has led to improved understanding of the nature of the impact of soot on NO_x conversion, and a greater level of understanding of strategies for improved SCR predictive modeling of integrated SCR-DPF systems.
- Fundamental understanding of the impact and nature of SCR reaction on passive soot oxidation has been developed, leading to a greater understanding of the potential pathways towards maximizing the passive soot oxidation exhibited in SCR-DPF systems for heavy-duty diesel deployment.

Future Directions

- No additional work is planned under this project.
- Additional efforts should look at optimized SCR-DPF integration through advanced washcoat development coupled with advanced SCR-DPF interrogation methods (e.g. micro-computed tomography).
- Additional efforts should pursue improved predictive modeling capability that is able to accurately simulate the empirical observations of SCR-DPF behavior from this work.

✧ ✧ ✧ ✧ ✧

INTRODUCTION

Exhaust after-treatment is considered an enabler for widespread adoption of more fuel efficient diesel engines. In the last decade extensive research has resulted in the development and advancement of many aftertreatment technologies. However, there are still many unanswered questions that relate to how these technologies can work together synergistically, especially when tightly integrated. Integration of catalytic SCR and DPF technologies is a relatively new area in exhaust aftertreatment systems. Integrated SCR/DPF technology combines NO_x reduction and soot filtration in a single two-way device. Its development is motivated by emission compliance in a manner that reduces aftertreatment system volume and cost, and increases packaging flexibility. Assuming adequate soot filtration efficiency is achievable with the wall-flow substrate employed, the requirements for successful SCR/DPF integration are maximizing NO_x reduction efficiency (at an acceptable pressure drop) while demonstrating acceptable passive soot oxidation capacity in order to

minimize the fuel penalty associated with increased active regeneration frequency.

APPROACH

The primary thrust is to study the synergies of SCR-DPF systems to develop a pathway to a singular catalytic brick that combines the function of both DPF and SCR. High porosity cordierite DPF samples were provided by a major substrate manufacturer for the purposes of this study. The DPF samples were subsequently loaded with SCR catalyst, predominantly within the filter microstructure, by a major catalyst vendor and coater to ~60 g/L, ~90 g/L, and ~150 g/L SCR catalyst density. The samples were empirically tested for pressure drop, SCR of NO_x, and passive soot oxidation through loading with soot to an initial concentration of 4 g/L.

RESULTS

Figure 1 shows an example of on-engine pressure drop across the 150 g/L and 90 g/L SCR-DPF samples loaded with soot in different configurations. Scanning electron microscopy imaging conducted on the samples in prior years has shown that SCR catalyst within the porous filter wall is predominantly loaded to one side of the filter wall for all of the samples, and in the case of the 150 g/L sample, accumulations of catalyst were also observed on the filter wall surface. The SCR catalyst itself had minimal impact on filter permeability. However, both catalyst amount and location significantly impacted the magnitude of increased pressure drop resulting from the collection of soot, primarily occurring during depth filtration of soot. It is believed that this effect is primarily centered upon pore throats: pore throats (and their surrounding volumes) appear to be affected by SCR catalyst, resulting in an increased extent of plugging during depth filtration of soot.

The presence of SCR catalyst on the inlet filter channel wall also has adverse impact on backpressure development during the cake filtration phase, whereas similar catalyst loadings on the outlet filter channel did not exhibit such effect. Of the four samples shown in Figure 1, only the 150 g/L sample in the upstream configuration has SCR catalyst on the inlet channel wall, resulting in significantly increased cake filtration pressure rise (3.4 kPa/[g/L soot]). The above results suggest improved SCR/DPF catalyst integration is possible, and increased SCR catalyst loading is feasible, if SCR catalyst is preferentially located on the downstream portion of the filter wall microstructure and on the outlet channel wall.

Figures 2 and 3 show NO_x reduction efficiency of the 150 g/L SCR/DPF samples in the presence of 4 g/L initial soot loading, compared to performance in the absence of soot. In Figure 2 at $NO_2/NO_x = 0.5$ and less, soot adversely impacted NO_x reduction beginning at ~240°C. This effect was observed by soot shifting the NO_x reduction efficiency to analogous performance at lower NO_2/NO_x ratios without soot. As an example, at $NO_2/NO_x = 0.5$, NO_x reduction performance above 280°C with soot tracked similarly to $NO_2/NO_x = 0.4$ in the absence of soot. Then above 330°C, NO_x reduction tracked similarly to $NO_2/NO_x = 0.35$ in the absence of soot. Conversely, in Figure 3 at $NO_2/NO_x > 0.5$, soot positively impacts NO_x reduction. As an example, at $NO_2/NO_x = 0.6$, NO_x reduction is significantly improved in the presence of soot, demonstrating comparable performance to $NO_2/NO_x = 0.5$ without soot.

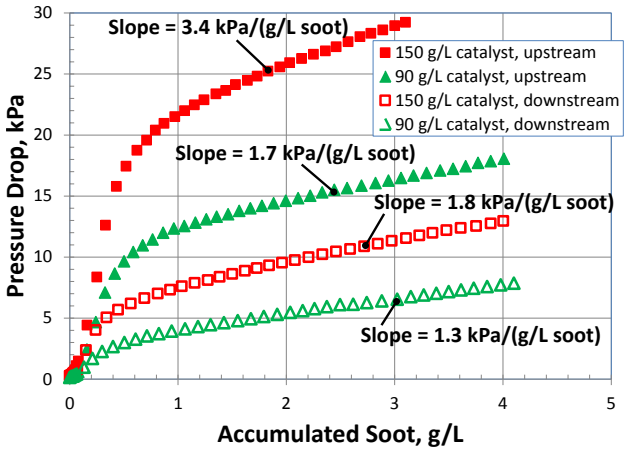

FIGURE 1. Soot loading characteristics of 90 g/L and 150 g/L SCR/DPF samples configured with catalyst located on the downstream versus upstream portion of the DPF filter wall.

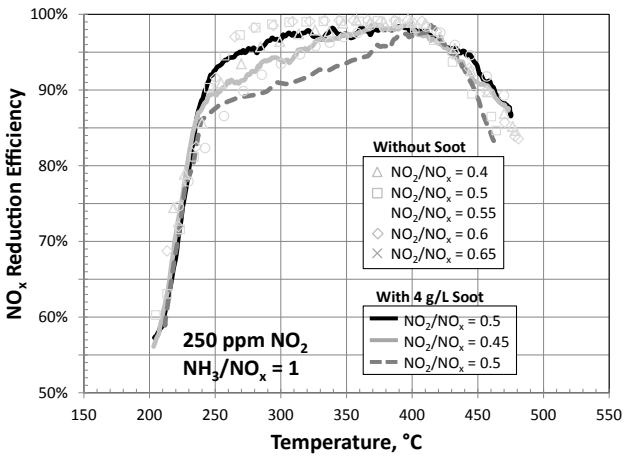

FIGURE 2. SCR/DPF NO_x reduction efficiency at 35,000 gas hourly space velocity, $NH_3/NO_x = 1$, $NO_2 = 250$ ppm, and $NO_2/NO_x = 0.5$ and less: effect of 4 g/L initial soot loading on NO_x reduction efficiency.

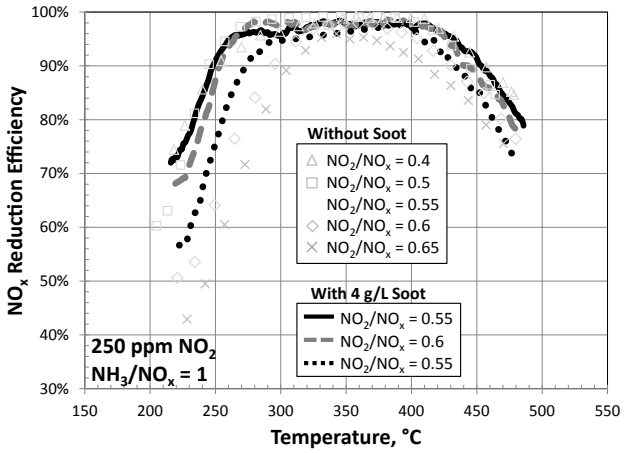

FIGURE 3. SCR/DPF NO_x reduction efficiency at 35,000 gas hourly space velocity, $NH_3/NO_x = 1$, $NO_2 = 250$ ppm, and $NO_2/NO_x > 0.5$: effect of 4 g/L initial soot loading on NO_x reduction efficiency.

Since NO_x reduction efficiency is dependent on the comparative magnitude of standard-SCR, fast-SCR, and NO_2-only SCR reactions, the impact of soot on NO_x conversion can largely be explained by the NO_2 balance in the system, the relative rates of various SCR reaction processes, and the interaction between the two. At $NO_2/NO_x < 0.5$, below ~380°C fast SCR dominates the kinetics of SCR depleting NO_2 until an abundance of NO remains, which is then consumed by the slower standard SCR reaction. Figure 4 (left) shows the NO and NO_2 concentrations in the catalyst effluent with and without soot at $NO_2/NO_x = 0.45$. At $NO_2/NO_x < 0.5$, NO_2 concentration in the effluent is minimally affected by soot as expected; however, the presence of soot oxidation converts NO_2 to NO increasing the dependency on standard SCR as evident by increased NO in the catalyst effluent. The result is inferior SCR performance in the presence of soot. At $NO_2/NO_x > 0.5$, fast SCR again dominates, but conversely depleting NO until an abundance of NO_2 remains, which is then consumed by the slower NO_2-only SCR reaction. It should be noted that, for $NO_2/NO_x > 0.5$, peak activity is limited by reductant availability due to the stoichiometry of the NO_2-only SCR reaction. Figure 4 (right) shows the NO and NO_2 concentrations in the catalyst effluent with and without soot at $NO_2/NO_x = 0.6$. NO concentration in the effluent is minimally affected by soot as expected for this case; however, the presence of soot oxidation converts NO_2 to NO, decreasing the dependency on NO_2-only SCR; this is evident by decreased NO_2 in the catalyst effluent. The result is significantly improved SCR performance in the presence of soot.

Figure 5 shows temperature programmed oxidation studies performed to characterize the passive soot oxidation in the presence of SCR, presented as normalized pressure drop across the samples as a function of temperature, with decrease in pressure drop employed as a means to characterize the on-set of soot oxidation. The data shows the effect of varying the NO_2/NO_x ratio between 0.4 and 0.65 while keeping the NO_2 constant at 250 ppm, for providing insight into the primary reactive drivers that are governing passive soot oxidation activity of the system. At $NO_2/NO_x \leq 0.5$, soot oxidation is relatively unaffected by NO_2/NO_x fraction, with light-off occurring at ~400°C. Comparatively, at $NO_2/NO_x > 0.5$ increased rate of soot oxidation is observed compared to $NO_2/NO_x \leq 0.5$, the magnitude of which is governed by the NO_2/NO_x fraction. These results suggest that at a given NO_2 concentration, passive soot oxidation behavior is dictated by the nature of the dominating SCR reaction mechanisms. At $NO_2/NO_x \leq 0.5$, fast-SCR reaction mechanisms dominate NO_2 availability in the reactor via diffusion. Only at NO_2/NO_x

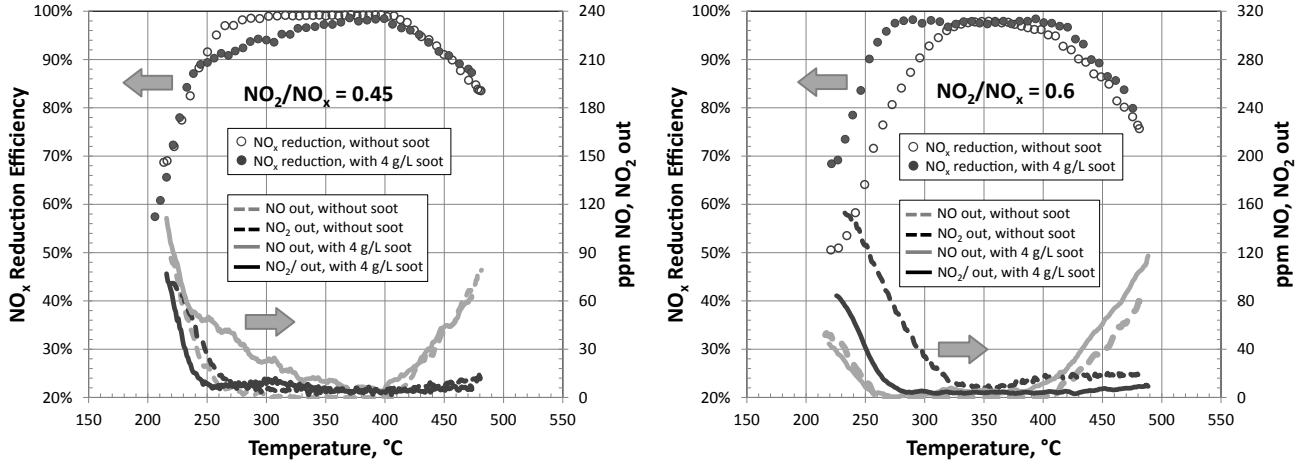

FIGURE 4. Effect of 4 g/L initial soot loading on NO and NO_2 concentration in the catalyst effluent at $NO_2/NO_x = 0.45$ (left) and 0.6 (right).

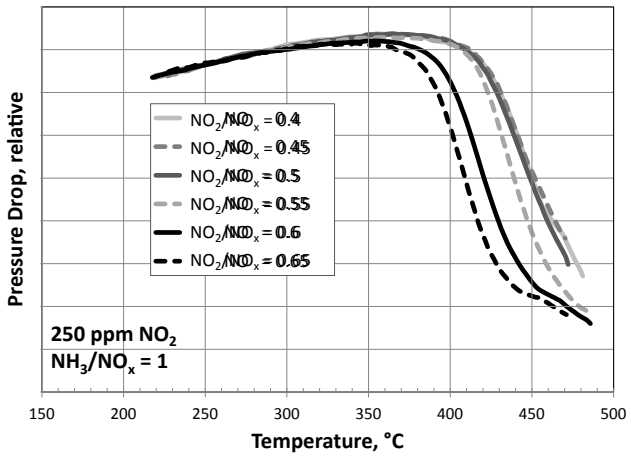

FIGURE 5. Temperature programmed oxidation of SCR/DPF with 4 g/L initial soot loading with 250 ppm NO_2 (varying total NO_x) at NO_2/NO_x = 0.4 through 0.65 and NH_3/NO_x = 1.

> 0.5 is a divergence from this observed. In this case, fast-SCR consumes NO equimolarly with NO_2 until NO is depleted and a relative abundance of NO_2 remains. The ensuing NO_2-only SCR reaction rates are comparatively slow on the Cu-zeolite catalyst employed, leading to decreased diffusion of the remaining NO_2 and increased availability for passive soot oxidation. This indicates that SCR reaction, and particularly the fast-SCR reaction, significantly effects NO_2 concentration in front of the filter wall and collected soot; this further highlights the impact of NO_2 diffusion on soot oxidation performance in the integrated SCR/DPF system, and how that rate of diffusion is governed by the nature of the SCR reaction network.

CONCLUSIONS

- The combined effect of SCR catalyst concentration and location has been shown to affect the pressure drop across the samples with accumulated soot. These studies suggest the potential for improved SCR/DPF catalyst integration, and increased SCR catalyst loading, if SCR catalyst is preferentially located on the downstream portion of the filter wall microstructure and on the outlet channel wall.
- The impact of soot on NO_x conversion can largely be explained by the NO_2 balance in the system, the relative rates of various SCR reaction processes, and the interaction between the two, leading to greater understanding of strategies for improved predictive modeling of integrated SCR-DPF systems.
- At a given NO_2 concentration, passive soot oxidation behavior is dictated by the nature of the dominating SCR reaction mechanisms. At $NO_2/NO_x \leq 0.5$, fast-SCR reaction mechanisms dominate NO_2 availability in the reactor, and only at NO_2/NO_x > 0.5 is a divergence from this observed. In this case, fast-SCR consumes NO equimolarly with NO_2 until NO is depleted and a relative abundance of NO_2 remains. The ensuing NO_2-only SCR reaction rates are comparatively small, leading to increased availability for passive soot oxidation.

FY 2014 PUBLICATIONS/PRESENTATIONS

1. Rappé, Kenneth G. "Integrated SCR-DPF Aftertreatment: Insights into Pressure Drop, NO_x Conversion, and Passive Soot Oxidation Behavior". INDUSTRIAL & ENGINEERING CHEMISTRY RESEARCH. OCT 2014. DOI: http://dx.doi.org/10.1021/ie502832f.

2. Rappé, Kenneth G. "Combination & Integration of DPF-SCR Aftertreatment". Presentation to DOE in Richland, WA. August 13, 2014.

3. Rappé, Kenneth G. "Combination & Integration of DPF-SCR Aftertreatment". Presentation to PACCAR in Richland, WA. June 6, 2014.

III.7 Low-Temperature Emissions Control

Todd J. Toops (Primary Contact),
James E. Parks, Andrew Binder, Sheng Dai,
Jae-Soon Choi, Mi-Young Kim
Oak Ridge National Laboratory (ORNL)
2360 Cherahala Boulevard
Knoxville, TN 37932

DOE Technology Development Manager
Ken Howden

Overall Objectives

- Develop emission control technologies that perform at low temperatures (<150ºC) to enable fuel-efficient engines with low exhaust temperatures to meet emission regulations
- Identify advancements in technologies that will enable commercialization of advanced combustion engine vehicles

Fiscal Year (FY) 2014 Objectives

- Identify novel/innovative technologies that can be implemented to address the challenges of advanced combustion strategies
- Characterize performance and surface morphology for a novel candidate catalyst

FY 2014 Accomplishments

- Completed support investigation of innovative Au@Cu (core@shell) catalyst for oxidation:
  - Found CeO_2-ZrO_2 support gives improved oxidation and better durability
  - Sulfur a concern
- Successfully added ZrO_2 to SiO_2 support for Pd catalyst to achieve high surface area support with better activity:
  - High activity in both CO and C_3H_6 oxidation due to acidity generated
  - Promising for sulfur tolerance
  - Characterized the accessible area of ZrO_2 layer on SiO_2 (critical for durability)
- Discovered a new catalyst that has no platinum-grade metal (PGM) based on Cu-Ce-Co (CCC) oxides that does not demonstrate inhibition between hydrocarbon (HC) and CO oxidation processes (which commonly limit PGM-based catalysts):
  - CO low-temperature oxidation not inhibited by HCs
  - HC oxidation temperature relatively high
  - Projected cost of catalyst is very low
- Initiated study of trapping materials:
  - New activity in project
  - Experimental design based on discussion with industry
  - Performed on several formulations at end of FY 2014

Future Directions

- Continue to investigate pathways to take advantage of the improved Pd/Zr reactivity to CO and HC oxidation:
  - Investigate additional synthesis techniques for improved durability and selective dispersion of the Pd on the Zr-phase of a Zr/SiO_2 or Zr/Al_2O_3 support
  - Also include ceria as part of the study
- Investigate durability of CCC catalysts and how it interacts with the PGM-based systems for HC conversion:
  - Interested in the introduction of low levels of PGM on the CCC for HC conversion
  - Also, zoned operation with CCC in front of PGM catalyst
- Low-temperature NOx and HC trap materials:
  - Investigate synergy of release kinetics with other technologies being studied
- Identify low-temperature NOx reduction strategies that can be used at 150°C:
  - Novel NH_3-SCR catalyst formulations; likely to be used with gaseous NH_3 introduction, e.g. Amminex
  - NOx storage reduction catalysis with low temperature release and highly active reduction chemistry
- Begin exploring how the technologies discussed above can work together to achieve 90% conversion of all exhaust constituents at 150°C

INTRODUCTION

Removing the harmful pollutants in automotive exhaust has been an intense focus of the automotive industry over the last several decades. In particular, the emissions regulations for fuel-efficient diesel engines that were implemented in 2007 and 2010 have resulted in a new generation of emissions control technologies. These catalysts usually reach 90% conversion of pollutants between 200°C and 350°C and consequently, more than 50% of the emissions occur in the first 2-3 minutes under "cold-start" or idling conditions [1]. Thus, as emissions regulations become more stringent [2] meeting the emission regulations will require increased activity during this warm-up period. To further complicate matters, the increased Corporate Average Fuel Economy standards that will be implemented over the next decade will result in the introduction of more fuel-efficient engines [3]. This will result in lower exhaust temperatures, which further necessitates the need for increased emissions control activity at low temperatures [4]; with this in mind the U.S. DRIVE Advanced Combustion and Emission Control Technology Team has set a goal of achieving 90% conversion of CO/HC/NOx at 150°C. Higher Pt/Pd loadings may help to increase the catalytic efficiency, but such methods are too expensive for long-term success. Other options to meet the emissions standards include hydrocarbon/NOx absorbers; however, while this pathway would help mitigate cold-start emissions, the lowering of the average exhaust temperature suggests this approach alone will be insufficient and ultimately a more complete solution will be necessary. One way to accomplish this goal is to develop new catalytic materials that are active at lower temperatures.

APPROACH

To reach the goal of 90% conversion at 150°C a multi-functional approach will be pursued. Currently, there is a large effort being pursued in Basic Energy Science programs that are focused on studying catalysts with very high activity regardless of the specific application. We initiate contact with these researchers to investigate their catalysts in the harsh conditions that are present in automotive exhaust, e.g. H_2O, CO_2, CO, HC, NOx and hydrothermal aging above 800°C. Often these catalysts show exceptional activity in single component exhaust streams, but there is significant inhibition from other exhaust species. With this in mind, we are aiming to understand the limitations of each system, but also look for synergistic opportunities when possible. This includes using traps to limit exposure of inhibiting species to active catalysts until temperatures are more amenable. Also, mixing catalytic components where the catalysts are limited by different species will be explored. Our efforts will aim to understand the processes at a fundamental level and illustrate where the shortcomings are of each catalyst we study, while striving to find compositions that will enable the very challenging goal of 90% conversion of CO/NOx/HC at 150°C. Improving this understanding of the potential limitations of catalysts will guide the reformulation of new catalysts.

RESULTS

The first area that we are exploring focuses on more conventional PGM-based emissions control catalysts, but with a focus on improved reactivity through catalyst-support interactions. In as much we are currently investigating Pd-based systems using ZrO_2 and SiO_2 supports (Pd/ZrO_2 and Pd/SiO_2, respectively). The theory of the approach is to optimize support for Pd catalysts by combining high acidity of ZrO_2 with high surface area of SiO_2, and thus we are dispersing ZrO_2 on SiO_2 followed by the addition of Pd (Pd/ZrO_2-SiO_2). High acidity should improve Pd dispersion, HC oxidation, and S tolerance. Figure 1 illustrates how the reactivity of these three catalysts is affected by gas composition and compares them to a commercially available diesel oxidation catalyst (DOC). With respect to CO oxidation (Figure 1a) there is little effect from the use of the ZrO_2 and SiO_2 supports, and in fact, when flowing CO+NO+HC, the commercial DOC shows the best performance. What is clear from this CO reactivity comparison is the influence of both NO and HC in the inhibition of the CO oxidation behavior. A different story is observed in the HC reactivity, Figure 1b. Although 90% conversion at 150°C is not observed, dispersing the ZrO_2 phase on the SiO_2 support resulted in the best HC reactivity with a $T_{90\%}$ of 257°C compared to 323°C for the commercial DOC. This improvement is significant and supports the continuation of the study to fully take advantage of the enhanced activity from the addition of the ZrO_2 phase. An area of improvement that will be the focus of future work is how to better disperse the ZrO_2-phase on the SiO_2 support (current estimates indicate only ~18% coverage), and how to anchor the Pd to the Zr-phase versus the silica phase. The ability to do this should help both the HC activity and the resistance to hydrothermal aging. This is illustrated in Figure 2, where transmission electron spectroscopy images of the Pd/ZrO_2, $PdSiO_2$ and Pd/ZrO_2-SiO_2 samples after hydrothermal aging at 800°C show finely dispersed Pd on the ZrO_2 sample but significant sintering when using SiO_2.

An important aspect from the Pd work is that the addition of the ZrO_2 improves HC oxidation compared to other catalysts, and while the results in Figure 1 and elsewhere show HCs inhibit CO oxidation [5,6], it is also

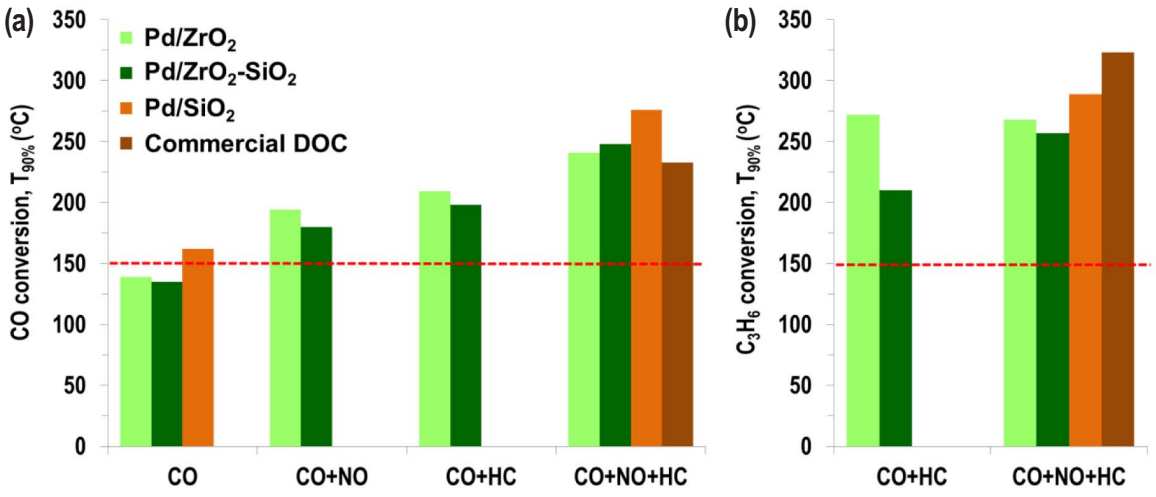

FIGURE 1. Temperature of 90% conversion ($T_{90\%}$) for either (a) CO or (b) C_3H_6 under a variety of reaction conditions using fresh catalysts. Reaction Conditions: 4,000 ppm CO/500 ppm NO/1,000 ppm C_3H_6 +10% O_2 + 5% H_2O in Ar, W/F = 0.19 g·h mol^{-1}.

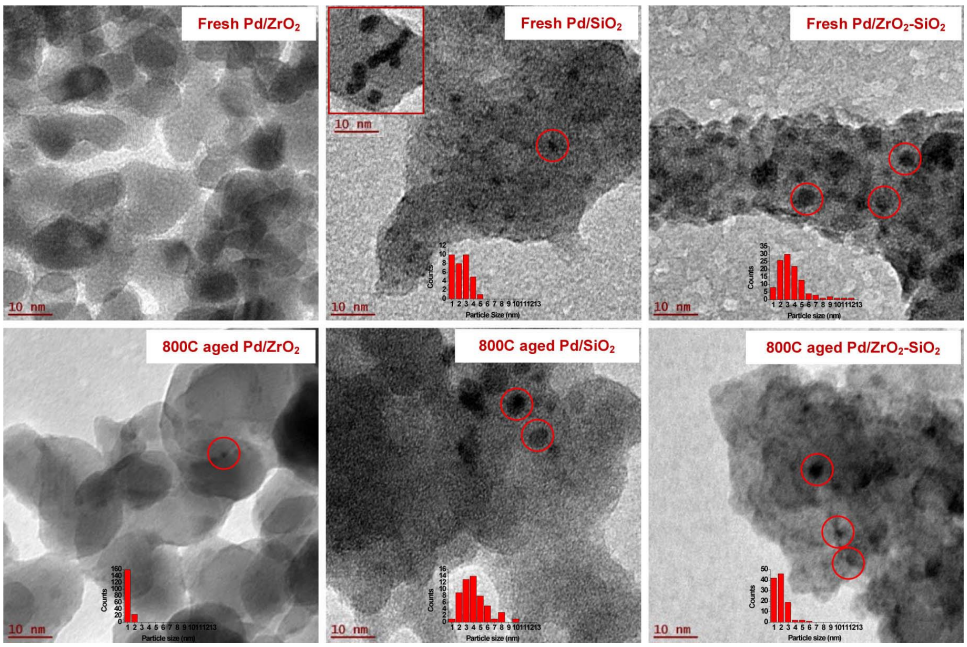

FIGURE 2. Transmission electron spectroscopy images of Pd/ZrO_2, Pd/SiO_2, and Pd/ZrO_2-SiO_2 in fresh and hydrothermally aged state; a few representative Pd particles are marked with circles in the images.

possible for CO to inhibit HC oxidation. Figure 3a shows that the removal of CO results in significantly improved HC oxidation. Thus having a catalyst that can remove CO in the presence of HC would be very beneficial. In working with a Basic Energy Science-funded group at the University of Tennessee we began exploring the potential of a PGM-free catalyst that demonstrated good stability and very good low temperature CO oxidation, less than 100°C in dry conditions [7]. The catalyst is a ternary oxide with the following general form: CuO_x-CoO_y-CeO_2 (CCC). We then incorporated this into our study to investigate its reactivity under simulated exhaust conditions. Figure 3b illustrates that this PGM-free catalyst has two exceptional traits: low-temperature CO reactivity and CO oxidation is unaffected by HC oxidation. The PGM-free CCC catalyst (red lines in Figure 3b) is in fact more reactive than the best Pd-based catalyst that we studied earlier, Pd/ZrO_2-SiO_2. The addition of 0.1% C_3H_6 has no effect on the reactivity which is a very unique trait and one that can be exploited in automotive exhaust.

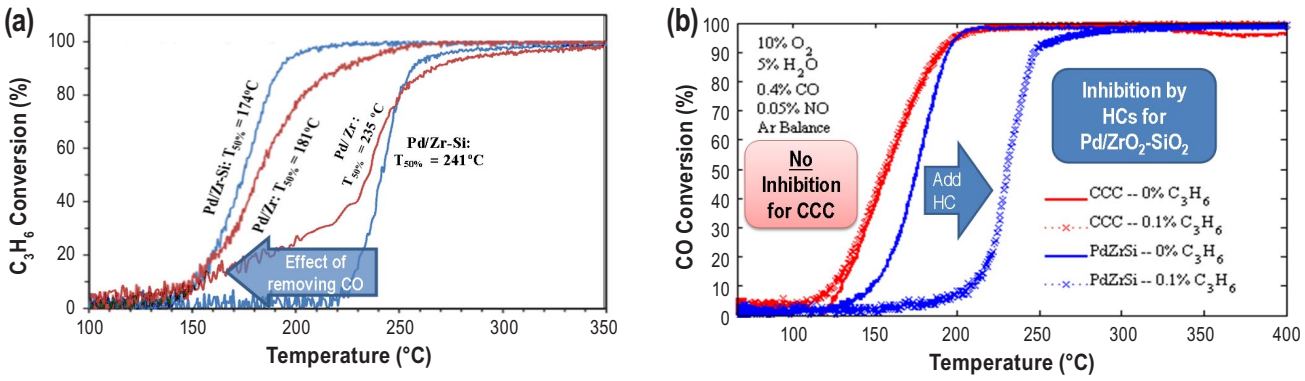

FIGURE 3. (a) C_3H_6 and (b) CO light-off curves of Pd/ZrO_2, Pd/ZrO_2-SiO_2, and CuOx-CoOy-CeO_2 (CCC) catalysts in simulated exhaust conditions. Arrows highlight significant change in the response to either C_3H_6 or CO.

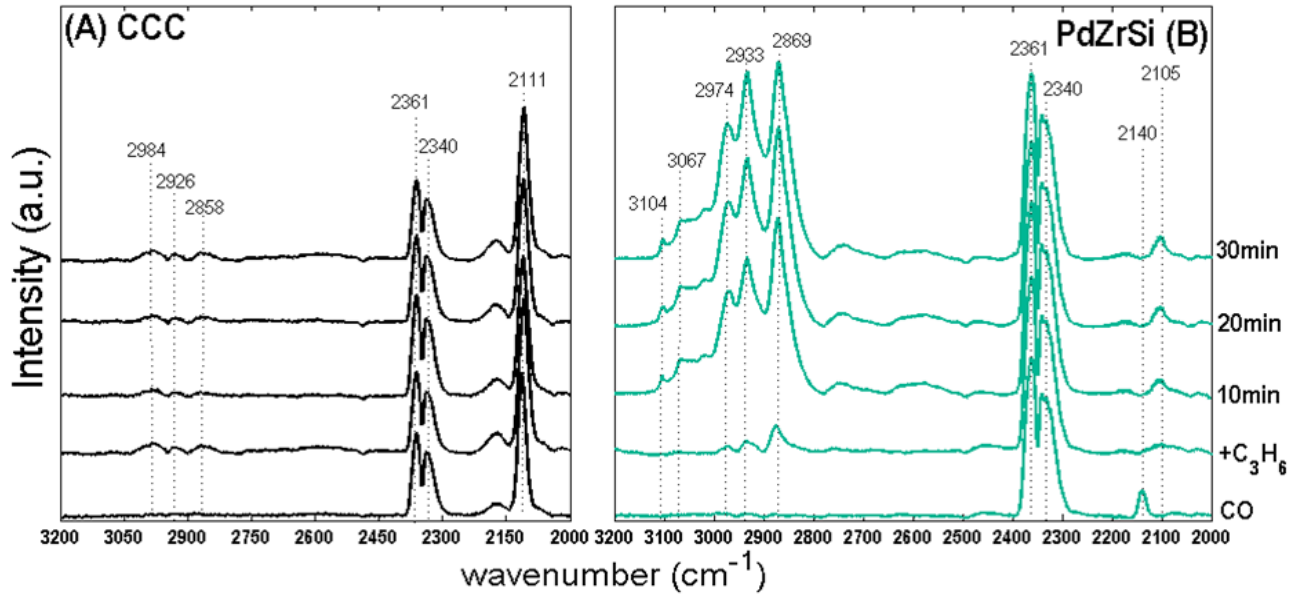

FIGURE 4. Diffuse reflectance infrared Fourier-transform spectroscopy data collected for (A) CCC at 120°C and (B) Pd/ZrO_2-SiO_2 at 140°C before and after introduction of [C_3H_6] = 0.1%. Initial stream: [O_2] = 10%, [CO] = 0.4%, Ar balance.

While the goal of this project is to identify catalysts that have the potential to be used in low-temperature exhaust environments, it is also a goal to understand how these catalysts function so that more catalysts can be studied that demonstrate similar traits. With this in mind we employed diffuse reflectance infrared Fourier transform spectroscopy to study the competitive adsorption of hydrocarbons and CO (Figure 4 with peak assignments defined in Table 1). The data shows that upon introduction of C_3H_6 to PdZrSi with pre-adsorbed CO, the Pd-CO band (2,105 cm^{-1}) immediately disappears and reappears with time at a significantly shifted position (Δ = -35 cm^{-1}) indicating a reduction in the oxidation state of the Pd metal and a change in the CO adsorption site on the active metal [8]. On the CCC catalyst, no disappearance of the Cu^+-carbonyl band is observed and only a slight shift occurs (Δ = -5 cm^{-1}), still within the region for Cu^+-carbonyl on CuO-CeO_2 [9]. Furthermore, the C-H stretching bands that appear upon C_3H_6 adsorption are significantly weaker and broader for the CCC catalyst compared to Pd/ZrO_2-SiO_2, suggesting a weaker C_3H_6 adsorption by CCC at lower temperatures where CO oxidation occurs.

TABLE 1. Peak Assignments from the DRIFT Spectra shown in Figure 4

Wavenumber	Assignment
2105	Pd^+-CO
2140	Pd^{2+}-CO
2111	Cu^+-CO
2340,2361	CO_2 gas
2800-3200	C-H stretch

To better understands which phases of the CCC catalyst are active for HC adsorption and CO oxidation a systematic study was commenced that removed one of the oxides, thus Cu-Co, Cu-Ce and Ce-Co catalysts were synthesized (details in Table 2). Figure 5 illustrates the light-off behavior of the three binary catalysts. It is interesting to note that all three of the samples exhibit similar CO oxidation behavior, with the CuCe sample having the lowest initiation temperature. These results suggest the Cu-phase is the likely most active component, but each phase may play a role. The HC oxidation behavior is significantly different for the Co-free CuCe catalyst, which suggests the Co-phase is responsible for both HC adsorption and thus reactivity. Also note that the CCC catalyst was superior to the three binary samples for CO oxidation, so there is an unexpected synergistic affect observed, which likely derives from the higher surface area that occurs when combining these three phases (Table 2). With these additional characterization experiments we can propose that its good low-temperature CO oxidation behavior is uninhibited by HCs, because CO and HC adsorb on different phases, with the CO likely adsorbing on the Cu-phase and the HC adsorbing on the Co-phase in small quantities.

While the low HC adsorption for the CCC catalyst is a primary reason that it is active near 150°C, some applications would benefit from having HC adsorb on them at low temperatures to allow light-off to occur and thus enable the catalyst to reach its active state faster. With this in mind we have embarked on a study of HC adsorbers. The first materials we will be investigating are zeolite-based and have pores large enough to allow adsorption of HC on their entire surface. These materials are listed in Table 3, and while some results have been recorded this year we will discuss these materials more next year.

TABLE 2. Compositional and Structural Properties of Ternary and Binary Catalysts

Sample	EDX atomic percentage[a]			Ratio (Cu:Co:Ce)	Crystallite size[b]		SSA ($m^2 g^{-1}$)
	Cu	Co	Ce		d_{Co3O4}	d_{CeO2}	
CCC	9 ± 2	46 ± 1	45 ± 1	1 : 5 : 5	18	8	41.8
CoCe	--	52 ± 2	48 ± 2	0 : 1 : 1	13	10	34.9
CuCe	9 ± 1	--	91 ± 1	1 : 0 : 10	--	17	26.7
CuCo	9 ± 2	91 ± 2	--	1 : 10 : 0	26	--	8.6

EDX - energy dispersive X-ray spectroscopy

TABLE 3. Hydrocarbon trapping materials that are being studied in a systematic variation of key zeolite properties: pore structure (Beta vs. ZSM-5), acidity (low vs. high SiO_2/Al_2O_3), and cation type (H+ vs. Ag+).

Zeolite type	SiO_2/Al_2O_3 molar ratio	Nominal cation form	Surface area (m^2/g)
Beta	25	H^+	680
Beta	25	Ag^+	NM
Beta	300	H^+	620
Beta	300	Ag^+	NM
ZSM-5	30	H^+	405
ZSM-5	30	Ag^+	NM
ZSM-5	280	H^+	400
ZSM-5	280	Ag^+	NM

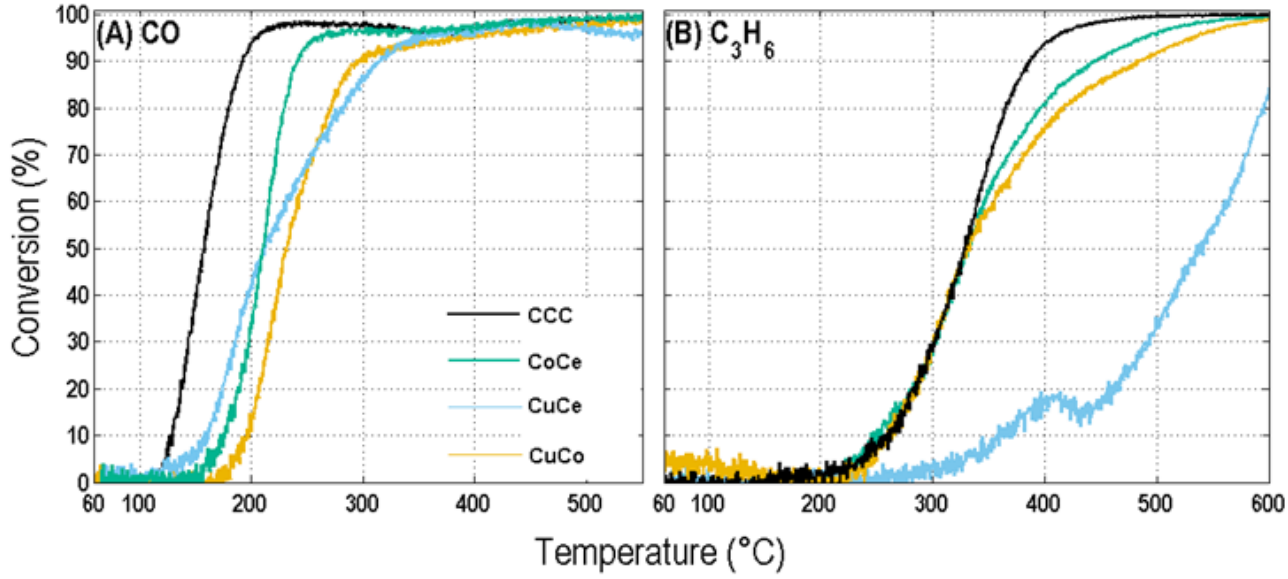

FIGURE 5. Light-off curves under simulated exhaust conditions for ternary CCC and binary catalysts. (A) CO oxidation. (B) C_3H_6 conversion. [O_2] = 10%, [H_2O] = 5%, [NO] = 0.05%, [CO] = 0.4%, [C_3H_6] = 0.1%, balanced with Ar at gas hourly space velocity ≈150,000^{-1}.

CONCLUSIONS

- Conventional PGM-based catalysts, particularly Pd, continue to show the best activity for HC oxidation. The supporting of Pd on a ZrO_2 support can improve both activity and durability, but dispersing this relatively low surface area support on a high surface area one like SiO_2 is the best path to 90% conversion at 150°C.
- Non-traditional catalysts continue to be a major focus of the project specifically a PGM-free ternary oxide, CuO_x-CoO_y-CeO_2 (CCC), which has demonstrated excellent low-temperature CO oxidation, high activity in the presence of HCs, and durability up to 800°C.
- Combining technologies is the best pathway towards achieving the goal of 90% conversion of NO, HC, and CO at 150°C and thus research will continue on a multifaceted approach that includes HC trap materials.

REFERENCES

1. Kašpar, J.; Fornasiero, P.; Hickey, N.; *Catal. Today* **2003**, *77*, 419–449.

2. U.S. Environmental Protection Agency, *EPA-420-F-13-016a* **2013**, 1-4.

3. U.S. Environmental Protection Agency, Department of Transportation, National Highway Traffic Safety Administration, *Federal Register* **2012**, *77:199*, 62623-63200.

4. Prikhodko, V.; Curran, S.; Parks, J.; and Wagner, R.; *SAE Int. J. Fuels Lubr.* **2013**, *6:2*, 329-335.

5. M.A. Harbi, R. Hayes, M. Votsmeier, W.S. Epling, *Can. J. Chem. Eng.* **90**, 1527–1538 (2012).

6. J.T. Kummer, *J. Phys. Chem.*, 4747–4752 (1986).

7. Z.-G. Liu, S.-H. Chai, A. Binder, Y.-Y. Li, L.-T. Ji, S. Dai, Appl. Catal. A 451 (2012) 282.

8. A. Martínez-Arias *et al.*, *Appl. Catal. B. - Environ* **31**, 51–60 (2001).

9. P. Bera, A.L. Cámara, A. Hornés, A. Martínez-Arias, *J Phys Chem C* **113**, 10689–10695 (2009).

FY 2014 PUBLICATIONS/PRESENTATIONS

1. J. Chris Bauer, Todd J. Toops, Yatsandra Oyola, S. Dai, S. Overbury, James E. Parks II, "Catalytic activity and thermal stability of Au-CuO/SiO_2 catalysts for the low temperature oxidation of CO in the presence of propylene and NO," Catalysis Today 231 (2014) 15-21.

2. Christopher D. DiGiulio, Josh A. Pihl, Jae-Soon Choi, James E. Parks II, Michael J. Lance, Michael D. Amiridis and Todd J. Toops, "NH_3 formation over a Lean NOx Trap (LNT) system: effects of lean/rich cycle timing and temperature", Applied Catalysis B: Environmental 147 (2014) 698-710.

3. Christopher D. DiGiulio, Josh A. Pihl, James E. Parks II, Michael D. Amiridis, Todd J. Toops, "Passive-Ammonia Selective Catalytic Reduction (SCR): Understanding NH_3 formation over close-coupled Three Way Catalysts (TWC)," Catalysis Today 231 (2014) 33-45.

4. Andrew Wong, Todd J. Toops, John R. Regalbuto, "Catalytic behavior of Pt-Pd Bimetallic Diesel Oxidation Catalysts Synthesized by Strong Electrostatic Adsorption," 2014 Southeastern Catalysis Society Fall Symposium, September 14-15, 2014.

5. Andrew J. Binder, Todd Toops, Sheng Dai, James E. Parks, "CO Oxidation over CuO_x-CoO_y-CeO_2 Ternary Oxide in Simulated Exhaust Conditions: Comparison to Platinum-Group Metal Catalysts," 8th International Conference on Environmental Catalysis, Asheville, NC, August 24-27, 2014.

6. Mi-Young Kim, Jae-Soon Choi, Todd J. Toops, Cyril Thomas, Andrew Binder, James E Parks II, Viviane Schwartz, Jihua Chen, "Enhancing Durability and Low-Temperature Activity of Pd-based Diesel Oxidation Catalysts Using ZrO_2 Supports," 8th International Conference on Environmental Catalysis, Asheville, NC, August 24-27, 2014.

7. James E. Parks, Todd Toops, Jae-Soon Choi, Miyoung Kim, Chris Bauer, Andrew Binder, "Low Temperature Emission Control to Enable Fuel-Efficient Engine Commercialization," presentation to the U.S. DOE Vehicle Technologies Office 2014 Annual Merit Review and Peer Evaluation Meeting, Washington D.C., June 19, 2014.

8. Todd J. Toops, James E. Parks, Jae-Soon Choi, Miyoung Kim, Chris Bauer, Andrew Binder, "Investigation of Low Temperature Emissions Control Catalysts to Enable Fuel-Efficient Engine Commercialization," 2014 Cross-cut Lean Exhaust Emissions Reduction Simulations (CLEERS) Workshop, Dearbon, MI, May 1, 2014.

III.8 Emissions Control for Lean-Gasoline Engines

Jim Parks (Primary Contact), Todd Toops, Josh Pihl, Vitaly Prikhodko
Oak Ridge National Laboratory (ORNL)
2360 Cherahala Blvd.
Knoxville, TN 37932

DOE Technology Development Manager
Ken Howden

Overall Objectives

- Assess and characterize catalytic emission control technologies for lean-gasoline engines.
- Identify strategies for reducing the costs, improving the performance, and minimizing the fuel penalty associated with emission controls for lean-gasoline engines.
- Identify a technical pathway for a lean-gasoline engine to meet U.S. emission regulations (U.S. Environmental Protection Agency Tier 3) with minimal fuel consumption and cost.
- Demonstrate the fuel efficiency improvement of a low-emission lean-gasoline engine relative to the stoichiometric-gasoline engine case on an engine dynamometer platform.

Fiscal Year (FY) 2014 Objectives

- Characterize the performance of Umicore three-way catalyst (TWC) prototypes for NH_3 production for downstream oxides of nitrogen (NOx) reduction over selective catalytic reduction (SCR) catalysts.
- Define the potential impact of NOx storage components added to TWC formulations.
- Measure the H_2 concentration as a function of air-to-fuel ratio in engine exhaust, and determine the effect of H_2 concentration on NH_3 formation.

FY 2014 Accomplishments

- Determined that H_2 concentration is not a limitation at air-to-fuel ratios associated with peak NH_3 production over the TWC.
- Evaluated the concept of adding a NOx storage component to the TWC for increasing net NH_3 production; discovered that the relative advantage of the NOx storage component addition is a strong function of temperature, with lower temperatures giving more improvement in fuel economy.
- Constructed and commissioned a synthetic exhaust gas catalyst aging apparatus with the capability to age catalysts under a stoichiometric-rich-stoichiometric-lean sequence per industry guidance (based on communication with collaborating partners General Motors and Umicore).

Future Directions

- Determine the effect of thermal aging on NH_3 production by TWCs.
- Measure the fuel penalty of the passive SCR approach for programmed load-step engine operation that simulates mode switching operation (between lean and rich) in transient drive cycles.

INTRODUCTION

Currently, the U.S. passenger car market is dominated by gasoline engine powertrains that operate at stoichiometric air-to-fuel ratios (sufficient fuel is mixed in air such that all of the oxygen in the air is consumed during combustion). Stoichiometric combustion leads to exhaust conditions suitable for TWC technology to reduce NOx, CO, and hydrocarbon (HC) emissions to extremely low levels. Operating gasoline engines at lean air-to-fuel ratios (excess air) enables more efficient engine operation and reduces fuel consumption; however, the resulting oxygen in the exhaust prevents the TWC technology from reducing NOx emissions. It is relatively straightforward to operate an engine lean over a significant portion of the load and speed operating range; so, the largest challenge preventing fuel-saving lean combustion in gasoline applications is the control of emissions, primarily NOx. This project addresses the challenge of reducing emissions from fuel-saving lean gasoline engines in a cost-effective and fuel-efficient manner to enable their market introduction.

APPROACH

This project utilizes the full suite of capabilities available at ORNL's National Transportation Research Center, including: a lean-gasoline engine on an engine dynamometer, a vehicle equipped with the same engine on a chassis dynamometer, flow reactors for detailed catalyst evaluations under carefully controlled operating

conditions, and vehicle system level modeling. The combination of catalyst studies on flow reactor and engine platforms is a key component of the project approach. Prototype catalyst formulations are first studied on flow reactors to understand catalytic function and establish operating parameters in a controlled setting; then, select catalyst combinations are studied on the engine platform to characterize performance under realistic exhaust conditions. The engine studies also enable direct measurement of fuel economy benefits from lean-gasoline engine operation as well as measurement of "fuel penalties" imposed by the emission control system to function properly.

The engine platform for the project is from a model year 2009 BMW 120i vehicle sold in Europe. The 4-cylinder, direct-injection, naturally aspirated engine operates in multiple modes including lean (excess air) and stoichiometric combustion. The BMW 120i employs both a TWC for stoichiometric operation and a lean-NOx trap (LNT) catalyst for NOx reduction during lean operation. Although this engine and aftertreatment combination met the 2009 emissions regulations in Europe, as configured its emissions are well above the current U.S. emissions standards. Furthermore, the LNT catalyst contains high loadings of platinum group metals, which add significantly to the overall cost of the vehicle. The goal for this project is to identify emissions control technologies that could meet the U.S. Environmental Protection Agency Tier 3 emission standards, which represent reductions of 70% for NOx and 85% for HCs compared to the previous Tier 2 standard. In addition to the emissions goal, the project aims to maximize the fuel efficiency benefit from lean-gasoline engine operation and minimize system cost.

To date, the project has primarily focused on an emission control concept known as "passive SCR" [1-3]. The key to the approach is to generate NH_3 over the TWC under slightly rich conditions and then store it on a downstream SCR. When returning to lean operation, the stored NH_3 reduces NOx that is not converted over the upstream TWC. In this manner, the TWC controls NOx during stoichiometric and rich operation of the engine, and the SCR catalyst controls NOx during lean-engine operation. This report highlights results from both engine and flow reactor experiments on a passive SCR emission control system. The catalysts used in the system were either supplied or recommended by Umicore, a major catalyst supplier to the automotive industry. Frequent interaction occurred with collaborating partners Umicore and General Motors to guide project progress and relevance.

RESULTS

In FY 2013, >98% reduction of NOx emissions was demonstrated on engine with the passive SCR approach using a commercial TWC and small pore copper zeolite SCR catalyst supplied by Umicore. The lean engine operation gave a 5.5% fuel efficiency gain over stoichiometric operation at a moderate load (2 bar), including the extra fuel required for NH_3 generation for the passive SCR approach. While excellent NOx reduction efficiency and significant fuel economy improvements were observed, the performance was still short of the long-term project goal of 15% better fuel economy. Thus, FY 2014 activities focused on specific approaches to better the system level fuel efficiency; corresponding experiments from an engine and a flow reactor study are presented here.

Improving the mass rate of NH_3 production during rich engine operation will increase the fuel efficiency of the passive SCR approach. One approach to increase NH_3 production is to generate more NOx emissions from the engine during rich operation; however, such an approach is only feasible when sufficient reductant is available to convert the NOx to NH_3 over the TWC. To determine whether or not the NOx to NH_3 conversion is limited by reductant supply, engine-based experiments were conducted to characterize the engine-out and TWC-out emissions as a function of lambda (λ), which represents the ratio of the actual air-to-fuel ratio to the stoichiometric air-to-fuel ratio (λ<1 indicates fuel-rich operation). Emissions downstream of the TWC at 2,000 rpm and 2 bar are shown in Figure 1. As λ decreases, higher levels of reductants (NH_3, CO, H_2, and HCs) are observed as expected; note that the NH_3 is generated by conversion of the engine-out NOx

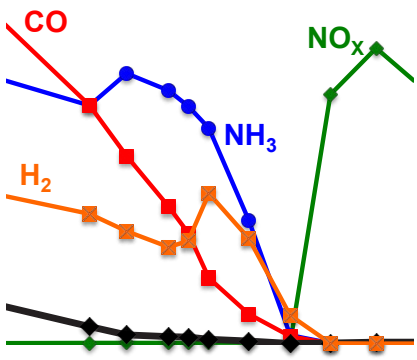

FIGURE 1. Emissions downstream of the TWC as a function of air-to-fuel ratio (expressed as lambda) showing the relative concentration of reductants CO, H_2, NH_3, and HCs.

over the TWC. The optimal λ to operate is dependent on many factors; importantly, as λ decreases, more fuel is consumed. Other factors impacting the choice of λ include selectivity of NOx reduction to NH_3 and emissions of CO and HCs, both of which must be controlled to the Tier 3 standard. Focusing on high NH_3 production and low HC emissions, λ=0.96 was chosen for rich operation for further engine experiments; however, this may not be the optimal point for fuel economy.

Data was collected at λ =0.96 and stoichiometric conditions (λ =1.00) for comparison at different engine speed and load combinations. The ratio of H_2 to NOx upstream of the TWC was measured and is shown in Figure 2. H_2 is of particular importance since H_2 can react directly with NOx to form NH_3 via the equation shown in Figure 2. As a reference, the ratio of H_2 to NO in this reaction (2.5) is shown on the graph as a dashed line. As apparent from the data, the H_2:NOx ratio is much higher than the NH_3 formation stoichiometry for all speed and load points at λ=0.96. Considering this data was collected at the TWC outlet, the data shows that plenty of excess H_2 is available for further conversion of NOx to NH_3 over the TWC. Thus, a limiting factor is the engine out NOx emission level under these conditions. This finding shows that approaches to improve NH_3 formation rates by increasing in-cylinder NOx formation are feasible approaches to pursue since sufficient reductant is available to convert a higher NOx mass to NH_3.

Another approach pursued to increase the NH_3 production was a modification of the TWC formulation. A catalyst including a NOx storage component was provided by Umicore for investigations in simulated exhaust gas. The concept behind this approach is to store NOx during the lean phase of operation so that more NOx is available on the TWC for conversion to NH_3 during rich operation. Thus, the stored NOx, released during rich operation, would join the NOx coming into the TWC from the engine to create more total NOx to convert to NH_3. An additional advantage is that NOx passing to the downstream SCR catalyst would be decreased during the lean phase, allowing longer lean operation with an equivalent amount of NH_3 stored on the SCR catalyst. Figure 3 shows lean-rich cycling of the TWC with NOx storage component at 300ºC. Here we observe that catalyst outlet NOx is less than the inlet concentration during lean operation (time: 10-13.2 min), indicating NOx storage. Furthermore, catalyst outlet NH_3 is more than the inlet NOx concentration during the rich phase (time: 13.2-14.4 min), which implies that some of the stored NOx is converted to NH_3, proving that the concept of NOx storage to boost NH_3 production works at 300ºC. However, note that there is a significant delay in the production of NH_3 during the rich phase. Such temporal lags in NH_3 production may be problematic for transient operation and control.

The formulation with NOx storage was also studied at many other catalyst temperatures. Figure 4 shows lean-rich cycling of the same catalyst at 500ºC. Here, the performance differs greatly from the 300ºC case. While some NOx is stored in the lean phase (time: 11.3-12.4 min), at the switch to the rich phase (time: 12.4 min),

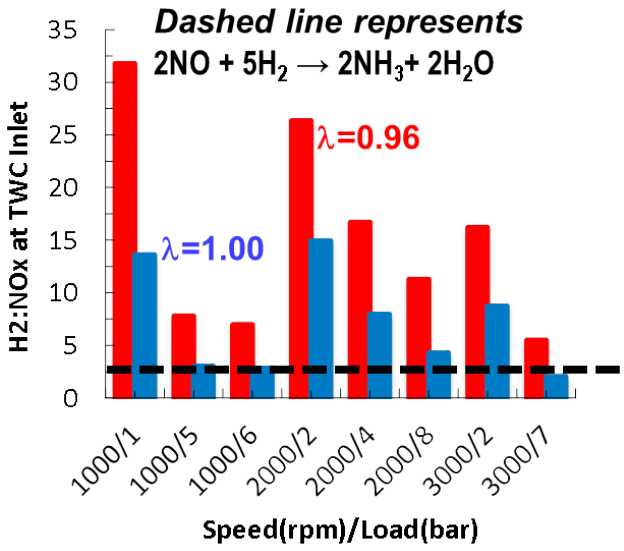

FIGURE 2. Ratio of H_2 to NOx upstream of the TWC at stoichiometric (λ=1.00) and rich (λ=0.96) conditions; results show the production of NH_3 (via chemical reaction shown) is not limited by H_2 supply.

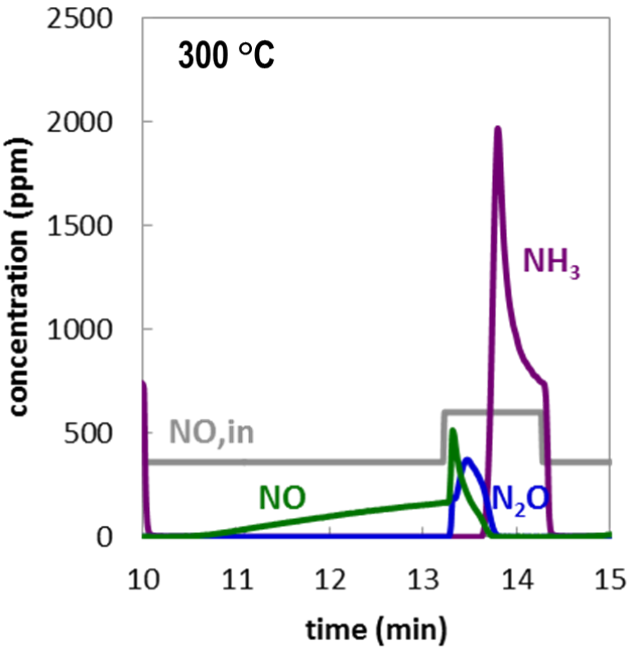

FIGURE 3. Nitrogen species over a lean-rich cycle at 300ºC as a function of time. During lean operation (time=10-13 min) NOx storage occurs which leads to higher NH_3 formation during rich operation (time=13-14.5 min).

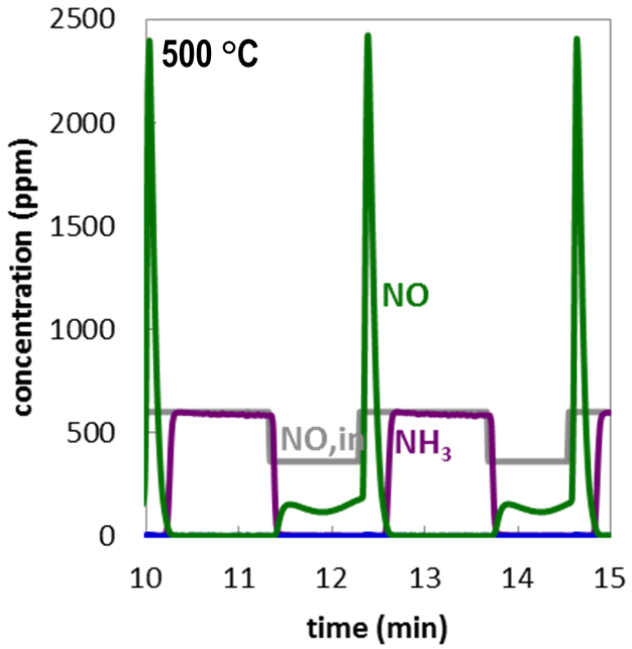

FIGURE 4. Nitrogen species over a lean-rich cycle at 500°C as a function of time. During the rich phase of operation (time=12.3-13.8 min), the release of stored NOx occurs rapidly at the onset of rich conditions, thereby preventing further reduction to NH_3.

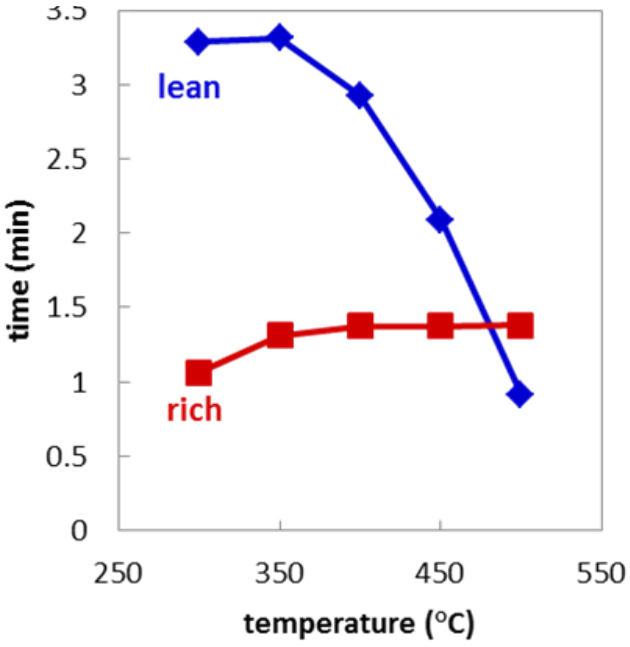

FIGURE 5. Periods of lean and rich operation required to achieve sufficient NH_3 for NOx reduction as a function of temperature.

a spike of NO comes out of the catalyst, representing stored NOx that is not converted to NH_3. Furthermore, no additional NH_3 above the amount associated with the inlet NOx level is observed. Thus, at high temperatures during rich operation, the release of the stored NOx from the NOx storage component does not correspond temporally with the presence of reductants, which limits the conversion of the stored NOx to NH_3.

Figures 5 and 6 show results for the NOx storage component addition across the temperature range associated with a lean gasoline engine. Figure 5 shows the experimentally defined lean and rich periods that produce equal NH_3 levels during rich operation to account for the NOx level entering the downstream SCR catalyst for reduction; this corresponds to the 1:1 NH_3:NOx stoichiometry that is typical of SCR operation. Here we observe that, at lower temperatures, longer lean operation can result from the improved NH_3 production during rich operation and reduced lean NOx at the TWC outlet enabled by the NOx storage component on the TWC. However, at high temperatures, the benefit decreases and ultimately disappears due to the temporal mismatch shown in Figure 4. Based on the percentage of lean operation relative to the entire lean-rich cycle (the "lean time fraction"), we can predict the fuel economy gain (relative to a stoichiometric gasoline engine) for a lean-gasoline engine operating with the TWC with NOx storage and a downstream SCR catalyst (assuming ideal NOx conversion over the SCR). The prediction is shown

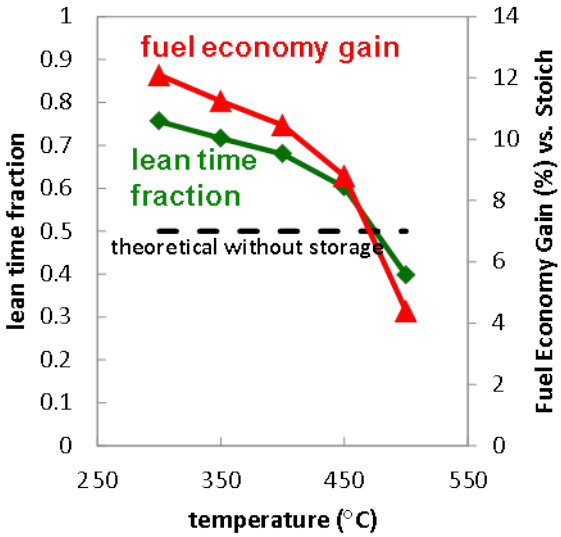

FIGURE 6. Lean time fraction and associated predicted fuel economy gain as a function of temperature; fuel economy gain is relative to stoichiometric-only operation.

in Figure 6 along with the lean-time fraction. At low temperatures, the fuel economy gain reaches 12%, but the lean gasoline benefit is reduced at high temperatures to near 6% (more consistent with performance the TWC that does not have a NOx storage component). Thus, we find that addition of a NOx storage component to the TWC can increase the fuel economy of the system, but catalyst

temperature and transient operation affect the gains from the NOx storage component dramatically. Ongoing studies of this approach will include engine-based studies and durability studies.

CONCLUSIONS

Two approaches have been studied for the purpose of increasing NH_3 production over a TWC to lessen rich operation and, thereby, increase the fuel economy gain of the lean gasoline engine. Findings in FY 2014 related to these approaches are:

- During rich engine operation for the production of NH_3 over the TWC, levels of H_2 have been observed that would enable further NH_3 production if higher engine-out NOx levels could be generated.
- The addition of a NOx storage component to the TWC can increase NH_3 production during lean-rich cycling and have a net benefit in the predicted fuel economy gain, but the gains are highly subject to the catalyst temperature and temporal release of stored NOx by the catalyst.

REFERENCES

1. Li, W., Perry, K., Narayanaswamy, K., Kim, C. et al., "Passive Ammonia SCR System for Lean-burn SIDI Engines," *SAE Int. J. Fuels Lubr.* 3(1):99-106, 2010, doi:10.4271/2010-01-0366.

2. Kim, C., Perry, K., Viola, M., Li, W. et al., "Three-Way Catalyst Design for Urealess Passive Ammonia SCR: Lean-Burn SIDI Aftertreatment System," SAE Technical Paper 2011-01-0306, 2011, doi:10.4271/2011-01-0306.

3. Guralp, O., Qi, G., Li, W., and Najt, P., "Experimental Study of NOx Reduction by Passive Ammonia-SCR for Stoichiometric SIDI Engines," SAE Technical Paper 2011-01-0307, 2011, doi:10.4271/2011-01-0307.

FY 2014 PUBLICATIONS/PRESENTATIONS

1. Vitaly Y. Prikhodko, James E. Parks, Josh A. Pihl, and Todd J. Toops, "Ammonia Generation over TWC for Passive SCR NOx Control for Lean Gasoline Engines", *SAE Int. J. Engines* 7(3):1235-1243, 2014, doi:10.4271/2014-01-1505.

2. Christopher D. DiGiulio, Josh A. Pihl, Jae-Soon Choi, James E. Parks II, Michael J. Lance, Todd J. Toops, and Michael D. Amiridis, "NH_3 formation over a lean NOx trap (LNT) system: Effects of lean/rich cycle timing and temperature", *Applied Catalysis B: Environmental* **147**, pp. 698-710 (2014).

3. Christopher D. DiGiulio, Josh A. Pihl, James E. Parks II, Michael D. Amiridis, and Todd J. Toops, "Passive-Ammonia Selective Catalytic Reduction (SCR): Understanding NH3 formation over close-coupled Three Way Catalysts (TWC)", *Catalysis Today* **231**, pp. 33-45 (2014).

4. Vitaly Y. Prikhodko, James E. Parks II, Josh A. Pihl, and Todd J. Toops, "Ammonia generation over TWC for passive SCR NOx control in lean gasoline engines", *2014 DOE Crosscut Workshop on Lean Emissions Reduction Simulation (CLEERS),* April 29 – May 1, 2014 (2014).

5. Alla Zelenyuk, Jacqueline Wilson, Mark Stewart, George Muntean, John Storey, Vitaly Prikdhodko, Samuel Lewis, and Mary Eibl, "Detailed Characterization of Particulates Emitted by Lean-Burn Gasoline Direct Injection Engine", *2014 DOE Crosscut Workshop on Lean Emissions Reduction Simulation (CLEERS),* April 29 – May 1, 2014 (2014).

6. Jim Parks, "Emission Control Challenges for Advanced Combustion Approaches", *SAE 2013 Fuels, Lubricants, and Aftertreatment Symposium*, Long Beach, CA, November 18-21, 2013.

7. Jim Parks, Todd Toops, Josh Pihl, Vitaly Prikhodko, "Emissions Control for Lean Gasoline Engines", 2014 DOE Annual Merit Review, Washington, DC, June 16–20, 2014.

III.9 Cummins-ORNL SmartCatalyst CRADA: NO_x Control and Measurement Technology for Heavy-Duty Diesel Engines

Bill Partridge[1] (Primary Contact), Neal Currier[2], Mi-Young Kim [1], Josh Pihl[1], Jae-Soon Choi[1], Krishna Kamasamudram[2], Alex Yezerets[2]
[1]Oak Ridge National Laboratory (ORNL)
[2]Cummins Inc.
2360 Cherahala Blvd.
Knoxville, TN 37932

DOE Technology Development Manager
Ken Howden

Overall Objectives

- Understand the fundamental chemistry of automotive catalysts
- Identify strategies for enabling self-diagnosing catalyst systems
- Address critical barriers to market penetration

Fiscal Year (FY) 2014 Objectives

- Characterize distributed performance of hydrothermally aged commercial Cu-SAPO-34 selective catalytic reduction (SCR) catalyst under standard and fast SCR conditions.
- Improve spatially resolved capillary inlet mass spectrometer (SpaciMS) analysis codes for better quantification and balances
- Compare de-greened and hydrothermally aged integral and intra-catalyst distributed performance
- Demonstrate the effectively noninvasive nature of intra-catalyst sampling and experimental methods for assessment

FY 2014 Accomplishments

- Characterized spatiotemporal intra-catalyst performance of hydrothermally aged commercial Cu-SAPO-34 SCR catalyst under standard and fast SCR conditions
- Developed improved SpaciMS analysis codes for improved quantification and enabling nitrogen and stoichiometry balances
- Demonstrated noninvasive nature of SpaciMS capillary sampling methodology used for Cooperative Research and Development Agreement (CRADA) measurements
- Many publications and presentations of CRADA work:
  - In collaboration with Professor Louise Olsson and Dr. Xavier Auvray at Chalmers University of Technology demonstrated fitting of kinetic parameters under normal catalyst operating conditions, and a model of distributed SCR performance.
  - In collaboration with the Cross-Cut Lean Exhaust Emissions Reduction Simulations (CLEERS) program, and Professor Marek and Dr. Petr Kočí at the Institute of Chemical Technology, Prague published mechanistic insights regarding N_2O formation in PGM catalysts.
  - In collaboration with the CLEERS program, and Professors Enrico Tronconi and Isabella Nova and Dr. Maria Pia Ruggeri of the Politecnico di Milano published insights regarding NO oxidation during the standard SCR reaction.
  - In collaboration with Professor Alexandre Goguet et al. at Queen's University Belfast published a rebuttal regarding the noninvasive nature of SpaciMS.
- One book chapter; three archival publications; two invited presentations; four oral presentations

Future Directions

Quantify spatiotemporal performance of commercial Cummins SCR catalyst under lab- and field-aged conditions

✧ ✧ ✧ ✧ ✧

INTRODUCTION

A combination of improved technologies for engine and aftertreatment control of oxides of nitrogen (NO_x) and particulate emissions are required to efficiently meet increasingly stringent emission regulations. This CRADA section focuses on catalyst technologies, while a parallel section (Characterization and Reduction of Combustion Variations) focuses on combustion and engine technologies. Improved catalyst-system efficiency, durability and cost can be achieved through advanced

control methodologies based on continuous catalyst state monitoring; the overarching goal of this CRADA section is to enable self-diagnosing or smart catalyst systems. Self-diagnosing catalyst technologies are enabled by basic and practical insights into the transient distributed nature of catalyst performance, improved catalyst models, insights suggesting control methodologies, and instrumentation to demonstrate and drive advanced control technologies. These catalysis advances require development and application of enhanced diagnostic tools to realize these technology improvements. While the CRADA has a strong diagnostic focus, it is involved, often through synergistic partnerships, in the other enabling research activities discussed previously.

APPROACH

The CRADA applies the historically successful approach of developing and applying minimally invasive advanced diagnostic tools to resolve spatial and temporal variations within operating engines and catalysts. Diagnostics are developed and demonstrated on bench reactors and engine systems (as appropriate) at ORNL prior to field application at Cummins. In some cases discrete sensor technology is a stepping stone and may be further developed and integrated in system components; e.g., to create self-diagnosing smart catalyst systems.

Diagnostics are applied at ORNL and Cummins to study the detailed nature and origins of catalyst performance variations; this may be spatial and temporal variations unique to each catalyst function (e.g., SCR, NH_3 storage and parasitic oxidation, NO_X storage and reduction, oxygen storage capacity, water-gas shift) during operating and how these vary with ageing (e.g., thermal, hydrocarbon, sulfur). This detailed information is applied to understand how catalysts function and degrade, develop device and system models, and develop advanced control strategies.

RESULTS

The integral and intra-catalyst distributed performance of a de-greened (700°C, 4 hrs) and hydrothermally aged (800°C, 50 hrs) commercial Cu-SAPO-34 SCR catalyst was assessed under standard and fast SCR conditions at 200, 300 and 400°C using a four-step protocol [1]. The ammonia capacity of the de-greened sample was measured without O_2 co-flow using 200 ppm NH_3 and a dedicated short protocol: NH_3 saturation at the target temperature (Total Capacity), subsequent isothermal desorption at the target temperature (Weakly Bound Capacity) and temperature-programmed desorption (Strongly Bound Capacity) in the absence of NH_3. At 200, 300 and 400°C, the Total Capacity was measured to be ca. 1.26, 0.73 and 0.34 grams NH_3 per liter catalyst based on mass spectrometry measurements. At the two higher temperatures, the vast majority of stored NH_3 desorbs in the isothermal desorption step. The measured values are consistent with separate work using spatially resolved capillary inlet Fourier transform infrared (SpaciIR) which indicated a Total Capacity of 1.2 g/L catalyst at 300°C using 500 ppm NH_3; assuming a simple single-site Langmuir Isotherm with ΔG = -40 kJ/mol approximate fit to intra-catalyst data, this corresponds to a value of 0.82 g/L catalyst if 200 ppm NH_3 had been used, and which is in excellent agreement considering the assumptions made for the comparison.

The de-greened and hydrothermally aged catalyst performance was compared on an integral and intra-catalyst distributed basis. Ageing impact on NH_3 capacity has been assessed from an integral basis and later work will focus on intra-catalyst distributed capacity components; the integral total capacity was degraded by 16, 25 and 25% at 200, 300 and 400°C, respectively. SpaciMS and the four-step protocol were used to assess the distributed performance of several aspects of SCR. In the de-greened state, the SCR conversion profiles were similar at 300 and 400°C, with the NO_X conversion being only ca. 5% greater at 400°C and the catalyst front 3/8 length; this is very different from the model Cu-Beta KCK (Chalmers University of Technology, Competence Center for Catalysis) SCR catalyst studied via SpaciMS previously, and which had very high conversion profile becoming increasingly step-like with increasing temperature [2]. The de-greened catalyst had both measurable NH_3 (neat) and parasitic oxidation at 400°C, but neither at 300°C. Hydrothermal ageing doubled the NH_3 oxidation at 400°C, but the parasitic NH_3 oxidation was identical for the de-greened and hydrothermally aged samples; this differing impact emphasizes how these are different reactions, likely occurring at different sites on the catalyst. Hydrothermal ageing had very little impact on the NO_X-conversion profiles, which were practically identical at 300°C. Similarly, the de-greened and hydrothermally aged NO_X conversion profiles were identical in the back 0.75 of the catalyst length at 400°C, but with some differences in the front 3/16; specifically, the NO_X conversion was degraded 59, 20 and 15% at the 1/16-, 1/8- and 3/16-length locations, with the NH_3 conversion being impacted similarly. The similar profiles in the catalyst back 0.75, where NH_3 conversion is 50-100%, indicates that the conversion catches up despite the front-end degradation. This is likely due to small differences in the catalyst loading on the two catalyst samples which could be amplified in the high-conversion-gradient region of the catalyst front. For the 400°C cases where parasitic NH_3 oxidation occurs, excellent overall NH_3:NO_X:N_2 balance was measured consistent with the partitioning of NH_3 between SCR and parasitic oxidation,

and all parasitic oxidation generating N_2. Furthermore, this is consistent with little to no N_2O being measured, which should increase with greater ageing. With respect to SCR performance, the 800°C, 50 hrs hydrothermal ageing was very mild, having little distributed and no integral impact, despite its impact on NH_3 total capacity; this also indicates that total NH_3 capacity is not limiting the integral performance, and further insights may come from the intra-catalyst capacity analysis. NH_3 oxidation was the most sensitive indicator of hydrothermal ageing in this case. Because of the mild impact of this initial hydrothermal ageing on SCR performance, we plan to perform additional lab ageing and selected analysis prior to analysis of a field-aged 2010CMI catalyst sample.

Improved SpaciMS analysis methodologies and codes were developed based on cross-sensitivity measurements which enabled better understand of reactions that occur in the reactor, catalyst and mass spectrometer ionizer. Initial work shows these new methods to improve the calculated NH_3:NO_X balance distributions compared to the old methods; e.g., the new analysis methodology enabled improved Total-N balances, typically within 5-10%, and in turn very good assessment of overall reaction stoichiometries.

Several archival journal papers and a book chapter based on CRADA work in collaboration with the DOE CLEERS project and university partners were published. One of these was in collaboration with Professor Louise Olsson at Chalmers University of Technology, and focused on determining kinetic parameters from SpaciMS data, and developing a model of distributed SCR-catalyst performance; this follows another similar joint paper related to lean-NO_X trap performance, and demonstrates the rich nature of SpaciMS data for determining kinetic parameters under normal operating conditions. Another was in collaboration with Dr. Kočí and Professor Marek at the Institute of Chemical Technology, Prague, and focused on N_2O formation mechanisms during operation of lean-NO_X trap catalysts; the mechanistic insights are believed to be general and applicable for N_2O formation over a broader class of platinum-group metal catalysts. A third was an invited publication in the form of a chapter focusing on iron-zeolite catalysis in a book on automotive SCR catalysis edited by Professors Nova and Tronconi of the Polytechnic University of Milan. A Letter to the Editor of Catalysis Today was published in electronic format; this was in collaboration with Professor Goguet et al. at Queens University, Belfast, and in response to published work incorrectly overstating the invasive nature of intra-catalyst SpaciMS capillary sampling.

Experiments to demonstrate the minimally invasive nature of intra-catalyst capillary probes, as used by SpaciMS and SpaciIR, were performed in response to some incorrect modeling-based results presented at the 2013 North American Catalysis Conference and published in the literature [3]; the basic incorrect message of those communications was that SpaciMS measurements are typically 50% wrong, and that only modeling is an appropriate way to demonstrate the invasive nature of intra-catalyst capillary sampling. In collaboration with partners at Queen's University Belfast, a separate response was published [4]. Figure 1 describes the background, experiments and results of the invasive-nature experimental study. The lower left portion of Figure 1 shows simulated catalyst conversion results for a probed and unprobed catalyst channel for a case where the intra-catalyst probe is invasive; in the figure flow is from left to right, blue represents reactants, red represents full conversion, and the black line in the lower channel represents the intra-catalyst probe. If indeed intra-catalyst sampling is invasive, it should lower the probed channel's flow rate, resulting in reduced space velocity, steeper conversion gradients closer to the catalyst front, and greater channel-out conversions compared to unprobed channels. Thus, increasingly invasive intra-catalyst sampling should cause (i) steeper intra-catalyst conversion gradients biased to the front, and (ii) a concentration step at the catalyst exit due to differing conversion in the probed and unprobed channels; these indicators of invasive nature are apparent in the lower-left portion of Figure 1.

The upper-left portion of Figure 1 details the intra-catalyst sampling methodologies used to generate five levels of catalyst-channel frontal-area blocking from 1.2% to 35%. Three different sampling capillary outside diameters (ODs) were used (150, 200 and 375 μm) to create different levels of channel blocking (1.2%, 2.2% and 7.7%, respectively); the three capillary sizes had the same 50-μm internal diameter to maintain consistent sample flow throughout the cases. To induce even greater catalyst channel blocking, the two larger capillary OD sizes were used along with a 700-μm OD optical fiber which was inserted the full length of the catalyst channel; these produced ca. 29% and 35% channel blocking for the 200- and 375-μm OD capillaries, respectively. The 300-cells-per-square-inch catalyst sample was oriented at ca. 45° so that the intra-catalyst probes rested along the bottom corner of the catalyst channel.

The right-hand portion of Figue 1 shows intra-catalyst distributed NH_3 oxidation with the de-greened 2010CMI SCR catalyst at three temperatures and five levels of channel blockage. For these experiments, reactant feed included 200 ppm NH_3, 10% O_2, 5% H_2O and Ar balance. The catalyst core was ca. 1-in long, and the spatial distribution is indicated as a fraction of this length; i.e., 0 is the inlet, 0.5 is half way along the catalyst channel, 1 is the channel exit, and 1.25 is

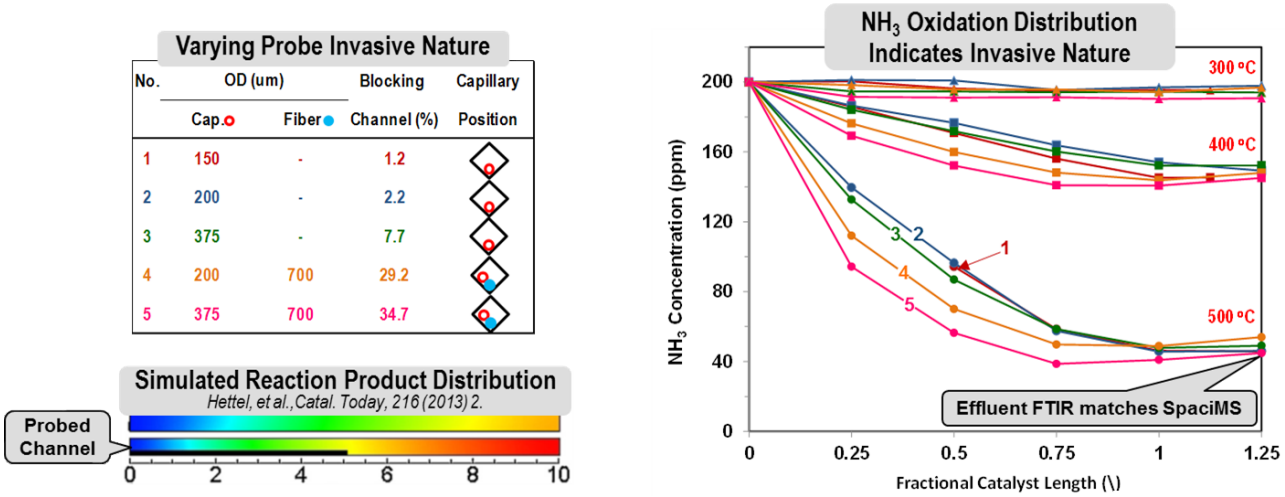

FIGURE 1. Experiment demonstrating the noninvasive nature of SpaciMS capillary sampling. Lower left figure shows modeling results for an invasive intra-catalyst sampling situation; blue represents reactants, red represents full reactant conversion, and the black line represents an intra-catalyst probe. Upper left table shows capillary configurations for generating five levels of capillary channel blocking; all capillaries have the same inside diameter for maintaining sample flow rate between the various configurations. Right hand graph shows NH_3 conversion distributions along a catalyst channel, and how equivalent distributed results with the 150- and 200-µm OD capillaries indicate practical noninvasive sampling.

0.25 in beyond the catalyst exit. By the 1.25 location, effluent from the probed channel has mixed with that from the surrounding unprobed channels. Separate Fourier transform infrared effluent measurements are in agreement with the outlet SpaciMS measurements (not shown here). As expected, the NH_3 oxidation proceeds to greater degrees and at steeper gradients with increasing temperature as measured by all five sampling configurations; there is no significant oxidation at 300°C, but the results are useful in demonstrating experimental variations. The 150- and 200-µm OD capillaries (configurations 1 and 2) give equivalent intra-catalyst results indicating that these probe sizes are effectively noninvasive for this reaction at the temperatures studied; this is particularly so at 500°C, which should be most sensitive to any capillary invasive nature, and suggests that any differences in these curves at 400°C is due to measurements scatter. The larger 375-µm OD capillary (configuration 3) seems to show increased gradients in the front catalyst half at 500°C, but even this unusually large capillary shows only 11.6% and 9.3% greater conversion at 0.25 and 0.5 length, and which is on the order of the observed scatter. Only at grossly unrealistic conditions where ca. 30% of the channel is blocked are enhanced conversions on the order of 50% observed. The 200-µm OD capillary with the 700-µm OD quartz rod (configuration 4) blocks ca. 29% of the channel open area, and at 500°C enhances the NH_3 conversion by 46% and 25% at 0.25 and 0.5 length, respectively, compared to the 150-µm and 200-µm OD capillary results. The most invasive situation observed (375-µm OD capillary with the 700-µm quartz rod; configuration 5) blocks ca. 35% of the channel open area, and at 500°C enhances the NH_3 conversion by 75% and 39% at the 0.25 and 0.5 locations, respectively, compared to the small capillary results. In general and when they exist, the enhanced conversion errors are greatest at the catalyst front where the NH_3 concentration is greatest. This analysis shows that the 180-µm OD capillaries used for SpaciMS measurements in this CRADA are effectively noninvasive. Furthermore, these results suggest that the larger capillaries used for other applications may be suitably minimally invasive. Moreover, this demonstrates a protocol that can be used to experimentally quantify these potential impacts of intra-catalyst sampling. It is possibly that different reactions will have different sensitivities to space velocity, and thus may experience differing influence of intra-catalyst probing.

Figure 1 shows that a decreasing conversion step across the catalyst exit is not a reliable indicator of invasive nature. Indeed, the forced invasive configurations (4 and 5) do not show such a step because sufficient catalyst length exists for conversion in the slower un-probed channels to catch up with that in the probed channel. However, Figure 1 shows that with a 0.5-in long catalyst such a step would have been observed. For that case, the most invasive capillary (configuration 5) would have a full-length NH_3 concentration of ca. 60 ppm, while the surrounding un-probed channels would have an NH_3 concentration of ca. 100 ppm; in that case, NH_3 measurement downstream of the shorter catalyst would be somewhere around 100 ppm, and more typical of conversion in the greater number of unprobed channels. Another interesting aspect

of these Figure 1 curves is the apparent decreasing conversion in the back catalyst quarter for configurations 4 and 5; this could be caused by wall diffusion or back diffusion. This demonstrates that the most reliable way to quantify invasive nature of an intra-catalyst sampling configuration via distributed measurements as described in Figure 1.

CONCLUSIONS

- Assessed distributed performance of a (800°C, 50 hrs) hydrothermally aged commercial Cu-SAPO-34 SCR catalyst under standard and fast SCR conditions and at a range of temperatures
  - Hydrothermal ageing conditions have little impact on SCR conversion or parasitic NH_3 oxidation reaction distributions
  - Hydrothermal ageing approximately doubles NH_3 oxidation
  - Hydrothermal ageing degrades integral total capacity 16, 25 and 25% at 200, 300 and 400°C, respectively
- Refined SpaciMS analysis provides for improved nitrogen and stoichiometry balances
- SpaciMS method use in CRADA for intra-catalyst distributed performance characterization is effectively noninvasive
- Multiple collaborations benefit DOE and CRADA objectives
  - SCR fundamentals including impact of NO oxidation on standard SCR
  - N_2O mechanistic pathways during catalyst operation
  - Determining kinetic parameters of catalyst-reactions under normal operating conditions

REFERENCES

1. K. Kamasamudram, N.W. Currier, X. Chen, A. Yezerets, Catalysis Today 151 (2010) 212–222.

2. Xavier Auvray, William P. Partridge, Jae-Soon Choi, Josh A. Pihl, Aleksey Yezerets, Krishna Kamasamudram, Neal W. Currier, Louise Olsson (2012). "Local ammonia storage and ammonia inhibition in a monolithic copper-beta zeolite SCR catalyst," Applied Catalysis B: Environmental 126, 144–152; http://dx.doi.org/10.1016/j.apcatb.2012.07.019.

3. Deutschmann 2013 NAM, and Hettel et al. Catalysis Today 216 (2013) 2-10.

4. Alexandre Goguet, William P. Partridge, Farid Aiouche, Christopher Hardacre, Kevin Morgan, Cristina Stere, Jacinto Sá (2014). Letter to the Editor, Comment on "The Critical evaluation of in situ probe techniques for catalytic honeycomb monoliths" by Hettel et al., Catalysis Today 2014, available online; http://dx.doi.org/10.1016/j.cattod.2014.02.034.

FY 2014 PUBLICATIONS/PRESENTATIONS

Book Chapters

1. Todd J. Toops, Josh A. Pihl and William P. Partridge (2014). "Chapter 4: Fe-Zeolite Functionality, Durability and Deactivation Mechanisms in the Selective Catalytic Reduction (SCR) of NO_x with Ammonia," in Urea-SCR Technology for deNO$_x$ After Treatment of Diesel Exhausts, Nova, Isabella, Tronconi, Enrico (Eds.). Springer, Series: Fundamental and Applied Catalysis, ISBN 978-1-4899-8071-7.

Archival Publications

1. Soran Shwan, William Partridge, Jae-Soon Choi and Louise Olsson (2014). "Kinetic Modeling of NO_x Storage and Reduction Using Spatially Resolved MS Measurements," Applied Catalysis B: Environmental 147, 1028-1041; doi: http://dx.doi.org/10.1016/j.apcatb.2013.10.023.

2. Šárka Bártová, Petr Kočí, Miloš Marek, Josh A. Pihl, Jae-Soon Choi, Todd J. Toops, William P. Partridge (2014). "New Insights on N_2O Formation Pathways during Lean/Rich Cycling of a Commercial Lean NO_x Trap Catalyst," Catalysis Today (Special NAM2013 Edition) 231, 145-154; http://dx.doi.org/10.1016/j.cattod.2013.11.050.

3. Alexandre Goguet, William P. Partridge, Farid Aiouche, Christopher Hardacre, Kevin Morgan, Cristina Stere, Jacinto Sá (2014). Letter to the Editor, Comment on "The Critical evaluation of in situ probe techniques for catalytic honeycomb monoliths" by Hettel et al., Catalysis Today 2014, available online; http://dx.doi.org/10.1016/j.cattod.2014.02.034.

Oral Presentations

1. David Mráček, Šárka Bártová, Petr Kočí, Miloš Marek, Jae-Soon Choi, Josh A. Pihl, Stuart Daw, William P. Partridge. "N_2O Formation During Lean NO_x Trap (LNT) Catalyst Regeneration," Southeastern Catalysis Society Meeting, Asheville, North Carolina, September 30, 2013.

2. Bill Partridge, Jae-Soon Choi, Jim Parks, Maggie Connatser, Jon Yoo, Rodrigo Sanchez, Vitaly Prikhodko, Neal Currier, Sam Geckler, Mike Ruth, Rick Booth, David Koeberlein, Alex Yezerets. "Diagnostic Developments & Applications for Enabling Advanced-Efficiency Automotive Systems," Knoxville-Oak Ridge Chapter of the American Institute of Chemical Engineers (AIChE), Knoxville, Tennessee, October 10, 2013. ***Invited***

3. Xavier Auvray, William Partridge, Jae-Soon Choi, Josh Pihl, Aleksey Yezerets, Krisha Kamasamudram, Neal Currier, Filipa Coehlo and Louise Olsson. "Modeling of NO_x SCR with NH_3 from axial species distribution measurements," Crosscut Workshop on Lean Emissions Reduction Simulation (CLEERS) Teleconference (intra- and international attendance via teleconference) Oak Ridge National Laboratory, October 17, 2013. ***Invited***

4. W.P. Partridge, N. Currier, M.-Y. Kim, J.A. Pihl, R.M. Connatser, J.-S. Choi, A. Yezerets, K. Kamasamudram, "Cummins/ORNL FEERC Combustion CRADA: NO_x Control & Measurement Technology for Heavy-Duty Diesel Engines, Self-Diagnosing SmartCatalyst Systems," 2014 DOE Vehicle Technologies Program Annual Merit Review, Washington, D.C., June 19, 2014.

5. Maria Pia Ruggeri, Isabella Nova, Enrico Tronconi, Josh A. Pihl, Todd J. Toops, William P. Partridge. "DRIFT in situ study of the NO oxidation and Standard SCR reactions on a Cu-CHA commercial catalyst," 8th International Conference on Environmental Catalysis (ICEC), Asheville, North Carolina, August 7th, 2014.

6. Petr Kočí, David Mráček, Miloš Marek, Jae-Soon Choi, Josh Pihl, Todd Toops, William Partridge. "N_2O and N_2 Formation Dynamics During and After the Regeneration of Lean NO_x Trap," 8th International Conference on Environmental Catalysis (ICEC), Asheville, North Carolina, August 8th, 2014.

III.10 Particulate Emissions Control by Advanced Filtration Systems for GDI Engines

Hee Je Seong (Primary Contact),
Seungmok Choi
Argonne National Laboratory
9700 South Cass Avenue
Argonne, IL 60439

DOE Technology Development Manager
Ken Howden

Overall Objectives

- Determine detailed mechanisms of gasoline particulate filter (GPF) filtration/regeneration processes.
- Evaluate filter performance in consideration of back pressure increase, particulate matter (PM) mass, and number emission reduction efficiencies to suggest an optimized filter substrate structure for gasoline direct-injection (GDI) engines.

Fiscal Year (FY) 2014 Objectives

- Investigate PM mass and number emissions from a GDI engine under various conditions.
- Examine PM properties such as carbon crystalline structure, surface chemistry, and ash fraction to understand key factors influencing soot oxidation reactivity.
- Perform filtration and regeneration tests for a selected filter and provide an appropriate experimental strategy targeted for a GDI engine.

FY 2014 Accomplishments

- With the installation of a particle measurement program-like dilution system, accurate soot number measurements were enabled using a scanning mobility particle sizer.
- Raman spectroscopy and pair distribution function analyses using synchrotron X-rays were used to evaluate carbon crystalline structures of GDI PM taken under various engine operating conditions.
- Extensive oxidation experiments by thermogravimetric analyzer (TGA) were performed for GDI soot containing different ash fractions to understand ash effects on soot oxidation kinetics.
- PM-reducing effects were examined with a three-way catalyst (TWC) as a function of engine operating conditions.
- GPF filtration and regeneration experiments were performed, along with micro-imaging, to evaluate unique characteristics of GPF filtration and regeneration processes.
- An environmental scanning electron microscope was employed to observe in situ soot oxidation on an aged filter.

Future Directions

- Define the role of ash components in soot oxidation:
  - Identify metal engine oil additives that enhance soot oxidation, on the basis of extensive TGA experiments and chemical state analyses of GDI soot containing targeted metal additives.
  - Evaluate ash effects on the filtration/regeneration performance of uncatalyzed and catalyzed filters with ash loading.
- Suggest filter types appropriate for GDI engines:
  - Evaluate the filtration/regeneration performance of various bare filter types with different wall thicknesses and micropore structures.
  - Investigate the effect of catalyst components on filter performance.

✧ ✧ ✧ ✧ ✧

INTRODUCTION

GDI engines, which feature direct injection of gasoline fuel into engine cylinders at high compression ratio, offer low fuel consumption and high power output. Although these benefits of GDI engines contribute to their increasing market share for passenger vehicles, their high PM emissions will need to be significantly reduced to comply with future PM regulations. To achieve this goal, GPFs have been developed for GDI engines, like diesel particulate filters (DPFs) for diesel engines. Despite the similarity in function of GPFs and DPFs, however, the unique exhaust conditions of GDI engines, such as low PM mass but high number emissions, high exhaust temperatures, and low O_2 and oxides of nitrogen concentrations under certain conditions, complicate the understanding of GPF

filtration/regeneration mechanisms. In addition, the low-back-pressure requirement of GDI engines for passenger vehicles means that GPFs will need to differ from DPFs in microstructure and wall thickness characteristics.

APPROACH

This project aims to provide a fundamental understanding of GPF filtration and regeneration processes, and examining the filtration and regeneration performance of various filter types, to help filter and vehicle manufacturers develop appropriate GPF filter substrates for low-back-pressure passenger vehicle engines. To understand the contribution of PM to filtration, PM mass and number emissions are examined using transmission electron microscopy, as well as a micro-soot sensor and aerosol measurement instrument with a particle measurement program-like dilution system, under various engine operating conditions ranging from cold start to transient mode. The PM mass and number emissions from different types of GPFs over time are measured during filtration and regeneration processes, in correlation with back-pressure increases. Since the impact of physicochemical properties of PM on soot oxidation is shown to be significant, the carbon fringe patterns, crystalline structure, and surface chemistry of GDI PM are examined to support and understand soot oxidation results from a TGA. Filtration and regeneration processes are visualized under a microscope and an environmental scanning electron microscope.

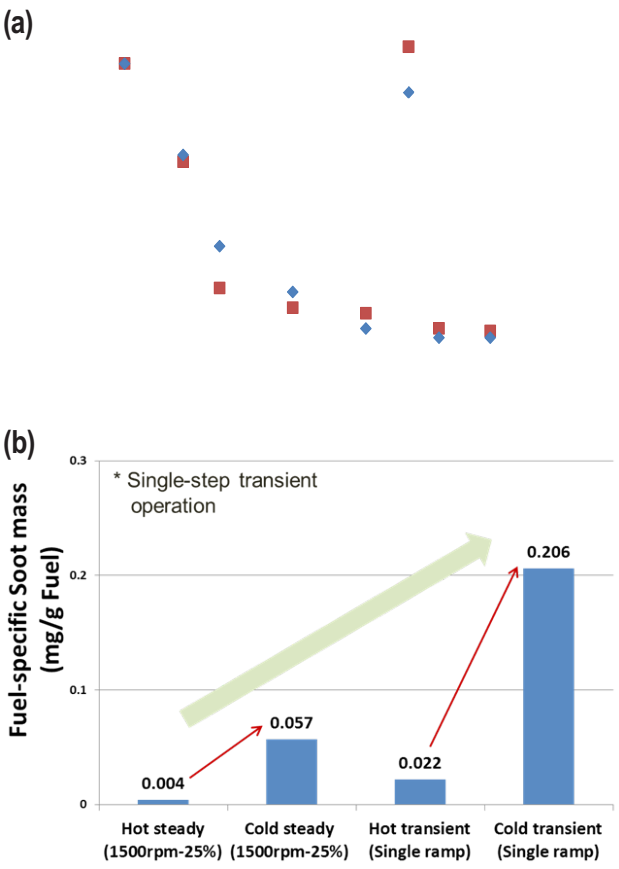

FIGURE 1. (a) PM mass and number emissions measured as a function of coolant-out temperature; (b) comparison of fuel-specific soot mass at steady and transient modes.

RESULTS

Soot mass and number emissions from a GDI engine were examined under varying engine operating conditions to understand PM emission characteristics. Soot mass concentrations were measured using a micro-soot sensor, and soot numbers were counted using an scanning mobility particle sizer coupled with a dilution system. Figure 1a shows soot mass and number emissions during the warm-up period as a function of coolant-out temperature at steady-state operation of 1,500 rpm/25% load. Soot mass and number emissions clearly decreased with increasing coolant-out temperature; emissions at 65°C were 10 times lower than at 32°C. This result reflects the observation that a cold cylinder wall inhibits evaporation of fuel, delaying fuel-air mixing. High soot emissions occur at advanced fuel injection timings because wall wetting, resulting from delayed evaporation of fuel, greatly increases soot mass and number emissions. As a combination effect of the cold wall and wall wetting, a cold transient condition such as cold start and rapid acceleration produced 50 times higher fuel-specific soot mass emissions than did a hot steady condition, as shown in Figure 1b.

The soot-reducing effect of installed TWCs is pertinent to understanding soot emissions from GDI engines with no GPF present. In the present study, soot mass and number emissions were measured at the upstream and downstream of a TWC using various engine modes. Space velocities were categorized as follows: idling and 1,500 rpm/25% load for a low space velocity, 1,500 rpm/75% load and 3,000 rpm/25% load for a medium space velocity, and 3,000 rpm/75% load for a high space velocity. Figure 2 indicates that soot mass reduction with the TWC was apparent at low and high space velocities, whereas soot number reduction was more significant at a low space velocity. The reason was that particles in an entire size range were trapped in the TWC at a low space velocity. Although small fractions of relatively small and large particles were captured in the catalyst in the case of high space velocity, the mass reduction was found to be non-negligible because of the higher weight of large particles.

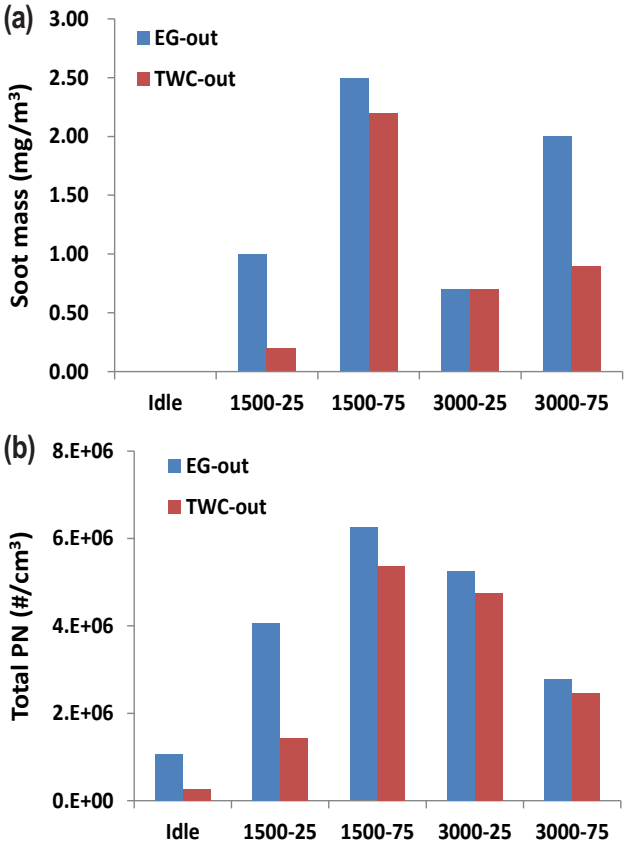

FIGURE 2. Comparison of engine-out and TWC-out emissions under various engine conditions: (a) PM mass and (b) total PM number.

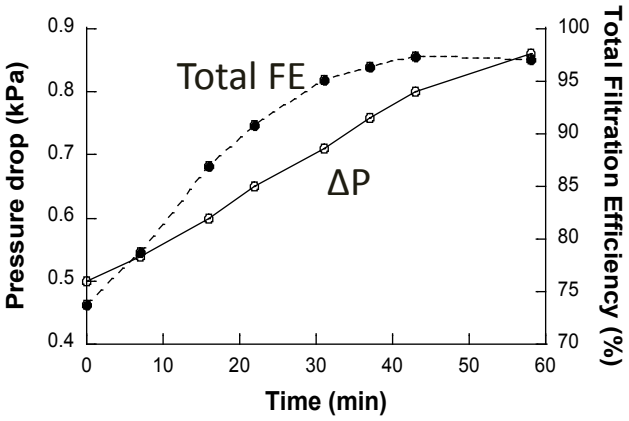

FIGURE 3. Pressure drop and number-based filtration efficiency (FE) as a function of time after PM loading in a filter.

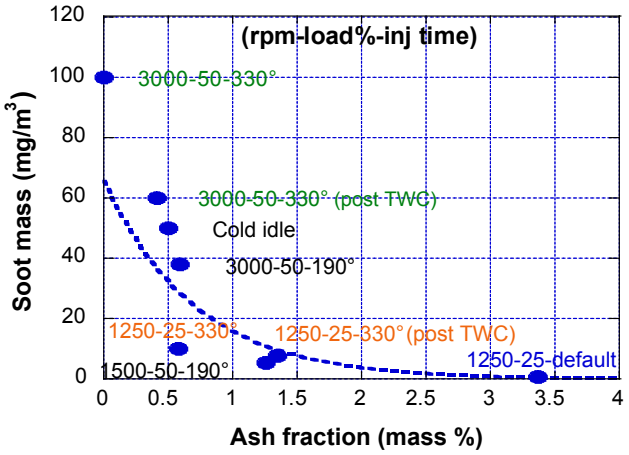

FIGURE 4. Plot of soot mass against ash fraction in mass %.

PM filtration experiments were performed for a bare filter with AC 200 cpsi/12 mil (0.012 inch) cell geometry at 1,500 rpm/25% load. To examine the filtration process, the tests were carried out at 200°C, a temperature that did not result in continuous soot oxidation. Figure 3 shows that with 2.5 mg/m^3 of soot mass, slow deep-bed filtration only was observed for 60 min; this finding was validated by micro-imaging, which showed that a number-based filtration efficiency ranging from 73 to 97% was achieved. When the exhaust temperatures increased, however, soot build-up in surface pores was even slower, owing to the soot oxidation.

The oxidation reactivity of GDI soot collected by a gravimetric sampler was evaluated from TGA experiments to simulate the regeneration process in GPFs. Unlike diesel soot, GDI soot appeared to contain high ash residues that remained after TGA tests. When the ash fractions in the soot were correlated with soot mass concentration (Figure 4), it became clear that low soot mass emissions will contain more ash particles, contributed mainly by consumed engine oil. In addition, physicochemical properties of diesel soot are known to have a significant impact on soot oxidation [1,2]. However, in Raman analyses (Figure 5) using D1 full width at half maximum, carbon crystalline structures of GDI PM samples collected under various conditions were observed to be quite comparable to each other; this finding was validated by pair distribution function analyses using synchrotron X-rays. The examination of surface chemistry, such as complex oxygen functional groups and aliphatic carbon, also showed no apparent differences among the samples examined. In comparison, the ash fraction in soot agrees well with soot oxidation reactivity, as noted in Figure 6. From the kinetic analyses of oxidation rates, it was determined that an ash fraction of 1% in soot increased the soot oxidation rate by a factor of 2.

The TGA results reflect early stages of the GPF regeneration process, in which the contact between ash and soot is likely tight. With increased ash loading, however, the contact tends to become loose. Consequently, it is important to verify whether the ash enhancing effect shown in TGA experiments can occur in

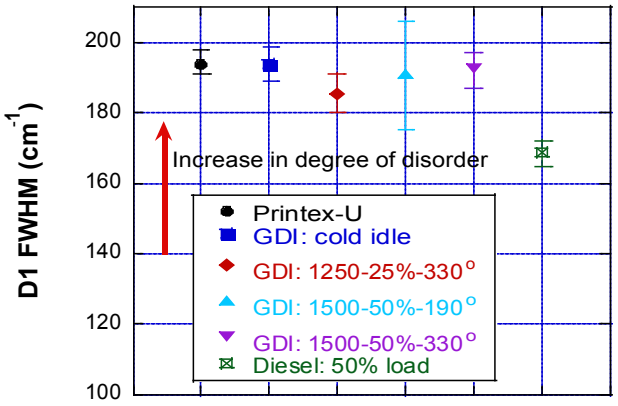

FIGURE 5. Raman analysis of carbon crystalline structure of various soot samples in terms of D1 full width at half maximum.

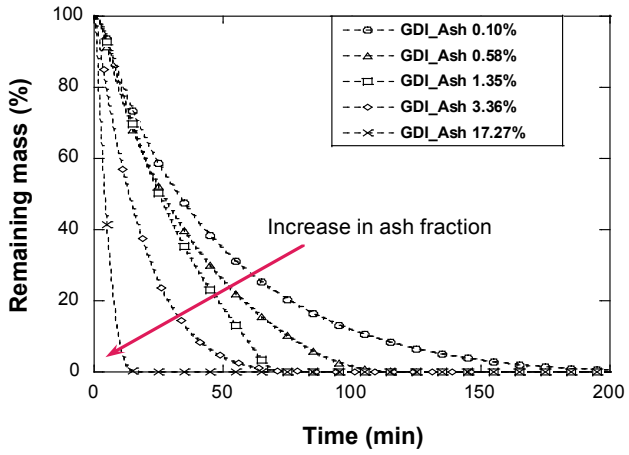

FIGURE 6. Thermogravimetric analysis of GDI soot containing different ash fractions.

GPFs with ash loading. To examine the impact of aging with ash loading, an engine-oil injector is being installed to accelerate ash loading in a modified GPF system.

CONCLUSIONS

- Owing to the combined effect of a cold cylinder wall and wall wetting, cold transient modes—including cold start and rapid acceleration—can be associated with 50-fold higher fuel-specific soot mass emissions than hot steady modes.
- The TWC effect on particle removal is space-velocity- and particle size-dependent, with high mass reduction observed at both low and high space velocities and high number reduction observed only at low space velocity.
- Transmission electron microscope images and Raman and synchrotron X-ray analyses suggest that unlike that of diesel soot, the carbon crystalline structure of GDI soot is not greatly impacted by operating conditions ranging from cold start to high load.
- With low soot mass emissions, the number-based filtration efficiency of a fresh bare filter (AC 200/12) slowly increases over time because of delayed deep-bed filtration, as micro-imaging observations confirmed.
- Ash has a stronger effect on GDI soot than on diesel soot:
  - GDI soot contains a higher ash fraction under normal operating conditions than does diesel soot, because of the low soot mass emissions from GDI engines.
  - The soot oxidation rate is proportional to the ash fraction in the soot.

REFERENCES

1. M. Knauer, M.E. Schuster, D. Su, R. Schlögl, R. Niessner, and N.P. Ivleva, Journal of Physical Chemistry A, 113, 13871–13880 (2009).

2. J. Song, M. Alam, A.L. Boehman, and U. Kim, Combustion and Flame, 146, 589–604 (2006).

FY 2014 PUBLICATIONS/PRESENTATIONS

1. Heeje Seong, Kyeong Lee, and Seungmok Choi, "Effects of Engine Operating Parameters on Morphology of Particulates from a Gasoline Direct Injection (GDI) Engine," SAE paper 2013–01–2574 (2013).

2. H. Seong, S. Choi, and K. Lee, "Examination of Nanoparticles from Gasoline Direct-Injection(GDI) Engines Using Transmission Electron Microscopy (TEM)," International Journal of Automotive Technology, 15, 175–181 (2014).

3. Heeje Seong, Kyeong Lee, and Seungmok Choi., "Oxidative Reactivity of Particulates from a Gasoline Direct Injection (GDI) Engine," FISITA 2014 World Automotive Congress, F2014-CET-106, Maastricht, The Netherlands, June 2–6 (2014).

4. Heeje Seong, Kyeong Lee, and Seungmok Choi, "Unique Properties of Gasoline Direct Injection (GDI) Engine Particulate Matter (PM): Morphology, Nanostructures, and Oxidative Reactivity," Cross-Cut Lean Exhaust Emissions Reduction Simulations (CLEERS) workshop, Dearborn, MI (USA), April 29–May 1 (2014).

5. Seungmok Choi, Heeje Seong, and Kyeong Lee, "Oxidation Characteristics of Soot from a Gasoline Direct-Injection (GDI) Engine," Cross-Cut Lean Exhaust Emissions Reduction Simulations (CLEERS) workshop, Dearborn, MI (USA), April 29–May 1 (2014).

6. Kyeong Lee, Heeje Seong, and Seungmok Choi, "Particulate Emissions Control by Advanced Filtration Systems for GDI Engines," 2014 DOE Hydrogen and Vehicle Technologies Merit Review, Washington, DC, June 16–20 (2014).

7. Seungmok Choi and Heeje Seong, "Oxidation Characteristics of Gasoline Direct-Injection (GDI) Engine Soot: Catalytic Effects of Ash and Modified Kinetic Correlation," Combustion and Flame, under review.

III.11 Fuel-Neutral Studies of PM Transportation Emissions

Mark Stewart (Primary Contact), Alla Zelenyuk
Pacific Northwest National Laboratory
902 Battelle Boulevard
Richland, WA 99352

DOE Technology Development Manager
Ken Howden

Subcontractor
University of Wisconsin Engine Research Center (ERC), Madison, WI

Overall Objectives

- Systematic particulate characterization with single-cylinder test engines, guided by industry
- Seek to shorten development time of filtration technologies for future engines
- Develop modeling approaches relevant to the likely key challenge for gasoline particulate filtration—high number efficiency at high exhaust temperatures

Fiscal Year (FY) 2014 Objectives

- Use image analysis of micro X-ray computed tomography (CT) data to identify morphological features and length scales affecting pressure drop and filtration efficiency
- Develop improved modeling tools for prediction of filtration performance as a function of exhaust particle size
- Carry out filtration experiments to develop fundamental understanding of system behavior and identify promising materials for filtration of spark-ignited, direct-injection (SIDI) engine exhaust
- Conduct additional characterization of SIDI engine exhaust particulates to elucidate soot formation mechanisms and quantify filter performance

FY 2014 Accomplishments

- Micro X-Ray CT data were obtained for seven additional substrate samples in support of ongoing filtration experiments
- Extensive analysis was carried out to characterize the three dimensional structure of porous filter materials and identify features and length scales tied to performance
- Three dimensional micro-scale simulations were carried out to support the development of improved reduced order device-scale modeling tools
- A third round of cooperative experiments at the ERC was successfully completed and analysis of the resulting data has begun

Future Directions

- Complete analysis of data collected during third round of cooperative experiments at the University of Wisconsin ERC
- Explore the use of new techniques, such as maximal inscribed sphere analysis, to characterize three-dimensional filter microstructure and quantify features tied to pressure drop and filtration performance
- Extend exhaust filtration analysis (EFA) experiments to multiple filter substrates from many manufacturers spanning a wide range of properties
- Re-design of the University of Wisconsin EFA system, including features to allow experiments with SIDI exhaust at temperatures representing close-coupled filter placement

INTRODUCTION

Technologies such as SIDI and gasoline compression ignition offer the possibility of dramatically increasing the fuel efficiency of engines that run on gasoline and associated fuel blends. Development of this technology will blur the lines that have traditionally existed between gasoline and diesel engines. Although some similarities have been observed between diesel soot and particulates generated by lean-burn engines designed to use other fuels, significant differences could require adaptation of existing aftertreatment technologies. Gasoline particles are generally smaller than diesel particles, and particulate matter (PM) production can vary widely between engine operating conditions.

Regulation of engine particulate emissions in Europe is moving from mass-based to number-based standards. This will place more emphasis on the reliable removal of smaller particles, which make up the vast majority of the particulates generated on a number basis. American manufacturers must already design systems to meet number regulations for the European market, and must also be prepared for the introduction of more stringent

particulate limits in the U.S. market. Experience thus far indicates that current and future SIDI engines will likely require filtration to meet number limits. It is also likely that filtration will be required if current mass limits are tightened significantly. Furthermore, many filtration systems currently used with diesel engines may not provide adequate filtration efficiency, or may result in unacceptable levels of back-pressure. Most current generation diesel particulate filters rely on a soot cake to achieve high capture efficiencies. High exhaust temperatures and relatively low rates of PM production may limit soot cake formation in gasoline exhaust filtration applications.

APPROACH

General Motors Research has provided components and guidance to develop advanced gasoline research engines at the University of Wisconsin's ERC. These research engines have been configured to run with a variety of fuels over a wide range of operating conditions. Two previous campaigns of joint experiments conducted by PNNL and ERC have generated an extensive set of data on particulate size, shape, and composition, using standard gasoline and ethanol blends.

The current focus of this project is to develop a fundamental understanding of the factors affecting filtration efficiency and back-pressure, in order to promote the development of optimum filtration systems for advanced gasoline vehicles. Detailed characterization of a number of different porous ceramic exhaust filter substrates were undertaken using data from mercury porosimetry and micro X-ray CT. Five substrates from two leading manufacturers have been examined to date, and data have been collected for seven additional substrates, selected to support planned filtration experiments using the EFA system at the University of Wisconsin, Madison. The entire set includes samples of cordierite, silicon carbide, and aluminum titanate filters from four different manufacturers, covering a wide range of properties. The three-dimensional CT data was examined in a number of ways, with the goal of identifying quantitative structural parameters and developing insight that will lead to better prediction of filter performance and optimization of future systems. Analysis included autocorrelation, chord length distributions [1], maximal inscribed sphere analysis [2], and simulations using the lattice-Boltzmann method. A third round of joint experiments at the ERC, conducted in the summer of 2014, focused on fuel and combustion effects on particulate formation, and on detailed interactions between particulates and filters. These datasets are currently being analyzed, and results will be discussed in a future report.

RESULTS

Figure 1 shows one example of a single frame from a micro X-Ray CT scan of a small filter sample. Each scan generates thousands of such images, with a resolution of approximately 1.6 micron. The raw images reveal a number of qualitative differences between various filter products and manufacturers. The cordierite substrate shown in Figure 1 exhibited pores with a comparatively narrow size distribution, many having a spherical shape, and relatively rough wall surfaces compared to other products.

Figure 2 shows a common feature among many of the filter samples examined: filter wall surfaces have a significantly lower porosity than the average wall porosity, which is the value measured by mercury porosimetry. This feature was most pronounced in cordierite filters, but was also observed to a lesser extent in other types of substrates, including silicon carbide. In only one of the 12 samples examined was this feature completely absent. The filter wall surfaces may play an important role in determining back-pressure during operation because of interactions with soot and catalyst washcoat layers.

One parameter of interest for modeling purposes is the representative equivalent volume (REV) [3], or minimum volume of the porous material needed to give representative behavior. Hundreds of lattice-Boltzmann simulations were carried out in order to define the REV for various substrates. Figure 3 shows distributions of permeabilties predicted for subdomains of various sizes from one particular sample. As the subdomains get

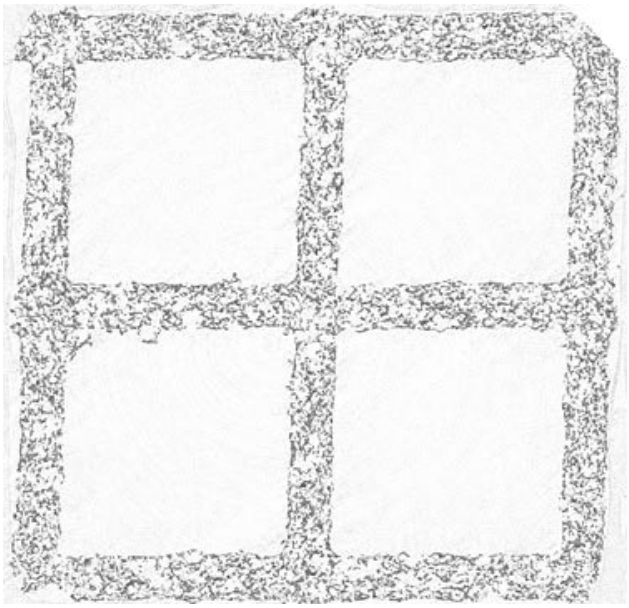

FIGURE 1. Example of one frame from a micro X-Ray CT scan.

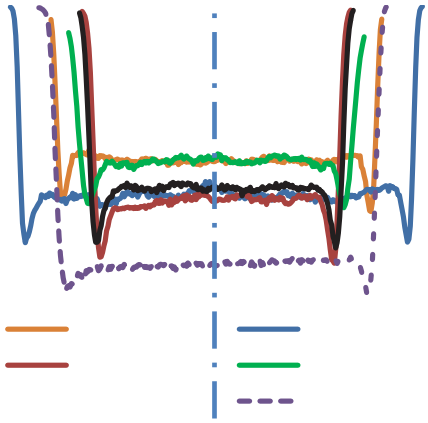

FIGURE 2. Variation in local porosity across filter walls in one silicon carbide and five cordierite samples.

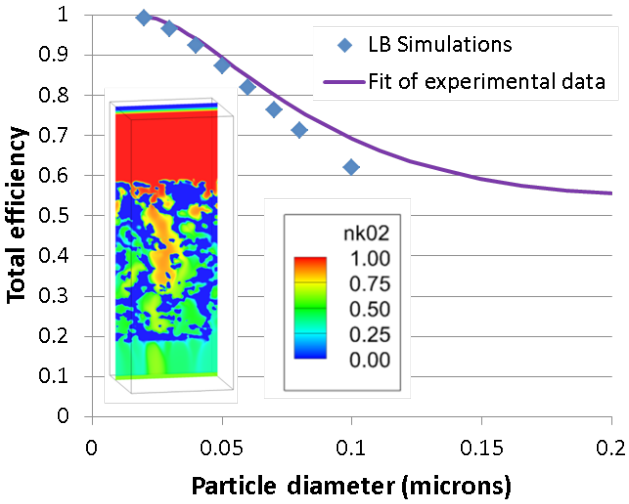

FIGURE 4. Predictions of filtration efficiency made using micro-scale lattice-Boltzmann simulations compared to a fit of experimental data.

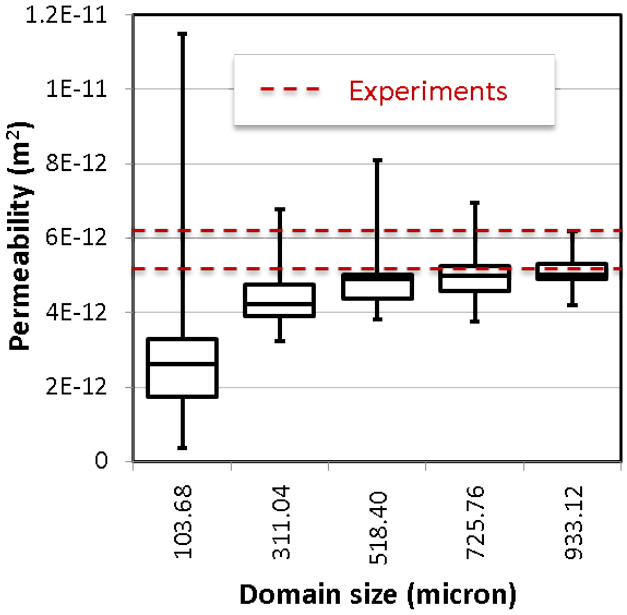

FIGURE 3. Distributions of permeabilities predicted with subdomains of various sizes from one particular filter sample. Whiskers show maximum and minimum permeabilties in a given set, while boxes show the second and third quartiles.

larger, the distributions get tighter and tend to converge toward experimentally observed values. The REV for permeability prediction varies somewhat between the substrates examined, but, in general, around 1 mm^2 of filter wall area seems to be the size needed for representative predictions in exhaust filter materials.

Lattice-Boltzmann filtration simulations were also explored as a means of improving device-scale filtration efficiency models. Previous work had shown that the ability of unit collector models to predict filtration efficiency as a function of particle size could be improved through the use of a modified diffusion efficiency term obtained by micro-scale simulations, using methods such as lattice-Boltzmann. Figure 4 shows predictions of filtration efficiency as a function of particle size from a lattice-Boltzmann filtration model which represents particles as a continuous concentration field. The simulations gave good agreement with experimental data for small particles, for which the diffusion capture mechanism is dominant.

Figure 5 shows the results of a parallel effort undertaken at the University of Wisconsin, Madison to improve the ability of the unit collector filter model to predict filtration efficiency as a function of particle size. The standard unit collector uses a single average collector size to represent the structure of the porous filter material, even though it is known that filter pores cover a spectrum of sizes. The Heterogeneous Multi-Scale Filtration model uses a range of collector sizes, obtained from analysis of pore size distributions, and is able to match size-resolved filtration efficiency data better than the standard unit collector model.

Figure 6 shows an example of recently acquired transient filtration efficiency data obtained with the EFA apparatus at the University of Wisconsin, Madison. The data shows how the filtration efficiency increases over time, and how the maximally penetrating particle size shifts to the left, affecting the relative removal efficiency of smaller particles, which make up most of the PM population on a number basis. This approach will allow filtration performance to be characterized for a wide

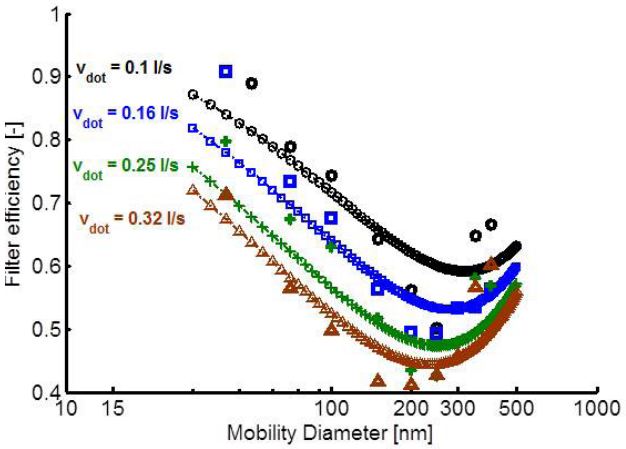

FIGURE 5. Filtration efficiency predictions made by the new Heterogeneous Multi-Scale Filtration model developed at the ERC, compared to experimental data.

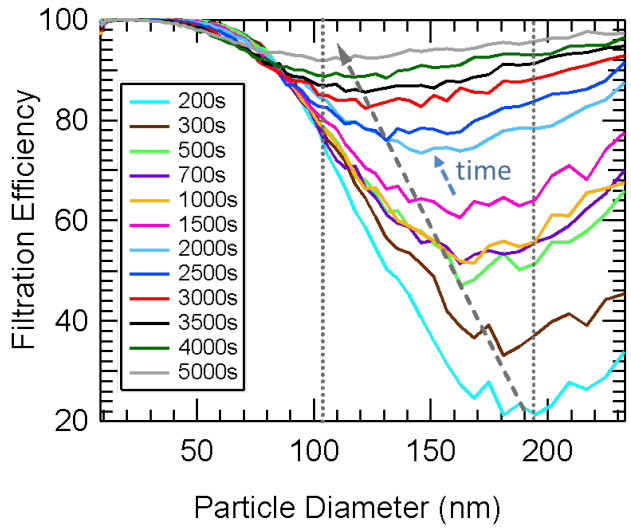

FIGURE 6. Filtration of SIDI particulates, examined using the ERC EFA system.

range of filter substrates. The EFA system is currently being re-designed to allow high temperature operation, mimicking the conditions seen in real SIDI exhaust passing through a close-coupled filter.

CONCLUSIONS

- Most, but not all, porous ceramic materials examined exhibited a relatively low porosity region at the filter wall surfaces. The effect was generally greatest for cordierite substrates.
- Approximately 1 mm^2 of filter wall appears to be a REV for the purposes of permeability prediction from three-dimensional microstructure, but the exact value varies somewhat between the filter products examined.
- Good agreement was observed between experimental filtration efficiency data for small particles and lattice-Boltzmann simulations that represented aerosol particles as a continuous field.
- The new Heterogeneous Multi-Scale Filtration model developed at the University of Wisconsin ERC provides better predictions of filtration efficiency as a function of particle size than the traditional single collector model.
- Filtration experiments with the ERC EFA apparatus show how size-resolved filtration efficiency evolves over time as a given filter substrate is exposed to exhaust particulate.

REFERENCES

1. Roberts, A and S Torquato, "Chord-distribution functions of three-dimensional random media: Approximate first-passage times of Gaussian processes". PHYSICAL REVIEW E, 1999. 59(5): p. 4953-4963.

2. Dong, H and MJ Blunt, "Pore-network extraction from micro-computerized-tomography images". Physical Review E, 2009. 80(3): p. 036307.

3. Bear, J, Dynamics of fluids in porous media. 1988, New York: Dover. XVII, 764 s.

4. Wirojsakunchai, E, C Kolodziej, R Yapaulo, and D Foster, "Development of the Diesel Exhaust Filtration Analysis system (DEFA)". 2008. 2008-01-0486.

FY 2014 PUBLICATIONS/PRESENTATIONS

1. Zelenyuk A, P Reitz, D Imre, M Stewart, P Loeper, C Adams, M Hageman, A Maier, S Sakai, D Foster, D Rothamer, M Andrie, R Krieger, K Naranayaswamy, P Najt, A Solomon. "Detailed Characterization of Particulates Emitted by Pre-commercial High-Efficiency Gasoline Engines". The 32nd Annual American Association for Aerosol Research (AAAR) Conference, Portland, OR, Sept 30 – Oct 4, 2013.

2. Zelenyuk A, P Reitz, M Stewart, D Imre, P Loeper, C Adams, M Andrie, D Rothamer, D Foster, K Narayanaswamy, P Najt, A Solomon. "Detailed Characterization of Particulates Emitted by Pre-commercial Single-cylinder Gasoline Direct Injection Compression Ignition Engine". COMBUSTION AND FLAME 2014.

3. Viswanathan, S, S Sakai, and D Rothamer. "Design & Evaluation of an Exhaust Filtration Analysis (EFA) System," SAE Technical Paper 2014-01-1558, 2014 SAE World Congress and Exhibition. Detroit, MI.

4. Stewart, ML. "Microstructural features of catalyzed and uncatalyzed DPFs." DOE CLEERS Workshop, Dearborn, MI, April 30, 2014.

5. Zelenyuk, A. "Detailed Characterization of Particulates Emitted by a Lean-Burn Gasoline Direct Injection Engine." DOE CLEERS Workshop, Dearborn, MI, April 30, 2014.

6. Stewart, ML. "Fuel-Neutral Engine Particulate Filtration Studies", General Motors Technical Center, Warren, MI, May 1, 2014.

7. Stewart, ML. "Microstructural features of catalyzed and uncatalyzed DPFs." Advanced Engine Crosscut Meeting, Southfield MI, May 8, 2014.

8. Stewart, ML. "Fuel-Neutral Studies of Particulate Matter Transport Emissions", 2014 DOE Hydrogen and Vehicle Technologies Merit Review, Washington, DC, June 19, 2014.

9. Stewart, ML. "Microstructural features of catalyzed and uncatalyzed exhaust particulate filters." (Invited Seminar) Corning Incorporated Sulivan Park R&D Center, Corning, NY, July 30, 2014.

10. Gong, J and C Rutland. "Filtration Characteristics of Fuel Neutral Particulates Using a Heterogeneous Multi-scale Filtration (HMF) Model", Proceedings of the ASME 2014 Internal Combustion Engine Division Fall Technical Conference, Columbus, Indiana, USA.

11. Viswanathan, S, S Sakai, M Hageman, D Foster, T Fansler, M Andrie, D Rothamer. "Effect of Particle Size Distribution on the Deep-Bed Capture Efficiency of an Exhaust Particulate Filter", Proceedings of the ASME 2014 Internal Combustion Engine Division Fall Technical Conference, Columbus, Indiana, USA.

ACKNOWLEDGEMENTS

General Motors Corporation: Kushal Naranayaswamy, Paul Najt, Arun Solomon, Wei Li

University of Wisconsin Madison: David Rothamer, David Foster, Christopher Rutland, Sandeep Viswanathan, Stephen Sakai, Jian Gong, Michael Andrie, Todd Fansler

PNNL: Jacqueline Wilson, David Bell, Carmen Arimescu, Jie Bao, Cameron Hohimer

A portion of the research was performed using the Environmental Molecular Sciences Laboratory, a national scientific user facility sponsored by the Department of Energy's Office of Biological and Environmental Research and located at Pacific Northwest National Laboratory.

III.12 Thermally Stable Ultra-Low Temperature Oxidation Catalysts

János Szanyi, Charles H.F. Peden
(Primary Contact)
Institute for Interfacial Catalysis
Pacific Northwest National Laboratory
P.O. Box 999, MS K8-93
Richland, WA 99354

DOE Technology Development Manager
Ken Howden

CRADA Partners
Chang H. Kim, Se H. Oh and Steven J. Schmieg
(General Motors)

Overall Objectives

- Investigate a number of candidate low-temperature oxidation catalysts as fresh materials, and after realistic laboratory- and engine-aging.
- Obtain a better understanding of fundamental characteristics and various aging factors in both thermal and chemical aspects that impact the long-term performance of these candidate low-temperature oxidation catalysts.
- Provide an assessment of the appropriateness of the laboratory aging protocols in realistically reproducing the effects of actual engine aging conditions.
- In this way, provide a viable pathway to commercialization of these very new and, thus, uncharacterized catalyst materials.

Fiscal Year (FY) 2014 Accomplishments

Two major thrusts this year:

- Synthesis and activity measurements on new Cu/CeO_2-ZrO_2 catalysts:
  - Cu/CeO_2-ZrO_2 catalyst have been prepared by impregnating Cu on both home-made (CZ and C_4Z_1) and commercial (GMR5 and GMR6) support materials.
  - Very high initial CO oxidation activity was observed on the home-made CZCu catalyst (50% CO conversion was achieved at 150°C). However, the activity of all Cu catalyst supported on home-made CeO_2-ZrO_2 dropped dramatically after high temperature hydrothermal aging.
  - After aging Cu catalysts supported on the commercial GMR6, significant improvement for CO oxidation was obtained (behaved exactly the same as the fresh CZCu catalyst).
- Physicochemical characterization of Cu/CeO_2-ZrO_2 catalysts revealed that:
  - Commercial CeO_2-ZrO_2 catalysts contain both Pr and La ions. These additives may stabilize the CeO_2-ZrO_2 mixed oxides, and also, may help to establish and maintain high Cu dispersion.
  - Ce^{4+} ions in the commercial support GMR6 can be reduced to Ce^{3+} much more extensively than in home-made mixed oxides. This probably enhances their oxygen donating abilities, and therefore, their oxidation activities.
- Based on initial results, one manuscript has been prepared and will be submitted soon.

Future Directions

- Conduct additional physical and chemical characterization studies to understand the activity variation patterns observed in CO oxidation over a home-made (CZ) and commercial CeO_2-ZrO_2 (GMR5 & 6) supported Cu catalysts (Fourier transform infrared spectroscopy, transmission electron microscopy [TEM], X-ray photoelectron spectroscopy [XPS]).
- Prepare model Cu/CeO_2 catalysts with well-defined CeO_2 crystal facets (cubes, rods, polyhedral). Investigate the reactivities of these model catalysts in the oxidation of both CO and hydrocarbons. These studies will focus on understanding the effect of the different crystal facets on the overall catalyst performances of Cu/CeO_2-ZrO_2 catalysts.
- Conduct physicochemical characterization studies on sulfur poisoned Cu/CeO_2-ZrO_2 catalysts to understand the deactivation mechanism caused by sulfation. Try to develop methods for efficient sulfur removal.

INTRODUCTION

New federally mandated Corporate Average Fuel Economy and greenhouse gas standards for light-duty vehicles in the U.S. will require a near doubling of the fuel economy by 2025. These new regulations are a direct response to the need to reduce emissions of greenhouse gases; notably, CO_2 in the case of the transportation

sector. To meet this challenge, automobile manufacturers are pursuing a variety of high risk stoichiometric and lean combustion strategies with downsize boosting that have the potential to dramatically increase the efficiency of engine operation. Invariably, these fuel efficient strategies result in significantly lower temperatures of their exhaust gases but also still yield significant quantities of hazardous combustion products whose emissions are also regulated. In fact, at the same time that these new Corporate Average Fuel Economy and greenhouse gas standards are phasing in, the emissions regulations are also becoming more stringent, with so-called Federal Tier 3 and California Low-Emission Vehicle 3 standards applying to passenger vehicles over the next 10-15 years. Exhaust gas temperatures from many of the new engine technologies are expected to be below 200°C for a considerable fraction of federal driving cycles. This presents an enormous challenge for the vehicle's emissions control system using today's technologies as illustrated in Figure 1. In this figure, it can be seen that common catalysts for gasoline (Pd-based commercial three-way catalysts) and diesel vehicles (Cu-based selective catalytic reduction [SCR] catalysts) do not show adequate performance below 200°C even after mild degreening.

Almost certainly, what is needed to meet this "low temperature challenge" for vehicle emissions control systems are revolutionary (rather than evolutionary) solutions. The fundamental catalysis science community has identified a number of candidate catalyst formulations that provide for sufficient activity below 200°C. Some of these have been briefly discussed recently (November, 2012) at a U.S. DRIVE-sponsored workshop on "*Future Automotive Aftertreatment Solutions: The 150°C Challenge*" [1]. A primary issue with all of these laboratory results is the absence of high-temperature hydrothermal stability. In fact, most of these catalysts do not display sufficient thermal durability even in model gases used for the fundamental studies.

General Motors Company (GM) and Battelle/Pacific Northwest National Laboratory (PNNL) will investigate a number of candidate low temperature oxidation catalysts as fresh materials, and after realistic laboratory- and engine-aging. Some specifics for the initial catalyst materials to be studied are contained in GM's recent patent disclosure (US20120291420A1) on non-platinum-group-metal-based ultra-low temperature oxidation catalysts. These studies will lead to a better understanding of fundamental characteristics and various aging factors that impact the long-term performance of catalysts, while also providing an assessment of the appropriateness of the laboratory conditions in realistically reproducing the effects of actual engine aging conditions.

APPROACH

This project will focus on the characterization of catalyst materials used for low temperature catalytic oxidation reactions with special attention to the materials' sensitivity to conditions of laboratory (e.g., oven and laboratory reactor) and engine (e.g., engine

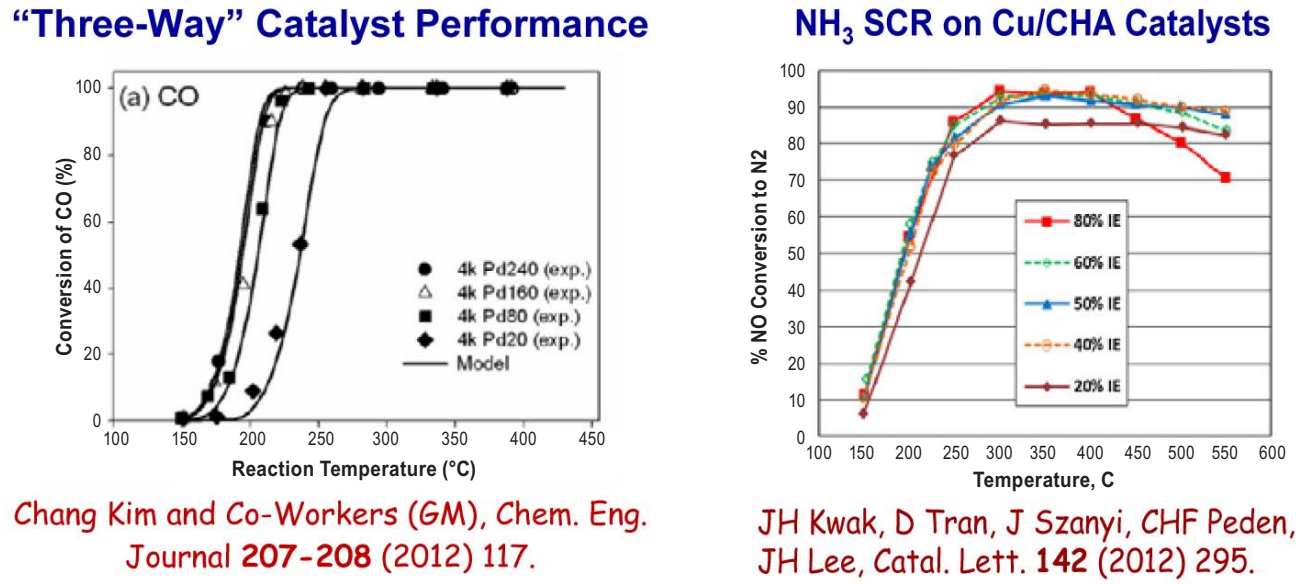

FIGURE 1. "Light-off curves" of performance for a three-way catalyst and for a Cu/CHA SCR catalyst used on current gasoline and diesel vehicles, respectively.

dynamometer) aging protocols. This information will aid the development of improved catalyst formulations and the optimal integration of new catalyst formulations into GM's aftertreatment systems. More importantly, the information will also aid in understanding of the mechanisms for catalyst degradation of newly developing low-temperature catalytic oxidation materials.

GM will provide both fresh and aged catalyst materials that are potentially useful for low-temperature oxidation, and examine changes in the catalytic performance of these materials before and after the aging. Battelle will provide state-of-the-art analytical techniques to investigate the surface and bulk properties of these catalysts, and the changes in these properties induced by the aging process. In this way, the mechanisms for low-temperature performance as well as the mechanisms of degradation will be assessed in the project. This work will utilize a group of model and development catalysts. By developing a good understanding of performance degradation mechanisms during the catalyst aging, Battelle and GM expect to be able to provide a framework for developing robust low temperature oxidation catalyst systems, a better definition of the operational window for these materials, and likely also suggesting formulation changes that have potential to demonstrate improved performance.

RESULTS

Support-Dependent Catalytic Performance of Cu-CeO_2-ZrO_2 Catalysts

A series of Cu-CeO_2-ZrO_2 oxidation catalysts were prepared by GM and tested in the catalytic oxidation of CO and hydrocarbons in both fresh and aged form. It was found that the CO oxidation activities of these catalysts (both fresh and aged) were strongly dependent on the support material. CO oxidation activities as a function of catalyst bed temperature are shown in Figure 2 for a number of Cu-CeO_2-ZrO_2 catalysts using a simulated exhaust gas mixture.

CZ and C_4Z_1 are home-made (GM), while GMR5 and GMR6 are commercial CeO_2-ZrO_2 support materials. Cu was loaded onto the support material either by impregnation (GMR5, GMR6, C_4Z_1) or by co-precipitation (CZCu). The CO oxidation activities of these Cu-CeO_2-ZrO_2 catalysts changes in the order of Cu/GMR5<Cu/GMR6<Cu/C_4Z_1<CZCu. The best performance was observed for the CZCu catalyst that exhibited 50% CO conversion at a catalyst bed temperature of ~150°C, while for the poorest performing fresh catalyst (Cu/GMR5), 50% CO conversion was achieved at ~225°C. Dramatically different CO oxidation activity patterns were observed after high temperature hydrothermal aging (at 750°C for 72 hrs) of these catalysts: notably, the CO oxidation activities of catalysts with home-made CeO_2-ZrO_2 supports (CZCu and Cu/C4Z1) declined significantly. On the other hand, the CO oxidation activities of Cu catalysts supported on commercial CeO_2-ZrO_2 (on both GMR5 and GMR6) improved, although to differing extents. Most notably, the CO oxidation activity of the Cu/GMR6 catalyst improved dramatically compared to its fresh counterpart: the temperature of 50% CO conversion (~160°C) was now comparable to that observed for the best fresh catalyst, CZCu.

Physicochemical Characterization of Cu-CeO_2-ZrO_2 CO Oxidation Catalysts

The two key questions we were seeking to answer from the physicochemical characterization studies were: 1) what are the key differences in the catalyst support materials (CeO_2-ZrO_2) that influence the CO oxidation

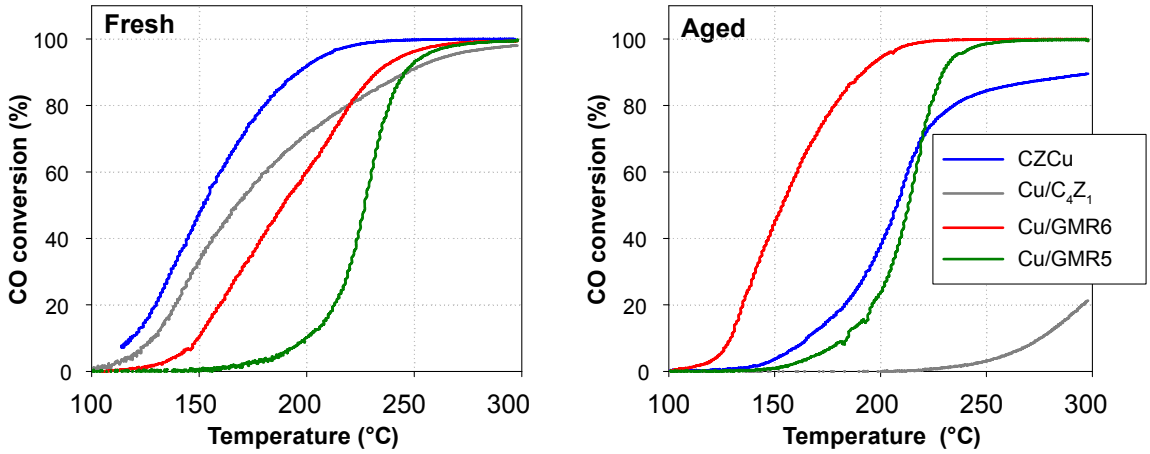

FIGURE 2. CO conversions over fresh and aged catalysts. Feed composition: 500 ppm CO, 260 ppm C_3H_6, 87 ppm C_3H_8, 200 ppm NO, 8% O_2, 8% H_2O and N_2 balance. Gas hourly space velocity = 170,000 h^{-1}. Catalyst aging: 750°C for 72 h in 10% H_2O/air.

activities so strongly; and 2) whether these different support materials have different redox properties that can also influence the activities of the active supported Cu phase. To this end we have conducted XPS, X-ray diffraction and TEM studies on these four samples.

XPS studies revealed the presence of both Pr and La in the commercial catalyst support materials, while the home-made supports contained only CeO_2 and ZrO_2. A representative sample of these results is shown in Figure 3. The Pr and La additives (especially La_2O_3) have been known to act as structure stabilizers in other oxide support materials (e.g., γ-Al_2O_3); thus, one of their key roles in our samples is to stabilize the CeO_2-ZrO_2 structures against structural damage during the high-temperature hydrothermal aging (thus preserving a higher surface area, and preventing Cu agglomeration). These additives may also enhance Cu dispersion since they can provide anchoring sites for the Cu clusters. Indeed, this may explain why the CO oxidation activities of the high temperature hydrothermally treated samples actually improve where, at the very high temperature of the aging process, the dispersion of large Cu cluster actually may increase.

Further information about the physical properties of the support materials was obtained using high-resolution TEM analysis. For example, results shown in Figur 4 demonstrate that the commercial GMR6 is a highly crystalline support material, and the distribution of both La and Pr additives is uniform.

XPS spectra of selected samples (GMR6, Cu/GMR6, Cu/GMR6-850 and CZCu) after 500°C reduction in a 10% H_2/He gas mixture are shown in Figure 5. The differences in reducibilities of the different samples can clearly be seen in these data. In particular, the intensities of the peaks at 904.2 and 885.7 eV binding energies are characteristic of the Ce^{3+} ions, while the feature at 917.0 eV originates only from Ce^{4+} ions. It is clear that the highest fraction of Ce^{3+} ions are in the GMR6 support, and the lowest are in the CZCu sample. Comparing the two Cu-containing samples before aging (Cu/GMR6 and CZCu), the catalyst with the commercial CeO_2-ZrO_2 support (Cu/GMR6) has a much larger fraction of Ce ions in the 3+ oxidation state than in the home-made CeO_2-ZrO_2. These observations are in line with their reactivity trends; notably, the sample that can be reduced easier (Cu/GMR6) exhibits higher activity in the oxidation of CO. This is due to the more facile release of oxygen from the support that then enhances the oxidation ability of the catalyst.

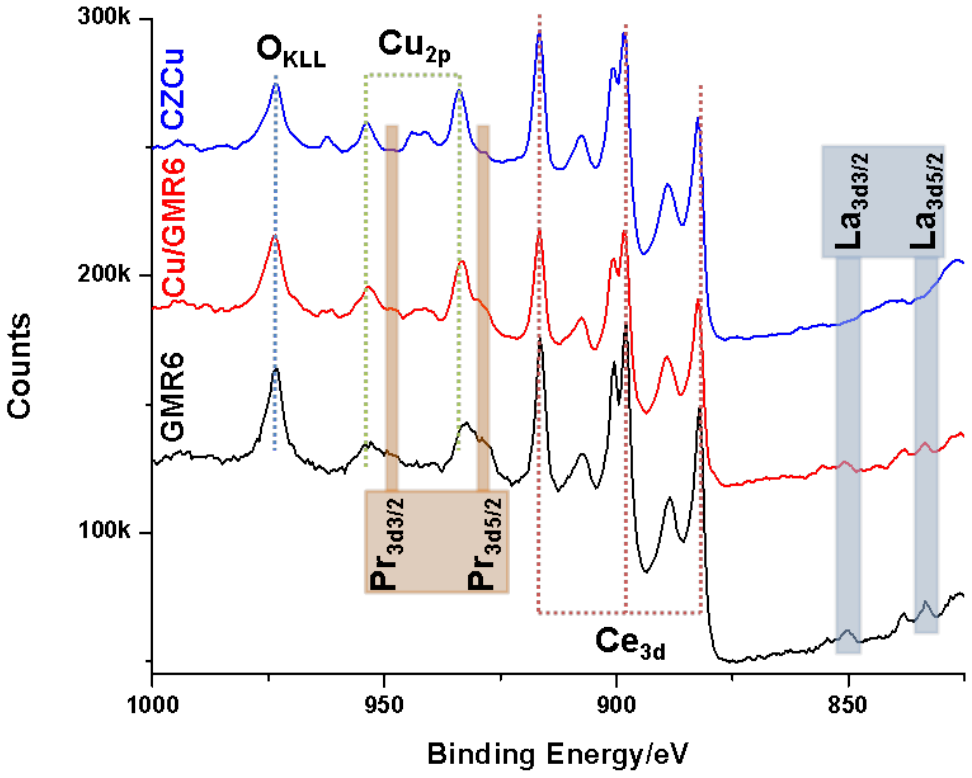

FIGURE 3. XPS spectra of CZCu, Cu-GMR5 and Cu-GMR5 catayst.

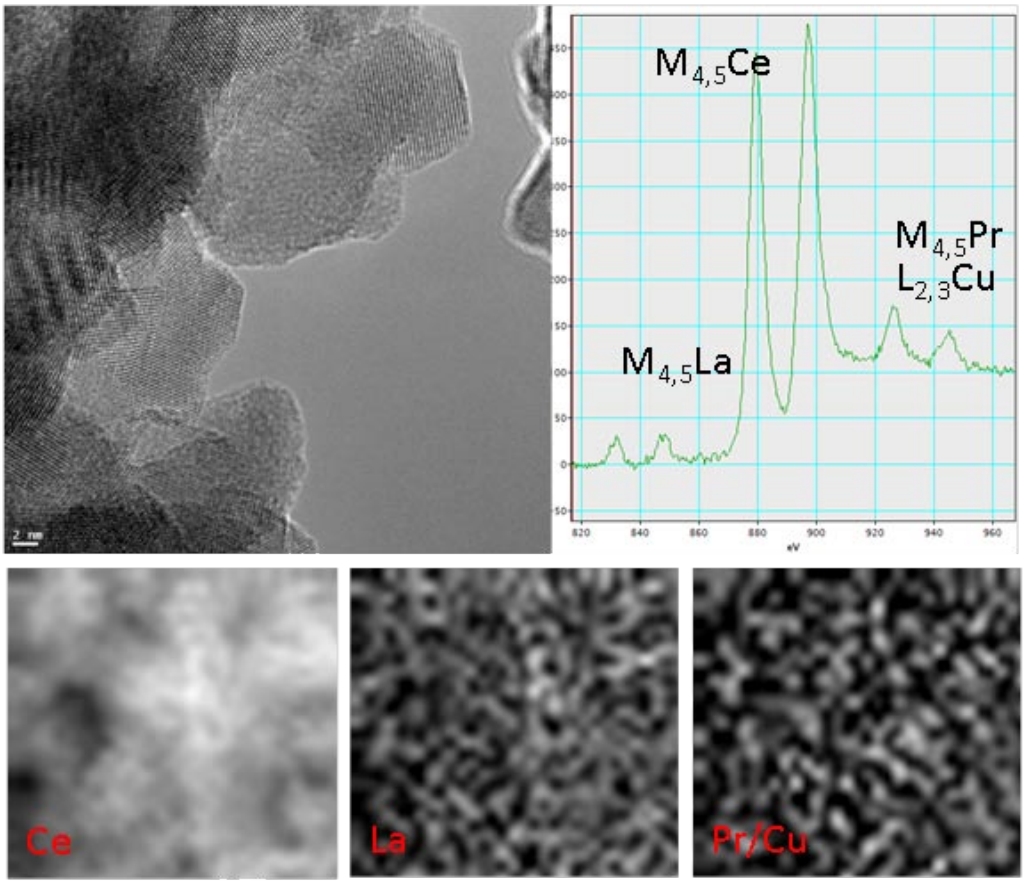

FIGURE 4. High-resolution TEM image of the Cu/GMR6 sample and elemental maps of Ce, La, Cu/Pr.

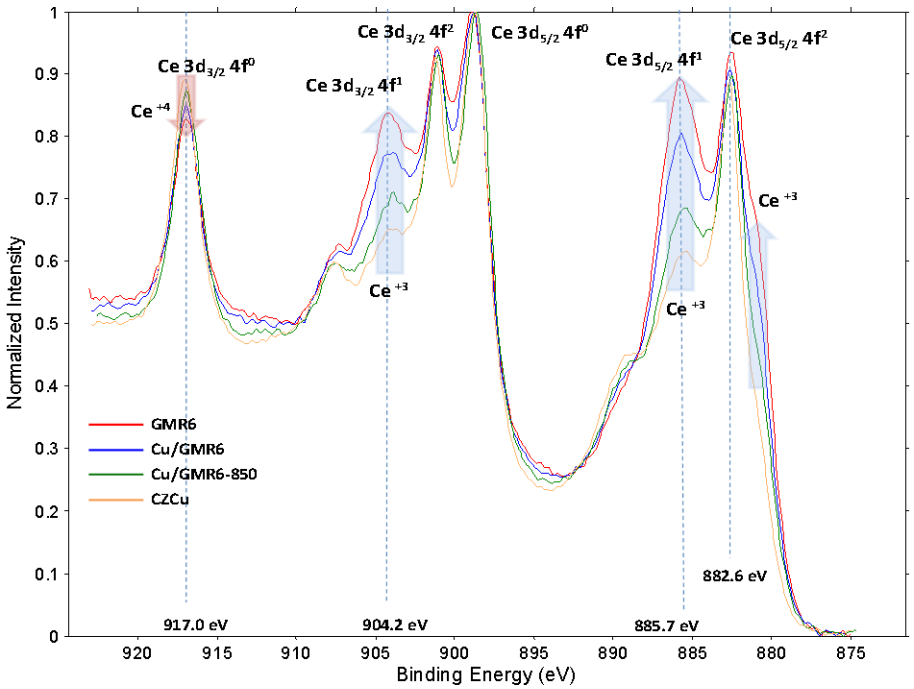

FIGURE 5. XPS spectra of GMR6, Cu/GMR6, Cu/GMR6-850 and CZCu in the Ce 3d binding energy region. Prior to spectral acquisition, the samples were reduced at 500°C in 10% H_2/He.

CONCLUSIONS

PNNL and its partners from GM are carrying out a project aimed at developing low-temperature oxidation catalysts for diesel engine aftertreatment applications. Results to date demonstrate that Cu/CeO_2-ZrO_2 catalysts are highly effective for the oxidation of CO and heavy hydrocarbons. Catalysts prepared on home-made CeO_2-ZrO_2 support materials have shown poor hydrothermal stability, as the CO oxidation activities of these catalysts dropped dramatically after hydrothermal aging at 750°C associated with its siginificant surface area loss. On the other hand, Cu supported on a commercial CeO_2-ZrO_2 (GMR6) has shown a remarkable activity increase during hydrothermal aging while its surface area has decreased. Physicochemical characterization has shown that the support material of the Cu/GMR6 catalyst is highly crystalline, and contains evenly distributed Pr and La ions. These additives may serve multiple functions in the catalyst: 1) stabilize the CeO_2-ZrO_2 support material against structural degradation during hydrothermal aging; and 2) also possibly helping to keep (or even enhance) the active Cu centers in a highly dispersed form. We have also shown that the commercial mixed oxide support material is much more reducible than the home made supports, likely also contributing to the enhanced catalytic performance of the Cu/GMR6 sample as it can supply oxygen for the catalytic reaction.

REFERENCES

1. Zammit M, CL DiMaggio, CH Kim, C Lambert, GG Muntean, CHF Peden, JE Parks, and K Howden. "Future Automotive Aftertreatment Solutions: The 150°C Challenge Workshop Report." Pacific Northwest National Laboratory Report #PNNL-22815.

FY 2014 PUBLICATIONS/PRESENTATIONS

1. Heo, I, SJ Schmieg, SH Oh, W Li, J Szanyi, CHF Peden, and CH Kim. "Improved Thermal Stability of a Ceria-based Catalyst Containing Copper for Low Temperature CO oxidation under Simulated Diesel Exhaust Conditions." ACS Catalysis, to be submitted.

2. Szanyi, J, CHF Peden, CH Kim, W Li, SH Oh, and SJ Schmieg. "Thermally Stable Ultra-Low Temperature Oxidation Catalysts." Presented by **Chuck Peden (Invited Speaker)** at Vehicle Technologies Program Annual Merit Review and Peer Evaluation Meeting, Washington DC, June 2014.

III.13 Understanding NOx SCR Mechanism and Activity on Cu/Chabazite Structures throughout the Catalyst Life Cycle

Fabio H. Ribeiro (Primary Contact),
W. Nicholas Delgass, Rajamani Gounder,
William F. Schneider, Jeffrey T. Miller,
Aleksey Yezerets, Jean-Sabin McEwen,
Charles H. Peden
Purdue University
School of Chemical Engineering
480 Stadium Mall Dr.
West Lafayette, IN 47907

DOE Technology Development Manager
Ken Howden

Overall Objectives

- Synthesize Cu-SSZ-13 catalysts that are exceptionally well defined at the microscopic level, including control of number and type of active sites
- Use *operando* spectroscopy to measure selective catalytic reduction (SCR) rates as a function of reaction conditions while simultaneously observing the catalyst state and nature of reaction intermediates
- Correlate experimental observations with first principles models to create microkinetic mechanisms, rate laws, and validated, predictive structure-function-activity relationships
- Integrate experiment and computation to characterize and quantify catalyst response to sulfur poisoning and to develop strategies to mitigate poisoning

Fiscal Year (FY) 2014 Objectives

- Synthesize SSZ-13 samples that cover a range of Si/Al ratios (6, 18, >100) and Cu loadings
- Measure and quantify standard SCR kinetics as a function of these composition variables
- Perform *operando* X-ray absorption spectroscopy (XAS) experiments to monitor the catalyst working state and infer the number and types of active Cu sites
- Create computational molecular models of candidate Cu sites and predict spectroscopy and reactivity

FY 2014 Accomplishments

- We showed that isolated Cu ions near the six member rings of SSZ-13 are the dominant active sites for standard SCR (473 K) and are present in both oxidized (Cu^{I}) and reduced (Cu^{II}) forms. We further showed that dry NO oxidation is a useful tool to detect the presence of Cu dimers or larger aggregates in catalyst samples.
- We performed *operando* XAS reactant cutoff experiments at Argonne National Laboratory to isolate the species that contribute to Cu reduction and oxidation during standard SCR. We integrated these results with first principles models to develop a standard SCR mechanism that accounts for all these experimental observations.
- We synthesized a series of SSZ-13 samples with varying Si/Al ratio (ranging from 4-140) using three different synthesis methods. For each synthesis method, we have developed a correlation to predict the gel composition required to make an SSZ-13 sample of desired Si/Al ratio. For three Si/Al ratios (~5, ~15, ~30) that resemble the Si/Al ratio of H-SSZ-13 catalysts used in commercial SCR applications, we have prepared a series of Cu-exchanged derivatives for further characterization and kinetic analysis.
- We have developed new experimental NH_3 titration methods to characterize the dynamic nature of active sites in Cu-SSZ-13 before and during SCR reactions.
- We computed spectroscopies of Cu sites and their interactions with a variety of reactants in SSZ-13 and SAPO-34 throughout the redox cycle.

Future Directions

- Develop synthesis procedures that control or optimize the SSZ-13 microstructure, specifically the Al and Cu active site type and density.
- Develop spectroscopies (X-ray, vibrational, and ultraviolet visible near–infrared), titrations (NH_3, H/D exchange) and probe reactions (NO oxidation, NH_3 adsorption) that provide decisive information about SCR active site structures, before and during SCR redox cycles.
- Develop first principles models that correlate with experiment and that predict reaction mechanism and rate as a function of site type.
- Use experiment and computation to characterize sulfur impact on catalyst state and performance.

INTRODUCTION

Oxides of nitrogen (NO_x) compounds contribute to acid rain and photochemical smog and have been linked to respiratory ailments. NO_x emissions regulations continue to tighten, driving the need for high performance, robust control strategies. The goal of this project is to develop a deep, molecular level understanding of the function of Cu-SSZ-13 and Cu-SAPO-34 materials that catalyze the SCR of NO_x with NH_3.

Approach

An integrated approach is necessary to develop robust descriptions of SCR catalyst systems. Our approach includes five tightly integrated tasks that take advantage of state-of-the-art experimental and computational catalytic capabilities.

- **Task 1 - Simulation**: First-principles density functional theory models are used to predict the structure, spectroscopy, and reactivity of various candidate Cu sites in SSZ-13 and SAPO-34 catalysts. These results are used as a basis of microkinetic models.
- **Task 2 - Kinetics**: Reaction rates are measured as a function of reaction conditions and catalyst composition. Two dedicated reactors, including one that is automated and can work unattended, are used for kinetic measurements.
- **Task 3 – Synthesis**: A series of SSZ-13 and SAPO-34 samples are synthesized with systematically varying Si, Al, P and Cu content and distribution, in order to use as model catalysts in characterization and kinetic studies.
- **Task 4 – Spectroscopies**: Mechanistic hypotheses generated from the kinetic and theoretical work are addressed using operando Fourier-transform infrared and X-ray absorption spectroscopies, including isotopic transients. XAS results provide a direct probe of Cu oxidation state, key information in relating structure and function.
- **Task 5 – Applications**: A critical element of our approach is regular communication and face-to-face meetings with our collaborators at Cummins to ensure that research follows a path that maximizes the impact on advances in engine efficiency.

RESULTS

The signature accomplishment of the first project year has been the definitive observation of the Cu redox cycle during SCR on Cu-SSZ-13 (Figure 1),

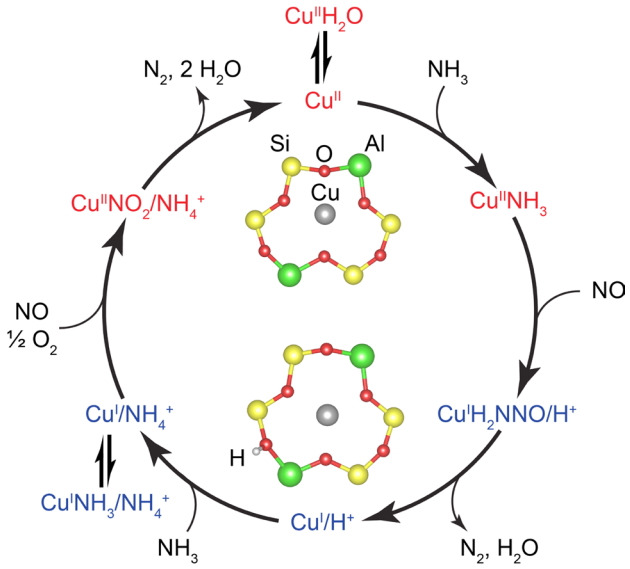

FIGURE 1. Proposed Catalytic Cycle for Standard SCR over Cu-SSZ-13 (T ~473 K)

which required combining experimental XAS spectra and H^+ site titrations measured *in operando* and after reactant cutoff from gas streams, and computational determination of the SCR reaction mechanism on isolated Cu^{2+} sites in Cu-SSZ-13. Density functional theory calculations on large supercell models of candidate exchange sites showed that Cu^{2+} sites were more stable when exchanged at six-membered rings (6-MR) in SSZ-13 containing two Al atoms. Furthermore, the fraction of framework Al atoms located in such 6-MRs containing 2 Al was computed as a function of Si/Al ratio using a stochastic lattice model, and matched with the Cu/Al ratio (~0.20) observed to maximize the SCR rates experimentally for Si/Al = 4.5. These results, along with other experiments, provided strong evidence for such sites giving rise to SCR activity. This information can be used to synthesize new SSZ-13 zeolites with higher SCR rates, by preparing them to contain higher densities of isolated Cu^{2+} cations.

Operando XANES spectra (Figure 2) showed the presence of ~30% Cu^{I} under steady-state SCR operated under differential conditions on two Cu-SSZ-13 catalysts (Si/Al = 4.5, Cu/Al = 0.11, 0.16), providing evidence of a Cu^{II}/Cu^{I} redox cycle during SCR. *Ab initio* potential mean force calculations were used to relate the Heyd-Scuseria-Ernzerhof-06 internal energies to free energies at reaction conditions. The results showed that co-adsorption of NH_3 and NO leads to exothermic, dissociative adsorption, cleavage of an N-H bond with the creation of a new N-N bond, and reduction of Cu^{2+} to Cu^{1+} and a proximal H^+ site. These predictions were consistent with XAS cutoff experiments (Figure 3),

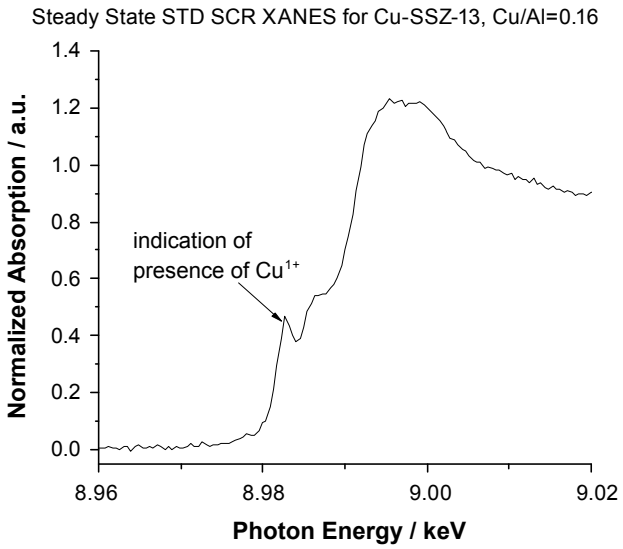

FIGURE 2. Steady-State X-Ray Absorption Near Edge Structure Spectrum for Cu-SSZ-13 (Cu/Al=0.16, Si/Al=4.5), Showing Presence of both Cu^{I} and Cu^{II}

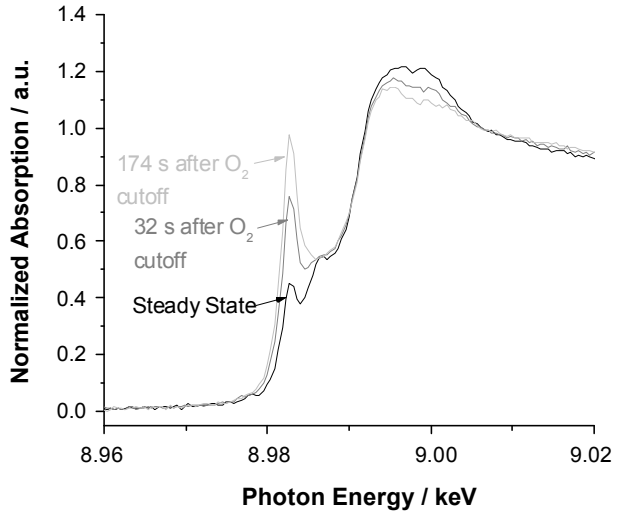

FIGURE 3. Time-Resolved X-Ray Absorption Near Edge Structure Spectra for Cu-SSZ-13 (Cu/Al = 0.16, Si/Al = 4.5) after O_2 Cutoff

which showed that removing O_2 from the feed reduced all Cu ions to Cu^{I}, and with NH_3 titrations performed after O_2 cutoff that detected one additional H^+ site formed per Cu^{I} (Figure 4).

We developed three different NH_3 titration methods and one n-propylamine titration method to consistently titrate H^+ sites on metal-exchanged zeolites, in order to learn more about their role in standard SCR. The methods were validated on medium-pore H-ZSM-5 and Cu-ZSM-5 samples with varying Si/Al ratio (17-90) and Cu/Al ratio (0-0.27). However, in SSZ-13 (Si/Al=4.5, Cu/Al=0-0.35),

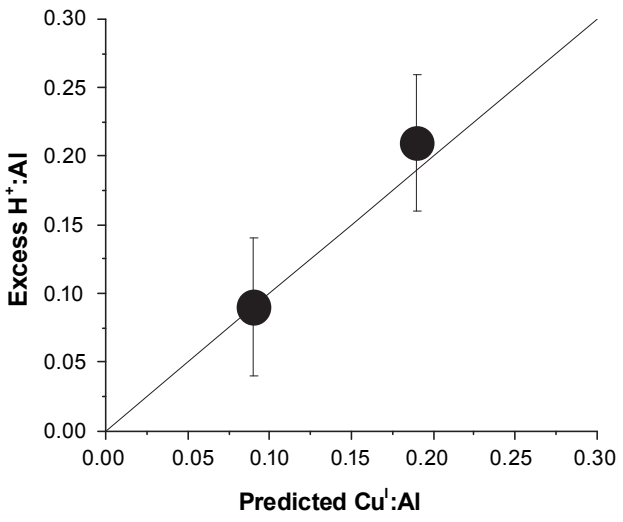

FIGURE 4. NH_3 Titration of Excess H^+ Sites Formed upon Reduction of Cu-SSZ-13 Samples after Treatment in Flowing NO+NH3 at 473 K

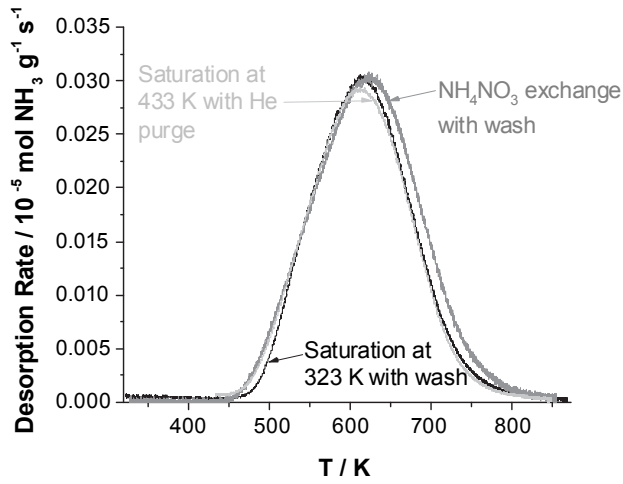

FIGURE 5. NH_3 – Temperature-Programmed Desorption Profiles for H-ZSM-5 (Si/Al=17) after Different NH3 Treatment Procedures

the number of H^+ sites titrated by NH_3 was >4 times higher than the number titrated by n-propylamine. NH_3 is more appropriately suited to titrate H^+ sites in small-pore Cu-SSZ-13 zeolites active for SCR, as it is also the reductant in standard SCR (Figure 5). SCR rates (per g) were zero-order in the number of residual H^+ sites for Cu-SSZ-13 (Si/Al = 4.5, Cu/Al = 0-0.2), but first-order in the number of proximal H^+ sites generated in situ upon Cu^{2+} reduction. The residual H^+ sites behave as NH_3 storage and binding sites during actual SCR operation, while the proximal H^+ sites are involved in the catalytic SCR redox cycle.

CONCLUSIONS

- Low-temperature standard SCR (T ~473 K) on Cu-SSZ-13 (Si/Al = 4.5) is primarily mediated by isolated Cu ions, stabilized by two framework Al atoms within SSZ-13.
- The working state of the catalyst, however, requires Cu ions to undergo a redox cycle during standard SCR in a way that appropriate reactants can be adsorbed and stabilized which can then enable reactions to form nitrogen and water.
- Residual Brønsted acid sites that remain after Cu exchange do not affect standard SCR rates, but can store ammonia during operation, while proximal Brønsted acid sites are generated upon reduction of Cu^{II} to Cu^{I} and participate in the SCR redox cycle.

FY 2014 PUBLICATIONS/PRESENTATIONS

1. S.A. Bates, A.A. Verma, C. Paolucci, A.A. Parekh, T. Anggara, A. Yezerets, W.F. Schneider, J.T. Miller, W.N. Delgass, F.H. Ribeiro, Identification of the active Cu site in standard selective catalytic reduction with ammonia on Cu-SSZ-13, J. Catal. 312 (2014) 87 – 97.

2. S.A. Bates, W.N. Delgass, F.H. Ribeiro, J.T. Miller, R. Gounder, Methods for NH_3 titration of Brønsted acid sites in Cu-zeolites that catalyze the selective catalytic reduction of NO_x with NH_3, J. Catal. 312 (2014) 26 – 36.

3. A.A. Verma, S.A. Bates, T. Anggara, C. Paolucci, A.A. Parekh, K. Kamasamudram, A. Yezerets, J.T. Miller, W.N. Delgass, W.F. Schneider, F.H. Ribeiro, "NO oxidation: A probe reaction on Cu-SSZ-13," J. Catal. 312 (2014) 179 – 190.

4. C. Paolucci, A.A. Verma, S.A. Bates, V.F. Kispersky, J.T. Miller, R. Gounder, W.N. Delgass, F.H. Ribeiro, W.F. Schneider, "Isolation of the Copper Redox Steps in the Standard Selective Catalytic Reduction on Cu-SSZ-13, "Angew. Chem. Int. Ed. 53 (2014) 11828-11833.

5. C. Paolucci and W.F. Schneider, "DFT Analysis of Reactivity of Isolated and Dimeric Cu Sites in SSZ-13 SCR Catalysts," AIChE National Meeting, November 2013.

6. S.A. Bates, W.N. Delgass, F.H. Ribeiro, R. Gounder, J.T. Miller "Methods for Brønsted acid site titration in Cu-zeolites that mediate the selective catalytic reduction of NO_X with NH_3." ACS Meeting, Dallas, TX, March 17, 2014.

7. R. Gounder, "New insights into the properties of and mechanistic roles of Brønsted acid sites in Cu-zeolites that catalyze NO_X SCR with NH_3." DOE CLEERS Workshop, Dearborn, MI, April 29, 2014. (Invited)

8. T. Anggara and W. F. Schneider, "First-Principles and Stochastic Simulation Study of NO Oxidation on Cu-Exchanged SSZ-13 Zeolite Catalysts," Chicago Catalysis Society Spring 2014 Meeting, Naperville, Illinois. (*Poster*)

9. C. Paolucci and W. F. Schneider, "A Molecular Level Understanding of NOx SCR in Cu-SSZ-13 from First Principles," Chicago Catalysis Society Spring 2014 Meeting, Naperville, Illinois. (*Poster*)

10. A.A. Parekh, S.A. Bates, A.A. Verma, C. Paolucci, T. Anggara, A. Yezerets, J.T. Miller, W.F. Schneider, R. Gounder, W.N. Delgass, F.H. Ribeiro, "Nature of the Active Site for Ammonia Standard SCR and NO Oxidation Reactions," Michigan Catalysis Society, Spring Symposium, 2014.

11. F.H. Ribeiro, W.N. Delgass, W.F. Schneider, J.T. Miller, A. Yezerets, T. Anggara, C. Paolucci, S.A. Bates, A. Verma, A. Parekh, "Exploring the Catalytic Properties of Cu/SSZ-13 using NO Oxidation and Standard Selective Reduction of NO with NH_3, Catalysis Club of Philadelphia," Spring Symposium, 2014.

12. F.H. Ribeiro, W.N. Delgass, R. Gounder, W.F. Schneider, J.T. Miller, A. Yezerets, A. A. Verma, A.A. Parekh, S.A. Bates, T. Anggara, C. Paolucci, "Exploring the Catalytic Landscape of Cu-SSZ-13 Using NO Oxidation and the Selective Reduction of NO with NH_3," TOCAT7, June 4th, 2014.

13. T. Anggara and W. F. Schneider, "First Principles Simulation of NO Oxidation on Cu-SSZ-13 Zeolite Catalyst, Gordon Research Conference on Catalysis, New London, NH, June 22, 2014. (*Poster*)

14. C. Paolucci and W. F. Schneider, "A Molecular Level Understanding of NOx SCR in Cu-SSZ-13 from First Principles," Gordon Research Conference on Catalysis, New London, NH, June 22, 2014. (*Poster*)

15. R. Zhang, J.-S. McEwen, "Thermodynamic stability of the location of Cu in Cu-SSZ-13: Influence of reactants, intermediates, and products in the SCR of NO_x", Gordon Research Conference on Catalysis, New London, NH, June 22, 2014. (*Poster*)

16. S.A. Bates, A.A. Verma, W.N. Delgass, F.H. Ribeiro, J.T. Miller, R. Gounder "New Insights into the Mechanistic Roles of Brønsted Acid Sites in Cu-zeolites for NOx Selective Catalytic Reduction." Gordon Research Conference on Catalysis, New London, NH, June 23, 2014. (*Poster*)

17. W.F. Schneider, T. Anggara, C. Paolucci, "Sites and mechanisms for NO_x transformations in CuSSZ13," ACS National Meeting, San Francisco, CA, August 14, 2014. (*Invited*)

SPECIAL RECOGNITIONS AND AWARDS/ PATENTS ISSUED

1. Outstanding oral presentation award at the Michigan Catalysis Society, Spring 2014 meeting.

2. Best Poster Award at Chicago Catalysis Society Spring 2014 Meeting, Naperville, Illinois.

3. 3rd place poster presentation award at the Purdue Chemical Engineering Graduate Student Organization Symposium, Fall 2014.

4. 3rd place poster presentation at Gordon Research Conference on Catalysis, June 2014.

III.14 Tailoring Catalyst Composition and Architecture for Conversion of Pollutants from Low-Temperature Diesel Combustion Engines

William Epling (Primary Contact), Vemuri Balakotaiah, Lars Grabow, Michael Harold, and Dan Luss
University of Houston (UH)
4800 Calhoun Rd.
Houston, TX 77002

DOE Technology Development Manager
Ken Howden

Subcontractor
Oak Ridge National Laboratory, Knoxville, TN

Overall Objectives

- Predict binary and ternary metal alloy catalyst compositions for enhanced CO, NO and hydrocarbon (HC) oxidation from first principles density functional theory (DFT) and verify through kinetic and mechanistic studies
- Develop enhanced low-temperature CO, HC and NO oxidation catalysts through zoning and profiling of metal and ceria components
- Develop zoned and layered catalysts that exploit the coupling between in situ NH_3 generation and oxides of nitrogen (NO_x) reduction
- Develop reactor models of these catalysts with active site gradients to elucidate the effects of catalyst architecture on performance for the oxidation and reduction catalysts

Fiscal Year (FY) 2014 Objectives

- Task 1.1 – Development of descriptor-based reaction model
- Task 1.2 – UH-synthesized catalyst characterization
- Task 1.3 – CO, NO and HC oxidation kinetic expression development
- Task 1.4 – Diesel oxidation catalyst (DOC) reactor-level model build
- Task 1.5 – NOx reduction kinetics with low-temperature combustion (LTC) exhaust

FY 2014 Accomplishments

- Discovered a novel water-mediated reaction mechanism for CO oxidation on supported metal catalysts at low temperatures
- Developed the first iteration of a computational screening model for simultaneous CO and NO oxidation
- Developed a kinetic model of NO_x reduction on a lean-NO_x trap (LNT) with H_2/CO/C_3H_6 as reductants
- Characterized the performance of Pt/Pd/Al_2O_3 oxidation catalysts with different Pt:Pd ratios for CO and C_3H_6 oxidation and developed kinetic expressions

Future Directions

- Improve the descriptor-based model by refining the included elementary reaction steps and tune the reaction energetics to match experimental data. The current model fails to predict Pt and Pd as most active oxidation catalysts.
- Calculate activation barriers for propylene oxidation and derive the corresponding scaling relationships that are needed as input for the descriptor-based microkinetic model.
- Develop a microkinetic model of CO and C_3H_6 oxidation, while incorporating the impact of different Pt/Pd ratios.
- Predict NH_3 generation on LNT at low temperature and impact on zoned or layered selective catalytic reduction (SCR).

✧ ✧ ✧ ✧ ✧

INTRODUCTION

Diesel engines are more fuel efficient than their gasoline counterparts, but even so, increases in fuel economy are needed. Coincidentally, environmental policies require significant decreases in tailpipe NO_x, HC, CO, CO_2 and particulate matter emissions from diesel engines. To meet these emissions regulations and fuel economy demands, the diesel engine community has developed LTC engines.

Most past research and development effort has focused on NO_x and particulate matter emissions control from "conventional" diesel engines. Current diesel

after-treatment systems contain catalysts in series, including a DOC, followed by some combination of a NO_x storage/reduction catalyst, an SCR catalyst and a diesel particulate filter. Although the relatively low temperature of conventional diesel engine exhaust is already a challenge, LTC engines have persistently lower exhaust temperatures. While NO_x and particulate matter emissions are reduced, there are substantially higher levels of CO and HC emissions. These trends put significantly more emphasis on the activity of the oxidation catalyst and low-temperature NO_x reduction performance.

APPROACH

Computational catalyst screening is being used to predict optimal metal alloy compositions for DOCs. The approach requires DFT-derived binding energies and activation barriers, which are subsequently reduced to a minimum set of reactivity descriptors. The use of descriptors allows subsequent combinatorial screening of binary and ternary metal alloys using high-performance computing infrastructure. The data obtained from reactor studies is being used as a source for the DFT studies, as well as for the micro-kinetic and reactor models being developed. The key is evaluating the impact of metal ratios and loading on oxidation reactions.

NOx reduction at low temperatures is also challenging, particularly with the inability to use urea as an NH_3 source, since urea will not hydrolyze at some LTC exhaust temperatures. Layered NO_x reduction catalysts are being utilized to take advantage if in situ NH_3 formation and the inherent reductants in the exhaust (H_2, CO and hydrocarbons).

RESULTS

Molecular Level Modeling (Task 1.1): A novel water-mediated reaction mechanism for room-temperature CO oxidation over Au/TiO_2 catalysts was discovered and is supported by direct experimental and theoretical evidence. A hydrogen/deuterium kinetic isotope effect of nearly 2 implicates O-H(D) bond breaking in the rate-determining step. Kinetics and in situ infrared spectroscopy experiments showed that the coverage of weakly adsorbed water on TiO_2 largely determines catalyst activity by changing the number of active sites.

NO oxidation barriers have been calculated on terrace and step sites of monometallic Fe, Ru, Co, Ni, Rh, Ir, Pt, Pd, Cu, Ag, and Au surfaces and a good linear relationship for the transition state energy as function of O* and CO* binding energy has been obtained (Figure 1 A,B). DFT results for NO oxidation were obtained on the DOE National Energy Research Scientific Computing Center supercomputers “Hopper” and “Edison,” as well as the NSF XSEDE systems “Stampede” and “Gordon,” while CO oxidation and O_2 dissociation energetics were obtained from the CatApp online database provided by the DOE Stanford Linear Accelerator Center National Laboratory [http://suncat.slac.stanford.edu/outreach/catapp/].

The first iteration of a descriptor-based microkinetic model with two reaction sites (terrace and step) for simultaneous NO and CO oxidation at T = 425 K, P_{NO} = 0.0001 bar, P_{CO} = 0.005 bar, and P_{O2} = 0.1 bar is given in Figure 1C. The model contains 15 elementary steps of which three are the diffusion of O*, CO* and NO* between terrace and step sites. Currently, a simple regression approach is being tested to improve the consistency between the energy input parameters.

Kinetic Modeling (Tasks 1.3, 1.4 and 1.5): Isothermal steady-state NO_x reduction on $Pt/BaO/Al_2O_3$ by H_2/CO/C_3H_6 mixtures was studied using a 1+1 dimensional two-phase model that accounts for washcoat diffusional limitations. The temperature dependence of the rate constants were quantified so that the surface chemistry is consistent with experimental observations. H_2 is known to be a more effective reductant than CO and C_3H_6. Figure 2 shows that a similar behavior is predicted by the model. H_2 rapidly diffuses in the washcoat and reacts, while CO and C_3H_6 are “stickier” compared to H_2 and occupy the vacant sites on the Pt surface thus inhibiting further reaction.

A predictive model has been developed for lean-NO reduction with propylene on a Cu/SSZ-13 SCR monolithic catalyst. The model captures all of the trends measured in bench flow reactor studies (Figure 3), including the existence of a cyanate-like surface species, produced from the reaction of NO with oxygenates, which blocks sites.

A monolith model was used to evaluate the ignition behavior of a CO + C_3H_6 mixture under typical conditions encountered for a DOC. Both are known to inhibit their own oxidation rates. The rates reveal a rate maximum at intermediate concentrations of the individual reactants.

Reactor Studies (Task 1.2): A series of Pt/Pd/Al_2O_3 catalysts were prepared and oxidation reaction performance evaluated in CO, C_3H_6 and NO mixtures. The results clearly show that the adsorption/desorption of the reactant molecules is key for light-off and that changing the Pt:Pd ratio leads to a mon-monotonic change in light-off characteristics due to differences in reactant molecule desorption characteristics. The 1:1 Pt:Pd sample has thus far shown best overall performance when based on 50% conversion of the species as a measure, although a 3:1 Pt:Pd blend leads to >90% CO

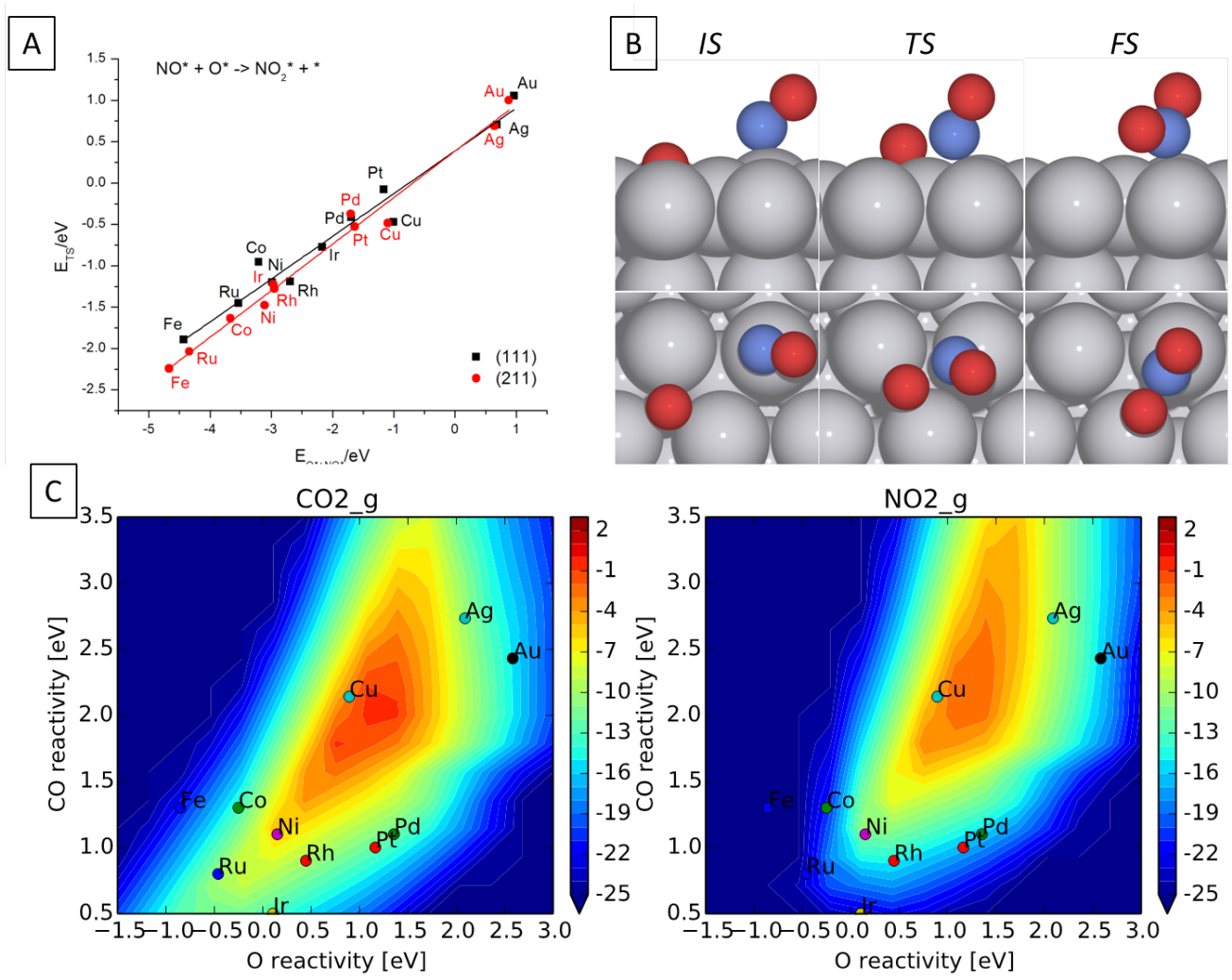

FIGURE 1. (A) Transition state scaling relationship for NO oxidation over flat (111) and stepped (211) transition metal surfaces. (B) Snapshots along the NO oxidation reaction over Pt(111). IS = initial state; TS = transition state; FS = final state; grey spheres = Pt, red spheres = O, blue spheres = N. (C) Descriptor-based microkinetic model for simultaneous CO (left) and NO (right) oxidation (T = 425 K, P_{NO} = 0.0001 bar, P_{CO} = 0.005 bar, P_{O2} = 0.1 bar).

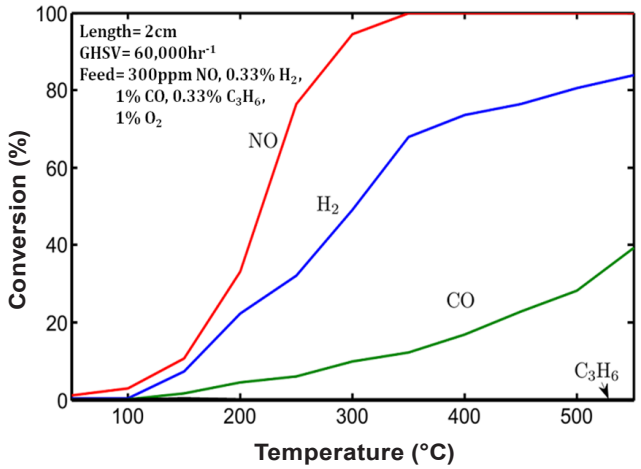

FIGURE 2. Steady-state reduction of NO_x on 2% Pt/16% BaO/Al_2O_3 catalyst with a feed consisting of H_2, CO, C_3H_6 at different temperatures with a feed containing 300 ppm NO, 1% O_2, 1% CO, 0.33% H_2, 0.33% C_3H_6.

conversion at the lowest temperature. The reactions have been spatially-resolved and the results demonstrate that CO is oxidized prior to the hydrocarbon species. Transmission electron microscopy data obtained at Oak Ridge National Laboratory reveal that the bimetallic samples typically form bimetallic clusters, i.e. not distinct Pt and Pd particles. These bimetallic phases appear responsible for the improved performance observed.

Dual-layer monolithic catalysts consisting of a SCR layer on top of a LNT layer were used to carry out periodic selective NOx reduction to N_2. Ammonia generated from the LNT layer is captured by the top SCR layer where it reacts with NO_x. Evidence also exists for a non-ammonia pathway at low temperature. Zoning of either or both the SCR and LNT in the dual-layer catalysts improved the low-temperature NO_x conversion, and minimized the high-temperature conversion loss

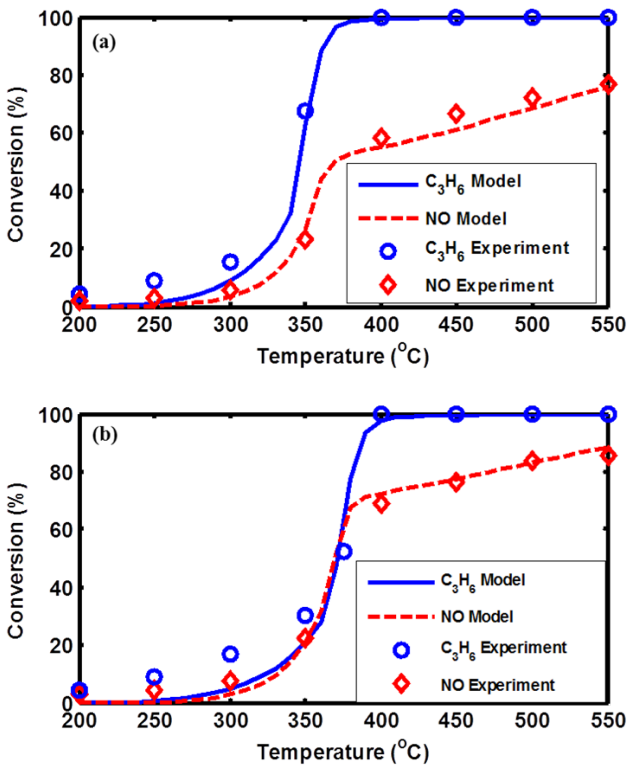

FIGURE 3. Measured and predicted C_3H_6 and NO conversion versus temperature: (a) 500 ppm C_3H_6, 250 ppm NO, 5% O_2, (b) 750 ppm C_3H_6, 250 ppm NO, 5% O_2, Ar balance.

caused by the SCR layer diffusion resistance and undesired NH_3 oxidation.

CONCLUSIONS

- The use of catalytic reactivity descriptors has for the first time been applied to two simultaneous oxidation reactions occurring on two types of active sites.
- A micro-kinetic model of NO_x reduction over a model NO_x trap catalyst has been developed to include washcoat diffusion and reactions with H_2, CO and C_3H_6 as reductants.
- Oxidation catalyst reactor testing demonstrates non-monotonic trends in oxidation performance as a function of Pt:Pd ratio.
- Layered and zoned NOx reduction catalysts have been evaluated.

FY 2014 PUBLICATIONS/PRESENTATIONS

1. J. Saavedra, H.A. Doan, C.J. Pursell, L.C. Grabow and B.D. Chandler, "The critical role of water at the gold-titania interface in catalytic CO oxidation", *Science* **345** (2014) 1599–1602.

2. "Water mediated proton transfer at metal/metal-oxide interfaces" L. C. Grabow, ACS Fall Meeting, San Francisco, CA, 2014.

3. "The Critical Role of Water in Catalytic CO oxidation over Au/TiO_2 Catalysts" H.A. Doan, J. Saveedra, C.P. Pursell, B.D. Chandler, L.C. Grabow, OChEGS Symposium, University of Houston, Houston, TX, 2014.

4. A.S. Kota, D. Luss and V. Balakotaiah, "Micro-kinetics of NO_x storage and reduction with $H_2/CO/C_3H_6$ on $Pt/BaO/Al_2O_3$ monolith catalysts", *Chemical Engineering Journal*, (2014), in press [DOI: 10.1016/j.cej.2014.09.060].

5. R.R. Ratnakar and V. Balakotaiah, "Reduced Order Multimode Transient Models for Catalytic Monoliths with Micro-Kinetics", Chemical Engineering Journal, 260, pp. 557-572 (2015).

6. B. Shakya, M. Harold and V. Balakotaiah, "Simulations and Optimization of Combined Fe- and Cu-Zeolite SCR Monolith Catalysts", Chemical Engineering Journal, ISCRE special issue (accepted with minor revision).

7. R. Raj, M.P. Harold and V. Balakotaiah, "Kinetic Modeling of NO Selective Reduction with C_3H_6 over Cu-SSZ13 Monolithic Catalyst", Chemical Engineering Journal, 254, pp.452-462 (2014).

8. Y. Zheng, M.P. Harold and D. Luss, "Optimization of LNT-SCR Dual-layer Catalysts for Lean NOx Reduction by H_2 and CO", *SAE Journal*, 2014-01-1544 (2014).

III.15 Low-Temperature NOx Storage and Reduction Using Engineered Materials

Mark Crocker (Primary Contact), Yaying Ji, Samantha Jones, Shuli Bai

University of Kentucky Center for Applied Energy Research
2540 Research Park Drive
Lexington, KY 40511

DOE Technology Development Manager
Ken Howden

Subcontractors
- MEL Chemicals, Flemington, NJ (John Darab)
- Oak Ridge National Laboratory, Oak Ridge, TN (Jae-Soon Choi)

Partners
Ford Motor Co., Dearborn, MI (Christine Lambert)

Overall Objectives

- Improve the low-temperature performance of catalyst-based oxides of nitrogen (NOx) mitigation systems by designing materials which can function as either passive NOx adsorbers (PNAs) or low-temperature lean-NOx trap (LNT) catalysts.
- Develop materials capable of storing NOx at low temperatures (<200ºC). These materials should also readily release NOx at higher temperatures (>200ºC) under lean conditions, at which point the NOx can be reduced by a downstream selective catalytic reduction (SCR) catalyst.
- Develop materials which can store NOx at low temperatures but which form thermally stable nitrites/nitrates under lean conditions. These materials should also display fast NOx release kinetics under reducing conditions, thereby facilitating both NOx storage and NOx reduction at low temperatures.

Fiscal Year (FY) 2014 Objectives

- Evaluate candidate metal oxide materials for (i) their low-temperature NOx storage capacity and (ii) the stability of the adsorbed NOx species with respect to thermal desorption.
- Examine the effect on NOx storage and release of promoting mixed metal oxides with small amounts of Pt (<1 wt%).
- Screen ceria-based mixed oxides (CeO_2-ZrO_2 and M_2O_3-CeO_2) for their NOx storage capacity at low temperatures (120-200ºC).

FY 2014 Accomplishments

- The fundamentals of NOx storage and release on Al_2O_3, Pt/Al_2O_3 and $Pt/La\text{-}Al_2O_3$ in the temperature range 80-160ºC were investigated by means of microreactor and in situ diffuse reflectance infrared Fourier transform spectroscopy (DRIFTS) experiments.
- Pt/CeO_2-ZrO_2 was identified as a promising material for PNA applications.
- Ceria-based mixed oxides incorporating Pr were identified as promising materials for LNT catalysts intended for low temperature operation, due to the fast kinetics of nitrate decomposition they exhibit under rich conditions.

Future Directions

- Study the benefits of using Pd as a promoter in PNA applications (as opposed to Pt), particularly for ceria-based materials
- Vary the Ce-Zr ratio in $MnFeOx/CeO_2$-ZrO_2 and CeO_2-ZrO_2 materials in order to assess how increasing the Zr content affects NOx uptake and release
- Examine the effect on low-temperature NOx storage capacity of fine tuning the M:Ce ratio in M_2O_3-CeO_2 mixed oxides
- Initiate DRIFTS studies on the most promising materials identified above in order to elucidate the mechanism of NOx adsorption
- Initiate NOx reduction studies on the most promising material(s) identified above

INTRODUCTION

The control of NOx emissions from lean-burn engines represents an on-going challenge to the automotive industry, particularly at the low exhaust temperatures associated with modern, fuel-efficient engines. For example, the slow rate of urea decomposition limits the ability to deploy urea-SCR at low operating temperatures.

Consequently, a system is required which combines low-temperature NOx storage with subsequent NOx reduction. In this regard, the use of a PNA device in combination with a urea-SCR catalyst is an attractive option which to date has been little explored. In this system, the PNA adsorbs NOx emitted from the engine during cold starts, and then releases the NOx at higher temperatures, e.g., ca. 200°C. At this point the SCR catalyst is sufficiently warm to function efficiently, while the temperature is also high enough to permit stoichiometric injection of urea. By developing materials tailored for this purpose, this project intends to fully develop this concept. Insights gained in this work should also aid the development of materials suitable for low-temperature NOx storage reduction, as applied in LNT catalysts.

This work will be of benefit to both urea SCR and LNT-SCR NOx reduction systems and will directly address the emission control R&D tasks pertaining to NOx control outlined in the DOE Vehicle Technologies Office 2011-2015 Multi-year Program Plan. Both urea SCR and LNT-SCR systems can be viewed as important enabling technologies: by facilitating the attainment of current Tier 2 emissions standards for lean-burn vehicles, as well as future Tier 3 standards, their use removes a major impediment to the widespread use of fuel-efficient engines. This holds the potential for savings in overall transportation fuel consumed and CO_2 emitted. An additional outcome of this project will be the training of students in key aspects of materials science, catalysis and environmental engineering.

APPROACH

The overarching goal of this proposal is to improve the low-temperature performance of catalyst-based NOx mitigation systems. Towards this goal, we are employing an approach that combines mechanistic studies, materials synthesis, and catalyst evaluation under realistic conditions. Specifically, we propose a two-pronged approach which may be summarized as follows:

- The development of passive NOx adsorbers. We will develop materials capable of storing NOx at low temperatures (<200ºC), either as nitrite (NO_2^-) and/or as nitrate (NO_3^-), and which readily release NOx at higher temperatures (>200ºC) under lean conditions, at which point the NOx can be reduced by a downstream SCR catalyst (with urea injection downstream of the NOx adsorber providing the necessary reductant).
- The design of materials for improved low-temperature NOx storage and reduction. Building on knowledge generated in the first activity, materials will be developed which can store NO at low temperatures but which form thermally stable nitrites/nitrates. Moreover, these materials will be designed to display fast NOx release kinetics under rich conditions, thereby facilitating both NOx storage and NOx reduction at low temperatures.

RESULTS

NOx storage on Al_2O_3, Pt/Al_2O_3 and $Pt/La\text{-}Al_2O_3$ in the temperature range 80-160ºC was investigated by means of microreactor and in situ DRIFTS experiments, to ascertain their suitability for passive NOx adsorber applications. Addition of 1 wt% La to Al_2O_3 resulted in the creation of new NOx storage sites and improved NOx storage efficiency (Figure 1). However, according to temperature-programmed reduction (TPD) measurements, $Pt/La\text{-}Al_2O_3$ exhibited slightly lower NOx desorption efficiency below 250ºC than Pt/Al_2O_3. In the absence of Pt, NOx adsorption efficiency on Al_2O_3 was poor, indicating that the oxidizing function of Pt plays an important role in NOx storage, even at low temperatures. During NOx adsorption-desorption cycling, repeated cycles resulted in a significant decrease in the NOx storage capacity, accompanied by a continuous decrease in low-temperature NOx desorption efficiency (<250ºC). These effects were more significant for the La-promoted Pt/Al_2O_3 sample, with the consequence that it desorbed smaller amounts of NOx below 250°C after five cycles than the Pt/Al_2O_3 analogue. Overall, these results highlight the fact that effective PNA design must balance adequate low temperature NOx storage capacity with facile NOx desorption.

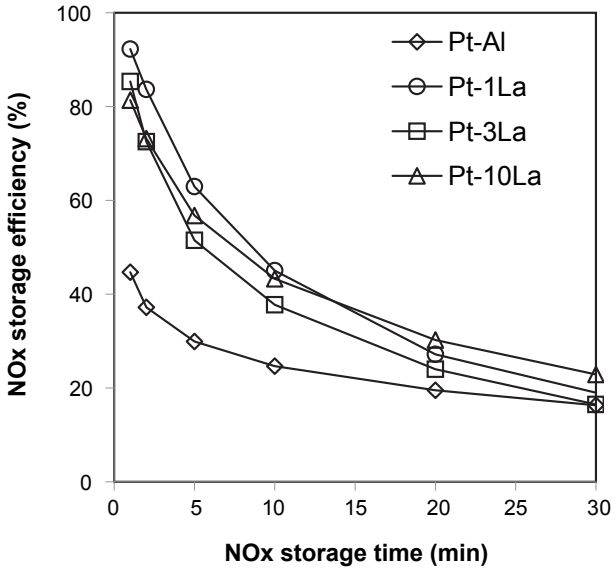

FIGURE 1. Comparison of NOx Storage Efficiency of Pt/Al_2O_3 and $Pt/La\text{-}Al_2O_3$ at 120°C (La loading = 1, 3 or 10 wt%). Feed: 300 ppm NO, 5% O_2, 5% CO_2, 3.5% H_2O, He as Balance

Ce-Zr mixed oxides are known to possess significant NOx adsorption capacity at low temperatures and are therefore also interesting candidates for PNA applications. Figure 2 shows NOx storage efficiency (NSE) as a function of time at different NOx storage temperatures for Pt/CeO_2-ZrO_2 (Pt = 1 wt%; Ce:Zr = 20:80 on a mole basis). A significant increase in NSE with storage temperature was observed, especially during the first few minutes of storage. Indeed, nearly 95% NSE was obtained at 160°C (vs. 33% at 80°C) for the first minute. Comparison of the NSE at 120°C for Pt/CeO_2-ZrO_2 and Pt/ZrO_2 indicates that incorporation of Ce into the ZrO_2 phase significantly improves the NSE.

NOx desorption behavior was studied after NOx storage for 15 min; Figure 3 displays the resulting NOx-TPD profiles. Two NOx desorption events are apparent, the first occurring below 300°C and the second occurring in the range 300-500°C. With increasing storage temperature, the first desorption peak slightly shifts to lower temperature, while the position of the second peak is largely unchanged. Similar NOx-TPD profiles were obtained after only 5 min of NOx storage, although the first desorption peak was relatively less intense. From this it follows that increasing the storage time is beneficial for low-temperature NOx release. As storage progresses, strong adsorption sites are filled first and hence at longer storage times NOx is increasingly stored on weak adsorption sites. Similarly, increasing the storage temperature, which results in increased NOx storage (in the range studied), is also beneficial for low-temperature NOx release (Figure 3). Hence, both storage temperature and storage time play important roles in the NOx desorption behavior.

In other work, $Pt/Ce_{0.9}Pr_{0.1}O_2$ materials were prepared for use in low temperature LNT catalysts. Model $Pt/Ce_{0.9}Pr_{0.1}O_2$ and Pt/CeO_2 NOx storage-reduction catalysts were prepared via nitrate calcination (N), urea-assisted co-precipitation (U) and carbon-templating routes (C). Raman spectroscopic data obtained on the catalysts indicated that the introduction of praseodymium into the ceria lattice increased the concentration of defect sites (vacancies), arising from the higher reducibility of the Pr^{4+} cation compared to Ce^{4+} (Figure 4). For the Pr-promoted samples, H_2-TPR profiles contained high temperature bulk reduction peaks which were less pronounced compared with their ceria analogs, indicating that the presence of praseodymium enhances oxygen mobility due to the creation of lattice defects (Figure 5). Under lean-rich cycling conditions, the cycle-averaged NOx conversion of the $Pt/Ce_{0.9}Pr_{0.1}O_2$ samples was in each case substantially higher than that of the Pt/CeO_2 analog, amounting to a difference of 10-15% in the absolute NOx conversion in some cases (Figure 6). This improvement is largely due to the superior NOx storage efficiency of the Pr-containing catalysts, which according to DRIFTS data is explained by the fact that the kinetics of nitrate decomposition under rich conditions are faster on $Pt/Ce_{0.9}Pr_{0.1}O_2$, leading to improved catalyst regeneration. These results suggest that ceria-based mixed oxides incorporating Pr are promising materials for NOx storage-reduction catalysts intended for low-temperature operation.

CONCLUSIONS

- From a study of NOx storage and release on Al_2O_3, Pt/Al_2O_3 and $Pt/La\text{-}Al_2O_3$ in the temperature range 80-160ºC, guidelines were established for the design of materials for PNA applications. In particular, effective PNA design must balance adequate low-temperature NOx storage capacity with facile NOx desorption. This points to the need for materials which adsorb NOx principally as nitrite and weakly bound nitrate species.

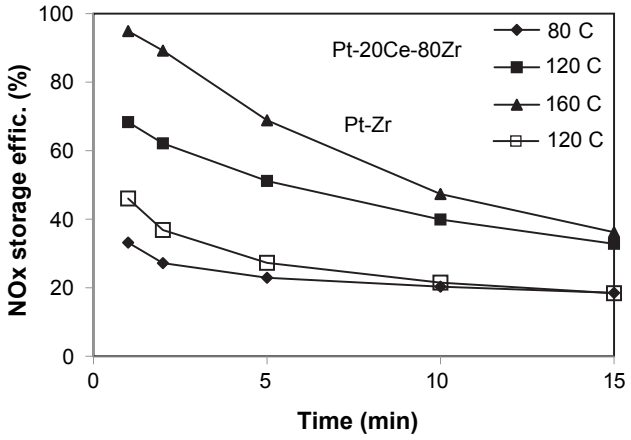

FIGURE 2. Comparison of NOx Storage Efficiency of Pt/CeO_2-ZrO_2 and Pt/ZrO_2 at Different Temperatures—Feed Gas as for Figure 1

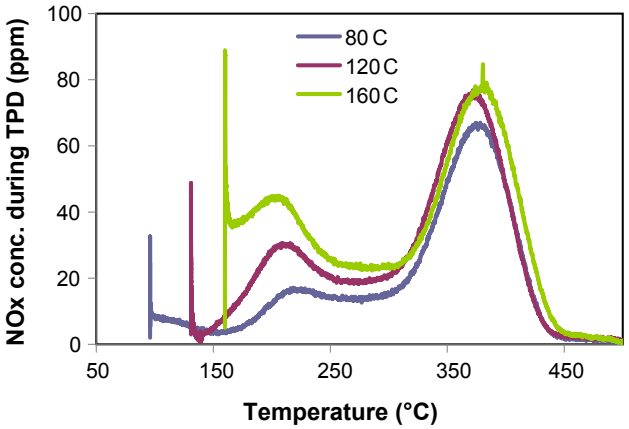

FIGURE 3. NOx-TPD Profiles for Pt/CeO_2-ZrO_2 (NOx stored for 15 min at the temperature indicated)

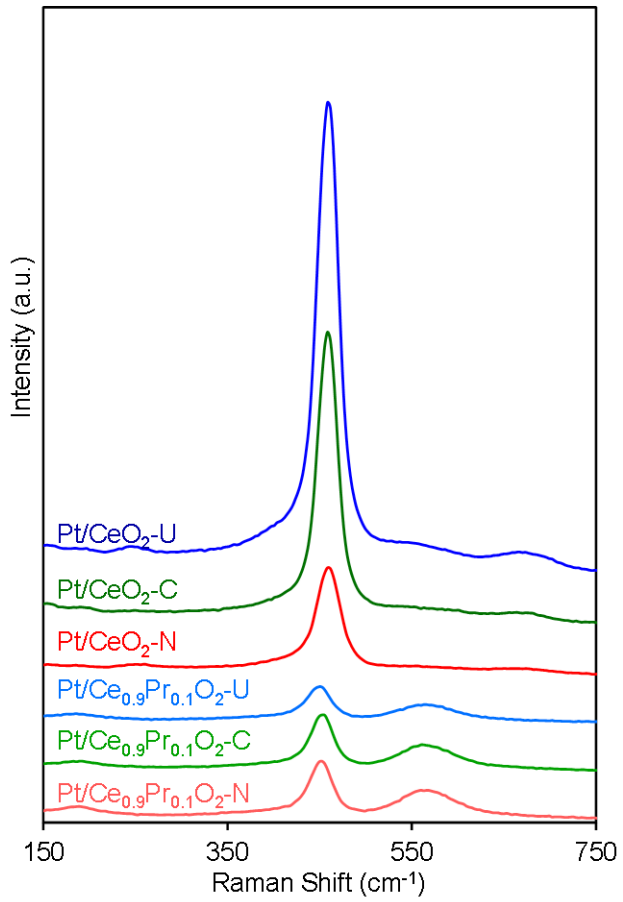

FIGURE 4. Raman Spectra of Model $Pt/Ce_{0.9}Pr_{0.1}O_2$ and Pt/CeO_2 Catalysts

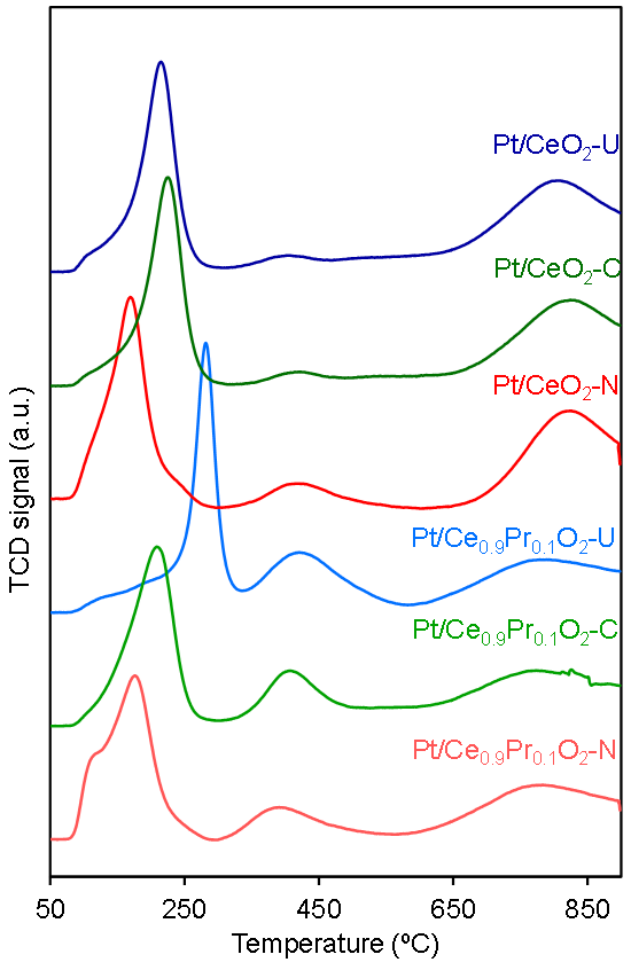

FIGURE 5. H_2-TPR Profiles of Model $Pt/Ce_{0.9}Pr_{0.1}O_2$ and Pt/CeO_2 Catalysts

- Pt/CeO_2-ZrO_2 was identified as a promising material for PNA applications based on its ability to thermally desorb significant amounts of NOx in the temperature range 200-350°C.
- Ceria-based mixed oxides incorporating Pr were identified as promising materials for LNT catalysts intended for low temperature operation, due to the fast kinetics of nitrate decomposition they exhibit under rich conditions.

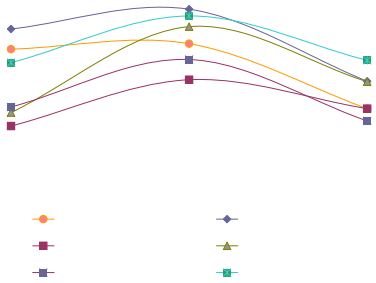

FIGURE 6. Cycle-Averaged NOx Conversion of Model Catalysts

FY 2014 PUBLICATIONS/PRESENTATIONS

1. V. Rico-Pérez, A. Bueno-López, D.J. Kim, Y. Ji, M. Crocker, "$Pt/Ce_xPr_{1-x}O_2$ (x = 1 or 0.9) NOx Storage-Reduction (NSR) Catalysts," *Appl. Catal. B*, 163 (2015) 313.

2. Y. Ji, M. Crocker, "Al_2O_3-based passive NOx adsorbers for low temperature applications," oral poster presentation EC-P-98, 8th ICEC, Asheville, NC, August 24–27, 2014.

3. M. Crocker, V. Rico-Perez, A. Bueno-Lopez, D.J. Kim, Y. Ji, "Model $Pt/Ce_xPr_{1-x}O_2$ (x = 1 or 0.9) NOx storage-reduction catalysts," poster presentation EC-P-15, 8th ICEC, Asheville, NC, August 24–27, 2014.

IV. HIGH EFFICIENCY ENGINE TECHNOLOGIES

IV.1 Technology and System Level Demonstration of Highly Efficient and Clean, Diesel-Powered Class 8 Trucks

David Koeberlein
Cummins Inc.
PO Box 3005
Columbus, IN 47201-3005

DOE Technology Development Manager
Roland Gravel

NETL Project Manager
Ralph Nine

OVERALL OBJECTIVES

- Objective 1: Engine system demonstration of 50% or greater brake thermal efficiency in a test cell at an operating condition indicative of a vehicle traveling on a level road at 65 mph.
- Objective 2:
  - a: Tractor-trailer vehicle demonstration of 50% or greater freight efficiency improvement (freight-ton-miles per gallon) over a defined drive cycle utilizing the engine developed in Objective 1.
  - b: Tractor-trailer vehicle demonstration of 68% or greater freight efficiency improvement (freight-ton-miles per gallon) over a defined 24-hour duty cycle (above drive cycle + extended idle) representative of real-world, line-haul applications.
- Objective 3: Technology scoping and demonstration of a 55% brake thermal efficiency engine system. Engine tests, component technologies, and model/analysis will be developed to a sufficient level to validate 55% brake thermal efficiency.

FISCAL YEAR (FY) 2014 OBJECTIVES

- Complete Demo 2 24-hr cycle freight efficiency testing.
- Complete Demo 2 drive cycle freight efficiency testing.
- Complete analysis and targeted testing for a 55% thermal efficient engine system.

FY 2014 ACCOMPLISHMENTS

- Demonstrated the SuperTruck Demo 2 vehicle with 86% freight efficiency improvement on a 24-hour cycle, which includes overnight hoteling and operating the Texas highway drive cycle route.
- Demo 2 also demonstrated a 76% freight efficiency improvement on the Texas highway drive cycle.
- Demonstrated a Li-ion battery pack auxiliary power unit (APU) capabilities to support full sleeper cab hotel loads.
- Validated an advanced transmission efficiency model.
- Completed an alternate fuel compression ignition (AFCI), i.e. dual-fuel multi-cylinder engine build and initial testing with cylinder-to-cylinder and cycle-to-cycle control system.
- Completed an initial conventional diesel engine technologies roadmap to 55% thermal efficiency.
- Completed selective analytical validation tests in a conventional diesel single-cylinder engine of revised injector and piston configurations.
- Completed multi-cylinder engine tests to validate analysis of both conventional diesel and AFCI technologies.

FUTURE DIRECTIONS

- Analysis and targeted testing of technologies for achievement of a 55% thermal efficient engine.
- Develop the technology roadmap for a 55% thermal efficient engine with supporting analysis and test results.

INTRODUCTION

Cummins Inc. is engaged in developing and demonstrating advanced diesel engine technologies to significantly improve the engine thermal efficiency while meeting U.S. Environmental Protection Agency 2010 emissions. Peterbilt Motors is engaged in the design and manufacturing of heavy-duty Class 8 trucks.

Together, Cummins and Peterbilt provide a comprehensive approach to achievement of a 68%

or greater increase in vehicle freight efficiency over a 24-hour operating cycle. The integrated vehicle demonstration includes a highly efficient and clean diesel engine with 50% or greater brake thermal efficiency including advanced waste heat recovery, aerodynamic Peterbilt tractor-trailer combination, reduced rolling resistance tire technology, advanced transmission, and a Li-ion battery APU for idle management. In order to maximize fuel efficiency, each aspect associated with the energy consumption of a Class 8 tractor-trailer vehicle will be addressed through the development and integration of advanced technologies.

In addition, Cummins will scope and demonstrate evolutionary and innovative technologies for a 55% brake thermal efficiency engine system.

APPROACH

Cummins and Peterbilt's approach to these project objectives emphasizes an analysis-led design process in nearly all aspects of the research. Emphasis is placed on modeling and simulation results to lead to attractive feasible solutions. Vehicle simulation modeling is used to evaluate freight efficiency improvement technologies. Technologies are evaluated individually along with combination effects resulting in our path to target measure of project status and for setting project direction.

Data, experience, and information gained throughout the research exercise will be applied wherever possible to the final commercial products. We continue to follow this cost-effective, analysis-led approach both in research agreements with the Department of Energy as well as in our commercial product development. We believe this common approach to research effectively shares risks and results.

RESULTS

- The SuperTruck Demo 2 vehicle (Figure 1) demonstrated an 86% freight efficiency improvement on a 24-hour cycle, which included both overnight hoteling and operating the Texas highway drive cycle route. On this test cycle, the Demo 2 fuel economy gains were 75%, and calculated greenhouse gas emission reduction of 43%. Test weight of both vehicles was 65,000 lb. Result is the average of three runs, where the 95% confidence was calculated at 4.5% and standard deviation of 2%. Freight efficiency runs include effects of the Cummins fuel quantity manager algorithm. All comparisons were made with the model year 2009 baseline Peterbilt 386 operating with the same test protocol on the same day, with the same weather conditions.

  On the 24-hour cycle the test protocol included both the Demo 2 truck and baseline trucks being hotel loaded to a prescribed load bank current draw profile. The baseline truck's engine idled during this period, while the Demo 2 vehicle drew power from its Li-ion battery APU. At the start of the drive cycle test, fuel flow measurement commenced upon startup of the Demo 2 engine. Both vehicles retrieved their respective trailers and proceeded on the 500-mile round trip route to/from Memphis,

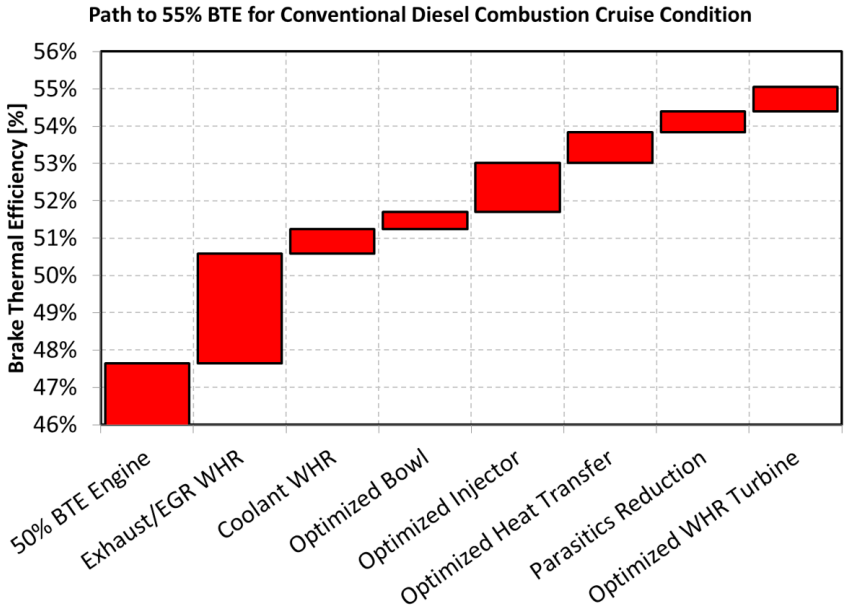

BTE - brake thermal efficiency; EGR - exhaust gas recirculation; WHR - waste heat recovery

FIGURE 1. SuperTruck Demo 2 Vehicle

TX from Peterbilt's Denton facility. This completed Objective 2b of the SuperTruck deliverables.

- The SuperTruck Demo 2 vehicle also demonstrated a 76% freight efficiency improvement on our drive cycle run on U.S. Route 287 between Fort Worth and Vernon, Texas. On this test cycle, the Demo 2 fuel economy gains were 66%. The tractor-trailer had a combined gross weight of 65,000 lbs. Result is the average of three runs, where the 95% confidence was calculated at 6% and standard deviation of 8%. The cruise control system had some operational issues on the last run which increased test variation. All comparison were made with the model year 2009 baseline Peterbilt 386 operating with the same test protocol on the same day, with the same weather. This repeated with improvements those accomplishments documented in the previous annual report. This completed Objective 2a of the SuperTruck (Figure 2).
- An AFCI multi-cylinder engine demonstrated a 49.4% brake thermal efficiency at a 10-bar brake mean effective pressure load. The alternate fuel substitution rate was 97%. The engine control system with in-cylinder pressure sensing adjusted each cylinders' operating parameters on a cylinder-to-cylinder and cycle-to-cycle basis for maximum efficiency. This combustion system technology enables higher efficiency with low emissions. Research continues to increase the load capacity of this engine. The initial cost analysis of this dual-fuel engine design appears attractive, if the engine requirements do not demand full engine operability and capability on each fuel independently, i.e. bi-fuel.
- Combustion bowl analysis was completed to identify bowl shape commensurate with a new injector specification. The analysis optimization work of bowl volume, shape factors and diameter resulted in a predicted 0.5% brake thermal efficiency improvement from that demonstrated on the SuperTruck 50% brake thermal efficiency engine.
- Single-cylinder engine test of a new injector specification which seeks to minimize combustion duration for maximum efficiency has shown a closed-cycle efficiency improvement of 1.3%. This single-cylinder engine validation testing confirms earlier combustion analysis work and will be followed with validation in multi-cylinder engine testing. The validation testing on this second injector iteration directionally points to a critical 55% technology roadmap element (Figure 3).
- Reduction of in-cylinder heat loss increases closed-cycle efficiency. Analysis of in-cylinder heat loss in conventional diesel engine showed that the piston rejects 50% of the in-cylinder heat losses, followed by the cylinder head at 30% and the cylinder liner at 20%. Since the piston is the largest component to in-cylinder heat losses, analysis of various piston materials and coatings and their influence to closed-cycle efficiency has been studied. Current analysis of multiple piston design variants relative to the baseline piston show a potential brake thermal

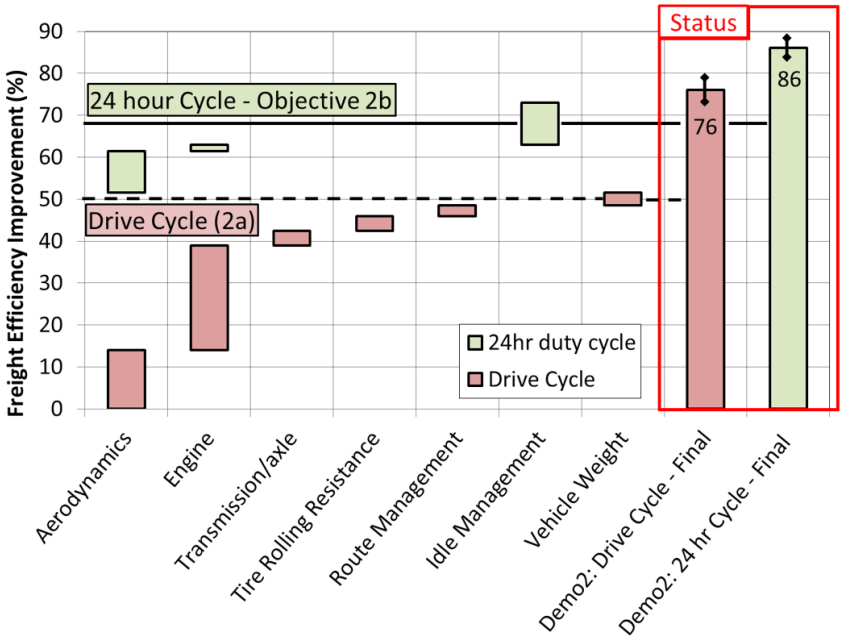

FIGURE 2. Final Freight Efficiency Roadmap and Status

FIGURE 3. Initial Diesel Technology Roadmap to Reach 55% Brake Thermal Efficiency

efficiency gain of 0.8%, through a combination of closed-cycle efficiency gains and increased exhaust energy.

- An advanced design of a waste heat recovery turbine expander has been rig tested with a 1.8-hp improvement over the turbine expander used on the SuperTruck Demo 2. This turbine expander improvement in addition to a plumbing 'pre-heat' circuit of the low-pressure-loop system is expected to increase engine cycle brake thermal efficiency by 0.7%.

CONCLUSIONS

The SuperTruck Engine and Vehicle System Level Demonstration of Highly Efficient and Clean, Diesel-Powered Class 8 Truck project has successfully completed the third year of the four-year project. The following conclusions have come from the third year:

- Demonstrated Class 8 truck freight efficiency improvements of 86% on a 24-hour cycle and drive cycle improvements of 76%.
- Demonstrated a Li-ion battery pack APU with capabilities all anticipated hoteling loads.
- Validated an advanced transmission efficiency model.
- Completed an AFCI, i.e. dual-fuel multi-cylinder engine build and initial testing with cylinder-to-cylinder and cycle-to-cycle control system.
- Completed an initial conventional diesel engine technologies roadmap to 55% brake thermal efficiency.
- Completed selective analytical validation tests in a conventional diesel single-cylinder engine of revised injector and piston configurations.
- Completed multi-cylinder engine tests to validate analysis of both conventional diesel and AFCI technologies.

FY 2014 PUBLICATIONS/PRESENTATIONS

Journal Paper Submissions

1. Gurneesh Jatana, Sameer Naik, Robert Lucht, and Gregory M. Shaver, High-speed diode laser measurements of temperature and water vapor concentration in the intake manifold of a diesel engine, *International Journal of Engine Research*, vol. 15 no. 7 773-78, October 2014.

2. Akash Garg, Mark Magee, Chuan Ding, Leighton Roberts, and Gregory M. Shaver, Exhaust Thermal Management Using Cylinder Throttling via Intake Valve Closing Timing Modulation, *Journal of Automobile Engineering,* revised version submitted 10-2014.

3. Leighton Roberts, Mark Magee, Akash Garg, Gregory M. Shaver, Eric Holloway, Edward Koeberlein, Raymond Shute, David Koeberlein, James McCarthy Jr., and Douglas Nielsen, Modeling the Impact of Early Exhaust Valve Opening on Exhaust Aftertreatment Thermal Management and Efficiency for Compression Ignition Engines, submitted for review to the *International Journal of Engine Research,* online Oct. 6th, 2014.

4. Gurneesh S Jatana, Sameer V Naik, Gregory M Shaver, and Robert P Lucht, Simultaneous high-speed gas property measurements in the turbocharger inlet, the EGR cooler exit, and the intake manifold of a multi-cylinder diesel engine using diode-laser-absorption-spectroscopy. Submitted for review to *Applied Optics*, 8-25-2014.

Public Presentations:

1. David Koeberlein, *Cummins SuperTruck Program - Technology and System Level Demonstration of Highly Efficient and Clean, Diesel Powered Class 8 Trucks*, Cummins, 2014 DOE Vehicle Technologies Program Annual Merit Review, Arlington, Virginia, June 20, 2014.

2. Ken Damon, *DoE SuperTruck Program - Technology and System Level Demonstration of Highly Efficient and Clean, Diesel Powered Class 8 Trucks*," 2014 DOE Vehicle Technologies Program Annual Merit Review, Arlington, Virginia, June 19, 2014.

3. Bill Partridge, *Cummins/ORNL FEERC Combustion CRADA: Characterization & Reduction of Combustion Variations*," 2014 DOE Vehicle Technologies Program Annual Merit Review, Arlington, Virginia, June 18, 2014.

SPECIAL RECOGNITIONS & AWARDS/ PATENTS ISSUED

1. 2014 Early Career Excellence in Research Award, Purdue University College of Engineering.

2. 2014 Purdue University Faculty Scholar.

3. 2014 DOE Vehicle Technologies Office R&D Award.

IV.2 SuperTruck – Improving Transportation Efficiency through Integrated Vehicle, Engine, and Powertrain Research: Fiscal Year 2014 Engine Activities

Sandeep Singh
Detroit Diesel Corporation
A08, 13400 Outer Drive West
Detroit, MI 48239-4001

DOE Technology Development Manager
Roland Grave

NETL Project Manager
Carl Maronde

Subcontractor
Massachusetts Institute of Technology, Cambridge, MA

Overall Objectives

- Demonstration of a 50% total increase in vehicle freight efficiency measured in ton-miles per gallon, with at least 20% improvement through the development of a heavy-duty diesel engine.
- Development of a heavy-duty diesel engine capable of achieving 50% brake thermal efficiency (BTE) on a dynamometer under a load representative of a level road at 65 mph.
- Identify key pathways through modeling and analysis to achieving 55% BTE on a heavy-duty diesel engine.

Fiscal Year (FY) 2014 Objectives

- Utilizing the results of the comprehensive analytical effort along with the component and system level development for engine and waste heat recovery (WHR) systems; the 2014 objective was to experimentally demonstrate a 50% engine BTE for the integrated systems.
- Finalize hardware builds, controls and calibration, for engine and WHR systems for SuperTruck vehicle integration.
- Functional integration and validation of vehicle and engine technologies, including WHR and hybrid systems on the SuperTruck A-sample vehicle.
- Build and commissioning of the final demonstrator SuperTruck vehicle in preparation of performance and freight efficiency testing next FY.
- Both, analytical and test-based technology scoping for the 55% engine BTE roadmap.

FY 2014 Accomplishments

- Demonstrated a combined 50.2% BTE in the laboratory on the SuperTruck demonstration engine and WHR systems, meeting the 2014 project targets.
- Development continued on the core diesel engine technology with the best results to date being an engine BTE of 47.9%.
- The WHR system design for vehicle integration is completed. Two complete systems fabricated and built for installation on the vehicles in FY 2014.
- Prototype A-sample SuperTruck vehicle built and utilized as a test bed for functional integration of the various complex technologies.
- Successful integration of WHR, hybrid and high voltage systems, controllers and network architecture, new cooling layout, new hydraulic systems, and powertrain.
- Lessons learned from A-sample build and integration in early FY 2014, applied to the build-up of final demonstration truck builds in late FY 2014.
- The final high efficiency engine hardware, including optimized turbocharger and aftertreatment systems, installed and running on the demonstration vehicle.
- Prototype model-based engine controls implemented on the vehicles, and operates the engine in primary control modes for over the road drive cycles.
- Within the scope of investigating higher efficiency combustion approaches, initiated a pilot project to evaluate advanced low-temperature combustion (LTC) regimes on a multi-cylinder stock engine.

Future Directions

- While the 50% BTE project goal has been achieved, further refinements will continue to be tested to further improve the efficiency of both engine and WHR systems.
- Refinement of various engine systems will continue to help fine tune their operating characteristics in support of final demonstrator testing on selected SuperTruck routes.

- Development of mechanical expanders for the WHR system to improve its performance characteristics by eliminating the inefficiencies of energy form conversion.
- Complete the pilot testing of advanced combustion regimes on a stock engine in collaboration with Oak Ridge National Laboratory (ORNL).
- Further development of engine and aftertreatment strategies to mitigate the challenges of controlling transient and LTC emissions.
- Continue the analytical effort to build a roadmap for higher efficiency approaches.

INTRODUCTION

SuperTruck is a five-year research and development project with a focus on improving diesel engine and vehicle efficiencies. The objective is to develop and demonstrate a Class-8, long-haul tractor-trailer that achieves a 50% vehicle freight efficiency improvement (measured in ton-miles per gallon) over a best-in-class 2009 baseline vehicle. The engine shall contribute 20% of the 50% improvement, specifically targeting a BTE of 50%, as tested on a dynamometer under conditions representative of the SuperTruck vehicle at 65 mph. In FY 2014, the engine specific goal of 50% BTE was demonstrated on a dynamometer. Further refinement in engine and WHR performance, controls and calibration was achieved. However, much of the focus was on design, hardware, and build for integration of engine and WHR systems on the hybrid SuperTruck vehicle.

APPROACH

The approach used is primarily centered on conventional diesel engine and testing of the systems required to achieve high BTE. Specific engine systems being refined and tested for high efficiency include the combustion system, air system, fuel system, engine controls, engine parasitics, aftertreatment, and waste heat recovery. In addition, the engine was significantly downsized relative to the baseline engine in order to improve the engine's efficiency at conditions representative of road-load operation.

RESULTS

The building blocks in reaching the 50% BTE milestone include the following elements:

- Downsizing to 10.7-L engine from the 14.8-L baseline engine
- Reduced exhaust gas recirculation (EGR) and optimized turbocharger and air system match
- Higher compression ratio, piston bowl optimization, matching injector nozzles
- Variable speed water pump
- Low viscosity oil and higher oil film temperatures
- Piston kit improvements
- High efficiency, lower restriction aftertreatment
- Exhaust and EGR waste heat recovery system

In previous years, many of these building blocks were evaluated analytically and individually in engine testing. All of these items have now been brought together to improve the efficiency of the demonstration engine. Over the last year, hardware design effort and controls and calibration development, have been the focus for transient over the road operation on the SuperTruck demonstration vehicle.

The combustion efficiency of the diesel engine has been enhanced by increasing the compression ratio and peak firing pressures, and optimizing the piston profile and injector geometry after extensive design of experiments. A combination of single-cylinder and multi-cylinder platforms were used for this investigation. This approach is promising for part-load efficiency and a SuperTruck-like efficient vehicle operation with low cruise power demands. High-load durability and resulting engine design changes were not in the scope of the project. The turbocharger was sized for reduced EGR and air mass, contributing to lower pumping losses. Essentially, the air system was tuned for a down sped engine operation over the road, with lower vehicle axle ratios and direct drive transmission. The air system design leverages a lower power rating required for the aerodynamically and parasitically efficient SuperTruck. The high-efficiency SuperTruck engine design also results in high engine-out oxides of nitrogen (NOx) which has to be mitigated with a very high-efficiency selective catalytic reduction and low-backpressure aftertreatment.

Research has been conducted in the area of parasitics reduction at the Sloan Automotive Laboratory of the Massachusetts Institute of Technology (MIT) as part of the SuperTruck sub-contract. Reduction of in-cylinder friction losses, which amount to 40-50% of the total engine mechanical losses, is an area of primary focus. Technologies related to piston kit friction reduction, oil circuit and flow optimization, and low viscosity oil are being explored, with testing taking place on the most promising of these ideas. Testing with reduced mid-stroke liner cooling has shown measureable fuel economy improvement and potential. Further evolution of this approach is ongoing by leveraging detailed liner

temperature measurements and thereby improving MIT models which predict the liner insulation profile. Another area of MIT contribution is lubricant formulation optimization working with an oil supplier. Focus is on fuel economy benefit that can be gained through different base engine oils and corresponding viscosity characteristics, including viscosity index improvers and anti-wear additives.

A novel method of engine controller is being utilized in this project, and these controls have been optimized for engine fuel efficiency improvement measures via dynamometer test cycles representative of over-the-road SuperTruck operation. The SuperTruck engine control logic is based on extensive mapping of engine operation, followed by training of neural network engine performance models. The resulting logic enables the control of engine actuators based on engine-out NOx set-points adapted to the driving conditions. The controls have been calibrated for the high-efficiency engine and much of the work recently focused on preparing the system for testing and evaluation on the demonstration vehicle. This year vehicle tests of SuperTruck engine systems, particularly focused on the neural network-based engine control algorithm, were conducted. Duty cycles included bobtail/urban routes for initial troubleshooting tasks, and culminated with loaded/highway routes to enable fine tuning of controller gains. The test performance metrics were controller stability, throttle response, engine-out and tailpipe-out NOx levels, fuel economy, turbo over-speed control, and the ability of the control algorithm to converge on pre-defined NOx and combustion timing set-points/targets. This novel approach resides on a prototype controller, and today stands far from a maturity to be implemented on an embedded controller, but has the potential to systemize the multi-dimensional controls complexity of today's engine technology.

Progress has been made in the development of a high-efficiency, low-backpressure aftertreatment system for the SuperTruck engine. One of the engine strategies is higher engine-out NOx for increased engine efficiency matched to a high-efficiency aftertreatment system. A number of aftertreatment designs were procured and tested, and the final system was selected in previous years. The steady-state performance yields compliant tailpipe NOx levels with fresh new catalysts. However, real world degradation of a system required to consistently perform at high efficiency is a concern. Further investigations is currently ongoing in developing a novel engine air system which can span a wide range of engine-out NOx operation in order to address the challenges of LTC transient aftertreatment.

The SuperTruck WHR system will employ a Rankine cycle to harness the heat energy in the engine's exhaust and EGR cooler. Currently, the Rankine heat engine is set up to generate high pressure ethanol vapor utilizing both exhaust and EGR heat, that then energizes an expansion machine to turn a generator to produce electrical power. Significant testing and refinements of both the hardware and control system were undertaken in the last year, and a BTE improvement of 2.3% was realized. This year the WHR system with electrical expander and associated cooling system was commissioned on the final demonstrator SuperTruck. Lessons learned from the A-sample vehicle functional integration were useful in optimizing the effort on the final demonstrator build. Accomplishments during the commissioning include automated and mature controls for cold start, shutdown, boiler steam quality and condenser cooling. Minimal impact on engine cooling and fan activation was observed. Further vehicle freight efficiency improvement tests are planned for the final demonstration vehicle.

Some of the WHR technology barriers identified during the SuperTruck project include the vehicle aerodynamic and underhood cooling flow tradeoffs; optimum working fluid selection with regards to its thermodynamics characteristics, system design and environmental impacts; complex payback, cost, reliability, durability, component packaging and weight scenarios.

The partnership with ORNL over the last year has been focused on dual-fuel investigation for both conventional diesel like combustion approaches, and advanced LTC regimes. The LTC regimes have a potential towards the stretch goal of 55% engine BTE. The efforts at ORNL focused on commissioning of the dual-fuel engine setup, shakedown and benchmarking of the Daimler engine in diesel mode, and programming the natural gas injection controller hardware. The set up work has now concluded, and the testing of the natural gas injection system and dual-fuel operation is set to begin early in the next FY. These advanced combustion studies in search for higher efficiencies are expected to run through the last year of the project.

CONCLUSIONS

A 50.2% BTE has been demonstrated with the engine and WHR systems. The high efficiency engine and subsystems have been implemented into the demonstration vehicle including functional validation of the technologies early in FY 2014 on the A-sample vehicle. Further development of controls and calibration for all systems will continue in order to support performance testing of the demonstration vehicle on selected SuperTruck routes in Oregon and Texas. In addition, analysis and testing continues for the roadmap to a higher BTE engine, such as LTC effort in partnership

with ORNL, mechanical expanders for WHR system, and other air system optimization and parasitics reduction-related simulation tasks.

FY 2014 PUBLICATIONS/PRESENTATIONS

1. Singh, Sandeep: "SuperTruck Program: Engine Project Review; Recovery Act -Class 8 Truck Freight Efficiency Improvement Project", Project ID: ACE058, DoE Annual Merit Review, June 20, 2014.

2. Rotz, Derek: "SuperTruck Program: Vehicle Project Review; Recovery Act -Class 8 Truck Freight Efficiency Improvement Project", Project ID: ARRAVT080, DoE Annual Merit Review, June 19, 2014.

IV.3 SuperTruck Initiative for Maximum Utilized Loading in the United States

Pascal Amar (Primary Contact),
Samuel McLaughlin, Arne Andersson,
John Gibble
Volvo
13302 Pennsylvania Avenue
Hagerstown, MD 21742

DOE Technology Development Manager
Roland Gravel

NETL Project Manager
Ralph Nine

Subcontractor
Penn State University, State College, PA

Collaborations
Delphi
Exxon Mobil
University of Michigan

Overall Objectives

- Identify concepts and technologies that have potential to achieve 55% brake thermal efficiency (BTE) on a heavy-duty diesel engine. Perform a thorough analysis of the limiting factors and potential areas for improving the engine's efficiency using analytical simulations, including research into alternative thermodynamic cycles, advanced component design, fuel formulation and new engine designs, as well as development of more advanced combustion modeling tools.
- Demonstrate a heavy-duty diesel engine capable of achieving 50% BTE at the end of the SuperTruck project.

Fiscal Year (FY) 2014 Objectives

- Develop and use simulation tools and models for partially premixed combustion (PPC) and other new concepts
- Evaluate and select a concept capable of 55% BTE
- Design and build the Phase 2 engine components capable of 50% BTE

FY 2014 Accomplishments

- Validated computational fluid dynamics (CFD) combustion models against 1-cylinder engine test data with primary reference fuel 87 surrogate fuel
- Evaluated several concepts capable of 55% BTE
- Engine test results together with verified sub systems add up to 47.9% BTE without waste heat recovery (WHR) for the 50% BTE demonstrator powertrain
- Transported probability density function (PDF) combustion CFD tool used for the 55% BTE concept engine work where we enter new regimes and explore advanced injection strategies

Future Directions

- Continue development of the combustion CFD tool to be able to simulate PPC, with focus on kinetic mechanisms and ways to speed them up
- Continue to use the transported CFD tool for 55% BTE concept engine combustion simulation
- Integrate closed-cycle CFD result into complete GT-POWER engine models
- Verify more subsystems including WHR to reach 50% BTE

INTRODUCTION

New combustion concepts like PPC and reactivity-controlled compression ignition have demonstrated very high indicated efficiencies together with a potential for low engine-out emissions, however the combustion is significantly more difficult to simulate than normal diesel diffusion combustion. The transported PDF combustion model has been developed to address this challenge and supports the 55% BTE concept engine work where we enter new regimes and explore advanced injection strategies.

The concept simulation work targeting 55% BTE has been successful. The model in GT-POWER reaches the target, but the 55% BTE concept pushes the rather simple GT-POWER sub-models into extrapolation. We are validating the sub-models for the new regimes one by one. So far the extrapolations have proved to be reasonably correct.

APPROACH

The Penn State University effort includes CFD modeling and laboratory experiments aimed at meeting the 55% BTE target. Several tests have been performed in order to create good validation data. One set of simulations targets high-pressure, constant-volume turbulent spray combustion in two configurations: a set of experiments available through the Engine Combustion Network and a set of experiments that is being performed at Penn State using a cetane identification 510 device. The constant-volume simulations are focused on model development and validation for different fuels. The second set of simulations targets a Volvo heavy-duty diesel engine running on primary reference fuel 87 in PPC mode. The engine simulations are focused on exploring advanced high-efficiency combustion strategies, including PPC and reactivity-controlled compression ignition. The modeling framework is a PDF method, with skeletal-sized chemical mechanisms (up to ~100 species) and soot models. The models are being implemented via user coding in a commercial CFD code (STAR-CD). It is anticipated that this modeling approach will be able to capture the multiple regimes of compression-ignition combustion that are of interest for this project, including conventional diesel combustion, low-temperature combustion, partially premixed combustion, and dual-fuel combustion.

The ignition test apparatus has been modified to introduce optical probes into the combustion chamber for high-speed fuel-spray imaging and chemiluminescence detection.

Our search for concepts capable of 55% BTE started with an analysis of where the losses in presently used cycles occur. We identified improvement potential in a number of areas, see Figure 1.

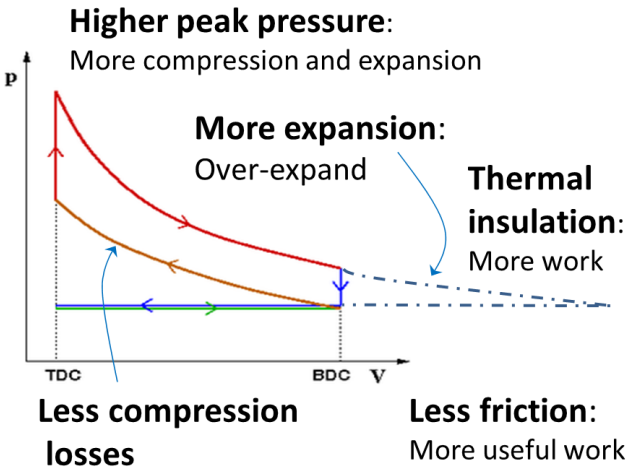

FIGURE 1. Opportunities for Higher Efficiency Cycles

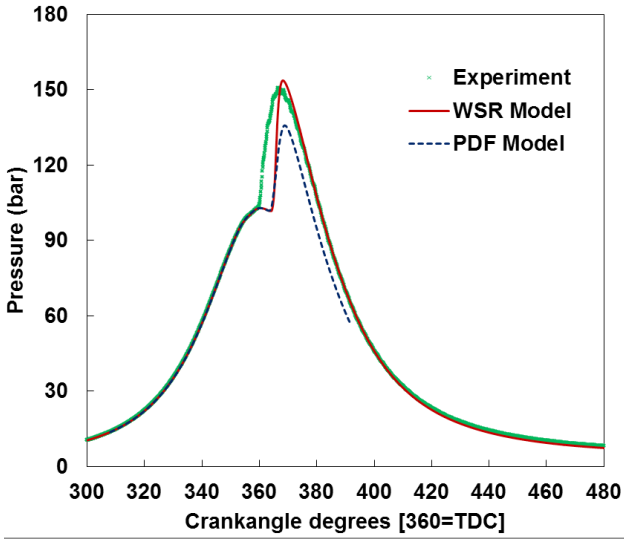

TDC - top-dead center

FIGURE 2. Pressure Traces for Experiment, Well Stirred Reactor (WSR) Model and PDF Model for a 12-Bar Indicated Mean Effective Pressure PPC Case

RESULTS

Combustion CFD Validation

Figure 2 shows that there is an issue with the heat release for the PDF method. A systematic investigation is on-going to find the root cause. One possible cause is the spray model. We have measured penetration lengths from cetane identification through the optical access, see Figure 3.

The simulations initially gave longer penetration lengths than observed in the experiments, and the reasons for this discrepancy were explored. These included parametric studies to determine which physical and numerical parameters in the simulations have the largest influence on computed liquid penetration length. Of the parameters tested, the only one that made a significant difference was the criterion used to define the liquid penetration length from the CFD. It is not clear what fraction of liquid fuel droplets is visible in the experiment. For example, Table 1 shows sensitivities of computed liquid penetration lengths and cone angles to variations in the liquid fuel temperature and to an assumed cut-off in liquid droplet size. For this operating condition, the measured penetration length is 16.8 mm and the measured cone angle is 8.1 degrees. The computed penetration length shows weak sensitivity to the assumed fuel temperature, but strong sensitivity to the assumed droplet size cut-off. A cut-off of 20 microns captures more than 99.9% of the liquid mass (mass

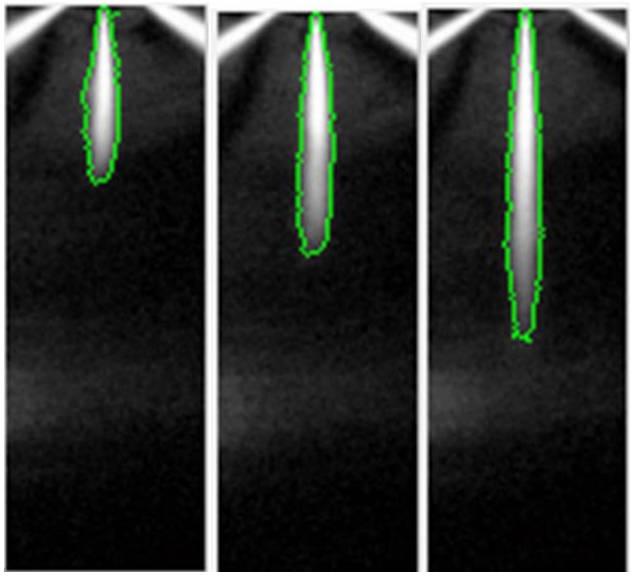

FIGURE 3. Spray Images of N-Heptane Post-Processed with Edge Detection

TABLE 1. Spray computed liquid penetration lengths and cone angles 1.5 ms after start of injection for a n-heptane spray in the cetane identification instrument, with variations in the liquid fuel temperature and the minimum droplet diameter threshold.

	Base Line			
Diameter Threshold	300 K		323.15 K	
	PL (mm)	MF	PL (mm)	MF
none	27.29	1.0	25.98	1.0
>1e-5 (m)	18.86	0.9999	18.50	0.9999
>2e-5(m)	17.38	0.9998	17.08	0.9998
>3e-5(m)	15.91	0.9992	15.63	0.9992
>4e-5(m)	14.47	0.9975	14.28	0.9976
Cone Angle	8.68		8.72	

fraction), and gives a computed penetration length that is in good agreement with experiment. This cut-off is somewhat arbitrary however, and further work is needed to determine the minimum size of droplets that can be seen in the experiment.

Using Combustion CFD to Analyze the 55% BTE Concepts

One uncertainty with the GT-POWER simulations is the heat losses. When analyzing different combustion engines and combustion modes, significant tuning of the heat loss factor is required. Sensitivity analysis on the heat loss factor shows a strong influence on BTE. Once the heat loss factors are validated they will be incorporated into the GT-POWER models.

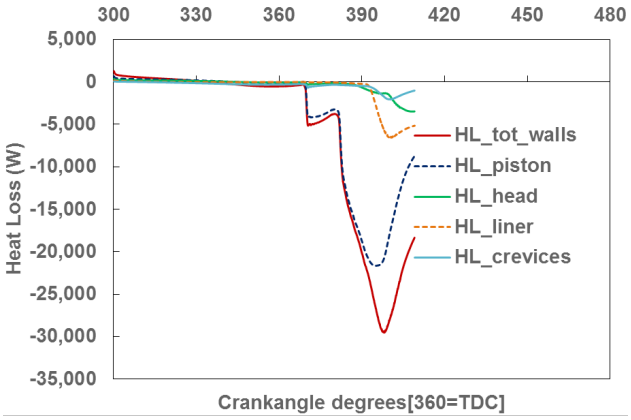

FIGURE 4. Heat Load on Different Combustion Chamber Components with the 55% BTE Combustion System

The combustion CFD is also used to evaluate the heat load on different components, see Figure 4.

50% BTE Powertrain

The engine for the 50% BTE powertrain is built, and components are being integrated onto the engine and verified. The engine has achieved 47.9% BTE without the addition of WHR, with some components remaining to be integrated and verified.

The next generation of WHR system for Phase 2 has been designed and components are on test. This generation is more compact and lighter than the system demonstrated on the mule vehicle in Phase 1.

CONCLUSIONS

PPC combustion is very demanding on simulation tools. A practical PPC engine involves combustion modes from premixed charge compression ignition to diffusion combustion.

The advanced transported PDF model is a valuable tool for combustion simulations of new regimes and advanced combustion strategies for the 55% BTE concepts.

FY 2014 PUBLICATIONS/PRESENTATIONS

1. V Raj Mohan, D.C. Haworth, Proc. Combust. Inst. (2014) Turbulence-chemistry interactions in a heavy-duty compression-ignition engine. Proc. Combustion Institute 35. In press.

2. V Raj Mohan, D.C. Haworth, Turbulence-chemistry interactions in a heavy-duty compression ignition engine, 35th International Combustion Symposium, San Francisco, CA, 4–8 August 2014.

3. D.C. Haworth, Radiative Heat Transfer in Engine-Relevant Environments, Advanced Engine Combustion Program Review Meeting, Southfield MI, 19–21 August 2014.

4. V Raj Mohan (2014) Development and application of a transported probability density function model for advanced compression-ignition engine, Ph.D. thesis, The Pennsylvania State University, University Park, PA.

5. Mayo, M.P., 2014, Effects of Air Temperature and Oxygen Dilution on the Ignition Behavior of Liquid Fuels in an Optical Spray Chamber, M.S. Thesis, Chemical Engineering, The Pennsylvania State University, University Park, PA.

6. Bhaskar Prabhakar; Srinivas Jayaraman; Randy Vander Wal; André L. Boehman, Experimental Studies of High Efficiency Combustion with Fumigation of DME and Propane into Diesel Engine Intake Air, J. Eng. Gas Turbines Power. 2014; GTP-14-1251, doi: 10.1115/1.4028616 (*To appear in)*

7. Prabhakar, B. and A. Boehman, High Efficiency Combustion with DME and Propane Fumigation into Diesel Engine Intake Air, in *Prepr. Pap.-Am. Chem. Soc., Div. Energy Fuels.* 2014*, 59(2), 617-618.*

IV.4 SuperTruck Advanced Combustion Development at Navistar

Russell Zukouski (Primary Contact),
James Cigler, Gengxin Han, James Park,
Raj Kumar, Ryan Vojtech, Andrew Ickes,
Thomas Wallner
Navistar, Inc.
2701 Navistar Drive
Lisle, IL 60531

DOE Technology Development Manager
Roland Gravel

NETL Project Manager
Ralph Nine

Overall Objectives

Using advanced engine technologies, develop a heavy-duty diesel engine capable of achieving 50% or better brake thermal efficiency (BTE) on a dynamometer under a load representative of a level road at 65 mph

Fiscal Year (FY) 2014 Objectives

- Quantitatively asses the compression ratio (CR) impact on engine BTE
- Quantitatively asses the peak cylinder pressure impact on engine BTE
- Optimize combustion duration for better thermal efficiency
- Investigate the turbo efficiency impact on combustion efficiency
- Demonstrate the improvement of engine BTE on test engines
- Assessment focusing on the impact of premixed fuel reactivity, using high octane gasoline alternatives in conjunction with varied effective CR

FY 2014 Accomplishments

- Resumed this project from "pause period"; supported one of the ongoing tasks with direct collaboration of Argonne National Laboratory (ANL)
- Conducted study on impact of effective CR, comparing early intake valve closing and late intake valve closing valve strategies for dual-fuel operation at a mid-load operating condition
- Completed investigation on important combustion parameters, such as CR, peak cylinder pressure and their impact on thermal efficiency; extensive investigation of conventional diffusive diesel combustion
- Conducted advanced combustion investigation by varying combustion parameters such as fuel injection strategy, combustion bowl geometry
- Demonstrated combustion efficiencies from 47.6% to 48.1% through contributing combustion system and engine system features

Future Directions

- Evaluate the implications of a downsized engine (10.5 L from 12.4 L)
- Continue investigation and development of high-efficiency solutions focusing on the impact of premixed fuel reactivity and the assessment of variable valve actuation (VVA) technologies under dual-fuel combustion
- Conduct three-dimensional computational fluid dynamics to analyze and develop the advanced combustion solution for high-efficiency combustion, both dual-fuel and conventional single-fuel combustion will be included under this study
- Investigate and evaluate the feasible technology of waste heat recover system for maximum net BTE gain to be applied on an engine and on the vehicle
- Conduct evaluation and optimization of aftertreatment system to optimize engine BTE

INTRODUCTION

The overall goal of this project is to develop and demonstrate a 50% total increase in vehicle freight efficiency measured in ton-miles per gallon. This overall goal will be achieved through efficiency improvements in advanced vehicle systems technologies and advanced engine technologies. At least 20% of this improvement will be through the development of a heavy-duty diesel engine capable of achieving 50% BTE on a test engine. Describing a pathway to an engine with 55% BTE is an additional deliverable of the DOE SuperTruck project.

In order to develop an engine with 50% BTE incorporating the compliance with prevailing U.S. Environmental Protection Agency emissions standards, certain advanced engine technologies need to be applied in order to help attain higher efficiency through

combustion optimization by maximizing work extraction from the combustion process and minimization of thermal and parasitic losses. Efficiency can be increased by improving combustion processes, minimizing engine losses such as friction, reducing the energy penalty of the emission control system and using recovered waste energy. Each technology improves efficiency in a different way, following major technology areas are being pursued during FY 2014:

- Combustion optimization - CR, combustion chamber and matching fuel injection strategies, down-sizing effects
- Improvements in the engine gas exchange efficiency (volumetric efficiency, air handling efficiency)
- Further assessment of dual-fuel combustion under different conditions
- Overall engine thermal management

APPROACH

The base engine efficiency gain was accomplished through improvements in combustion, gas flow optimization, reduction in pumping losses. For advanced combustion of diesel fuel, burning predominantly takes place simultaneously with the mixing of fuel and air, known as diffusion combustion. Automotive diesel combustion process enables very efficient engine architecture, and is the key motivation behind this strategy.

Task 1: Combustion Improvement. Combustion improvements include increased CR, optimized piston bowl shape and injector match, thermal management and calibrations. These engine design changes account for most BTE improvement during FY 2014. A 13-L diesel engine at Navistar was utilized for this task. This engine, with a geometric CR of 17, equipped with Bosch's common rail fuel injection system. This 2010-compliant engine was modified from a series of combustion chamber designs with optimum fuel nozzle spray matches. The CR changes are obtained by changing the volume of combustion chamber. Effects of advanced fuel injection strategies (e.g., multiple fuel injections, higher injection pressure, smaller orifices, orifice geometry and patterns, etc.) are also included under this task. In conjunction with injection timing, the BTE impact from an engine designed peak cylinder pressure is also investigated. To contain the combustion energy for useful work, the overall thermal managements on in-cylinder insolation, cooling system, lube system is investigated and applied on test engines.

Task 2: Air System Improvement. The expanded investigation of an optimized air system is conducted under this task. Air utilization, air motion, or/and fuel-air mixing are key enablers for advanced combustion. Increasing the turbo efficiency by not increasing engine pumping loss will hence increase the thermal efficiency. The different configuration of turbochargers was investigated from two-stage fixed geometry to a single variable geometry turbocharger. With simulation guidance, the selected turbochargers are tested on a development engine, with emphasis on the project goal, the road cruise condition is emphasized during the turbocharger match process. Comparing with baseline turbocharger, the newly matched high-efficiency turbocharger does show BTE gain on the test engine.

Task 3: Investigation of Dual-fuel Combustion. In cooperation with ANL, the engine test under this task was conducted at ANL's test cell. The FY 2014 activities focus on evaluating the use of higher octane gasoline alternatives, E85 (85% ethanol and 15% gasoline) and compressed natural gas (CNG), in dual-fuel combustion with the upgraded hardware incorporating higher effective CR and variable intake valve closing timing enabled with the VVA system. The specific focus is on maximizing BTE using an optimized combination of dual-fuel operation and effective CR. Specifically, by increasing the knock resistance of the low-reactivity fuel, expanded high-load operation, with higher efficiency, is sought. Effective CR can be optimized in conjunction with the low-reactivity fuel. The engine system was benchmarked on a single-fuel (diesel) variant of a Navistar 13-L engine, and on gasoline-diesel dual-fuel operation with late intake valve closure strategies. As noted in the previous reports, the VVA-equipped dual-fuel engine utilizes a higher geometric CR than the previous dual-fuel engine (17:1 vs 14:1) used during earlier phases of this project. The higher base geometric CR is aligned with other tasks within the project for CR investigation and peak cylinder pressure (PCP) impact for FY 2014.

RESULTS

To achieve maximum BTE gain from advanced combustion, the efforts were made on the optimization of combustion chamber, compression ratio, fuel injection system, engine designed PCP, air system, etc. The following sections highlight the major achievements during FY 2014.

Task 1: Comprehensive efforts have been made to optimize combustion efficiency. A series of new cumbustion chambers with different shape and different CR (from 17:1 to 22:1) have been designed and tested on the engine (Figure 1). The engine tests showed that the shape of the combustion chamber is very depandent of the engine-out oxides of nitrogen (NOx) level and fuel injection strategies. For the current project, the CR

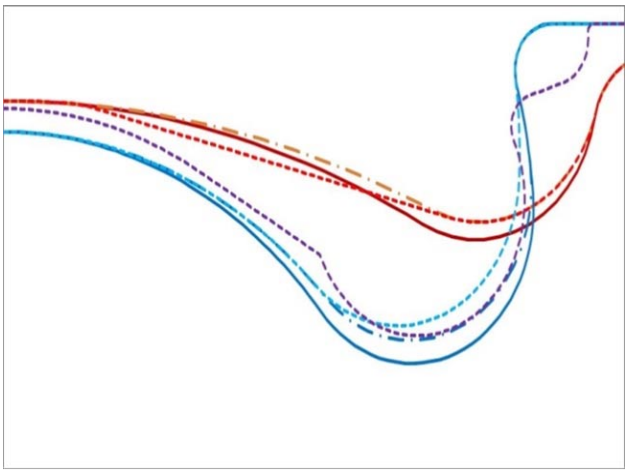

FIGURE 1. Combustion Chambers with Different Shape and Different CR (from 17:1 to 22:1)

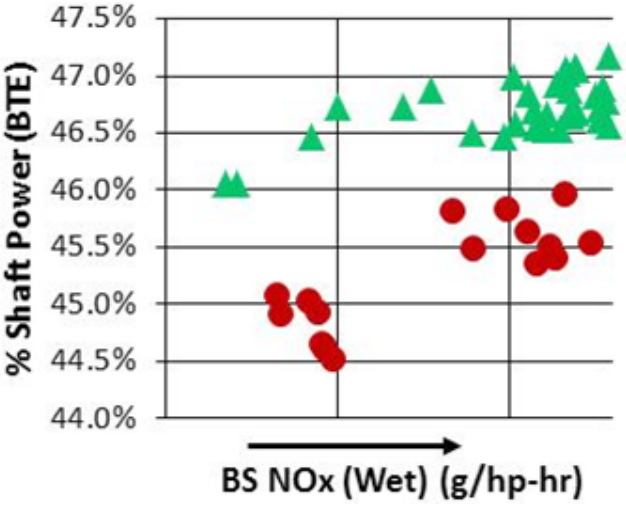

FIGURE 2. Advanced Combustion Match with Different Combustion Chambers: ●- Combustion Chamber 1 ▲- Combustion Chamber 2

started from 17:1, and CR changed in the range from 17:1 to 22:1. The example of combustion optimization is shown in Figure 2, where it is shown more than 1% (absolute) BTE gain with the optimized combustion design; the major BTE gain comes from the the increase of CR. During this optimal process, the fuel injection strategies are applied and optmized. The new engine design for higher PCP due to the CR increase is considered in the course of this task. The reasonable higher PCP ensures the utilization of combustion efficiency. Figure 3 clearly demonstrates the BTE effect with PCP difference of 400 psi from PCP1 to PCP3.

Task 2: Air utilization is one of the important factors for high-efficiency combustion, and the turbocharger plays key role for the air system. With simulation guidance, different turbocharger systems were designed

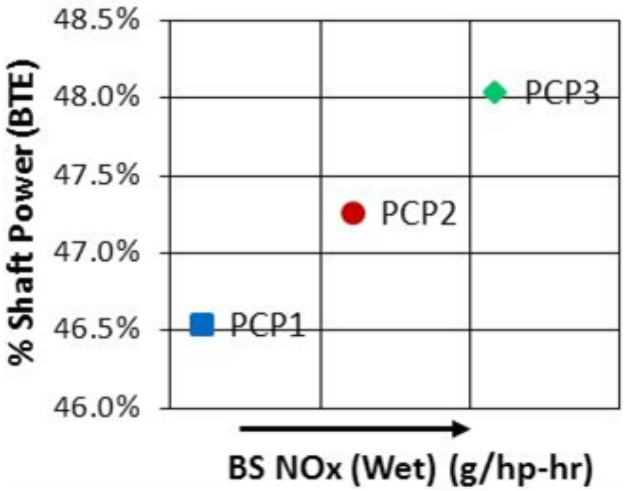

FIGURE 3. Peak cylinder pressure effect on BTE. The tests are under the same condition with most relaxed PCP at PCP3, PCP3 is 400 psi higher than PCP1.

and investigated, from two-stage fixed geometry turbochargers to single-stage variable geometry turbochargers, the main pupose is to investigate the air system impact on BTE. It is clearly shown that the high-efficiency turbo with minimum engine pumping loss is very beneficial to a high-BTE engine. Combustion data analysis from cylinder pressure traces indicated that with higher air/fuel ratio (AFR), the increasing premixed fraction leads to short duration of combustion providing the higher thermal efficiency. A typical comparison for a turbo system is shown in Figure 4, where two groups of turbo systems with different turbo efficiency indicated on the figure. When turbo efficiency is improved from 48% to 53%, the corresponding BTE gains over 1% (absolute) with higher AFR. On the other hand, if AFR increase is not coming directly from turbo efficiency, but from high engine exhaust back pressure, the high AFR does not gurantee the net BTE gain due to the increase in engine pumping loss.

Task 3: The conducted investigation details the performance behavior of E85-diesel dual-fuel combustion in conjunction with the higher CR behavior and VVA-enabled alternate valve strategies. Figure 5 compares the peak efficiency achieved with E85-diesel dual-fuel combustion across a range of engine loads at 1,200 rpm for two series of tests: (1) 14:1 CR with non-VVA cylinder head and conventional valve timing, and (2) 17:1 CR with VVA-enabled varied intake valve closing timings (values are noted in the figure). At lower load conditions, there is an efficiency advantage to using the higher geometric CR with conventional intake valve closing timing. At 9.6 bar brake mean effective pressure (BMEP), the higher CR configuration yielded a +1.4 percentage point increase in peak BTE (from 41.7% to 43.1%). CR with VVA

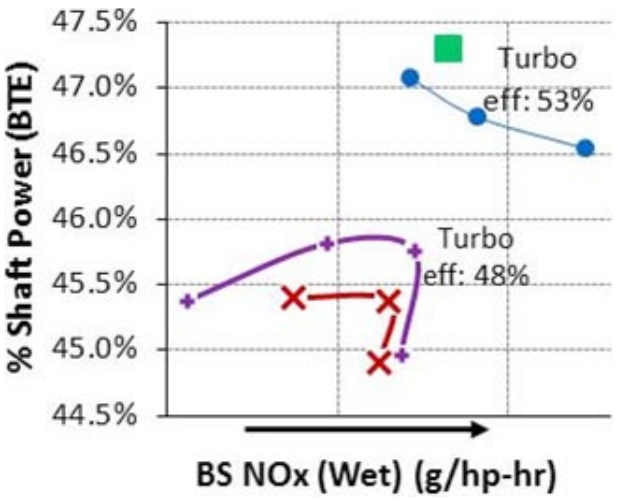

FIGURE 4. Air system effect on BTE. With same combustion system, the BTE gains over 1% (absolute) with an increase of 5% (absolute) turbo efficiency.

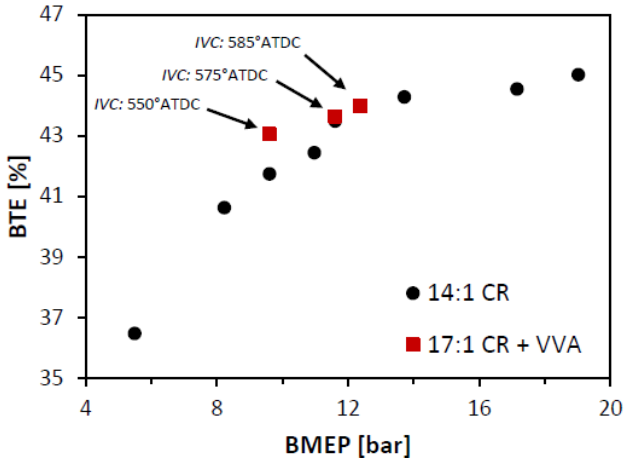

IVC - intake valve closing; ATDC - after top-dead center

FIGURE 5. BTE as a function of load for optimized E85-diesel dual fuel combustion with CR of 14:1 and 17:1+VVA.

case (16.4:1) is higher than the 14:1 geometric CR case (13.6:1). Accordingly, the overall charge reactivity will be higher due to higher pressure and temperature conditions at the end of compression. This enables the use of a greater premixed E85 fraction (82% for the 17:1 + VVA case versus 59% for the 14:1 case) without yielding a long combustion duration which compromises thermal efficiency.

Figure 6 shows peak BTE achieved across a range of engine loads at 1,200 rpm for the CNG-diesel dual-fuel combustion. Three different data series are shown, representing different specified NOx levels. With the proper NOx level, peak efficiency is delivered at 16.5 bar BMEP, yielding a 45.9% BTE at 2.0 g/kW-hr

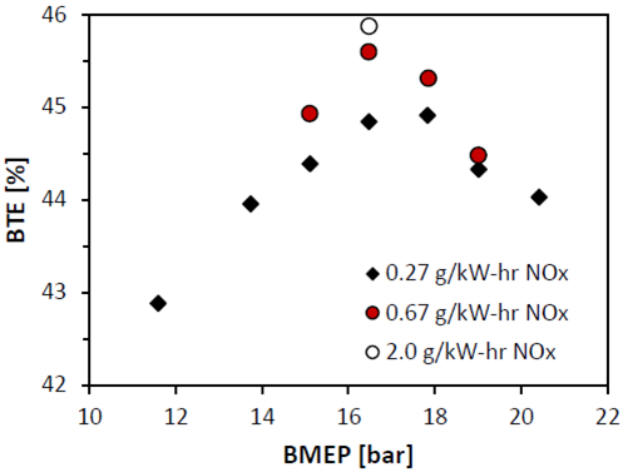

FIGURE 6. BTE as a function of load for optimized CNG-diesel dual-fuel combustion with different NOx levels.

(2.68 g/hp-hr) NOx emissions level. The general increase in efficiency with load up to 16-17 bars of BMEP is expected due to the reduced contribution of parasitic losses as load increases. The decrease in BTE at loads above 16-17 bar (dependent on targeted NOx emissions levels) is due to the later combustion phasing required to avoid exceeding the engine PCP limit, when the PCP is further relaxed, the BTE gain will be expected as shown in Task 1.

CONCLUSIONS

Engine efficiency was optimized by advanced combustion strategies including new combustion chambers, start of injection, injection pressure, and relaxed PCP to shorten the combustion duration; the combined efforts leads to an optimized combustion phasing for about 1.5% (absolute) BTE gain. The higher turbo efficiency providing better AFR accounts for further BTE gain, with increasing 5% (absolute) of turbocharger efficiency, an improvement of 1% (absolute) BTE gain was attained. The fuel's low-reactivity in dual-fuel combustion allows higher effective CR with a corresponding increase in the premixed fuel fraction, enabling higher efficiencies, potentially increasing BTE.

FY 2014 PUBLICATIONS/PRESENTATIONS

1. Ickes, A., Wallner, T., Zhang, Y., and De Ojeda, W., "Impact of Cetane Number on Combustion of a Gasoline-Diesel Dual-Fuel Heavy-Duty Multi-Cylinder Engine," *SAE Int. J. Engines* 7(2):860-872, 2014, doi:10.4271/2014-01-1309.

IV.5 Gasoline Ultra Fuel Efficient Vehicle with Advanced Low-Temperature Combustion

Keith Confer (Primary Contact), Dr. Peter Olin, Mark Sellnau

Delphi
3000 University Drive
Auburn Hills, MI 48326

DOE Technology Development Manager

Ken Howden

NETL Project Manager

Ralph Nine

Subcontractors

- John Juriga, HATCI, Superior Township, MI
- Dr. Rolf Reitz, WERC LLC, Madison, WI
- Dr. Ming-Chia Lai, Wayne State University, Detroit, MI

Overall Objectives

- Develop, implement, and demonstrate fuel consumption reduction technologies using a new low-temperature combustion process: gasoline direct-injection compression ignition (GDCI).
- Refine and demonstrate several near-term fuel consumption reduction technologies including advanced valvetrain and parasitic loss reduction.
- Design and build engine hardware required.
- Develop engine control strategies.
- Demonstrate benefits of new hardware and refined engine operation.

Fiscal Year (FY) 2014 Objectives

- Map and refine GDCI operation using multi-cylinder dynamometer engines.
- Debug Phase 2 development vehicle with GDCI multi-cylinder engine.
- Continue development of GDCI controls.
- Refine and test Phase 2 development vehicle with GDCI multi-cylinder engine.

FY 2014 Accomplishments

- Engine calibration mapping tests were performed over a broad speed and load range on performance dynamometers in support of vehicle controls development.
- GDCI engine on the start cart was used for algorithm and control system development.
- GDCI vehicle, which was completed at the end of FY 2013, underwent a full debug of controllers and wiring.
- Control algorithms for the GDCI combustion system and control hardware were integrated into the demonstration vehicle including cooled exhaust gas recirculation (EGR) control, cold-start improvements, fuel timing control and transient control algorithms.
- GDCI vehicle achieved milestone events of the first firing in November 2013 and first chassis dyno operation in December 2013. Other vehicle milestones included running steady-state break-in test points in January 2014, completion of constant speed fuel economy and emissions tests in March 2014 and ability to be driven from a stop up to highway speed without aid from an external operator in May 2014.
- Completed GDCI vehicle warm Federal Test Procedure (FTP) testing revealing a 39% improvement in fuel economy over the baseline port fuel-injected (PFI) vehicle. Tailpipe emissions, however, did not meet the targeted Tier 2 Bin 2 standard.

Future Directions

Future GDCI development work should concentrate on combustion control during vehicle transient operation and on improved exhaust aftertreatment targeted for the lower temperatures resulting from this low temperature combustion scheme.

✧ ✧ ✧ ✧ ✧

INTRODUCTION

This project focused on development, implementation and demonstration of fuel consumption reduction technologies which are focused on the improvement of thermal efficiency from in-cylinder combustion complemented by a reduction of friction and parasitic losses.

The investigation includes extensive simulation efforts combined with bench, engine and vehicle testing in a comprehensive four-year project conducted in two phases. The conclusion of each phase is marked by an on-vehicle technology demonstration.

The single largest gain in fuel economy is from development and demonstration of a breakthrough low-temperature combustion scheme called GDCI as developed in Phase 2 of the project. Initial steady-state dynamometer testing of this new combustion scheme showed that thermal efficiencies can be greater for GDCI combustion than for diesel combustion. During the project, substantial development work was done in the areas of combustion control, base engine design, fuel system design and valve train design to fully validate and reduce to practice a combustion scheme implementing GDCI in a gasoline engine which could be suitable for mass production. Phase 2 development work spanned the full four years of this project and was completed in September 2014.

Phase 1 concentrated on nearer-term technologies to reduce friction and parasitic losses. The on-vehicle implementation of these technologies was performed using a systems engineering approach to optimize the collective value of the technologies. The duration of Phase I was two years and was completed in June of 2012.

APPROACH

Phase 1 technologies were divided into two demonstration vehicles. These two vehicles were equipped with different Phase 1 technologies and hardware. Broadly, Vehicle 1 focused on technologies to reduce engine friction and accessory loads. Vehicle 2 focused on pumping losses and engine idling reduction. Both demonstration vehicles met the same tailpipe emissions standards as the original production vehicle from which they were derived.

For Phase 2, a wide range of analytical and experimental tools were assembled and used by small expert teams. Detailed FIRE and KIVA simulations were used in combination with spray chamber tests of physical injectors. Single-cylinder engine tests using the Design of Experiments method were combined with response surface modeling and custom combustion analysis macros to quickly process large amounts of test data. GT-POWER was used to evaluate and develop an efficient boosting system via simulation. While the multi-cylinder engine design work addressed all aspects of the engine, extra design effort was placed on valvetrain, fuel injection, thermal management and boost systems as they are key enablers for the new combustion process. Multi-cylinder GDCI engines were built for the performance dynamometer, engine start-cart, and development vehicle. A test vehicle was built specifically for GDCI operation including GDCI engine, transmission with down-speeded gearing, full GDCI thermal management system, and development controllers for engine control and watchdog functions (see Figure 1).

RESULTS

Phase 1

Phase 1 of this project was successfully completed in FY 2012. Two demonstration vehicles were constructed, refined and tested during that phase. One vehicle realized a combined unadjusted fuel economy improvement of 13.1% compared to the PFI baseline vehicle. The second vehicle achieved a combined unadjusted fuel economy improvement of 13.4% compared to the PFI baseline vehicle. Minimal overlap between technologies implemented on the two vehicles suggested that the combination of compatible technologies from the two vehicles would likely offer further improvement on a single vehicle.

Phase 2

Multi-Cylinder Engine Mapping of GDCI

Multi-cylinder engine steady-state mapping was completed over a broad speed-load range. Indicated specific fuel consumption was in the 170 to 200 g/kWh range over a broad region and increased some at low speed and low load. The brake specific fuel consumption (BSFC) was in the range of diesel engines with the minimum BSFC of 213 g/kWh occurring at 1,800 RPM and 12 bar. Oxides of nitrogen (NOx) levels were low and showed a decreasing trend with increasing load which shows good potential for engine down-speeding strategies. During steady-state testing, hydrocarbon and CO emissions were in the range of spark-ignition engines. Hydrocarbon makeup did however contain a much higher

FIGURE 1. GDCI demonstration vehicle at the Delphi Technical Center in Auburn Hills Michigan

percentage of aldehydes and ketones compared to a standard spark-ignition engine.

Engine Controls

Controls work comprised algorithm development for closed loop fuel control, boost pressure control, combustion phasing control, transient EGR control and coolant system control. Continuing improvements to controls capability throughout the year led to several accomplishments for the GDCI development vehicle including first fire and idle, first road load motion, first catalyst light off and first transient drive cycle.

Phase 2 Demonstration Vehicle

The GDCI demonstration vehicle achieved many milestone events from the first firing in November 2013 through completed warm FTP testing in September 2014.

A summary of the results including the percentage improvement in Corporate Average Fuel Econony combined fuel economy is given in Table 1. The GDCI vehicle achieved 39.3% improvement in combined fuel economy relative to the baseline vehicle. This far exceeds the DOE ATP-1 target of 25% improvement and also exceeds the project target of 35% improvement. Performance improvements on the individual drive cycles were 42% City (warm) and 33% Highway and are given in Figure 2.

While fuel economy targets for the project were exceeded, the emissions performance target (Tier 2, Bin 2) was not met. Emissions performance of the GDCI vehicle on the warm City and Highway cycles are listed in Figure 3 which plots these emissions results against the Tier 2 Bin 2 standard and Tier 2 Bin 5 standard as a ratio to the standard. A ratio of 1 or lower thus indicates meeting that standard. All data provided are for tailpipe bag emissions. Clearly, there remains a great deal of work to do to reduce the emissions of the GDCI vehicle to acceptable levels. Engine loads and fuel consumption are higher during the accelerations which lead to higher

TABLE 1. Vehicle Fuel Economy Results in Miles Per Gallon

Cycle	Run 1	Run 2	Run 3	Avg.
City - EPAIII (Warm, unadjusted E10 fuel)	38.19	38.47	38.44	**38.37**
Hwy (unadjusted E10 fuel)	57.04	57.86	59.54	**58.15**
CAFE method Combined FE (Warm, adjusted)	46.21	46.66	47.11	**46.66**
Percent Improvement over Baseline				
Combined FE comparison (Warm, adjusted)	38.0	39.3	40.7	**39.3**

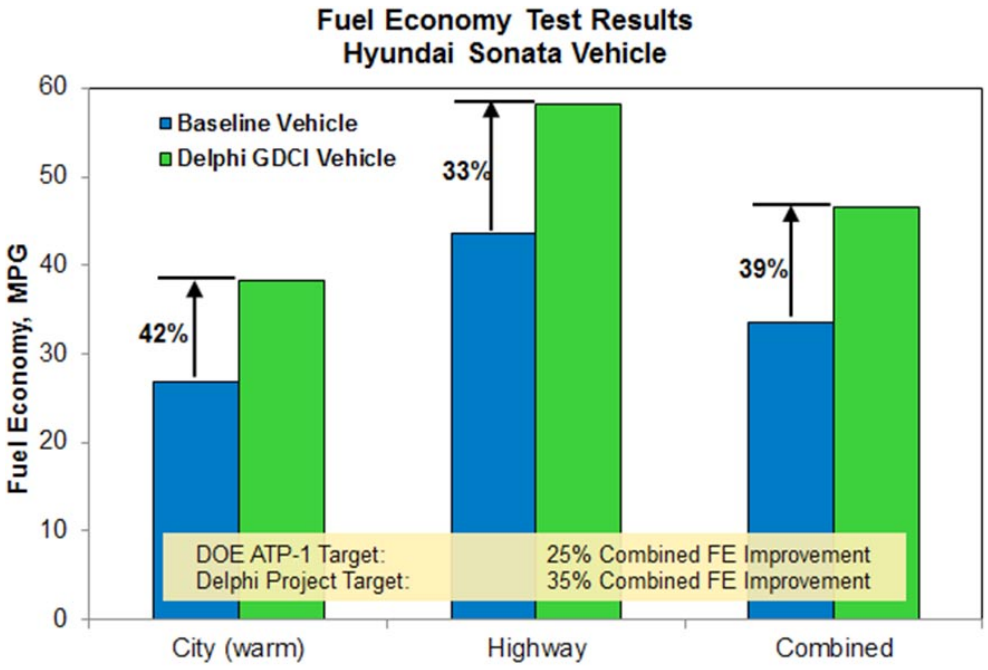

FIGURE 2. GDCI Vehicle Fuel Economy Results Compared to the 2009 PFI Baseline Vehicle

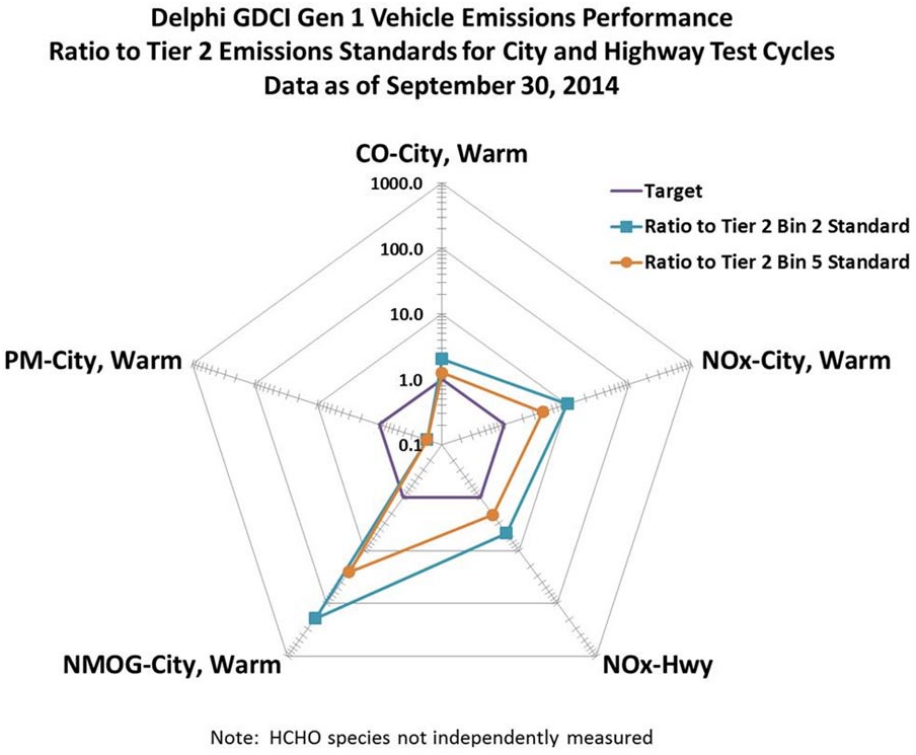

FIGURE 3. GDCI Vehicle Emissions Results

emissions rates. The highly transient nature of these sections of the drive cycle increases the control challenge and thus the likelihood of sub-optimal engine operation. In addition, low-temperature combustion produces correspondingly low exhaust temperatures which cause lower than desired catalyst efficiencies. The vehicle as tested contained an oxidation catalyst aftertreatment system without NOx aftertreatment. Figure 4 shows the potential effects of improved aftertreatment. Plotted in the figure are simulated results over the Urban Dynamometer Driving Schedule predicting warmed-up performance of a low-temperature oxidation catalyst and a selective catalytic reduction system at measured exhaust temperatures. Future work should therefore concentrate on improved transient control and improved exhaust aftertreatment targeted for the lower temperatures resulting from low-temperature combustion.

CONCLUSIONS

Phase 2

- Efficient GDCI combustion can be controlled over a wide speed/load range including idle. Mixed-mode combustion therefore is not required.
- During multi-cylinder steady-state mapping, the GDCI engine NOx, smoke, and coefficient of variation indicated mean effective pressure targets were fully met. BSFC at all conditions was very good with minimum BSFC of 213 g/kWh observed at 1,800 rpm-12 bar brake mean effective pressure and indicated specific fuel consumption was below 180 g/kWh over a wide operating range.
- Vehicle level testing of the GDCI engine, accomplished for the first time during this past FY, was very promising. Combined fuel economy, for a warm FTP cycle, was improved by over 39% when compared to the baseline 2009 PFI vehicle. This performance surpassed both the ATP-1 target of 25% and the project target of 35%.
- Vehicle level emissions did not meet the target objectives but steady-state dyno testing showed promise for treatment with tailpipe emissions similar to spark-ignition engines. Transient operation and aftertreatment were determined to be the areas that could yield the highest gains in emissions improvements.

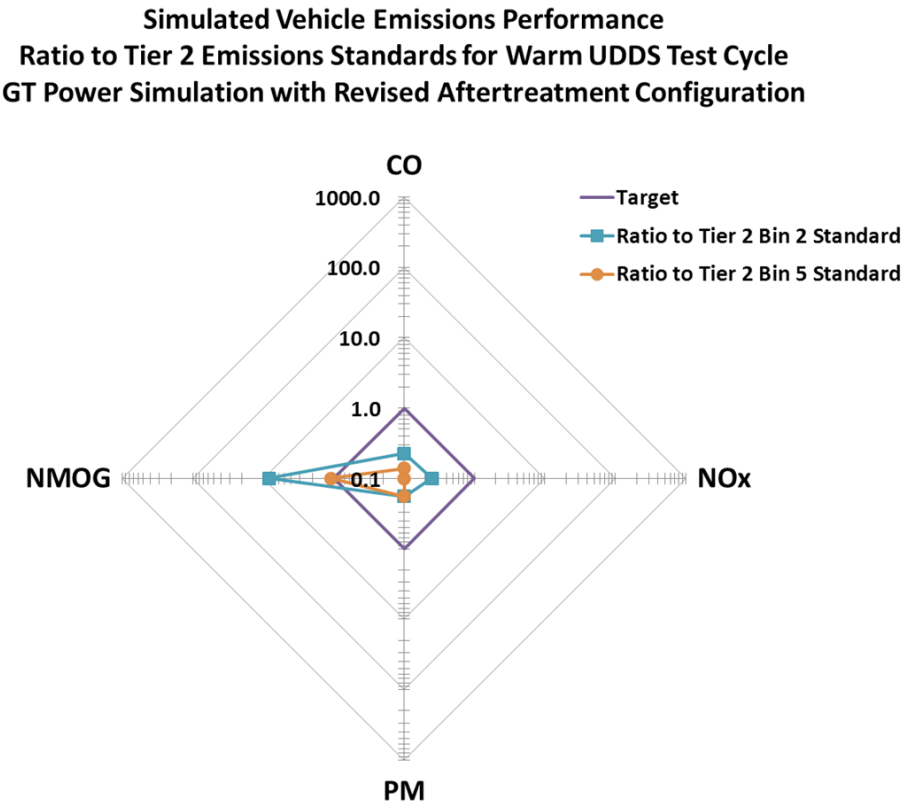

FIGURE 4. Vehicle Emissions with Simulated Low-Temperature Aftertreatment

2014 PUBLICATIONS/PRESENTATIONS

1. "*Protecting Development Engines during Controls Development and Calibration*", J. Kraenzlein et al., SAE 2014-01-1172 SAE World Congress, April 2014.

2. *"Development of Gasoline Direct-Injection Compression Ignition (GDCI) Engine", Sellnau et al.,* SAE 2014-01-1300, SAE World Congress, April 2014.

IV.6 Advanced Gasoline Turbocharged Direct Injection Engine Development

Terry Wagner
Ford Motor Company
2101 Village Road
Dearborn, MI 48121

DOE Technology Development Manager
Ken Howden

NETL Project Manager
Ralph Nine

Subcontractor
Michigan Technological University (MTU), Houghton, MI

Overall Objectives

Ford Motor Company Objectives:

- Demonstrate 25% fuel economy improvement in a mid-sized sedan using a downsized, advanced gasoline turbocharged direct injection (GTDI) engine with no or limited degradation in vehicle level metrics.
- Demonstrate vehicle is capable of meeting Tier 3 Super Ultra-Low Emissions Vehicle (SULEV) 30 emissions on the Federal Test Procedure (FTP)-75 cycle.

MTU Objectives:

- Support Ford Motor Company in the research and development of advanced ignition concepts and systems to expand the dilute/lean engine operating limits.

Fiscal Year (FY) 2014 Objectives

- Vehicle build, instrumented, and development work started (deferred from 12/31/2013 to 02/14/2014)
- Vehicle demonstrates greater than 25% weighted City/Highway fuel economy improvement and Tier 3 SULEV30 emissions on the FTP-75 test cycle (deferred from 12/31/2014 to 09/30/2015)

FY 2014 Accomplishments

Engine Design/Procure/Build:

- Completed build of a total of 12 engines for project support. Engine #1 for combustion system/mechanical verification; Engine #2 for transient emissions verification testing; Engine #3 for steady-state mapping; Engine #4 for mechanical friction/noise, vibration, and harshness (NVH) studies; Engine #5 for performance development testing; Engine #6 for thermal management studies; Engine #7 for mechanical development studies; Engine #8 for spare; and Engines #9–12 for vehicle build.
- Rebuilt various engines following completion of their intended usage in anticipation of further project support.

Engine Development on Dynamometer

- Completed Engine #2 transient emissions verification testing, including steady-state cold fluids development and transient cold start development. Testing to date indicates combustion system satisfies target metrics.
- Continued Engine #3 steady-state mapping (replaced in process by Engine #7), effectively utilizing AutoTest control for autonomous engine mapping. Principal tasks include: i) electric twin independent variable cam timing optimization, ii) direct-injection (DI) fuel injection timing optimization, iii) DI fuel rail pressure optimization, iv) naturally-aspirated air charge – throttle sweeps, v) boosted air charge – scroll/wastegate control sweeps, vi) full-load performance – borderline detonation/maximum brake torque spark sweeps, vii) preliminary “auto” calibration. Continued mapping validation testing and additional detailed mapping factorials as required to ensure accuracy.
- Completed Engine #4 instrumentation and dynamometer prep for subsequent mechanical development studies.
- Completed Engine #6 instrumentation, dynamometer prep, dynamometer install, and engine commissioning. Completed thermal management studies, including detailed metal temperature and heat rejection surveys.
- Completed Engine #8 instrumentation, dynamometer prep, dynamometer install, and engine commissioning (exchanged assignment with Engine #5). Substantially progressed performance development studies including speeds sweeps, load sweeps, charge air temperature sensitivity surveys, and fuel research octane sensitivity surveys.

- Completed Engine #3 (rebuilt) instrumentation, dynamometer prep, dynamometer install, and engine commissioning. Substantially progressed vehicle calibration support testing, including verification of multiple software releases and feature functionality.
- Continued dynamometer facility and engine instrumentation planning in support of 2014–2015 development plans.

Vehicle Build

- Completed powertrain/vehicle integration tasks for Vehicles #1–4, including removal of existing powertrain, prep for new powertrain, prep for new advanced integrated and supporting powertrain systems, and installation of new powertrain.
- Completed Vehicles #1–4 powertrain/vehicle mechanical verification and prep for commissioning and first drives.

Vehicle Calibration

- Completed Vehicles #1–4 powertrain/vehicle control verification on hoist; all systems functional and responsive per design intent.
- Completed Vehicles #1–4 commissioning and first drives.
- Initiated and progressed vehicle calibration tasks on Vehicles #1–4, including basic startability (crank, run-up, cold/warm idle stability) and basic driveability (tip-in/tip-out stability, accel/decel stability, transmission scheduling).
- Initiated and progressed vehicle calibration tasks on Vehicles #1–4 supporting project fuel economy and emissions objectives.
- Continued vehicle controls and calibration releases supporting Vehicles #1–4 calibration tasks.

Future Direction

Vehicle will demonstrate greater than 25% weighted city/highway fuel economy improvement and Tier 3 SULEV30 emissions on FTP-75 test cycle.

INTRODUCTION

Ford Motor Company has invested significantly in GTDI engine technology as a cost-effective, high-volume, fuel economy solution, marketed globally as EcoBoost technology. This project is directed toward advancing the EcoBoost technology, as well as related additional technologies, in order to achieve the project objectives:

- Demonstrate 25% fuel economy improvement in a mid-sized sedan using a downsized, advanced GTDI engine with no or limited degradation in vehicle level metrics.
- Demonstrate vehicle is capable of meeting Tier 3 SULEV30 emissions on the FTP-75 cycle.

APPROACH

Engineer a comprehensive suite of gasoline engine systems technologies to achieve the project objectives, utilizing:

- Aggressive engine downsizing in a mid-sized sedan from a large V-6 to a small I-4
- Mid- and long-term EcoBoost advanced technologies such as:
  - Dilute combustion with cooled exhaust gas recycling and advanced ignition
  - Lean combustion with direct fuel injection and advanced ignition
  - Boosting systems with active and compounding components
  - Cooling and aftertreatment systems
- Advanced friction reduction technologies, engine control strategies, and NVH countermeasures
- Progressively demonstrate the project objectives via concept analysis/modeling, single-cylinder engine, multi-cylinder engine, and vehicle-level demonstration on chassis rolls

RESULTS

The team progressed the project through the engine design/procure/build, engine development on dynamometer, vehicle build, and vehicle calibration tasks with material accomplishments. The team completed build of a total of 12 engines (detailed previously) for project support, and rebuilt various engines following completion of their intended usage in anticipation of further project support. Figure 1 shows a representative completed engine build.

The team progressed Engines #2–8 to a high level of dynamometer development productivity, completed transient emissions verification testing, including steady-state cold fluids development and transient cold-start development, and completed thermal management studies, including detailed metal temperature and heat rejection surveys. Additionally, the team continued steady-state mapping and mapping validation testing, and substantially progressed performance development studies and vehicle calibration support testing. Testing

FIGURE 1. Multi-Cylinder Engine Build

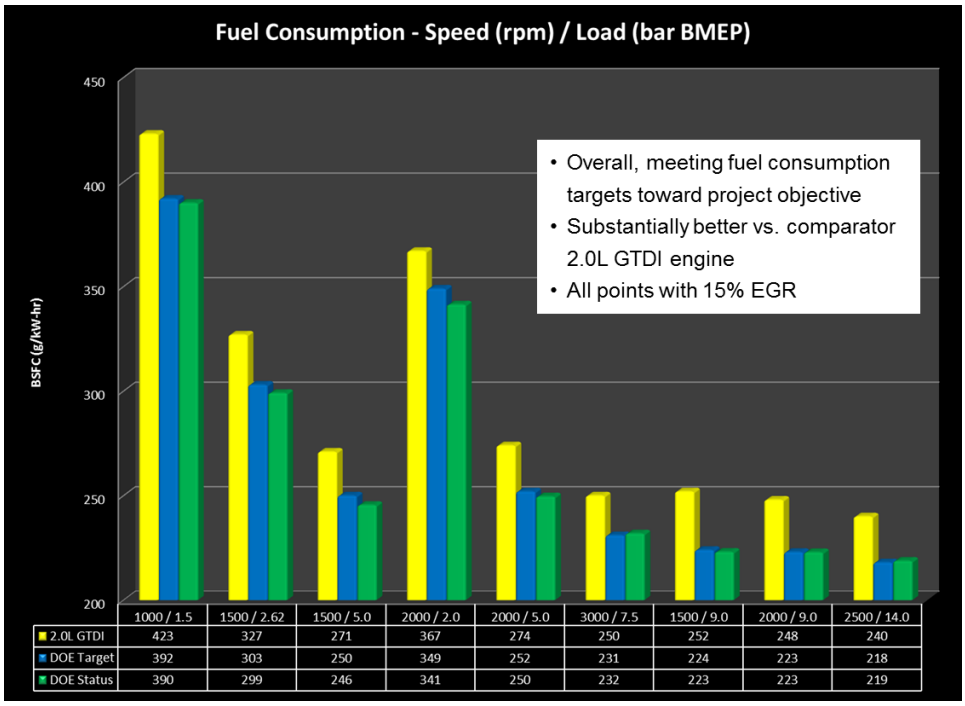

	1000 / 1.5	1500 / 2.62	1500 / 5.0	2000 / 2.0	2000 / 5.0	3000 / 7.5	1500 / 9.0	2000 / 9.0	2500 / 14.0
2.0L GTDI	423	327	271	367	274	250	252	248	240
DOE Target	392	303	250	349	252	231	224	223	218
DOE Status	390	299	246	341	250	232	223	223	219

FIGURE 2. Engine Fuel Consumption

to date indicates that the engine system satisfies the target metrics, which are critical to satisfy the project objectives. For example, Figure 2 shows mapped engine fuel consumption at critical speed/load points, all with 15% exhaust gas recirculation; as shown, the engine overall meets the fuel consumption targets toward the project objective, and is substantially better than a comparator 2.0-L GTDI engine. Notably, the engine

meets the CO and particulate matter emissions at the same critical speed/load points, all with 15% exhaust gas recirculation, indicating good air/fuel mixing.

Figure 3 shows engine full-load torque across the engine speed range; as shown, the engine meets the full-load performance targets at all engine speeds. Meeting the full-load performance targets of 20 bar brake mean effective pressure at 2,000–4,500 rpm and 80 kW/L at 6,000 rpm at 11.5:1 compression ratio was challenging and required detailed parameter optimization to balance compressor outlet temperatures, peak cylinder pressures, exhaust gas temperatures, overlap oxygen blowthrough, and other critical constraints. Notably, the engine operates with stoichiometric air/fuel to 3,500 rpm, which forecasts good on-road fuel consumption; also, the engine operates with typical GTDI combustion phasing (50% mass fraction burned between 25-30 deg after top-dead center) across the speed range, which indicates a good attribute balance.

Table 1 shows the results of the transient emissions verification testing, including steady-state cold fluids development and transient cold-start development; as shown, the engine meets the transient emissions targets toward the project objective. For reference, the 20°C cold-start feedgas targets are derived from the tailpipe standards, and are evaluated at a coordinated Strategy for Emissions Reduction heat flux that achieves ~350°C catalyst mid-bed to 20 seconds after engine start. The team had received concurrence in 2013 on transitioning from Tier 2 Bin 2 to Tier 3 SULEV30 emissions, and both are shown for reference.

TABLE 1. Engine CO Emissions

Tailpipe Standards	Tier 2 Bin 2	Tier 3 SULEV30
NMOG	10 mg / mi	--
NOx	20 mg / mi	--
NMOG + NOx	--	30 mg / mi
PM	10 mg / mi	3 mg / mi

Cold Start Attribute	Units	Target[1]	Status
0-20s Cumulative FGHC + FGNOx	mg	< 227	224
0-20s Cumulative Particulate Mass (PM)	mg	< 3.0	1.3
5-15s CSER stability (RMS_SDIMEP)	bar	< 0.350	0.375

Evaluated at a CSER heat flux that achieves ~350°C catalyst mid-bed @ 20 seconds after engine start

NMOG - non-methane organic gases; FGHC - feed gas hydrocarbon; FGNOx - feed gas oxides of nitrogen; CSER - Coordinated Strategy for Emissions Reduction

The team continued development of the advanced lean combustion system "micro" stratified charge capability. Figure 4 shows a pictorial of "micro" stratified charge, as well as a complement of engine data at 1,500 rpm/5 bar brake mean effective pressure. Advantages of "micro" stratified charge include good fuel economy, low oxides of nitrogen (NOx) emissions, low particulate matter emissions, practical controls, acceptable NVH, and good stability. Most importantly, "micro" stratified charge extends the lean combustion

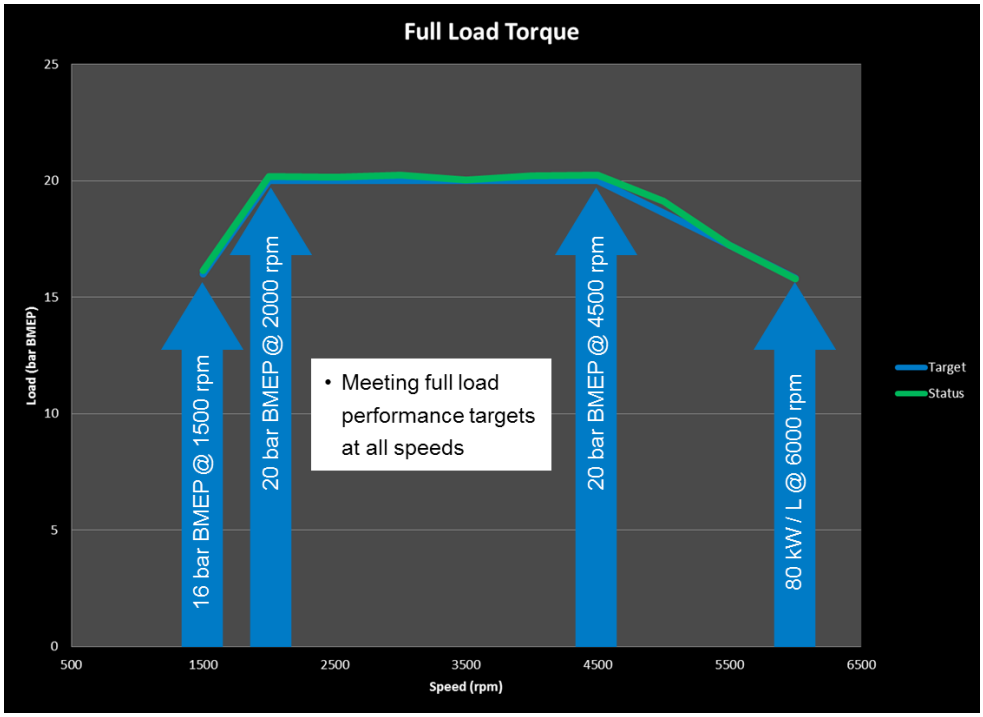

FIGURE 3. Engine Stability

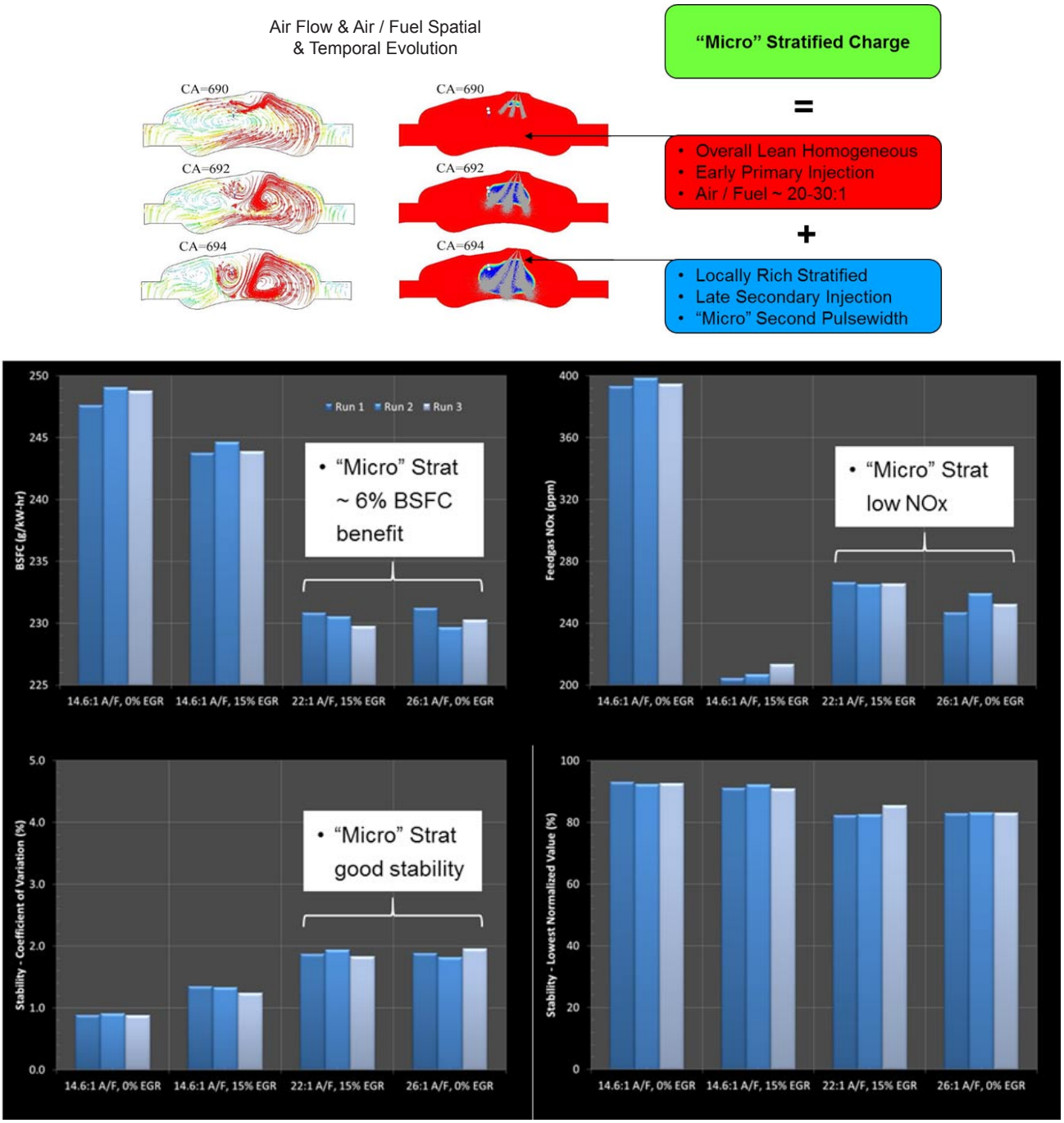

FIGURE 4. Computer-Aided Design Powertrain as Installed in Vehicle

capability to a region of good aftertreatment efficiency, potentially enabling a lean-NOx trap (LNT)/selective catalytic reduction (SCR) or passive SCR system. Given the desulfurization challenges of a three-way catalyst + LNT/SCR system, and the uncertainty of a three-way catalyst + passive SCR system, the team received concurrence in 2012 on lean aftertreatment transitioning to stoichiometric at the vehicle level. Despite persistent lean aftertreatment challenges, the team continued development of the advanced lean combustion system at the engine level.

The team completed the powertrain/vehicle integration tasks for Vehicles #1–4, including removal of the existing powertrain, prep for the new powertrain, prep for the new advanced integrated and supporting powertrain systems, and installation of the new powertrain. Additionally, the team completed mechanical verification, control verification, commissioning and

first drives for Vehicles #1–4. Figure 5 shows the actual powertrain as installed in Vehicle #1. Following first drives, the team initiated and progressed vehicle calibration tasks on Vehicles #1–4, including basic startability and basic driveability supporting project fuel economy and emissions objectives. The team is proud to have met all engine level part-load fuel consumption, full-load performance, and transient emissions targets, and to have four fully commissioned and driving vehicles entering the final phase of the project.

FIGURE 5. Actual Powertrain as Installed in Vehicle

CONCLUSIONS

- The project will demonstrate a 25% fuel economy improvement in a mid-sized sedan using a downsized, advanced GTDI engine with no or limited degradation in vehicle level metrics, while meeting Tier 3 SULEV30 emissions on the FTP-75 cycle.
- Ford Motor Company has engineered a comprehensive suite of gasoline engine systems technologies to achieve the project objectives and progressed the project through the concept analysis, design, development, and evaluation tasks with material accomplishments.

FY 2014 PUBLICATIONS/PRESENTATIONS

1. Completed presentation at 2014 U.S. Department of Energy (DOE) Hydrogen and Fuel Cells Program and Vehicle Technologies Program Annual Merit Review and Peer Evaluation Meeting (AMR), held June 16–20, 2014, Wardman Park Marriott, Arlington, Virginia.

IV.7 Cummins Next Generation Tier 2 Bin 2 Diesel

Michael J. Ruth
Cummins Inc.
PO Box 3005
Columbus, IN 47201-3005

DOE Technology Development Manager
Roland Gravel

NETL Project Manager
Carl Maronde

Subcontractor
Johnson Matthey Inc., Wayne, PA

Overall Objectives

- Demonstrate 40% fuel economy improvement over baseline gasoline V-8 pickup truck
- Demonstrate Tier 2 Bin 2 tailpipe emissions compliance

Fiscal Year (FY) 2014 Objectives

- Demonstration of Tier 2 Bin 5 tail pipe emissions on ATLAS vehicle and engine
- Demonstration of Tier 2 Bin 2 engine-out emissions in a test cell using an ATLAS engine
- Demonstration of Tier 2 Bin 2 tailpipe emissions in a test cell using ATLAS engine and vehicle

FY 2014 Accomplishments

- Completed demonstration of Tier 2 Bin 5 demonstration with ATLAS engine and vehicle
- Completed demonstration of Tier 2 Bin 2 engine-out emissions demonstration in a test cell using an ATLAS engine.

Future Directions

Development and optimization of the ATLAS engine Tier 2 Bin 2 ATLAS engine-out emission demonstration in a test cell and vehicle environment.

INTRODUCTION

The overall objective of this project, Cummins Next Generation Tier 2 Bin 2 Diesel, is to design, develop, and demonstrate a state-of-the-art light-duty (1/2 ton pickup truck) diesel engine that meets U.S. Environmental Protection Agency Light-Duty Tier 2 Bin 2 Emission Standards and increases fuel efficiency by at least 40% compared with a state-of-the-art port-fuel-injected gasoline engine.

The U.S. new, personal use vehicle fleet has changed slightly over the past few years, with car purchases increasing, making the fleet split slightly more favorable for cars over that of trucks and full-sized sport utility vehicles (SUVs). By and large, pickup trucks and SUVs still account for nearly half of sales in this segment. An improvement in fuel economy by 40% in the light truck and SUV segment would reduce the U.S. oil consumption by 1.5M bbl/day and reduce greenhouse gas emissions by 0.5 MMT/day.

The final targets for this project would be to demonstrate oxides of nitrogen (NOx) emissions of 0.02 g/mi or less with 0.01 g/mi hydrocarbons (HCs) or less while achieving a fuel economy of at least 22.4 miles per gallon (mpg) over the Federal Test Procedure-75 test procedure and at least 34.3 mpg on the highway fuel economy test. The fuel economy targets are based on 40% improvement over the baseline gasoline powertrain.

APPROACH

The project has four phases. The first phase included the baseline establishment for the target vehicle (2010 Nissan Titan) as well as the fuel consumption and emission rate of the Cummins 2.8-L ISF Euro III engine. Model development in phase one directed technology testing and development to create a technical profile for a new engine design. The second phase of work determined viable technologies to carry forward. Phase three entailed the development work required to bring the new engine to achieve Tier 2 Bin 5 emissions with the majority of all systems working properly. The fourth and final phase is to develop the emission control system and the newly designed and integrated engine to meet the final Tier 2 Bin 2 tailpipe emissions level while maintaining a 40% fuel economy improvement over the baseline gasoline power train.

The fourth phase is intended to demonstrate the ultimate goal of Tier 2 Bin 2 emissions with at least 40% fuel economy improvement over the baseline gasoline powertrain. Work is focused on ensuring the engine-out emissions are achieved utilizing the most fuel efficient means and the aftertreatment utilizing the latest formulation for cold-start emission storage and reduction. The efficient engine system development includes

low-pressure exhaust gas recirculation, high-efficiency turbocharging and close-coupled aftertreatment. The aftertreatment development focus includes not only formulation, but also ensuring the most effective substrate materials are utilized to yield the most effective aftertreatment possible. The fourth phase of this project is expected to conclude in the first quarter of calendar year 2015.

RESULTS

The vehicle development team has demonstrated Tier 2 Bin 5 emission levels on the ATLAS equipped vehicle. The vehicle delivered very good NOx and HC emissions even without the addition of the diesel Cold Start Concept (CSC®) and two-loop exhaust gas recirculation (EGR) systems. The emission results were very near Tier 2 Bin 2 levels, yielding significant margin to the Tier 2 Bin 5 levels (full Federal Test Procedure-75 NOx = 0.03 g/mi, HC = 0.02 g/mi). The fuel economy remains above target, at greater than 25 mpg, leaving the team the option to trade fuel economy for tailpipe emissions if the prime path is unable to deliver. The engine-out and tailpipe data for the Tier 2 Bin 5 run show the effectiveness of the selective catalytic reduction (SCR) system is very near that of the target, albeit without the use of the cold-start storage catalyst. As would be expected the most significant emissions are realized in the cold phase, bag one. In this demonstration test the tailpipe NOx in bag one was 0.12 g/mi, where bags two and three were much less than 0.02 g/mi.

Engine-out emissions are not regulated, however, the values are important to understand how well the aftertreatment system is performing in each phase of the test. For the demonstration test, the NOx effectiveness of the aftertreatment system was greater than 90% for the test as a whole. Again the bag one effectiveness shown the lowest performance at just greater than 70% NOx effectiveness, while bags two and three were 99% and 95%, respectively. The data does suggest the system is capable of meeting the needs once the cold-start catalyst is employed, assuming it can meet the targets set for its own performance.

The development team has progressed toward the demonstration of the Tier 2 Bin 2 embodiment. The following points are highlights from the work completed:

- Progress made with air-handling controller development, including transient calibration
- Development of refined algorithms and improved calibration during cold bag portions of the transient cycle
- Demonstrated engine-out modal steady-state targets for Tier 2 Bin 2
- Functional low-pressure EGR and liquid charge air cooler on the ATLAS engine

The performance and controls team have been working to develop a control system capable of controlling the dual-loop EGR systems. The performance team has demonstrated a marked improvement on engine-out emissions. The controls team continues to refine the control system to react to the transient operation without sacrificing fuel consumption, HC or particulate matter (PM) emissions. The controls team has written code to move a large section of the controls from the development controller to electronic control module-based control.

Engineers continue to refine the steady-state calibration to reduce engine-out emissions. The opportunities for improvement are mainly due to the team gaining experience with the multitude of tuning options with the air handling and fuel system. The most recent work has been to maintain fuel economy and NOx while reducing HC and soot where possible. Data is being gathered to understand the implications of reducing NOx if that is a requirement to meet the Tier 2 Bin 2 tailpipe goals.

The dual-loop EGR and cooling system hardware set-ups have been successfully deployed and calibration efforts have been able to demonstrate the performance of the architecture by meeting the targeted engine-out NOx, PM and fuel economy over the steady-state modal operating conditions. The data from the Tier 2 Bin 2-trimmed ATLAS engine shows improved fuel economy by 16% versus that of the mule engine on the same composite test rollup while meeting the targeted level of NOx emissions at engine-out.

One challenge toward achieving the demonstration was the addition of the two-loop EGR and cooling systems. The addition of these systems has created a quite complex control system for a single controller. Previously the team used standalone or open-loop controllers to cover the steady-state operation for demonstration purposes. Now, the objective of running transient on a controller suitable to fit in a vehicle, has posed the challenge of system capacity.

The team has been working on “sociability” of the engine—meaning noise emissions. There has been little focus on the radiated noise until now. The team has only had a short time to focus attention on this important issue. The most recent calibration was able to maintain the target on engine-out NOx and HC while reducing noise by nearly 5 dBa while only increasing PM emissions by 0.02 g/mi, estimated from steady-state modal conditions, without any loss in fuel economy.

Johnson Matthey has continued working to improve the cold-start emission control. Johnson Matthey has

shown in their test work the effectiveness of the diesel Cold Start Concept (CSC®) and SCR on Filter (SCRF®) system can be improved by using a lower weight filter. The lower weight filter heats faster and reaches the "light-off" temperature in time to reduce a larger fraction of the NOx released from the CSC®. Additionally, the team is considering improvements can be made to the CSC® formulation to raise the release temperature allowing the SCR system to further warm and become more effective.

CONCLUSIONS

The Cummins next generation Tier 2 Bin 2 light-duty diesel engine project has completed its fourth year. The following successes have come from the most recent year of development:

- Vehicle level demonstration of Tier 2 Bin 5 with emissions margin and more than 40% improvement in fuel economy over the baseline gasoline powertrain with current technology aftertreatment system.
- Very capable aftertreatment system operating at Tier 2 Bin 2 target level effectiveness.
- Test cell environment demonstration of Tier 2 Bin 2 engine-out emissions.
- The control system has demonstrated capability to control dual-loop EGR system.
- Johnson Matthey has demonstrated a plan to improve the utilization of the diesel CSC®.

IV.8 Advanced Combustion Concepts – Enabling Systems and Solutions (ACCESS)

Hakan Yilmaz (Primary Contact), Oliver Miersch-Wiemers, Li Jiang, Jeff Sterniak
Robert Bosch LLC
38000 Hills Tech Drive
Farmington Hills, MI 48331

DOE Technology Development Manager
Ken Howden

NETL Project Manager
Ralph Nine

Subcontractors
- AVL Powertrain, Plymouth, MI
- Emitec, Auburn Hills, MI
- University of Michigan, Ann Arbor, MI
- Stanford University, Palo Alto, CA

Overall Objectives

- Improve fuel economy by 25% with minimum performance penalties
- Achieve super ultra-low emission vehicle (SULEV) level emissions with gasoline
- Demonstrate multi-mode combustion engine management system

Fiscal Year (FY) 2014 Objectives

- Complete powertrain hardware integration and engine management system development for two prototype vehicles
- Evaluate drive-cycle fuel economy and emissions performance of target technologies, apart from advanced combustion, on prototype vehicles
- Evaluate real-world driving performance of advanced combustion on prototype vehicles

FY 2014 Accomplishments

- Upgraded two 2009 Cadillac CTS vehicles with 3.6-L port-fuel-injection 6-cylinder engines to ACCESS prototype vehicles with 2.0-L turbocharged direct injection 4-cylinder multi-mode combustion capable engines
- Achieved the project target of greater than 25% fuel economy improvement in prototype vehicle on combined Federal Test Procedure-75 (FTP-75) and Highway Fuel Economy Test (HWFET) drive cycles over the baseline vehicles, and identified measures to attain SULEV emissions
- Demonstrated spark-ignition, spark-assisted compression ignition (SI-SACI) multi-mode combustion in the prototype vehicle during real-world driving conditions, relying on ACCESS-developed mode switch algorithms

Future Directions

- Evaluate drive-cycle fuel economy and emissions performance of multi-mode combustion on prototype vehicles
- Improve real-world driving performance on prototype vehicles for demonstration
- Analyze fuel efficiency and emission results from vehicle, identifying commercial potentials of the proposed technology solutions

✧ ✧ ✧ ✧ ✧

INTRODUCTION

Due to availability and security of energy resources, environmental concerns, and cost factors, the automotive industry is facing the challenge of improving fuel economy and reducing the emissions without sacrificing performance. Although there are promising developments in electrification of powertrain with hybrid systems, battery electric vehicles and fuel cell electric vehicles; internal combustion engines are expected to be the mainstream power source of future high-efficiency vehicles for the next decade. The feasible future advanced engine and powertrain configuration must address the topics such as emission and fuel economy requirements for worldwide applications, transition to bio fuels, and synergies with future powertrain trends.

The ACCESS project has the primary objective of developing highly capable and flexible advanced control concepts with enabling system, sub-system and component level solutions for the management of multi-mode combustion events in order to achieve 25% fuel economy improvement in a gasoline-fueled light-duty vehicle without compromising its performance while meeting future emission standards as outlined in DOE solicitation targets.

APPROACH

The ACCESS project, through a three-phase approach, addresses the development, testing, and demonstration of the proposed advanced technologies and the associated emission and fuel economy improvement at an engine dynamometer and on a full-scale vehicle. The project investigates the synergistic mainstream advanced combustion and system concepts such as:

- Spark-ignited combustion with high compression ratio assisted with cooled external exhaust gas recirculation
- Spark-assisted compression ignition assisted with external exhaust gas recirculation, spark, valve and fueling strategies
- Multi-hole direct injection with individual nozzle geometry design for improved mixture preparation and combustion efficiency
- Improved thermal management system for enhanced engine warm-up behaviors
- Start-stop system to eliminate fuel consumption at idling conditions

As a result, a substantial improvement in fuel efficiency by exploiting the advantages of multi-mode combustion on a turbocharged downsized engine with high compression ratio is proposed. The research engine platform, equipped with the flexible capabilities of external exhaust gas recirculation system, electric dual cam phasing, dual cam profile switching, enables the investigation and development of combustion strategies to expand advanced combustion operation range. In order to cope with the complexity in combustion as well as air management, cylinder pressure sensors and Bosch's prototype intake manifold oxygen sensor supported with Bosch's in-production engine control unit MED17 are introduced, which enables development of control strategies for multi-mode combustion.

RESULTS

Vehicle-Level Fuel Economy and Emissions Performance

In order to demonstrate the suite of technologies included in the ACCESS project and support the fine tuning of the driving characteristics of the multi-mode combustion control system, the two development vehicles pictured in Figure 1 are equipped with prototype ACCESS multi-mode combustion engines. Initial drive cycle testing with the prototype engine has confirmed the effectiveness of the intended approach. Compared to measurements taken with the initial three-vehicle fleet in baseline V-6 trim, Figure 2 shows that a combined 25.6% fuel economy benefit has been achieved on the first demonstration vehicle with the prototype ACCESS engine. Start-stop and a final drive ratio update to that of the direct-injected variant of the baseline Cadillac CTS, enabled by the low end torque characteristics of the boosted prototype engine, also contributed to the fuel economy improvement. Confirmatory testing with the second prototype vehicle, as well as activation of the advanced combustion mode during the test cycles, will enable valuation of the multi-mode combustion concept. Additional conventional emissions reduction technologies, enabled by the full-time stoichiometric operation of the multi-mode combustion concept, are

FIGURE 2. Up-to-Date ACCESS Prototype Vehicle Drive-Cycle Fuel Economy Results

		FTP-75	HWYFET		Combined Calc.
Baseline	Base V6 [MPG]	17.80	33.64		22.59
ACCESS Prototype	ACCESS P2b [MPG]	22.99	39.78		28.38
	FE Improv. [%]	29.13	18.25		25.63

FIGURE 1. ACCESS Prototype Vehicle

being employed to close the remaining cold start and catalyst control gaps to the SULEV target.

The challenges of further extension of the advanced combustion operating region beyond what has been demonstrated in-vehicle are actively being addressed by collaboration with the University of Michigan and Stanford University. In particular, boosted SACI has been demonstrated experimentally on a multi-cylinder engine, and potential for mitigation of ringing during high-load non-dilute homogenous charge compression ignition has been observed in simulation and free-piston engine experiments.

Engine Management System Development for Multi-Mode Combustion

The ACCESS-developed engine management system is developed based on Bosch's torque-driven modular software architecture, as illustrated in Figure 3, which impacts multiple subsystems including the torque and mode coordinator (TC), air system (AS), fuel system (FS) and ignition system (IS). In order to achieve smooth transition between spark-ignition and SACI combustion modes, key functions grouped into the supervisory controller, multi-mode combustion controller and exhaust gas recirculation system controller are developed and integrated into the engine control unit.

Figures 4 and 5 demonstrate SI-SACI combustion mode switch performance on the ACCESS multi-cylinder prototype engine at 2,000 RPM, 5-bar brake mean effective pressure (BMEP) and 3-bar BMEP conditions, respectively. Figure 4 illustrates that the engine is able to obtain smooth transitions using several metrics, including indicated mean effective pressure (IMEP), desired combustion phasing (crank angle at 50% mass fraction burn, MFB50) and stoichiometric air/fuel mixture measured in lambda, during the switches into and out of spark-assisted combustion mode. Figure 5 illustrates the key control actuators including throttle angle, valve timings, and spark angle during the mode switches. It also quantifies the fuel economy impact of SACI and the mode switches that are primarily achieved through improved combustion efficiency due to charge composition and reduced pumping losses. The multi-mode combustion engine management system is also evaluated on the ACCESS prototype vehicle during real-world driving conditions. Figure 6 illustrates the engine and vehicle measurements during one of the city drives, in which the time durations highlighted in grey are run under SACI. Further vehicle-level calibration is currently ongoing to optimize its drivability.

CONCLUSIONS

- Two baseline 2009 Cadillac CTS vehicles are upgraded with ACCESS multi-mode combustion capable prototype engines equipped with central-mounted direct injection, electric cam phasing, 2-step cam profile switching, cylinder pressure sensing, and high-pressure cooled external exhaust gas recirculation.

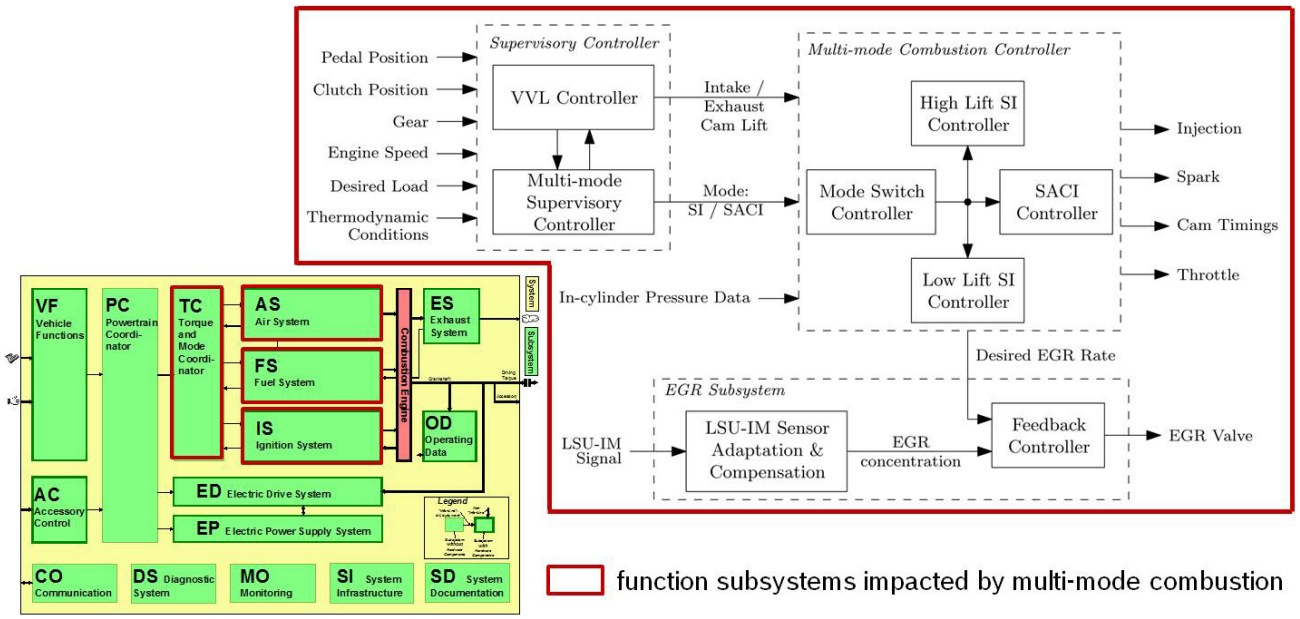

EGR - exhaust gas recirculation; LSU-IM - ?; VVL - variable valve lift

FIGURE 3. Engine Management System Development for Multi-Mode Combustion

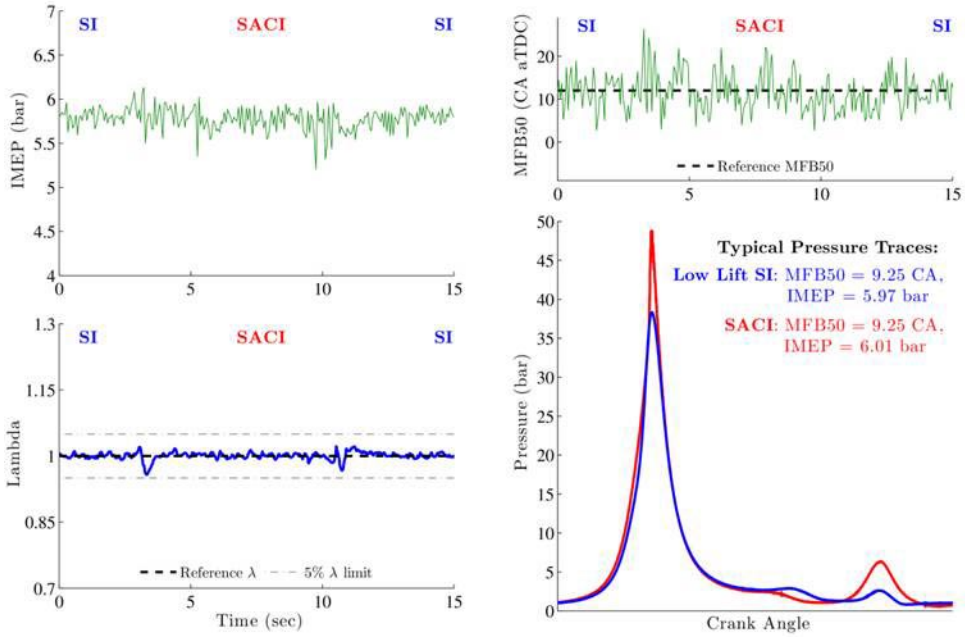

FIGURE 4. SI-SACI Mode Switch Performance at 2,000 RPM, 5-Bar BMEP on ACCESS Prototype Engine

- Multi-mode combustion is functional in the prototype vehicle running with the ACCESS engine management system based on Bosch's in-production MED17 engine control unit. Initial evaluation of the real-world driving performance is completed and vehicle calibration is currently ongoing for demonstration.
- A combined 25% fuel economy improvement on the FTP-75 and HWFET drive cycles is demonstrated on a prototype vehicle against the average performance measured on three baseline vehicles utilizing spark-ignition combustion mode and powertrain measures. Fuel economy benefits of SACI combustion mode are currently being evaluated.
- SACI assisted with boosting and positive valve overlap strategies, and ringing mitigation with high-load pre-mixed non-diluted homogenous charge compression ignition are identified as promising solutions to advanced combustion operation region extension through the collaboration with University of Michigan and Stanford University

FY 2014 PUBLICATIONS/PRESENTATIONS

1. J. Blumreiter and C. Edwards, "Overcoming Pressure Waves to Achieve High Load HCCI Combustion," SAE Technical Paper 2014-01-1269, 2014, doi:10.4271/2014-01-1269.

2. S. Jade, J. Larimore, E. Hellström, L. Jiang, and A.G. Stefanopoulou. Controlled load and speed transitions in a multi-cylinder recompression HCCI engine. *IEEE Transactions on Control Systems Technology*, 2014. to appear.

3. E. Hellström, A.G. Stefanopoulou, and L. Jiang. A linear least-squares algorithm for double-Wiebe functions applied to spark-assisted compression ignition. *Journal of Engineering for Gas Turbines and Power*, 136(9):091514, 2014.

4. E. Hellström, J. Larimore, S. Jade, L. Jiang, and A.G. Stefanopoulou. Reducing cyclic variability while regulating combustion phasing in a four-cylinder HCCI engine. *IEEE Transactions on Control Systems Technology*, 22(3):1190–1197, 2014.

5. Jade, S.; Larimore, J.; Hellstrom, E.; Stefanopoulou, A.G.; Jiang, L., "Controlled Load and Speed Transitions in a Multicylinder Recompression HCCI Engine," Control Systems Technology, IEEE Transactions on , vol.PP, no.99, pp.1,1 doi: 10.1109/TCST.2014.2346992

6. International Journal of Engine Research 1468087414552616, first published on October 8, 2014 doi:10.1177/1468087414552616.

7. S. Nüesch, E. Hellström, L. Jiang, and A.G. Stefanopoulou. Mode switches among SI, SACI, and HCCI combustion and their influence on drive cycle fuel economy. In *Proc. American Control Conference*, pages 849–854, Portland, OR, USA, 2014.

8. J. Su (SJTU and UM AL), W. Lin (UM AL), J. Sterniak (Bosch), M. Xu (SJTU), S. Bohac (UM AL). Particulate Matter Emission Comparison of Spark Ignition Direct Injection (SIDI) and Port Fuel Injection (PFI) Operation of a Boosted Gasoline Engine. JEGTP, 2014.

9. P. Shingne (UM AL), M. Gerow (UM AL) V. Triantopoulos (UM AL), S. Bohac (UM AL), J. Martz (UM AL). A Comparison of Valving Strategies Appropriate for Multi-Mode Combustion within a Downsized Boosted Automotive

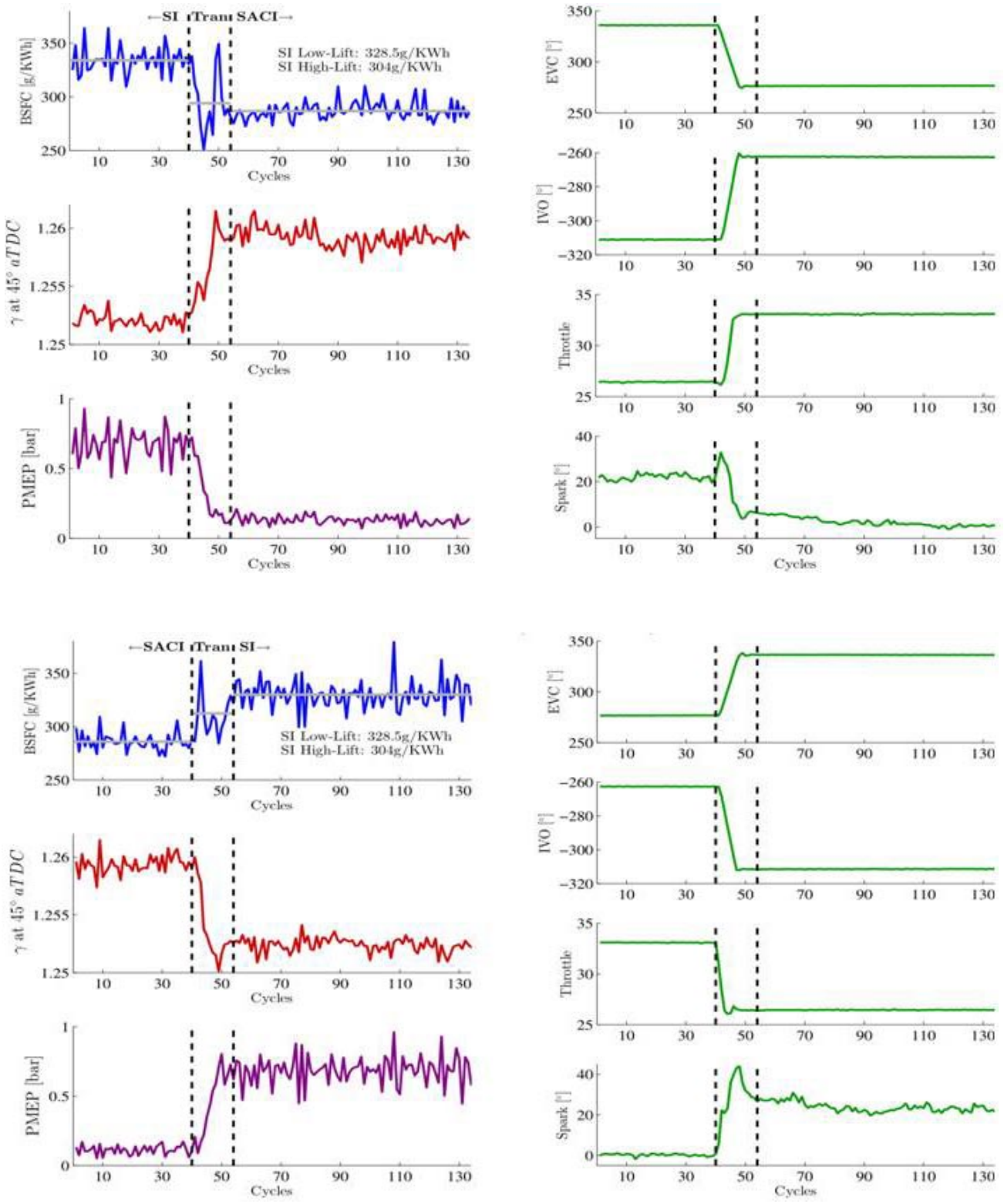

FIGURE 5. SI-SACI Mode Switch Performance at 2,000 RPM, 3-Bar BMEP on ACCESS Prototype Engine

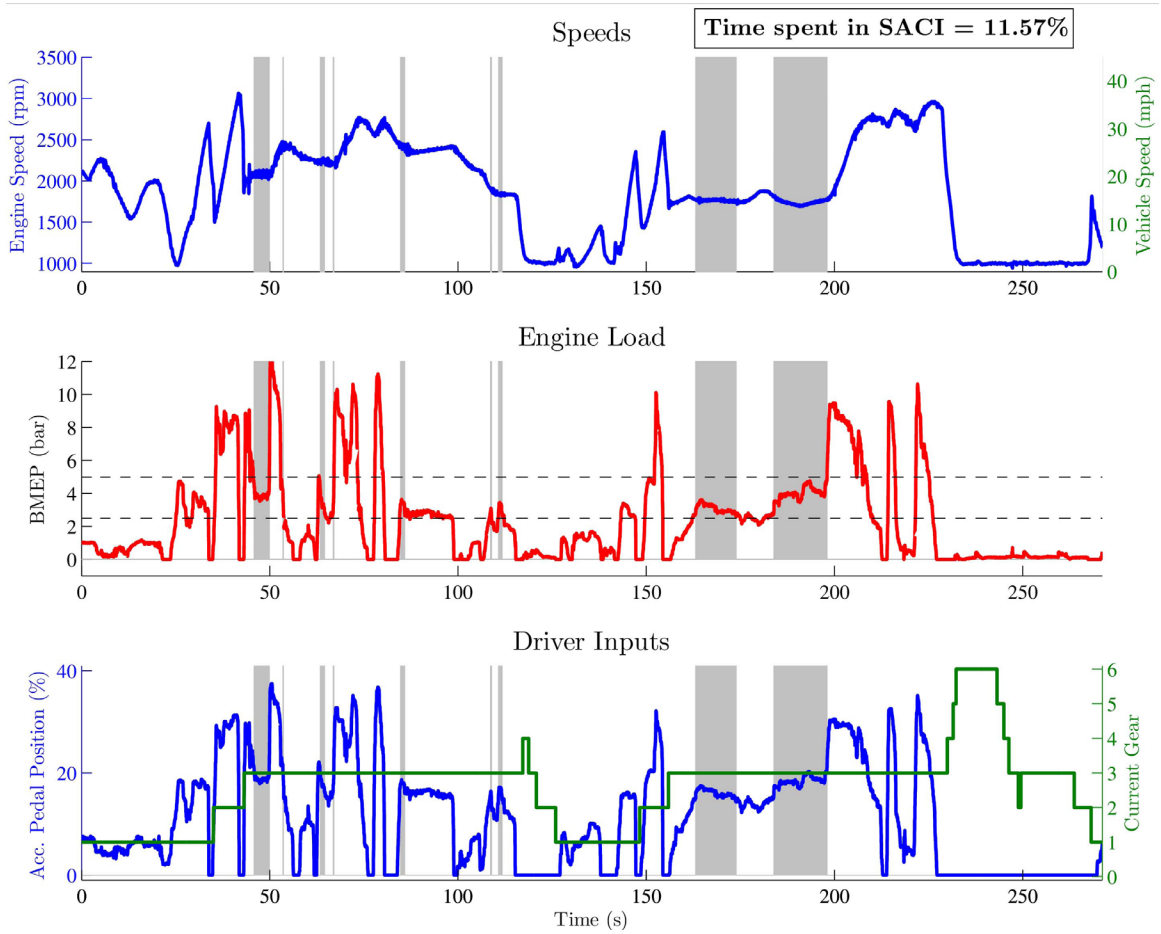

FIGURE 6. Multi-Mode Combustion Performance during Real-World Operations on ACCESS Prototype Vehicle

Engine Part A: High Load Operation within the SI Combustion Regime. JEGTP, 2014.

10. M. Gerow (UM AL), P. Shingne (UM AL), V. Triantopoulos (UM AL), S. Bohac (UM AL), J. Martz (UM AL). A Comparison of Valving Strategies Appropriate for Multi-Mode Combustion within a Downsized Boosted Automotive Engine Part B: Low to Moderate Load Operation within the SACI Combustion Regime. JEGTP, 2014.

11. Y. Chen (UM AL), V. Sima (UM-AL), W. Lin (UM-AL), J. Sterniak (Bosch), S. Bohac (UM-AL). Lean HCCI / Rich SACI Combustion Cycling and Three-Way Catalyst for Fuel Efficiency and NOx Reduction. ASME ICEF, 2014.

12. J. Kodavasal (UM-AL), G. Lavoie (UM-AL), D. Assanis (Stony Brook), J. B. Martz (UM-AL). Reaction-space analysis of premixed and direct injected fueling in the context of homogeneous charge compression ignition combustion under positive and negative valve overalp conditions. Spring Tech Meeting - Combustion Institute, 2014.

13. J. Kodavasal (UM-AL), G. Lavoie (UM-AL), D. Assanis (Stony Brook), J. B. Martz (UM-AL). The effect of diluent composition on homogeneous charge compression ignition auto-ignition and combustion dudration. Combustion Symposium, 2014.

14. J. Kodavasal (UM-AL), G. Lavoie (UM-AL), D. Assanis (Stony Brook), J. B. Martz (UM-AL). The effect of thermal and compositional stratification on the ignition and duration of homogeneous charge compression ignition combustion. Combustion and Flame, 2014.

15. V. Janakiraman (UM AL), X. Nguyen (UM), J. Sterniak (Bosch), D. Assanis (UM AL). Modeling the Stable Operating Envelope for Partially Stable Combustion Engines Using Class Imbalance Learning. IEEE Transactions on Neural Networks and Learning Systems, 2014.

16. Kivanc Temel, Jeff Sterniak. Characterization of SACI Combustion for Use in Model Based Controls. SAE, 2014.

17. Sandro Nüesch, Erik Hellström, Li Jiang, Anna Stefanopoulou. Mode Switches among SI, SACI, and HCCI Combustion and their Influence on Drive Cycle Fuel Economy. American Control Conference. Jun, 2014.

18. Nuesch, A.G. Stefanopoulou, L. Jiang, J. Sterniak, "Methodology to Evaluate the Fuel Economy of a Multimode Combustion Engine With Three-Way Catalytic Converter," ASME J. DSMC, Oct 2014.

19. Sandro Nuesch, Li Jiang, Jeff Sterniak and Anna Stefanopoulou. "Methodology to Evaluate the Fuel Economy of a Multimode Combustion Engine with Three-Way Catalytic

Converter." ASME Dynamic Systems and Control Conference (DSCC), San Antonio, October 2014.

20. Patrick Gorzelic, Prasad Shingne, Jason Martz, Anna Stefanopoulou, Jeff Sterniak, Li Jiang, "A Low-Order HCCI Model Extended to Capture SI-HCCI Mode Transition Data with Two-Stage Cam Switching," ASME Dynamic Systems and Control Conference (DSCC), San Antonio, October 2014, DSCC2014-6275.

SPECIAL RECOGNITIONS AND AWARDS/ PATENTS ISSUED

1. L. Jiang, J. Sterniak, and J. Schwanke, "Combustion Control with External Exhaust Gas Recirculation (EGR) Dilution", Application US 13/951,658, Filed on July 26, 2013. *Pending*

2. J. Larimore, L. Jiang, E. Hellström, S. Jade, and A. Stefanopoulou, "Real-Time Residual Mass Estimation with Adaptive Scaling", Application US 14/185,673, Filed on February 20, 2014. *Pending*

3. N. Ravi, J. Oudart, N. Chaturvedi, and D. Cook, "System and Method for Control of a Transient Between SI and HCCI Combustion Modes", Application US 14/185,278, Filed on February 20, 2014. *Pending*

4. J. Oudart, N. Ravi, and D. Cook, "System and Method for Control of a Transient Between SI and HCCI Combustion Modes", Application US 14/185,357, Filed on February 20, 2014. *Pending*

5. E. Hellström, A. Stefanopoulou, L. Jiang, J. Sterniak, N. Ravi, J. Oudart, J. Schwanke, "Mixed-Mode Combustion Control", Application US 14/221,989, Filed on March 21, 2014. *Pending*

6. E. Doran, D. Cook, J. Oudart, and N. Ravi, "Method of estimating duration of auto-ignition phase in a spark assisted compression ignition operation", Application US 61/821,102, Filed on May 8, 2014. *Pending*

IV.9 Recovery Act – A MultiAir/MultiFuel Approach to Enhancing Engine System Efficiency

Ron Reese
Chrysler Group LLC
800 Chrysler Drive
Auburn Hills, MI 48326

DOE Technology Development Manager
Ken Howden

NETL Project Manager
Ralph Nine

Subcontractors
- The Ohio State University, Columbus, OH
- Bosch, Farmington, MI
- Delphi, Troy, MI
- Argonne National Laboratory (ANL), Argonne, IL

Overall Objectives

- Demonstrate 25% improvement in combined Federal Test Procedure (FTP) City and Highway fuel economy for the Chrysler minivan.
- Accelerate the development of highly efficient engine and powertrain systems for light-duty vehicles, while meeting future emissions standards.
- Create and retain jobs in support of the American Recovery and Reinvestment Act of 2009.

Fiscal Year (FY) 2014 Objectives

- Complete system controls and calibration of the Alpha 2 engine in dyno and vehicle to meet all performance, emissions, fuel economy and drivability targets by utilizing the implemented technologies including twin turbochargers, cooled exhaust gas recirculation (EGR), secondary air and multi-fuel.
- Complete thermal management system control and calibration to improve fuel economy.
- Optimize shift schedule and lock-up in vehicle to fully utilize the capability of the pendulous crankshaft in improving operating efficiency.
- Continue diesel micro-pilot (DMP) combustion learning through continued engine testing and simulation efforts at ANL.
- Perform FTP testing on rolls to demonstrate fuel economy improvement and emission levels.
- Demonstrate in-vehicle drivability and performance to compare with baseline vehicle.

FY 2014 Accomplishments

- Base calibrations were developed and refined. Base engine calibration has been completed and incorporated into powertrain test cell and vehicle testing.
- The second vehicle build was completed, including exhaust and aftertreatment upgrades.
- In late 2013/early 2014 significant progress was made by ANL in the Reynolds-averaged Navier Stokes and large-eddy simulation simulations of the diesel and gasoline fuel sprays with good correlation. In 2014, ANL completed their engine and simulation work. Engine testing with Fischer Tropsch diesel fuel and E85 (85% ethanol and 15% gasoline) achieved over 45% brake thermal efficiency.
- Cold start/FTP calibration and testing in powertrain test cell has been completed.
- Several FTP tests have been run and cold-start calibration improvements evaluated.
- Hardware changes to improve the engine warm-up rate were procured and installed in the Alpha 2 engines.
- Thermal and ancillary load management refinement continued in development vehicle, but was not used during the demonstration vehicle tests.
- Several FTP tests were completed with calibration refinements that helped exceed the fuel economy goal.
- Chrysler hosted DOE management on October 8th in Auburn Hills, for a ride-and-drive demonstration.
- Final reports have been completed by Ohio State University, Delphi and ANL. Chrysler is working with Mid Michigan Research to complete the final report to be submitted to the DOE.

Future Directions

- Complete final report.
- Evaluate and apply learnings to future vehicles, where appropriate.

INTRODUCTION

The intent of the project is to demonstrate a 25% improvement in fuel economy while maintaining comparable vehicle performance to the baseline engine, which is a state-of-the-art 4.0-L V-6. Tier 2, Bin 2 tailpipe emissions are also intended to be demonstrated. The technical approach is to downsize and down-speed the engine through combustion improvements via a combination of engine technologies with concurrent development of other system enhancements. Main technologies explored as part of development project include in-cylinder combustion improvements, waste heat recovery and thermal management strategies, friction reduction, ancillary load management and emissions controls.

APPROACH

Complete two engine design/development iterations. Each iteration encompassed two development phases—one for design/simulation efforts, the second for procurement, engine build and test. The combination of Phases 1/2 resulted in the Alpha 1 engine. Phases 3/4 incorporated learning from early phases to produce the Alpha 2 engine. This engine was used in Phase 5 for the fuel economy and emissions demonstration.

RESULTS

Efforts for this FY focused on refinement of calibrations and technologies to achieve the targeted fuel economy and tailpipe emissions goals. Significant changes were made including transmission shift schedule, thermal management calibration, secondary air optimization, and catalyst light-off calibration. These changes have been made in order to optimize the balance between fuel economy and emissions while maintaining drivability. An emission test using the belt starter generator for stop/start functionality was attempted unsuccessfully due to unforeseen transmission and vehicle electronics incompatibility for the hardware used.

The steady-state dynamometer test results of the Alpha 2 engine with the targeted technology showed that the 25% improvement goal for the combined FTP City and Highway fuel economy should be exceeded. The nine-speed transmission allows the engine to operate at speeds/loads where the engine runs at high efficiency for the majority of the test.

The DMP system had several challenges which led to it not being included in the Alpha 2 engine design and vehicle demonstration. The benefit of DMP was limited to loads of 11-bar brake mean effective pressure and higher and required a precisely controlled amount of EGR. Too little EGR resulted in knock and too much led to unstable combustion. In all, the benefits offered by DMP operation were not significant enough to warrant addressing all of the challenges it presented for this project. Further work at ANL this year increased the range of benefit and reached a peak brake thermal efficiency of over 45% at specific points with unique fuels, but these points would rarely be reached during FTP cycle operation, for this application.

Shift schedule adjustments further enabled an engine down-speeding approach to improve fuel economy. The pendulous crankshaft was a key enabler in this approach; it functioned well in the challenging operating area of lower speeds and higher loads.

Testing in the powertrain test cell focused on increasing the catalyst temperature warm-up during cold starts to improve catalyst efficiency and reduce tailpipe emissions. The mass of the twin-turbo system provided a large heat sink, absorbing much of the heat from the exhaust before it reached the catalyst. A turbo bypass system was developed to route the exhaust flow directly to the catalyst (Figure 1). The bypass system was enabled during the first 20 seconds after a cold start which significantly increased the catalyst brick temperature (Figure 2).

Final testing was done on the target vehicle to determine the fuel economy and emissions results for the FTP City and Highway tests. This testing was done at Chrysler's Emission Test Facility at the Chrysler Technical Center in Auburn Hills, MI (Figure 3).

Chrysler exceeded the fuel economy goal of the project using the developed engine and a 9-speed transmission in the Chrysler minivan. The baseline powertrain was the state-of-the-art gasoline port fuel-injected 4.0-L V-6 equipped with a 6-speed 62TE transmission. The best fuel economy result

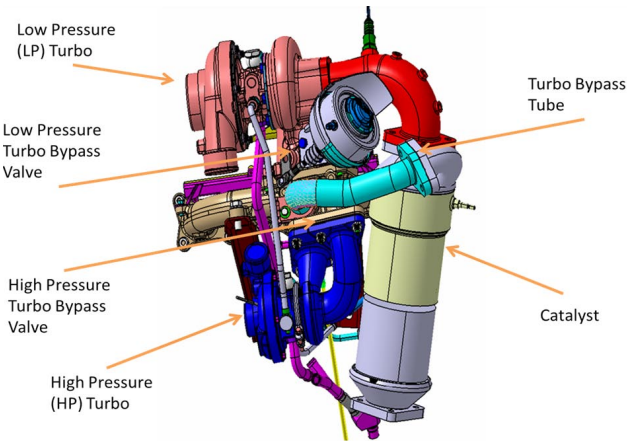

FIGURE 1. Engine After-Treatment

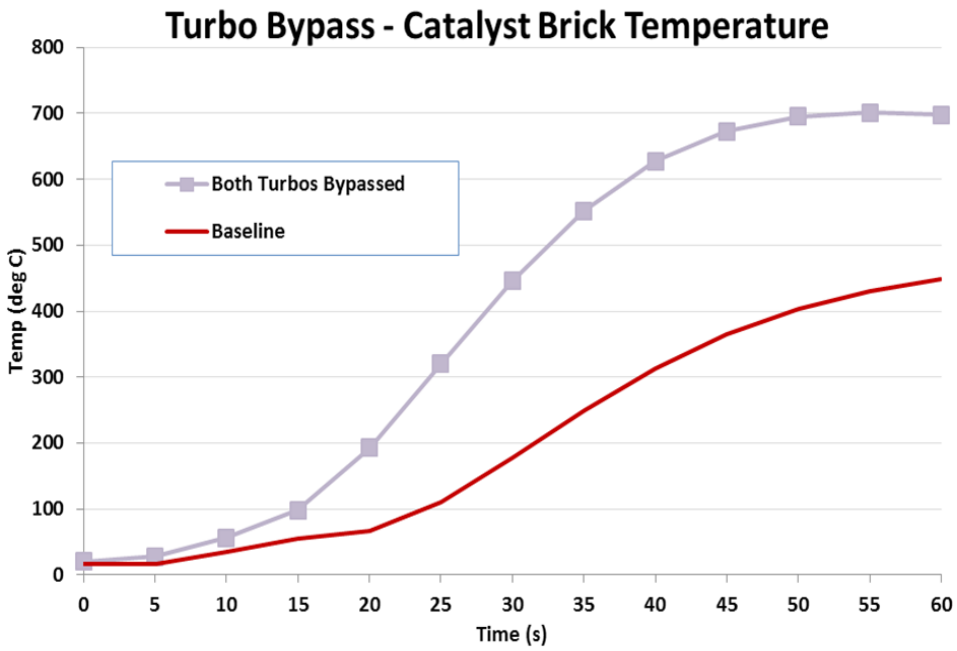

FIGURE 2. Turbo Bypass Catalyst Brick Temperature

FIGURE 3. Vehicle Installed in Chassis Rolls Emissions Test Cell

achieved during the testing demonstrated a 27.4% improvement in combined FTP City and Highway fuel economy, exceeding the project goal of 25%. The emissions measured during the FTP City cycle were 0.0179 grams/mile non-methane organic gases (NMOG), 0.2927 grams/mile CO, and 0.0182 grams/mile oxides of nitrogen (NOx). These results were demonstrated while maintaining comparable vehicle performance to the baseline engine. The average results for the final six tests were 0.0173 grams/mile NMOG, 0.3541 grams/mile CO, and 0.0192 grams/mile NOx with a 26.7% improvement in fuel economy.

The tailpipe emissions goal for the demonstration vehicle was Tier 2, Bin 2. The vehicle emissions did not quite meet the Bin 2 NMOG standard of .010 g/mile, but were below the NOx and CO standards. The super ultra-low emission vehicle-30 standard of .030 g/mile for NMOG and NOx combined (which is the new standard that effectively replaces the Tier 2, Bin2 standard) was met during two tests. The cold start and transient portions of the test created the greatest difficulty in meeting the emissions goal.

CONCLUSIONS

- Overall, Chrysler exceeded the goal of 25% improvement in combined FTP City and Highway fuel economy in a Chrysler minivan.
- DMP is a complex combustion strategy that has some limitations, but the efficiency gains warrant further investigation of its operation.
- Additional calibration work and further reduction of the mass in the exhaust/dual turbo system may have enabled the emissions goal to be met.
- The complexity of controlling the various technologies required significant controls and calibration effort beyond what was estimated and scoped on the project.

FY 2014 PUBLICATIONS/PRESENTATIONS

1. 2014 DOE Vehicle Technologies Program Annual Merit Review (AMR), June 19, 2014.

IV.10 Development of Radio Frequency Diesel Particulate Filter Sensor and Controls for Advanced Low-Pressure-Drop Systems to Reduce Engine Fuel Consumption

Alexander Sappok (Primary Contact), Leslie Bromberg, Paul Ragaller
Filter Sensing Technologies, Inc. (FST)
P.O. Box 425197
Cambridge, MA 02141

DOE Technology Development Manager
Roland Gravel

NETL Project Manager
Ralph Nine

Subcontractors
- Corning, Inc., Corning, NY
- FEV Inc., Auburn Hills, MI
- Oak Ridge National Laboratory, Knoxville, TN
- SemiGen, Inc., Manchester, NH

Overall Objectives

- Demonstrate and quantify improvements in efficiency and greenhouse gas reductions through improved diesel particulate filter (DPF) sensing, controls, and low-pressure-drop components
- Design, develop, and validate radio frequency (RF) sensor performance for accurate real-time measurements of DPF loading with low-pressure-drop substrates
- Achieve breakthrough efficiencies via use of advanced combustion modes, alternative fuels, and advanced aftertreatment enabled by improved sensing and controls
- Develop production sensor designs and commercialization plans on the scale required to significantly impact reduction in greenhouse gas emissions and fuel consumption

Fiscal Year (FY) 2014 Objectives

- Develop second generation, pre-production RF sensors for real-time measurements of DPF loading to optimize the combined engine and DPF efficiency
- Quantify RF sensor accuracy to measure DPF soot and ash levels relative to gravimetric standards, laboratory instruments, and pressure- and model-based approaches
- Demonstrate on-road durability of RF sensors and quantify fuel savings and efficiency benefits enabled via RF sensing relative to original equipment controls over a 12-month fleet test
- Develop RF-based aftertreatment control system relying solely on the RF sensor to control filter operation and quantify fuel savings relative to the current state-of-the-art
- Evaluate additional potential for fuel savings through the use of alternative fuels in conjunction with RF-based DPF soot loading measurements and control

FY 2014 Accomplishments

- Developed pre-production RF sensors capable of fast response (<1 second) and both single- and dual-antenna vector measurements, which received a 2014 R&D 100 Award
- Achieved Phase II performance targets of sensor accuracy within 10% of full-scale measurements relative to gravimetric standard with new and ash-aged DPFs simulating over 380,000 miles of on-road aging and ash accumulation
- Achieved 2014 technical objective of developing a stand-alone RF control system for a model year (MY) 2013, 13-L heavy-duty engine, which demonstrated a reduction in regeneration duration of 15% to 30% with RF-based sensing and control
- Demonstrated on-road RF sensor durability through a 12-month fleet test of two sensor units installed on heavy-duty Volvo/Mack vehicles operated in New York City
- Attained project objective of demonstrating on-road fuel savings with RF-based sensing through shorter regenerations and increase in regeneration interval by up to a factor of two based on fleet test data with MY 2009 Volvo/Mack vehicles
- Demonstrated additional fuel savings with biodiesel blends, enabled through real-time RF sensing, via increase in regeneration interval and faster soot oxidation

Future Directions

- Quantify RF sensor performance and efficiency gains with a wide range of light-duty and heavy-

duty engines with cordierite and aluminum titanate particulate filters

- Confirm on-road durability and quantify fuel savings through an additional 12-month fleet test on MY 2010+ heavy-duty vehicles; testing initiated ahead of schedule
- Investigate additional efficiency gains possible through the use of advanced combustion modes with real-time feedback control enabled by fast RF sensor response
- Develop production sensor designs and commercialization plans on the scale required to significantly impact reduction in greenhouse gas emissions and fuel consumption

INTRODUCTION

Diesel engines present one of the most promising, readily-available technologies to achieve efficiency improvements in light-duty applications and are the power plant of choice for most heavy-duty vehicles. However, the need to use advanced aftertreatment systems, and DPFs in particular, to meet current emissions regulations is a significant hurdle. The DOE Vehicle Technologies Multi-Year Program Plan has identified challenges associated with the use of diesel particulate filters, namely: (1) additional cost and energy usage, (2) lack of "ready to implement" sensors and controls required for sophisticated feedback systems, and (3) demanding durability requirements for both light- and heavy-duty applications [1].

This project directly addresses these challenges by developing an RF sensor and control system, for use with next-generation, low-pressure-drop aftertreatment devices, to reduce engine fuel consumption while still meeting emissions requirements. A pre-production RF sensor was developed and tested during the second year of this project. System design targets of less than 1 second sensor response time, and an electronics footprint comparable to that of conventional particulate matter (PM) and oxides of nitrogen sensors were achieved. Sensor testing quantified measurement accuracy over a range of operating conditions, including accelerated aging and ash loading comparable to 380,000 miles of on-road use. Fleet testing with Volvo/Mack trucks confirmed the potential to reduce the fuel required for DPF regenerations by 50% to 75%, based on RF sensor measurements with these vehicles. In parallel, a stand-alone RF-based aftertreatment control system was developed and validated on an MY 2013, DD-13 engine. Benchmarking of the RF controls with the stock controls showed a reduction in regeneration duration of 15% to 30% with the RF-based approach. RF-based control with engines operated on biodiesel blends also indicated the potential to extend the time between regenerations and shorten regenerations due to the biodiesel-derived PM's more favorable oxidation characteristics, enabled via in situ measurements of the DPF loading state, which is not possible with current technologies.

APPROACH

The approach taken in this project is to identify, address, and overcome key technical challenges to successful RF sensor implementation early on, by leveraging knowledge gained from past research and development efforts conducted by Filter Sensing Technologies and in collaboration with national laboratories, industry, and academia [2-3]. This approach, implemented in four project phases, will develop several RF sensor prototypes, and conduct an extensive series of evaluations to quantify measurement accuracy and potential sources of error, relative to a gravimetric standard. Evaluation of the RF sensor will be carried out on a range of light- and heavy-duty applications through engine testing at Corning, Oak Ridge National Laboratory (ORNL), and FEV, as well as over 48 months of cumulative on-road testing with the New York City Department of Sanitation.

Following this phased approach, a second generation sensor was developed in this project phase, guided by RF system simulations and test results from the prior project phase. Successful sensor evaluations over the course of the previous year have validated sensor accuracy and quantified fuel savings enabled by the technology over a range of on-road and engine dynamometer tests. Ongoing work is focused on further optimizing engine and aftertreatment system control strategies based on input from the RF sensor in a range of light- and heavy-duty applications with various filter materials. Ultimately, the sensor performance data will be used to quantify efficiency gains and estimate aftertreatment system costs reduction and extended component life enabled by RF sensing and feedback control to meet the project objectives.

RESULTS

The work over the course of this project phase has resulted in an R&D 100 Award, several publications, a patent application, and most importantly demonstrated real-world fuel efficiency gains enabled through RF-based DPF sensing and control. The second generation, pre-production RF sensor and control unit developed during this project phase is shown in Figure 1(a). The RF

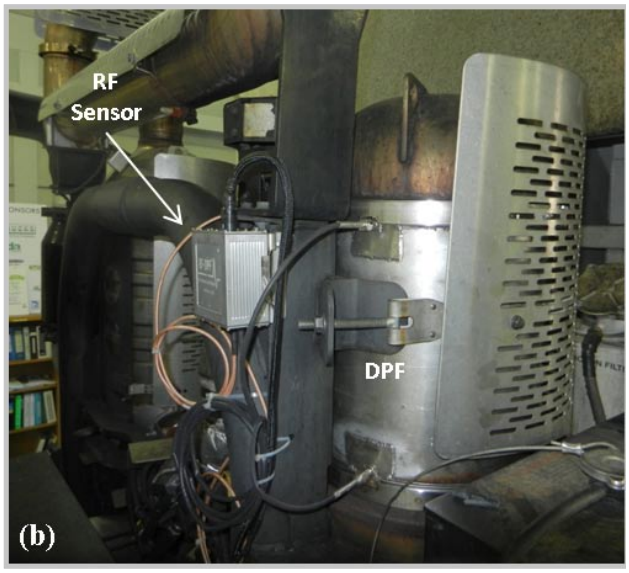

FIGURE 1. FST RF-DPF™ control unit and sensor (a) and RF-DPF™ system installed on MY 2010+ Volvo/Mack diesel aftertreatment system.

probe or antenna is of similar size and form factor to a conventional exhaust temperature sensor and the subject of a patent application. The RF control unit is capable of vector measurements in either single antenna (reflection) or dual antenna (transmission) configurations, with a response time of less than 1 second. Figure 1(b) shows the RF system installed next to the DPF on a MY 2010+ Volvo/Mack aftertreatment system during the first phase of a 24-month fleet test conducted with vehicles operated by the New York City Department of Sanitation.

Results from the first 12 months of the fleet tests have confirmed RF system durability in the field and compared RF measurements of DPF operation with the stock original equipment controls. An example of the fleet test data over approximately 150 hours of vehicle operation is provided in Figure 2. All engine and DPF operation was managed by the stock original equipment controls for the fleet tests, with the RF system passively monitoring filter soot levels and operation. Over the 150-hr period, shown in Figure 2, the vehicle spent between 4% to 5% of its operating time in

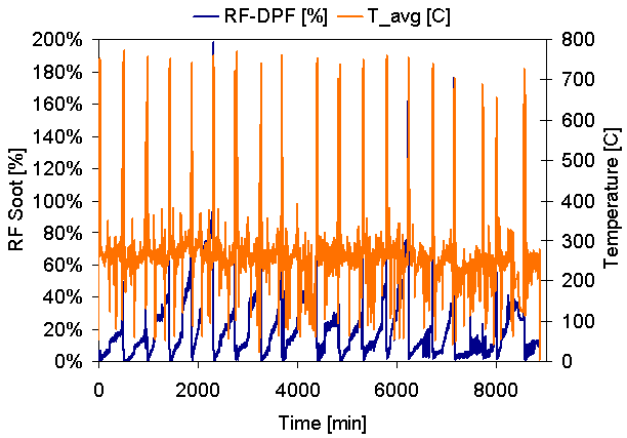

FIGURE 2. DPF RF-measured soot levels and temperature over a 150-hr fleet test period on Volvo/Mack vocational truck operated on urban drive cycle in New York City.

regeneration, with 21 regeneration events measured, and each regeneration event lasting around 18 minutes. All regenerations were triggered by the stock aftertreatment control system.

Comparison with the RF measurements show the actual DPF soot load at the start of regeneration triggered by the stock controller to vary significantly, with a large number of regenerations initiated with relatively low DPF soot levels (below 50%). The RF measurements further showed rapid soot oxidation during the active, burner-based, regeneration process employed on these vehicles, indicating the potential to decrease the regeneration duration as well. Relative to the frequent regenerations, triggered every 7-8 hours by the stock controller, in situ, RF measurements of the DPF loading state were estimated to reduce the frequency and duration of the regenerations by up to a factor of two for these vehicles.

Investigations of RF sensor transient response were also conducted during this project phase at ORNL. The testing, conducted on a 1.9-L General Motors turbo-diesel engine compared the RF sensor response to throttle tip-in events with measurements of engine-out soot emissions using the AVL microsoot sensor. The results, presented in Figure 3, compare the derivative of the RF-measured PM level on the DPF with the exhaust PM concentration upstream of the DPF measured using the AVL instrument. The testing at ORNL was conducted at the beginning of this project phase with the slower response, first generation RF sensor (before the second generation system became available). Relative to the AVL system, which operated at a sampling rate of 1 Hz, the first generation RF sensor exhibited a response time of 12 seconds. Despite the slower response, good qualitative agreement is observed between the derivative of the RF signal and the AVL measurements for these transient

events. Testing with the fast response, second-generation RF sensor, slated for the upcoming project phase.

A significant portion of the project work during FY 2014 was dedicated to developing a DPF control system based solely on measurements from the RF sensor. Figure 4(a) presents the overview of the system architecture, which was developed on a MY 2013 DD-13 engine platform at FEV with considerable input and support from Detroit Diesel/Daimler Trucks. The control system development also marked the first demonstration of the FST RF sensor operated with a single antenna, shown in Figures 4 (a) and (b). Initial work at FEV focused on developing and validating the single antenna RF system calibration over a range of conditions. Output from the sensor was integrated into the aftertreatment controller to trigger the start and end of the regeneration.

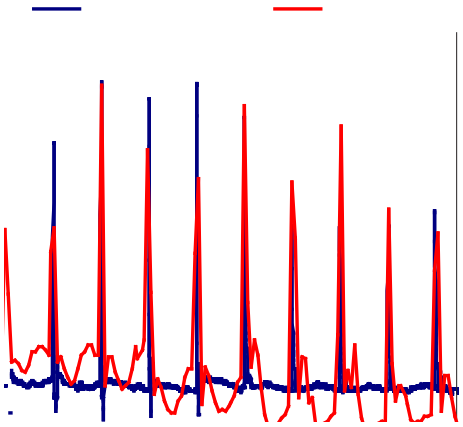

FIGURE 3. Comparison of transient response for AVL microsoot sensor with the derivative of RF-measured DPF soot level to throttle tip-in events on a General Motors 1.9-L turbo-diesel engine.

Figure 5 presents test results with the RF-based DPF control system at FEV. The testing compared the duration of active regenerations triggered by the stock controller to the duration of active regenerations triggered by the RF-based controls. The DPF soot loading state was designated as low (LSL), medium (MSL), or high (HSL) soot load. Relative to the stock controls, a reduction in regeneration duration from 15% to 30% was observed with the RF control system. The reduction in regeneration duration is attributed to the capability to end the regeneration event based on the actual measured DPF soot level with the RF system. In other words, the

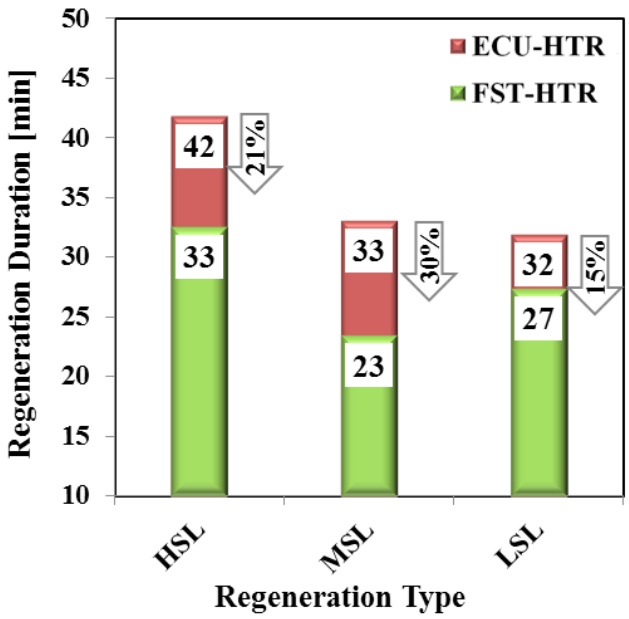

FIGURE 5. Comparison between stock regeneration duration and RF-controlled regeneration duration for regenerations initiated at low (LSL), moderate (MSL) and high (HSL) DPF soot levels.

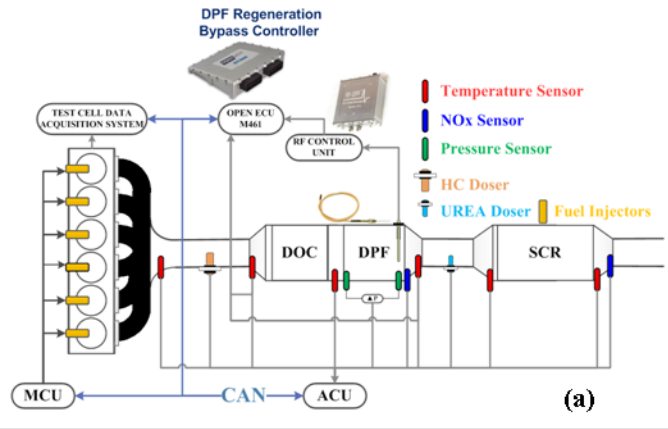

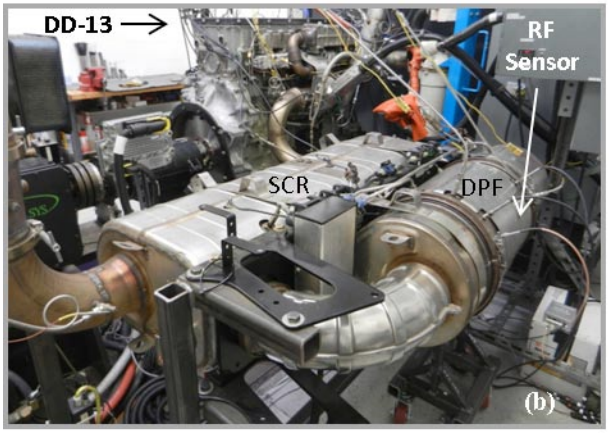

FIGURE 4. RF-based aftertreatment system controls architecture (a) and single-antenna RF measurement system installed on MY 2013, DD-13 aftertreatment system at FEV (b).

RF controller ends the regeneration once the DPF soot level has dropped below a threshold value indicative of a clean DPF. In contrast, current control systems generally conduct the regeneration for a fixed amount of time, consistent with the fleet test results observed in New York.

Measurements of DPF soot levels before and after the regeneration events further quantified the RF sensor's variability with respect to the gravimetric soot load. The mean variation between RF estimated and gravimetrically determined soot loads was found to be 3.66 g, or 0.17 g/l during soot loading and -0.67 g, or 0.03 g/l following regeneration. Confirmation of sensor accuracy and DPF-related fuel savings through the engine dynamometer tests at FEV and on-road fleet tests in New York, therefore achieved the objectives and performance targets of this project phase to quantify potential efficiency gains enabled through in situ RF sensing and control.

Additional work at ORNL towards the end of this project period investigated additional efficiency gains possible through the use of biodiesel blends in conjunction with direct RF measurements of the filter loading state. It is well-known that the use of biodiesel results in lower engine-out PM emissions, and that biodiesel-derived PM exhibits more favorable oxidation characteristics (lower light-off temperature and faster oxidation). Direct measurements of the DPF loading state are required, however, to enable extended regeneration intervals and shorter regeneration duration, when different biodiesel blends are used. Figure 6 clearly shows faster soot oxidation, measured by the RF sensor, for B20- and B100-derived PM relative to the B0 (neat petroleum diesel) case. The results, thus, confirmed RF sensor performance with biodiesel and demonstrated additional potential to optimize DPF operation for use with alternative fuels.

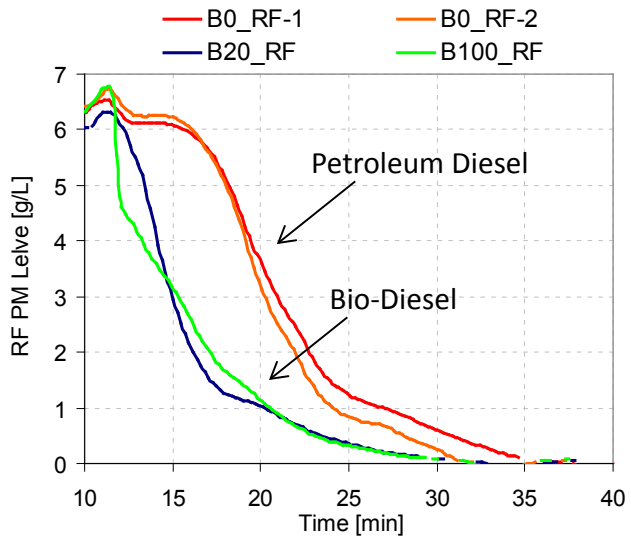

FIGURE 6. RF-measured soot oxidation during DPF regeneration with neat petroleum diesel (B0), 20% biodiesel (B20), and 100% biodiesel (B100) for testing conducted at ORNL.

CONCLUSIONS

Completion of the second phase of this project has resulted in significant progress toward achieving the overall project objectives. Specific accomplishments are the following:

- Developed a second generation, fast response RF sensor capable of either single- or dual- antenna vector measurements, which received a 2014 R&D 100 Award.
- Demonstrated RF sensor durability through an initial 12 month on-road fleet test and confirmed RF measurement accuracy with aged DPFs simulating over 380,000 miles of on-road thermal aging and ash accumulation.
- Achieved performance targets, demonstrating on-road regeneration-related fuel savings by up to a factor of two for MY 2009 Volvo/Mack vocational vehicles, and demonstrated reduced regeneration duration from 15% to 30% on a modern (MY 2013) DD-13 engine relative to the stock control system.
- Benchmarked the RF measurement transient response and observed good agreement with the AVL microsoot sensor, and confirmed additional aftertreatment-related efficiency gains through RF-based controls optimization with biodiesel blends.

REFERENCES

1. U.S. Department of Energy, "Freedom Car and Vehicle Technologies Multi-Year Program Plan: 2006-2011," September 2006.

2. Bromberg, L., Sappok, A., Parker, R., and Wong, V., "Advanced DPF Loading Monitoring with Microwaves," CLEERS Workshop, Dearborn, MI, May 2006.

3. Sappok, A., Bromberg, L., Parks, J., and Prikhodko, V., "Loading and Regeneration Analysis of a Diesel Particulate Filter with a Radio Frequency-Based Sensor," SAE Technical Paper 2010-01-2126, 2010, doi:10.4271/2010-01-2126.

FY 2014 PUBLICATIONS/PRESENTATIONS

1. Sappok, A., Bromberg, L., "Development of Radio Frequency Diesel Particulate Filter Sensor and Controls for Advanced Low-Pressure Drop Systems to Reduce Engine Fuel Consumption (06B)," 2014 DOE Merit Review, Washington, D.C., June 2014.

2. Sappok, A. and Bromberg, L., "Radio Frequency Diesel Particulate Filter Soot and Ash Level Sensors: Enabling Adaptive Controls for Heavy-Duty Diesel Applications," SAE Int. J. Commer. Veh. 7(2):468-477, 2014.

3. Sappok, A., and Bromberg, L., " Radio Frequency Sensing for Direct, In-Situ Emissions Aftertreatment State Monitoring and Optimized Control," Advanced Engine Cross-Cut Team Meeting, March 13, 2014.

4. Sappok, A., "Radio Frequency Sensing for Direct, In-Situ Emissions Aftertreatment State Monitoring and Optimized Control," CLEERS Teleconference, August 21, 2014.

5. Masoudi, M., and Sappok, A., "Soot (PM) Sensors," DieselNet Technology Guide, 2014.

6. Sappok, A., Bromberg, L., Ragaller, P., Prikhodko, V., Storey, J., and Parks, J., "Diesel Particulate Filter-Related Fuel Efficiency Improvements using Biodiesel Blends in Conjunction with Advanced Aftertreatment Sensing and Controls," Biodiesel Technical Workshop, October 28-29, 2014.

SPECIAL RECOGNITIONS AND AWARDS/ PATENTS ISSUED

1. R&D 100 Award for RF-DPF™, received from R&D Magazine for development of one of the top 100 new technologies of the year.

2. Diesel Progress Magazine, "A Matter of Frequency: Radio frequency technology key to Filter Sensing Technologies' DPF monitoring system," July 2014.

3. Bromberg, L., Sappok, A., Koert, Parker, R., and Wong, V., "Microwave Sensing for Determination of Loading of Filters," United States Patent 7,679,374 (2010), European Patent granted 2014.

4. Bromberg, L., Sappok, A., and Koert, P., "Method and System for Controlling Filter Operation," United States Patent No. 8,384, 397, (2013), Japanese Patent granted 2014.

5. Sappok, A., Smith III, R., Bromberg, L., "Advanced Radio Frequency Sensing Probe," United States Patent Application No. 61,897,825, Filed 2013.

IV.11 The Application of Ignition, Fuel System, Charge Motion and Boosting Enabling Technologies to Increase Fuel Economy in Spark Ignition Gasoline Engines by Increasing EGR Dilution Capability

Edward J. Keating
General Motors Co. (GM)
GM Powertrain – Pontiac Engineering Center
895 Joslyn Ave.
Pontiac, MI 48340

DOE Technology Development Manager
Roland M. Gravel

NETL Project Manager
Ralph Nine

Subcontractor
Southwest Research Institute®, San Antonio, TX

Overall Objectives

- Apply and evaluate the enabling technologies of hydrogen-augmented exhaust gas recirculation (EGR), two spark plugs per cylinder, increased compression ratio with a low surface area to volume ratio combustion chamber, increased charge motion (tumble and/or swirl), dual gasoline direct injection (GDI)/port fuel injection (PFI) fuel system and a variable geometry turbocharger system to a current GM-boosted spark ignition engine.
- Demonstrate that this GM-boosted spark ignition gasoline engine operating with extensive, "high quality" EGR dilution achieves a 12% fuel economy benefit relative to a conventional 2.4-L naturally aspirated gasoline engine at equivalent or better performance.
- Demonstrate that this GM-boosted spark ignition gasoline engine solution is capable of U.S. introduction packaged in a mid-sized GM vehicle in the near- to medium-term and has the capability of meeting current and anticipated future emission standards while maintaining or exceeding competitiveness with alternate technologies.

Fiscal Year (FY) 2014 Objectives

- Design, acquire components, and test a current GM 2.0-L turbocharged engine updated to Phase 4 specification through the addition of the following features while packaging in a current GM mid-sized vehicle:
  - Addition of a redesigned cylinder head featuring a two spark plug per cylinder combustion system
  - Addition of redesigned pistons to achieve a 12.0:1 compression ratio
  - Addition of a cooled, dedicated EGR system [1]
  - Addition of a dedicated EGR bypass system
  - Addition of an intake port swirl plate system
  - Addition of a variable geometry turbocharger assembly
  - Addition of a port fuel injection system
- Design and acquire components to update the Phase 4 GM 2.0-L turbocharged engine to Phase 5 by adding the following features while packaging in a current GM mid-sized vehicle:
  - Addition of a redesigned cylinder head featuring a four valve per cylinder, low surface to volume ratio combustion system

FY 2014 Accomplishments

- Phase 4 turbocharged 2.0-L engine with dedicated EGR, 12.0:1 compression ratio, two spark plugs per cylinder, intake port swirl plate, dual GDI/PFI fuel system and variable geometry turbocharger has been tested to establish the fuel consumption and full load performance of this specification compared to the baseline.
- Phase 5 turbocharged 2.0-L engine with dedicated EGR, 12.0:1compression ratio, Dual Coil Offset (DCO™) ignition system [2], intake port swirl plate, dual GDI/PFI fuel system and variable geometry turbocharger is being tested to establish the fuel consumption and full-load performance of this specification compared to the baseline.

Future Directions

Evaluate results of Phase 4 and Phase 5 testing to determine performance to objectives.

✧ ✧ ✧ ✧ ✧

INTRODUCTION

In order to support the federal government's objective of achieving breakthrough thermal efficiencies

while meeting U.S. Environmental Protection Agency emission standards, this project focuses on the enabling technologies of hydrogen-augmented EGR, two spark plugs per cylinder, increased compression ratio with a low surface area to volume ratio combustion chamber, increased charge motion (tumble and/or swirl), dual GDI/PFI fuel system and a variable geometry turbocharger system. These technologies have been shown to enable engine operation with very high EGR dilution levels leading to significant thermal efficiency improvements across the engine operating range. The mechanisms for thermal efficiency improvement include lower thermal losses, improved ideal cycle efficiency, improved combustion phasing, improved combustion efficiency, and reduced pumping losses. The enabling technologies involved are production viable in the near- to medium-term.

APPROACH

Simulation: One-dimensional engine performance simulations have been developed to evaluate the potential of the enabling technologies. An output of the engine simulations was the definition of various options for recirculating EGR that will best support the enhanced EGR dilution tolerance provided by the enabling technologies. An additional output was the determination of potential novel boost systems to efficiently generate charge boosting and enhance mixing with EGR.

A vehicle simulation was conducted following the engine simulation to define the engine dynamometer test points that are being used to predict vehicle fuel efficiency as installed in a current mid-size GM vehicle.

Engine System Development: Components were designed and procured to update GM turbocharged engine(s) with dilution enabling technologies and the appropriate EGR system as determined by simulation. Design work confirmed that the systems added to the engine(s) are capable of installation in the engine compartment of a current mid-size GM vehicle. The engine(s) have been installed in the test cell and are being developed to operate at the highest thermal efficiency possible based upon the EGR dilution tolerance established with the addition of the hydrogen augmented EGR, increased compression ratio with a low surface area to volume ratio combustion chamber, increased charge motion (tumble and/or swirl), dual GDI/PFI fuel system and variable geometry turbocharger system.

RESULTS TO DATE

Simulation

A vehicle simulation of a current mid-size GM vehicle was conducted using the current U.S. Federal City/Highway/US06 drive cycles. The engine speed and load operating points were compiled over these vehicle test cycles and the fuel energy used was determined. Based on this work, 11 engine speed and load operating points were established that represent approximately 95% of the fuel energy used by the mid-size GM vehicle during these test cycles. These engine speed and load points form the basis for engine testing to establish fuel consumption performance of the current baseline engine and the technologies under study.

Install and Test the Baseline Engine

A baseline 2.4-L Ecotec engine was installed in a test cell and the baseline test matrix was fully executed.

The engine test matrix was determined by vehicle simulation (see previous) to best represent engine fuel consumption over the Federal City/Highway/US06 drive cycles. This matrix includes 11 modes. Best brake specific fuel consumption (BSFC) points were determined at each of the 11 modes. Best BSFC was determined by performing sweeps of intake and exhaust cam phasers at each speed/load condition. The spark timing was adjusted to minimum for best torque (MBT), or knock-limited spark advance (KLSA). The full-load curve from 1,250 rpm to 6,000 rpm was acquired to verify performance.

Install and Test the Phase 3 Low-Pressure-Loop (LPL) EGR GM 2.0-L Turbocharged Engine

The engine assembled to Phase 3 LPL EGR specification (Figure 1) was installed and evaluated in the test cell. Various engine, EGR, and ignition performance testing was completed for the turbocharged GM 2.0-L

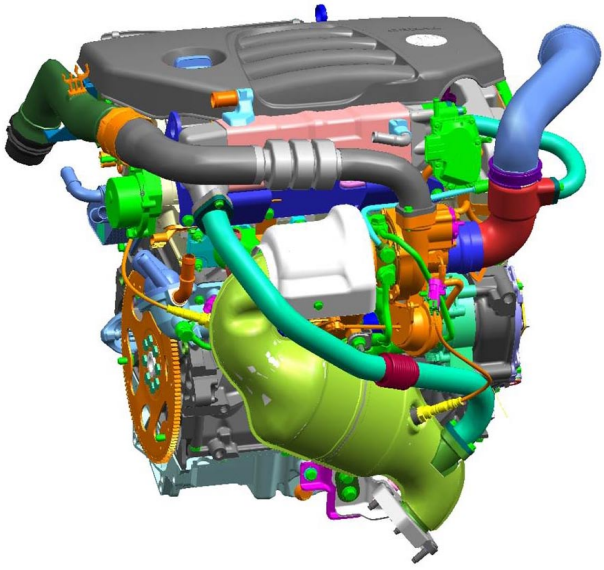

FIGURE 1. Phase 3 LPL EGR Engine Packaged for a GM Mid-sized Vehicle

4-cylinder engine specified with 11:1 compression ratio, high-energy, extended-duration DCO™ ignition system and the baseline (LPL) cooled EGR system. The best BSFC settings were determined at each of the 11 modes. Best BSFC was determined by performing sweeps of intake and exhaust cam phasers in conjunction with cooled external EGR at each speed/load condition. The spark timing was adjusted to MBT, or KLSA. The fuel consumption at the selected 11 mode points of the Phase 3 2.0-L turbocharged engine as specified above is shown compared to the 2010 2.4-L baseline engine in (Figure 2) and also compared to the 2012 2.4-L baseline engine in (Figure 3).

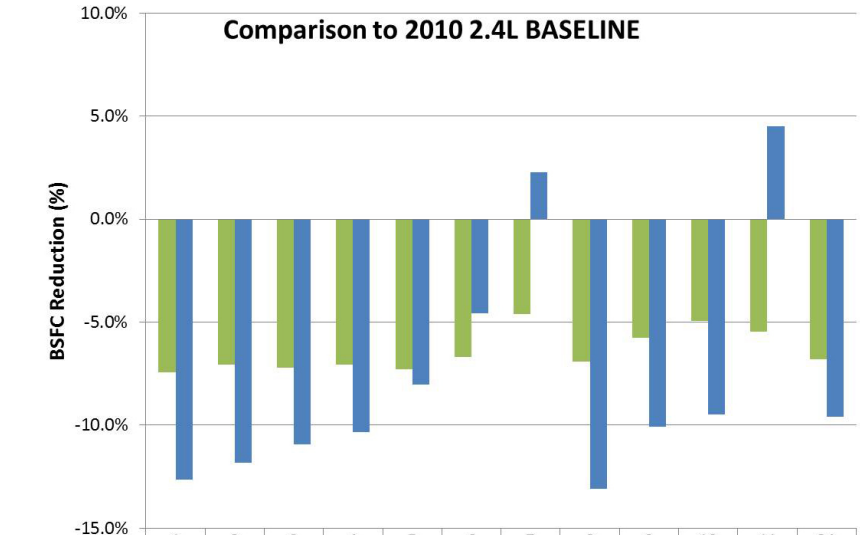

	1	2	3	4	5	6	7	8	9	10	11	OA
LPL-EGR Phase 3	-7.4%	-7.1%	-7.2%	-7.1%	-7.3%	-6.7%	-4.6%	-6.9%	-5.8%	-5.0%	-5.5%	-6.8%
D-EGR Phase 4	-12.6%	-11.8%	-10.9%	-10.3%	-8.0%	-4.6%	2.3%	-13.1%	-10.1%	-9.5%	4.5%	-9.6%

FIGURE 2. BSFC Comparison of Phase 3 and Phase 4 2.0-L Turbocharged Engine to 2010 2.4-L Baseline Engine

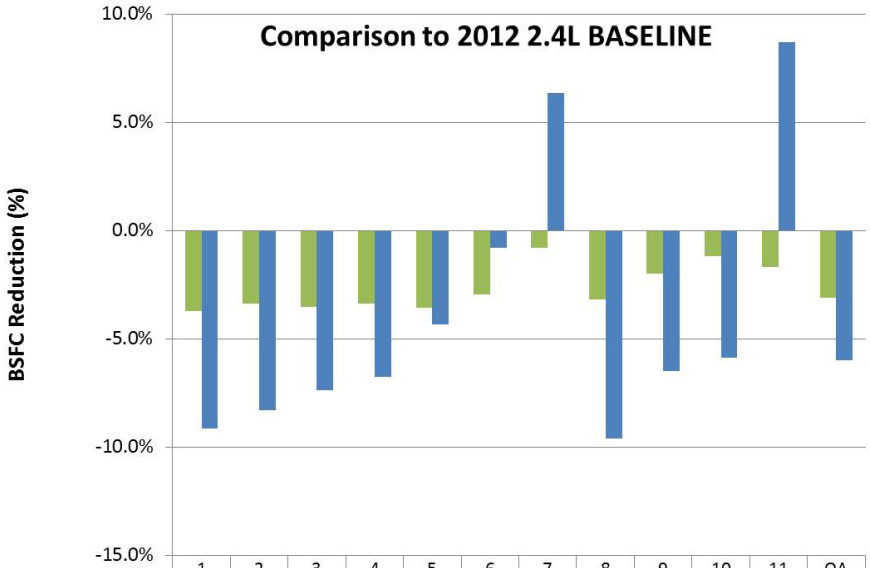

	1	2	3	4	5	6	7	8	9	10	11	OA
LPL-EGR Phase 3	-3.7%	-3.4%	-3.5%	-3.4%	-3.6%	-2.9%	-0.8%	-3.2%	-2.0%	-1.2%	-1.7%	-3.1%
D-EGR Phase 4	-9.2%	-8.3%	-7.4%	-6.8%	-4.4%	-0.8%	6.3%	-9.6%	-6.5%	-5.9%	8.7%	-6.0%

FIGURE 3. BSFC Comparison of Phase 3 and Phase 4 2.0-L Turbocharged Engine to 2012 2.4-L Baseline Engine

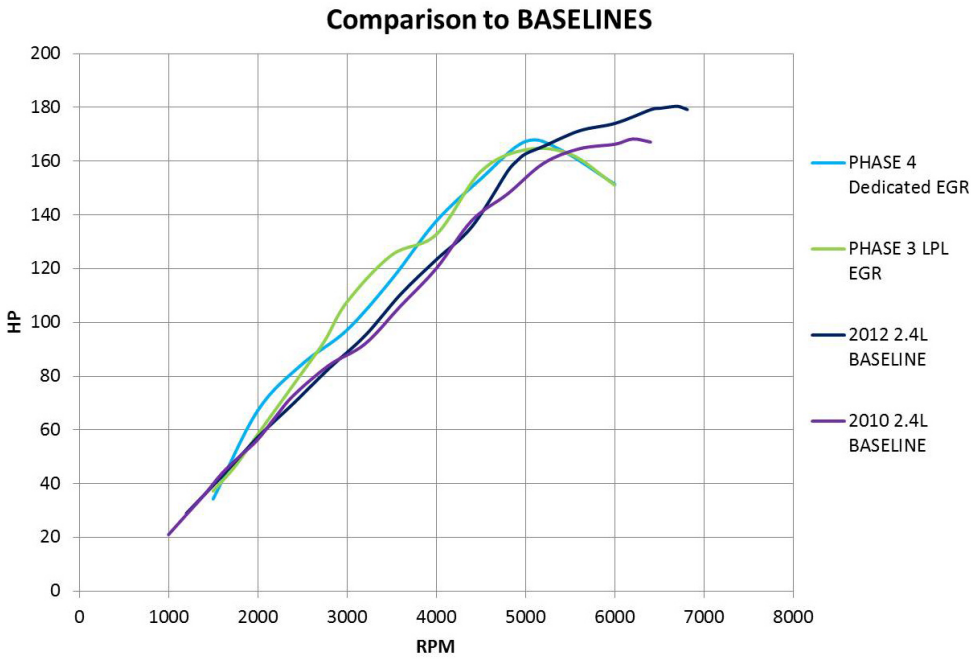

FIGURE 4. Full-Load Performance Comparison of Phase 3 and Phase 4 2.0-L Turbocharged Engine compared to 2.4-L Baseline Engines

Engine full-load performance testing has been completed for the Phase 3 LPL EGR turbocharged GM 2.0-L 4-cylinder engine. Best power was determined by performing sweeps of intake and exhaust cam phasers in conjunction with 20%+ cooled external EGR at each rpm point. A stoichiometric air/fuel ratio was maintained as the turbocharger turbine inlet temperatures remained within the allowable range due to the addition of cooled EGR and excess fuel dilution was not required. The spark timing was adjusted to MBT, or KLSA. The full-load performance of the Phase 3 2.0-L turbocharged engine as specified above is shown compared to the 2.4-L naturally aspirated baseline engines in (Figure 4).

Install and Test the Phase 4 Dedicated EGR GM 2.0-L Turbocharged Engine

The engine assembled to Phase 4 dedicated EGR specification (Figure 5) was installed and evaluated in the test cell. Various engine, EGR, and ignition performance testing was completed for the turbocharged GM 2.0-L 4-cylinder engine specified with dedicated EGR, 12.0:1 compression ratio, two spark plugs per cylinder, intake port swirl plate, dual GDI/PFI fuel system and variable geometry turbocharger. The best BSFC settings were determined at each of the 11 modes. Best BSFC was again determined by performing sweeps of intake and exhaust cam phasers in conjunction with cooled dedicated EGR at each speed/load condition. The spark timing was adjusted to MBT, or KLSA. The fuel consumption at the selected 11 mode points of the Phase 4 2.0-L turbocharged engine as specified above is shown compared to the Phase 3 and 2010 2.4-L baseline engine in (Figure 2) and also compared to the Phase 3 and 2012 2.4-L baseline engine in (Figure 3).

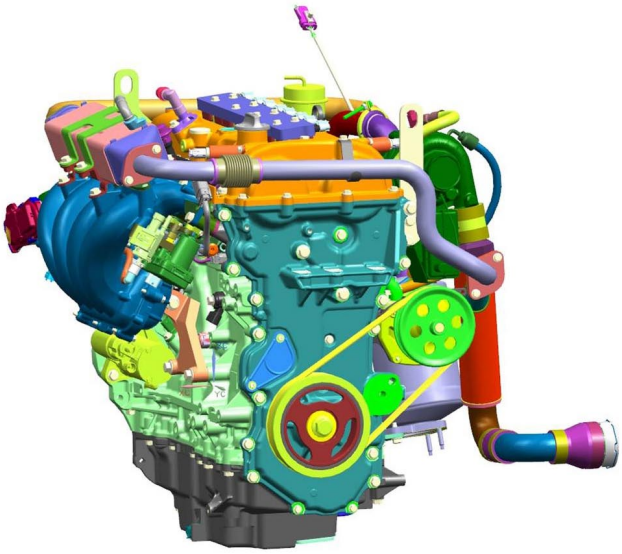

FIGURE 5. Phase 4 Dedicated EGR Engine Packaged for a GM Mid-sized Vehicle

Engine full-load performance testing has been completed for the Phase 4 dedicated EGR turbocharged GM 2.0-L 4-cylinder engine. Best power was determined by performing sweeps of intake and exhaust cam phasers

in conjunction with cooled dedicated EGR at each rpm point. Air/fuel ratio was specified as required so as not to exceed the maximum turbine inlet temperature specification of the "Diesel" specification variable geometry turbocharger utilized. The spark timing was adjusted to MBT, or KLSA. The full-load performance of the Phase 4 2.0-L turbocharged engine as specified above is shown compared to the Phase 3 and the 2.4-L baseline engines in (Figure 4).

CONCLUSIONS TO DATE

The project activities conducted to date have supported the basic assumptions used for the performance improvement projections. The activities have been completed within the constraints of the project timeline. Execution of the remaining engine test cell evaluations will establish the performance benefits of the enabling technologies identified.

- Engine, EGR, and DCO™ performance testing has been completed for the Phase 3 LPL EGR turbocharged 2.0-L 4-cylinder engine. The overall weighted fuel consumption is improved by 6.8% compared to the 2010 2.4-L baseline and 3.1% compared to the 2012 2.4-L baseline.
- Engine, EGR augmentation, fuel system and intake charge motion performance testing has been completed for the Phase 4 dedicated EGR turbocharged 2.0-L 4-cylinder engine. The overall weighted fuel consumption is improved by 9.6% compared to the 2010 2.4-L baseline and 6.0% compared to the 2012 2.4-L baseline.

REFERENCES

1. T. Alger, B. Mangold, "Dedicated EGR: A New Concept in High Efficiency Engines", SAE paper 2009-01-0694, March 2009.

2. T. Alger, J. Gingrich, B. Mangold, "A Continuous Discharge Ignition System for EGR Limit Extension in SI Engines" Preliminary SAE paper number 2011-01-0661.

FY 2014 PUBLICATIONS/PRESENTATIONS

1. 2014 U.S. DOE Vehicle Technologies Program Annual Merit Review and Peer Evaluation Meeting.

IV.12 Heavy-Duty Diesel Engines Waste Heat Recovery Using Roots Expander Organic Rankine Cycle System

Swami Subramanian (Primary Contact), William N. Eybergen

Eaton Corporation
Global Research and Technology (GRT)
Advance Mechanical Systems
26201 Northwestern Hwy.
Southfield, MI 48076

DOE Technology Development Manager
Roland Gravel

NETL Project Manager
Ralph Nine

Subcontractors
- AVL Powertrain Engineering, Inc., Plymouth, MI
- John Deere, Waterloo, IA
- Electricore, Inc., Valencia, CA

Overall Objectives

- Demonstrate fuel economy improvement through organic Rankine cycle (ORC) waste heat recovery (WHR) systems utilizing a roots expander in heavy-duty diesel applications of:
  - 5% (baseline objective) if only energy from the exhaust gas recirculation loop is recovered.
  - 8% (target objective) if exhaust energy from downstream of the turbine is also used for recovery.
- Demonstrate green house gas improvement with WHR systems in heavy-duty diesel applications of:
  - 5% (baseline objective) if only energy from the exhaust gas recirculation loop is recovered.
  - 8% (target objective) if exhaust energy from downstream of the turbine is also used for recovery.
- Demonstrate that other pollutants, such as oxides of nitrogen, hydrocarbons, carbon monoxide, and particulate matter will not be increased as part of the overall engine/WHR/exhaust after-treatment optimization.
- Demonstrate a plan for cost reduction by incorporation of a Roots type expander.

Fiscal Year (FY) 2014 Objectives

- Refinement of thermodynamic analytical model for ORC system with roots expander
- Prototype and evaluate the multistage roots expander in an ORC system utilizing water
- Verification of multistage roots expander analytical results with objective test data
- Finalize system design layout, specifications and prototype heat exchangers, working fluid pump, valves and fluid conveyance lines
- Develop engine controls and build a heavy-duty diesel engine ORC system with integrated roots expander for John Deere 13.5-L diesel engine
- Demonstrate roots expander capability of meeting DOE project objective utilizing the developed heavy-duty diesel engine ORC system

FY 2014 Accomplishments

- Refined and updated thermodynamic system model for ORC with roots expander
- Built and evaluated multistage roots expander with water as working fluid on ORC test stand
- Correlated objective ORC test data to the analytical predictions for the multistage expander
- Procured all ORC components including heat exchangers, working fluid pump, valves and fluid conveyance lines
- Developed engine controls for the ORC system with roots expander
- Completed ORC system installation on a 13.5-L John Deere engine

Future Directions

Demonstrate roots expander capability of meeting DOE project objective utilizing the developed heavy-duty diesel engine ORC system

INTRODUCTION

Nearly 30% of fuel energy is not utilized and is therefore wasted in engine exhaust. ORC WHR systems offer a promising approach for waste energy recovery

and improving the efficiency of heavy-duty diesel engines. One of the major technological barriers in the ORC WHR system is the turbine expander. A turbine expander is grossly mismatched for use with diesel engine exhaust heat recuperation. Eaton Corporation's comprehensive project will develop and demonstrate advanced component technology to reduce the cost of implementing ORC WHR systems to heavy-duty diesel engines. Accelerated adaptation and implementation of new fuel efficiency technology into service is critical for reduction of fuel used in the commercial vehicle segment.

Eaton's solution is to adapt an Eaton-designed Roots compressor (currently in use for supercharger boosting applications) as an expander of the ORC WHR system. Roots-based expanders will have multiple advantages over turbine expanders, including minor down speeding to match engine speed, caliber to handle multiphase flow, high volumetric efficiency, and a broad efficiency island. This configuration will enable faster commercialization of ORC WHR technology capable of improving engine fuel efficiency and total power output (performance). The expander technology to be demonstrated during this project will be validated during engine dynamometer testing using a John Deere 13.5-L heavy-duty diesel engine.

APPROACH

The project has been structured to baseline the 13.5-L heavy-duty diesel engine, characterize and quantify the potential waste energy sources for construction of thermodynamic analysis models. The impacts of various WHR heat exchanger layouts on system performance have been assessed, leading to specifications of WHR components. The expander development utilized computational fluid dynamics analysis, bench testing, calibration, and validation to maximize efficiency and durability. The developed expander with ORC system will be tested on an engine operated over the same speed and load conditions of the baseline engine. These results will be compared to the baseline engine data at the same oxides of nitrogen emission levels to provide a back-to-back demonstration of the expander technology and impact on fuel efficiency and engine system performance.

RESULTS

An expander, heat exchangers, working fluid, and working fluid pump are the major components within an ORC system. Expander design and development is being executed by Eaton. A collaborative team effort between Eaton, AVL, John Deere and ORC component vendors has been utilized to develop the system and all specifications.

Thermodynamic Analytical Model for ORC System with Roots Expander

The model of the ORC system with roots expander has been refined to incorporate a correlated thermodynamic multistage expander sizing tool, vendor inputs for all ORC components, fan loss estimation, working fluid properties, and baseline engine data. Figure 1 shows that most operating points with the three-stage root expander achieving nearly 5% or greater brake specific fuel consumption (BSFC) improvement.

Expander Development

The multistage expander depicted in Figure 2 has been designed and developed to achieve optimal performance and efficiency at a wide range of operation in heavy-duty diesel engines. The displacement of each expander stage and the drive ratios relative to the pulley speed is defined by outputs from the ORC system thermodynamic model based on operating conditions. The isentropic efficiency of the roots expander has been

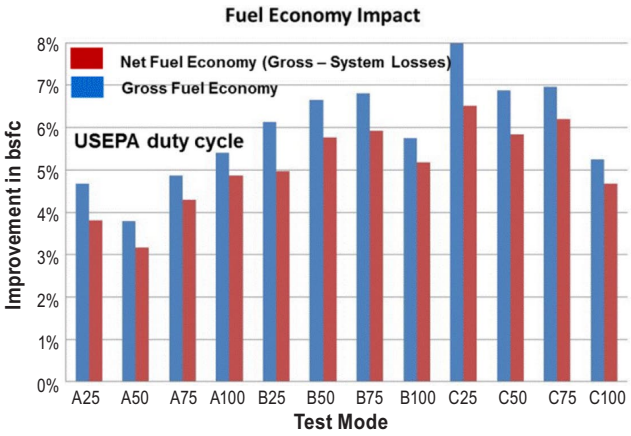

FIGURE 1. BSFC Prediction

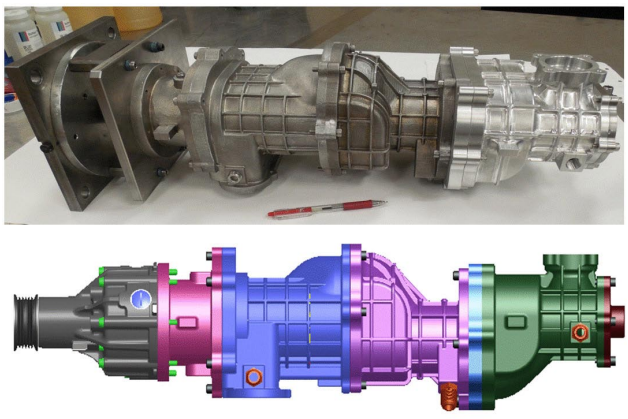

FIGURE 2. Multistage Expander

optimized through computational fluid dynamics to investigate the effect of different inlet and outlet porting configurations, rotor geometry changes, component material selection to alter the coefficient of thermal expansion and working fluid selection.

The multistage expander has been evaluated on the ORC stand (Figure 3) with water as the working fluid. The expander has mechanically operated as expected with no functional issues experienced during testing and the objective test results correlate to the analytical prediction. For a multistage roots expander, the drive ratios for each stage relative to pulley speed need to be altered depending on the selected working fluid due to expansion ratio differences of different working fluids. Stage bypassing is an alternative method to compensate for different expansion ratios of working fluids and has been implemented into the prototype roots multistage expander design. Depending on the working fluid and overall operating conditions, varying levels of stage bypassing is possible to maximize output power of the expander. The prime path for the working fluid is ethanol, but a mixture of ethanol and water is planned for evaluation. All ORC components have been designed to be able to handle the mixtures.

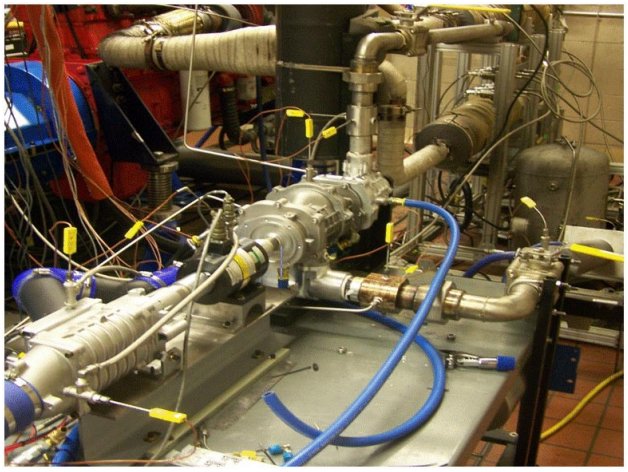

FIGURE 3. Multistage Expander Test Setup on ORC Stand

ORC System Integration onto the Engine

Specifications for all ORC components were developed and system layout design completed for the 13.5-L John Deere engine (Figure 4). Procurement of components and installation onto the engine was successfully completed as outlined in Figure 5.

Development of Engine Controls

The roots expander has tolerance to two-phase working fluids which reduces the system control complexity relative to competing technologies. MATLAB® models of the three-stage roots expander WHR system using expander performance equations and efficiency data derived by Eaton and boiler steady-state function were utilized to generate an open-loop model to establish operating points for the Simulink® control code. The Simulink® control code is target compiled for an open electronic controller. Simulations are illustrating that the output response of the roots ORC system is significantly insensitive to mass flow rate variance which simplifies closed-loop controllability. An iterative approach has been taken for the controls development. As engine data becomes available the MATLAB® model, Simulink® components and target code will be refined.

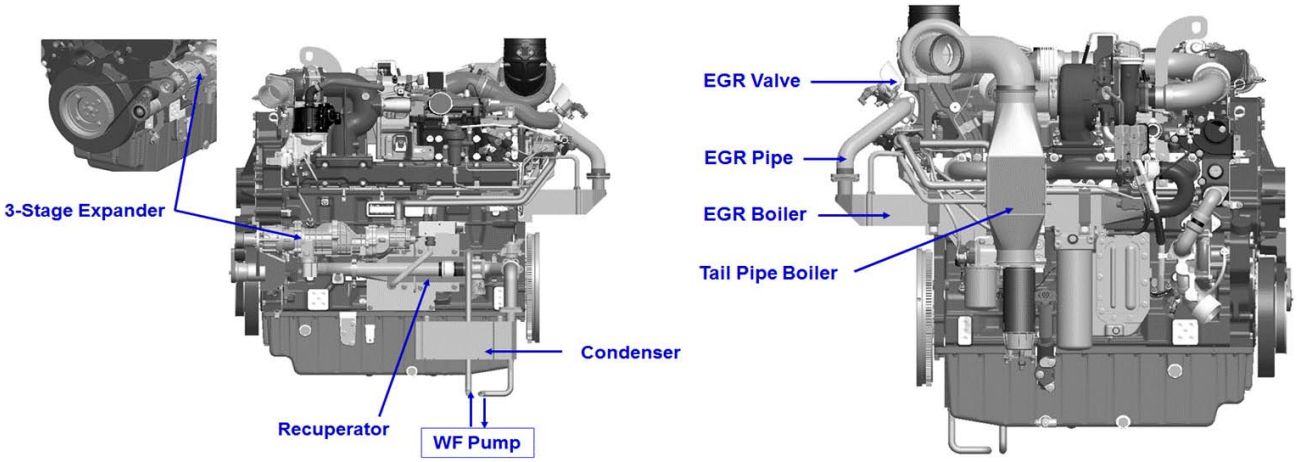

WF - working fluid

FIGURE 4. Roots ORC System Design Layout

FIGURE 5. Roots ORC System Integrated onto the Engine

CONCLUSIONS

Based on the studies documented in this report, the following summary is made:

- Refined simulation results for the multistage roots expander system show a BSFC improvement of approximately 5% for most operating points as outlined in Figure 1.
- No functional issues have been experienced after limited testing of the roots multistage expander and all indications are positive regarding achieving the predicted performance targets.
- Simulations are showing that tight control of mass flow is not necessary which simplifies closed-loop controllability of the Roots ORC system.
- The Roots ORC system has been successfully installed on a 13.5-L John Deere engine and preparation of the engine dynamometer is 95% complete to enable evaluation.

FY 2014 PUBLICATIONS/PRESENTATIONS

1. The Project Principal Investigator, Swami Subramanian, presented at the 2014 DOE Vehicle Technologies Program Review.

2. The Project Principal Investigator, Swami Subramanian, presented at the SAE 2014 Thermal Management Systems Symposium in Denver Colorado on September 22nd, 2014.

3. Eaton Engineering Specialist, Matthew Fortini presented at the SAE 2014 Commercial Vehicle Engineering Congress in Rosemont, Illinois on October 9, 2014.

IV.13 Next Generation Ultra-Lean Burn Powertrain

Hugh Blaxill (Primary Contact), Michael Bunce, Kristie Boskey, Prasanna Chinnathambi, Eric Smith, Luke Cruff
MAHLE Powertrain
23030 MAHLE Dr.
Farmington Hills, MI 48377

DOE Technology Development Manager
Roland Gravel

NETL Project Manager
Ralph Nine

Partner
Ford Motor Co., Dearborn, MI

Subcontractor
Delphi Corporation, Rochester, NY

Overall Objectives

- Demonstrate thermal efficiency of 45% on a light-duty gasoline engine platform while demonstrating potential to meet U.S. Environmental Protection Agency emissions regulations.
- Demonstrate using ultra-lean burn technology, a 30% predicted vehicle drive cycle fuel economy improvement over an equivalent conventional port-fuel-injected gasoline engine with variable cam phasing.
- Demonstrate potential to maintain typical levels of passenger vehicle performance.
- Demonstrate a cost-effective system, capable of being installed in production engines with minimum modification and showing a clear route to production.
- Develop MAHLE Powertrain's Turbulent Jet Ignition (TJI) concept, in conjunction with turbocharging, as the enabling technology to accomplish these objectives.

Fiscal Year (FY) 2014 Objectives

- Complete boosted single-cylinder thermodynamic engine testing.
- Continue TJI pre-chamber and nozzle design optimization.
- Initiate development of TJI operating strategy.
- Develop a computational fluid dynamics (CFD) model correlated to experimental results.

FY 2014 Accomplishments

- Completed boosted single-cylinder thermodynamic engine testing with Phase 2A TJI designs and Phase 2B TJI designs.
- Completed pre-chamber injector spray targeting optimization.
- Initiated TJI operating strategy development.
- Successfully correlated CFD model to wide open throttle, lean, auxiliary fueled pre-chamber experimental results.

Future Directions

- Identify optimal TJI pre-chamber and nozzle geometry for peak thermal efficiency, drive cycle fuel consumption, and lean limit extension.
- Identify optimal TJI operating strategy across engine operating map for peak thermal efficiency, drive cycle fuel consumption, and lean limit extension.
- Build boosted multi-cylinder TJI engine.
- Complete boosted multi-cylinder TJI engine testing and analysis.
- Complete one-dimensional TJI drive cycle analysis utilizing multi-cylinder engine data.
- Utilize correlated CFD model to increase understanding of and optimize the pre-chamber mixture preparation process.

INTRODUCTION

Regulation and industry trends have sought to produce engines with higher efficiency, lower fuel consumption, and lower exhaust emissions than their predecessors. Lean-burn operation provides thermal efficiency benefits but may result in higher NO_x emissions, requiring expensive emissions aftertreatment. Ultra-lean burn has been shown to improve thermal efficiency and simultaneously reduce NO_x formation by significantly reducing in-cylinder temperatures. However, there are challenges associated with ignition of the charge and combustion stability. In order to improve light-duty spark ignition (SI) engine efficiency and vehicle fuel economy, the industry is moving towards downsizing

(smaller displacement, boosted direct injection engines), but these engines typically display poor thermal efficiency. MAHLE Powertrain intends to use two key enabling technologies for its ultra-lean burn combustion concept: TJI and turbocharging.

APPROACH

TJI is a pre-chamber-initiated distributed ignition system that enables reliable ignition of ultra-lean main chamber air-fuel mixtures. TJI differs from other pre-chamber-based systems in that it incorporates auxiliary fueling directly in the pre-chamber, and the design of the nozzle interface between pre-chamber and main chamber promotes flame quenching, thereby seeding the main chamber with active radical species. This project seeks to apply this concept to a light-duty SI engine platform in an effort to achieve 45% peak thermal efficiency, 30% drive cycle fuel economy improvement, and low NO_x emissions levels.

To meet these objectives, the FY 2013 workscope included optical engine and single-cylinder thermodynamic engine testing. Optical engine testing was employed to qualitatively explore effects of the turbulent radical jets on main chamber ignition and combustion. Single-cylinder thermodynamic engine testing was employed to determine combustion and engine performance differences as functions of different nozzle designs. Optical and metal engine data are compared to quantitatively determine the physical characteristics of the jets and their comparative effect on combustion and engine performance.

The FY 2014 workscope continues the design optimization study begun in FY 2013. The addition of boost capability to the single-cylinder thermodynamic engine enables multiple engine operating strategies to be employed. An initial TJI operating strategy is developed to identify optimal pre-chamber fuel injection settings for system performance. This optimization work is coupled with correlated three-dimensional simulations which provide a greater understanding of the nuances of in-pre-chamber phenomena.

RESULTS

Data demonstrate that TJI effectively extends the lean limit of the base engine. Unfueled TJI results in a lean limit of approximately λ=1.4; fueled TJI can extend this limit past λ=2.0. A major contributor to stable combustion at significantly higher λs is the reduction in crank angle (CA) 0-10 degree burn duration. This duration remains much flatter over the λ sweep with fueled TJI than with unfueled TJI. This indicates that fueled TJI provides an increased ignition potential, allowing it to continue to ignite the main charge relatively easily despite the decreasing ignitability of the main charge as it is enleaned. These data are presented in Figure 1.

Figure 1 illustrates the progress made to date on utilizing TJI to increase the net thermal efficiency (NTE) of the system above that of the base engine. Due to the gamma effect, enleanment has been shown to increase NTE [1]. An additional gain in NTE results from the ability to increase compression ratio without enduring a knock penalty. The lower temperature combustion accompanying lean combustion coupled with the distributed ignition qualities of TJI enable this increase in compression ratio from 10:1 of the base engine to 14:1. Base engine peak NTE has been established as approximately 36.5% at stoichiometric. Previous internal TJI research [2-5] has demonstrated peak NTE reaching approximately 42% with TJI. Data presented at the higher compression ratio demonstrates parity with these previous results.

Due to the lack of boost and thus the inability to maintain constant indicated mean effective pressure (IMEP) at wide-open throttle (WOT) as λ is varied, thermal efficiency decreases as the engine is enleaned. The addition of boost capability during the FY 2014 workscope prevents this decline in IMEP and thus thermal efficiency increases during enleanment due to reduced heat loss and reduced pumping loss.

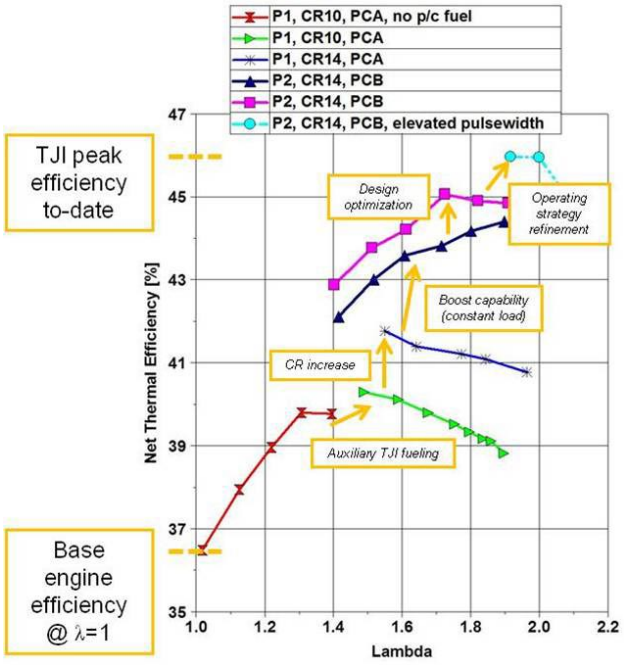

FIGURE 1. NTE vs. λ, 2,500 rpm, 47 kg/hr Air Flow (Phase 1), 11.7 bar IMEPg (Phase 2)

Design optimization undertaken in FY 2013 and continued in FY 2014 results in a further increase in thermal efficiency from a peak of approximately 44% to 45%. As the design optimization work concludes at the end of FY 2014, this figure may be increased further.

Auxiliary fuel is injected into the pre-chamber to initiate pre-chamber combustion but, generally, this fuel does not contribute to the work output of the engine. This fuel is largely confined to the pre-chamber combustion event which in the case of TJI is an ignition source and not a contributor to the pressure rise event in opposition to piston motion. This fuel quantity is, however, included in the calculation of thermal efficiency since it is consumed during the system combustion event. It was therefore assumed that limiting the quantity of the auxiliary fuel would produce higher overall thermal efficiency. Analysis of engine data reveals that in fact the opposite may be the case. Increasing auxiliary fuel quantity in the pre-chamber results in an increase in peak thermal efficiency from 45% to 46%, as depicted in Figure 1.

Figure 2 provides insight into the reason for this effect. Increased auxiliary fuel flow enables advances in the crank angle at which 50% of the combustion heat release has occurred (CA50), resulting in reduced main chamber fuel flow to achieve the same IMEP. This leads to increased thermal efficiency. It is hypothesized that increasing auxiliary fuel flow increases the energy content of the turbulent radical jets, reducing instability in main chamber combustion and enabling greater control over combustion phasing. Subsequent testing, analysis, and simulation will focus more fully on this effect and its underpinning logic.

A correlated multi-dimensional computational fluid dynamics (CFD) model has been successfully developed during FY 2014 for TJI operation with auxiliary fuel injection. Primary CFD runtime workload is allocated in performing key CFD parameter sweeps that were required to arrive at critical boundary condition inputs which are not available from the test bed. The CFD model is tested and developed against two experimental test points under WOT conditions. The test points have different compression ratios (CR) (10 vs. 14) achieved with different piston geometries and intake conditions (naturally aspirated vs. boosted) but have the same pre-chamber design. Operating conditions are detailed in Table 1. Correlation of modeled in-cylinder and in-pre-chamber pressure traces with experimental results for the CR_10 and CR_14 models are shown in Figures 3 and 4, respectively.

A similar type of analysis as is described in the following for model CR_10_BaseP/C was performed for the other correlated test point CR_14_BaseP/C.

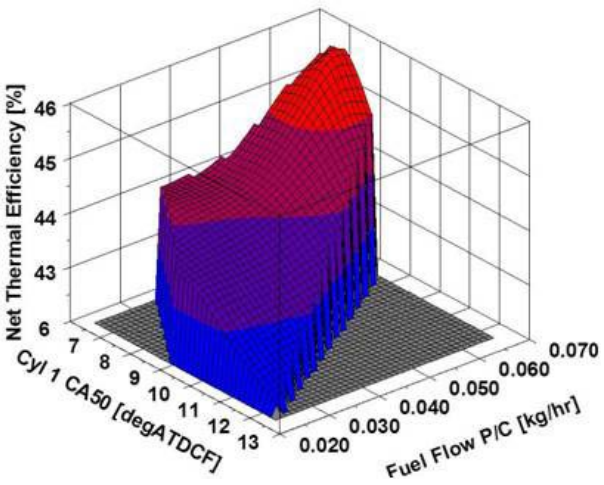

FIGURE 2. NTE vs. CA50 vs. Pre-Chamber Fuel Flow, 2,500 rpm, 11.7 bar IMEPg, CR = 14 – TJI Design P2A PCB.

TABLE 1. Engine Operating Conditions

CFD Model	Speed (RPM)	Exhaust λ	Pre-chamber Fuel	Intake Pressure (Kpa)	Compression Ratio
CR_10_BaseP/C	2,500	1.9	Yes	98 (WOT)	10
CR_14_BaseP/C	2,500	1.75	Yes	147 (WOT)	14

Unlike conventional internal combustion engine environment, within the pre-chamber, spray interaction initially happens with a cross flow of incoming main-chamber charge and subsequently impinges on the wall. The spray-wall interaction physics dominate the pre-chamber mixture preparation process. The splashed spray particles are later transported to other regions in the pre-chamber by the flow features created inside the pre-chamber (based on design) by the action of incoming charge forced through the nozzles. The strong inflow of main-chamber charge creates three distinct stratification zones within the pre-chamber as shown in Figure 5. The rich zones are cornered around the spark plug and the injector location. For design consideration purposes it is better to maintain a richer zone near the spark plug region compared to the injector location to minimize injector durability issues. The transport pattern of the spray also indicates the need to reduce crevice regions associated with placement of the spark plug and the pre-chamber injector. The incoming charge of ultra-lean mixture also affects and alters the flame propagation process within the pre-chamber after the onset of spark.

Figure 6 provides a three-dimensional visualization of jet penetration and consumption of the main chamber charge. The asymmetry in the initial jet penetration,

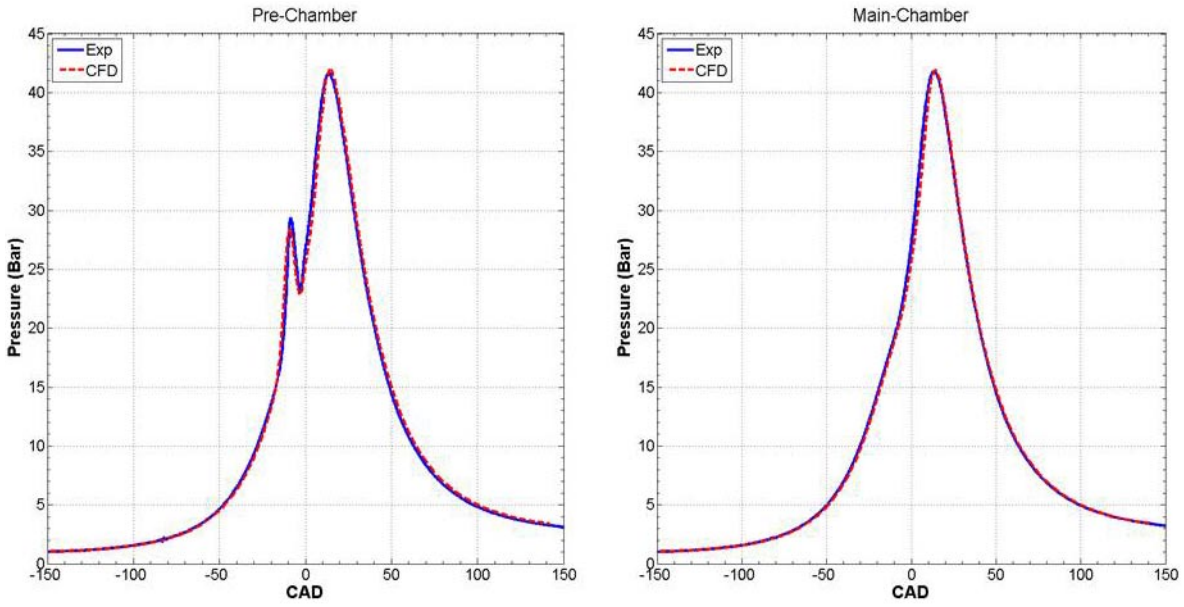

FIGURE 3. In-Cylinder and In-Pre-Chamber Pressure vs. Crank Angle Degree (CAD) for CFD Condition 1

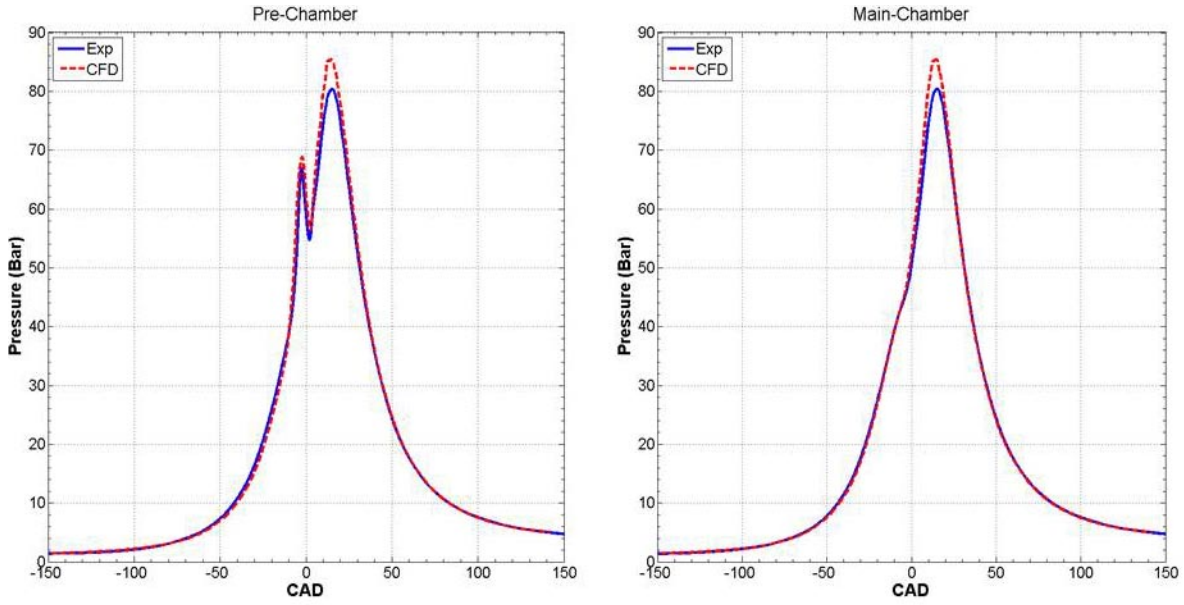

FIGURE 4. In-Cylinder and In-Pre-Chamber Pressure vs. Crank Angle Degree (CAD) for CFD Condition 2

location of the reignition zones at the jet tips and subsequent combustion in the main-chamber can be observed across crank angle degrees. The re-ignition zones are usually located just above the piston surface and the appearance of these mushroom shaped reaction zones occurs analogous with rapid a decrease in jet velocity.

These results indicate the importance of both design optimization and operating parameter optimization for TJI performance. Design optimization encompasses both pre-chamber and nozzle geometry features that can have a strong impact on both the mixture preparation process and the main chamber reignition process, such as component location.

Pre-chamber fuel injector parameters have a direct impact on the mixture preparation process by dictating the quantity of available fuel in the pre-chamber at time of spark, degree of homogeneity inside the pre-chamber, and λ at the spark plug at time of spark. These parameters have an indirect though important impact on

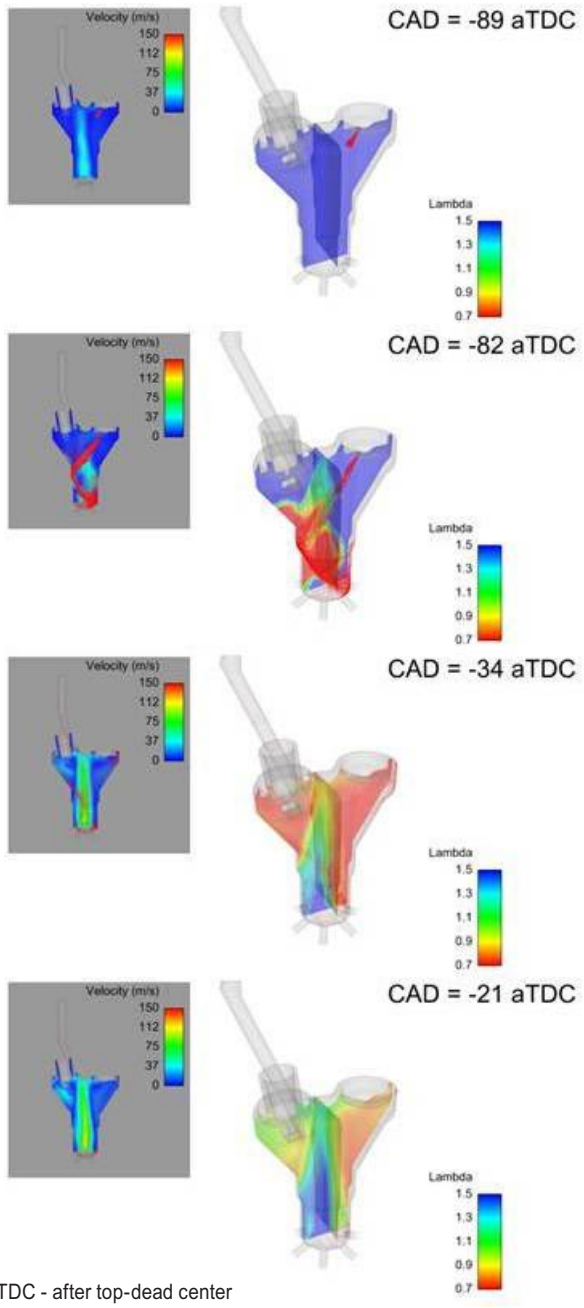

aTDC - after top-dead center

FIGURE 5. CFD Visualization on Two-Dimensional Contour Planes Indicating Spray Particles, Lambda Stratification, and Velocity Magnitude at Different Crank Angle Degrees

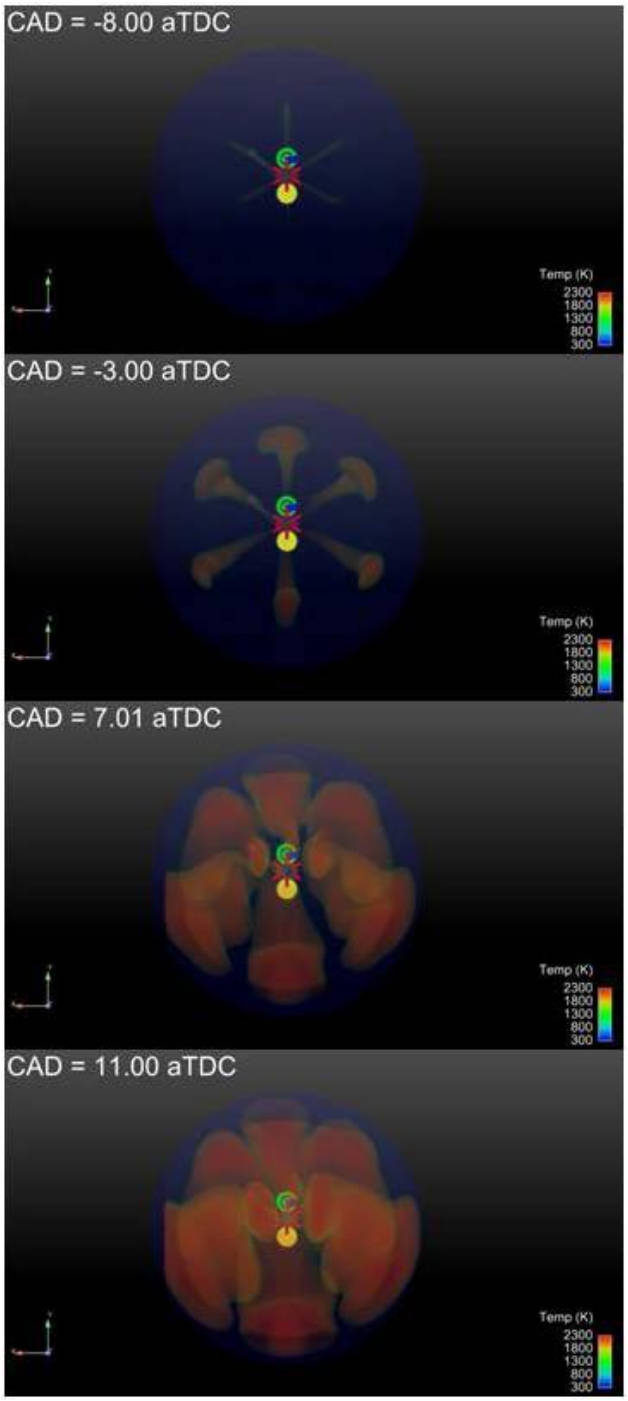

FIGURE 6. CFD Volume Rendering of Multiple Iso-Surfaces Representing Different Temperature Zones with a Pre-Set Transparency Providing Three-Dimensional Visualization of the Jet and Reaction Zones

main chamber combustion quality via control over jet characteristics.

CONCLUSIONS

Previous studies [2-5] have demonstrated the potential of TJI as an enabling technology for ultra-lean SI combustion to significantly increase NTE and reduce NO_x emissions. This project examines comparative performance of TJI designs and operating strategies in an effort to achieve the NTE, fuel economy, and emissions targets enumerated in the objectives.

Experimental results demonstrate the successful progress of design and operating strategy optimization work, with a combination thereof achieving a peak net

thermal efficiency of 46%. This exceeds the primary objective of this project.

CFD simulation provides a greater degree of understanding in relation to the hypotheses underpinning both TJI operation and the optimization work undertaken on this project. Successful correlation of the models to experimental data is a key first step to ensuring that this enhanced understanding has a real-world bearing.

REFERENCES

1. Germane, G., Wood, C., Hess, C., "Lean Combustion in Spark-Ignited Internal Combustion Engines – A Review," SAE Technical Paper 831694, 1983.

2. Attard, W., Toulson, E., Fraser, E., Parsons, P., "A Turbulent Jet Ignition Pre-Chamber Combustion System for Large Fuel Economy Improvements in a Modern Vehicle Powertrain," SAE Technical Paper 2010-01-1457, 2010, doi:10.4271/2010-01-1457.

3. Attard, W., Kohn, J., Parsons, P., "Ignition Energy Development for a Spark Initiated Combustion System Capable of High Load, High Efficiency and Near Zero NO_x Emissions," SAE Journal Paper JSAE 20109088, 2010.

4. Attard, W., Blaxill, H., "A Gasoline Fueled Pre-Chamber Jet Ignition Combustion System at Unthrottled Conditions," SAE Technical Paper 2012-01-0386, 2012, doi:10.4271/2012-01-0386.

5. Attard, W., Blaxill, H., "A Lean Burn Gasoline Fueled Pre-Chamber Jet Ignition Combustion System Achieving High Efficiency and Low NO_x at Part Load," SAE Technical Paper 2012-01-1146, 2012, doi:10.4271/2012-01-1146.

FY 2014 PUBLICATIONS/PRESENTATIONS

1. "The Effects of Turbulent Jet Characteristics on Engine Performance Using a Pre-Chamber Combustor", SAE Technical Paper 2014-01-1195.

2. "The Development of a Pre-Chamber Combustion System for Lean Combustion of Liquid and Gaseous Fuels", CRC Advanced Fuels and Combustion Conference 3/14.

3. 2014 DOE Annual Merit Review and Peer Evaluation presentation - Washington, DC, 6/16/2014 - 6/20/2014.

4. "Methodology for Combustion Analysis of a Spark Ignition Engine Incorporating a Pre-Chamber Combustor", SAE Technical Paper 2014-01-2603.

IV.14 High Efficiency Variable Compression Ratio Engine with Variable Valve Actuation and New Supercharging Technology

Charles Mendler
ENVERA LLC
Los Angeles, CA 90068

DOE Technology Development Manager
Roland Gravel

NETL Project Manager
Ralph Nine

Subcontractors
- Eaton Corporation, Marshall, MI
- Eaton Corporation, Southfield, MI

Overall Objectives

The primary objective of this project is to develop a high-efficiency variable compression ratio (VCR) engine having variable valve actuation (VVA) and an advanced high-efficiency supercharger to obtain up to a 40% improvement in fuel economy when replacing current production V-8 engines with the new small displacement VCR engine.

- Target power range: 281 to 360 hp
- Target light- and medium-load efficiency: 230 g/kWh

Fiscal Year (FY) 2014 Objectives

- Computer-aided design design and development of the VCR cranktrain, mechanism, actuator system and crankcase
- Generate mass-production feasible valve lift and duration profiles
- Construct GT-POWER model of the VCR engine
- Evaluate boosting system options using GT-POWER modeling. Down-selection of the boosting system to be used on the VCR engine will occur in FY 2015.
- Engine management component and system needs specification

FY 2014 Accomplishments

- Computer-aided design and development of the VCR cranktrain, mechanism, actuator system and crankcase
- Generated mass-production feasible valve lift and duration profiles
- Constructed GT-POWER model of the VCR engine
- Initiated evaluation of boosting system options using GT-POWER modeling. Down-selection of the system to be used on the VCR engine will occur in FY 2015.
- Developed engine management system component and needs specification

Future Directions

- During FY 2015 development work will be conducted in the following areas:
- Engine tuning using GT-POWER modeling
- VCR boosting system down-selection
- Advanced supercharger development—to be determined based on down-selected system
- Cam development as needed based on GT-POWER modeling
- VCR engine design/build

INTRODUCTION

This project is directed towards development of a high-efficiency VCR engine having VVA and new supercharging technology. Aggressive engine down-sizing and the high-efficiency Atkinson cycle will be used during most driving conditions to attain large improvements in fuel economy. New supercharging technology will be used to provide V-8-like driving performance from the down-sized 4-cylinder VCR engine. Fleet operators are potential early adopters of the Envera VCR engine technology for use in light-duty delivery vans and pickup trucks. Replacing current V-8 engine offerings in these vehicles with a 4-cylinder VCR engine has the potential for improving fuel economy by about 40% while retaining full engine power. The VCR engine can provide similar fuel economy benefits in other vehicle types such as passenger cars and sport utility vehicles.

Under the current project Envera plans to demonstrate the benefits of the Envera VCR engine to prospective early adopters of the VCR technology, while concurrently pursuing mass-market commercialization of the VCR engine, the Eaton VVA and advanced supercharging technologies.

APPROACH

The current project includes three phases. In Phase 1 the general feasibility of attaining performance goals will be assessed. The assessment will also include a detailed assessment of boosting system options using GT-POWER modeling, and down-selection of the boosting system approach to be used for the project. Durability of the VCR engine power take-off coupling will also be assessed. In Phase 2 the VCR engine will be designed and built, including the VCR crankcase, VVA-equipped cylinder head, and advanced supercharging installation. In Phase 3 the engine will receive baseline calibration and testing. Engine and chassis dynamometer testing will then be conducted to quantify baseline fuel economy improvements and performance. The current project builds on earlier development efforts, including a VCR crankcase and actuator development, and a 1.8-L VCR engine built for Oak Ridge National Laboratory for combustion research.

RESULTS

Engine Efficiency

The Toyota Prius engine is a benchmark for engine efficiency for the current project. The Prius engine attains high efficiency through use of the Atkinson cycle, exhaust gas recirculation (EGR) and low internal engine friction. The engine has a peak efficiency of about 220 g/kWh at 2,000 rpm 7.0-bar brake mean effective pressure (SAE International Paper 2009-01-1061).

Prius cam timing and compression ratio values are fully attainable with the Envera VCR engine. GT-POWER modeling has shown that the higher compression ratio capability of the Envera VCR engine provides additional benefits.

The Prius EGR system is a highly successful mass production technology that further enhances the fuel efficiency of the Atkinson cycle. Success of the Prius EGR system and its current mass production status are the principal reasons why Envera is using this EGR approach.

The Prius engine has exceptionally low internal friction losses. Attaining similarly low friction losses in the VCR engine will be challenging. VCR technology enables peak cylinder pressures to be lowered, which is beneficial for designing lower friction bearings and piston ring packs. The supercharging system will include clutch-out technology to reduce engine friction at lower power levels. Other friction reduction technologies will be used, including an electric water pump and roller cam followers.

Engine down-sizing is a core strategy used throughout the automotive industry, but not with the Toyota Prius (or Mazda SkyActiv, another high-efficiency Atkinson Cycle engine). The Atkinson cycle is achieved using late intake valve closing and a long duration intake cam. When high-power levels are needed, the intake camshaft is phase shifted to close sooner for trapping more air in the cylinders to generate more power. Unfortunately, the phase shifting also causes the intake valve to open sooner, well before the piston top-dead center position. The early intake valve opening results in high levels of internal EGR, and the heat of this exhaust gas can cause engine knock. To prevent knock, engine torque is limited, which prevents use of the down-sizing strategy.

With the Envera VCR engine, the fuel economy benefits of the Prius engine are combined with aggressive engine downsizing. This is made possible with the Eaton cam profile switching rocker arm. With the switchable cam profiles, internal EGR can be restricted, enabling higher boost levels to be attained without detonation. Furthermore, compression ratio can be lowered with the VCR. With the Envera VCR engine the Atkinson Cycle and downsizing strategies can both be used for improving fuel economy.

Engine Performance Targets

Pickup trucks, utility vans, and light aircraft have been identified as potential early adopter markets for the Envera VCR engine technology. The market for utility vans is much larger in Europe. Because of these higher sales volumes, Europe needs to be included in the utility van commercialization game plan for the VCR engine. The power and torque required for European vans is less demanding than for the U.S. market.

The power and torque needs are significantly higher for full-size U.S. pickup trucks. The major manufacturers of full-size pickup trucks offer a large range of engine power and torque values. Envera will target the power and torque values of the highest sales volume engines used in full-size pickup trucks. These values are approximately 360 hp and 360 ft-lb torque.

The Envera VCR engine will attain high mileage through engine down-sizing plus use of the Atkinson cycle. The VCR engine will also be supercharged to provide high-power levels to meet U.S. commercial needs.

VCR Engine Power and Torque Assessment

The ability of the Eaton VVA mechanism (shown in Figure 1) to provide both Atkinson and high-power cam profiles was assessed. Envera generated baseline valve lift and valve timing values for attaining high efficiency using the Atkinson cycle and also for attaining high power levels with supercharging. Eaton then developed valve lift profiles to the specifications provided by Envera to determine if the target values are attainable. Kinematic

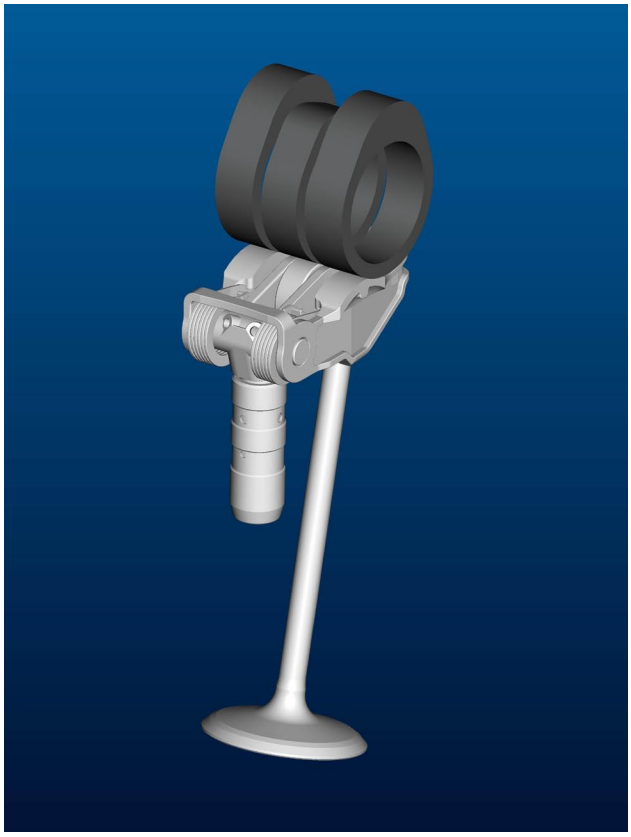

FIGURE 1. Eaton Variable Valve Control Rocker Arm

calculations conclude that the Eaton VVA mechanism can be utilized for late intake valve closing to enable a switchable Atkinson cycle combustion strategy. The analysis indicates that the target values can be attained. A more detailed assessment is currently in progress using computer GT-POWER modeling.

VCR engine performance targets were assessed with Eaton's advanced supercharger technology and VVA. The preliminary analysis indicated that the minimum performance targets for the current project are feasible, however, which boosting system provides the least risk and the highest power and torque results is unclear. Several boosting system technologies are currently being evaluated using GT-POWER computer software modeling.

Engine Management System

An engine management component specification has been developed. Engine management and calibration efforts can be very costly. A goal is to lessen those costs through advanced development work. The advanced development work includes component specification and characterization and calibration approach.

Engine Design

The General Motors 2.5-L model year 2014 Ecotec engine has been selected as the platform engine model for the project. Under the current project, a VCR crankcase has been developed that mates with the Ecotec cylinder head. Advanced supercharging and variable valve control will also be added to the engine.

Figures 2 through 4 show design details for the VCR engine. The VCR crankcase and cradle packaging design

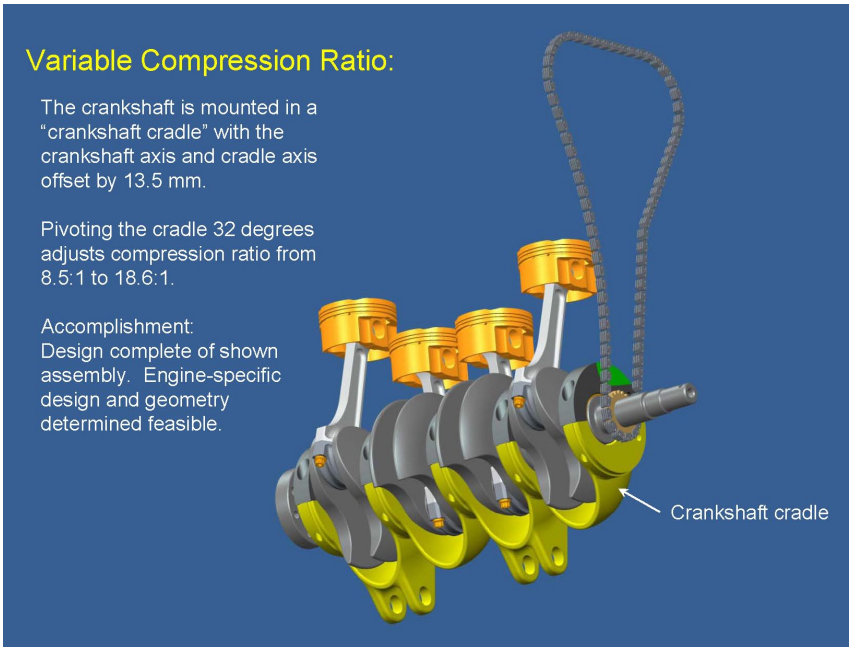

FIGURE 2. Envera VCR Mechanism

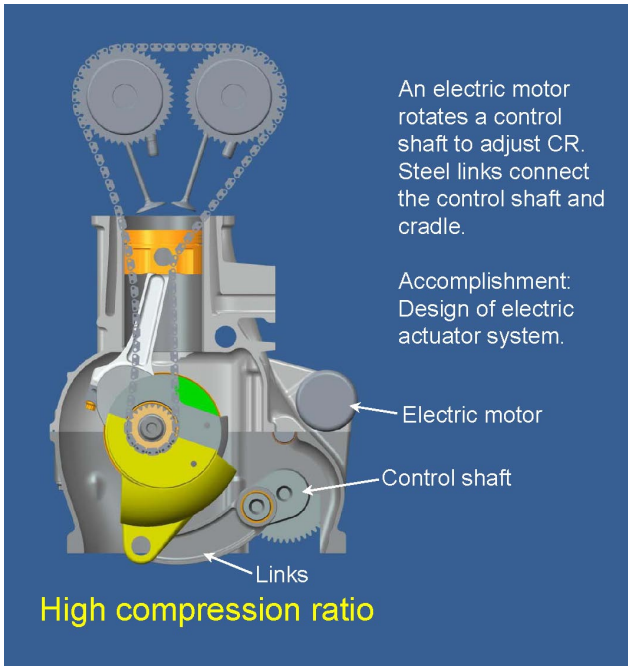

FIGURE 3. Envera VCR Engine Shown at High Compression Ratio

has exceeded expectations. Design upgrades from prior VCR engine builds include:

- Ring dowels used on all main fasteners for added stiffness
- Large clearances between the main bolt columns and cradle for lower-cost casting tolerances
- Raised cradle bearing race for easier and lower cost machining
- Off-set rails on the cradle bearing backs for easier assembly
- No cutout in the cradle for actuator space, to provide a stiffer cradle

CONCLUSIONS

the Envera VCR engine, the efficiency benefits of Atkinson cycle engines (such as the Toyota Prius engine) are being combined with aggressive engine downsizing to attain large gains in fuel economy.

Valve lift and duration values needed for Atkinson and Otto Cycle operation were projected to meet project needs. GT-POWER modeling is currently in progress to determine which boosting configuration to use on the current project. During FY 2015 a high-efficiency VCR engine will be designed and built.

FY 2014 PUBLICATIONS/PRESENTATIONS

1. DOE Annual Merit Review presentation, June 20, 2014.

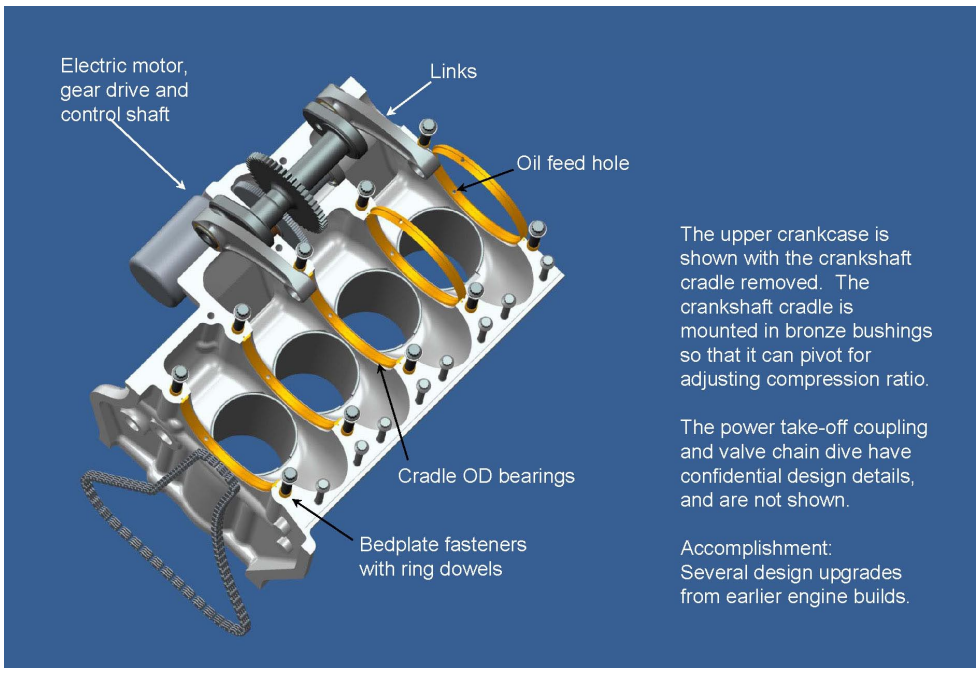

FIGURE 4. Envera VCR Crankcase

IV.15 Recirculated Exhaust Gas Intake Sensor (REGIS) Enabling Cost-Effective Fuel Efficiency Improvement

Claus Schnabel (Primary Contact), Karen Carwile, Julia Miersch

Robert Bosch LLC
38000 Hills Tech Drive
Farmington Hills, MI 48331

DOE Technology Development Manager
Roland Gravel

NETL Project Manager
Ralph Nine

Subcontractors
- Clemson University, Robert Prucka, PhD, Greenville, SC
- Oak Ridge National Laboratory, Scott Sluder, Knoxville, TN

Overall Objectives

- The primary objective of this project is to develop an intake air oxygen (IAO2) sensor which directly and accurately measures the oxygen concentration in the intake manifold.
- This project will address the technical barriers in fundamental research, technology application, and system implementation to accelerate the development of an IAO2 sensor to directly and accurately measure the oxygen concentration in the intake manifold for gasoline engines using external exhaust gas recirculation (EGR).

Fiscal Year (FY) 2014 Objectives

- Development of a control algorithm that uses the accurate IAO2 sensor oxygen concentration measurement to maximize combustion efficiency, and improve fuel economy.
- Quantify fuel economy gain potential when using IAO2 sensors for EGR control in a turbocharged direct-injection spark-ignition engine.
- Fabrication of IAO2 sensors.
- Validation of first generation IAO2 sensor design (component and engine durability).
- Identification of further improvement potential on base of component validation and cooled EGR (cEGR) system analysis.
- Set up and conduct design work to incorporate lessons learned from component validation and cEGR system analysis performed in Phase I and Phase II.

FY 2014 Accomplishments

- An EGR control algorithm that utilizes an IAO2 sensor was developed, calibrated, and implemented in a rapid-prototype engine control unit (ECU) for dynamometer cell validation at Clemson University. The control algorithm predicts cylinder-by-cylinder EGR percentages based on intake system models and IAO2 sensor readings. Experimental validation/refinement of the new algorithm is currently in progress.
- Engine and vehicle simulation results suggest that maximum fuel economy gain potential when using an IAO2 sensor for EGR control is approximately 1-2% for spark-ignition engines. This is compared to current state-of-the-art model-based EGR control systems.
- Testing and validation of design concept for IAO2, which was completed in Phase I. Focus of component design and research continued to be on the subsystems sensor connector and housing as well as the protection tube.
- Development of protection tube led to benchmark functional performance in its design space.
- Testing also identified need to explore design space in terms of robustness against deposits.
- Testing and validation of the IAO2 design variant resulted in positive results for function, thermal shock, and vibration. Test results identified further development and improvements for deposits and sealing.

Future Directions

- Engine dynamometer testing of sensors and control algorithm to validate the fuel economy, emissions, and durability performance of the IAO2 sensor and control algorithm.
- Develop concept for second generation IAO2 sensor.

INTRODUCTION

The primary objective of the REGIS project is to develop an IAO2 sensor which directly and accurately measures the oxygen concentration in the intake manifold. This capability affords vehicle manufacturers the ability to estimate the EGR percentage to a level of accuracy currently not possible. Accurate EGR estimation and resultant finer control improves engine efficiency, reduces fuel consumption, and maintains or improves exhaust emission. More specifically, measurement of the actual EGR percentage enables a significant reduction in the calibrated safety margins required due to the inclusion of component tolerances in current EGR modeling approaches. Controlling EGR usage near optimized set points with improved combustion control is an enabler for gasoline engine fuel economy improvements in modern and advanced engine concepts including conventional stoichiometric engines, advanced turbocharged and downsized engines, and homogeneous-charge compression-ignition engines.

APPROACH

The project will redesign the current generation of wideband exhaust gas oxygen sensors to meet the requirements of the intake manifold environment. The major challenges, as identified by Bosch internally and reported in the technical literature, of thermal shock, contamination, accuracy, pressure dependency, and response time will be addressed through design improvements. Clemson University, in collaboration with Bosch, will develop and validate robust control algorithms using the IAO2 measured oxygen concentration to improve combustion efficiency. Engine dynamometer tests will verify fuel economy improvements and sensor robustness to function and environment for gasoline engines with high concentrations of external EGR.

RESULTS

Simulation-based fuel economy improvement predictions due to intake oxygen sensor use were completed at Clemson University. The study investigated the benefits of using low-pressure (LP) cooled EGR with IAO2 sensing on a modern spark ignition engine. Simulations were run for low-load and high-load operation, and compared IAO2 use with the current state-of-the-art methods for controlling EGR. Fuel efficiency benefits of LP cooled EGR for part-load operation when using a intake oxygen sensor show approximately 3% fuel economy improvement over a vehicle drive-cycle. These results are based on steady-state engine efficiency assumptions, and real-life results with a realistic transient control strategy are expected to be in the range of 1-2%. At high engine loads, where knock and exhaust temperature constraints reduce fuel economy, the use of intake oxygen sensing for EGR control has the potential in improve fuel consumption in the range of 5% or more (some points produced gains above 15%). These fuel economy predictions suggest that the price per fuel economy gain of an IAO2 sensor is extremely competitive with other technologies, and will likely be accepted by automobile manufacturers. A key project objective is to produce a product that allows for a cost-effective fuel economy gain, and these results suggest that this objective is achievable.

An IAO2-based LP EGR control system was developed and implemented in the engine dynamometer cell at Clemson University during this period. The control-oriented model for estimation of EGR transport delays in the air-path was developed using GT-POWER, MatLAB® and Simulink®, as shown in Figure 1. Initial model testing was done by interfacing Simulink® with GT-POWER to compare control performance with simulation predictions. The control model was then tested in real-time on-engine using the setup shown in Figure 2 that utilizes an ETAS-910 rapid prototyping controller. Initial testing results in Figure 3 of calculated EGR transport delays by the control model from IAO2 sensor to throttle plate (one of three transport delay regions calculated by the model) show prediction accuracy in the range of one engine cycle at most operating conditions. Transport delays from exhaust oxygen sensor to EGR valve and from EGR valve to intake oxygen sensor were also validated, and a real-time closed-loop EGR valve control algorithm is currently being tested. Initial control model results suggest that IAO2 sensors will be

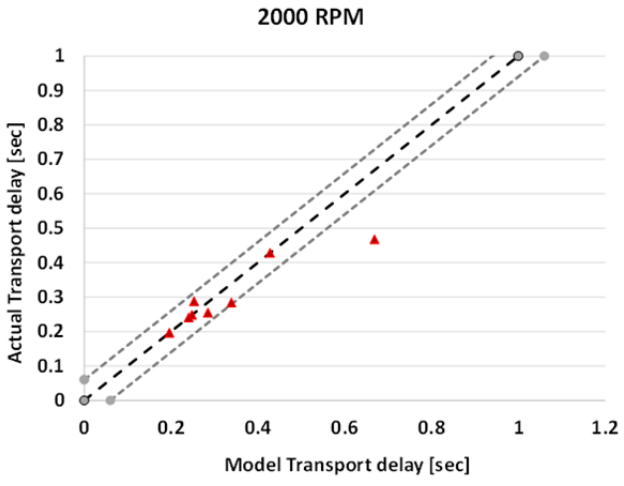

FIGURE 1. The IAO2-Based LP-EGR Control Strategy Accounts for Transport Delays Through the Engine Air Path to Accurately Determine EGR Cylinder-By-Cylinder

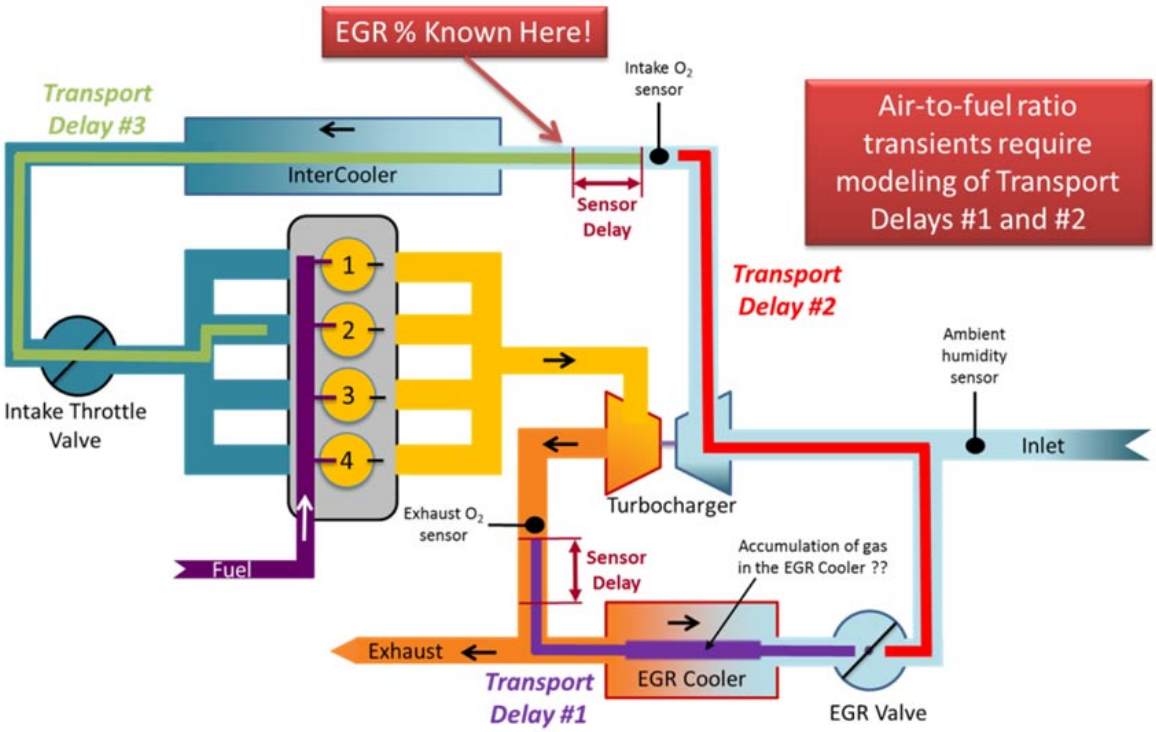

FIGURE 2. Software and Hardware Architecture being utilized to Assess IAO2-Based EGR Control Strategies at Clemson University

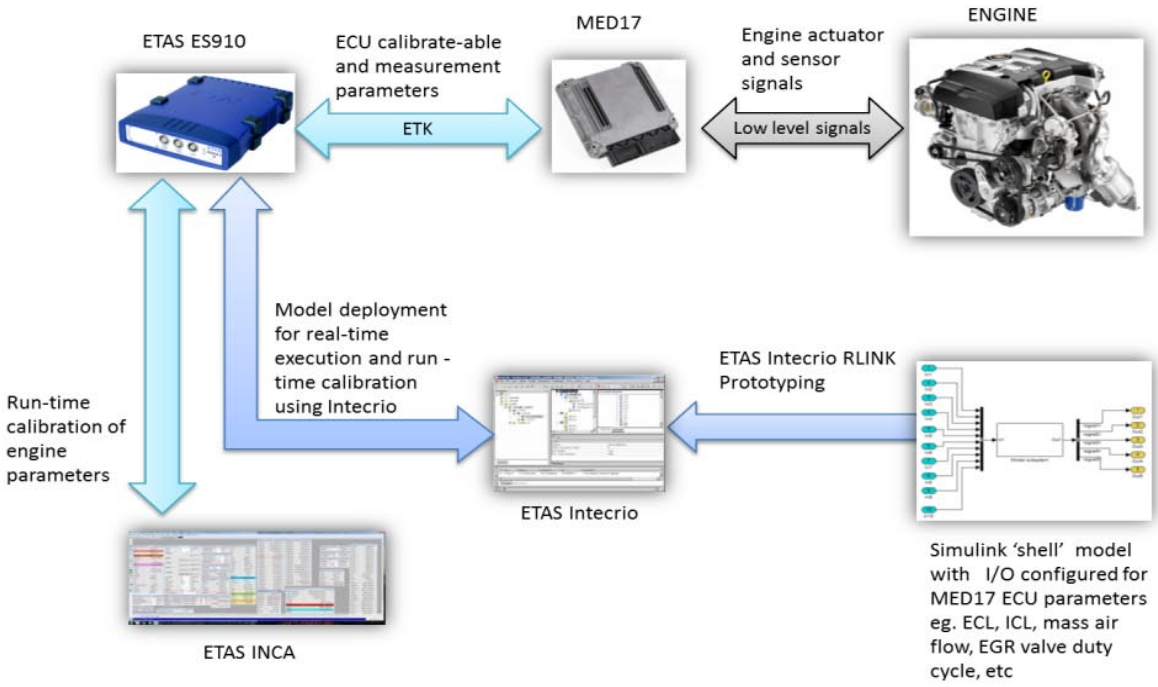

FIGURE 3. Comparison of Actual and Control Model Transport Delays from Engine Experiments

a very effective way to adapt feed-forward EGR control models over time. Traditional feed-forward models tend to become inaccurate over time due to lack of feedback, so the new sensor and control algorithm can help solve a significant performance issue during engine aging. The controls system also seems to be accurate enough to allow nearly cycle-by-cycle correction of air flow prediction (and hence more accurate fuelling), as well as combustion phasing control. Both of these aspects have the potential to further improve fuel economy in real-world operation.

The IAO2 sensor improves EGR path control, and allows for higher EGR levels than traditional model-based control approaches. The use of higher EGR levels improves fuel economy, but has the potential to further complicate transient engine control, particularly in aggressive throttle tip-outs. An engine control strategy to mitigate this issue was started during this period. The strategy is used to control both external and internal EGR levels during transient operation. It will use variable valve timing actuation to limit the burned gas dilution to an acceptable level, since any EGR valve actuation is associated with long transport delays to the cylinders. The base control algorithm to address aggressive transients was developed during this phase, and extensive GT-POWER simulations are currently in progress to provide the required data needed to populate control models

Sensor concept evaluation was based on the 35-mm diesel element for use in lean environments. This element is stable in lean conditions, has a low pressure dependency and has a strong heater that is optimized for high and cold flow rates even when using open type protection tubes making it suitable for the intake application. Adopting a direct connector for packaging constraints under the hood in the engine was important for the tight space. Other inputs into the design concept were a serious consideration for high communality to the existing production line to allow quick access into serial production and an optimized protection tube for use the severe intake environment. A decision to go forward with a duel bolt design for fixturing in the application was made based on customer input.

Testing of the IAO2 sensor demonstrated that the durability of the parts were acceptable for the intake environment. Parts were evaluated for static temperature mapping in the vehicle showing that the temperature distribution did not exceed the materials rating for the connector. Additionally, functional testing before and after thermal shock testing in a range from -40°C to 150°C for 500 cycles showed no failures. This was also the case for the Brine Thermal shock testing and the two types of vibration testing performed—Sine Vibration and wideband vibration. Two parts did not pass the bubble leak test with one bubble after 5 minutes. Further analysis is in process.

To evaluate deposit behavior, parts were placed in a test established to evaluate deposit behavior in exhaust sensors. In parallel, a test is being designed for intake oxygen sensors. The result of the exhaust sensor test identified the need for some improvements against deposits. Current results for the IAO2 designed protective tube demonstrated that it behaved in a similar manner to the current protective tubes.

For the second recursion on the IAO2 sensor, further investigation will be made into the sealing of the connector housing the sleeve. Also, additional investigation into deposit robustness using an intake system model which would include an extended look at the unique environment of the intake.

CONCLUSIONS

- Engine and vehicle simulation results show a potential of 1-2% gain in fuel economy of cEGR systems running with oxygen sensors compared to systems running on model base EGR control.
- To support this work an EGR control algorithm that utilizes an IAO2 sensor was developed, calibrated, and implemented in a rapid-prototype ECU at Clemson University.
- IAO2 prototypes were manufactured on base of comprehensive system and component research during Phase I and Phase II.
- Testing and validation of the build IAO2 prototypes resulted in positive results for function, thermal shock, and vibration. Test results identified further development and improvements for deposits and sealing to be addressed and validated in Phase III.

FY 2014 PUBLICATIONS/PRESENTATIONS

1. Clemson University published one paper titled “Assessment of Simulation-Based Calibration for Fuel Economy Optimization,” that summarizes and evaluates the fuel economy estimation study. The results were presented at the IAV 3rd Conference on Design of Experiments (DoE) in Engine Development, Plymouth, MI.

IV.16 Robust Nitrogen Oxide/Ammonia Sensors for Vehicle Onboard Emissions Control

Rangachary Mukundan[1] (Primary Contact), Cortney Kreller[1], Vitaly Y. Prikhodko[2], Josh A. Pihl[2], Scott Curran[2], James E. Parks II[2], Wenxia Li[3], Ponnusamy Palanisamy[3] and Eric L. Brosha[1]

Los Alamos National Laboratory (LANL)
MS D429, PO Box 1663
Los Alamos, NM 87544

DOE Technology Development Manager
Roland Gravel

No Cost Partner
[2]Oak Ridge National Laboratory (ORNL),
Oak Ridge, TN

Subcontractor
[3]ESL ElectroScience, King of Prussia, PA

Overall Objectives

- Develop prototype oxides of nitrogen (NO_x) sensor based on mixed-potential technology using a $La_{1-x}Sr_xCrO_{3-d\delta}$ (LSC) sensing electrode.
- Develop prototype NH_3 sensor based on mixed-potential technology using an Au sensing electrode.

Fiscal Year (FY) 2014 Objectives

- Demonstrate quantitative NO_x sensor performance in engine dynamometer environment.
- Demonstrate 10 ppm NH_3 sensitivity in commercially manufacturable sensor prototype.
- Optimize electrode composition and operating conditions for NO_x sensor to improve sensitivity and response time.

FY 2014 Accomplishments

- Sensor quantitatively tracks NO_x and hydrocarbon (HC) concentration in engine dynamometer testing performed both during start up and when operated in EGR step mode.
- Demonstrated 5 ppm NH_3 sensitivity in a Pt/ytrria-stabilized zirconia (YSZ)/Au sensor manufactured by ESL ElectroScience (ESL). Also demonstrated stable performance over 1,000 hours of operation in the laboratory.
- Demonstrated an effective overcoat layer to improve sensor durability in engine environments.

Future Directions

- Validate NH_3 sensor in an engine environment for the first time.
- Extend validation of HC and NO_x sensors to a lean-burn gasoline engine environment.
- Evaluate sulfur tolerance of both NO_x and NH_3 sensor.
- Demonstrate improved sensor selectivity/sensitivity through use of catalyst over coat and electrode composition optimization.
- Explore commercialization partners for unique sensing technology.

INTRODUCTION

The 2010 Environmental Protection Agency (EPA) emissions regulation for NO_x is 0.2 g/bhr-hr, and the EPA has started to certify vehicles that can actually meet this regulation. Most manufacturers had initially opted instead to meet a family emission limit around 1.2-1.5 g/bhp-hr NO_x with most of their vehicle emissions lying between the two standards [1]. Currently the EPA has certified engines with both the exhaust gas recirculation (EGR) and selective catalytic reduction (SCR) technologies to meet the strict 0.2 g/bhr-hr NO_x standard. While there is only one EGR system that has been certified by the EPA as meeting 2010 emissions regulations (Navistar, Inc.), there are several SCR systems that can meet this requirement (Cummins, Detroit Diesel, Volvo, etc.). Moreover the SCR system in addition to meeting emissions regulations can result in a 3 to 5.5% increase in fuel efficiency [2].

The SCR system typically uses a zeolite NO_x adsorption catalyst that can selectively adsorb NO_x molecules during lean-burn operation and convert it to N_2 and H_2O with the injection of a urea water solution called diesel exhaust fluid. It is the technology of choice for emissions control in Europe and several manufacturers have adopted this for the United States. SCR systems require tuning to work properly and systems can be tuned with either preexisting engine performance curves or with NO_x/NH_3 sensors. The use of NO_x/NH_3 sensors

can provide closed-loop control of the SCR system that can optimize the system for improved NO_x reduction efficiencies and low NH_3 slip. According to a recent review "Reliable and accurate NO_x sensors will be the key to the management of adsorption catalysts" [3]. The optimized use of SCR systems can increase the value for the customer with fuel and diesel exhaust fluid savings (including reduced frequency and costs of the dealer servicing of the emissions system consumables) over the life of the vehicle helping defray the added cost of the system.

APPROACH

LANL has previously developed a new class of mixed-potential sensors that utilize dense electrodes partially covered with porous and/or thin film electrolytes [4-8]. This unique configuration stabilizes the three-phase (gas/electrode/electrolyte) interface resulting in sensors with exceptional response stability and reproducibility. This configuration also minimizes heterogeneous catalysis resulting in high sensor sensitivity. Moreover, the electrode composition of these sensors can be varied to tune the selectivity relative to desired exhaust gas species. For example, a gold electrode has high NH_3 selectivity while a LSC electrode provides high HC or NO_x selectivity. When the sensors using LSC electrodes are operated at open circuit, the voltage response is proportional to non-methane hydrocarbons and when they are operated under a current/voltage bias mode, the response is proportional to total NO_x.

The unique mixed potential electrochemical sensors developed at LANL were experimental, laboratory devices. Moreover, the sensors were bulk, hand made devices that required a large external furnace for precise temperature control during operation. In this project LANL is working closely with ESL to apply commercial manufacturing methods to LANL laboratory NO_x sensor configurations. Through an iterative process of prototype preparation at ESL, laboratory testing and materials characterization at LANL, and a free exchange of performance and characterization data between LANL and ESL, the performance of the bulk sensors will be reproduced in a commercially manufacturable device. These devices are being evaluated under realistic engine exhaust conditions at the National Transportation Research Center in ORNL. Interest in this technology from commercial sensor manufacturing companies and end users of this technology is currently being evaluated in order to find a commercialization partner for this promising technology.

RESULTS

In FY 2013, we reported on the initial testing and performance of LANL patented mixed potential sensors manufactured by ESL using a commercial high-temperature co-fired ceramic process. The NO_x sensors exhibited a sensitivity of ± 5 ppm and showed little drift over 1,000 hours of operation. Preliminary testing at ORNL in engine conditions provided qualitative correlation of sensor response to NO_x concentration in the exhaust stream. However, temperature control of these sensors was identified as critical and LANL worked closely with Custom Sensor Solutions Inc. to manufacture heater control boards for heater feedback control.

In FY 2014 we continued extensive testing at ORNL's National Transportation Research Center on a 1.9-Liter Opel (General Motors) turbocharged diesel engine equipped with exhaust gas recirculation (EGR), a diesel particle filter and a diesel oxidation catalyst. The sensor setup was significantly modified from the first round of testing performed in FY 2013. The sensor holder was updated to avoid liquid water condensation on the sensor body and a new heater resistance control and measurement circuit was added. This modification allowed the sensor to be placed directly in the gas stream in front of the analytical equipment that measured the NO_x (Fourier transform infrared spectroscopy) and HC (FID) concentrations. The sensor was operated in both HC mode (no current bias) and NO_x mode (under positive current bias) and the response was compared to the gas composition measured using the analytical equipment. Figure 1a illustrates the relationship observed between the HC sensor response and the natural logarithm of the FID diesel concentration. The slope of the line was constant (0.02) irrespective of the HC concentration and mode of operation (start-up, EGR on/off) or location of sensor (engine-out, diesel oxidation catalyst-out). This slope was greater than the slope (0.016) measured with propane in the laboratory, consistent with the fact that the carbon number in the diesel exhaust is greater than 3. Figure 1b illustrates a similar relationship for the NO_x sensor where the sensor is operated under bias. Although there are variations between the EGR on/off and EGR step experiments, the sensor response matched the laboratory calibration as long as the NO/NO_2 concentration was kept constant.

In FY 2014 ESL prepared for the first time an NH_3 sensor using platinum and gold electrodes and a YSZ electrolyte. The response of this sensor to varying NH_3 concentration is illustrated in Figure 2a where a response of ≈10 mV was observed for 10 ppm of NH_3. The step response illustrates a fast (≈ 1 sec response time) and reproducible response to NH_3. The selectivity of the sensor is illustrated in Figure 2b where the NH_3

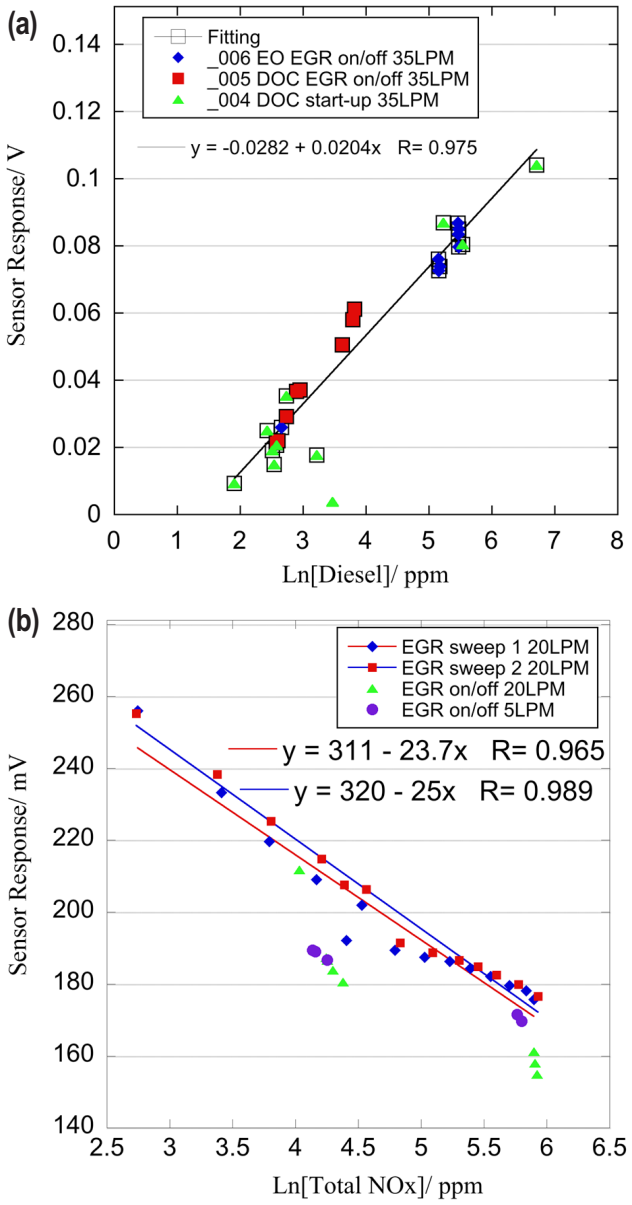

FIGURE 1. Response of LANL sensor operated in an engine environment compared to the a) HC and b) NO_x concentration measured by analytical instrumentation.

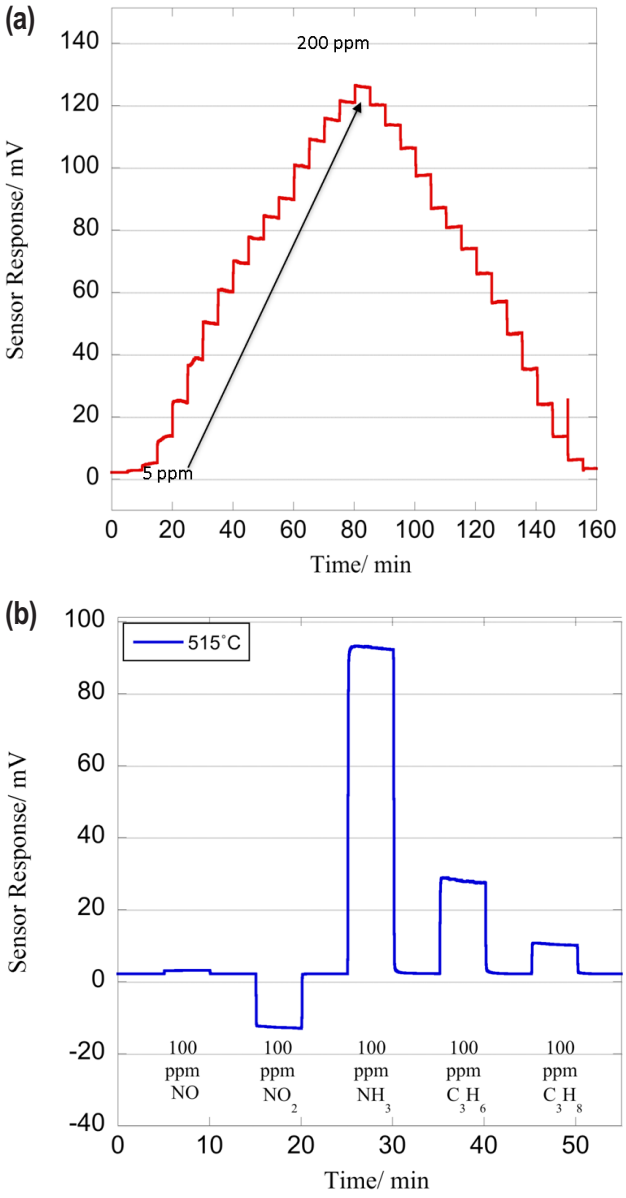

FIGURE 2. a) Sensitivity and b) Selectivity of a Pt/YSZ/Au NH_3 sensor operated in the laboratory.

response is at least three times greater than the response to any other gas. The main interferent gas under these conditions is expected to be NO, to which the sensor is insensitive. The selectivity of the sensor can be further improved by increasing the operating temperature. However the response to NH_3 decreases with increasing temperature. The optimum operating temperature of the NH_3 sensor was found to be between 500 and 525°C. The stability of the NH_3 sensors was also evaluated and is shown in Figure 3. While there is little change in sensor response during the 1,000 hour of testing, when the sensors were temperature cycled, X-ray tomography and scanning electron microscopy analysis reveled that the Au electrode was susceptible to peeling off from the electrolyte. Furthermore this effect could potentially be avoided, and the durability of the sensors significantly increased by use of an overcoat.

The sensing elements of most electrochemical sensors are protected by an overcoat material and in FY 2014 ESL prepared the first LANL-patented sensors using an overcoat. These sensors are illustrated in Figure 4a and their response to various gases at different temperatures is shown in Figure 4b. The sensor response is qualitatively similar to the uncoated sensor with the response decreasing with increasing temperature with

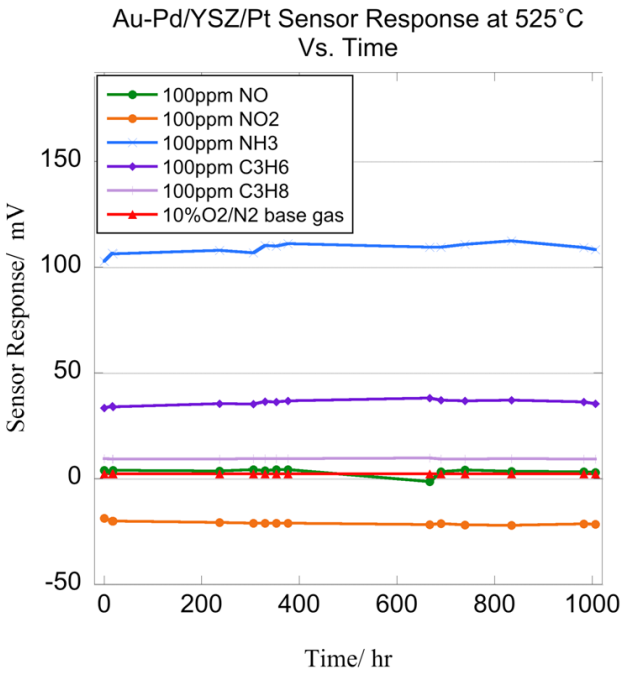

FIGURE 3. Stability of the NH_3-sensor over 1,000 hours at an operating temperature of 525°C.

maximum selectivity towards NO and NO_2. However, comparison to the un-coated sensor revealed that the sensor temperature was hotter for any given heater power, indicating that the overcoat served as a heat blanket. In addition to lowering the heater power the overcoat has the potential to increase the electrode stability under thermal cycling. Finally the overcoat will serve as a substrate to deposit/coat a catalyst layer to improve sensor selectivity.

CONCLUSIONS

- The NO_x sensor quantitatively tracked the NO/NO_2 concentration in a 1.9-L diesel engine:
  - NO_x response was proportional to the logarithm of the NO_x concentration measured by Fourier transform infrared spectroscopy.
  - Calibration is dependant on the NO/NO_2 ratio since response to NO and NO_2 are not identical.
- The HC sensor quantitatively tracked the HC concentration in a 1.9-L diesel engine:
  - HC sensor response was proportional to the logarithm of the HC concentration measured by the FID under varying conditions (EGR on/off, stepped EGR) at various locations (engine-out and diesel oxidation catalyst-out).

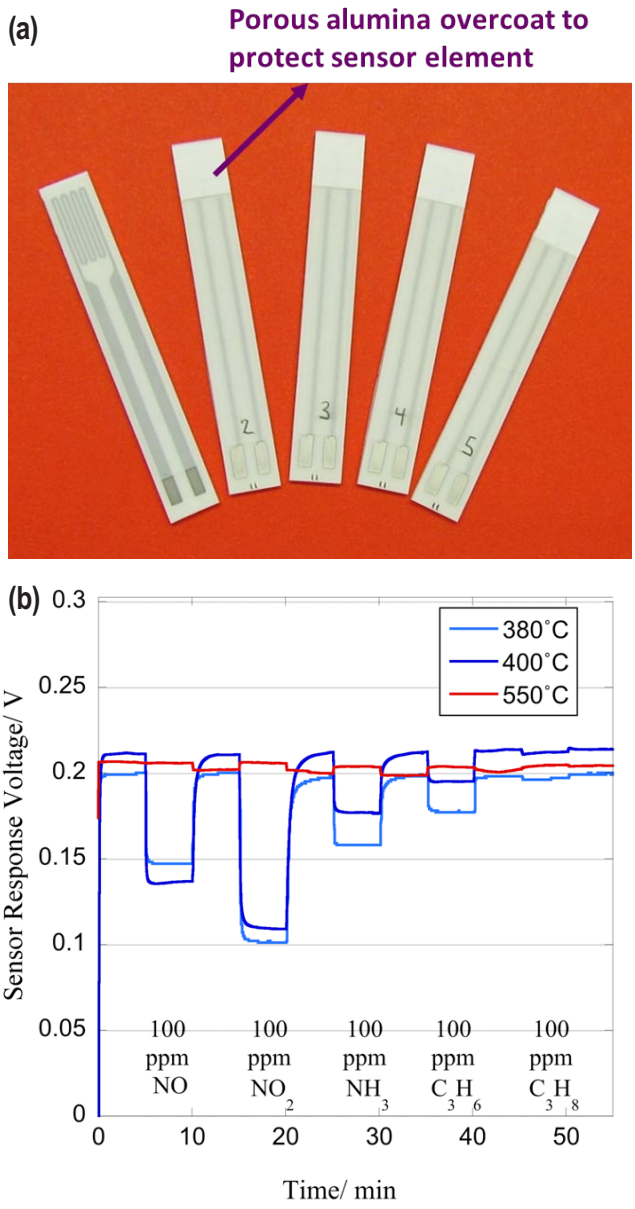

FIGURE 4. a) Picture of the NO_x sensor showing the overcoat, and b) response of the sensor with overcoat operated under various gases at different temperatures.

  - Calibration is dependant only on the carbon number of the HCs.
- ESL utilized the high-temperature co-fired ceramic process to successfully manufacture NH_3 sensors based on the LANL sensor design.
  - The NH_3 sensitivity was ≈ 10 mV for 10 ppm of NH_3.
  - The NH_3 selectivity was three times that of propylene and >10 times that of NO.
- Protective overcoat was applied to the NO_x sensors:

  - Overcoat results in lowered heater power.
  - Overcoat results in better sensor stability to thermal cycling and can serve as substrate to add an additional catalyst layer.
- LANL will seek industrial partners to commercialize this promising technology.

REFERENCES

1. Diesel Power: Clean Vehicles for Tomorrow. Vehicle Technologies Program, U.S. Department of Energy, July 2010.

2. T.V. Johnson, "Review of Diesel Emissions and control," International Journal of Engine Research, V10. No 5, 275 (2009).

3. N. Docquier, S. Candel, "Combustion control and sensors: a review," Progress in Energy and Combustion Science, V 28, 107 (2002).

4. R. Mukundan, E.L. Brosha and F. H. Garzon. US Patent # 7,575,709 B2, "Tape Cast Sensors and Method of Making;" August 18, 2009.

5. F.H. Garzon, E.L. Brosha and R. Mukundan. US Patent # 7,264,700, "Thin Film Mixed Potential Sensors;" Sept. 4, 2007.

6. R. Mukundan, K. Teranishi, E.L. Brosha, and F.H. Garzon, "Nitrogen oxide sensors based on Yttria-stabilized zirconia electrolyte and oxide electrodes." *Electrochemical and Solid-State Letters*, **10(2)**, J26-J29 (2007).

7. F.H. Garzon, E.L. Brosha, and R. Mukundan, "Solid State Ionic Devices for Combustion Gas Sensing." *Solid State Ionics*, **175(1-4)**, 487-490 (2004).

8. R. Mukundan, E.L. Brosha and F.H. Garzon. US Patent # 7,575,709 B2, "Tape Cast Sensors and Method of Making;" August 18, 2009.

FY 2014 PUBLICATIONS/PRESENTATIONS

1. C.R. Kreller, D. Spernjak, W. Li, P. Palanisamy, E.L. Brosha, R. Mukundan, and F.H. Garzon, "Mixed-Potential NO_x and NH_3 Sensors Fabricated by Commercial Manufacturing Methods," Presented at 226th ECS Meeting, Cancun, Mexico, October 2014.

2. C.R. Kreller, R. Mukundan, F.H. Garzon, and E.L. Brosha, "Mixed-potential NO_x, HC, and NH_3 Sensors for Vehicle On-Board Emissions Control," Poster presented at 2014 DOE Crosscut Workshop on Lean Emissions Reduction Simulation. April 29th – May 1st, 2014.

3. C.R. Kreller, P.K. Sekhar, V.Y. Prikhodko, J.A. Pihl, S. Curran, J.E. Parks II, E.L. Brosha, R. Mukundan, and F.H. Garzon, "Dynamometer Testing of Planar Mixed-Potential Sensors," Presented at the 225th ECS Meeting, Orlando, May 2014.

4. E.L. Brosha, C.R. Kreller, R. Lujan, D. Spernjak, R. Mukundan, F.H. Garzon, W. Li, P. Palanisamy, V.Y. Prikhodko, J.A. Pihl, S. Curran, J.E. Parks II, "Robust Nitrogen Oxide/Ammonia Sensors for Vehicle On-Board Emissions Control," Presented at CLEERS Teleconference (Feb 2014) and USCAR teleconference (March 2014).

5. J. Tsitron, C.R. Kreller, P.K. Sekhar, R. Mukundan, F.H. Garzon, E.L. Brosha, A.V. Morozov, "Bayesian decoding of the ammonia response of a zirconia-based mixed-potential sensor in the presence of hydrocarbon interference," *Sensors and Actuators B*, **V 192**, 283-293 (2014).

V. SOLID STATE ENERGY CONVERSION

V.1 Gentherm Thermoelectric Waste Heat Recovery Project for Passenger Vehicles

V. Jovovic (Principle Investigator) [1], D.Lock[1], C. Maranville[2], C. Haefele[3], M. Miersch[4]
[1]Gentherm Inc.
5462 Irwindale Ave.
Irwindale, CA 91706
[2]Ford Motor Company
[3]BMW AG
[4]Tenneco GmbH

DOE Technology Development Manager
Gurpreet Singh

NETL Project Manager
Carl Maronde

Subcontractors
- BMW, Palo Alto, CA and Munich, Germany
- Ford Motor Company, Dearborn, MI
- Tenneco GmbH, Grass Lake, MI and Edenkoben, Germany

Overall Objectives

- A detailed production cost analysis for a thermoelectric generator (TEG) for passenger vehicle volumes of 100,000 units per year and a discussion of how costs will be reduced in manufacturing.
- A 5% percent fuel economy improvement by direct conversion of engine waste heat to useful electric power for light-duty vehicle (LDV) application. For light-duty passenger vehicles, the fuel economy improvement must be measured over the US06 cycle.
- Confirmatory testing of the hardware to verify its performance in terms of fuel economy improvement.
- Build a scaled-up TEG for the TARDEC Bradley Fighting Vehicle (BFV).

Fiscal Year (FY) 2014 Objectives

- Scale up thermoelectric (TE) engine subassembly (tooling and process development)
- TE engine scalability and power form
- TE engine durability
- Scale up TEG subsystem joining technologies
- Scale up TEG fabrication concept
- Design of LDV TEGs.
- Begin bench testing of LDV TEGs.
- Complete assembly of heavy-duty vehicle (HDV) TEG and related system components.

FY 2014 Accomplishments

- Developed manufacturing processes for fabrication of TE materials
- Developed manufacturing processes for fabrication of TE engines
- Designed, built and tested TE cartridges
- Scaled up manufacturing of cartridges
- Developed models of cartridge and TEG, integrated these in vehicle
- Experimentally confirmed cartridge model
- Designed LDV and HDV generators
- Scaled up TEG fabrication concept by developing mass production design and tooling
- Bench tested partial LDV TEGs
- Developed test tools
- Developed and installed materials manufacturing tools

Future Directions

- Produce LDV TEGs for installation in Ford and BMW vehicles
- Test vehicles and measure fuel efficiency improvement at vehicle manufacturer sites
- Perform independent testing at the National Renewable Energy Laboratory (NREL)
- Analyze vehicle level test results and compare test and model data
- Deliver TEG system for the BFV to TARDEC
- Conclude project

INTRODUCTION

Rising levels of CO_2 in the atmosphere are driving stricter vehicle emission regulations aimed at reducing CO_2 generation or providing equivalent fuel efficiency improvements. Engine waste heat recovery strategies are

used to manage engine or transmission oil temperatures in order to minimize friction or to convert portions of waste heat directly into kinetic or electrical energy.

This project focuses on converting exhaust gas thermal energy into electric power. The converter is a solid state device—TEG. The first objective of this project is to design and implement TEG devices which demonstrate 5% fuel efficiency improvement for passenger vehicles. Demonstrating scalability of this design by building and testing a TEG for a BFV for TARDEC is the second objective. The ratio of the engine sizes, and thus the TEG size, for the BFV and passenger vehicles is roughly 20:1.

APPROACH

The team is led by Gentherm and structured to follow a traditional automotive supply chain hierarchy. Figure 1 shows the cartridge, the power generation device developed by Gentherm utilizing Gentherm's new technology of manufacturing thermoelectric materials. Gentherm's goal is to optimize the design of this device by maximizing power output and minimizing manufacturing cost. Products of this development are the cartridge and accompanying performance model. The cartridge (Figure 1) is the fundamental building block, a fully contained power generation device, which can be used in various configurations to design TE generators. The role of the Tier 1 exhaust supplier, Tenneco, is to design and build the complete TE power generation unit. Tenneco is applying technologies developed in packaging catalytic converters, particulate filters and other exhaust components. Tenneco uses one- and three-dimensional modeling tools in their design process to minimize the risk of mechanical failures and to optimize the number of cartridges and TEG installation position along the exhaust line. Products of Tenneco's development are the TEG and its one-dimensional performance model. Ford and BMW North America have advisory roles and act as the end customer. In the design process, the vehicle manufacturers define the vehicle level constraints and analyze the vehicle level performance of the device. In this program NREL has been tasked to perform LDV TEG testing and provide independent confirmation of device performance.

In addition to developing the demonstration TEG platform, the team's long-term goal revolves around developing a low cost manufacturing process while improving TE material performance. In this portion of the process Gentherm acts as the process developer while The California Institute of Technology (Caltech) has the role of analyzing fundamental material properties and developing future materials.

RESULTS

The objective of this project is to address the barriers to the widespread market adoption of TE power generation. This includes the production readiness of TE materials and generators, the underfloor exhaust system bypass valve, gas and liquid heat exchanger integration with the TEG, and the power management strategy for insertion of electrical power onto the vehicle bus.

To fulfill the requirements of this project Gentherm has developed methods of manufacturing TE elements which have the potential of reducing overall device cost. To increase our process throughput, Gentherm has used DOE funds to purchase and install additional powder handling and pressing equipment, doubling the process development capacity. In this project, we are addressing the reduction of TE material manufacturing cost as a parallel activity to working with current production materials required to build TE devices. Basic process parameters are defined and today we have stable processes used to manufacture metalized net shaped TE materials. Our cost studies indicate a significant reduction of the manufacturing cost as shown in Figure 2. Normalizing to cost per kg of TE materials we see that our process results in an approximate 30% reduction of

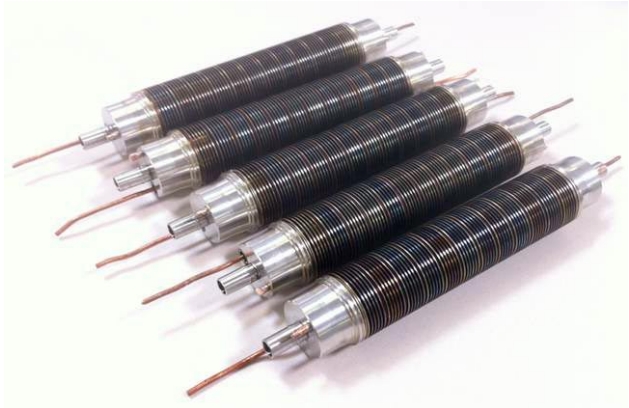

FIGURE 1. TE power generation device—cartridge.

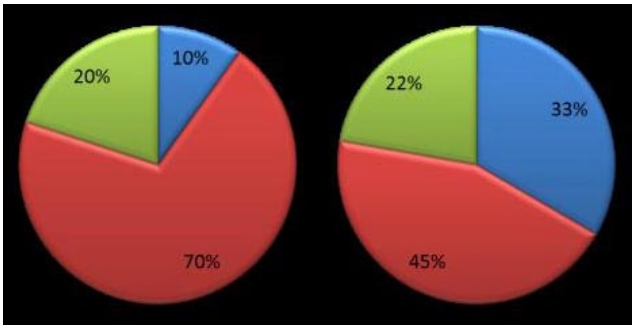

FIGURE 2. Comparison of manufacturing cost breakdown for traditional TE manufacturing process as compared to new Gentherm process.

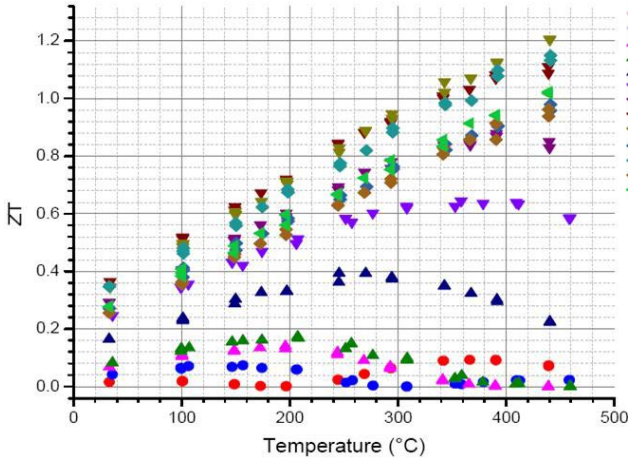

FIGURE 3. ZT values of n-type Skutterudite materials prepared at Caltech. Variations in ZT values demonstrate ability to control dopant and impurity levels and by doing so vary ZT.

the overall cost when compared to the process in which disks of TE materials are metalized and cut to size.

Process stability is monitored by measuring basic material properties such as Seebeck, electrical conductivity, thermal conductivity and calculating the resulting non-dimensional figure of merit, ZT. This data is used as reference in collaborative work with Caltech and analysis of material properties as a function of the starting materials purity, chemical composition, processing temperatures, etc. In summary, the Caltech group has developed a methodology which is required to better understand N-type $CoSb_3$ based materials. Through systematic analysis of material structure and measured properties they were able to develop material phase diagrams and characterize the electronic structure of these materials. The end result is better control of the materials' ZT as shown in Figure 3. In addition, the ZT values demonstrated by the Caltech team are 10-20% higher than those produced by materials manufactured at Gentherm.

The goal of this project is to develop a TE device concept which can be designed as a scalable system and have power output in the range from approximately ½ to 2 kW. The solution that was developed is the TEG cartridge shown in Figure 4. This device consists of internal (cold-side) and external (hot-side) heat exchangers, closely integrated with functional TE materials. The performance of this device shows improvement over that of the previous generation presented in our 2013 report. Tests indicate an additional 10-15% improvement in performance of the cartridge as a consequence of the improved assembly.

As a basic building block, the TEG cartridge is a self-contained power generation unit. This unit is used to build both light-duty vehicle TEGs with 10-12 TEG cartridges and a HDV TEG system with 56 cartridges. The power generation of these systems is 500 W and 1.5 kW, respectively. The complete design of the light-duty TEG system is shown in Figure 5. The system is developed by Tenneco and consists of a central canning section used to place 10 cartridges, bypass line and two control valves controlling the flow of gas to the TEG. Soft tooling for prototype level manufacturing of stamped components was manufactured by Tenneco and 20 sets of components were prepared for final assembly. A HDV package, design per TARDEC specifications for the BFV was prepared in the period covered by this report. The

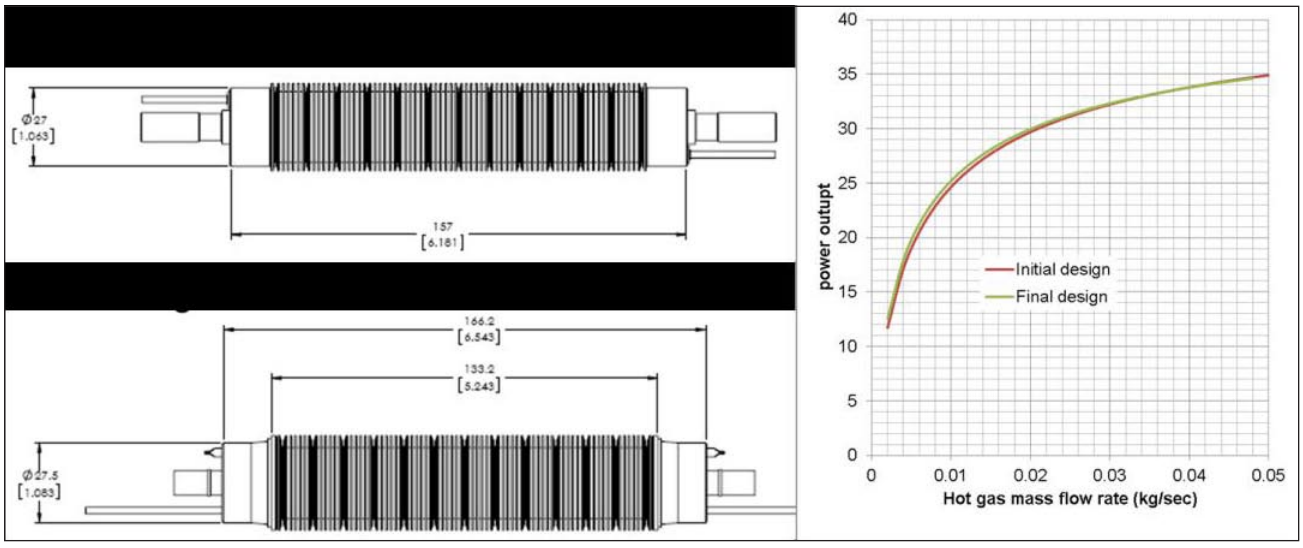

FIGURE 4. Evolution of cartridge design (left). Bottom left: geometry of cartridge for final delivery. Right: performance curves for cartridges at 600°C hot gas temperature and variable hot gas flow rate.

system shown in Figure 6 illustrates the TEG canning designed to hold 56 cartridges (4x14 units), radiators, fans, water pump and manifolds. This is a self-contained system with integrated cooling designed to fit in 2x2x4 ft space allocated by TARDEC. All system components are prepared and are waiting for delivery of cartridges.

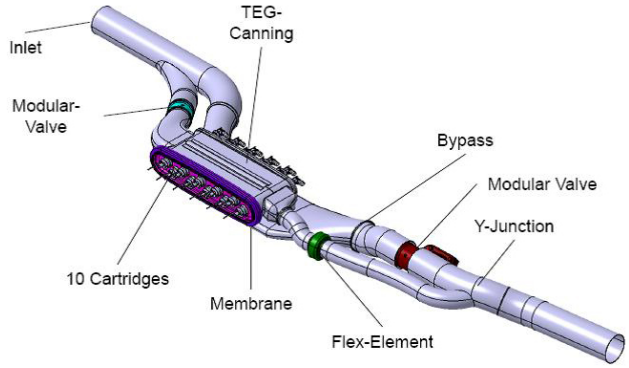

FIGURE 5. Design of LDV TEG system designed by Tenneco.

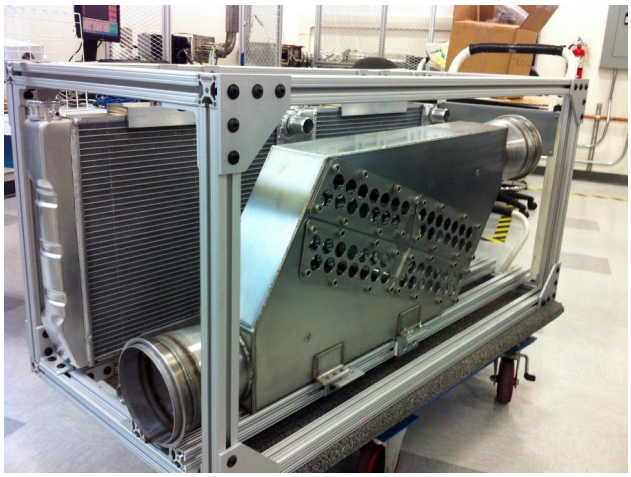

FIGURE 6. BFV test TEG device in a frame.

The project will conclude by building seven LDV TEG systems which will be tested on vehicles and in Gentherm, Tenneco and NREL laboratories. The HDV TEG will be tested at Tenneco and TARDEC. The ultimate goal of this project is to correlate these test results and results coming from vehicle level performance models in order to calculate the true benefits to fuel efficiency.

CONCLUSIONS

The team is continuing to progress towards final delivery of working systems installed in vehicles.

- Method of producing high-performance TE materials is developed and properties are verified in the experiments.
- Material cost model is developed and it will be verified with development of pilot-scale equipment.
- Cartridge, as a building block, is designed, modeled and its performance is verified experimentally.
- The TEG system is designed and modeled. Experimental performance confirmation is expected in late 2014.
- Vehicle level integration is modeled. Experimental trials are scheduled for early 2015.

FY 2014 PUBLICATIONS/PRESENTATIONS

1. "Waste heat recovery in passenger cars" Michael Mirsch, March 31, 2014, presentation at the VDI conference, Dusseldorf, Germany.

V.2 Development of Cost-Competitive Advanced Thermoelectric Generators for Direct Conversion of Vehicle Waste Heat into Useful Electrical Power

James R. Salvador (Primary Contact), Norman K. Bucknor, Gregory P. Meisner, Kevin Rober, Edward R. Gundlach, and Richard W. Leach

General Motors
30500 Mound Rd. MC 480-106-RA3
Warren, MI 48090

DOE Technology Development Manager
Gurpreet Singh

NETL Project Manager
Carl Maronde

Subcontractors
- Brookhaven National Laboratory, Upton, NY
- Dana Canada Corp. Oakville, Ontario, Canada
- Delphi Electronics and Safety. Kokomo, IN
- Eberspaecher, Novi, MI
- Jet Propulsion Laboratory, Pasadena, CA
- Marlow Industries (II-VI), Dallas, TX
- Michigan State University, East Lansing, MI
- Molycorp (formerly Magnequench), Singapore
- Oak Ridge National Laboratory, Oak Ridge, TN
- Purdue University, West Lafayette, IN
- University of Washington, Seattle, WA

Overall Objectives

- Overcome major obstacles to the commercialization of automotive thermoelectric generator (TEG) systems
- Develop an overall TEG system including all necessary vehicle controls and electrical systems and fully integrated onto a light-duty vehicle
- Demonstrate fuel economy improvement of 5% over the US06 drive cycle

Fiscal Year (FY) 2014 Objectives

- Develop a unified transient thermal model for heat exchanger and thermoelectric (TE) converter system co-optimization using target platform vehicle mass flow and temperature data
- Establish design targets for TEG components and subsystems
- Fabricate skutterudite thermoelectric modules (TEMs) for incorporation into the initial TEG prototype
- Complete a preliminary estimate of initial TEG performance
- Begin fabrication and testing of the initial prototype

FY 2014 Accomplishments

- Produced 6,300 skutterudite TE legs with diffusion barriers and metallization layers, and these legs were used to fabricate over 120 skutterudite TEMs for the initial TEG prototype
- Verified that the skutterudite modules maintain beginning-of-life (BOL) performance after 2,000 hours continuous in-gradient operation and 250 thermal cycles
- Used a thermal model to predict that a peak power of 1,600 W and an average power of 900 W are achievable in a full-size truck over the US06 drive cycle
- Completed computer-aided design of initial TEG
- Fabricated and acquired all hardware required to build the initial TEG
- Developed an enamel-based oxidation suppression method that is compatible with both n-type and p-type skutterudites
- Demonstrated that rare earth (RE)-free p-type skutterudites can exhibit comparable thermoelectric figure of merit (zT) values to RE-containing p-type skutterudite formulations

Future Directions

- Complete fabrication, assembly, and testing of initial TEG
- Evaluate initial TEG performance and durability; identify and address the root causes of component failures
- Evaluate the feasibility of modified TE module architecture to reduce clamp load requirements for the Phase 2 TEG
- Continue to develop strategies for skutterudite oxidation suppression

- Design, fabricate, and test a Phase 2 TEG that incorporates improvements based on initial TEG results

INTRODUCTION

The development of a practical and fully integrated TEG for a production vehicle will be a significant step toward reducing energy consumption and lowering emissions associated with the U.S. transportation sector. Considerable innovation, however, is needed to overcome the major obstacles to TEG technology commercialization. This effort will culminate in the first application of high-temperature TE materials for high-volume use, and it will establish new industrial sectors with scaled-up production capabilities for TEG materials and components. TE waste heat recovery is a new area of commercial technology that will be implemented without the added burden of displacing other existing technology. Moreover, this effort to commercialize TE-based recovery of waste energy has significant potential beyond the automobile industry. Our work on automotive TEGs focuses on several key tasks: (1) enhancing p-type material performance via band structure modification through doping and other compositional modifications, (2) optimizing TE material fabrication and processing to reduce thermal conductivity and improve fracture strength, (3) accelerating novel routes to high volume production for successful market introduction of skutterudite TEMs, (4) achieving high-efficiency heat flows and optimum temperature profiles under the highly variable exhaust gas flow conditions of typical automotive drive cycles by applying new designs to both the heat exchanger and TEG subsystem, (5) developing new modeling and simulation capabilities, and (6) applying new, highly thermally insulating substances such as aerogels, as potentially inexpensive encapsulation and insulation materials for TE technology. At the completion of this four-year project, we will have created a potential supply chain for automotive TEG technology and identified manufacturing and assembly processes for large-scale production of TE materials and components that include scale-up plans for the production of 100,000 TEG units per year.

APPROACH

Our current project builds on prior DOE-funded work with new goals for moving advanced TE materials and module fabrication from the laboratory scale to mass production and for developing a fully integrated and viable TEG design suitable for commercialization by the automotive industry. We have made significant advances in TE material performance through collaborative research and development for more than a decade, and our TE material research partners all have extensive accomplishments in advanced TE technology. Our project team's expertise includes (a) TE material research, synthesis, and characterization [1], (b) thermal and electrical interfaces and contacts [2], and (c) skutterudite-based TE module fabrication and testing [1,3]. We are working on improving the performance of TE materials simultaneously with the development of high-volume methods for TE material synthesis, and TEM production. Further, our team has considerable expertise in heat exchanger design, computational fluid dynamics, and packaging of automotive exhaust systems that includes the design and commercialization of several exhaust gas heat exchangers for other waste heat recovery applications. We will rely on these core competencies as we develop TEG heat exchanger designs that optimize heat extraction for maximum TE conversion of heat into usable electrical power. We are developing and implementing effective strategies for module interconnection and power management that are crucial to manufacturability and system efficiency. We are leveraging the team's expertise in hybrid electric vehicle technology and integrated circuits to both design an electrical subsystem for the TEG and develop integrated circuit solutions in TE module interconnections and TE module output power management hardware. Our focus is on durability and low-cost assembly strategies.

RESULTS

Last year, we developed a unified heat exchanger and TEM thermal model. These modeling tools capture transient behavior, comprehend heat flow in three dimensions, and use a combination of a proprietary heat exchanger design code developed by Dana and a multi-physics COMSOL model for the TEMs. The final combined model was coupled using the COMSOL Multiphysics® code. These modeling tools are a significant improvement over those developed in our previous project, which were limited to a one dimensional heat flow analysis. Our current thermal modeling in conjunction with manufacturability and packaging constraints have driven the TEG design to be a plurality of heat exchangers in a parallel flow arrangement in the exhaust gas stream with the TEMs positioned on the heat exchanger surfaces in a cross flow configuration. The modularity of our TEG subassembly design will facilitate adoption of this TEG technology to a wide variety of vehicle platforms and engine displacements. Figure 1(a) is an image of one TEG subassembly, which is $1/10^{th}$ of the full generator suitable for a 5.3-liter V-8 engine. In Figure 1(a) the exhaust gas flow direction is highlighted by the red arrows, and the row of isothermal TEMs

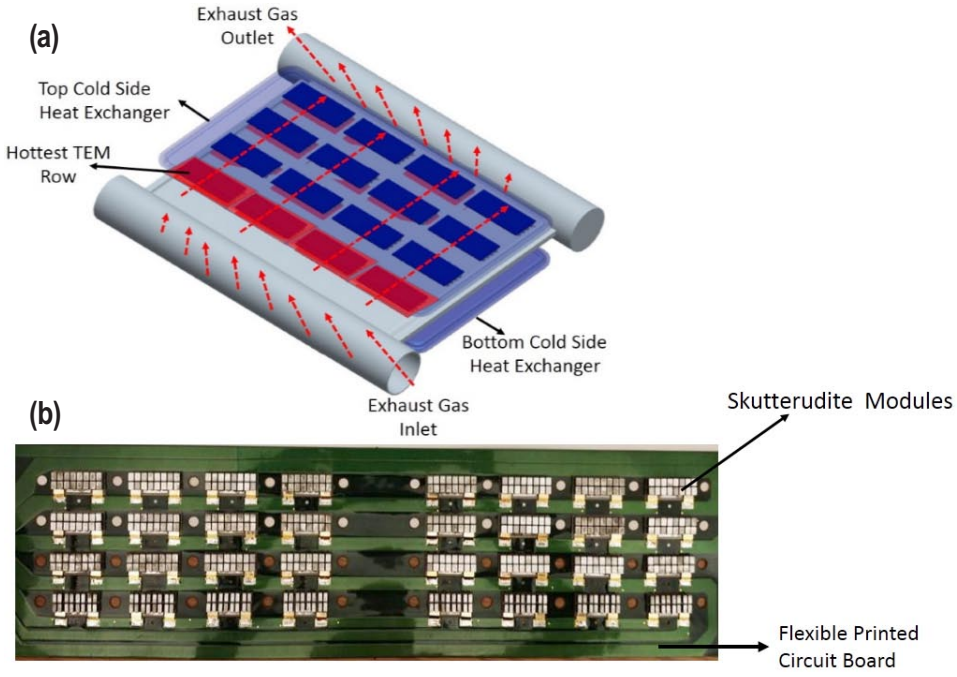

FIGURE 1. (a) Computer-aided design drawing of one TEG subassembly of the initial TEG prototype; the red arrows depict hot gas flow, and the string of modules highlighted in red are the hottest isothermal row. Subsequent rows will be heated to progressively lower temperatures. (b) The flexible printed circuit board with skutterudite modules soldered in place.

highlighted in red attain the highest hot side temperatures in operation. The subsequent rows of TEMs will attain progressively lower temperatures. The eight TEMs in each isothermal row (four on the top and four on the bottom of the central heat exchanger) are connected in series, and each of these rows is treated independently for maximum power delivery. Figure 1(b) shows a flexible integrated circuit designed to interconnect the TEMs and carry the current out of the TEG and into an external load. This design greatly simplifies the interconnection of TEMs, reduces the likelihood of short-circuits, and minimizes parasitic I^2R electrical losses. Figure 2 shows the unified model's predicted power output for a full-size TEG (ten subassemblies) in a full-size truck application. The exhaust gas temperatures and flow rates, as measured on the demonstration vehicle over the US06 drive cycle, were used as model inputs. By summing the power output contributions from each of the four isothermal rows of TEMs, a total peak power output of nearly 1.6 kW and an average power of 900 W over the cycle can be achieved. Incorporation of this TEG power output into the vehicle electrical system indicates that fuel economy can be improved by 2.5% to 3% over the US06 drive cycle based on unified vehicle model data. Further fuel economy gains are possible with improved utilization of the available TEG electrical power output at all points in the drive cycle.

Once the TEM layout (i.e., TE leg fill factor and aspect ratio) was defined from our thermal modeling, skutterudite TEM fabrication commenced. A total of 6,300 TE legs were produce through a combination of melt spin processing to form pre-reacted skutterudite alloys. This was followed by powder commutation, a brief heat treatment process, and then consolidation and diffusion barrier/metallization layer application using a hot-pressing process. Compacts were cut into the desired cross-sectional area and then assembled into TEMs by brazing the legs to metal interconnects that were patterned directly onto a dielectric substrate. Figure 3(a) shows the process flow from melt spun ribbons to metalized TE legs, and Figure 3(b) shows a close-up image of the skutterudite TEMs after assembly and brazing. Of the 120 TEMs produced, greater than 90% had a BOL AC resistance within 5% of the predicted value. We identified electrical contact resistance between the metallization layers and the TE leg as a potential source of parasitic electrical power loss. We measured the electrical contact resistance at this interface for both n-type and p–type skutterudite legs and found them to range from 0.24 $\mu\Omega\text{-cm}^2$ to 0.30 $\mu\Omega\text{-cm}^2$, which is well within specifications. The narrow distribution of AC resistance and the minimal geometric variability between the TEMs demonstrate a high level of process control. We evaluated several test TEMs (i.e., half size of those shown in Figure 3(b)) for performance and durability. For

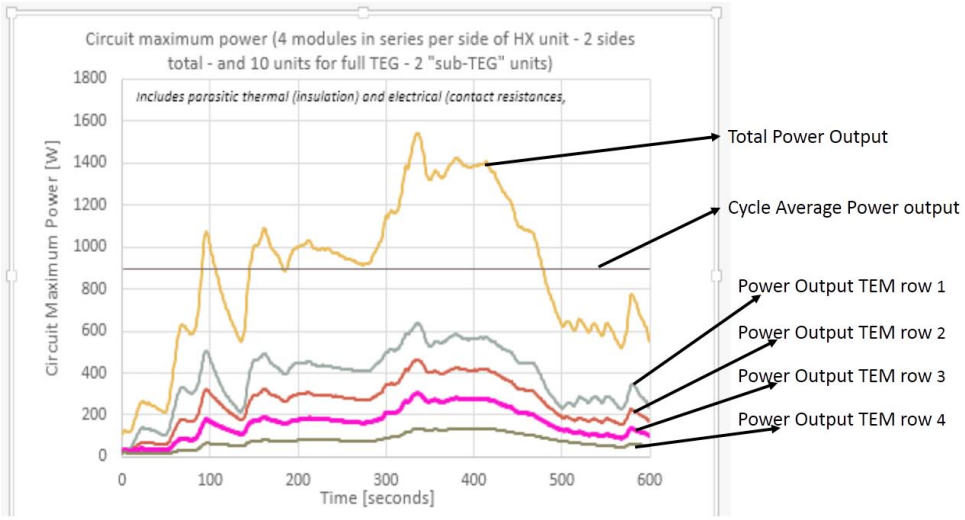

FIGURE 2. Modeled power output of the TEG for a full-size truck over the US06 drive cycle. The power output of each of the four strings of TEMs is shown together with the sum total of these contributions (gold line) and the drive cycle average power output (grey line).

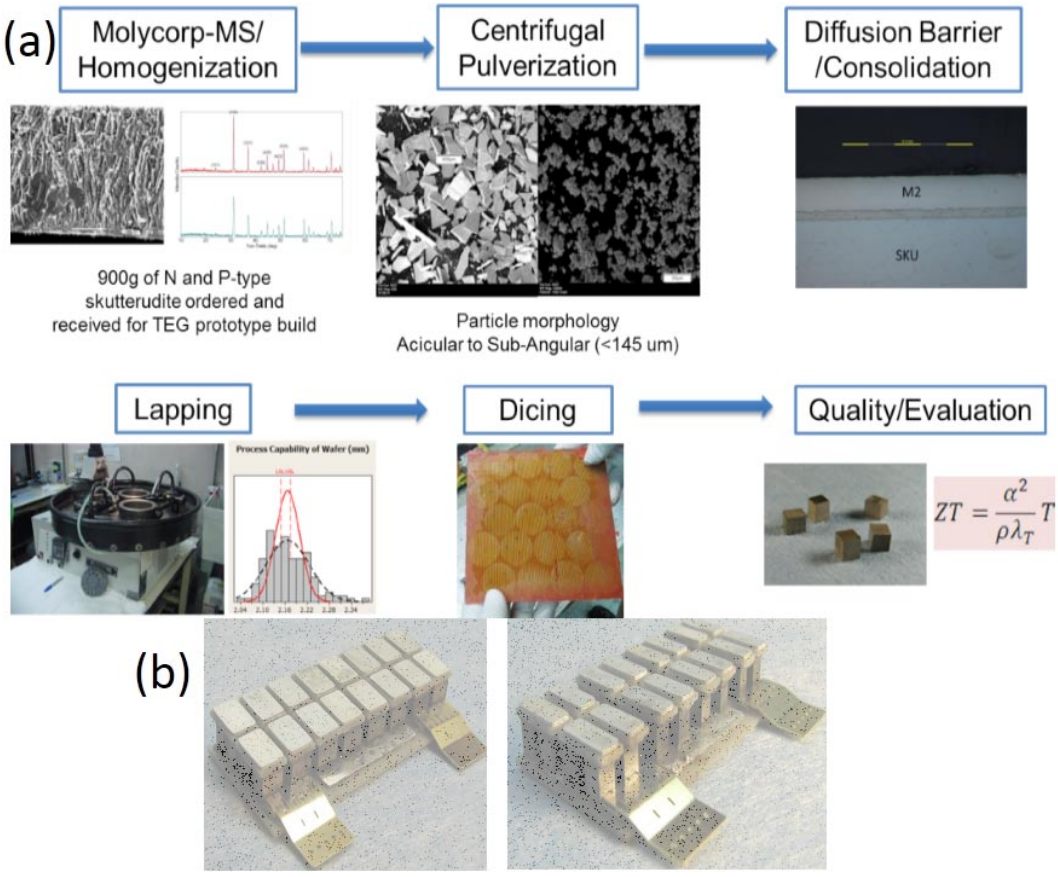

FIGURE 3. (a) Flow diagram for the processing of melt spun ribbons into metalized and consolidated wafers and then TE leg. (b) Photograph of the two types of skutterudite TE modules used for the initial TEG prototype build.

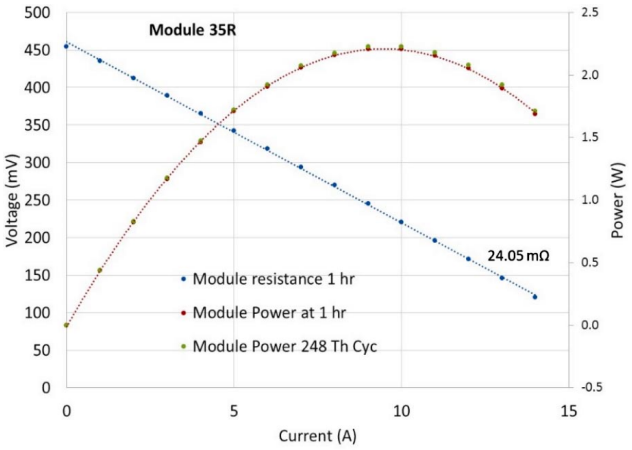

FIGURE 4. Power and voltage versus current for a skutterudite test TE module operating at a hot-side temperature of 500°C and a cold side of 100°C. The figure demonstrates steady power output of the module before and after 250 thermal cycles between 300°C and 500°C.

steady-state testing, the TEMs were heated to a hot-side temperature of 500°C with the cold side temperature held at 100°C. Power output of 2.2 W was obtained under these conditions as shown in Figure 4, and this power output was maintained both for several hundred hours of continuous in-gradient operation and for 250 thermal cycles, where one cycle was ramping from 500°C to 300°C and back to 500°C in 10 minutes.

A 1/10th scale TEG prototype (i.e., one TEG subassembly) was built in the last quarter of the year and is shown in Figure 5. The area bound by the width of the exhaust gas inlet and outlet and the length of the cold side heat exchanger assembly is about the size of a standard sheet of paper (8.5" x 11"), and the total assembly thickness is 6.4 cm. This TEG subassembly will be bench tested in the last quarter of 2014.

Materials development work in this past year has focused on reducing on the amount of critical REs in our skutterudite formulations while still achieving superior TE performance. For n-type materials, we found that adding a small amount of electron deficient transition metals onto the 8*c* site in the skutterudite structure increases the filling fraction limit of the noncritical RE element, cerium (Ce). This has the effect of increasing the TE power factor and reducing the lattice thermal conductivity, both of which contribute to improving zT by over 20% as compared to samples without transition metal doping. For p-type materials, calcium (Ca) was found to be an excellent filler atom for both achieving high power factors (>33 μW/cm·K^2) and lower lattice thermal conductivity. The loosely bound nature of Ca in the antimony cage of the crystal structure introduces a low frequency optical phonon mode, whose energy is comparable to those found in lanthanum-filled skutterudites. This low frequency optical mode imparts an avoided crossing of an acoustical mode, and this leads to low group velocities and low thermal conduction. A zT >0.8 at 773 K is realized for optimized p-type skutterudite formulations. A summary of the optimized zT values for the n-type and p-type materials are shown in Figures 6(a) and 6(b), respectively.

CONCLUSIONS

- Developed a fully integrated COMSOL multi-physics transient thermal TEG model.
- Developed a thermal and physical design for TEG based on modeling and constraints imposed by manufacturability and packaging.

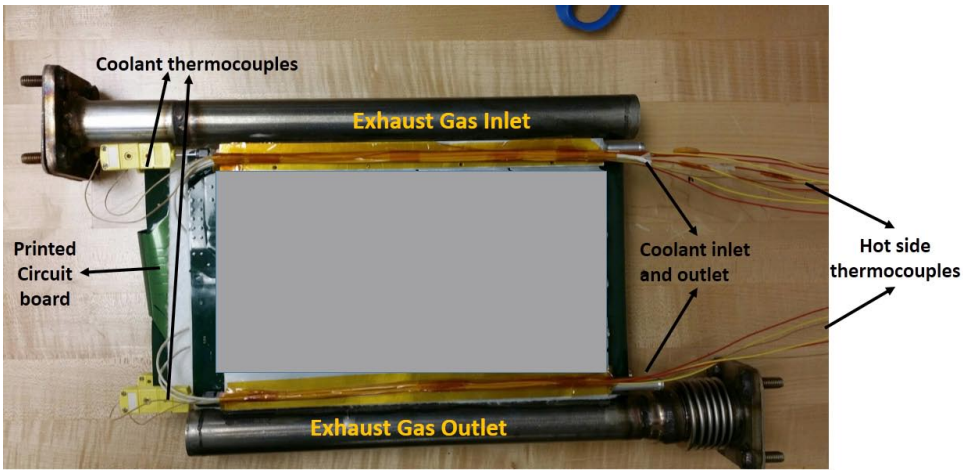

FIGURE 5. A single TEG subassembly (i.e., the 1/10th scale initial TEG prototype) with salient parts labeled. The area of the TEG subassembly shown is about the same as a standard sheet of paper, with a stack height of 6.4 cm.

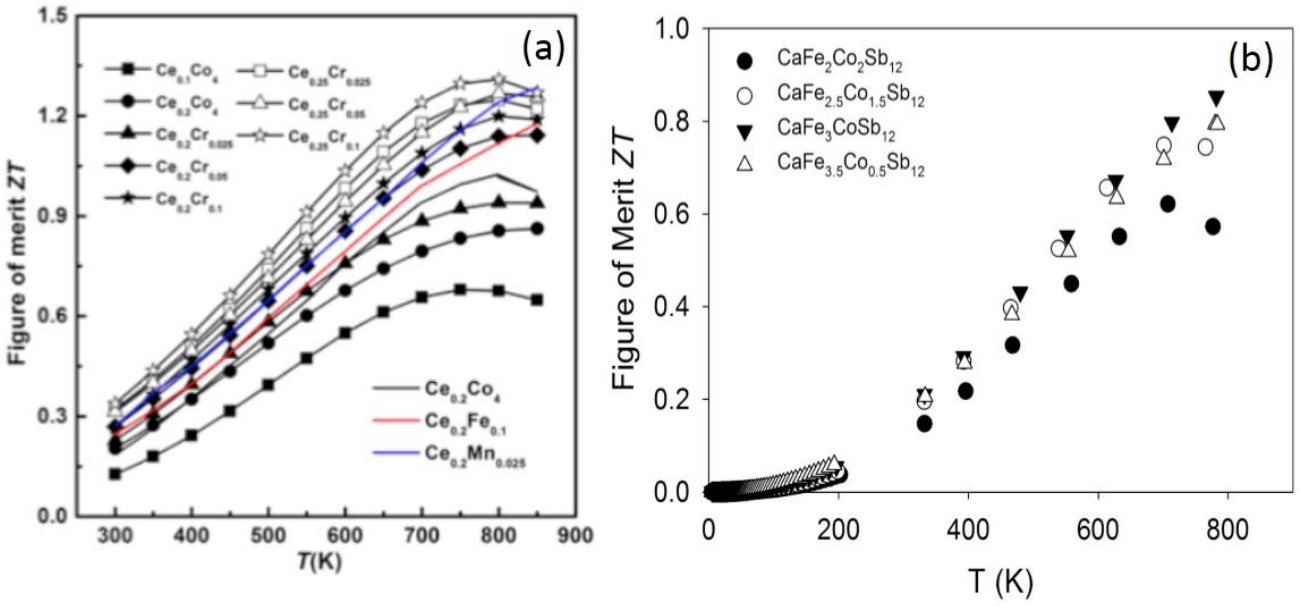

FIGURE 6. (a) Figure of merit zT for Cr-doped Ce-filled n-type skutterudites. (b) Figure of merit zT for Ca-filled p-type skutterudites.

- Developed manufacturing processes for the skutterudite TE legs and TE modules and executed a pilot build of 120 skutterudite TE modules.
- Fabricated and acquired all parts necessary to build a 1/10th scale TEG prototype. This initial TEG prototype has been assembled and will be bench tested within the next month.
- Demonstrated that Ca-filled p-type skutterudites have comparable TE performance to RE-filled skutterudites, and showed that doping n-type skutterudites with small amounts of certain transition metals can increase the Ce filling fraction and thereby improve TE performance. Both approaches significantly reduce TE materials cost.

REFERENCES

1. (a) X. Shi, H. Kong, C.P. Li, C. Uher, J. Yang, J.R. Salvador, H. Wang, L. Chen, W. Zhang, *Appl. Phys. Lett.* 2008, 92, 182101; (b) X. Shi, J. Yang, J.R. Salvador, M.F. Chi, J.Y. Cho, H. Wang, G.Q. Bai, J.H. Yang, W.Q. Zhang, L.D. Chen, *J. Amer. Chem. Soc.* 133(20), 7837 (2011).

2. Purdue's thermal resistance measurements using a photoacoustic technique showed thermal resistances as low as 1.7 mm^2 kW^{-1} for bonded VACNT films 25–30 µm in length and 10 mm^2 kW^{-1} for CNTs up to 130 µm in length. See: R. Cross, B.A. Cola, T.S. Fisher, S. Graham, *Nanotechnology*, 2010, *21,*445705.

3. T. Caillat "*Advanced High-Temperature Thermoelectric Devices*" DOE Thermoelectrics Applications Workshop, San Diego, 29 September 2009*"*.

FY 2014 PUBLICATIONS/PRESENTATIONS

1. J.R. Salvador, R.A. Waldo, C.A. Wong, M.M. Tessema, D.N. Born, D.J. Miller H. Wang, A.A. Wereszczak and W. Cai "*Thermoelectric and Mechanical Properties of Melt Spun and Spark Plasma Sintered n-type Yb-and Ba-filled skutterudites*" J. Mater. Sci. and Eng. B **178**, 1087 (2013).

2. J.R. Salvador, J.Y. Cho, Z. Ye, J.E. Moczygemba, A.J. Thompson, J. W. Sharp, J. D. Koenig, R. Maloney, T. Thompson, J. Sakamoto, H. Wang, A. A. Wereszczak. "*Conversion Efficiency of Skutterudite-Based Thermoelectric Modules*" J. Phys. Chem. Chem. Phys. **24**, 12510 (2014).

3. C. Liu, D.R. Thompson J.R. Salvador J. Yang J. Yang L. Guo and X.F. Xu *"Low Thermal Conductivity in Ca-filled p-type Skutterudites" Contributed Talk* Symposium BB 9.10 Materials Research Society Fall Meeting 2013 Boston, MA.

4. J.R. Salvador "*Skutterudite Materials and Modules for Automotive Waste heat Recovery Applications" Invited Talk* Symposium BB 2.01 Materials Research Society Fall Meeting 2013, Boston, MA.

5. G.P. Meisner *"Thermoelectric Technology for Generating Useful Electrical Power from Automotive Waste Heat,"* Invited presentation at IDTechEx 2013: Energy Harvesting & Storage USA Conference, Santa Clara, CA, 20 November 2013.

6. H. Wang, R. McCarty J.R. Salvador, A. Yamamoto, J. Koenig, "*Determination of Thermoelectric Module Efficiency: A Survey*" J. Electronic Mater. **43** 2274 (2014).

7. Z.H. Ge, J.R. Salvador, G.S. Nolas "*Selective Synthesis of Cu_2SnSe_3 and Cu_2SnSe_4 Nanocrystals"* Inorg. Chem. **53** 4445 (2014).

9. Y. Dong, A.R. Khabibullin, K. Wei, Z.-H. Ge, J. Martin, J.R. Salvador, L.M. Woods, and G.S. Nolas *"Synthesis,*

Transport Properties and Electronic Structure of $u_2CdSnTe_4$" Appl. Phys. Lett. **104** 252107 (2014).

10. Y.C. Liang, J. Yang, X. Yuan, W.J. Qiu, Z. Zhong, J. Yang, & W. Zhang, "*Polytypism in superhard transition-metal triborides*", Scientific Reports **4**, 5063, DOI: 10.1038/srep05063 (2014).

11. W.J. Qiua, L. Xi, P. Wei, X. Ke, J. Yang, and W. Zhang, "*Part-crystalline part-liquid state and rattling-like thermal damping in materials with chemical-bond hierarchy*", PNAS Early Edition, www.pnas.org/cgi/doi/10.1073/pnas.1410349111, (2014).

12. G.P. Meisner *"Low Cost Advanced Thermoelectric Technology for Automotive Waste Heat Recovery,"* Contributed talk: American Physical Society (APS) March Meeting, Denver, CO, 6 March 2014.

13. S. Kumar, A. Dubitsky, S.D. Heister, X. Xu "*Jet Impingement concept for Thermoelectric Generators*," International Conference on Thermoelectrics – ICT 2014, Nashville, Tennessee July, (2014).

14. S. Kumar, (2014). Thermoelectric Waste Heat Recovery in Automobile Exhaust Systems: Topological Studies and Performance Analysis. Ph.D. Thesis. Purdue University, IN, USA.

15. G.P. Meisner *"On the Development of Low Cost Thermoelectric Generators for Automotive Waste Heat Recovery,"* Invited talk: International Conference on Thermoelectrics, Nashville, TN, 7 July 2014.

16. J.R. Salvador "*Opportunities and Challenges for Automotive Thermoelectric Waste Heat Recovery Applications*" Invited lecture at HEATER summer school, University of Toronto, Toronto, ON. July 2014.

17. Y.S. Park, T. Thompson, Y.S. Kim, J.R. Salvador J.S. Sakamoto, "Protective EnamelC for n- and p-type Skutterudite Thermoelectric Materials". Accepted: J. Mater. Sci.

18. D.R. Thompson, C. Liu, N.D. Ellison, J.R. Salvador, M.S. Meyer, D.B. Haddad, H. Wang, and J.R. Salvador "*Improved Thermoelectric Performance of n-type Ca- and Ca-Ce Filled Skutterudites*" Accepted: J. Appl. Phys.

SPECIAL RECOGNITIONS AND AWARDS/ PATENTS ISSUED

1. "*Encapsulation of High Temperature Thermoelectric Modules*" (7029.3495.001). The patent authors are James R. Salvador, Jeffrey S. Sakamoto, and Young-Sam Park.

2. *"Exhaust bypass control for exhaust heat recovery,"* M.G. Reynolds, J. Yang, G.P. Meisner, F.R. Stabler, P.H. De Bock, T.A. Anderson, **P-006665** Chinese Patent CN 102,235,212: issued **16 October 2013**, (U.S. patent 8,256,220 was issued 4 September 2012).

3. *"Thermoelectric generators incorporating phase-change materials for waste heat recovery from engine exhaust"* G.P. Meisner and J. Yang, US Patent 8,646,261 Issued 11 February 2014.

V.3 Nanostructured High-Temperature Bulk Thermoelectric Energy Conversion for Efficient Automotive Waste Heat Recovery

Martin Cleary[1] (Primary Contact),
Xiaowei Wang[1], Boris Kozinsky[2], Zhifeng Ren[3],
Jim Szybist[4], Zhiming Gao[4], Yanliang Zhang[5]
[1]GMZ Energy
11 Wall St.
Waltham, MA 02453

DOE Technology Development Manager
Gurpreet Singh

NETL Project Manager
Carl Maronde

Subcontractors
[2]Bosch of North America, Farmington Hills, MI
[3]University of Houston, Houston, TX
[4]Oak Ridge National Laboratory, Oak Ridge, TN
[5]Boise State University, Boise, Idaho

Overall Objectives

- Demonstrate a robust, thermally cyclable thermoelectric exhaust waste heat recovery system that will provide approximately a 5% fuel efficiency improvement for a light-duty vehicle platform.
- Develop an initial design/concept for a 1-kW thermoelectric generator (TEG) in the exhaust stream of a Bradley Fighting Vehicle (BFV).

Fiscal Year 2014 (FY) Objectives

- Fabricate a half-Heusler device with >5% efficiency and <10% performance degradation after 100 thermal cycles.
- Finalize the heat exchanger (HEX) design for the automotive TEG, and fabricate the automotive TEG.
- Develop an advanced vehicle model, and generate an advanced testing plan to assess the impact of installing a TEG on the fuel economy of a mid-sized passenger vehicle.
- Perform an advanced cost analysis for manufacture and integration of an automotive TEG.
- Fabricate a 1-kW TEG for a BFV.

FY 2014 Accomplishments

- A device efficiency of 6.5% was measured, where the hot-side and cold-side temperatures were 600ºC and 100ºC, respectively. A 2% degradation in power output was measured for a thermoelectric module subjected to 1,000 thermal cycles, between 600°C and 100ºC.
- The HEX design for the automotive TEG was finalized. The TEG is predicted to generate ~190 W for the average exhaust conditions over the US06 drive cycle. The TEG is currently in fabrication.
- New NbFeSb-based half-Heuslers compositions have been developed. An analysis based on the cost of raw materials indicate that the cost of these new compositions is >50% less than conventional half-Heusler materials with a high Hf content.
- An advanced testing plan for measuring the effect of a TEG on the fuel economy of a mid-sized passenger vehicle has been developed. Chassis dynamometer testing has been performed on the vehicle platform in order to establish a fuel economy baseline.
- A 1/5th scale TEG, for the BFV application, was fabricated and tested. A power output of over 200 W was achieved, which validated the design of the 1-kW TEG. The 1-kW TEG for a BFV was fabricated, and is currently under testing.

Future Directions

- The TEG will be subjected to extensive thermal and mechanical reliability testing.
- The automotive TEG currently under fabrication will be installed onboard a Honda Accord vehicle platform, and the vehicle fuel economy will be compared with the baseline data in order to establish the improvement in fuel economy due to the TEG installation.

INTRODUCTION

The improvement of automotive vehicle efficiency is crucial to the conservation of petroleum and energy sustainability. Moreover, government regulations require increased vehicle fuel economy and reduced greenhouse emissions. In order to meet these demands the use of a TEG in the engine exhaust to achieve a 5% fuel efficiency improvement for a light-duty vehicle platform is considered. Engine waste heat accounts for >30% of the total energy consumption in a vehicle. TEGs are

robust solid-state devices that utilize the Peltier effect to directly convert heat into electrical power, which makes them ideal for waste heat recovery from engine exhaust.

APPROACH

This project is following a multi-tiered approach to achieve the outlined program goals. At the materials level, theoretical simulations, composition optimization, and production scale up are being pursued to achieve high-efficiency thermoelectric materials with reduced cost. The half-Heusler thermoelectric materials are then integrated into high-temperature thermoelectric modules, which are designed to maximize power, efficiency and reliability. A TEG, consisting of an exhaust gas HEX, modules and water-cooled cold plates, will be designed. The optimized TEG design will be fabricated, characterized and installed on a vehicle platform. The TEG will be fully integrated with vehicle exhaust, cooling, and electrical systems. The vehicle platform will be tested on a chassis dynamometer to measure the improvement in fuel economy after the TEG installation

RESULTS

There are a number of steps in the materials fabrication process including melting, ball milling and hot-pressing. The efforts at GMZ Energy initiated in FY 2013 to scale up material production by increasing the batch size during melting, ball milling, and the diameter of the disc hot-pressed has continued in FY 2014. GMZ Energy is currently exploring techniques that will allow batch size to be increased to the kg scale, and have developed a clear road map to mass production. New NbFeSb based half-Heuslers compositions have been developed. The performance of the new thermoelectric materials is shown in Figure 1, where it can be seen that the performance of the new composition is comparable to the current production material. However, an analysis based on the cost of raw materials indicate that the cost of these new compositions is >50% less than conventional half-Heusler materials with a high Hf content.

The vehicle exhaust stream is a very challenging environment, where components are subjected to repeated thermal cycling and peak temperatures in excess of 800ºC. In FY 2013 the reliability of the thermoelectric devices under thermal cycling was established. This year, a thermoelectric module (containing multiple thermoelectric devices) was subjected to a cyclical temperature profile where the hot-side temperature peaked at 560ºC while the cold-side was maintained at 60ºC, which is representative of conditions in a TEG automobile application. The thermal cycling was performed on a custom-designed device characterization apparatus. It was found that there was only 2.03%

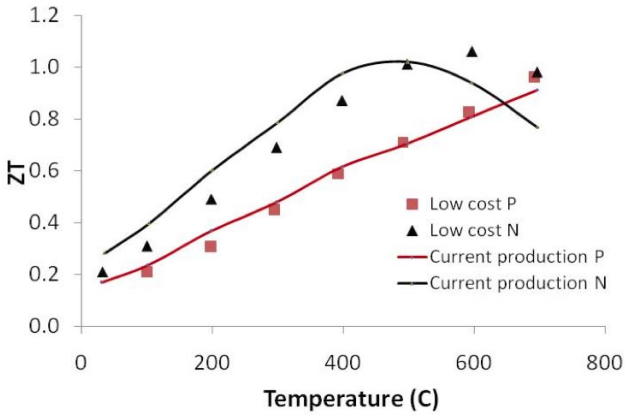

FIGURE 1. Comparison of ZT, a thermoelectric figure-of-merit, of arc-melted, ball-milled and hot-pressed 2nd generation low-cost (No/Low Hf) thermoelectric materials with the current 1st generation half-Heusler compositions.

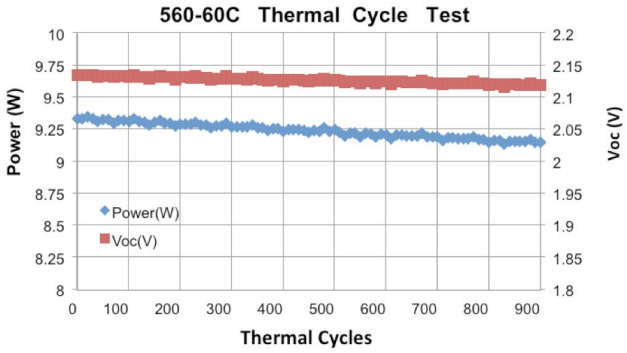

FIGURE 2. Power output and open circuit voltage (V_{oc}) for a thermoelectric module with a new device architecture subjected to 1,000 thermal cycles between 560°C and 60°C. A power degradation of just 2.03% was observed.

degradation in module power output after 1,000 thermal cycles, as shown in Figure 2, which indicates that the thermoelectric modules are robust and can operate under challenging thermal conditions.

A TEG design was developed for the passenger vehicle application. The HEX design was optimized to maximize the electrical power output of the TEG, while minimizing the weight backpressure. Based upon extensive computational fluid dynamics simulations, the TEG average power output over the US06 cycle is predicted to be 192 W, while the pressure drop across the TEG is predicted to be 800 Pa. A computer-aided design model of the TEG integrated onboard the vehicle platform is shown in Figure 3. The TEG location, under the oil pan beneath the engine, was selected to have the TEG as close to the engine as possible so as to maximize the exhaust gas temperature at the inlet to the TEG.

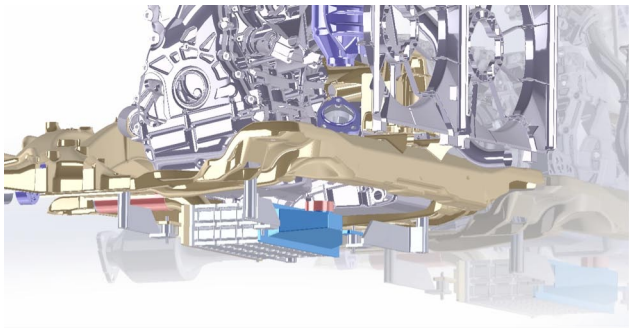

FIGURE 3. Computer-aided design model of the vehicle platform engine with an integrated TEG.

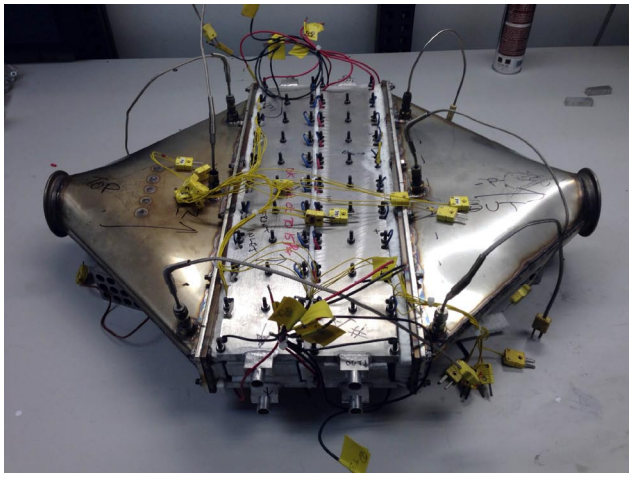

FIGURE 4. 200-W TEG assembly, with the exhaust inlet and outlet manifolds attached.

A 1/5th scale TEG prototype for the BFV application is shown in Figure 4. The TEG consists of a hot side HEX with Ni fins, 80 thermoelectric modules, and four aluminum cold plates. The thermoelectric modules are placed between the exhaust gas HEX and cold plates, and the assembly is held together with an array of spring-loaded bolts. The TEG was measured under representative diesel exhaust conditions. A power output of 220 W, where the exhaust gas and coolant inlet temperatures were 540ºC and 60ºC, respectively, was measured as shown in Figure 5. A pressure drop of 4,600 kPa was measured across the TEG, which is within the specified allowable range. A 1-kW TEG for the BFV application was fabricated, and is shown in Figure 6 attached to the exhaust of a diesel engine dynamometer. This TEG is currently being tested.

CONCLUSIONS

- A thermoelectric module has been subjected to 1,000 thermal cycles, between 560ºC and 60ºC, with only 2% degradation in power output performance.

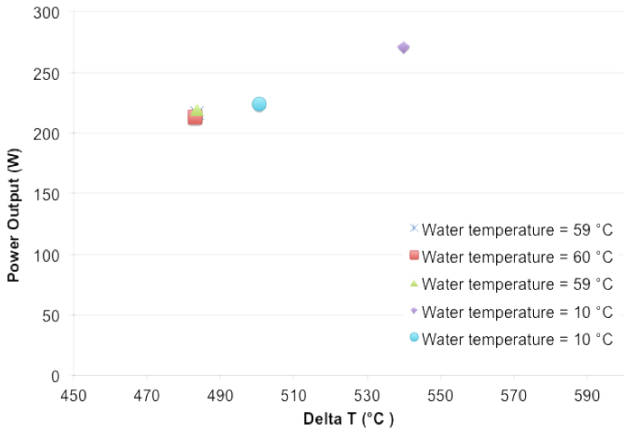

FIGURE 5. Power output of the 200-W TEG, shown in Figure 4, as a function of Delta T. Note: Delta T is defined as the temperature difference between the average exhaust gas inlet temperature and the water inlet temperature.

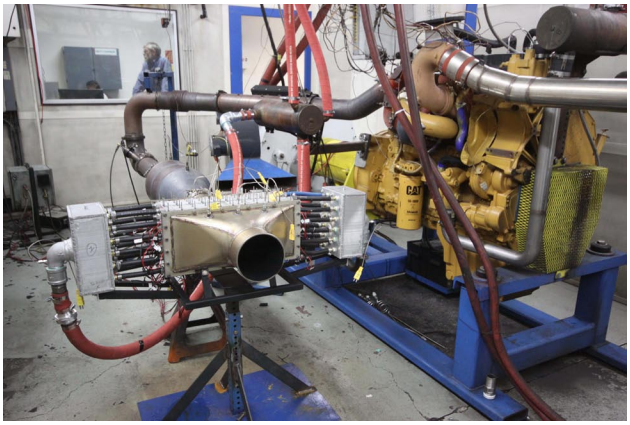

FIGURE 6. 1-kW TEG for a BFV attached to a diesel engine dynamometer.

- New NbFeSb-based half-Heuslers compositions, with performance comparable to the existing production materials, have been developed. The material cost of the new compositions is >50% less than conventional half-Heusler materials.
- A 200-W TEG was successfully fabricated and tested under representative diesel exhaust conditions. These results validated the 1-kW TEG design, which is currently being tested on a diesel engine dynamometer.

FY 2014 PUBLICATIONS/PRESENTATIONS

1. "NbFeSb based p-type half-Heusler materials for power generation applications", G. Joshi et al. Energy and Environmental Science 2014, DOI: 10.1039/c4ee02180k.

2. "Low cost half-Heusler materials for power generation applications," Giri Joshi, Ran He, Mike Engber, Ekraj Dahal,

Jian Yang, Boris Kozinsky, Xiaowei Wang, Martin Cleary and Zhifeng Ren, International Conference on Thermoelectrics, Nashville, TN, 2014.

3. "The Development of a 200 W Thermoelectric Generator for Exhaust Waste Heat Recovery from a Diesel Engine" by Martin Cleary, Yanliang Zhang, Lakshmikanth Meda, Xiaowei Wang, Giri Joshi, Jian Yang, Mike Engber and Yi Ma, International Conference on Thermoelectrics, Nashville, TN, 2014.

4. "Effects of tin doping on p-type $Hf_{0.5}Zr_{0.5}CoSb_{1-x}Sn_x$ for power generation applications" by Jian Yang, Giri Joshi, Mike Engber, Xiaowei Wang, Martin Cleary and Zhifeng Ren, International Conference on Thermoelectrics, Nashville, TN, 2014.

5. "Nanostructured Bulk High-Temperature Thermoelectric Generators for Efficient Power Generation." Luke Schoensee et al., International Conference on Thermoelectrics, Nashville, TN, 2014.

6. "A comprehensive multi-physics model on thermoelectric generators for waste heat recovery applications," Yanliang Zhang, International Conference on Thermoelectrics, Nashville, TN, 2014.

SPECIAL RECOGNITIONS AND AWARDS/ PATENTS ISSUED

1. Patent application number: 61969344, "NbFeSb-Based Half-Heusler Thermoelectric Materials and Methods of Making," G. Joshi, 2014.

2. Best poster award for "Nanostructured Bulk High-Temperature Thermoelectric Generators for Efficient Power Generation." by Luke Schoensee et al., at the International Conference on Thermoelectrics, Nashville, TN, 2014.

V.4 Energy Impact of Thermo Electric Generators (TEGs) on EPA Test Procedures

Ram Vijayagopal
Argonne National Laboratory
9700 South Cass Avenue
Argonne, IL 60439-4815

DOE Technology Development Manager
Gurpreet Singh

Overall Objectives

- Establish requirements for a TEG to provide cost-effective power for hybrid electric vehicles (HEVs) when subjected to U.S. Environmental Protection Agency (EPA) standard test procedures.
- Quantify fuel economy benefits from the EPA two-cycle procedure.
- Develop a TEG model based on published information that can simulate the effect of exhaust flow interruptions.
- Estimate the net present value (NPV) of the fuel savings.

Fiscal Year (FY) 2014 Accomplishments

- Analyzed the fuel-saving potential of auxiliary power sources over the two-cycle procedure for three types of vehicles:
  - Conventional
  - Belt-integrated starter alternator (BISG) mild hybrid
  - Split strong hybrid
- Developed a TEG model that reflects the effect of heat stored on the hot and cold surfaces of TEG.
- Evaluated the impact of thermal reservoirs and the possibility of optimizing the number of TEG modules.

Future Directions

- The TEG model can be improved if more module test data are made available from the original equipment manufacturers (OEMs).
  - More advanced models to factor detailed material and cost data can be used for optimization studies involving cost.

INTRODUCTION

TEGs can be used for a variety of applications in automobiles. Waste heat recovery and more efficient heating, ventilation, and air conditioning are two areas of research. This work is related to recovering the waste heat from the engine exhaust.

Argonne National Laboratory (Argonne) previously conducted a study to quantify the potential of TEGs for conventional and hybrid vehicles. In FY 2013, TEGs in HEVs were evaluated.

In FY 2014, we looked at the benefits these vehicles will see when subjected to EPA test procedures. The TEG module data used for this study were taken from previous studies. On the system design side, changes were implemented to factor in the thermal reservoir effect occurring due to the hot and cold surfaces of the TEG. The specific heat capacity of the materials used in the system will result in some heat energy being used to increase the temperature of the materials. This plays an important role when the exhaust flow is intermittent.

APPROACH

This study looked at the impact of TEGs on different types of light-duty vehicles. Urban Dynamometer Driving Schedule (UDDS), Highway, and combined two-cycle procedures were used to evaluate the fuel economy benefits in these vehicles. These benefits were then translated to gasoline savings and NPV of the monetary benefits.

Previous studies used TEG models that depend on exhaust flow traces recorded from the test bench. A better TEG model was developed which can estimate exhaust mass flow and respond to variations in the exhaust flow. This model can also predict temperature variations on the hot and cold side of the TEG modules. Better TEG modules were also modeled based on published data from General Motors (GM). The heat dissipation through the TEG between the source and sink was modeled, but various other losses, such as contact losses or thermal losses within the TEG, were not modeled.

Finding the right balance between fuel savings and the cost incurred by adding more and more modules is a challenge faced by OEMs. This study will provide guidance on how to find that balance. The TEG model developed has sufficient accuracy to predict trends in

potential fuel savings. Previous model versions and the simulation results were validated against test data provided by OEMs.

RESULTS

Fuel Saving Potential of TEGs

About 40% of the energy input to an engine is lost in the exhaust. TEGs provide an elegant way to recover waste heat and utilize that energy within the vehicle. Based on the electric load, vehicle technology, engine use, and drive cycle, the fuel saving potential for waste heat recovery varies. Our analysis showed that if 1 kW of power is produced by an auxiliary electric source (this could be a TEG module, solar cells, or a wireless charger), it can provide a significant (5%–15%) improvement in the fuel economy of a midsize car. In a conventional vehicle, the ability to utilize the recovered energy (assuming it is electrical energy) is limited, as it can only be used to meet the electric loads in the vehicle. Thus Figure 1 shows the benefits flattening out after the base load (250 or 750 W) is met.

For mild and strong hybrid vehicles, there is ample potential to utilize more than 1 kW of electrical power.

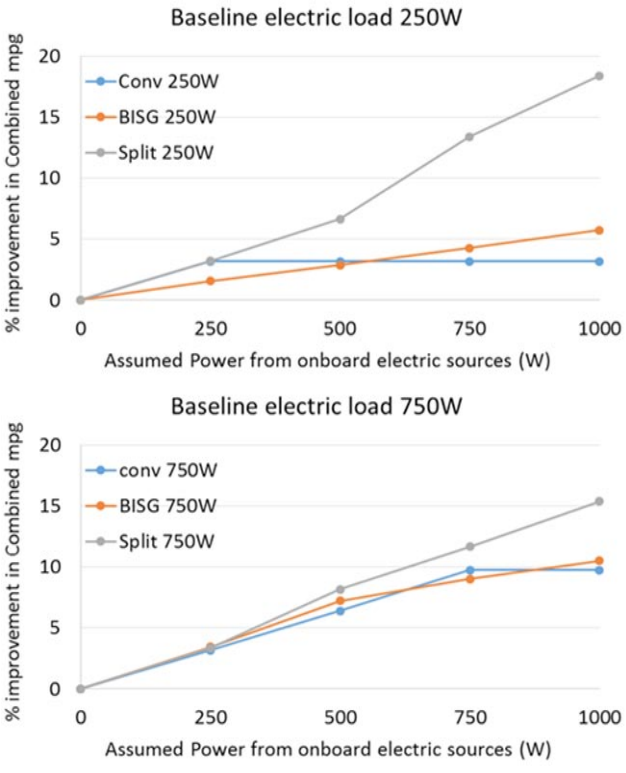

FIGURE 1. Sensitivity of Fuel Economy to Electric Power from Auxiliary Sources

This accounts for the steady rise in fuel economy when the power available from electric sources increases.

Current vehicles have only about 250 W of electric base load when subjected to dynamometer testing. However, many OEMs expect to convert some of the existing mechanical loads to electrical loads, to improve overall efficiency. This was the basis of looking at a second baseline case with 750 W as the electric load.

Monetary Value of Auxiliary Electric Sources in Vehicles

Fuel economy improvements can be translated to gasoline savings spread over the lifetime of the vehicle. To estimate what investment will justify such a future savings, the NPV of gasoline savings is computed. This gives us a clear idea of the worth of a technology to the consumer (Figure 2).

DOE has stated that its goal is to obtain 5% improvement in fuel economy through waste heat recovery. The above analysis shows that such a goal is achievable on a combined two-cycle procedure, if we recover an average of about 400 W.

TEG System Overview

GM follows a TEG system design which takes heat energy from the exhaust line of the vehicle. The engine

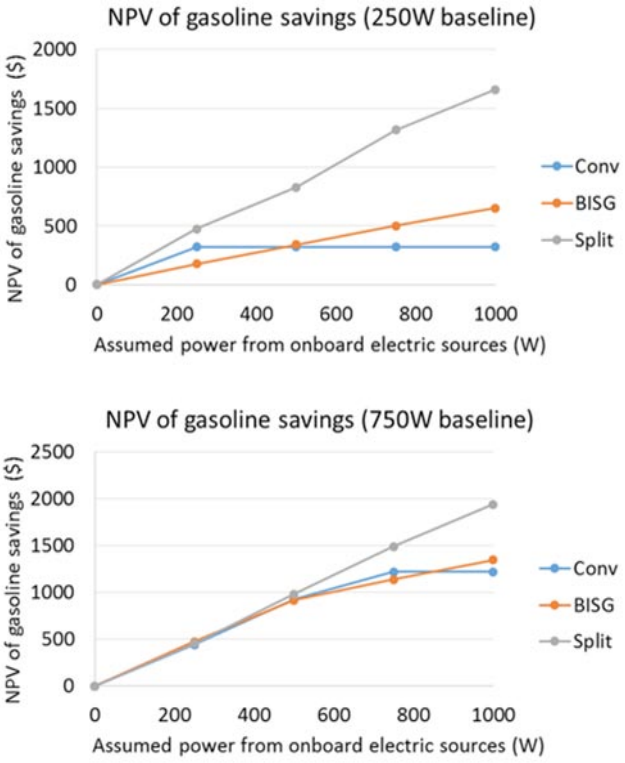

FIGURE 2. NPV of Having Auxiliary Electric Power in Vehicles

coolant serves as the cold side sink. Some OEMs have a separate coolant loop for TEGs. This study used the GM system as reference. Early prototypes used BiTe and PbTe modules; the new generation modules used by GM, however, rely on skutterudites. Past studies have shown that skutterudites have material properties better suited to be used as TEG modules in automotive applications. This study focused on how much of this benefit can be obtained when we use such TEG modules for waste heat recovery. The basic requirement for this analysis is a model for a TEG subsystem, which was developed using the data published by GM. Figure 3 shows the system architecture.

Part of the heat energy provided to the TEG is converted to electrical energy. The models for the TEG modules which use skutterudite modules were validated against the test data provided by GM (done in Phase 2 studies in FY 2013). Further reduction in internal resistance and more power output from each module are needed to meet the goal of obtaining 5% improvement in fuel economy. As more material test data become available, Autonomie models can also be updated with the new assumptions and test data.

Figure 4 gives an overview of the TEG model. The exhaust flow keeps the hot side plates of TEG warm, and the cold side plates are kept at a lower temperature by the coolant flow. The thermal reservoir concept was introduced to account for the heat energy stored in these plates. This allows us to model how the surface temperature would vary if there is any variation or interruption in the exhaust flow. Hybrids are especially

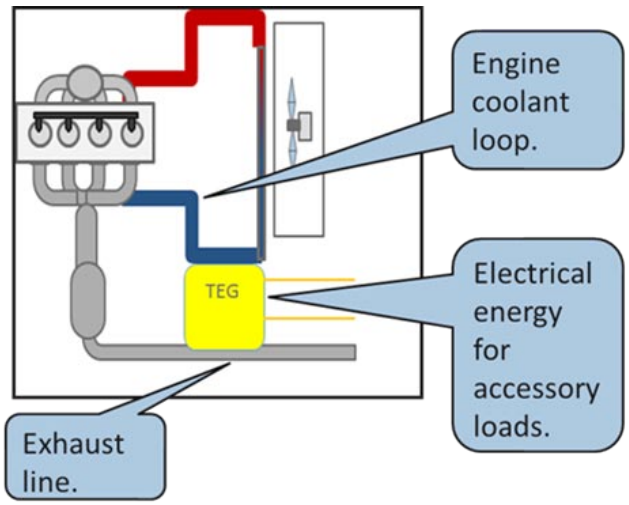

FIGURE 3. TEG System Integration to Vehicle

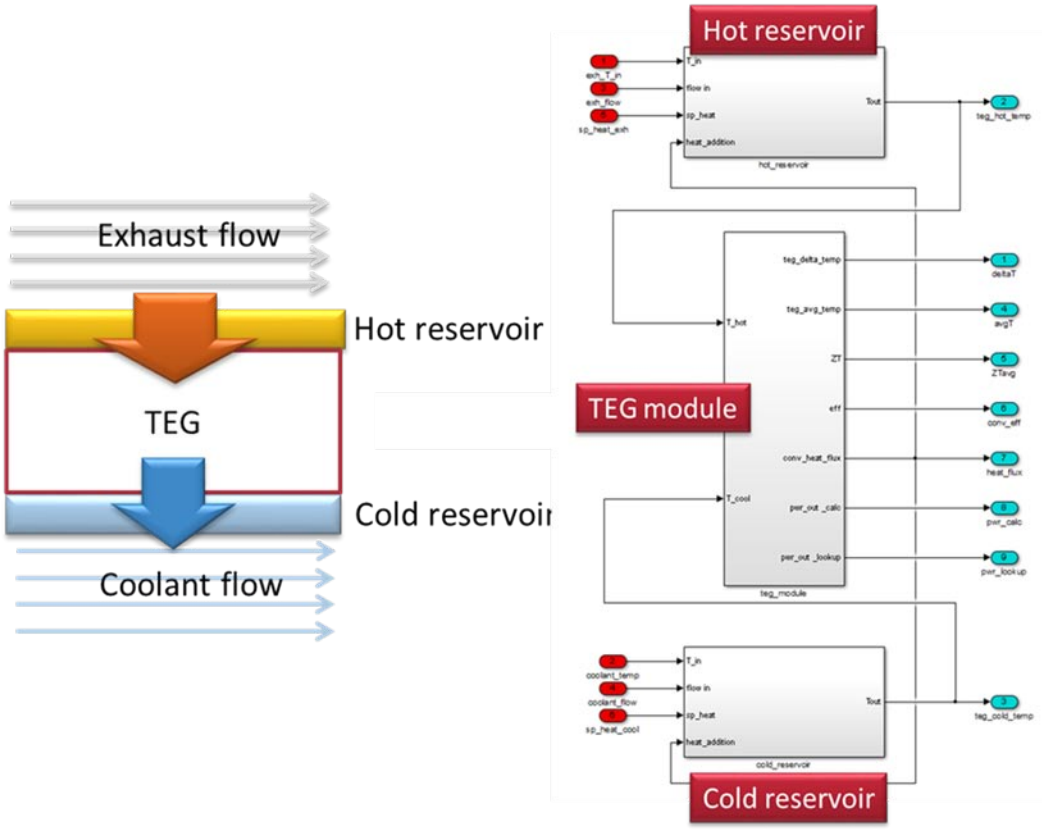

FIGURE 4. Overview of the TEG Module Model

prone to intermittent operation of the engine, and this could affect the power output we observe from the TEG.

Effect of Thermal Reservoirs on TEG Operation

The presence of thermal reservoirs (or the effect of the heat stored in the hot and cold surfaces on a TEG system) can modify TEG operating conditions. This stored energy may not cause much difference in real world driving, but on shorter regulatory cycles, the impact of the thermal reservoir is significant.

Depending on the drive cycle, vehicle technology, and number of TEG modules, the benefit of having a reservoir might vary. In conventional vehicles, we see that with an appropriately sized reservoir, the amount of energy recovered can be increased. This is attributed to the ability of reservoirs to store the heat energy from the exhaust surges and make it available to the TEG during periods such as idling, where there is input energy to the TEG. The average temperature of the TEG also drops when thermal reservoirs are considered. This could lower the operating temperature of the TEG and can reduce the overall conversion efficiency. The benefit of reservoirs diminishes if the number of modules is increased. When there are enough modules to handle the energy from these exhaust surges, then it is better to operate the TEG at higher temperatures and convert at higher efficiencies.

When the cost of TEG modules is considered, it might be better to use 20 modules with a reservoir, than to use 40 without a reservoir, as both can recover an average power of about 100 W in a midsize conventional vehicle over a UDDS cycle (Figure 5).

While the reservoir does not add much to the fuel economy benefits in certain cases, this study shows that it is surely one of the parameters that can be calibrated to maximize the benefits from TEGs.

When we test the impact of TEGs on the EPA test procedure, there are other adjustment factors that might affect the benefit we see in the mpg numbers. In the simulation analysis, overall improvement due to TEGs was in the range of 0.4 to 0.8 mpg for the vehicles we considered. This translates to roughly a 2% to 2.5% improvement in the fuel economy predicted by the adjusted two-cycle procedure. The percentage improvement in combined adjusted mpg is shown in Figure 6.

CONCLUSION

TEGs offer a way to improve fuel economy through waste heat recovery. When subjected to the EPA combined two-cycle procedure, they can provide

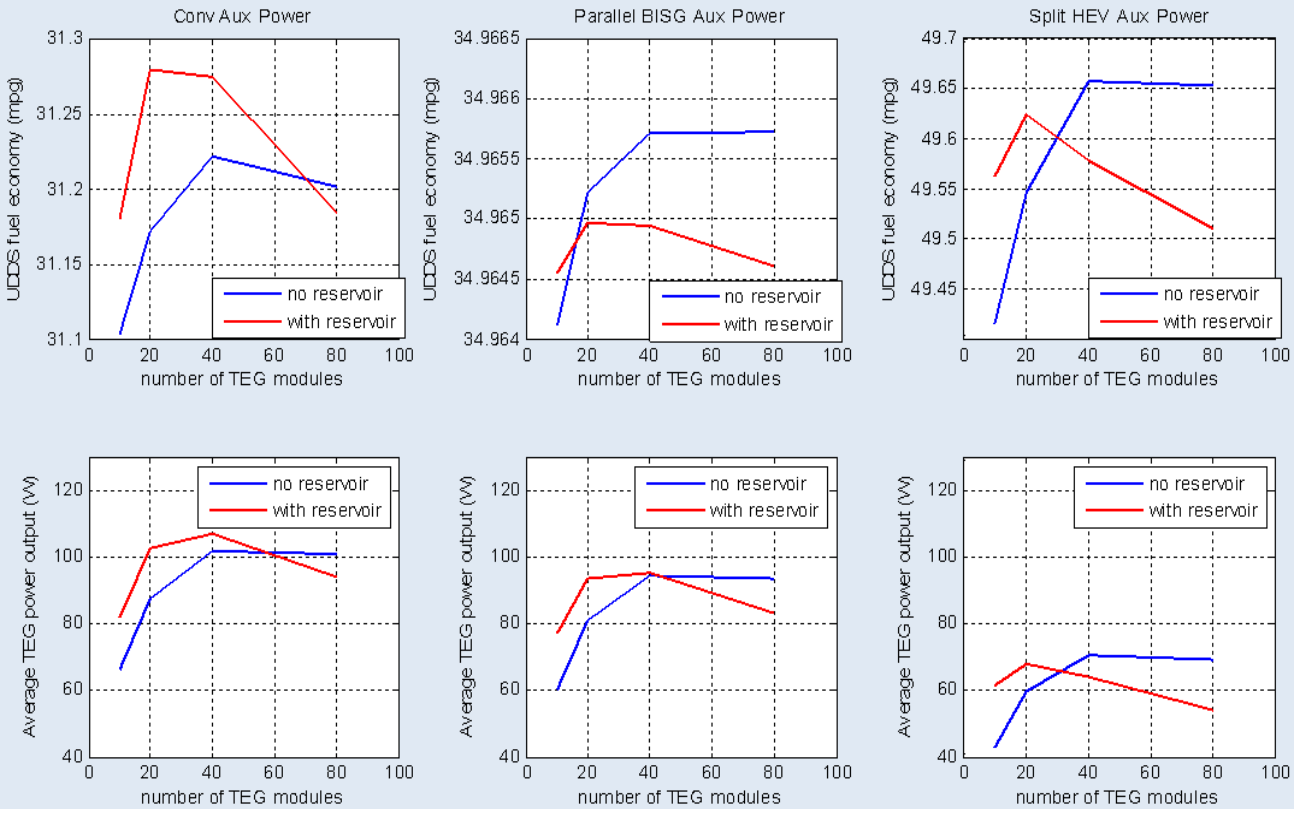

FIGURE 5. Benefit of TEGs on the UDDS Cycle

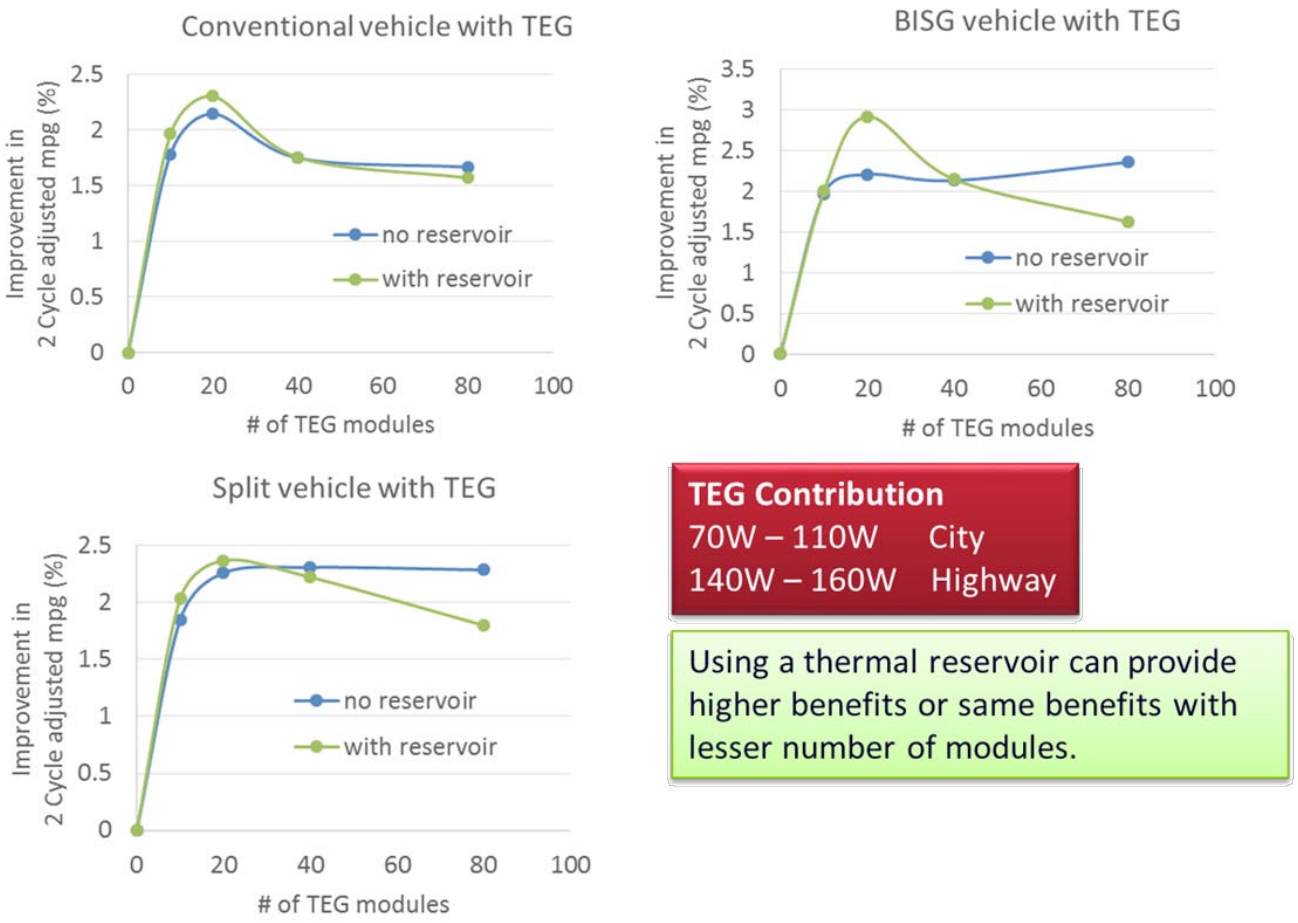

FIGURE 6. Fuel Economy Improvements in Two-Cycle Procedure Due to a TEG

between 2% and 3% improvement in mpg, depending on the vehicle technology and number of TEG modules. We have seen steady improvements in TEG modules over the last few years. Better materials/modules with higher conversion efficiencies may be able to provide more waste heat recovery. The monetary benefits of TEG vary with the type of vehicle selected for the analysis. The justifiable investment for generating 1-kW auxiliary electric power (whether it is from a TEG or other similar devices) is about $1,200. This amount is the NPV of the gasoline savings obtained due to the higher fuel economy. In the case of a split hybrid, the NPV of 1 kW of average TEG power can be as high as $2,000.

FY 2014 PUBLICATIONS

1. Vijayagopal, R., and Shidore, N., et al., "Estimating the Fuel Displacement Potential of a Thermoelectric Generator in a Conventional Vehicle, Using Simulation and Engine in the Loop Studies," EVS27, 2013.

VI. Acronyms, Abbreviations, and Definitions

η_g	Gross indicated thermal efficiency
γ	Ratio of specific heats (c_p/c_v)
κ	Thermal conductivity
λ	Stoichiometric ratio; air/fuel equivalence ratio
φ	Fuel/air equivalence ratio
σ	Electrical conductivity
µs	Micro-second
°C	Degrees Celsius
°CA	Degrees crank angle, 0° = TDC
°F	Degrees Fahrenheit
ΔP	Pressure change
ΔT	Delta (change in) temperature
0-D	Zero-dimensional
1-D, 1D	One-dimensional
2EHN	2-ethylhexyl nitrate
2-D, 2D	Two-dimensional
3-D, 3D	Three-dimensional
ABDC	After bottom-dead center
AC	Alternating current
AC, A/C	Air conditioning
ACCESS	Advanced Combustion Controls—Enabling Systems and Solutions
ACE	Advanced Combustion Engine
ACEC	Advanced Combustion and Emissions Control
ACES	Advanced Collaborative Emissions Study
AFCI	Alternate fuel compression ignition
A/F, AFR	Air/fuel ratio
Ag	Silver
AHR	Apparent heat release
AHRR	Apparent heat release rate
a.k.a.	Also known as
AKI	Anti-knock index
Al	Aluminum
Al_2O_3	Aluminum oxide
ALE	Arbitrary Lagrangian-Eulerian
ANL	Argonne National Laboratory
ANR	NH_3/NOx ratio
APS	Advanced Photon Source
APU	Auxiliary power unit
ASME	American Society of Mechanical Engineers
ASOI	After start of injection
atdc, ATDC, aTDC	After top-dead center
atm	Atmosphere
a.u.	Arbitrary units
Au	Gold
Avg.	Average
B	Boron
Ba	Barium
$BaAl_2O_4$	Barium aluminate
$Ba(NO_3)_2$	Barium nitrate
BaO	Barium oxide
bar	unit of pressure (14.5 psi or 100 kPa)
BBDC	Before bottom-dead center
BDC	Bottom-dead center
BES	Basic Energy Sciences
BET	Named after Brunauer, Emmett and Teller, this method for determining the surface area of a solid involves monitoring the adsorption of nitrogen gas onto the solid at low temperature and, from the isotherm generated, deriving the volume of gas required to form one monolayer adsorbed on the surface. This volume, which corresponds to a known number of moles of gas, is converted into a surface area though knowledge of area occupied by each molecule of adsorbate.
BFV	Bradley Fighting Vehicle
bhp-hr	Brake horsepower hour
BISG	Belt-integrated starter-generator
BiTe	Bismuth telluride
BMEP	Brake mean effective pressure
BOL	Beginning of life
Bsfc, BSFC	Brake specific fuel consumption
bsNOx, BSNOx	Brake specific NOx emissions
BTDC, btdc	Before top-dead center
BTE	Brake thermal efficiency; Boltzmann transport equation
C_2H_4	Ethene
C_2H_6	Ethane
C_3H_6	Propylene
ca.	About, approximately
CA	Crank angle

CA10	Crank angle at which 10% of the combustion heat release has occurred
CA50	Crank angle at which 50% of the combustion heat release has occurred
CAC	Charge air cooler
CAD	Crank angle degrees, computer-aided design
CAE	Computer-aided engineering
cc	Cubic centimeter
CCC	Cu-Ce-Co
CCD	Charge-coupled device
CDC	Conventional diesel combustion
CDI	Compression direct injection
CDPF	Catalyzed diesel particulate filter
Ce	Cerium
CEMA	Chemical explosive mode analysis
CeO_2	Cerium oxide
CFD	Computational fluid dynamics
CH_4	Methane
CHA	Chabhazite zeolite
CI	Compression ignition
CIDI	Compression ignition direct injection
CLC	Chemical looping combustion
CLCC	Closed-loop combustion control
CLEERS	Cross-Cut Lean Exhaust Emissions Reduction Simulations
cm	Centimeter
cm^3	Cubic centimeters
CMOS	Complementary metal oxide semiconductor
CN	Cetane number
CNG	Compressed natural gas
CNL	Combustion noise level
CO	Carbon monoxide
CO_2	Carbon dioxide
COV	Coefficient of variation (variance)
COV_{IMEP}	Coefficient of variation of indicated mean effective pressure
cP	Centipoise
CPF	Catalyzed particulate filter
cpsi	Cells per square inch
CPU	Central processing unit
Cr	Chromium
CR	Compression ratio
CRADA	Cooperative Research and Development Agreement
CRC	Coordinating Research Council
CRF	Cycloalkane reference fuel
CSC®	Cold Start Concept
CT	Computed tomography
CTE	Coefficient of thermal expansion
Cu	Copper
Cu-CHA	Copper chabazite zeolite
Cu-CTA	Copper chabazite zeolite
CV	Combustion vessel
DC, dc	Direct current; dynamic capacity
DCN	Derived cetane number
DCO™	Dual Coil Offset
deg	Degrees
°CA	Degrees crank angle, 0° = TDC
ΔT	Delta (change in) temperature
DFT	Density function theory
DI	Direct injection, direct-injected
DI PFS	Direct injection partial fuel stratification
DME	Dimethyl ether
DMP	Diesel micro-pilot
DNS	Direct numerical simulation
DOC	Diesel oxidation catalyst
DOE	U.S. Department of Energy
DOHC	Double overhead camshaft
dP	Differential pressure
DPF	Diesel particulate filter
DRIFTS	Diffuse reflectance infrared Fourier-transform spectroscopy
DSC	Differential scanning calorimeter
E10	10% ethanol, 90% gasoline fuel blend
E15	15% ethanol, 85% gasoline fuel blend
E20	20% ethanol, 80% gasoline fuel blend
E85	85% ethanol, 15% gasoline fuel blend
EC	Elemental carbon
ECM	Electronic (engine) control module
ECN	Engine Combustion Network
ECU	Electronic (engine) control unit
EDS	Energy dispersive spectroscopy
EDX	Energy dispersive X-ray
EE	Eulerian-Eulerian
EELS	Electron energy loss spectroscopy
EERE	Energy Efficiency and Renewable Energy
EEVO	Early exhaust valve opening
EFA	Exhaust filtration analysis
EGR	Exhaust gas recirculation

EHN	Ethyl hexyl nitrate
EIT	Engine in the loop
EOI	End of injection
EPA	U.S. Environmental Protection Agency
ERC	Engine Research Center
ESL	ElectroScience Inc.
et al.	Et Alii: and others
EV	Exhaust valve
EVC	Exhaust valve closing
EVO	Exhaust valve opening
EXAFS	Extended X-ray absorption fine structure
FACE	Fuels for Advanced Combustion Engines
Fe	Iron
FE	Fuel economy
FEA	Finite element analysis
FEM	Finite element method
FFVA	Fully flexible valve actuation
FID	Flame ionization detector
FMDF	Filtered mass density function
FMEA	Failure mode and effects analysis
FMEP, fmep	Friction mean effective pressure
FSN	Filter smoke number
FTIR	Fourier transform infrared
ft-lb	Foot-pound
FTP	Federal Test Procedure
FTP-75	Federal Test Procedure for light-duty vehicles
FY	Fiscal year
g, G	Gram
g/bhp-hr	Grams per brake horsepower-hour
GC	Gas chromatography
GC-FID	Gas chromatograph combined with a flame ionization detector
GCI	Gasoline compression ignition
GC-MS	Gas chromatography – mass spectrometry
GDCI, GDICI	Gasoline direct injection compression ignition
GDI	Gasoline direct injection; Gasoline direct injector
Ge	Germanium
g/hphr	Grams per horsepower-hour
GHSV	Gas hourly space velocity
gIMEP	Gross indicated mean effective pressure
GM	General Motors
g/mi	Grams per mile
GPF	Gasoline particulate filter
GPU	Graphical processing unit
GTDI	Gasoline turbocharged direct injection
H_2	Diatomic (molecular) hydrogen
H_2CO	Formaldehyde
H_2O	Water
H_2O_2	Hydrogen peroxide
HAADF STEM	High angle annular dark field scanning transmission electron microscopy
HC	Hydrocarbons
HCCI	Homogeneous charge compression ignition
HD	Heavy-duty
He	Helium
HECC	High Efficiency Clean Combustion
HEUI	Hydraulically activated electronic unit injector
HEV	Hybrid electric vehicle
HEX	Heat exchanger
HFIR	High Flux Isotope Reactor
HHV	Higher heating value
HIL	Hardware in the loop
hp	Horsepower
HPC	High-performance computing
HPL	High pressure loop
HPLB	High pressure, lean-burn
hr	Hour
HR	Heat release
HRR	Heat release rate
HRTEM	High-resolution transmission electron microscopy (microscope)
HVA	Hydraulic valve actuation
HVAC	Heating, ventilation and air conditioning
HWFET	Highway Fuel Economy Test
HWG	Hollow waveguide
Hz	Hertz
IAO2	Intake air oxygen
IC	Internal combustion
ICCD	Intensified charged-coupled device
ICE	Internal combustion engine
ID	Internal diameter
IMEP	Indicated mean effective pressure
$IMEP_g$	Indicated mean effective pressure, gross
$IMEP_{net}$	Indicated mean effective pressure, net
IR	Infrared
ISFC	Indicated specific fuel consumption

ISX	Cummins Inc. 15-liter displacement, inline, 6-cylinder heavy duty diesel engine
ITE	Indicated thermal efficiency
ITHR	Intermediate temperature heat release
IV	Intake valve
IVC	Intake valve closing
IVO	Intake valve opening
J	Joule
k	thousand
K	Kelvin, potassium
kg	Kilogram
kHz	Kilohertz
KIVA	Combustion analysis software developed by Los Alamos National Laboratory
KIVA-CMFZ	KIVA Coherent Flamelet Multi-Zone
kJ	Kilojoules
kJ/L	Kilojoules per liter
kJ/m^3	Kilojoules per cubic meter
KLSA	Knock-limited spark advance
KMC	Kinetic Monte Carlo
kPa	Kilopascal
kW	Kilowatt
L	Liter; Length; as in 0.5L is half catalyst full length
La	Lanthanum
LANL	Los Alamos National Laboratory
lb ft	Pound foot
lb/min	Pounds per minute
lbs	Pounds
lbs/sec	Pounds per second
LD	Light-duty
LDB	Lean Downsize Boost
LDT	Light-duty truck
LDV	Light-duty vehicle
LE	Lagrangian-Eulerian
LED	Light-emitting diode
LES	Large-eddy simulation
LHV	Lower heating value
LIF	Laser-induced fluorescence
LII	Laser-induced incandescence
LLNL	Lawrence Livermore National Laboratory
LMO	$LaMnO_3$
LNT	Lean-NOx trap
LOL	Lift-off length
LP	Low pressure
LPL	Low pressure loop
LSC	$La_{1-x}Sr_xO_{3-\delta}$
LSCO	$(La,Sr)CoO_3$
LSMO	$(La,Sr)MnO_3$
LTC	Low-temperature combustion
LTGC	Low-temperature gasoline combustion
LTHR	Low-temperature heat release
m^2	Square meters
m^2/gm	Square meters per gram
m^3	Cubic meters
mA	Milliamps
MAP	Manifold air pressure
mbar	Millibar
MBT	Minimum (spark advance) for best torque; Maximum brake torque
MCE	Multi-cylinder engine
MCP	Micro-channel plate
MD	Medium-duty
MER	Molar expansion ratio
Mg	Magnesium
mg/cm^2	Milligrams per square centimeter
mg/mi	Milligram per mile
mg/mm^2	Micrograms per square millimeter
mg/scf	Milligrams per standard cubic foot
mi	Mile
µs	Micro-second
min	Minute
MIT	Massachusetts Institute of Technology
µm	Micrometer
mm	Millimeter
mmols	Micro-moles
Mn	Manganese
Mo	Molybdenum
mol	Mole
mol/s	Moles per second
MON	Motor Octane Number
MOU	Memorandum of understanding
MPa	Megapascals
mpg	Miles per gallon
mph	Miles per hour
MPI	Message Passing Interface
MPICH2	Portable Implementation of MPI
MPRR	Maximum pressure-rate rise
MPT	MAHLE Powertrain

mRIF	Multiple representative interactive flamelet
ms	Millisecond
MS	Mass spectrometry
MSU	Michigan State University
MTU	Michigan Technological University
MZ	Multizone
N_2	Diatomic nitrogen
N_2O	Nitrous oxide
N_2O_3	Nitrogen trioxide
Na	Sodium
NA	Naturally aspirated
NETL	National Energy Technology Laboratory
NH_3	Ammonia
nm	Nanometer
Nm	Newton meter
NMEP	Net mean effective pressure
NMHC	Non-methane hydrocarbon
NMOG	Non-methane organic gases
NO	Nitric oxide
NO_2	Nitrogen dioxide
NOx, NO_X	Oxides of nitrogen
NPV	Net present value
NRE	NOx reduction efficiency
ns	Nanosecond
NSC	NOx storage capacity
NSE	NOx storage efficiency
NSR	NOx storage and reduction
NTC	Negative temperature coefficient
NTE	Net thermal efficiency; Negative thermal expansion
NVH	Noise, vibration, and harshness
NVO	Negative valve overlap
NW	Nanowire
O_2	Diatomic (molecular) oxygen
O_3	Ozone
OBD	On-board diagnostics
OC	Organic carbon
OD	Outside diameter
OEM	Original equipment manufacturer
OH	Hydroxyl
OH PLIF	Planar laser-induced fluorescence of OH
ORC	Organic Rankine cycle
ORF	Olefin reference fuel
ORNL	Oak Ridge National Laboratory
OSC	Oxygen storage capacity
P	Pressure
PAH	Polycyclic aromatic hydrocarbon
PCCI	Premixed Charge Compression Ignition
PCI	Premixed compression ignition
PCP	Peak cylinder pressure
PCS	Predictor-corrector split
PDF	Probability density function
PDI	Port-assisted direction injection
PI	Particulate filter
PFI	Port fuel injected; Port fuel injection
PFS	Partial fuel stratification
P-G	Petrov-Galerkin
PGM	Platinum-grade metal, platinum group metal
PIV	Particle image velocimetry
P_{in}	Intake pressure
PLIF	Planar laser-induced fluorescence
PLII	Planar laser-induced incandescence
PM	Particulate matter; Premixed
PNA	Passive NOx adsorber
PNNL	Pacific Northwest National Laboratory
ppb	Parts per billion
PPC	Partially premixed combustion
PPCI	Partially premixed compression ignition
ppi	Pores per square inch
ppm	Parts per million
PRF	Primary reference fuel
PRF80	PRF mixture with an octane number of 80 (i.e., 80% iso-octane and 20% n-heptane)
PRR	Pressure-rise rate
PSAT	Powertrain Systems Analysis Toolkit
PSD	Power spectral density
psi	Pounds per square inch
psig	Pounds per square inch gauge
Pt	Platinum
PTO	$PbTiO_3$
PV, P-V	Pressure-volume
PVT	Pressure-volume-temperature
Q	Heat
Q1, Q2, Q3, Q4	First, second, third and fourth quarters
R&D	Research and development
RANS	Reynolds-averaged Navier-Stokes
RCCI	Reactivity-controlled compression ignition

RCM	Rapid compression machine
Re	Reynolds number; radius of gyration
RE	Rare earth
REV	Representative equivalent volume
RF	Radio frequency
Rh	Rhodium
RI	Ringing intensity
ROI	Rate of injection
RON	Research Octane Number
RPM, rpm	Revolutions per minute
S	Seebeck coefficient
S	Sulfur
SA	Spark assist(ed)
SACI	Spark-assisted compression ignition
SAE International	Technical association formerly known as the Society of Automotive Engineers
SA-HCCI	Spark-Assisted Homogeneous Charge Compression Ignition
sccm	Standard cubic centimeters
SCE	Single-cylinder engine
SCF/min	Standard cubic feet per minute
SCR	Selective catalytic reduction
SCRF®	Selective catalytic reduction on filter; integrated DPF and SCR technologies
sec	Second
SEM	Scanning electron microscopy
Si	Silicon
SI	Spark ignition, Spark-ignited
SIDI	Spark-ignited direct injection
SI-SACI	Spark ignition, spark-assisted compression ignition
SFC	Specific fuel consumption
SFSM	Sequential function specification method
SG5	Spray Guided Engine version 5
SMPS	Scanning mobility particle sizer
SNL	Sandia National Laboratories
SO_2	Sulfur dioxide
SOC	Start of combustion; soluble organic compound
SOI	Start of injection
SOF	Soluble organic fraction
SOFC	Solid oxide fuel cell
SO_x	Oxides of sulfur
SpaciIR	Spatially resolved capillary inlet Fourier transform infrared
SpaciMS	Spatially resolved capillary inlet mass spectrometer
SPPS	Solution precursor plasma spray
Sr	Strontium
SU	Stanford University
SULEV	Super Ultra-Low Emissions Vehicle
SUV	Sport utility vehicle
SwRI®	Southwest Research Institute®
T	Temperature
T2B2	Tier 2 Bin 2
T2B5	Tier 2 Bin 5
T_{90}	90% volume recovered temperature
TARDEC	Tank Automotive Research, Development and Engineering Center
TBC	Thermal barrier coating
TC	Turbocompound; total capacity
TCC	Transparent combustion chamber
TCR	Thermochemical recuperation
TCRI	Turbulence-chemistry-radiation interactions
TDC	Top-dead center
TE	Thermoelectric; Thermal efficiency
TED	Thermoelectric device
TEG	Thermoelectric generator
TEM	Transmission electron spectroscopy; thermoelectric module
TGA	Thermal gravimetric analysis (analyzer)
THC	Total hydrocarbon
T_{in}	Intake temperature
TJI	MAHLE Powertrain's Turbulent Jet Ignition
TPD	Temperature-programmed desorption
TPO	Temperature-programmed oxidation
TPR	Temperature-programmed reduction or reaction
TRF	Toluene reference fuel
TS	Thermal stratification
T_{wall}	Temperature, wall
TWC	Three-way catalyst
UCB	University of California, Berkeley
UDDS	Urban Dynamometer Driving Schedule
UEGO	Universal exhaust gas oxygen
UHCs	Unburned hydrocarbons
UHP	Ultra-high porosity
ULSD	Ultra-low sulfur diesel
UM	University of Michigan

US06	Supplemental Federal Test Procedure (SFTP) drive cycle
U.S. DRIVE	United States Driving Research and Innovation for Vehicle efficiency and Energy sustainability
USSET	U.S. Supplemental Emission Testing
UV	Ultraviolet
UW	University of Wisconsin
UW-ERC	University of Wisconsin Engine Research Center
UWS	Urea-water solution
V	Volt
VAC	Volts, alternating current
VCR	Variable compression ratio
VDC	Volts – direct current
VGC	Variable geometry compressor
VGT	Variable geometry turbocharger
VNT	Variable nozzle turbine
VOCs	Volatile organic compounds
VVA	Variable valve actuation
VVT	Variable valve timing
W	Watt
WC	Tungsten carbide
WGS	Water-gas shift
WHR	Waste heat recovery
WOT	Wide-open throttle
wt%	Weight percent
WTT	Well-to-tank
XAFS	X-ray aborption fine structure
XAS	X-ray absorption spectroscopy
XPS	X-ray photoelectron spectroscopy
XRD	X-ray diffraction
Y	Yttrium
yr	Year
YSZ	Ytrria-stabilized zirconia
Zn	Zinc
Zr	Zirconium
zT	Dimensionless thermoelectric figure of merit; equal to: (electrical conductivity) (Seebeck coefficient)^2(temperature)/ (thermal conductivity)
ZTO	Zn_2SnO_4

VII. Index of Primary Contacts

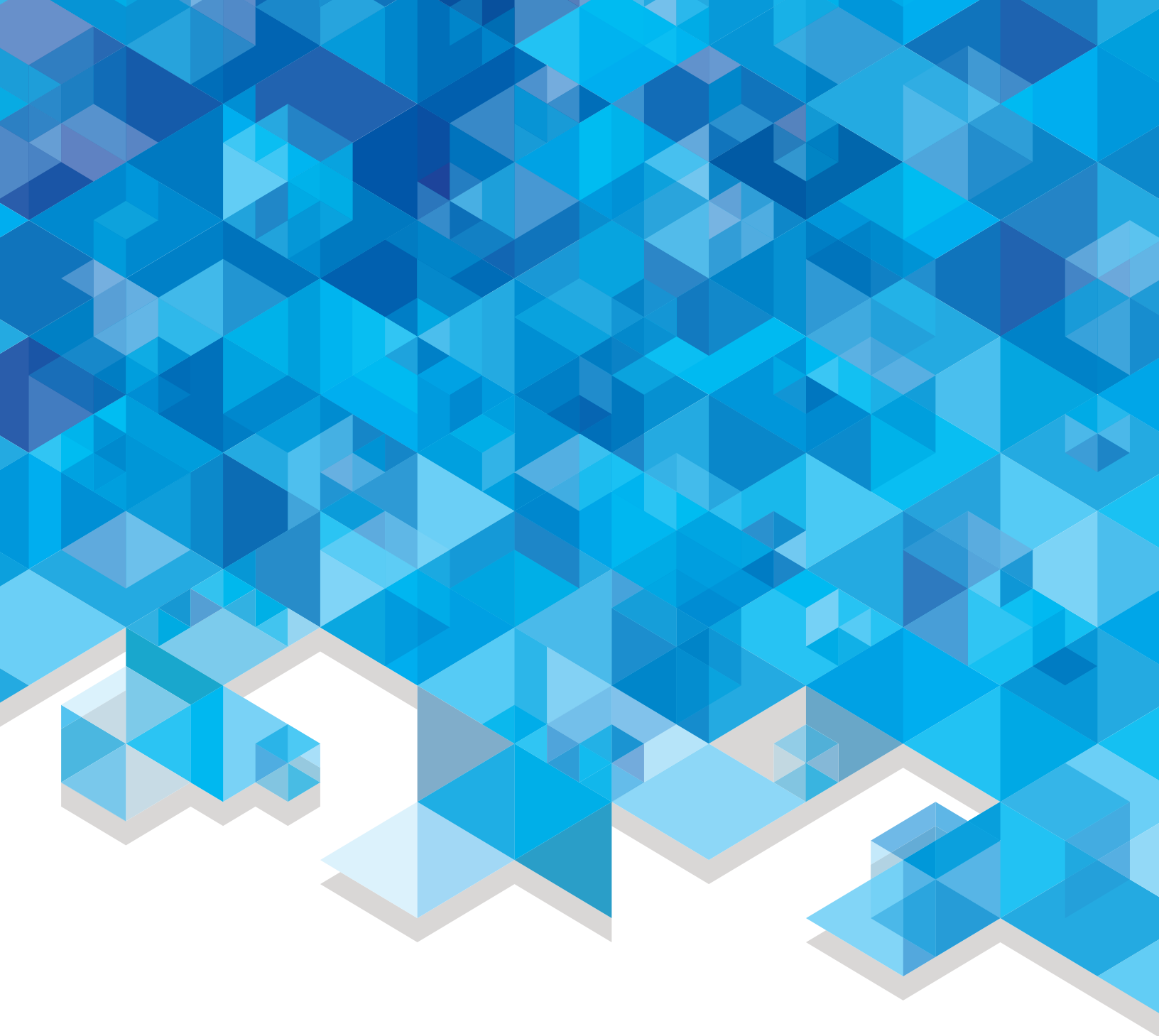

U.S. DEPARTMENT OF
ENERGY
Energy Efficiency &
Renewable Energy

For more information, visit: energy.gov/eere

DOE/EE-1156 • March 2015